MICROFUNGI IN THAI COASTAL WETLANDS: INSIGHTS INTO FRESHWATER POALES

AMUHENAGE THARINDU BHAGYA MAITHREEPALA

DOCTOR OF PHILOSOPHY

IN

BIOLOGICAL SCIENCE

SCHOOL OF SCIENCE

MAE FAH LUANG UNIVERSITY

2025

MICROFUNGI IN THAI COASTAL WETLANDS: INSIGHTS INTO FRESHWATER POALES

AMUHENAGE THARINDU BHAGYA MAITHREEPALA

THIS DISSERTATION IS A PARTIAL FULFILLMENT OF THE REQUIREMENTS FOR THE DEGREE OF MASTER OF PHILOSOPHY IN BIOLOGICAL SCIENCE

SCHOOL OF SCIENCE
MAE FAH LUANG UNIVERSITY
2025

DISSERTATION APPROVAL

MAE FAH LUANG UNIVERSITY

FOR

DOCTOR OF PHILOSOPHY IN BIOLOGICAL SCIENCE

Dissertation Title: Microfungi in Thai Coastal Wetlands: Insights into Freshwater Poales

Author: Amuhenage Tharindu Bhagya Maithreepala

Examination Committee:

Assistant Professor Mark Seasat Calabon, Ph. D.	Chairperson
Assistant Professor Pattana Kakumyan, Ph. D.	Member
Adjunct Professor Kevin David Hyde, Ph. D.	Member
Chitrabhanu Sharma Bhunjun, Ph. D.	Member
Associate Professor Wei Dong, Ph. D.	Member

Advisor:

.....Advisor

(Assistant Professor Pattana Kakumyan, Ph. D.)

Dean:

.....

(Professor Surat Laphookhieo, Ph. D.)

ACKNOWLEDGEMENTS

I would like to express my sincere gratitude to Adjunct Professor Dr. Kevin D. Hyde for providing me with the opportunity to pursue and complete my PhD under his invaluable guidance. The immense wealth of knowledge and experience he generously shared during field collections, laboratory experiments, and the preparation of publications has been truly invaluable. I am also deeply grateful to Professor E. B. Gareth Jones for his continuous motivation, guidance, and for sharing his immense knowledge, which helped me realize my dream of completing a PhD. Their expertise in aquatic and marine mycology has illuminated my path throughout this journey. The guidance, mentorship, and encouragement provided by both professors were truly key factors in the success of my work.

I would like to express my heartfelt gratitude to my supervisor, Dr. Chayanard Phukhamsakda, for introducing me to the first steps of mycology and guiding me through each stage of this journey. Her remarkable knowledge of mycology and exceptional management skills made my learning process smooth and effective. I am deeply grateful to Dr. Chayanard for training me to withstand the pressures of a PhD and for helping me transform those challenges into valuable outcomes.

My sincere thanks go to Assistant Professor Dr. Pattana Kakumyan, School of Sciences, Mae Fah Luang University, Thailand, for undertaking the challenging responsibility of serving as the main advisor for my research project. I am deeply grateful for her insightful comments and the attention she provided throughout the entire process. I would also like to thank Assistant Professor Mark S. Calabon, University of the Philippines Visayas, Philippines, for sharing his wisdom on aquatic fungi, guiding me to overcome challenges, and helping me understand the broader perspective of aquatic mycology.

Furthermore, I extend my gratitude to Dr. Chitrabhanu S. Bhunjun, School of Sciences, Mae Fah Luang University, Thailand, for his continuous support and guidance. His expertise in bioinformatics and the knowledge he shared enabled me to navigate the scientific strategies required to address challenges in taxonomy, phylogeny, and diversity investigations.

I would like to extend my heartfelt thanks to all the academic members of the Center of Excellence in Fungal Research, including Assistant Professor Dr. Ruvishika Jayawardena, Assistant Professor Dr. Thilini Chethana, Dr. Saranyaphat Boonmee, and Dr. Ausana Mapook, for their guidance and support. I am also deeply grateful to all the seniors spread across the globe, including Professor Sajeewa Maharachchikumbura, Professor Dhanushka N. Wanasinghe, Professor Samantha Karunarathna, Assistant Professor Hiran A. Ariyawansa, Dr. Ishara Manawasinghe, Dr. Chinthani Senanayake, Dr. Danushka Thennakoon, Dr. Milan Samarakoon, Dr. Pranami Abewisrama, Dr. Asha J. Dissanayake, Dr. Monika Dyarathne, Dr. Achala Ratnayake, Dr. Nuwanthika Subodhini, Dr. Dayana Marasinghe, Dr. Vinidini Thiyagaraja, Dr. Binu Samarakoon, Dr. Janith Aluthmushandiram, Dr. Nethmini Samaradiwakara, and Dr. Erandi, for their continuous encouragement and academic inspiration. I would also like to express my gratitude to my collaborators on publications, including Professor Eric McKenzie, Dr. Sinang Hongsanan, Dr. Shaun Pennycook, and Dr. Kasayuki Tanaka, whose insightful comments and advice greatly enhanced the quality of my work. My sincere thanks also go to Sornram Sukpisit, Wilawan Punyaboon, and Kasiphat Limsakul for their invaluable assistance. Without their generous support, it would not have been possible to complete this research successfully. Last but certainly not least, I wish to express my deepest gratitude to my parents, my brother, my wife, and my friends for their unwavering love, encouragement, and support, which have been my strength throughout my PhD journey and life in general.

Amuhenage Tharindu Bhagya Maithreepala

Dissertation Title	Microfungi in Thai Coastal Wetlands: Insights into Freshwater Poales
Author	Amuhenage Tharindu Bhagya Maithreepala
Degree	Doctor of Philosophy (Biological Science)
Advisor	Assistant Professor Pattana Kakumyan, Ph. D.

ABSTRACT

Wetlands are diverse ecosystems that provide numerous ecological niches and support long-term stability through biodiversity, nutrient cycling, and balanced ecosystem processes. In Thailand, coastal freshwater wetlands are largely dominated by Poales, a major monocot group that originated in the mid-Cretaceous and rose to global ecological importance in the Oligocene. Key families such as Poaceae, Cyperaceae, Juncaceae, and Typhaceae occupy varied habitats, support whole ecosystems, and supply major agricultural crops. Their fungal associations contribute to nutrient cycling, plant health, and ecosystem resilience, yet studies on microfungal diversity in tropical wetland Poales remain limited. This study therefore investigates saprobic microfungi associated with dominant Poales families in coastal freshwater wetlands of central and southern Thailand, providing taxonomic data, detailed morphology, illustrations, and an updated review of Ascomycota in these habitats.

Decomposing emergent and submerged plant materials were collected from wetlands in Khao Sam Roi Yot, Pran Buri, and Narathiwat, and a polyphasic approach was used for fungal identification. The study discovered 14 novel species new to science, including *Bambusicola loticola, Beltrania typhacearum, Distoseptispora paracrassispora, Distoseptispora pranburensis, Jalapriya saccata, Hongkongmyces typhacearum, Paraphaeosphaeria siamensis, Phaeoisaria pranburensis, Phaeoacremonium bambusae, Sporidesmium siamense, Poaceascoma fluviale, Stagonospora narathiwatensis, Tetraploa fusiformis,* and *Triadelphia parafusiformis*. In addition, 35 other species were recorded as new host or geographical records. Detailed descriptions, illustrations, and updated phylogenetic analyses are provided for each taxon. The distribution of saprobic microfungi across host families, and their ecological adaptations and geographical patterns, are also

discussed. This study highlights the high microfungal diversity in coastal freshwater wetlands of Thailand and supports future fungal taxonomic research in these ecosystems.

Research on the vertical distribution of saprobic fungi associated with Poales in Thailand's wetlands remains limited. In this study, decomposing material of *Typha angustifolia*, an invasive wetland plant with both submerged and aerial parts, was examined to assess vertical patterns of microfungal communities in Pran Buri and Khao Sam Roi Yot wetlands, Prachuap Khiri Khan Province. Sampling targeted three plant segments: (1) aerial leaves near the tip, (2) the portion between the tip and waterline, and (3) submerged leaves below the water surface. Fungi were identified using morphology and multigene phylogeny, and each taxon was recorded by vertical level.

From 360 samples, 73 saprobic genera were recorded. The middle segment showed the highest richness (48 genera; $H' = 3.4452$), while the aerial segment was least diverse (34 genera; $H' = 3.0412$). ANOVA ($Pr(>F) = 0.224$) showed no significant difference in α-diversity among levels. β-diversity analyses indicated distinct communities: Bray–Curtis showed the highest similarity between aerial and middle parts, and Sørensen showed the lowest dissimilarity between middle and submerged parts. PERMANOVA revealed significant compositional differences (39% and 35% explained by Bray–Curtis and Sørensen), while PERMDISP confirmed these were not due to dispersion. Generalist fungi occurred across all levels, while Halosphaeriaceae, Diplocladiella, and Jalapriya were restricted to submerged parts. Overall, the middle segment functioned as a transitional zone. Heatmaps, boxplots, and NMDS ordinations support these findings.

Keywords: Aquatic Fungi, α-diversity, β-diversity, Freshwater Fungi, Fungal Ecology, Fungal Taxonomy, Habitat Filtering

TABLE OF CONTENTS

TABLE OF CONTENTS

LIST OF TABLES

LIST OF FIGURES

LIST OF FIGURES

LIST OF FIGURES

LIST OF FIGURES

LIST OF FIGURES

LIST OF FIGURES

LIST OF FIGURES

LIST OF FIGURES

LIST OF FIGURES

ABBREVIATIONS AND SYMBOLS

cm	centimeter
com.	combination
diam.	diameter
e.g.	for example
et al.	and others
gen.	genus (singular) and genera (plural)
i.e.	that is
mm	millimeter
nov.	novum (Latin for new thing)
sp.	species
spp.	species (plural)
$\bar{x}$	average
°C	degree centigrade
=	heterotypic (taxonomic, facultative) a synonym
≡	homotypic (nomenclatural, obligate) a synonym
µm	micrometer
µl	microliter
%	percent

CHAPTER 1

INTRODUCTION

1.1 Wetlands

Wetlands are ecologically and socio-economically important ecosystems in the biosphere with a long geologic history. They are dynamic and robust systems (Finlayson et al., 2018). The most accepted definition was provided by the RAMSAR Convention, which defines wetlands as "areas of marsh, fen, peatland or water, whether natural or artificial, permanent or temporary, with water that is static or flowing, fresh, brackish or salt, including areas of marine water the depth of which at low tide does not exceed six meters". The RAMSAR Convention states that the global wetlands cover roughly 6% of the total land surface.

The origin of the first wetlands dates back to the mid-Paleozoic period (440 to 419 million years ago), and the organization of different wetland environments occurred parallel to plant diversification (Greb et al., 2022). With the evolution and diversification of the earliest land plants, the differentiation of wetland types has begun (Greb et al., 2006). The origin of vascular plants such as shrubs in the Emsian age (407 to 393 million years ago) and large trees in the Eifelian age (393 to 387 million years ago), led to the development of marshes and swamps in the mid-Devonian era (393 to 382 million years ago). They contributed by holding soil particles tightly from their developing root systems (Delwiche & Cooper, 2015). Differentiation of wetlands into various niches resulted in territorialization of arthropods and tetrapods in the Silurian and the late Devonian periods, respectively (Greb et al., 2006). In the Cretaceous period, the evolution of angiosperms has been occurred and it led to the expansion of aquatic species and the earliest true mangroves (Greb et al., 2006). Angiosperm diversifications were increased in the Tertiary (65 to 2.5 million years ago) and the expansion of grasses, rushes, and sedges into wetland habitats were started. This expansion had allowed the evolution of both freshwater and saltwater reed marshes (Greb et al., 2006).

1.2 Poales Hosts in Wetland Ecosystems

Wetland ecosystems are one of the most productive environments on earth, consist of rich biodiversity including plants and animals. The origin of the order Poales in Angiosperms has been reported in the late Cretaceous period (145 to 66 million years ago). At the end of the Paleogene era (66 to 23 million years ago), those early monocotyledonous plants diversified into modern families such as Cyperaceae, Juncaceae, Poaceae, and Typhaceae in Poales (Bouchenak-Khelladi et al., 2014). The physiology and anatomical features of those families facilitated their colonization of diverse habitats including wetlands. According to that, at the end of the Oligocene epoch (34 to 23 million years ago), the marshes and swamps were colonized with grasses and grass-like plants resembling today (Greb et al., 2006; Greb et al., 2022). This rich diversity of Poales hosts in wetlands including coastal ecosystems, facilitates the successful colonization of microorganisms, especially fungi.

1.3 Microfungal Communities in Wetlands

The wetland ecosystems provided nutrient-rich substrates, hosts, and facilitative environmental conditions for fungi. Those features may aid their establishment, colonization, and evolution in wetlands (Yarwood, 2018). Wind can disperse fungal spores for great distances. The lightweight conidia and ascospores are capable of blowing with the wind and landing on wetland ecosystems (Golan & Pringle, 2017). Water associated with wetland ecosystems could function as a vector for fungi. Rivers, tributaries, and rainwater have the potential to bring floating fungal spores to wetlands. Ocean currents and tides can deposit floating fungal spores into coastal wetlands. For example, Ingoldian fungi exhibit specifically shaped spores that facilitate their disposal via water. *Lignicola laevis* shows wide distribution in many marine ecosystems, suggesting that this fungus uses water current to disperse its spores over oceans (Pang et al., 2013). Live plants can float on freshwater or via the ocean and settle in wetlands. The fungal communities that were available on those plant materials can take a foothold to establish new populations in wetland ecosystems (Pang et al., 2013). According to

that, fungal communities are a part of the rich diversity available in wetlands (Voglmayr, 2011).

Many investigations of microfungal associated with aquatic ecosystems including wetlands have been reported throughout the world (Calabon et al., 2022; Calabon et al., 2023; Bhagya et al., 2024; Bhgya et al., 2025). However, taxonomic studies, distribution and diversity studies of microfungi associated with Poales hosts in coastal wetlands in Asian region are currently limited.

1.4 Coastal Wetland Ecosystems in Thailand

Wetlands can be categorized based on several factors, including water flow patterns, pH level, soil properties, nutrient availability, and geographic locations. That segregates wetlands into six main categories such as marine, estuarine, lacustrine, riverine, and palustrine (marshes) (Clarksoon & Peters, 2010). Among them, marine and estuarine wetlands are primarily located along coastal regions and comprise ecosystems such as coastal lagoons, rocky shorelines, mangrove forests, and tidal marshes (Figureueroa et al., 2018).

Thailand is a tropical Asian country with a rich accumulation of flora and fauna. Wetlands play a huge part in harboring the country's biodiversity and providing economic resources like sites for eco-tourism and aquaculture (Hempattarasuwan et al., 2021). Thailand's wetlands include marine wetlands, marshes, estuarine, and mangrove swamps. Those ecosystems extend approximately 36,600 km^2 and cover 7.5% of the available land surface of the country. Coastal wetlands are distributed in many areas in southern Thailand such as Thale Noi Non (Phatthalung province), Don Hoi Lot (Samut Songkhram Province), and the Gulf of Thailand including Khao Sam Roi Yot and Pran Buri (Prachuap Khiri Khan Province). Those wetlands are dominated by plants related to the order Poales (Trisurat, 2006) and other monocotyledons and dicotyledons.

Investigations related to coastal wetland-inhabiting fungi including fungi on wetland-dwelling Poales in Thailand are scarce and far between. The majority of the existing studies are centered around understanding the importance of mycorrhizal fungi communities occupying Poales in tropical wetlands (Miller & Bever, 1999; Zhang et

al., 2024). Therefore, a comprehensive investigation of microfungal diversity and distribution in coastal wetland habitats in southern Thailand are currently limited.

1.5 Importance of Investigating Microfungi in Coastal Wetlands

Fungi are successfully colonized with plants by adopting various lifestyles through parasitism, mutualism, and saprotrophy. Among these, saprobic taxa play an important role in the decomposition of organic matter and nutrient cycling in different ecosystems including wetland habitats. This research investigates the saprobic fungi associated with coastal wetland ecosystems that are responsible for decomposing dead plant materials on three selected families under order Poales, which dominate in coastal freshwater habitats in Thailand. The selected plant families are Cyperaceae, Poaceae, and Typhaceae. The target geographic areas of this study are Khao Sam Roi Yot and Pran Buri wetlands in Prachuap Khiri Khan Province, and Narathiwat peat swamp (Narathiwat Province) as sampling sites due to the limited microfungal studies in these areas. Also, these coastal wetlands have a rich diversity of Poales hosts and high socio-economic and ecological importance. Therefore, expanding the current understanding of microfungi associated with Poales hosts in coastal wetlands will provide significant findings for both mycologists and ecologists to understand the fungal biodiversity in coastal ecosystems. Further, studies in fungal taxonomy based on modern approaches; morphology and multigene phylogeny, including fungal ecology and diversity lead to produce and share accurate mycological data to the world.

1.6 Research Gaps

1.6.1 Lack of a comprehensive review on ascomycetes associated with wetland habitats in Asia, including Thailand

1.6.2 Lack of taxonomic studies on ascomycetes associated with Poales hosts in coastal wetland habitats in Thailand

1.6.3 Lack of investigation on the vertical diversity of ascomycetes and their ecological functions in coastal wetland habitats

1.7 Research Objectives

1.7.1 To study taxonomy of ascomycetes associated with Poales hosts in coastal wetland ecosystems in Thailand based on morphology and multi-locus phylogeny

1.7.2 To compare the occurrences of ascomycetes associated with hosts from Typhaceae, Poaceae, and Cyperaceae in coastal wetland ecosystems in Thailand

1.7.3 To conduct a comprehensive review of ascomycetes associated with wetland habitats, highlighting their ecological roles and global distribution

1.7.4 To investigate the vertical distribution of saprobic microfungi on Typhaceae hosts in coastal wetland ecosystems

1.8 Research Contents

This thesis is divided into six chapters.

Chapter 1 is the general introduction, which provides background on wetlands, their origin and diversification, emphasizing the coastal wetlands and importance of studying microfungi associated with Poales hosts in coastal freshwater wetlands in Thailand, as well as the research gaps, objectives of this research and the outline of the thesis.

Chapter 2 provides a comprehensive literature review on the current knowledge related to freshwater wetlands and Poales-associated fungi, including the applications of these studies and future perspectives.

Chapter 3 provides 50 entries covering both *Dothideomycetes* and *Sordariomycetes* related to Poales-associated fungal taxa identified from wetlands, with detailed illustrations accompanied by notes containing their main characteristics, ecological roles, geographical distribution, nutritional modes, and taxonomic placements.

Chapter 4 presents a detailed taxonomic study of saprobic microfungi associated with wetland-dwelling Poales in freshwater coastal wetlands of Thailand. The study covers three main host families: Cyperaceae, Poaceae, and Typhaceae. The assemblage

comprises 59 taxa, including 31 *Dothideomycetes*, 2 *Eurotiomycetes*, and 26 *Sordariomycetes*, with 20 new species. Updated phylogenetic trees, detailed morphological photoplates, taxonomic descriptions, notes, and in-depth discussions are provided.

Chapter 5 presents a vertical diversity study conducted on saprobic microfungi associated with freshwater wetland-dwelling *Typha angustifolia* host, including statistical analyses with graphics and detailed discussions.

Chapter 6 contains the overall conclusion, research highlights, suggestions for future studies and research articles resulted from the investigation.

CHAPTER 2

LITERATURE REVIEW

2.1 Wetlands

Wetlands are dynamic ecosystems that process soil, either covered by water or saturated by water. The water level in wetlands can be changed based on the season, location, and available vegetation. Water level, water quality, and water flow mainly define the inhabitants of these environments (Finlayson et al., 2018). The RAMSAR Convention provides a comprehensive definition, describing wetlands as encompassing marshes, fens, peatlands, and aquatic areas, whether natural or artificial, with water that may be static or flowing, and varying in salinity from freshwater to marine environments (RAMSAR Information Paper no. 1). These ecosystems cover approximately 6% of the Earth's total land area and are classified based on water flow patterns, pH levels, soil characteristics, nutrient availability, and geographic location.

The RAMSAR Convention recognizes six types of wetlands, viz. marine, estuarine, lacustrine, riverine, and palustrine (marshes). Lacustrine wetlands are associated with lakes. They are fed with fresh water from a lake and nearby waterways. Riverine wetlands are situated along the river and banks of tributaries. They are also known as floodplains. The water level, nutrient content, and water quality always fluctuate with the water level of the nearby river (Clarksoon & Peters, 2010). Marshes show a relatively high-water table and low peat content than bogs and swamps in riverine environments. Water level in marshes shifts with the season, and vegetation shows special adaptations to synchronize with seasonal water table changes (Clarksoon & Peters, 2010; Figureueroa et al., 2018).

Marine and estuarine wetlands are primarily located along coastal regions and comprise ecosystems such as coastal lagoons, rocky shorelines, mangrove forests, and tidal marshes. (Figureueroa et al., 2018). These environments span gradients of elevation, from shallow subtidal depths that allow light penetration for photosynthetic organisms at the bottom and benthic plants. Towards the ocean, benthic algae and

seagrasses dominate the vegetation but the landward niches are filled by organisms that can tolerate adverse environmental conditions such as salinity, water table, and pH fluctuations (Hopkinson et al., 2019).

2.1.1 Evolution of Wetland Ecosystems

Wetland ecosystems host distinct communities of flora and fauna, shaped by interactions between biotic and abiotic factors. Co-evolution between landscape geology and related organisms could be the underlying reason for this close association between wetlands and their resident organisms (Greb et al., 2006). Geological and paleoecological evidence suggests that wetlands originated during the mid-Paleozoic era (Greb et al., 2022).

The development of wetland types paralleled major events in plant evolution. The origin of vascular plants such as shrubs in the Emsian age and large trees in the Eifelian age led to the development of marshes and swamps in the mid-Devonian era. They contributed by holding soil particles tightly from their developing root systems (Delwiche & Cooper, 2015). The late Cretaceous saw the origin of the order *Poales*. At the end of the Paleogene era, those early monocotyledonous plants diversified into modern families such as *Cyperaceae*, *Juncaceae*, *Poaceae*, and *Typhaceae* (Bouchenak-Khelladi et al., 2014). The physiology and anatomical features of those families facilitated their colonization in wetland habitats. According to that, at the end of the Oligocene epoch, marshes and swamps were colonized with grasses and grass-like plants resembling today (Greb et al., 2006; Greb et al., 2022).

2.1.2 Fungal Colonization of Wetlands

Fungi may exploit available niches in developing wetlands, which offer nutrient-rich substrates, hosts, and favorable environmental conditions that support their establishment and evolution (Yarwood, 2018). Fungal spores can reach wetlands through several pathways. Wind disperses lightweight conidia and ascospores across long distances; some have been detected 10 km from their origin, with Fusarium graminearum spores found over 500 m above Earth's surface (Peay et al., 2010; Golan & Pringle, 2017). Water also serves as an effective dispersal vector. Rivers, tributaries, rain, and ocean tides can transport spores into wetland environments. Water protects spores from desiccation, UV radiation, and extreme temperatures (Golan & Pringle, 2017). Certain fungi, like Ingoldian species, and marine fungi, have spore morphologies

adapted for waterborne dispersal. For instance, Lignicola laevis is widely distributed in marine habitats, likely due to ocean currents aiding its spread (Pang et al., 2013). Thus, fungi from upstream leaf litter or nearby vegetation can travel as propagules and colonize downstream wetlands (Wong et al., 1998).

Fungi colonize both living and dead plant material. Wetlands often receive driftwood and herbaceous debris through water currents, which may carry fungal thalli or reproductive structures (Hellmann et al., 2013). The dispersal of plant propagules, such as seeds bearing endophytes, mycorrhizal fungi, or pathogens, can introduce fungi from other regions to wetlands (Hayward & Hynson, 2014). Floating live plants can also transport fungal communities, which may establish in new wetland habitats upon settlement (Pang et al., 2013). Animals, including humans, act as fungal dispersal agents. Biodiverse wetlands serve as feeding and breeding grounds for wildlife, and the movement of animals in and out facilitates fungal transfer. Migratory birds, for instance, have been shown to carry fungi like Cladosporium cladosporioides and Alternaria alternata between aquatic environments (Alfonzo et al., 2013). Human activities, including agriculture and trade can introduce new organisms to wetlands, some of which may harbor fungi that eventually become established (Barrett, 2007).

2.1.3 Evolution of Fungi in Wetlands

Fungi evolved alongside plants and wetlands, diversifying as decomposers, symbionts, and pathogens. True fungi with chitinous cell walls originated around 760 million years ago, and molecular clock estimates place the divergence of Ascomycota at 500–650 million years ago (Lücking et al., 2009).

Aero-aquatic fungi are a significant group in wetlands and aquatic habitats. These saprobes decompose submerged plant litter and produce conidia with adaptations for dispersal through air in freshwater environments. Although polyphyletic, their conidial forms evolved independently across lineages in response to aquatic conditions, a case of convergent evolution, as seen in *Spirosphaera*. This genus, currently in *Leotiomycetes* (*Sordariomycetes*), has the type species phylogenetically aligned with *Dothideomycetes* (Voglmayr, 2011; Yamaguchi, 2023). Genera like *Pseudaegerita* and *Helicodendron* produce both large macroconidia and small microconidia. While microconidia rarely germinate, they are considered the true conidia, whereas macroconidia likely evolved as aquatic propagules (Abdullah et al., 2000; Yamaguchi

et al., 2012). The emergence of wetlands created new ecological opportunities, driving fungal adaptations and contributing to the structure and diversity of wetland fungal communities (Lücking et al., 2009; Yamaguchi 2023).

2.1.4 Wetlands in Thailand

Thailand, a tropical Asian nation, hosts diverse flora and fauna, with wetlands playing a crucial role in supporting biodiversity and offering economic benefits such as eco-tourism and aquaculture (Hempattarasuwan et al., 2021). The country's wetlands, comprise marine wetlands, marshes, estuaries, and mangrove swamps that cover about 36,600 km², or 7.5% of the land area. The important areas include Thale Noi Non, Don Hoi Lot, the Mekong River, and coastal zones like Khao Sam Roi Yot and the Pran Buri estuary (Trisurat, 2006). However, these ecosystems face significant threats from resource overexploitation, including logging, land conversion for shrimp farming, poaching, and unsustainable agriculture, leading to the loss of nearly 2,000 km² of mangroves between 1961 and 1996 (Barbier, 2011).

Preserving and studying Thailand's wetlands is essential not only for wildlife conservation but also for advancing our understanding of wetland-associated microbial diversity. Focused research on wetland fungi can clarify taxonomic relationships and community structures, contributing to a more comprehensive picture of the region's microbial ecology.

2.2 Fungal-Like Taxa Found in Wetlands

2.2.1 Zoosporic Fungi and Chytridiomycota

Wetlands are ecologically diverse habitats offering a wide range of niches for fungal colonization, supporting nearly all major fungal groups and fungi-like organisms (Greb et al., 2022). These include zoosporic fungi (*Chytridiomycota*, *Myxomycota*, and *Oomycota*), as well as higher fungi such as *Zygomycota*, *Glomeromycota*, *Ascomycota*, and *Basidiomycota* (Stephenson et al., 2013). Lichens, though present in wetlands, often on macrophytes or inert substrates like rocks, are not addressed in this review, as they represent symbioses between fungal thalli and photosynthetic partners such as algae or cyanobacteria (Hawksworth & Grube, 2020).

Zoosporic fungi are characterized by their motile, flagellated zoospores (Grossart et al., 2016). Chytridiomycota, one of the principal zoosporic fungal phyla along with Oomycota, is considered the oldest lineage of true fungi. Though unicellular, chytrids possess true fungal traits and are globally distributed (Hurdeal et al., 2023; Voigt et al., 2021). In wetlands, they function primarily as parasites or saprobes, thriving in dynamic conditions and tolerating broad pH ranges (Longcore, 2001; Gleason et al., 2010). Saprobic chytrids have been recorded on decaying plant materials, including submerged wood and herbaceous tissues (Stephenson et al., 2013). As an example, the genus *Batrachochytrium*, notably *B. dendrobatidis*, is pathogenic to amphibians in tropical aquatic habitats. However, no records of this pathogen exist from wetlands in Thailand (Freitas et al., 2019).

2.2.2 Oomycota

Oomycota resemble true fungi in forming mycelium-like thalli and digesting substrates extracellularly, but they differ significantly in structure and genetics. Their coenocytic hyphae contain diploid nuclei and have cell walls composed of β-glucans and cellulose (Rossman & Palm, 2006). Primarily saprophytes and pathogens of plants, animals, and fungi, Oomycota inhabit diverse ecosystems including freshwater, marine, and terrestrial habitats (Saelee et al., 2021). In Korea, species such as *Pythium diclinum*, *P. heterothallicum*, *P. inflatum*, *P. intermedium*, and *P. oopapillum* were isolated from sediments and decaying plant matter in freshwater systems (Nam & Choi, 2019). Studies in the Arctic Ocean revealed that Oomycota account for about 6% of the eukaryotic microbial community, with diatom parasites like *Olpidiopsis drebesii* dominant in saline environments. Additionally, *Pythiogeton* species have been implicated in the die-back of *Phragmites australis*, supported by ITS metabarcoding data (Cerri et al., 2017). These findings highlight the ecological range and widespread occurrence of *Oomycota* in aquatic systems, including wetlands.

2.3 Higher Fungi Found in Wetlands

2.3.1 Glomeromycota

Glomeromycetes are true fungi residing in the rhizosphere, forming endomycorrhizal (Arbuscular Mycorrhizal Fungi) associations within plant root cells (Cornwell et al., 2001; Stephenson et al., 2013). Characterized by aseptate hyphae and large multinucleate spores, they lack observed sexual reproduction and are difficult to culture, making metagenomics the primary approach for study. Although data on AMF in wetlands are limited, their presence underscores ecological significance (Bohrer et al., 2004).

In Thailand's coastal freshwater wetlands, *Typha* species dominate, creating monocultures that influence AMF diversity. Studies in *Phragmites australis* wetlands identified *Glomus* species, especially *G. mosseae* and *G. fasciculatum*, as dominant (Wirsel, 2004). Coastal wetland conditions, such as flooding and hypoxia, impact AMF community structures. Santillán-Manjarrez et al. (2019) reported population declines under anoxic stress. Meanwhile, Silvani et al. (2017) identified 14 AMF species from *Glomeraceae* and *Claroideoglomeraceae* in similarly extreme environments using both molecular and morphological approaches. Given the fluctuating hydrology, oxygen limitation, and Poales-dominated vegetation of Thai wetlands, AMF in these ecosystems likely exhibit dynamic and stress-adapted population structures, warranting further investigation.

2.3.2 Yeast

Yeasts are a group of unicellular fungi that inhabit various aquatic ecosystems, including wetlands. Members of yeasts are found in both the *Ascomycota* and *Basidiomycota* phyla. The vegetative cells of most yeasts are obovoid, ellipsoid, or spherical in shape, they are occasionally known to produce pseudohyphae depending on environmental conditions, while Mrakia aquatica forms tetraradiate propagules in nature (Jones & Sloof, 1966). *Candida albicans, Mrakia aquatica*, *Papiliotrema laurentii*, and *Saccharomyces cerevisiae* are among the most commonly reported yeast species from freshwater ecosystems, with *Saccharomycetales* being the most dominant

order (Calabon et al., 2023; Nagahama, 2006; Monapathi et al., 2020; Calabon et al., 2022).

Yeasts in aquatic ecosystems predominantly propagate asexually via budding, although sexual structures have occasionally been reported in *Saccharomyces* species (Wallen & Perlin, 2018). In freshwater environments, yeasts are known to function as decomposers (e.g., *Saccharomyces* and *Mrakia*), endophytic organisms (e.g., *Rhodotorula*), and pathogenic organisms associated with aquatic fauna (e.g., *Candida*, *Debaryomyces hansenii*, and *Metschnikowia bicuspidata*) (Monapathi et al., 2020; Leme et al., 2011; Hagler et al., 2017). Although most yeast studies in freshwater environments have focused on sediments and aquatic fauna, in-depth taxonomic investigations of yeasts associated with freshwater wetlands remain limited. Therefore, a polyphasic taxonomic approach is recommended to better understand the yeast diversity in these habitats.

2.3.3 Ascomycota

Ascomycota is the most abundant and diverse fungal phylum, with widespread occurrence across ecosystems. A large proportion of fungi in wetlands belong to this group, functioning as saprobes, endophytes, and pathogens. They are well-studied due to their ecological significance and their reproductive strategies, producing either asci-bearing sexual morphs or conidial asexual morphs, which contribute to ecosystem balance and resilience by their ecological functions (Stephenson et al., 2013; Calabon et al., 2023).

Four major classes of Ascomycota are commonly associated with plants and plant-derived substrates, viz. *Dothideomycetes***,** *Eurotiomycetes***,** *Leotiomycetes***,** and *Sordariomycetes*. *Eurotiomycetes* are mostly represented by asexual forms, with limited cleistothecial ascomata and primitive asci reported in their sexual morphs. *Leotiomycetes* produce apothecial or cleistothecial ascomata. *Dothideomycetes*, the largest class, are defined by their diverse ascomata and bitunicate asci with fissitunicate dehiscence. *Sordariomycetes*, the second largest, are characterized by perithecial ascomata and inoperculate unitunicate asci. These classes are well represented in aquatic environments, including wetlands, and are frequently associated with Poales vegetation (Geiser et al., 2006; Hyde et al., 2013; Maharachchikumbura et al., 2016; Hongsanan et al., 2020; Calabon et al., 2022).

Note (a) *Hongkongmyces*; (b) *Aspergillus*; (c) *Tubeufia*; (d) *Pseudorhypophila*; (e) *Phaeoacremonium*; (f) *Ophiosphaerella*; (g) *Apiospora*; (h) *Triangularia*; and (i) *Corynascus*. Scale Bars: (a) 500 µm; (b-c) 250 µm; (d-e) 500 µm; (f) 100 µm; (g) 200 µm; (h) 500 µm and (i) 100 µm.

Figure 2.1 Ascomata diversity in wetland-dwelling Poales, associated microfungi in coastal wetlands of Thailand

Freshwater fungi, defined as "all ascomycetes isolated from submerged or partially submerged substrates in aquatic environments" (Shearer, 1993), are well represented in wetland ecosystems shaped by hydrological factors such as water source, volume, and flow dynamics (Finlayson et al., 2018). Most ascomycetes in freshwater wetlands fall within this functional group and exhibit key evolutionary adaptations for aquatic life (Figure 2.1).

Aquatic *Dothideomycetes* and *Sordariomycetes* develop spores with specialized features including thick walls (*Hongkongmyces*), appendages (*Tetraploa*, *Menisporopsis*),

gelatinous sheaths (*Phaeonectriella appendiculata*), and hydrophobic surfaces (*Annulatascus*), that enhance survival, dispersal, and substrate attachment under submerged conditions (Raja et al., 2018; Dong et al., 2020; Luo et al., 2019; Magaña-Dueñas et al., 2021; Calabon et al., 2023). Additionally, genera such as *Lophiostoma* and *Massarina* demonstrate slow growth, spore dormancy, and delayed germination to endure nutrient-poor or fluctuating environments (Baltussen et al., 2020; Seekles 2023). These traits enable freshwater fungi to persist in dynamic wetland systems and distinguish them from many terrestrial relatives (Figure 2.1 and Figure 2.2).

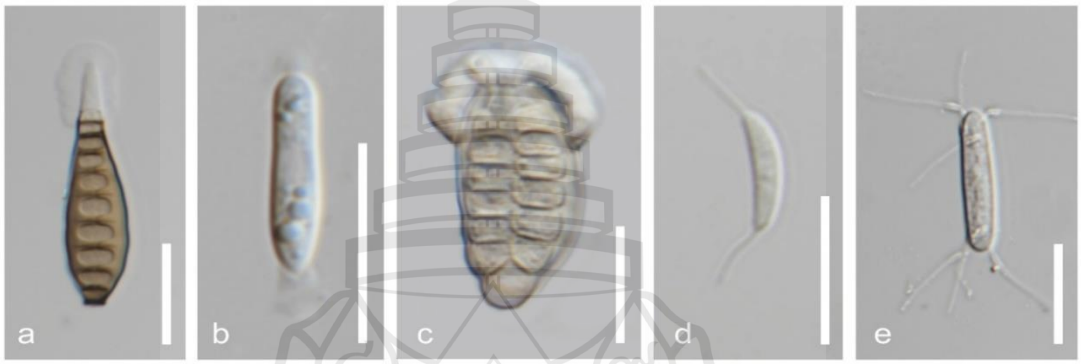

Note (a) Gelatinous apical appendage in *Sporidesmium*; (b) Flabellate apical appendage in *Acrocalymma*; (c) Gelatinous apical appendages in *Vikalpa*; (d) Filiform bipolar appendages in *Menisporopsis*; and (e) Capillaceous appendages in *Chaetospermum*. Scale Bars: (a) 20 µm; (b) 10 and (c-e) 20 µm.

Figure 2.2 Adaptations for effective conidial dispersal in wetland-dwelling fungi in habiting coastal Thailand

Calabon et al. (2022) reported substantial fungal diversity in freshwater ecosystems, documenting 49 genera of *Eurotiomycetes*, 82 of *Leotiomycetes*, 229 of *Dothideomycetes* (677 species), and 298 genera of *Sordariomycetes* (823 species). Similarly, Karunarathna et al. (2022) listed over 2,500 fungal species associated with grasses and other Poales plants. Despite Thailand's coastal freshwater wetlands being Poales-dominated and classified as freshwater ecosystems, fungal records from these habitats remain scarce in the literature (Table 2.1).

Table 2.1 Species of *Ascomycota* isolated from Poales hosts in freshwater wetlands of Thailand

Species Name	Host Material	Reference
Acrogenospora sphaerocephala	Bamboo	Hyde et al. (2019)
Aquaphila albicans	Bamboo	Dong et al. (2020)
Aquihelicascus thalassioideus	Bamboo	Dong et al. (2020)
Astrosphaeriella stellata	Bamboo	Kurniawati et al. (2010)
Clohesyomyces aquaticus	Bamboo	Zhang et al. (2012)
Flammeascoma bambusae	Bamboo	Liu et al. (2015)
Halobyssothecium unicellulare	Poaceae	Hyde et al. (2024)
Lindgomyces ingoldianus	*Typha latifolia*	Zhang et al. (201)3
Longipedicellata aptrootii	Bamboo	Goh and Hyde (1999)
Lophiostoma frondisubmersum	Bamboo	Kurniawati et al., 2010
Neohelicascus elaterascus	Bamboo	Hyde et al. (2020)
Occultibambusa aquatica	Bamboo	Hyde et al. (2016)
Poaceascoma aquaticum	Bamboo	Luo et al. (2016)
Pseudoastrosphaeriella africana	Bamboo	Phookamsak et al. (2015)
Pseudoastrosphaeriella bambusae	Bamboo	Phookamsak et al. (2015)
Pseudoastrosphaeriella longicolla	Bamboo	Phookamsak et al. (2015)
Pseudoastrosphaeriella papillata	Bamboo	Pinruan et al. (2014)
Stagonospora samroiyotensis	*Typha* sp.	Bhagya et al. (2024)
Xenoastrosphaeriella tornata	Bamboo	Cai et al. (2003)
Zopfiella cyperacearum	*Cyperaceae*	Bhagya et al. (2025) in Prep

These findings highlight the critical importance of conducting taxonomic studies on fungi in Thailand's coastal freshwater wetlands and other tropical regions because in-depth taxonomic study will unravel the hidden fungal diversity in these environments and the community structures shaped by the unique environmental conditions presented by wetlands. Such research will enhance our understanding of

fungal community structures, support conservation efforts, and underscore the ecological and economic significance of these sensitive ecosystems.

2.3.4 Basidiomycota

Basidiomycota, the second largest fungal phylum, is distinguished by well-developed fruiting bodies and specialized spore-producing hyphae. Most members lack asexual morphs and are commonly recognized as wood-decaying fungi. In freshwater wetlands, they function as saprobes on decomposing wood, typically in drier microhabitats (Stephenson et al., 2013). Calabon et al. (2022) documented 218 *Basidiomycota* species across approximately 100 genera in freshwater ecosystems, with *Agaricomycetes* and *Ustilaginomycetes* being the most prevalent classes. Similar to *Ascomycota*, research on wetland-associated *Basidiomycota* remains limited, indicating a need for further studies to elucidate their ecological roles in tropical coastal freshwater wetlands.

2.4 Ecological Roles of Wetland-Associated Fungi

The contribution of fungi can be observed in various aspects of wetland ecosystems, where they play a crucial role in maintaining the functionality of these intricate and complex environments. As decomposers, fungi contribute to nutrient cycling, while symbiotic fungi, including endophytes, ectomycorrhizal, and endomycorrhizal species support the plant physiology and health. Additionally, pathogenic fungi affect both plants and wetland-dwelling animals, significantly influencing the longevity and balance of these ecosystems (Thormann, 2006, Jones & Pang, 2012; Stephenson et al., 2013; Calabon et al., 2023).

2.4.1 Nutrient Recycling

Nutrient cycling in wetlands is largely driven by saprobic fungi that decompose dead vegetation, including submerged, moist, or dry plant materials (Calabon et al., 2023). Woody debris, particularly abundant in tropical wetlands, supports fungi capable of all three wood decay types including white rot, brown rot, and soft rot, that depending on the enzymatic capacity of each fungal group (Stephenson et al., 2013; Tsui et al., 2016; Rodríguez-Couto, 2017). White rot fungi degrade both cellulose and lignin, while

brown and soft rot primarily target cellulose, leaving lignin intact (Shen et al., 2022). Soft rot typically occurs in moist wood under aquatic conditions, producing dense dark cores that are later colonized by white or brown rot fungi in a succession process (Simonis et al., 2008; Hyde & Jones, 2002).

Thailand's coastal freshwater wetlands are dominated by Poales, including *Cyperaceae, Poaceae*, and *Typhaceae*. These monocotyledonous plants yield relatively soft and fast-decomposing herbaceous substrates that support fungal communities distinct from those on wood (Stephenson et al., 2013). Freshwater discomycetes, for example, are frequently isolated from decomposing grasses and sedges (Jones & Pang, 2012). Larger Poales leaves can trap aero-aquatic fungal spores via their bristled surfaces even before senescence. The location where these leaves fall influences fungal colonization, like the submerged litter is decomposed by aquatic fungi such as Ingoldian hyphomycetes, *Halosphaeriaceae*, and *Pleosporaceae*, while litter in drier areas supports soil-associated *Ascomycota* and *Basidiomycota* (Gulis, 2001; Thambugala et al., 2017). These fungi are involved in decomposition and recycle essential nutrients such as carbon, phosphorus, potassium, and magnesium, thus promoting wetland stability and longevity (Kuehn et al., 2011; Stephenson et al., 2013).

Fungi also form symbiotic associations with wetland plants, particularly as endophytes. These fungi, including *Trichoderma*, *Cladosporium*, and various Fusarium species, colonize healthy plant tissues without causing physiological harm, offering benefits such as stress resistance. For instance, *Cladosporium tenuissimum* has been shown to enhance drought tolerance in the wetland species *Alternanthera philoxeroides* (Jayaram et al., 2023; Sandberg et al., 2014).

2.4.2 Endophytic and Mycorrhizal Relationships

Wetland-associated endophytes disperse in the ecosystem by two main pathways. They may shift from a symbiotic to a saprobic or pathogenic lifestyle depending on host condition, producing sexual or asexual propagules for dispersal (Shen et al., 2022; Calabon et al., 2023). Alternatively, endophytes can be transmitted through seeds and vegetative tissues. Ingoldian hyphomycetes like *Lunulospora curvula* and *Tricladium splendens* are known to spread via host tissues (Selosse et al., 2008). In Thailand's coastal freshwater wetlands, seed-mediated dispersal is especially

significant, as lightweight monocot seeds carrying endophytes are easily transported by wind and water (Sandberg et al., 2014; Bärlocher & Boddy, 2016).

Mycorrhizal fungi represent another vital symbiotic group in wetlands. They are broadly classified as ectomycorrhizal (mostly *Basidiomycetes*) and endomycorrhizal (primarily *Glomeromycota*). Ectomycorrhizal fungi form external sheaths around roots without penetrating the cortex, while endomycorrhizal fungi colonize root cortical cells without causing damage. These mutualistic interactions enhance plant nutrient uptake, particularly phosphorus, in exchange for host-derived carbohydrates (Cornwell et al., 2001). Although mycorrhizal associations occur in wetlands, waterlogged conditions limit ectomycorrhizal colonization, confining it to drier microhabitats or the dry season (Bohrer et al., 2004). Endomycorrhizal fungi, including *Glomus*, *Funneliformis*, and *Rhizophagus*, have been widely reported in wetland plants, especially non-monocotyledonous hosts. Despite oxygen limitations in flowing-water wetlands, endomycorrhizal fungi remain ecologically important for supporting monocot plants in such environments (Ray & Inouye, 2006; Wang et al., 2023).

2.4.3 Fungal Pathogens in Wetlands

Fungal pathogens play an important role in ecosystems by regulating natural populations and exerting selective pressures on both plants and animals. Wetland ecosystems are no exception to fungal pathogens. These fungi infect healthy organisms and induce adverse physiological conditions that can be detrimental to the host's health (Aumentado et al., 2024). Although studies on fungal pathogens in wetland ecosystems are limited, numerous reports document pathogenic genera associated with members of the order Poales (Lofgren et al., 2018). Ascomycota members, including *Colletotrichum*, *Nigrospora*, *Pestalotiopsis*, and *Lasiodiplodia*, have been isolated from grasses, while rust pathogens have been frequently reported from grasses and other related host plants (Thambugala et al., 2017; Calabon et al., 2023).

Other inhabitants of wetlands, such as animals, are affected by fungal pathogens in these ecosystems. For example, *Candida* species are known to infect fish and disperse through freshwater bodies by using them as vectors. *Veronaea botryosa* has been reported in freshwater-associated amphibians in North America and has been documented at pandemic levels (Mayer et al., 2022; Calabon et al., 2023). Accordingly, wetland-associated fungi, including saprobes, endophytes, mycorrhizal fungi, and

fungal pathogens, play a crucial role in maintaining ecosystem balance in these delicate environments.

2.5 Industrial and Ecological Utilization of Wetland Fungi

2.5.1 Wastewater Treatment and Constructed Wetlands

Wetland ecosystems are defined by their close association with water, which shapes both their structure and resident biota. Consequently, many fungi inhabiting wetlands are aquatic or possess aquatic adaptations (Calabon et al., 2023). These features make them particularly suitable for applications in bioremediation and wastewater treatment, alongside their host plants (Chaturvedi et al., 2015). Bioremediation involves the use of living organisms, primarily fungi and bacteria, to break down hazardous substances into less harmful forms (Chaturvedi et al., 2015; Vaksmaa et al., 2023). Early fungal applications in wastewater treatment focused on decolorizing textile effluents. *Candida tropicalis* was found effective in degrading dyes under acidic conditions (Longhinotti et al., 1998), highlighting the potential of fungi from tannin-rich or blackwater wetlands for purification (Gleason et al., 2010). Fungi, as saprobes, secrete extracellular enzymes like laccases that oxidize aromatic compounds. Notable laccase producers include Basidiomycetes such as *Coprinus cinereus* and *Trametes versicolor*, and Ascomycetes like *Melanocarpus albomyces*, species well-adapted to aquatic and wetland habitats (Dias et al., 2007).

The natural purification capabilities of wetlands have inspired the development of constructed wetlands for wastewater treatment, where fungi native to such ecosystems contribute to pollutant removal (Mustafa et al., 2024). Among these, Arbuscular Mycorrhizal Fungi (AMF) play a key role. AMF colonization in constructed wetlands can occur through plant propagules, water, wind, animals, or artificial introduction, often requiring minimal intervention (Zhouying et al., 2016). Stable AMF-host associations are critical for bioremediation efficacy. Most host plants in constructed wetlands, including *Carex*, *Typha*, and other Poales, support AMF colonization. Phosphorus availability influences these interactions, while low phosphorus limits AMF colonization (Van Hoewyk et al., 2001), phosphorus-rich

wastewater facilitates it. Intern, AMF and other wetland-adapted fungi are integral to the success of constructed wetlands, underscoring their value as biological agents in environmental remediation.

2.5.2 Wetland Fungi as Bioindicators

Aquatic hyphomycetes, common in wetland ecosystems, are highly sensitive to environmental factors, making them effective bioindicators of ecosystem health. Their populations respond markedly to changes in water quality, pollutants, and temperature fluctuations (Maharachchikumbura et al., 2016; Calabon et al., 2023; Barros et al., 2024). A redundancy analysis (RDA) by Solé et al. (2008) demonstrated that species such as *Anguillospora longissima*, *Clavatospora longibrachiata*, *Clavariopsis aquatica*, *Flagellospora curvula*, *Heliscus lugdunensis*, *Tumularia aquatica*, and *Lemonniera aquatica* experienced significant population declines in freshwater rivers contaminated with organic matter, heavy metals, sulfates, and nitrates. These species' absence or reduction serves as a clear indicator of freshwater pollution.

Bai et al. (2018) analyzed fungal communities in three polluted freshwater reservoirs using ITS sequencing and chemical profiling. Ecosystems with anthropogenic disturbances and high fertilizer residues showed a notable decline in fungal diversity and abundance, although *Schizosaccharomyces* showed increased relative abundance. These findings, supported by recent studies including Siriarchawatana et al., (2024), emphasize the role of aquatic fungi, including those in freshwater wetlands, as reliable bioindicators for monitoring ecological integrity and pollution levels.

2.6 Threats, Challengers and Modern Conservation for Fungal Fauna in Coastal Freshwater Wetlands

2.6.1 Threats and Challenges

Wetland ecosystems are vital for environmental sustainability and the well-being of adjacent communities. However, expanding human settlements and unsustainable land use have placed these ecosystems under increasing pressure. Anthropogenic drivers including climate change, invasive species, and habitat

disturbance are negatively impacting wetland biodiversity globally (Barros & Seena, 2022). Targeted conservation strategies are essential to protect wetland habitats and their inhabitants, including microfungi (Calabon et al., 2023).

In tropical countries like Thailand, improper agricultural expansion poses one of the greatest threats to freshwater wetlands. Wetland water is frequently diverted for crop irrigation, reducing water levels and altering the hydrological balance. Land clearing for cultivation leads to biodiversity loss, particularly among wetland flora and fauna (Ferreira et al., 2006; Pereira & Ferreira, 2021). As a result, fungi that depend on these plants and animals, whether as pathogens, endophytes, symbionts, or saprobes are also adversely affected (Barros & Seena, 2022). Intensive agriculture further introduces chemical pollutants into wetlands through the use of fertilizers, pesticides, and fungicides. These substances often enter wetlands from surface runoff, disrupting nutrient dynamics and causing eutrophication (Chandrashekar & Kaveriappa, 1989; Gulis et al., 2006). Fungicide residues, in particular, can disturb aquatic fungal communities, diminishing diversity and ecological function (He et al., 2025).

The introduction of invasive plant species also contributes to alter the fungal community structures. Non-native species can outcompete native flora, indirectly displacing specialized fungi adapted to native hosts. In contrast, fungi capable of utilizing invasive plant material may proliferate, potentially leading to long-term dominance and loss of fungal diversity (Steiner et al., 2008; Barros & Seena, 2022; Calabon et al., 2023). For instance, in Thailand's coastal wetlands, invasive Poales species outcompete native *Nymphaeaceae*, shifting fungal associations and community dynamics.

Climate change is an overarching threat, with rising global temperatures affecting wetland hydrology and fungal physiology. Aquatic fungi are particularly sensitive to thermal stress, and elevated temperatures can reduce their diversity and metabolic function (Pérez et al., 2018; Calabon et al., 2023). Furthermore, polar ice melt is expected to alter oceanic and riverine flow patterns, disrupting nutrient delivery and water distribution in wetland systems (Döll & Zhang, 2010; Barros & Seena, 2022). These compounded impacts pose significant risks to fungal diversity and ecological stability in freshwater coastal wetlands.

2.6.2 Conservation

The conservation of wetland-dwelling fungi is best achieved through the protection and sustainable management of their habitats. The current global framework allows for coordinated responses to environmental challenges, including the preservation of coastal freshwater wetlands, critical ecosystems that support fungal biodiversity (Tittensor et al., 2014). International organizations such as the Ramsar Convention, IUCN, and WWF actively contribute to wetland conservation, indirectly safeguarding fungal communities (Tickner et al., 2020; Barros & Seena, 2022). National governments, particularly in countries like Thailand, can play a pivotal role by formulating conservation policies and raising public awareness about wetland protection (Leadley et al., 2014; Tittensor et al., 2014). Such efforts not only conserve biodiversity but also support local livelihoods that rely on wetlands for fisheries, agriculture, and eco-tourism (Trisurat, 2006; Hempattarasuwan et al., 2021).

Research in fungal ecology, taxonomy, and applied mycology provides essential guidance for conservation planning. Detailed studies help identify priority areas for protection, inform management strategies, and support the sustainable use of freshwater wetland resources (Barros & Seena, 2022; Calabon et al., 2023). Fungal taxonomic research, in particular, is fundamental to conservation efforts, as it reveals the richness and ecological roles of fungal communities, enabling more targeted and effective protection of wetland biodiversity.

2.7 Discussion

Although knowledge of freshwater wetlands is expanding, many aspects remain underexplored, particularly in relation to fungal diversity. Phang et al. (2014) and Calabon et al. (2023) noted the limited investigation of specific substrates in aquatic environments, including freshwater-associated grasses and other Poales, which dominate coastal wetlands in Thailand. These plants offer promising opportunities for detailed fungal taxonomic studies. Additionally, the ecological roles and phylogenetic significance of fungal morphological traits, such as appendages and mucilaginous sheaths remain insufficiently understood in freshwater fungi (Calabon et al., 2024).

Most taxa are known only from a single morph, and understudied habitats may reveal connections between sexual and asexual forms, alongside new molecular data for insufficiently characterized species (Stephenson et al., 2013).

Wetlands provide a range of microhabitats that support fungal specialization and diversification (Dong et al., 2020; Luo et al., 2019). In freshwater coastal wetlands, the same plant species can present multiple fungal niches including submerged, aerial, or intermediate, each influenced by fluctuating water levels. These zones expose fungi to distinct environmental stresses and ecological opportunities (Jones, 2011; Stephenson et al., 2013). However, vertical stratification of fungal communities in such habitats remains insufficiently studied. Filling this knowledge gap could lead to the discovery of novel taxa and illuminate unique ecological interactions between fungi and their host substrates.

CHAPTER 3

ASSEMBLAGE OF SELECTED MICROFUNGAL GENERA RECORDED FROM WETLANDS

3.1 Introduction

Grasses, belonging to the order Poales, represent one of the largest and most widely distributed groups of monocotyledonous plants. The origin of grasses and their close relatives can be traced back to the mid-Cretaceous period, approximately 105 to 125 million years ago, when they constituted a significant component of the Cretaceous undergrowth (Greb et al., 2022). Fossil evidence indicates that the extensive diversification of grasses and related taxa began around 55 million years ago, reaching a notable expansion during the Oligocene epoch (55 to 23 million years ago) (Schubert et al., 2019). By the end of the Paleogene period, several major plant families within Poales, including Cyperaceae, Juncaceae, Poaceae, and Typhaceae, were well established. Among these, the Poaceae (true grasses) occupy key ecological niches, often alongside related families that perform similar ecological functions (Bouchenak-Khelladi et al., 2014; Hodkinson, 2018). The physiological and anatomical adaptations of these families have facilitated their colonization of diverse habitats, including grasslands and wetlands (Thambugala et al., 2017; Karunathna et al., 2022).

Grasses hold considerable ecological and economic significance. Ecologically, they function as primary producers, forming the foundation of many ecosystems by providing food and habitat for a wide range of organisms, including microorganisms such as fungi (Spalink et al., 2016; Thambugala et al., 2017). The population structure of grasses varies across habitats; for example, species within Poaceae commonly dominate open landscapes, whereas bamboos (also members of Poaceae) are typically found along riverbanks. Other families within the order Poales, such as *Cyperaceae*, *Juncaceae*, and *Typhaceae*, are frequently associated with wetland ecosystems. Economically, several species within Poales, including *Oryza sativa*, *Triticum aestivum*, and *Hordeum vulgare*, have been cultivated extensively beyond their native

ranges and serve as staple carbohydrate sources for human populations (Karunathna et al., 2022). In addition to their role in agriculture, grasses are important as livestock forage and are used as building materials in many regions worldwide. Thus, research on grasses highlights their critical roles in both ecological systems and human economies (Thambugala et al., 2017).

Despite the considerable ecological and economic significance of the Poales, studies addressing the diversity of fungi associated with this group remain comparatively limited. Although Karunathna et al. (2022) mentioned more than 2500 fungal taxa from grasses and other closely related hosts, other existing literature has primarily concentrated only on crop-associated or pathogenic fungi in grasses, with relatively limited attention given to saprobic and endophytic taxa, particularly those inhabiting aquatic or wetland grass ecosystems. Importantly, tropical coastal wetlands, which support a high diversity of grasses and sedges, continue to be markedly underrepresented in fungal biodiversity research (Quaedvlieg et al., 2013; Thambugala et al., 2017; Calabon et al., 2023).

Fungi play a vital role in ecosystems, interacting with both plants and animals, and grasses and grass-like plants are no exception. Fungi establish a range of associations with plants, including pathogenic, saprobic, and endophytic relationships. These interactions are fundamental to nutrient cycling and the maintenance of ecological balance (Spalink et al., 2016). However, lack and limitation of molecular data for many grass-associated fungi continues to hinder taxonomic resolution and phylogenetic placement, emphasizing the need for multilocus sequence analysis in modern fungal systematics. Investigating fungal communities associated with members of the Poales across diverse ecosystems worldwide is crucial for advancing our understanding of fungal diversity and offers significant potential for future research (Thambugala et al., 2017).

This study presents a comprehensive account of fungal genera associated with members of wetland or freshwater associated Poales, incorporating detailed morphological descriptions, illustrations, ecological data, distribution records, nutritional modes, and phylogenetic placements based on available molecular data. This compilation aims to enhance the understanding of fungal diversity in these critical,

Poales dominated ecosystems and to highlight areas for future fungal taxonomic research

3.2 Methodology

Microfungal genera associated with wetland-dwelling Poales were identified based on The Worldwide Checklist on Grass Fungi: What Do We Know So Far in Ascomycota by Karunarathna et al. (2022).

Updated taxonomic classifications and phylogenetic placements were documented using recent literature, including Hyde et al. (2024), Wijayawardene et al. (2022), and curated online databases such as:

1. Index Fungorum: https://www.indexfungorum.org/names/names.asp
2. Species Fungorum: https://www.speciesfungorum.org/
3. MycoBank: https://www.mycobank.org/Simple%20names%20search
4. Faces of Fungi: https://www.facesoffungi.org/
5. GenBank Overview: https://www.ncbi.nlm.nih.gov/genbank/
6. Freshwater Fungi: https://freshwaterfungi.org/

Morphological characteristics, geographical distribution, nutritional modes, and molecular markers were compiled through a comprehensive review of published literature. Illustrations were redrawn based on existing sources, giving priority to type specimens or species isolated from Poales or wetland ecosystems.

3.3 Results and Discussion

Class ***Dothideomycetes***

Sub-Class ***Dothideomycetidae***

Order ***Asterinales***

Family *Asterinaceae*

Asterina Lév.

Citation when using this entry: Amuhenage et al., in prep – Fungalpedia, grass and wetland fungi.

Index Fungorum, Faceoffungi, MycoBank, GenBank, Figure 3.1

Classification: *Asterinaceae*, *Asterinales*, *Dothideomycetidae*, *Dothideomycetes*, *Pezizomycotina*, *Ascomycota*, Fungi

Genus *Asterina* was introduced by Léveillé in 1845 and typified by *Asterina melastomatis* (Wijayawardene et al., 2022; Hyde et al., 2024). *Asterina* was initially placed as a member of *Sphaeriaceae* along with *A*. *azarae*, *A*. *compacta*, *A*. *pulla*. According to current phylogenetic studies the genus resides under *Asterinaceae* as the largest genus of the family with over 1100 entries in Index Fungorum. Most *Asterina* species are unculturable and only nine species have reliable molecular data (Hongsanan et al., 2020). *Asterina* species are saprobic, pathogenic and endophytic. Saprobic members produce circular thyriothecia with lateral appressoria, on decomposing host materials. Those thyriothecia protect globose to sub-globose asci. Each ascus bears eight, 1-septate, light brown to dark brown ascospores (Hongsanan et al., 2020). *Asterina* species occur worldwide in both terrestrial and aquatic habitats, on both monocotyledonous and dicotyledonous host materials. As examples, *Asterina microscopica* was isolated from *Chusqueae* sp. in Chile, and *A*. *pelliculosa* was isolated from decomposing *Rottboellia* materials (Karunarathna et al., 2022). The introduction of *Asterina magnolia* in 2018 utilized available LSU data from the genus with other related taxa in the *Asterinaceae*. That indicate the importance of using LSU sequences coupled with molecular evidences to delineate species of *Asterina* (Hongsanan et al., 2020). Lack of molecular data for the genus has made phylogenetic placement of *Asterina* questionable. Fresh collections and in-depth phylogenetic investigation using multilocus phylogenetic approaches are recommended.

Type species: ***Asterina melastomatis*** Lév.

Other accepted species: see Species Fungorum, search *Asterina* for names.

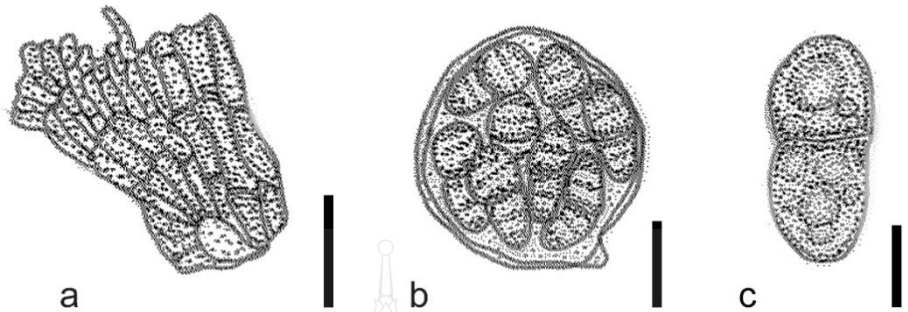

Note (a) Part of thyriothecium; (b) Ascus (c) Ascospore. Scale bars: (a) 50 µm; (b) 20 µm; (c) 10 µm.

Source Redrawn from Hongsanan et al. (2020)

Figure 3.1 *Asterina magnoliae* (MFLU 16-0071)

Family ***Capnodiaceae***

Leptoxyphium Speg.,

Citation when using this entry: Amuhenage et al., in prep – Fungalpedia, grass and wetland fungi.

IndexFungorum, Facesoffungi, MycoBank, GenBank: Figure 3.2

Classification: *Capnodiaceae*, *Capnodiales*, *Dothideomycetidae*, *Dothideomycetes*, *Pezizomycotina*, Ascomycota, Fungi

Leptoxyphium is a monophyletic and anamorphic genus that belongs to family *Capnodiaceae* in *Dothideomycetes* (Hongsanan et al., 2020). This genus was introduced by Spegazzini in 1918 and is typified by *Leptoxyphium graminum* (Wijayawardene et al., 2022; Hyde et al., 2024). Chomnunti et al. (2011) examined phylogenetic relationships between related genera in family *Capnodiaceae* with multigene phylogeny. *Leptoxyphium* formed a well-supported clade with 100% bootstrap support in maximum likelihood analysis and 1.0 bootstrap support in Bayesian posterior probability analysis (Chomnunti et al., 2011). *Leptoxyphium* species are sooty molds that grow in close proximity to glands and trichomes on leaves. They are saprobes on sugary exudates from insects. Colonies are superficial on host, velvety, black or brown. Mycelium is septate and branched. Conidiophores are synnematous, sub-cylindrical, brown, clustered and process a bulbous base. Phialidic conidiogenous cells produce aseptate, hyaline conidia with rounded ends (Karunarathna et al., 2022).

Wijayawardene et al. (2022) accepted 19 species but *L. unedonis* was synonymized with *Polychaeton brasiliense* (Index Fungorum, 2023). They have a wide distribution and host range. As examples, *L. graminum* was found on *Citrus* plants (Karunarathna et al., 2022) and *L. zeae* was recorded from *Zea maydis* (Karunarathna et al., 2022). According to Faces of Fungi only five species have molecular data. Chomnunti et al. (2011) used SSU and LSU sequences for a molecular investigation. Therefore, further phylogenetic studies involving other gene regions is needed to provide in depth view of *Leptoxyphium*.

Type species: ***Leptoxyphium graminum*** (Pat.) Speg. 1918

Other accepted species: see Species Fungorum, search *Leptoxyphium* for names.

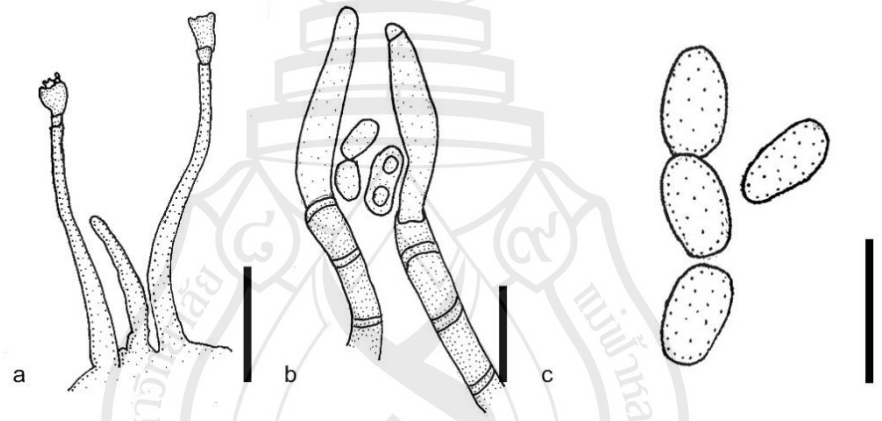

Note (a) Stalked pycnidia with wider base; (b) Conidiogenous cells; (c) Conidia. Scale bars: (a) 200 µm; (b-c) 20 µm.

Source Redrawn from Chomnunti et al. (2011)

Figure 3.2 *Leptoxyphium graminum* (holotype)

Family ***Mycosphaerellaceae***

Annellophora S. Hughes

Citation when using this entry: Amuhenage et al., in prep – Fungalpedia, grass and wetland fungi.

Index Fungorum, Faceoffungi, MycoBank, GenBank, Figure 3.3

Classification: *Incertae sedis*, *Incertae sedis*, *Incertae sedis*, *Incertae sedis*, *Pezizomycotina*, *Ascomycota*, Fungi

Annellophora was proposed by S. Hughes in 1951 to accommodate species from the genus *Chaetotrichum*, and *Annellophora ochracea* is the type species (Wijayawardene et al., 2022; Hyde et al., 2024). The genus has pathogenic and saprobic members. They are characterized by epiphyllous, occasionally branched, erect, straight, dark brown to light brown conidiophores that develop from lobed base cells. Conidiogenous cells are terminal, narrowing towards apex with percurrent extensions. Conidia are smooth, thick walled, border at the base with distoseptate, yellowish brown to pale brown, and broadly clavate or obclavate (Kirschner et al., 2018). *Annellophora* has worldwide distribution and affinity towards many plants including members of the order Poales (Kirschner et al., 2018). As an example, *A. arundinariae* was isolated from *Arundinaria* sp. in Delhi, India (Karunarathna et al., 2022). There are thirteen morphologically known species and all lack molecular data, leading to the uncertain taxonomic placement of *Annellophora*. More fresh collections from different habitat are recommended to obtain taxonomic insight in to the genus.

Type species: ***Annellophora ochracea*** S. Hughes

Other accepted species: see Species Fungorum, search *Annellophora* for names.

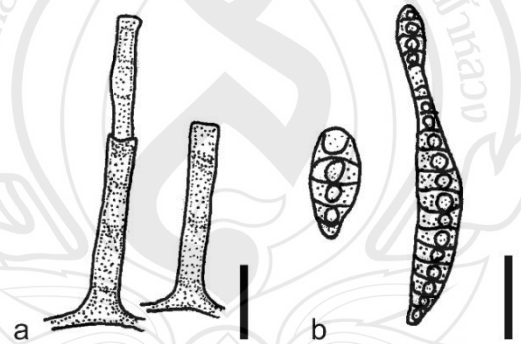

Note (a) Conidiophores; (b) Conidia. Scale bars: (a-b) 10 µm.

Source Redrawn from Kirschner et al. (2018)

Figure 3.3 *Annellophora phoenicis*

Neoramularia Braun

Citation when using this entry: Amuhenage et al., in prep – Fungalpedia, grass and wetland fungi.

Index Fungorum, Faceoffungi, MycoBank, GenBank, Figure 3.4

Classification: *Incertae sedis*, *Incertae sedis*, *Incertae sedis*, *Incertae sedis*, *Pezizomycotina*, Ascomycota, Fungi

Braun introduced *Neoramularia* in 1991 with *Neoramularia eurotiae* as type species (Wijayawardene et al., 2022; Hyde et al., 2024). *Ramularia eurotiae* Gamalizk was transferred to the genus (Andrianova, 2020). *Neoramularia* species are mainly recognized as asexual morphs, with worldwide distribution and are well known pathogens of dicotyledonous plants (Ruszkiewicz-Michalska & Wolczanska, 2008). *Neoramularia phragmitis* was isolated from *Phragmites communis* in Russia (Karunarathna et al., 2022). *Neoramularia* is characterized by straight conidiophores that give rise to terminal, polyblastic, sympodial and percurrent conidiogenous cells. Conidiogenous loci are inconspicuous and hyaline. Conidia are hyaline, oblong with blunt ends, solitary or catenate. They can be arranged in unbranched connected chains where each terminal conidium functiona as a conidiogenous cell and adds new conidia to the existing conidia chain. Species such as *N. bidentis*, *N. esfandiarii* and *N. phragmitis* produce catenate conidia (Ruszkiewicz-Michalska & Wolczanska, 2008; Andrianova, 2020). Molecular data is not available for any species of *Neoramularia* and thus, the genus is placed in *Incertae sedis* (Andrianova, 2020). More fresh collections and investigations with both morphology and multigene phylogeny are required to understand proper placement of the genus *Neoramularia* in fungal kingdom.

Type species: ***Neoramularia eurotiae*** (Gamalizk.) by U. Braun

Other accepted species: see Species Fungorum, search *Neoramularia* for names

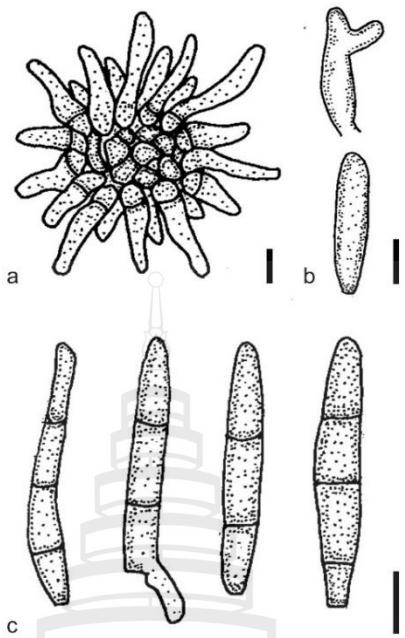

Note (a) Conidiophores in fascicle; (b) Conidiophores; (c) Conidia. Scale bars: (a-c) 10 μm.

Source Redrawn from Braun et al. (2005)

Figure 3.4 *Neoramularia karelii* (BRIP 5658)

Family ***Dothideaceae***

Vestergrenia Rehm

Citation when using this entry: Amuhenage et al., in prep – Fungalpedia, grass and wetland fungi.

Index Fungorum, Faceoffungi, MycoBank, GenBank, Figure 3.5

Classification: *Botryosphaeriaceae*, *Botryosphaeriales*, *Dothideomycetidae*, *Dothideomycetes*, *Pezizomycotina*, *Ascomycota*, Fungi

Vestergrenia was introduced by Rehm in 1901 and typified by *Vestergrenia nervisequia* (Wijayawardene et al., 2022; Hyde et al., 2024). This genus is predominantly saprobic on dead plant leaves. Members of genus *Vestergrenia* species form dark brown to black, coriaceous, subglobose or globose ascomata that are found scattered or loosely aggregated on leaf veins (Liu et al., 2012). Peridium consists of a single stratum containing 3–4 layers of brown pseudoparenchymatous cells. Peridium cell structures can vary from *textura angularis* to *textura globulosa*. Pseudoparaphyses are absent and peridium protects bitunicate, broadly clavate to ovoid asci. Asci have a

long pedicel and the apex is round with a well-defined ocular chamber. Each ascus bears eight ascospores. Ascospores are ellipsoidal to ovoid, hyaline, aseptate, and arranged in either diseriate or triseriate manner (Liu et al., 2012). Asexual morphs are not known. *Vestergrenia* was placed under *Sphaeriaceae* as a monophylitic genus. Luttrell transferred the genus to *Dothideaceae* considering its singe celled ascospores, separate ascomata, broad clavate to ovoid asci on thin stalks with different lengths which results in asci reaching differing heights in the locule (Liu et al., 2012). This transfer was not supported by other morphological data because there are considerable morphological differences between *Dothidea*, the type genus of *Dothideaceae*, and *Vestergrenia*. Considering the thick brown *textura angularis* to *textura globulosa* cells in ascomata, broadly clavate asci with well-defined pedicels and unicellular ascospores Liu et al. (2012) transferred *Vestergrenia* to *Botryosphaeriaceae*. This is not supported by phylogeny, as the genus is inadequately studied and no molecular data is available. Most recent species were added by Wulandari et al. (2014). They transferred four species from *Guignardia* to *Vestergrenia* considering morphological evidence. More fresh collections, and multigene phylogenetic studies are required to understand the proper placement of *Vestergrenia* in *Dothideomycetes*.

Type species: ***Vestergrenia nervisequia*** Rehm

Other accepted species: see Species Fungorum, search *Vestergrenia* for names.

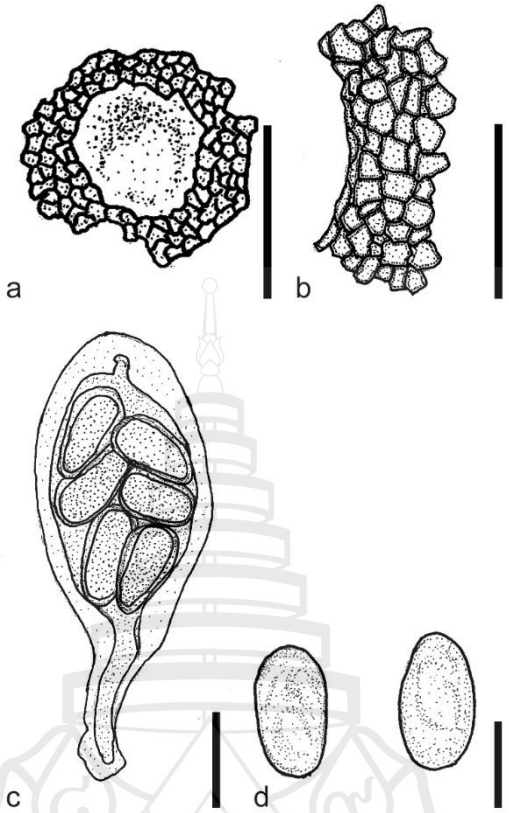

Note (a) Section of ascoma; (b) Ascomata wall; (c) Ascus; (d) Ascospores. Scale bars: (a) 100 µm; (b) 50 µm; (c-d) 10 µm.

Source Redrawn from Liu et al. (2012)

Figure 3.5 *Vestergrenia nervisequia* (SF10703, holotype)

Family ***Saccotheciaceae***

Saccothecium Fr.

Citation when using this entry: Amuhenage et al., in prep – Fungalpedia, grass and wetland fungi.

Index Fungorum, Faceoffungi, MycoBank, GenBank, Figure 3.6

Classification: *Saccotheciaceae*, *Dothideales*, *Dothideomycetidae*, *Dothideomycetes*, *Pezizomycotina*, *Ascomycota*, Fungi

Saccothecium was proposed by Fries in 1835 by synonymizing several species from *Metasphaeria* Sacc., *Phaeodothiora* Petr., *Pleosphaerulina* Pass. and *Schizostege* Theiss. (Wijayawardene et al., 2022; Hyde et al., 2024). Initially the genus was not typified but was late typified by *Saccothecium sepincola* Clements and Shear in 1931

(Li et al., 2016). The genus was first assigned to *Dothioraceae*, based on similarities in peridium, asci and ascospores morphology to other members in the family. Thambugala et al. (2014) used multigene phylogeny to study phylogenetic placement of several genera under *Dothideomycetidae* and categorized *Saccothecium* under *Saccotheciaceae*, order *Dothideales*. *Saccothecium* species show both parasitic or saprobic life modes in nature. Sexual morph generates black, thick walled, globose or subglobose, uniloculate ascomata that individually or gregariously arranged on host tissue and immersed or erumpent (Thambugala et al., 2014; Li et al., 2016). Several layers form cells in pseudoparenchymatous*, textura angularis* producing the peridium. Peridium protects bitunicate, fissitunicate, broad-clavate, to cylindric-clavate or saccate asci with short bifurcate pedicel. They have a rounded apex with a distinct ocular chamber (Thambugala et al., 2014; Li et al., 2016). Each ascus contains eight ascospores arranged in overlapping biseriate or triseriate manner (Thambugala et al., 2014; Li et al., 2016). Ascospores are hyaline, muriform to phragmosporous, obovoid or elliptic, tri-septate or multiple septate with blunt ends. Aureobasidium-like asexual morphs produce hyaline to brownish, ovate, aseptate conidia (Thambugala et al., 2014). *Saccothecium* has a wide distribution and is isolated from monocotyledenous plants, as example *S. luttrellii* was isolated from *Pennisetum typhoides*, Maharashtra, India (Karunarathna et al., 2022). Introduction of a new species *S. rubi* utilized only LSU, SSU and ITS loci for phylogenetic analysis (Li et al., 2016). According to that use of multigene phylogeny with more loci are required to obtain more robust view of the genus.

Type species: ***Saccothecium sepincola*** Clements & Shear

Other accepted species: see Species Fungorum, search *Saccothecium* for names.

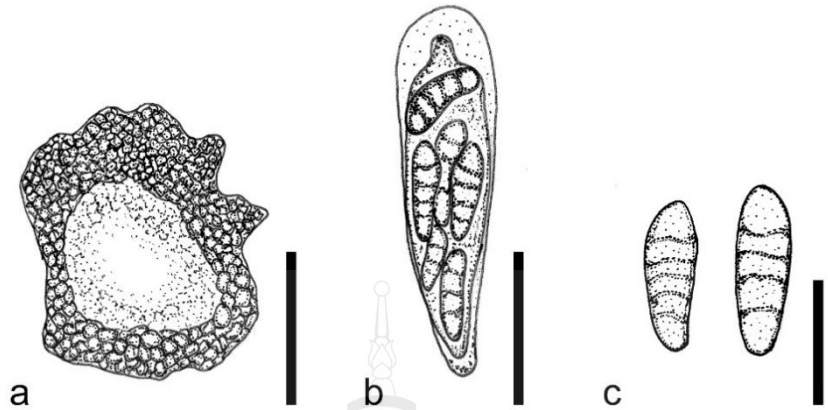

Note (a) Section of ascoma; (b) Ascus; (c) Ascospores. Scale bars: (a-b) 50 μm; (c-d) 25 μm; (e-f) 10 μm.

Source Redrawn from Thambugala et al. (2014)

Figure 3.6 *Saccothecium sepincola* (MFLU 14–0276)

Selenophoma Maire

Citation when using this entry: Amuhenage et al., in prep – Fungalpedia, grass and wetland fungi.

Index Fungorum, Faceoffungi, MycoBank, GenBank, Figure 3.7

Classification: *Saccotheciaceae*, *Dothideales*, *Dothideomycetidae*, *Dothideomycetes*, *Pezizomycotina*, *Ascomycota*, Fungi

Selenophoma is a polyphyletic genus introduced by Maire in 1907 and typified with *Selenophoma catananches* (Wijayawardene et al., 2022; Hyde et al., 2024). This genus is known by asexual morphs and a sexual morph has yet to be confirmed. *Selenophoma* species are characterized by pale brown to brown immersed, septate, thick-walled, branched, immersed or superficial mycelium that gives rise to pycnidial or avervular structures on shoot tissue. The fruiting bodies lack ostioles (Thambugala et al., 2014). Conidiophores are reduced to conidiogenous cells or are 1–3-septate, irregularly branched, hyaline and short. Hyaline to pale brown, determinate, subglobose, obpyriform conidiogenous cells are enteroblastic and phialidic. Conidia are hyaline or light brown, smooth or rough walled, unicellular, occasionally guttulate, holoblastic, fusiform, or ellipsoidal (Thambugala et al., 2014). Index Fungorum (2024) list 83 morphological species of *Selenophoma* but only 6 species have molecular data. The genus is widely distributed on various hosts. The genus is saprobic and occasionally

pathogenic (Cheewangkoon et al., 2009). As example *S. aristidae* was isolated from *Aristida pennata* in Russia, *S. baldingerae* on *Baldingera arundinacea* in Denmark and *S. tritici* isolated from *Triticum aestivum* in China (Karunarathna et al., 2022). Thambugala et al. (2014) revisited *Dothideales* and evaluated the phylogenetic placement of *Selenophoma* using multigene phylogenetic approaches. They noticed that *Selenophoma* produces three different clades in *Dothideales*. Epitification and reevaluation of natural placement of *Selenophoma* is recommended.

Type species: ***Selenophoma catananches*** Maire

Other accepted species: see Species Fungorum, search *Selenophoma* for names.

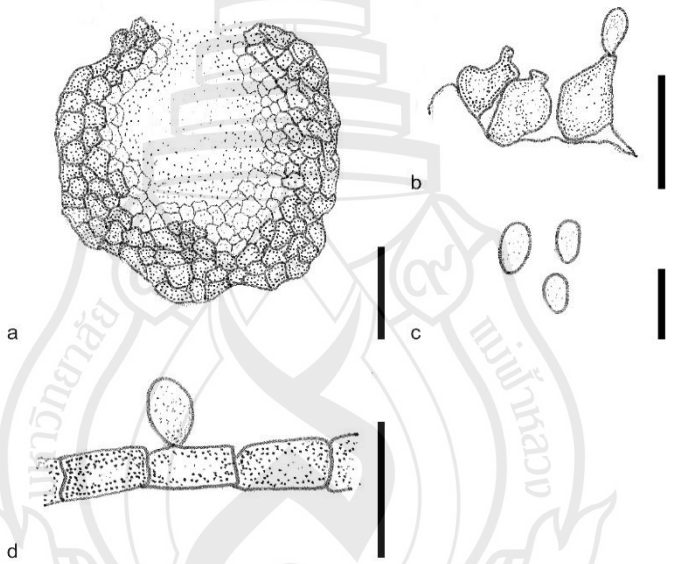

Note (a) Cross section through pycnidium; (b) Conidiogenous cells; (c) Conidia; (d) Conidia produced from hyphal cells. Scale bars: (a-d) 10 µm.

Source Redrawn from Cheewangkoon et al. (2009)

Figure 3.7 *Selenophoma australiensis* (Holotype)

Order ***Mycosphaerellales***

Family ***Incertae sedis***

Janetia Ellis

Citation when using this entry: Amuhenage et al., in prep – Fungalpedia, grass and wetland fungi.

Index Fungorum, Faceoffungi, MycoBank, GenBank, Figure 3.8

Classification: *Incertae sedis, Mycosphaerellales*, *Dothideomycetidae*, *Dothideomycetes*, *Pezizomycotina*, *Ascomycota*, Fungi

Janetia was introduced by M.B. Ellis in 1976 and typified by *Janetia euphorbiae* (Wijayawardene et al., 2022; Hyde et al., 2024). *Janetia* species are hyphomycetes and characterized by micronematous to mononematous, smooth, thick walled, pale brown to brown conidiophores bearing denticulate, integrated, individual or aggregated, monoblastic or polyblastic, smooth, pale brown conidiogenous cells. Conidia development is schizolytic, and conidia are dematiaceous, obclavate to cylindrical, and euseptate or distoseptate (Dubey, 2021). *Janetia* comprises 14 morphologically known species and 2 species with molecular data. Species are predominantly saprobic, occasionally weak pathogens and have worldwide distribution (Dubey, 2021). They have a wide host range and are reported from Poales. As an example, *J. synnematosa* was isolated from dead *Miscanthus floridulus* in Taiwan, China (Karunarathna et al., 2022). Dorchin et al. (2019) investigated the diversification rates of fungi and utilized, *COI*, 16S. ITS1, *CAD* and LSU loci in their analysis. Although they used protein cording loci sequences, the molecular data are limited. Fresh collections and in-depth phylogenetic investigations involving both morphology and multilocus phylogeny are recommended.

Type species: ***Janetia euphorbiae*** Ellis

Other accepted species: see Species Fungorum, search *Janetia* for names.

Note (a-b) Conidiophores with conidia. Scale bars: (a) 5 µm; (b) 10 µm.

Source Redrawn from Dubey. (2021)

Figure 3.8 *Janetia heterospora*

Family ***Mycosphaerellaceae***

Piricauda Bubák

Citation when using this entry: Amuhenage et al., in prep – Fungalpedia, grass and wetland fungi.

Index Fungorum, Faceoffungi, MycoBank, GenBank, Figure 3.9

Classification: *Mycosphaerellaceae*, *Mycosphaerellales*, *Dothideomycetidae*, *Dothideomycetes*, *Pezizomycotina*, *Ascomycota*, Fungi

Piricauda is an asexual genus introduced by Bubák in 1914, and typified by *Piricauda uleana* (Wijayawardene et al., 2022; Hyde et al., 2024). *Piricauda* is characterized by micronematous or semimacronematous, mononematous, simple or occasionally branched conidiophores that possess anastomosing loops. Conidiogenous cells are terminal or intercalary, monotretic, integrated and bear conspicuous dark scars and a prominent pore in the middle (Sierra et al., 2005). *Piricauda* exhibits complex and variable conidia morphology within different species. Conidia are pleurogenous, muriform, smooth or verrucose or spinulose, thick walled, broadly ellipsoidal, ovoid, obconical, spherical, subspherical, pyriform, obpyriform, turbinate, cylindrical, oblong, fusiform or obclavate, predominantly rostrate. They are brown, golden brown, dark brown or blackish brown (Sierra et al., 2005). *Piricauda* has a worldwide distribution and they are saprobic organisms. The host range includes Poales. As an example, *P. serendipita* was isolated from *Zea mays* in Iowa, USA (Karunarathna et al., 2022). *Piricauda* comprises around 30 morphological species but only 2 species have molecular data. Those sequences are limited only to LSU locus (Sierra et al., 2005). Thus, fresh collections and in-depth phylogenetic investigations utilizing both morphology and multilocus phylogeny are recommended.

Type species: ***Piricauda uleana*** Bubák

Other accepted species: see Species Fungorum, search *Piricauda* for names.

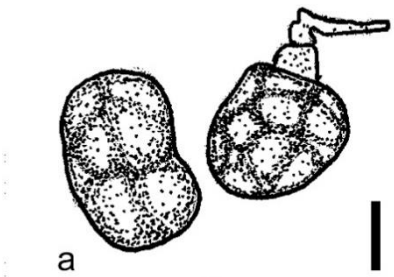

Note (a) Conidia. Scale bars: (a) 10 μm.

Source Redrawn from Sierra et al. (2005)

Figure 3.9 *Piricauda pseudarthriae*

Order ***Myriangiales***

Family ***Elsinoaceae***

Elsinoe Racib.

Citation when using this entry: Amuhenage et al., in prep – Fungalpedia, grass and wetland fungi.

Index Fungorum, Faceoffungi, MycoBank, GenBank, Figure 3.10

Classification: *Elsinoaceae*, *Myriangiales*, *Dothideomycetidae*, *Dothideomycetes*, *Pezizomycotina*, *Ascomycota*, Fungi

Elsinoe is a species rich genus, introduced by Raciborski in 1900, and typified by *Elsinoe canavaliae* (Wijayawardene et al., 2022; Hyde et al., 2024). The genus has both sexual and asexual morphs. The sexual morphs are characterized by brown to black, superficial, globose to subglobose, multi-loculate, pseudoascostromata which develop scab or wart appearance (Jayawardena et al., 2019). Asci are bitunicate, fissitunicate, apedicellate, and each ascus bears 8, hyaline, oblong to fusiform ascospores with 2–3 transverse septa. Asexual morphs are classified under *Sphaceloma*. They are immersed or erumpent, dark brown to black acervuli with hyaline, smooth, phialidic or annellidic, integrated, and terminal conidiogenous cells. Conidia are hyaline, smooth, cylindrical, oblong, ellipsoidal, or reniform, predominantly aseptate or occasionally 1-septate (Jayawardena et al., 2019). *Elsinoe* contains over 200 morphologically known species and around 80 species with molecular data. They are distributed worldwide and mainly known as plant pathogens (Jayawardena et al., 2019). The host range of *Elsinoe* includse grasses and closely related plants. As an example,

E. panici was reported from *Panicum virgatum* in USA (Karunarathna et al., 2022). Jayawardena et al. (2019) conducted in-depth phylogenetic study for *Elsinoaceae*, and they utilized ITS, LSU, SSU, *rpb2* and *tef1-α* sequences to obtain precise phylogenetic placement to members in genus *Elsinoe*. That emphasis the importance of those loci in phylogenetic analysis to obtain proper identification to the species.

Type species: ***Elsinoe canavaliae*** Racib.

Other accepted species: see Species Fungorum, search *Elsinoe* for names.

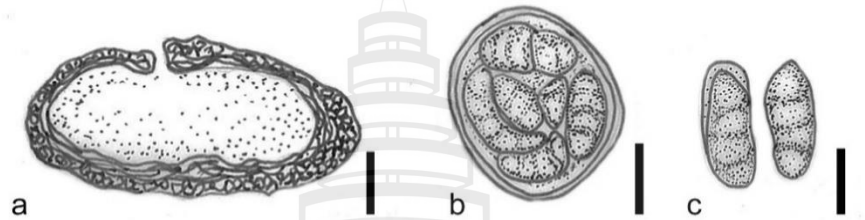

Note (a) Ascoma cross section; (b) Ascus; (c) Ascospores. Scale bars: (a) 100 µm; (b) 20 µm; (c) 10 µm.

Source Redrawn from Jayawardena et al. (2019)

Figure 3.10 *Elsinoe canavaliae* (isotype)

Sub-Class ***Incertae sedis***

Order ***Acrospermales***

Family ***Acrospermaceae***

Acrospermum Tode

Citation when using this entry: Amuhenage et al., in prep – Fungalpedia, grass and wetland fungi.

Index Fungorum, Faceoffungi, MycoBank, GenBank, Figure 3.11

Classification: *Acrospermaceae*, *Acrospermales*, *Incertae sedis*, *Dothideomycetes*, *Pezizomycotina*, *Ascomycota*, Fungi

Acrospermum was introduced by Tode in 1783 and is typified by *Acrospermum unguinosum*. This genus has 12 valid species (Wijayawardene et al., 2022; Hyde et al., 2024). Minter, et al., reported *Acrospermum chilense* from *Chusquea quila* stems in the USA (Karunarathna et al., 2022). The genus is found saprobic on dead and decaying plant materials. The species form club-shaped superficial ascomata that are loosely aggregated or scatted on the surfaces. Ascomata are uni-locular, erect, and brown or

brownish-black. Peridium has three layers. Outermost layers are composed of dark, pigmented cells of *textura angularis*. The middle layer has elongated like gelatinized hyphae and the inner layer contains highly compressed, small light brown cells (Hyde et al., 2013). Peridium protects the hamathecium encompassing long tread-like pseudoparaphyses and bitunicate, subcylindrical to cylindrical, and short pedicellate asci. Each ascus bears eight ascospores and has an ocular chamber. Ascospores are filamentous, hyaline and multi-septate (Hyde et al., 2013). The asexual morph is hyphomycetous and produces pale brown, septate, straight micronematous conidiophores. Each conidiophores bears holoblastic, long, brown, and cylindrical conidiogenous cells. They produce yellowish-brown, 1–3-septate, ellipsoidal conidia with a rounded apex (Hernandez-Restrepo et al., 2017). Hongsanan et al. (2020) used LSU and SSU sequences to introduce *A. urticae* to the genus. More taxon sampling and the use of more loci are required to obtain in in-depth view of the genus.

Type species ***Acrospermum unguinosum*** Tode

Other accepted species: see Species Fungorum, search *Acrospermum* for names.

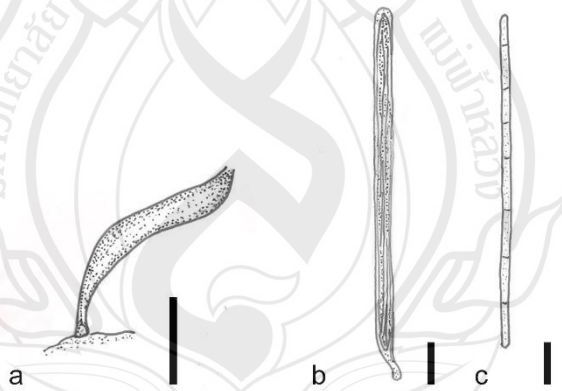

Note (a) Ascoma on the host; (b) Ascus; (c) Ascospore. Scale bars: (a) 0.5 mm; (b-c) 10 µm.

Source Redrawn from Minter et al. (2007)

Figure 3.11 *Acrospermum chilense*

Order ***Botryosphaeriales***

Family ***Botryosphaeriaceae***

Botryobambusa Phook.

Citation when using this entry: Amuhenage et al., in prep – Fungalpedia, grass and wetland fungi.

Index Fungorum, Faceoffungi, MycoBank, GenBank, Figure 3.12

Classification: *Botryosphaeriaceae*, *Botryosphaeriales*, *Incertae sedis*, *Dothideomycetes*, *Pezizomycotina*, *Ascomycota*, Fungi

Botryobambusa is a monophyletic genus introduced by R. Phookamsak in 2012 and typified by *Botryobambusa fusicoccum* (Liu et al., 2012; Wijayawardene et al., 2022; Hyde et al., 2024). The genus is characterized by gregarious or loosely aggregated, dark brown to black, coriaceous ascomata, immersed under epidermis to erumpent in the host tissue. Ascomata are multiloculate, individual locules are globose to subglobose or fused and produce a central ostiole. *Botryobambusa* possess bitunicate, fissitunicate, clavate to cylindro-clavate asci with pedicels and conspicuous ocular chambers. Each ascus bears eight aseptate, hyaline, ellipsoidal to obovoid ascospores with velvety, smooth, and thick walls and a mucilaginous sheath (Liu et al., 2012). Pycnidia are aggregated in stromatic clusters, multiloculate, globose to subglobose. They are broader at the base, the outer layer of the peridium comprises dark, thick-walled cells of *textura angularis* and inner layers exhibit hyaline thin-walled cells. Conidiogenous cells originate from inner layer of the peridium and are hyaline, smooth, cylindrical, or ellipsoidal and holoblastic (Liu et al., 2012). Conidia are hyaline, aseptate, cylindrical to cylindro-clavate, with thin-walls. Initially *Botryobambusa* was isolated only from bamboo in southeast Asia (Karunarathna et al., 2022), but Niranjan and Sharma (2018) reported *B. apiculiformispora* on *Calamus andamanicus* from Andaman Islands. The ITS, LSU, SSU, *EF1-α* and *β-tubulin* loci were used during the introduction of the genus (Liu et al., 2012) and that indicate the importance of those loci while introducing new species.

Type species: ***Botryobambusa fusicoccum*** Phook.

Other accepted species: see Species Fungorum, search *Botryobambusa* for names.

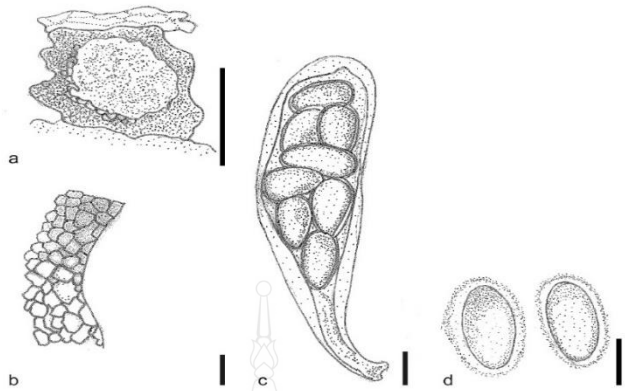

Note (a) Ascoma cross section; (b) Peridium; (c) Ascus; (d) Ascospores. Scale bars: (a) 200 µm; (b) 20 µm; (c) 10 µm; (d) 5 µm.

Source Redrawn from Liu et al. (2012)

Figure 3.12 *Botryobambusa fusicoccum* (MFLU 11–0179, Holotype)

Family ***Planistromellaceae***

Loratospora Kohlm. & Volkm.

-Kohlm.

Citation when using this entry: Amuhenage et al., in prep – Fungalpedia, grass and wetland fungi.

Index Fungorum, Faceoffungi, MycoBank, GenBank, Figure 3.13

Classification: *Planistromellaceae*, *Botryosphaeriales*, *Incertae sedis*, *Dothideomycetes*, *Pezizomycotina*, *Ascomycota*, Fungi

Loratospora was introduced by Jan Kohlmeyer, and Brigitte Volkmann-Kohlmeyer in 1993 and typified by *Loratospora aestuarii* (Wijayawardene et al., 2022; Hyde et al., 2024). Initially the genus was placed under *Dothideales*, *incertae sedis*, but was later transferred to *Phaeosphaeriaceae* following multilocus phylogeny (Monkai et al., 2013; Hyde et al., 2020). *Loratospora* is characterized by immersed, scatted and subglobose ascomata that produce dark patches on host tissue. The peridium is composed of 4-5 layers of thick-walled cells. Asci are bitunicate, fissitunicate, clavate to ovoid with knob-like pedicels and an apical ocular chamber. Each ascus bears eight, hyaline, obovoid, fusoid or clavate, 3-septate ascospores which taper towards the ends and are slightly constricted at each septum. They are covered with a thin mucilaginous

sheath (Monkai et al., 2013; Hyde et al., 2020). *Loratospora* species are saprobic, and known distribution includes marine habitats of North Carolina and woodlands of Italy. The genus is only recovered from *Juncus*. As an example, the type species *L. aestuarii* was isolated from both submerged and immersed sections of dead *Juncus roemerianus* (Monkai et al., 2013; Karunarathna et al., 2022). The most recently described species *L. arezzoensis* utilized ITS, LSU and SSU loci in the analysis. That emphases the importance of those loci in species delineation in the genus (Hyde et al., 2020). The phylogenetic placement of the genus is debatable. According to that more collections and in-depth investigations utilizing both morphology and multilocus phylogeny are recommended.

Type species: ***Loratospora aestuarii*** Kohlm. & Volkm.-Kohlm.

Other accepted species:

Loratospora arezzoensis Bundhun, Wanas., R. Jeewon & K.D. Hyde

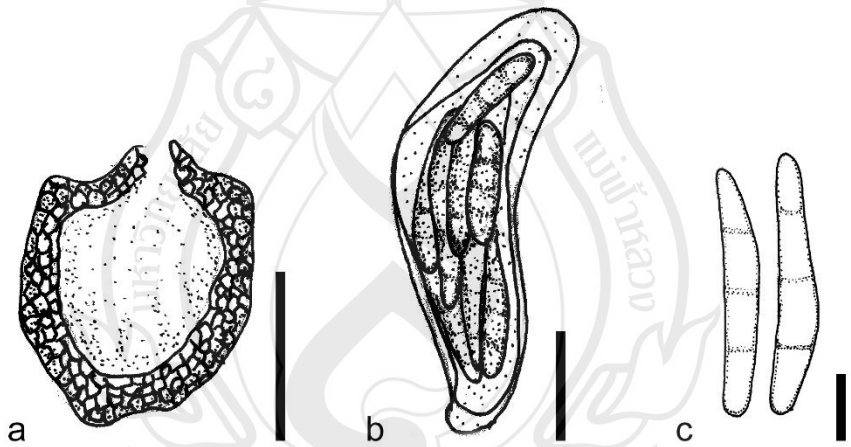

Note (a) Cross section of ascoma; (b) Ascus; (c) Ascospores. Scale bars: (a) 100 µm; (b) 25 µm; (c) 5 µm.

Source Redrawn from Monkai et al. (2013).

Figure 3.13 *Loratospora aestuarii* (Holotype)

Order ***Dyfrolomycetales***

Family ***Pleurotremataceae***

Melomastia Nitschke ex Sacc.

Citation when using this entry: Amuhenage et al., in prep – Fungalpedia, grass and wetland fungi.

Index Fungorum, Faceoffungi, MycoBank, GenBank, Figure 3.14

Classification: *Pleurotremataceae*, *Dyfrolomycetales*, *Incertae sedis*, *Dothideomycetes*, *Pezizomycotina*, *Ascomycota*, Fungi

Melomastia was introduced by Nitschke in 1875 and is typified by *Melomastia friesii* (Wijayawardene et al., 2022; Hyde et al., 2024). An initial lack of molecular data led this genus to be placed under *Ascomycota* genera *incertae sedi*s. Norphanphoun et al. (2017) reclassified the genus under *Pleurotremataceae* based on molecular phylogeny and morphological evidence. Later authors synonymsed *Melomastia* under *Dyfrolomyces* (Senanayake et al., 2023). Kularathnage et al. (2023) resurrected *Melomastia* based on multilocus phylogeny. *Melomastia* species are characterized by producing coriaceous to carbonaceous, ascomata that are scattered or solitary on host tissue. Each ascoma produces conical periphysate papilla and pseudoparaphyses are narrow, septate and abundant (Dong et al., 2023; Senanayake et al., 2023).Asci are bitunicate, cylindrical with eight ascospores that are arranged in an uni-seriate to overlapping uni-seriate manner. Ascospores are predominantly hyaline, ellipsoid to fusiform and 1–10-septate (Senanayake et al., 2023). *Melomastia* is found from a wide range of habitats including terrestrial, freshwater, and marine habitats such as mangrove forests. The species show a wide host range including both monocotyledonous and dicotyledonous plants. For example, *M. graminicola* was isolated from *Sorghum vulgare* in Equatorial Africa and *M. yezoensis* was found on *Sasa kurilensis* from Japan (Karunarathna et al., 2022). More collections and eptypification for older species are recommended to obtain clear robust view into the taxonomic relationships in genus *Melomastia*.

Type species: ***Melomastia friesii*** Nitschke ex Sacc

Other accepted species: see Species Fungorum, search *Melomastia* for names.

Note (a) vertical section of ascoma; (b) peridium; (c) pseudoparaphyses; (d-e) asci with short pedicel; (f-h) ascospores. Scale bars: (a) 100 µm; (b-c) 50 µm; (d-e) 20 µm; (f-h) 10 µm.

Figure 3.14 *Melomastia* species

Order ***Incertae sedis***

Family ***Balladynaceae***

Balladyna Racib.

Citation when using this entry: Amuhenage et al., in prep – Fungalpedia, grass and wetland fungi.

Index Fungorum, Faceoffungi, MycoBank, GenBank, Figure 3.15

Classification: *Balladynaceae*, *Incertae sedis*, *Incertae sedis*, *Dothideomycetes*, *Pezizomycotina*, *Ascomycota*, Fungi

Balladyna is a mono phyletic genus introduced by Raciborski in 1900 and typified by *Balladyna gardenia*. Although the genus lacks molecular data, morphologically around 35 species have been introduced (Wijayawardene et al., 2022; Hyde et al., 2024). They are parasitic life style on plants. Ascomata are globose or subglobose in shape. They are scattered on host tissue and situated superficial on hyphae. Peridium contains greenish dark cells of *textura angularis* and protect a single ascus. That ascus is bitunicate, subglobose or globose in shape. The sscus is sessile and there are no pseudoparaphyses. Ascus holds eight ornamented ascospores. They are 1-spetate with large superior cell, olive green and arranged in a multi-seriate manner (Boonmee et al., 2017). Asexual morphs are members of *Clasterosporium* and *Tretospora* (Seifert et al., 2011). *Balladyna* was reported from monocotledenus plants like grasses. As examples, *B. lelebae* was reported from *Leleba shimadai* in Chain Taiwan and *B. muroiana* was reported from *Nipponobambusa* in Japan (Karunarathna et al., 2022). Lack of molecular data is the main obstacle to understand proper taxonomic placement of the genus More research and isolations are need to get in-depth view to the phylogeny of genus *Balladyna*.

Type species ***Balladyna gardeniae*** Racib.

Other accepted species: see Species Fungorum, search *Balladyna* for names.

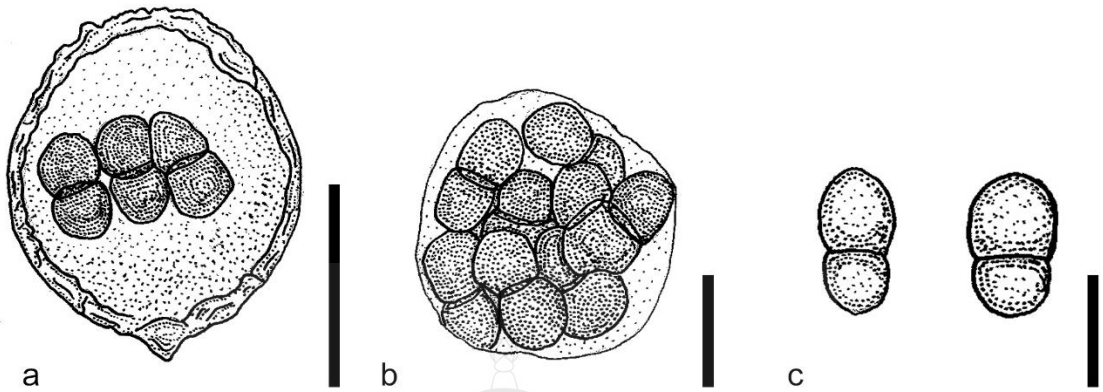

Note (a) Squash mount of ascomata; (b) Ascus; (c)Ascospore. Scale bars: (a) 50 μm; (b-c) 20 μm.

Source Redrawn from Boonmee et al. (2017)

Figure 3.15 *Balladyna gardenia* (BPI 691469, isotype)

Family ***Phaeothecoidiellaceae***

Septoriella Oudem

Citation when using this entry: Amuhenage et al., in prep – Fungalpedia, grass and wetland fungi.

Index Fungorum, Faceoffungi, MycoBank, GenBank, Figure 3.16

Classification: *Phaeosphaeriaceae*, *Incertae sedis*, *Incertae sedis*, *Dothideomycetes*, *Pezizomycotina*, *Ascomycota*, Fungi

Septoriella was first proposed by Oudem in 1889 and typified to *Septoriella phragmitis* (Wijayawardene et al., 2022; Hyde et al., 2024). Members of the genus characterized by both sexual and asexual morphs. Sexual morphs process loosely aggregated, semi-immersed or erupting black, globose to sub-globose ascomata with short ostiole. Pseudoparaphyses are hyaline, asepatae and thread like. Asci are bitunicate, cylindrical and process well developed ocular chambers at the top. Eachh ascus bear 6-8 sepatate, fusiform, hyaline, smooth ascospores. Asexual morphs of the genus *Septoriella* produces globose to subglobose, unilocular, black, short ostiolet, glabrous pycnidia. Conidiogenous cells are ampulliform to lageniform and give rise to smooth to verruculose, pale brown, fusiform to subcylindrical conidia (Crous et al., 2015; Wanasinghe & Maharachchikumbura, 2023). *Septoriella* was subjected to significant number of revisions. The most recent and the widely accepted revision was

done by Crous et al. (2015) and they accommodated the in *Phaeosphaeriaceae* and considered *Wojnowicia* as a synonym to the genus. Wanasinghe and Maharachchikumbura (2023) introduced *S. shoemaker* to the genus as a new species and synonymized *Amarenomyces dactylidis* and *Phaeopoacea muriformis* to the genus as *S. paradactylidis* and *S. neomuriformis*. According to that genus *Septoriella* process 55 morphological species and 26 species with molecular data. Genus *Septoriella* are prominently saprobic organisms, showcase cosmopolitan distribution and showcase affinity towards herbaceous plants. As an examples *Septoriella canadensis* was found on Bamboo in Canada, and *Septoriella dactylidicol* was isolated from *Dactylis* sp. in Italy (Karunarathna et al., 2022). Wanasinghe and Maharachchikumbura (2023) used ITS, LSU, SSU, *tef1-α* and *rpb2* loci in their investigation. That emphasis the importance of using those loci in species delineation in genus *Septoriella*.

Type species: ***Septoriella phragmitis*** Oudem

Other accepted species: see Species Fungorum, search *Septoriella* for names.

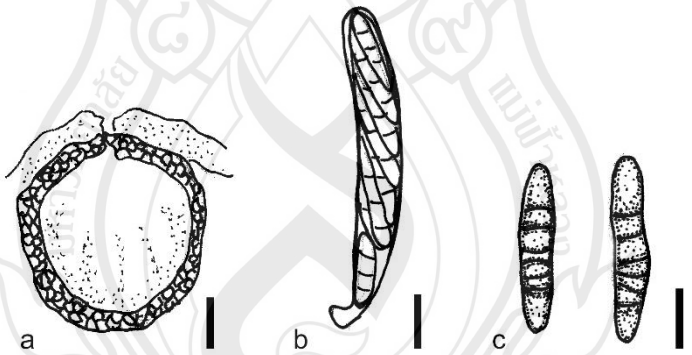

Note (a) Cross section of the ascomata; (b) Ascus; (c) Ascospores. bars: (a) 20 µm; (b-c) 10 µm.

Source Redrawn from Wanasinghe and Maharachchikumbura (2023)

Figure 3.16 *Septoriella paradactylidis* (HKAS 129216)

Family ***Pseudoperisporiaceae***

Juncaceicola Tennakoon

Citation when using this entry: Amuhenage et al., in prep – Fungalpedia, grass and wetland fungi.

Index Fungorum, Faceoffungi, MycoBank, GenBank, Figure 3.17

Classification: *Phaeosphaeriaceae*, *Pleosporales*, *Pleosporomycetidae*, *Dothideomycetes*, *Pezizomycotina*, *Ascomycota*, Fungi

Genus *Juncaceicola* was introduced by Tennakoon, Camporesi, Phook. & K.D. Hyde in 2016 and typified to *Juncaceicola luzulae* (Wijayawardene et al., 2022; Hyde et al., 2024). This monophyletic genus resides under Phaeosphaeriaceae and characterized by immersed or erumpent, scatted or loosely aggregated, globose to subglobose, and uni-loculate ascomata on host tissue. The pseudoparaphyses are dense, cellular with smooth walls and embedded in a gelatinous matrix. Asci are bitunicate, fissitunicate, cylindrical or cylindric-clavate. They are short pedicellate and process well-developed ocular chambers at the apexes. Each ascus bears eight, hyaline, to pale brown, 3-4-septate ascospores with wider second cells and rounded ends. Asexual morphs of the genus *Juncaceicola* known to exhibit similar characteristics to *Stagonospora* (Tennakoon et al., 2016). *Juncaceicola* comprise with eight species and all the members process molecular data. Their distribution limited to Europe and Australian continents. Members of this genus are known to lead saprobic lifestyle and isolated from monocotyledonous plants (Tennakoon et al., 2016). As an example, *Juncaceicola alpine* was isolated from *Phleum alpinum* in Switzerland (Karunarathna et al., 2022). The initial introduction of the genus utilized ITS, LSU and SSU loci. That indicate the importance of those loci to delineate species in genus *Juncaceicola* (Tennakoon et al., 2016). More collections from other locations and host species are recommended to widen the understanding of the ecological role of the genus.

Type species: ***Juncaceicola luzulae*** Tennakoon, Camporesi, Phook. & K.D. Hyde

Other accepted species:

Juncaceicola achilleae Wanas., Tennakoon, Camporesi & K.D. Hyde

Juncaceicola alpina (Leuchtm.) Tennakoon, Phook. & K.D. Hyde

Juncaceicola dactylidis Wanas., Tennakoon, Camporesi & K.D. Hyde,

Juncaceicola italica Tibpromma, Camporesi & K.D. Hyde

Juncaceicola oreochloae (Leuchtm.) Tennakoon, Phook. & K.D. Hyde

Juncaceicola padellana (Leuchtm.) Tennakoon, Phook. & K.D. Hyde

Juncaceicola queenslandica Y.P. Tan, Bishop-Hurley & R.G. Shivas

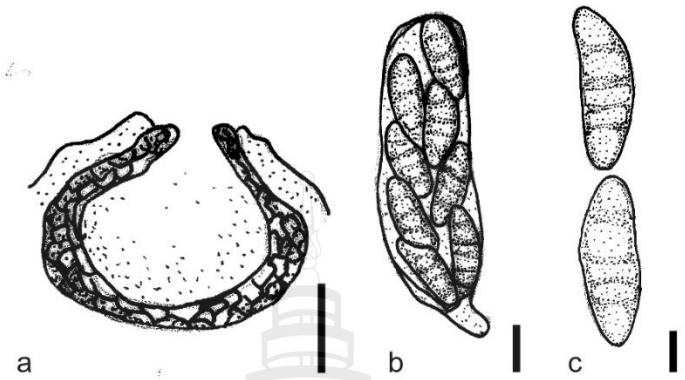

Note (a) Cross section of the ascomata; (b) Ascus; (c) Ascospores. Scale bars: (a) 50 μm; (b) 10 μm; (c) 5 μm.

Source Redrawn from Tennakoon et al. (2016)

Figure 3.17 *Juncaceicola achilleae*

Order ***Jahnulales***

Family ***Aliquandostipitaceae***

Xylomyces Goos, Brooks & Lamore

Citation when using this entry: Amuhenage et al., in prep – Fungalpedia, grass and wetland fungi.

IndexFungorum; Facesoffungi; MycoBank; GenBank; Figure 3.18

Classification: *Aliquandostipitaceae*, *Jahnulales*, *Incertae sedis*, *Dothideomycetes Pezizomycotina*, *Ascomycota*, Fungi

Xylomyces is a polyphyletic genus introduced by Goos, Brooks & Lamorein in 1977 and typified to *Xylomyces chlamydosporus* (Goh et al., 1997). Genus *Xylomyces* belongs to *Aliquandostipitaceae*, *Jahnulales* in *Dothideomycetes* (Wijayawardene et al., 2022; Hyde et al., 2024). This genus is known to contain anamorphs of genus *Jahnula*. The type species of genus *Xylomyces*, *Xylomyces chlamydosporus* was reported to be the anamorph of *Jahnula aquatica*. This connection was made by using only morphological analysis related to Jahnula aquatic and chlamydospores produced in the culture (Sivichai et al., 2011). Multigene phylogenetic analysis is required to firmly establish this link between genera. Genus *Xylomyces* are aquatic saprobic

hyphomycetes that produces large, broadly fusiform, septate, thick walled and dematiaceous chlamydospores. They are light brown to greenish dark in color (Goh et al., 1997). Members of genus *Xylomyces* are mainly found associated with submerged wood. Colonies are effuse and anastomosing mycelium can be immersed or slightly superficial. Conidiophores are indistinct, semi-macronematous or micro-macronematous. Chlamydospores are connected to each other from end to end and create chain like structure (Dong et al., 2020). *Xylomyces aquaticus* and *Xylomyces elegans* were excluded from the genus based on multigene phylogenetic analysis (Tanaka et al., 2015). Due to that genus *Xylomyces* consist with seven recognized species. Only *Xylomyces chlamydosporus* process molecular data (Dong et al., 2020). More investigations based on both phylogenetic and morphological approaches are required to generate robust understanding and with insight to the genus.

Type species: ***Xylomyces chlamydosporus*** Goos, Brooks & Lamore

Other accepted species: see Species Fungorum, search *Xylomyces* for names.

Note (a) Chlamydospores of *X. chlamydosporus* developed on culture. Scale bars: (a) 10 μm.

Source Redrawn from Suetrong et al. (2011)

Figure 3.18 *Xylomyces chlamydosporus*

Order ***Monoblastiales***

Family ***Monoblastiaceae***

Heleiosa Kohlm., Volkm. -Kohlm. & O.E. Erikss

Citation when using this entry: Amuhenage et al., in prep – Fungalpedia, grass and wetland fungi.

Index Fungorum, Faceoffungi, MycoBank, GenBank, Figure 3.19

Classification: *Monoblastiaceae*, *Monoblastiales*, *Incertae sedis*, *Dothideomycetes*, *Pezizomycotina*, *Ascomycota*, Fungi

Heleiosa is a monophyletic genus introduced by Kohlm., Volkm. -Kohlm. & O.E. Erikss in 1996, and typified to *Heleiosa barbatula* (Wijayawardene et al., 2022; Hyde et al., 2024). Members of the genus characterized by solitary to aggregated, brown to black, immersed to erumpent, globose to ampulliform ascomata with central, and cylindrical ostiole. Peridium comprise with multiple layers, the outer pigmented thick layer frequently unites with plant tissue, and inner thin layer composed by hyaline, thin-walled cells in *textura prismatica*. Hamathecium process gelatinous matrix, and pseudoparaphyses are hyaline, branched, and septate. The asci in the genus *Heleiosa* are bitunicate, cylindrical with furcated base, short pedicellate, and ocular chamber (Yang et al., 2023). Ascospores are hyaline to pale brown, ellipsoidal with obtuse ends, 1-septate, slightly constricted at the septum. Originally *Heleiosa* was monotypic, and Sun et al. (2025) incorporated three species such as *Heleiosa brunnea*, *H. guizhouensis* (≡ *Neoheleiosa guizhouensis*), *H. lincangensis* (≡ *Neoheleiosa lincangensis*) to the genus based on multilocus phylogeny and morphological evidences. They utilized ITS, LSU and SSU loci for their investigation, emphasizing the importance of those loci to species delineation in the genus. Members under genus *Heleiosa* are saprobic organisms, which were isolated from USA and Asia (Yang et al., 2023; Sun et al., 2025). The host range of the *Heleiosa* includes monocotyledonous plants. As example the type species *Heleiosa barbatula* was initially isolated from *Juncus* sp. in North Carolina, USA (Karunarathna et al., 2022). More fresh collections from diverse environments and different habitats are recommended.

Type species: ***Heleiosa barbatula*** Kohlm., Volkm. -Kohlm. & O.E. Erikss

Other accepted species:

Heleiosa brunnea Y.R. Sun, Yong Wang bis & K.D. Hyde

Heleiosa guizhouensis (Jin F. Zhang & K.D. Hyde) Y.R. Sun, Yong Wang bis & K.D. Hyde

Heleiosa lincangensis (P.E. Mortimer) Y.R. Sun, Yong Wang bis & K.D. Hyde

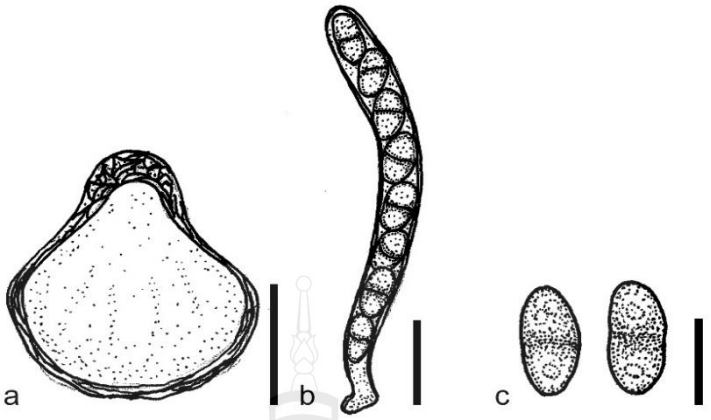

Note (a-b) Ascomata; (b) Ascus; (c) Ascospores. Scale bars: (a) 150 µm; (b-c) 25 µm.
Source Redrawn from Yang et al. (2023)

Figure 3.19 *Heleiosa barbatula* ((HKAS 122668)

Order ***Tubeufiales***

Family ***Tubeufiaceae***

Xenosporium Penz. & Sacc

Citation when using this entry: Amuhenage et al., in prep – Fungalpedia, grass and wetland fungi.

Index Fungorum, Faceoffungi, MycoBank, GenBank, Figure 3.20

Classification: *Tubeufiaceae*, *Tubeufiales*, *Incertae sedis*, *Dothideomycetes*, *Pezizomycotina*, *Ascomycota*, Fungi

Genus *Xenosporium* was proposed by Penz. & Sacc in 1901 and typified to *Xenosporium mirabile* (Wijayawardene et al., 2022; Hyde et al., 2024). This is a hyphomycetes genus wish shear morphological and phylogenetica affinity towered closely related genus *Tubeufia*, *Tubeufiaceae*. Members of *Xenosporium* characterized by macronematous, erect, simple or branched, pale brown to hyaline conidiophores that produces dorsiventrally curved, muriform conidia (Zhao et al., 2006). *Xenosporium* showcase worldwide distribution and recovered for both terrestrial and aquatic habitats (Karunarathna et al., 2022). They are menially known as saprobic organisms and contribute to material recycling cycling, and longevity of sensitive ecosystems such as wetlands. As an example, *Xenosporium formosiforme* was introduced from submerged decomposing vegetation freshwater body (Kuo & Goh. 2021). Genus contains 8

morphological species and only two species preprocess molecular data. Kuo and Goh. (2021) utilized ITS, LSU, *rpb2* and *gpd1* to introduced *X. formosiforme* and that emphasis the importance of those loci in species delineation to the genius *Xenosporium*. Fresh collections and in-depth phylogenetic studies are recommended to obtain a robust understanding of the genus and to determine its proper phylogenetic placement in relation to other closely related members within *Tubeufiaceae*.

Type species: ***Xenosporium mirabile*** Penz. & Sacc

Other accepted species: see Species Fungorum, search *Xenosporium* for names

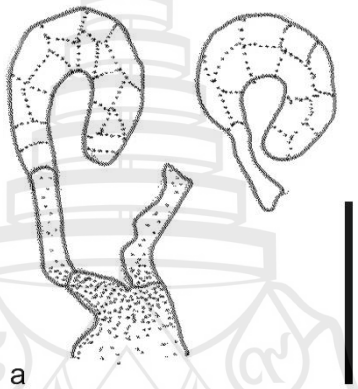

Note (a) Conidiophores with conidia. Scale bars: (a-c) 25 µm.

Source Redrawn from Zhao et al. (2006)

Figure 3.20 *Xenosporium helicominum*

Sub-Class ***Pleosporomycetidae***

Order ***Pleosporales***

Family ***Astrosphaeriellaceae***

Astrosphaeriella Syd & Syd

Citation when using this entry: Amuhenage et al., in prep – Fungalpedia, grass and wetland fungi.

Index Fungorum, Faceoffungi, MycoBank, GenBank, Figure 3.21

Classification: *Astrosphaeriellaceae*, *Pleosporales*, *Pleosporomycetidae*, *Dothideomycetes*, *Pezizomycotina*, *Ascomycota*, Fungi

This genus classifies under order Pleosporales and family *Melanommataceae* in fungal kingdom. It was introduced by Syd & P. Syd in 1913 (Lumbsch & Huhndorf, 2007). The resent analysis on order Pleosporales sported that original classification.

That investigation was a multi gene phylogenetic analysis conducted by using gene regions such as ITS5 and ITS4, LROR, LR5, NS1 and NS4. Pylogenetic tree was constructed based on Maximum-parsimony (MP) and Bayesian analyses. That phylogenetic tree illustrated the segregation of *Astrosphaeriella* as a separate genus in order *Pleosporales* (Liu et al., 2011). Genus *Astrosphaeriella* shows wide range of distribution. The predominate hosts are Monocotyledon plants. Aquatic species called *Astrosphaeriella aquatica* was recorded from freshwater habitat in Western Province of Papua New Guinea (Hyde, 1994). Ascomata of the genus *Astrosphaeriella* is black, conical, clustered at the bases and unilocular. They live scattered the host and found immersed, sub epidermal or superficial. Ascomata produces mammiform or elongated black ostiole and entire structure is supported by thick carbonaceous peridium. Asci are bitunicate, cylindric-clavate in shape and pedicellated. They hold eight spores as usual and harbor an ocular chamber They can elongate in spore discharge. Ascospores 2-3–seriate, elongate and narrowing to the apexes. Spores are mostly five septate and color change from hyaline to reddish brown. This ascospaore shape make this genus morphologicaly distinguishable from closely related genera such as genus *Trematosphaeria* and genus *Caryospora* (Liu et al., 2011).

Type Species ***Astrosphaeriella fusispora*** Syd & Syd

Other accepted species: see Species Fungorum, search *Astrosphaeriella* for names.

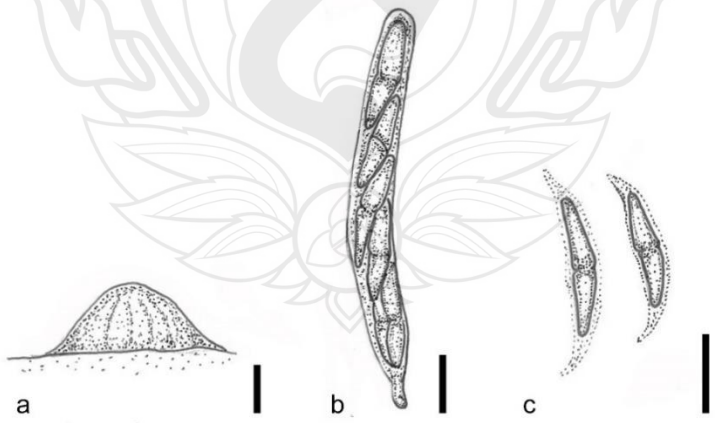

Note (a) Ascomata on host surface; (b) Ascus; (c) Ascospores. Scale bars: (a) 100 µm; (b-c) 10 µm.

Source Redrawn from Hyde KD. (1994)

Figure 3.21 *Astrosphaeriella aquatica*

Family ***Didymellaceae***

Leptosphaerulina McAlpine

Citation when using this entry: Amuhenage et al., in prep – Fungalpedia, grass and wetland fungi.

Index Fungorum, Faceoffungi, MycoBank, GenBank, Figure 3.22

Classification: *Didymellaceae*, *Pleosporales*, *Pleosporomycetidae*, *Dothideomycetes*, *Pezizomycotina*, *Ascomycota*, Fungi

Genus *Leptosphaerulina* was introduced in 1902 by McAlpine, accommodating the type species *Leptosphaerulina australis* form Australia (Wijayawardene et al., 2022; Hyde et al., 2024). Members of this genus are known as plant pathogen and saprobes on bead vegetation. The genus *Leptosphaerulina* resides in *Didymellaceae*, but initially categorized under the *Pleosporaceae*. The transfer was supported by molecular phylogenetic data and lack of pseudoparaphyses in the members of genus *Leptosphaerulina* (Kodsueb et al., 2006). Genus characterized by several morphological features. They produce pseudothecial, obpyriform to subglobose ascomata with single central ostiole that appear individually or loosely aggregated on host tissue. Pseudoparaphyses not available and asci are bitunicate, obovoid to sub-cylindrical, process conspicuous apical chambers, and bear eight spores in each mature ascus. Ascospores are hyaline, ellipsoid to obovoid, narrowing towards ends, more pointed towards base, exhibit thin mucoid sheath, and arranged in multiseriate manner. Ascospores process transverse septa, vertical, oblique septa, and slightly constricted at the septa (Crous et al., 2011). Genus *Leptosphaerulina* was isolated from variety of monocotyledonous plants from wide geographical range. As example *Leptosphaerulina calamagrostidis* was found from *Calamagrostis epigejos*, Kazakhstan, and *Leptosphaerulina fontium* isolated from *Carex frigida* in Austria (Karunarathna et al., 2022). Although genus *Leptosphaerulina* mainly considered as a phytopathogenic assembly of fungi, recent investigation utilized pathogenicity tests for grass inhabiting *Leptosphaerulina* species showcased that genus *Leptosphaerulina* lean more towards saprobic life style than pathogenic (Liang et al., 2021). That indicates there are more in-depth studies, incorporating modern technologies are necessary to understand the ecological role and evolutionary relationships in genus *Leptosphaerulina*.

Type species: ***Leptosphaerulina australis*** McAlpine

Other accepted species: see Species Fungorum, search *Leptosphaerulina* for names.

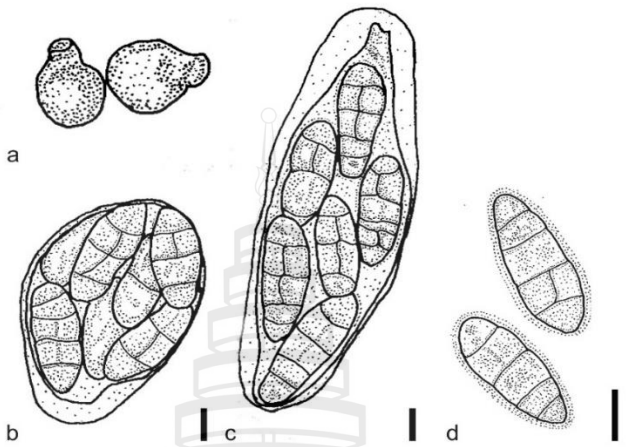

Note (a) Ascomata *in vitro*; (b-c) Asci; (d) Ascospores; Scale bars: (b-d) 10 μm.
Source Redrawn from Crous et al. (2011)

Figure 3.22 *Leptosphaerulina australis* (CBS 116307)

Neoascochyta Qian Chen & L. Cai

Citation when using this entry: Amuhenage et al., in prep – Fungalpedia, grass and wetland fungi.

Index Fungorum, Faceoffungi, MycoBank, GenBank, Figure 3.23

Classification: *Didymellaceae*, *Pleosporales*, *Pleosporomycetidae*, *Dothideomycetes*, *Pezizomycotina*, *Ascomycota*, Fungi

Genus *Neoascochyta* was proposed by Qian Chen & L. Cai in 2015 and typified to *Neoascochyta exitialis* (Wijayawardene et al., 2022; Hyde et al., 2024).The accommodated taxa from genus *Ascochyta* to this new genus following the phylogenetic avoidances provided by multigene phylogenetic analysis the conducted to *Didymellaceae* (Chen et al., 2015). Genus *Neoascochyta* characterized by following morphological features. Pseudothecial ascomata are found solitary or tightly aggregated, they are either immersed or erumpent in host material. Ascomata hold bitunicate, cylindrical to subclavate, slightly curved asci with eight ascospores. Asci are observed to process short pedestal or remain sessile. Ascospores are hyaline, cylindrical to ellipsoidal, 1-septate, constricted at the septum, show biseriate or irregular uniseriate

arrangement in ascus (Chen et al., 2015). Members of the genus produce asexual morphs with pycnidial, globose to subglobose, or irregularly shaped conidiomata with single, short ostiole. They are found individually or merged together on the substrate. Multiple layers of pseudoparenchymatous cells form the pycnidial wall and peripheral layers are pigmented and dark. Inner hyaline layer give rise to flask-shaped to ampulliform or doliiform, hyaline smooth and phialidic conidiogenous cells. Conidia that originate from those conidiogenous cells are hyaline, smooth walled, fusoid, cylindrical, obclavate, occasionally curved. Majority of the conidia are unicellular and some are 1-septate (Chen et al., 2015). Genus *Neoascochyta* was reported from monocotyledonous plants and from both hemispheres. *Neoascochyta europaea* was isolated from *Hordeum vulgare* in Great Britain, *Neoascochyta graminicola* was found from *Lolium* sp. seeds in Germany, and *Neoascochyta paspali* was isolated from *Paspalum dilatatum* in New Zealand (Karunarathna et al., 2022). Chen et al. (2015) utilized LSU, ITS, *rpb2*, and *tub2* loci in their phylogenetic analysis to establish genus *Neoascochyta*. They emphasis the important of using those loci to obtain robust view in to the evolutionary relationships in genus *Neoascochyta* and family *Didymellaceae*.

Type species: ***Neoascochyta exitialis*** (Morini) Qian Chen & L. Cai

Other accepted species: see Species Fungorum, search *Neoascochyta* for names.

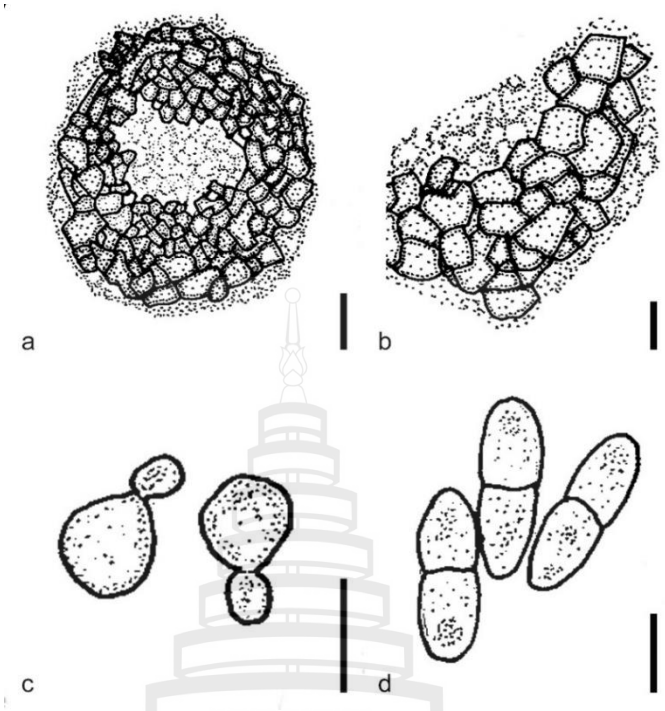

Note (a) Section of Pycnidia; (b) Pycnidial wall; (c) Conidiogenous cells; (d) Conidia. Scale bars: (a) 20 μm; (b-d) 10 μm.

Source Redrawn from Chen et al. (2015)

Figure 3.23 *Neoascochyta exitialis* (CBS 389.86)

Family ***Didymosphaeriaceae***

Kalmusia Niessl

Citation when using this entry: Amuhenage et al., in prep – Fungalpedia, grass and wetland fungi.

Index Fungorum, Faceoffungi, MycoBank, GenBank, Figure 3.27

Classification: *Didymosphaeriaceae*, *Pleosporales*, *Pleosporomycetidae*, *Dothideomycetes*, *Pezizomycotina*, *Ascomycota*, Fungi

Niessl introduced the genus *Kalmusia* in 1872 typified to *Kalmusia ebuli* (Wijayawardene et al., 2022; Hyde et al., 2024). Lack of molecular data from the type species made the phylogenetic placement the genus *Kalmusia* questionable and provided subject for argument in taxonomic world. Neotypification for *Kalmusia ebuli* and reexamining of *Kalmusia* phylogeny was taken place in 2014. That study placed genus *Kalmusia* under family *Montagnulaceae* based on phylogenic evidences and morphological features such as asymmetric ascospores and clavate asci that process

long pedicels (Zhang et al., 2014). Ariyawansa et al. (2014) conducted extensive taxonomic study on *Pleosporales* by utilizing ITS, LSU, SSU and *β-tubulin* loci. Based on the molecular evidence provided by that study authors synonymized *Montagnulaceae* under *Didymosphaeriaceae*, providing priority to the older taxon name. Genus *Kalmusia* characterized by sexual morphs that produce globose to subglobose or laterally flattened, coriaceous black ascomata without papilla. They are observed to be loosely aggregated and immersed to erumpent in host tissue. Septate, filliform, delicate, branching and anastomosing pseudoparaphyses produces dense Hamathecium. bitunicate, clavate asci with a long, furcate pedicel bear eight, ovoid to clavate, 3-distoseptate, light brown ascospores in each ascus. Asexual morphs in genus *Kalmusia* are not observed (Ariyawansa et al., 2014). The host range of this genus include plants reside under family Poaceae. As example *Kalmusia orysopsidis* was isolated from *Oryzopsis miliacea* stems in Portugal (Karunarathna et al., 2022). Understanding of proper taxonomic placement of genus *Kalmusia* demand the utilization of ITS, LSU, SSU and *β-tubulin* loci based multigene phylogeny and morphological investigations. That emphasis the importance of those loci to obtain robust view in to evolutionarily relationships between members in the genus *Kalmusia* and family *Didymosphaeriaceae*.

Type species: ***Kalmusia ebuli*** Niessl

Other accepted species: see Species Fungorum, search *Kalmusia* for names

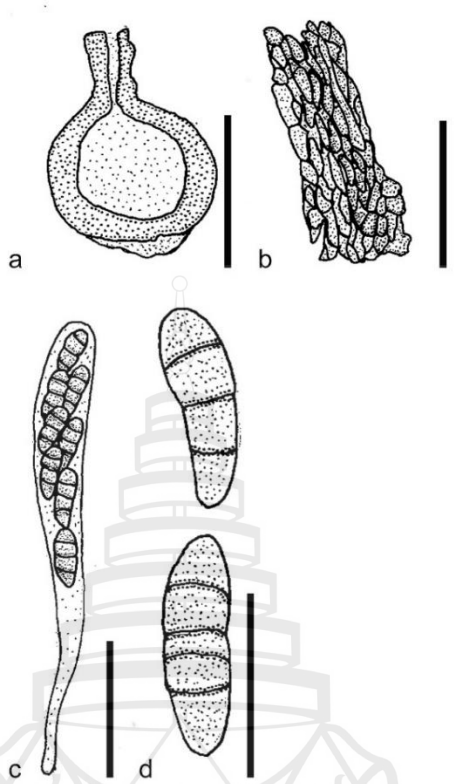

Note (a) Horizontal section of immersed ascomata; (b) Part of the peridium; (c) Ascus; (d) Ascospores. Scale bars: (a) 0.5 mm; (b-c) 20 µm; (d) 10 µm.

Source Redrawn from Zhang et al. (2014)

Figure 3.24 *Kalmusia ebuli* (neotype)

Paraconiothyrium Verkely

Citation when using this entry: Amuhenage et al., in prep – Fungalpedia, grass and wetland fungi.

Index Fungorum, Faceoffungi, MycoBank, GenBank, Figure 3.25

Classification: *Didymosphaeriaceae*, *Pleosporales*, *Pleosporomycetidae*, *Dothideomycetes*, *Pezizomycotina*, *Ascomycota*, Fungi

Paraconiothyrium is a polyphyletic genus introduced by Verkley in 2004 and typified to *Paraconiothyrium estuarinum* (Verkley et al., 2004; Wijayawardene et al., 2022; Hyde et al., 2024). The genus was erected to accommodate four *Coniothyrium*-like anamorphic isolates that showcase biological control and potential bioremediation properties. Maximum parsimony analysis incorporating ITS sequences supported the establishment of the genus *Paraconiothyrium*. This genus characterized by scattered or

loosely aggregated, dark brown to black, unilocular, pycnidial conidiomata that comprise from a peridium that process multiple layers of thick-walled pigmented cells of *textura angularis*. Conidiogenous cells that resides inside the conidiomata are hyaline, smooth, subcylindrical or ampulliform, discrete to integrated, phialidic or occasionally percurrent. Conidia are hyaline when immature and turn sub-hyaline to light brown at maturity, ellipsoidal to cylindrical, aseptate or 1-septate, smooth-walled, or minutely warted at maturity (Verkley et al., 2004; Xiong et al., 2024). Members of the genus *Paraconiothyrium* are mainly saprobic and were isolated from variety of substrates including soil, decomposing leaf litter and decomposing wood. As examples *Paraconiothyrium thysanolaenae* were reported from *Thysanolaena maxima* in Thailand (Karunarathna et al., 2022) and *Paraconiothyrium guangdongensis* was isolated from genus *Arecaceae* in Guangzhou, China (Xiong et al., 2024). Xiong et al. (2024) conducted the most recent phylogenetic analysis to the genus, and they utilized LSU, ITS, SSU, *rpb2* and *tef 1-α* sequences. That emphasis the importance of those loci in phylogenetic analysis and new species declaration to genus *Paraconiothyrium*.

Type species: ***Paraconiothyrium estuarinum*** Verkley

Other accepted species: see Species Fungorum, search *Paraconiothyrium* for names.

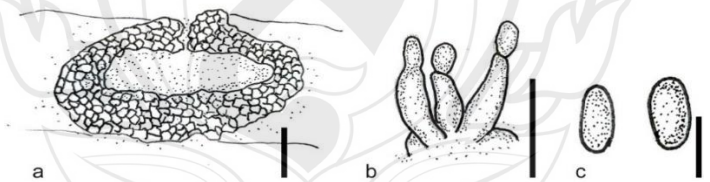

Note (a) Cross section of the conidiomata; (b) Peridium; (c) Conidiogenous cells; (d) Conidia. Scale bars: (a) 100 µm; (b-c) 10 µm; (d) 5 µm.

Source Drawn from Xiong et al. (2024)

Figure 3.25 *Paraconiothyrium guangdongensis* (MHZU 22-0176, Holotype)

Family ***Hysteriaceae***

Graphyllium Clem

Citation when using this entry: Amuhenage et al., in prep – Fungalpedia, grass and wetland fungi.

Index Fungorum, Faceoffungi, MycoBank, GenBank, Figure 3.26

Classification: *Hysteriaceae*, *Pleosporales*, *Pleosporomycetidae*, *Dothideomycetes*, *Pezizomycotina*, *Ascomycota*, Fungi

Genus *Graphyllium* was proposed by Clem in 1901 to accommodate *Pleospora chloes* and typified to *Graphyllium chloes* (Wijayawardene et al., 2022; Hyde et al., 2024). Initially genus *Graphyllium* was placed under *Diademosa*. Extensive study conducted on *Diademaceae* by Ariyawansa et al. (2014) transferred genus *Graphyllium* to family *Hysteriaceae* considering presence of hysterothecium-like ascomata with a longitudinal opening. Members of the genus form coriaceous, glabrous, black hysteriform like ascomata with central, longitudinal ostiolar opening. Often semi-immersed to immersed and arranged in rows on host tissue (Zhang et al., 2011). Several layers of thick-walled, pigmented cells in *textura angularis* compose the peridium. Innermost layer of the peridium showcase flatter cells than peripheral layers. Pseudoparaphyses are absent and asci originate from hyaline basal pseudoparenchyma layer in the ascomata (Zhang et al., 2011). Asci bear eight ascospores in each ascus. They are bitunicate, clavate or cylindrical with short stalks. Ascospores are brown to dark brown, applanate and muriform, showcase 3-4 transverse septa and 1-2 longitudinal septa (Zhang et al., 2011). Members of genus *Graphyllium* show cosmopolitan distribution and found saprobic on both dicotyledonous and monocotyledonous plant materials. As example *Graphyllium panduratum* was isolated from *Chusquea subtessellata* in Costa Rica (Karunarathna et al., 2022). Majority of the species under genus *Graphyllium* lack molecular data. Fresh collections and utilization of multigene phylogeny is required to obtain clear view to phylogenetic placement of the genus.

Type species: ***Graphyllium chloes*** Clem

Other accepted species: see Species Fungorum, search *Graphyllium* for names.

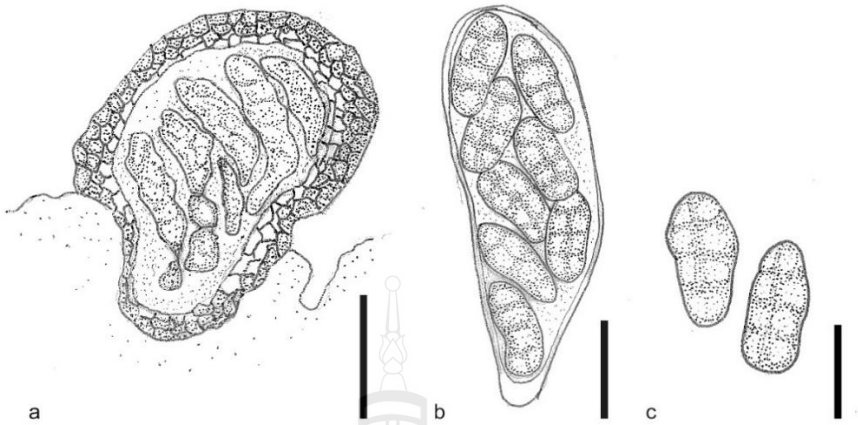

Note (a) Horizontal section of ascomata; (b) Ascus; (c) Ascospores. Scale bars: (a) 50 µm; (b-c) 20 µm.

Source Redrawn from Zhang et al. (2011)

Figure 3.26 *Graphyllium chloes* (NEB 158190, Lectotype)

Family ***Lindgomycetaceae***

Lolia Abdel-Aziz & Abdel-Wahab

Citation when using this entry: Amuhenage et al., in prep – Fungalpedia, grass and wetland fungi.

Index Fungorum, Faceoffungi, MycoBank, GenBank, Figure 3.27

Classification: *Incertae sedis, Incertae sedis, Incertae sedis, Incertae sedis, Pezizomycotina, Ascomycota*, Fungi

This mono phyletic genus was initially introduced as a monotypic genus by Abdel-Aziz & Abdel-Wahab in 2011. They described the asexual morph of type species *Lolia aquatica* from decayed stem of *Phragmites australis* found in an irrigation canals of the River Nile, Egypt (Abdel-Aziz & Abdel-Wahab, 2011). Sexual morph of *Lolia aquatica* and second species of the genus, *Lolia dictyospora* was introduced by Abdel-Aziz in 2016 from decayed submerged wood from Nile River. Authors used morphological and multigene phylogenetic evidence (SSU and LSU) for the classification and taxonomic placement of those isolates (Abdel-Aziz, 2016).Those findings made sexual asexual morph connection between *Lolia aquatica,* and *Lolia dictyospora* was introduced as a sexual morph. Asexual morph of genus Lolia produces acervular, superficial, loosely aggregated conidiomata on host tissue. Conidiomata wall

containing cells in *textura intricate*. Conidiophores arise from innermost layer. They are hyaline, smooth, branched and septate. Conidiogenus cells sub-cylindrical and hyaline, each bearing one conidium from apex. Single celled conidia are hyaline, thin walled and clavate. Conidia bear three to five apical appendages and one basal appendage (Abdel-Aziz & Abdel-Wahab, 2011). *Lolia aquatica* produces globose to subglobose ascomata that immersed in host tissue. They are observed to be loosely aggregated. Ascomata are black or dark brown, coriaceous in nature, produces an ostiole (Abdel-Aziz, 2016).Peridium containing two leyers. Outer layer consists with hic pigmented cells in *textura angularis* and inner layer consist with hyaline tin walled polygonal cells. Pseudoparaphyses in genus *Lolia* are hyaline, septate and branched. They protect bitunicate, cylindric to clavate and pedicellated asci that bear eight ascospores in each ascus. Ascospores fusiform, yellowish brown, showcase four to six septa and constricted at each septum. They process rounded ends, the third cells from the tip is enlarged. Ascospores consist with ornamented surfaces and surrounded by gelatinous sheath (Abdel-Aziz, 2016). Genus *Lolia* is known only from Egypt and new isolated from the same region or from throughout the world in necessary to understand the species diversity, worldwide distribution, higher classification and evolution of the genus.

Type species ***Lolia aquatica*** Abdel-Aziz & Abdel-Wahab

Other accepted species: *Lolia dictyospora* Abdel-Aziz, 2016

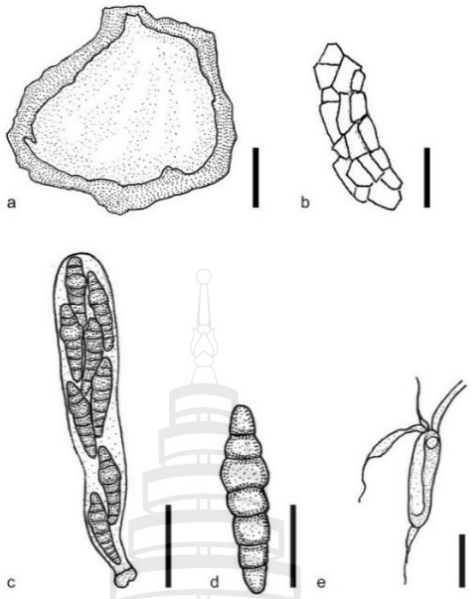

Note (a) Vertical section of ascomata; (b) Peridium; (c) Ascus; (d) Ascospore; (e) Conidia from asexual morph. Scale bars: (a) 100 µm; (b-c) 10 µm; (d-e) 5 µm.

Source Redrawn from Abdel-Aziz (2016)

Figure 3.27 *Lolia aquatica* (CBS H-22130, holotype)

Family ***Pleosporaceae***

Clathrospora Rabenh

Citation when using this entry: Amuhenage et al., in prep – Fungalpedia, grass and wetland fungi.

Index Fungorum, Faceoffungi, MycoBank, GenBank, Figure 3.28

Classification: *Pleosporaceae*, *Pleosporales*, *Pleosporomycetidae*, *Dothideomycetes*, *Pezizomycotina*, *Ascomycota*, Fungi

Clathrospora is a polyphyletic genus introduced by Rabenh in 1857 and typified to *Clathrospora elynae* (Wijayawardene et al., 2022; Hyde et al., 2024). Originally the genus was placed under family *Diademaceae* but based on the multilocus phylogenetic evidences the genus was excluded from *Diademaceae* and transferred to *Pleosporaceae*. Members of the genus characterized by semi immersed to scattered, brown to black, subglobose or globose ascomata with circular lid- like opening at central sunken ostiole. Peridium process 3-4 layers of thick walled pigmeneted cells in *textura angularis* where inner cell layers are fatter than other cell layers.

Pseudoparaphyses are longer than the asci, dance, hyaline, and filiform. Asci are bitunicate, fissitunicate, cylindrical or clavate. They are compized with short pedicles at the base and shallow ocular chambers at the tips (Ariyawansa et al., 2014). Asci bear eight fusiform 7-transseptate, brown muriform ascospores with numerous longitudinal septa and hyaline thin mucilaginous sheath. *Clathrospora* process 36 morphological specie and only *C. elynae* (CBS 196.54) and *C. diplospora* (IMI 68086) process molecular data. The members of the genus known as both pathogenic and saprobic organisms on variety of host species and showcase worldwide distribution (Ariyawansa et al., 2014). As an example, *Clathrospora bakeri* was reported from *Juncus* sp. in Colorado, USA (Karunarathna et al., 2022). The phylogenetic studies conducted with Clathrospora was utilized ITS, LSU, SSU and *rpb2* loci in the investigations, emphasizing the impotent of those loci in studies related to genus *Clathrospora* (Ariyawansa et al., 2014). Fresh collections and in-depth phylogenetic analysis with more representatives from the genus are recommended.

Type species: ***Clathrospora elynae*** Rabenh

Other accepted species: see Species Fungorum, search *Clathrospora* for names.

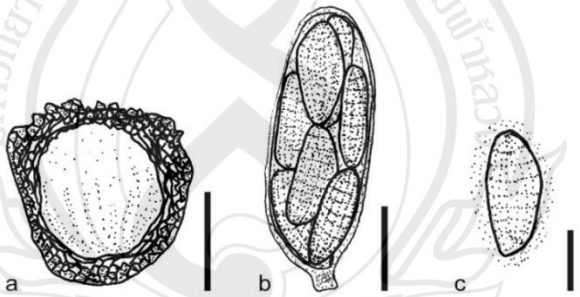

Note (a) Cross section of ascomata; (b)Ascus; (c) Ascospore. Scale bars: (a) 10 µm; (b) 60 µm; (c) 30 µm.

Source Redrawn from Ariyawansa et al. (2014)

Figure 3.28 *Clathrospora elynae* (Isotype)

Pyrenophora Fr

Citation when using this entry: Amuhenage et al., in prep – Fungalpedia, grass and wetland fungi.

Index Fungorum, Faceoffungi, MycoBank, GenBank, Figure 3.29

Classification: *Pleosporaceae*, *Pleosporales*, *Pleosporomycetidae*, *Dothideomycetes*, *Pezizomycotina*, *Ascomycota*, Fungi

Pyrenophora is a species rich genus, introduced by Fr in 1849 and typified to *Pyrenophora phaeocomes* (Wijayawardene et al., 2022; Hyde et al., 2024). Members include both sexual and asexual morphs. Sexual morphs are characterized by globose to subglobose, uniostilulate ascomata that appear immersed, erumpent or superficial on host tissue. This genus lacks pseudoparaphyses and asci are bitunicate, fissitunicate, clavate to sub-cylindrical with large epical ring in well-developed ocular chamber. Each ascus process eight hyaline, smooth walled muriform, ascospaores which are constricted at the septum (Dokhanchi et al., 2022). Asexual morphs of the genus *Pyrenophora* are hyphomycetous. They produce macronematous, mononematous, straight or flexuous, unbranched, and brown conidiophores. They bear polytretic, integrated, terminal, sympodial, and cylindrical conidiogenous cells, that give rice to acropleurogenous, simple, straight or curved, clavate, cylindrical. Smooth, brown septate conidia (Dokhanchi et al., 2022). Members of the genus are known mainly as plant pathogens and showcase worldwide distribution and isolated from both aquatic and terrestrial habitats (Dokhanchi et al., 2022). As an examples *Pyrenophora bondarzewii* was isolated from *Triticum* sp. in Ukraine, and *Pyrenophora japonica* was reported from *Secale cereal* in USA (Karunarathna et al., 2022). *Pyrenophora* comprise with more than 100 morphologically know species and 16 species with molecular data. ITS, LSU, SSU, *tef1-α*, and *rpb2* loci were used in many species' delineations and that emphasis the importance of those loci to obtain clear view in to the evolutionary relationships among *Pyrenophora* species (Dokhanchi et al., 2022).

Type species: ***Pyrenophora phaeocomes*** Fr

Other accepted species: see Species Fungorum, search *Pyrenophora* for names

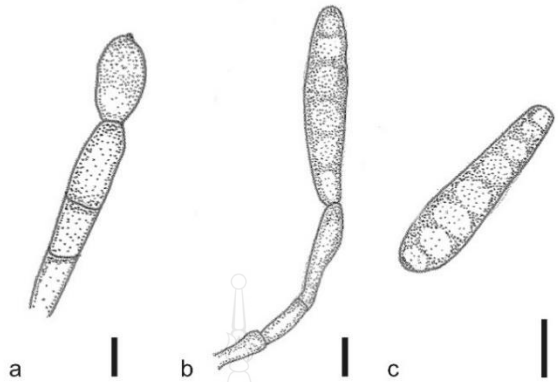

Note (a-b) Conidiophores with conidia; (c) Conidiam. Scale bars: (a-c) 10 µm.
Source Redrawn from Dokhanchi et al. (2022)

Figure 3.29 *Pyrenophora semeniperda*

Family ***Pseudodidymellaceae***

Petrakia Syd. & P. Syd

Citation when using this entry: Amuhenage et al., in prep – Fungalpedia, grass and wetland fungi.

IndexFungorum; Faceoffungi; Mycobank; Genbank; Figure 3.30

Classification: *Pseudodidymellaceae*, *Pleosporales*, *Pleosporomycetidae*, *Dothideomycetes*, *Pezizomycotina*, Ascomycota, Fungi

Petrakia is a mono-phyletic genus that belongs to the family *Melanommataceae*, in *Dothideomycetes* (Wijayawardene et al., 2022; Hyde et al., 2024). Genus *Petrakia* was introduced by Sydow and Sydow in 1913 and typified by *Petrakia echinata*. The anamorph of *Petrakia paracochinensis* was found saprobic on Miscanthus *floridulus* (family Poaceae) on Hong Kong Island, providing evidences to the association of genus *Petrakia* with grasses. (Wong et al., 2002). Sexual morph of genus *Petrakia* produces black, epiphyllous ascomata that appear solitary and partly immersed in host leaves. Each fruiting body produces one ostiole, peridium pseudoparenchymatous and hamathecium process pseudoparaphyses. Those pseudoparaphyses are hyaline and septate. Asci hold eight spores and they are cylindrical, bitunicate and fissitunicate. Ascospores are biseriately arranged, fusoid with submedian primary euseptum. Spores can be straight to slightly curved and tapering towards the apexes. Mature spores can be hyaline to light brown (Jaklitsch et

al., 2017). Asexual morph produces sporodochial conidiomata with macronematous, short, branched or straight and septate conidiophores. Conidiogenous cells are terminal and conidiogenesis happen in holoblastic manner. Hyaline or brown conidia are multicellular They show variety of shapes such as irregularly subglobose, fusoid and falcate (Jaklitsch et al., 2017). Phylogenetic revision of the genus *Petrakia* in 2020, have used LSU, ITS, *RPB2*, and *TEF1* multigene phycology to obtain proper phylogenetic segregation among the members associated with genus *Petrakia*. That indicated LSU, ITS, *RPB2*, and *TEF1* loci can produces in-depth phylogenetic information about the genus *Peratika* (Beenken et al., 2020).

Type species ***Petrakia echinata*** (Peglion) Syd. & P. Syd

Other accepted species: see Species Fungorum, search *Petrakia* for names.

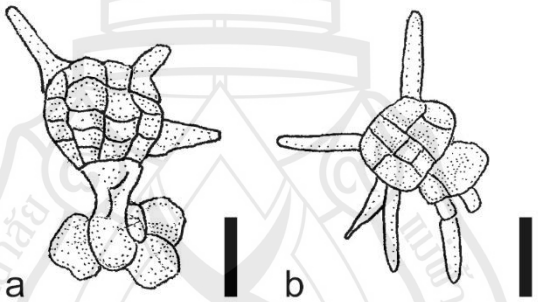

Note (a) Developing conidia with conidiogenus cell; (b) Conidia. Scale bars: (a-b) 20 μm.

Source Redrawn from Wong et al. (2002)

Figure 3.30 *Petrakia echinata* (holotype)

Order ***Venturiales***

Family ***Venturiaceae***

Arkoola Walker & Stovold

Citation when using this entry: Amuhenage et al., in prep – Fungalpedia, grass and wetland fungi.

Index Fungorum, Faceoffungi, MycoBank, GenBank, Figure 3.31

Classification: *Venturiaceae*, *Venturiales*, *Pleosporomycetidae*, *Dothideomycetes*, *Pezizomycotina*, *Ascomycota*, Fungi

Genus *Arkoola* was introduced by Walker & Stovold in 1986 (Wijayawardene et al., 2022; Hyde et al., 2024) from leaf blight of soybean in New South Wales. This monotypic taxon typified to only known species called *Arkoola nigra* (Walker & Stovold, 1986). The main life mode of genus *Arkoola* is phytopathogenic but reported from both and alive dead soybean leaves (Walker & Stovold, 1986). Host range of *Arkoola* nigra extends beyond the soybean plants. As example it was isolated from *Glycine max* leaves in New South Wales (Karunarathna et al., 2022). *Arkoola* develops subglobose, broadly ovoid to obpyriform, dark *Pseudothecia* that superficial or erurnpent on dead tissue material of infected plants. Predominantly covered from dark, septate, thick-walled superficial mycelium. Multi layered Peridium composed with several black to brown cells in *textura angularis*. Hyaline, cellular and filiform Pseudoparaphyses protects bitunicate with fissitunicate, cylindrical or sub cylindrical, short stipitate asci with eight ascospores. Ascospores are ellipsoidal to fusiform, light greenish, 1-septate, slightly constricted at septum and contain thin gelatinous sheath (Walker & Stovold, 1986). Molecular data for the genus *Arkoola* is not available and other members apart from type species are yet to be discovered. According to that new collections are required to understand proper taxonomic placement, and ecological role of the genus.

Type species: ***Arkoola nigra*** Walker & Stovold

Other accepted species: N/A

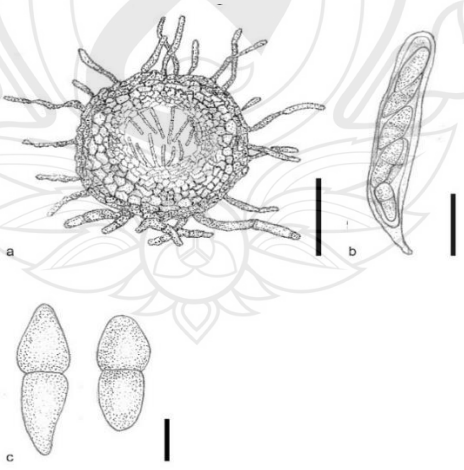

Note (a) Horizontal section of ascomata; (b) Ascus; (c) Ascospores. Scale bars: (a) 200 µm; (b-c) 20 µm.

Source Redrawn from Walker and Stovold (1986)

Figure 3.31 *Arkoola nigra* ((DAR 43446)

Class *Saccharomycetes*

Sub-Class *Saccharomycetidae*

Order *Saccharomycetales*

Family *Incertae sedis*

Nakazawaea Y. Yamada, K. Maeda & Mikata

Citation when using this entry: Amuhenage et al., in prep – Fungalpedia, grass and wetland fungi.

Index Fungorum, Faceoffungi, MycoBank, GenBank, Figure 3.32

Classification: *Incertae sedis*, *Saccharomycetales*, *Saccharomycetidae*, *Saccharomycetes*, *Saccharomycotina*, Ascomycota, Fungi

Nakazawaea was first proposed by Y. Yamada, K. Maeda & Mikata in 1994 (Wijayawardene et al., 2022; Hyde et al., 2024) to transfer *Pichia holstii* to a new genus (Yamada et al., 1994). This heterothallic and haploid genus typified to *Nakazawaea holstii* and considered as ascomycetous yeast (Polburee et al., 2017). This transfer was conducted by following the molecular evidence based on D1/D2 region of the large subunit (LSU) and the small subunit (SSU) rRNA genes of *Pichia holstii* (Polburee et al., 2017). Later researchers supported the proposed genus by using protein cording loci such as actin (*ACT1*), the RNA polymerase largest subunit (*RPB1*), second largest subunit (*RPB2*), and second subunit of the mitochondrial cytochrome oxidase (*COX2*) in phylogenetic analysis (Polburee et al., 2017). Genus *Nakazawaea* bear around 15 species which include 10 taxa transferred from genus Candida (Polburee et al., 2017). The most resend addition was *Nakazawaea siamensis* on *Saccharum* sp from Thailand (Karunarathna et al., 2022). Members in this genus produces globose, ellipsoid, ovoid or rarely cylindrical cells. They are arranged in mucoid colonies (Yamada et al., 1994). Pseudomycelium are observed and cells demonstrate multilateral budding. Cell conjugation develop asci that bear 2 to 4 pileiform ascospores (Yamada et al., 1994). More collections from different habitats including different host substrates are important to obtain solid idea about the distribution of this genus in the world.

Type species: ***Nakazawaea holstii*** (Wick.) Y. Yamada, K. Maeda & Mikata

Other accepted species: see Species Fungorum, search *Nakazawaea* for names.

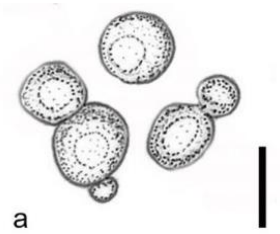

Note (a) Budding cells. Scale bars: (a) 10 µm.

Source Redrawn from Kaewwichian and Limtong (2014)

Figure 3.32 *Nakazawaea siamensis*

Class *Sordariomycetes*

Sub-Class *Diaporthomycetidae*

Order *Annulatascales*

Family *Annulatascaceae*

Annulatascus K. D. Hyde

Citation when using this entry: Amuhenage et al., in prep – Fungalpedia, grass and wetland fungi.

Index Fungorum, Faceoffungi, MycoBank, GenBank, Figure 3.33

Classification: *Annulatascaceae*, *Annulatascales*, *Diaporthomycetidae*, *Sordariomycetes*, *Pezizomycotina*, *Ascomycota*, Fungi

Annulatascus is a polyphyletic genus introduced by K. D. Hyde in 1992 to accommodate *A. velatispora* and *A. bipolaris*. Genus isolated with freshwater habitats and typified to *Annulatascus velatispora* (Dayarathne et al., 2016; Wijayawardene et al., 2022; Hyde et al., 2024). Phylogenetic revision of the *Annulatascus* demanded an epitypication. Based on molecular and phylogenetic evidence Dayarathne et al. (2016) introduced an epitype from submerged wood in a river, at Millaa Falls, north Queensland, Australia. Genus characterized by scattered to gregariously arranged, black, coriaceous ascomata, with erumpent, black, ellipsoidal, centric or lateral ostiole. Peridium composed with multiple layers of cells in *textura angularis* where peripheral cells are wider and pigments, while cells close to the ascomatal cavity turns hyaline. Genus *Annulatascus* process hypha-like, septate, Paraphyses which get narrow towards the apex (Hu et al., 2013; Dayarathne et al., 2016; Dong et al., 2021). Asci are unitunicate, cylindrical, apex truncate and exhibit well developed reflective apical ring.

They process long pedicelles and each ascus bear eight fusiform, straight to slightly curved, aseptate, hyaline, smooth, thin-walled ascospores which are arranged in uniseriate manner. Ascospores are minutely guttulate and process irregular mucilaginous sheath (Hu et al., 2013; Dayarathne et al., 2016; Dong et al., 2021). *Annulatascus* was collected mainly from Southeast Asia, China and Australia (Hu et al., 2013; Dayarathne et al., 2016). Majority of the isolations originated from submerged wood, but *Annulatascus hongkongensis* was isolated from Bamboo in Hong Kong and *Annulatascus liputii* was reported from Bamboo in Philippines (Karunarathna et al., 2022). Recent introductions to the genus were done by Dong et al. (2021) and they utilized LSU, ITS *tef* and *rpb2* loci in the phylogenetic analysis. Based on that those loci are critical to identify the correct phylogenetic placement of members in *Annulatascus*. Majority of the members in the genus *Annulatascus* do not process molecular data. Thus, new collections and investigations based on multilocus phylogeny is required to obtain clear view to the *Annulatascus*.

Type species: ***Annulatascus velatispora*** K. D. Hyde

Other accepted species: see Species Fungorum, search *Annulatascus* for names.

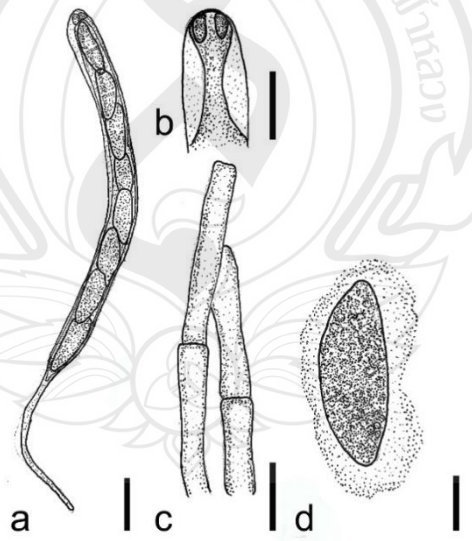

Note (a) Ascus; (b) Apical ring of the ascus; (c) Paraphyses; (c) Ascospore. Scale bars: (a) 200 µm; (b-d) 5 µm.

Source Redrawn from Hu et al. (2013)

Figure 3.33 *Annulatascus velatispora* (Holotype)

Order *Diaporthales*

Family *Gnomoniaceae*

Mamianiella Höhn

Citation when using this entry: Amuhenage et al., in prep – Fungalpedia, grass and wetland fungi.

Index Fungorum, Faceoffungi, MycoBank, GenBank, Figure 3.34

Classification: Gnomoniaceae, Diaporthales, Diaporthomycetidae, *Sordariomycetes*, *Pezizomycotina*, *Ascomycota*, Fungi

Mamianiella was purposed by Höhn in 1917 and typified to *Mamianiella coryli* (Wijayawardene et al., 2022; Hyde et al., 2024). This genus characterized by dark brown to black, immersed to erumpent, globose to subglobose, perithecial ascomata, compoased with a central, papillate ostiole, and preridium containing thick walled cells in *textura angularis* (Morgan-Jones, 1981; Senanayake et al., 2018). Asci in genus are unitunicate, cylindrical to clavate and develop prominent apical rings at the apexes. Each ascus bears eight hyaline, smooth-walled, 1-septate, ellipsoidal to fusiform asospores (Senanayake et al., 2018). Members of the genus *Mamianiella* are known as saprobic organisms and opportunistic pathogens. The distribution is limited to the Germany and Japan, and the host range include members under plant family Poales (Senanayake et al., 2018). As an example, *Mamianiella yukawana* was reported from *Sasa hirtella* in Japan (Karunarathna et al., 2022). *Mamianiella* contain only two morphologically known species and one strain with molecular data. The limited molecular data result the taxonomic placement of the gens is debatable (Senanayake et al., 2018). More fresh collections are recommended.

Type species: ***Mamianiella coryli*** (Batsch) Höhn.

Other accepted species:

Mamianiella yukawana (I. Hino & Katum.) M. Monod

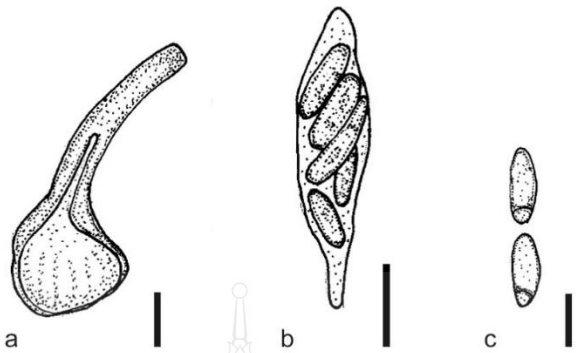

Note (a) Ascomata cross section; (b) Ascus; (c) Ascospores. Scale bars: (a) 100 µm; (b) 20 µm; (c) 5 µm.

Source Redrawn from Senanayake et al. (2018)

Figure 3.34 *Mamianiella coryli* (F144462, F144463)

Order *Distoseptisporales*

Family *Distoseptisporaceae*

Distoseptispora K.D. Hyde, McKenzie & Maharachch

Citation when using this entry: Amuhenage et al., in prep – Fungalpedia, grass and wetland fungi.

Index Fungorum, Faceoffungi, MycoBank, GenBank, Figure 3.35

Classification: *Distoseptisporaceae*, *Distoseptisporales*, *Incertae sedis*, *Sordariomycetes*, *Pezizomycotina*, *Ascomycota*, Fungi

Distoseptispora is a monophyletic genus, introduced by K.D. Hyde, McKenzie & Maharachch in 2016, and typified to *Distoseptispora fluminicola* (Wijayawardene et al., 2022; Hyde et al., 2024). The majority of *Distoseptispora* species are asexual, and characterized by macronematous, mononematous, solitary, or fasciculate conidiophores that bear blastic, terminal, mainly cylindrical conidiogenous cells. These conidiogenous cells produce obclavate, ellipsoidal, obovoid, or fusiform, euseptate, distoseptate, or rarely muriform conidia (Xia et al., 2017; Karimi et al., 2024). *Distoseptispora* is a large genus with 94 morphologically know species and 51 species with molecular data. Members of the genus Distoseptispora are saprobic organisms, showcase worldwide distribution predominantly found in aquatic environments (Xia et al., 2017; Karimi et al., 2024). The host range of the *Distoseptispora* cover both monocotyledonous and dicotyledonous plants. As an example, *Distoseptispora martinii* was reported from

Carex elata in Poland (Karunarathna et al., 2022). Recently Karimi et al. (2024) introduced three new species to the genus and they utilized ITS, LSU, *rpb2* and *tef1-α* loci in their investigation, emphasizing the importance of using those loci to delineate species in *Distoseptispora*.

Type species: ***Distoseptispora fluminicola*** K.D. Hyde, McKenzie & Maharachch

Other accepted species: see Species Fungorum, search *Distoseptispora* for names.

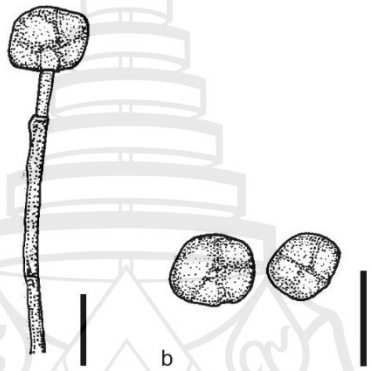

Note (a) Conidiophore with attached conidia; (b) Conidia. Scale bars: (a-b) 20 µm.
Source Redrawn from Xia et al. (2017)

Figure 3.35 *Distoseptispora martini*

Sub-Class *Hypocreomycetidae*

Order *Amphisphaeriales*

Family *Bartaliniaceae*

Truncatella Steyaert

Citation when using this entry: Amuhenage et al., in prep – Fungalpedia, grass and wetland fungi.

Index Fungorum, Faceoffungi, MycoBank, GenBank, Figure 3.36

Classification: *Bartaliniaceae*, *Amphisphaeriales*, *Xylariomycetidae*, *Sordariomycetes*, *Pezizomycotina*, *Ascomycota*, Fungi

Genus *Truncatella* is a polyphyletic genus introduced by Steyaert in 1949 and typified to *Truncatella truncate* (Wijayawardene et al., 2022; Hyde et al., 2024). Members of this genus are mainly anamorph, known pathogens and saprobes in both

dicotyledons and monocotyledons plants. They show worldwide distribution reported from terrestrial and aquatic habitats. As example *Truncatella angustata* was isolated from leaf spots on *Olea europaea* in Iran and saprobic on *Triticum* sp (Arzanlou et al., 2012; Karunarathna et al., 2022). *Truncatella* form scatted or loosely aggregated dark conidiomata which are immersed or semi-immersed in host tissue. Conidiomata wall composed from small *textura angularis*, cells with thick walls. Conidiophores are smooth, hyaline, erect, sparsely septate, and unbranched to irregularly branched. Conidiogenous cells hyaline, smooth, terminal, discrete or integrated, lageniform to cylindrical, holoblastic, and showcase percurrent enteroblastic proliferations by replacement wall-building apices (Andrianova, 2014). Conidia that originate form genus *Truncatella* are 3-sepatae, fusiform, slightly curved, thick-walled, bearing appendages. The basal cell obconic, hyaline, process a truncate base, both central cells are doliiform, with unequal lengths and pigmented. Apical cell hyaline, conical, smooth, process 2-3, irregularly or dichotomously branched, filiform, flexuous apical appendage (Andrianova, 2014). Perera et al. (2018) examined *Truncatella*-like coelomycete isolates and they used ITS, LSU and SSU loci for the phylogenetic analysis. According to that it is critical to use those loci for species identification in *Truncatella*. Fresh collections and utilizing protein cording loci in phylogenetic analysis for genus *Truncatella* are recommended to obtain robust view to the evolutionary placement of the genus.

Type species: ***Truncatella truncate*** Steyaert

Other accepted species: see Species Fungorum, search *Truncatella* for names.

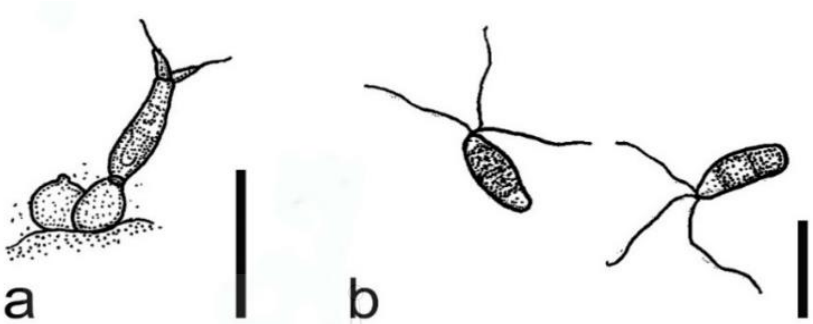

Note (a) Conidiophores with developing conidia; (b) Conidia. Scale bars: (a-b) 20 µm.
Source Redrawn from Andrianova (2014)

Figure 3.36 *Truncatella angustata*

Order *Hypocreales*

Family *Nectriaceae*

Hydropisphaera Dumort

Citation when using this entry: Amuhenage et al., in prep – Fungalpedia, grass and wetland fungi.

Index Fungorum, Faceoffungi, MycoBank, GenBank, Figure 3.37

Classification: *Nectriaceae*, *Hypocreales*, *Hypocreomycetidae*, *Sordariomycetes*, *Pezizomycotina*, *Ascomycota*, Fungi

Hydropisphaera is a polyphyletic genus introduced by Dumort in 1822 and typified to *Hydropisphaera peziza* (Wijayawardene et al., 2022; Hyde et al., 2024). Genus show affinity towards genus *Nectria* and process nectria-like sexual morphs, but certain characteristics make *Hydropisphaera* distinct from *Nectria* (Hou et al., 2023). Genus *Hydropisphaera* characterized by perithecial or cleistothecial, light yellow to orange, globose, subglobose or doliiform ascomata that appear superficial on host tissue. Ascomata can de deeply cupulate, smooth or process fasciculate hairs, process negative results or no color change with both KOH and lactic acid. Peridium comprise with two layers, where outer layer processes thin-walled, globose cells. Asci are clavate and each ascus holds eight hyaline, 1-septate or occasionally multiseptated, coarsely striate, smooth or spinulose ascospores Hou et al. (2023). Asexual morphs of the genus *Hydropisphaera* were accommodated into several genera including *Cephalosporium* and *Gliomastix* (Hou et al., 2023). Members of this genus are mainly saprobic

organisms that inhabit wide range or geographical regions and host types. As example *Hydropisphaera bambusicola* was isolated from Bamboo in Martinique (Lechat et al., 2010), West Indies, and *Hydropisphaera sinensis* was collected from unknown grass (Poaceae) in Guangdong, China (Karunarathna et al., 2022). Multilocus phylogenetic study conducted by Hou et al. (2023) utilized ITS, LSU, *rpb2* and *tef-1α* loci in their analysis. The result indicated the genus *Hydropisphaera* separate into eight different clades and differ from each other with phylogenetic and morphological characters. According to that more collections and in-depth phylogenetic analysis are recommended to obtain robust view into the genus *Hydropisphaera*.

Type species: ***Hydropisphaera peziza*** Dumort

Other accepted species: see Species Fungorum, search *Hydropisphaera* for names.

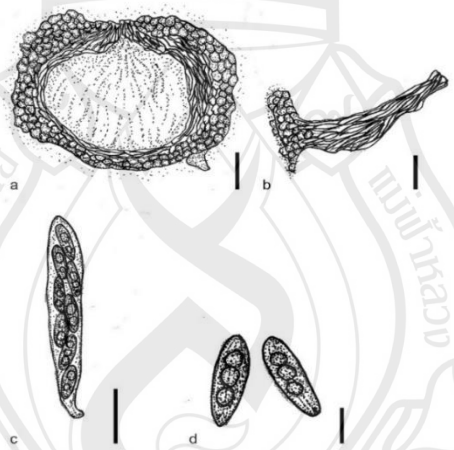

Note (a) Ascomata; (b) Fasciculate hairs; (c) Ascus; (d) Ascospores. Scale bars: (a) 50 µm; (b-c) 20 µm; (d) 10 µm.

Source Redrawn from Lechat et al. (2010)

Figure 3.37 *Hydropisphaera bambusicola* (Holotype)

Order *Pleurotheciales*

Family *Pleurotheciaceae*

Rhexoacrodictys W.A. Baker & Morgan-Jones

Citation when using this entry: Amuhenage et al., in prep – Fungalpedia, grass and wetland fungi.

Index Fungorum, Faceoffungi, MycoBank, GenBank, Figure 3.38

Classification: *Pleurotheciaceae*, *Pleurotheciales*, *Hypocreomycetidae*, *Sordariomycetes*, *Pezizomycotina*, *Ascomycota*, Fungi

Genus *Rhexoacrodictys* was introduced by W.A. Baker & Morgan-Jones in 2002 to accommodate *Rhexoacrodictys erecta* as the type species (Wijayawardene et al., 2022; Hyde et al., 2024).This monophyletic, anamorphic genus characterized by the production of mononematous conidiophores that erect from thy mycelium, and each conidiophore bear terminal, percurrent individual conidiogenous cell (Bao et al., 2023). Conidiogenesis happen holoblastic and separation is rhexolytic. and conidia are highly muriform, pigmented at maturity, acrogenous, ellipsoidal or obovoid, thick and smooth-walled (Bao et al., 2023) .Genus *Rhexoacrodictys* inhabit wide host rage, cosmopolitan distribution and mainly saprobic in life style (Bao et al., 2023) .As example *Rhexoacrodictys erecta* was isolated from *Bambusa multiplex* in USA and *Rhexoacrodictys fimicola* was found saprobic on *Dendrocalamus* in Hong Kong (Karunarathna et al., 2022). Boonmee et al. (2021) placed the genus under *Savoryellaceae*, but latter Luo et al. (2018) used more taxa in phylogenetic analysis and transferred genus *Rhexoacrodictys* to *Pleurotheciaceae* with good statistic support. Most recent species was added to the genus by Bao et al. (2023) as *Rhexoacrodictys melanospora*, isolated from decaying wood in Yunnan, China. They have utilized SSU, ITS, LSU, and *rpb2* loci in the phylogenetic analysis (Bao et al., 2023). That indicate the requirement of those loci to obtain robust view in to phylogenetic placement of genus *Rhexoacrodictys*.

Type species: ***Rhexoacrodictys erecta*** (Ellis & Everh.) W.A. Baker & Morgan-Jones

Other accepted species: see Species Fungorum, search *Rhexoacrodictys* for names.

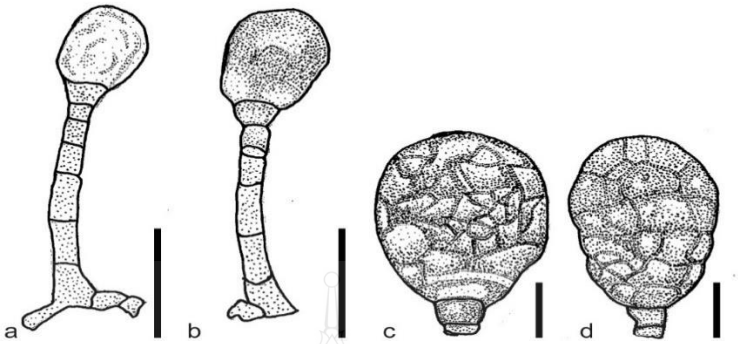

Note (a-b) Conidiophores with conidia; (c-d) Conidia. Scale bars: (a-b) 20 μm; (c-d) 10 μm.

Source Redrawn from Bao et al. (2023)

Figure 3.38 *Rhexoacrodictys melanospora* (HKAS 124580, holotype)

Sub-Class *Incertae sedis*

Order *Incertae sedis*

Family *Halosphaeriaceae*

Pileomyces K.L. Pang & J.S. Jheng

Citation when using this entry: Amuhenage et al., in prep – Fungalpedia, grass and wetland fungi.

Index Fungorum, Faceoffungi, MycoBank, GenBank, Figure 3.39

Classification: *Halosphaeriaceae*, *Incertae sedis*, *Incertae sedis*, *Sordariomycetes*, *Pezizomycotina*, *Ascomycota*, Fungi

Pileomyces is a monotypic genus, introduced by K.L. Pang & J.S. Jheng in 2012 (Wijayawardene et al., 2022; Hyde et al., 2024), from decomposing bamboo stem in coast of Taiwan, China (Karunarathna et al., 2022). This genus in known only from a sexual morph and characterized by erumpent, pyriform with globose to subglobose, black ascomata with short ostiole. The peridium composed with single layer of dark, thick-walled cells. Asci in genus *Pileomyces* are unitunicate, broadly clavate, short pedunculated with thickened apexes. Each ascus bears eight, hyaline, smooth, thin-walled, ellipsoidal ascospores with prominent appendage covering the end of the ascospore. The appendage dislodges with the spore dispersal (Pang & Jheng, 2012).

Type species: ***Pileomyces formosanus*** K.L. Pang & J.S. Jheng

Other accepted species: N/A

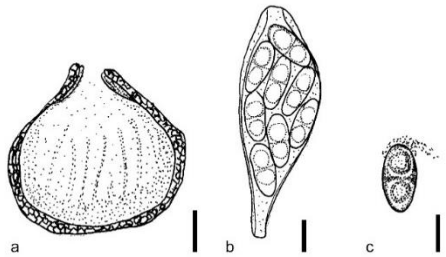

Note (a) Ascomata cross section; (b) Ascus; (c) Ascospore. Scale bars: (a) 50 µm; (b-c) 10 µm.

Source Redrawn from Pang and Jheng (2012)

Figure 3.39 *Pileomyces formosanus*

Order *Junewangiaceae*

Family *Junewangia*

Junewangia Baker & Morgan-Jones

Citation when using this entry: Amuhenage et al., in prep – Fungalpedia, grass and wetland fungi.

Index Fungorum, Faceoffungi, MycoBank, GenBank, Figure 3.40

Classification: *Junewangia*, *Junewangiaceae*, *Incertae sedis*, *Sordariomycetes*, *Pezizomycotina*, *Ascomycota*, Fungi

Junewangia is a monophyletic genus, introduced by W.A. Baker & Morgan-Jones in 2002, and typified to *Junewangia sphaerospora* (Wijayawardene et al., 2022; Hyde et al., 2024). This hyphomycetes genus characterized by dark brown, effuse colonies on the substrate with partly superficial to immersed mycelia. Conidiophores that develop by genus *Junewangia* are erect, brown at the base, hyaline towards the apexes, smooth, thick –walled, straight or flexuous, cylindrical and unbranched. Those conidiophores develop brown to pale brown or subhyaline, smooth to verrucose, monoblastic, integrated, terminal, cylindricala, and collarette conidiogenous cells (Zhao et al., 2011; Xia et al., 2017). Conidia arise in the genus *Junewangia* are brown to dark brown, smooth, oval, ellipsoidal to spherical. *Junewangia* process 9 morphologically known species and 5 species with molecular data. Members of this genus show case saprobic lifestyle and distribution concentrated to Asia (Zhao et al., 2011; Xia et al., 2017). The host range of Junewangia includes plants under order Polaes. As an example *Junewangia globulosa* was isolated from *Bambusa* sp. in Hong

Kong (Karunarathna et al., 2022). *Junewangia* shear morphological resemblances to *Acrodictys*, but conspicuous, cuneiform or funnel- shaped basal cells in Acrodictys made both genera distinguishable. Initially *Junewangia* was placed under *Incertae sedis*, and Xia et al. (2017) introduced *Junewangiaceae* to accommodate genus *Junewangia*. They utilized ITS, LSU, SSU and *tub2* sequences in their analysis (Xia et al., 2017). That indicate the importance of using those loci for species delineation in *Junewangia*.

Type species: ***Junewangia sphaerospora*** W.A. Baker & Morgan-Jones

Other accepted species:

Junewangia aquatica H.Y. Song & D.M. Hu

Junewangia globulosa (Tóth) W.A. Baker & Morgan-Jones

Junewangia guangxiensis W.P. Wang & Z.L. Luo

Junewangia lamma (Whitton, McKenzie & K.D. Hyde) W.A. Baker & Morgan-Jones

Junewangia obliqua (M.B. Ellis) W.A. Baker & Morgan-Jones

Junewangia queenslandica (Matsush.) J.W. Xia & X.G. Zhang

Junewangia synnematica W.P. Wang & Z.L. Luo

Junewangia thailandica W. Dong, H. Zhang & K.D. Hyde

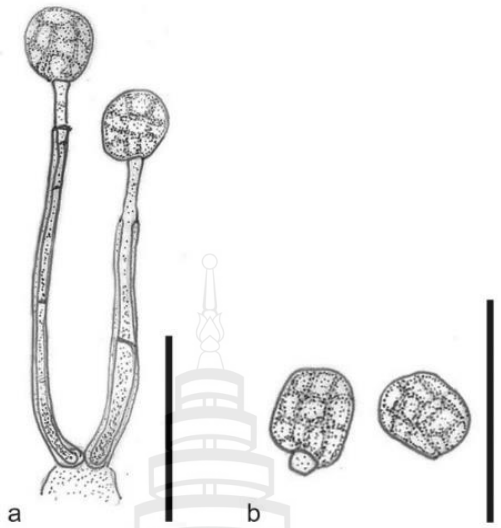

Note (a) Conidiophores with conidia; (b) Conidia. Scale bars: (a-b) 50 µm.

Source Redrawn from Zhao et al. (2011)

Figure 3.40 *Junewangia globulosa* (HSAUP992154)

Order *Chaetosphaeriales*

Family *Australiascaceae*

Codinaea Maire

Citation when using this entry: Amuhenage et al., in prep – Fungalpedia, grass and wetland fungi.

Index Fungorum, Faceoffungi, MycoBank, GenBank, Figure 3.41

Classification: *Chaetosphaeriaceae*, *Chaetosphaeriales*, *Sordariomycetidae*, *Sordariomycetes*, *Pezizomycotina*, *Ascomycota*, Fungi

Genus *Codinaea* was proposed by Maire 1937 and typified to *Codinaea aristate* (Wijayawardene et al., 2022; Hyde et al., 2024,). Based on the currant molecular and morphological studies the genus bears 14 accepted species with diverse morphology (Wu & Diao, 2022). Members of the genus *Codinaea* are characterized by dark brown to black, hairy colonies with aggregated setae and conidiophores. Setae are single, thick-walled, erect, straight, or flexuous, septate, dark brown to black, process a single terminal phialide or several lateral openings. Conidiophores are single macronematous, mononematous, originate from fascicles, erect, straight, or flexuous, undulate, unbranched, or branched, smooth, septate, dark brown at the base and hyaline to light

brown at the tips, end with a phialide or with a sterile setiform extension (Wu & Diao, 2022). Conidiogenous cells that available with conidiophores are, funnel shaped, mono- or polyphialidic, integrated, terminal, or discrete are showcase percurrent or sympodial proliferation. Conidia belongs to genus *Codinaea* are mainly hyaline, falcate, lunate, or oblong-falcate, ellipsoid to ellipsoid-fusiform or broadly oblong, vermiform, with a straight or gently curved setula at each end. Some species generate conidia that are globose to pyriform with setulae distributed over the surface aseptate (Wu & Diao, 2022).

Type species: ***Codinaea aristate*** Maire

Other accepted species: see Species Fungorum, search *Codinaea* for names.

Note (a-b) Conidiophores and conidiogenous cells with funnel-shaped collarettes; (c) Conidia. Scale bars: (a-c) 5 μm.

Source Redrawn from Wu and Diao (2022)

Figure 3.41 *Codinaeella brevissima* (Wu17241, Holotype)

Dendrophoma Sacc

Citation when using this entry: Amuhenage et al., in prep – Fungalpedia, grass and wetland fungi.

Index Fungorum, Faceoffungi, MycoBank, GenBank, Figure 3.42

Classification: *Chaetosphaeriaceae*, *Chaetosphaeriales*, *Sordariomycetidae*, *Sordariomycetes*, *Pezizomycotina*, *Ascomycota*, Fungi

Genus *Dendrophoma* was introduced by Sacc in 1880 by typifying to *Dendrophoma cytisporoides*. This accommodation was done by synonymizing *Phoma cytisporoides* Sacc genus *Dendrophoma* (Wijayawardene et al., 2022; Hyde et al., 2024). Morphological comparison conducted between genus *Dinemasporium* and

Dendrophoma lead scientist to synonymized *Dendrophoma* to genus *Dinemasporium* (Réblová et al., 2020).In depth phylogenetic study conducted by Crous et al. (2012) using LSU and ITS loci indicated genus *Dendrophoma* form a separate lineage from genus D*inemasporium*, under *Chaetosphaeriaceae*. Thus, the genus *Dendrophoma* re-established as a monophyletic taxon. Until 2020, Members of genus *Dendrophoma* was known only with their asexual morphs. Sexual morph and asexual morph connection for this genus was first proposed by Réblová et al. (2020).Ascomata of genus *Dendrophoma* are loosely aggregate or arraigned dense caespitose clusters on host. They are perithecial, dark brown to black, to broadly conical, glabrous, papillate, normally immersed and turn erumpent at maturity. Ascomata process one periphysate ostiole (Réblová et al., 2020). Peridum carbonaceous, and composed with outer layer containing brown thick walled cells in *textura prismatica* and inner layers featuring thin-walled, hyaline, flattened cells in *textura prismatica* (Réblová et al., 2020). Paraphyses are septate and anastomosing. Asci conatin eight ascospaores in each ascus, long in the sporiferous section, unitunicate, cylindrical or cylindrical-clavate, apically broad and rounded with an indistinct, non-amyloid apical annulus (Réblová et al., 2020). Ascospores are arranged in uniseriate manner. They are fusiform, hyaline, mono septate and not constricted at the septum (Réblová et al., 2020). Conidiomata of genus *Dendrophoma* are stromatic, stipitate, setose and discrete or integrated from distribution. They bear lageniform to subcylindrical conidiogenous cells that generate naviculate to botuliform hyaline conidia with unbranched cellular appendage at both terminals (Réblová et al., 2020). Although many members of this genus found on woody subtracts, they are recorded as pathogens and on monocotyledonous plants as well. As example *Dendrophoma petrakii* was isolated from *Phragmites communis* in Portugal (Karunarathna et al., 2022). More fresh collections and more investigations based on molecular phylogeny is required to obtain proper understanding towards the phylogenetic relationships among the members of the genus.

Type species: ***Dendrophoma cytisporoides*** (Sacc.) Sacc

Other accepted species: see Species Fungorum, search *Dendrophoma* for names

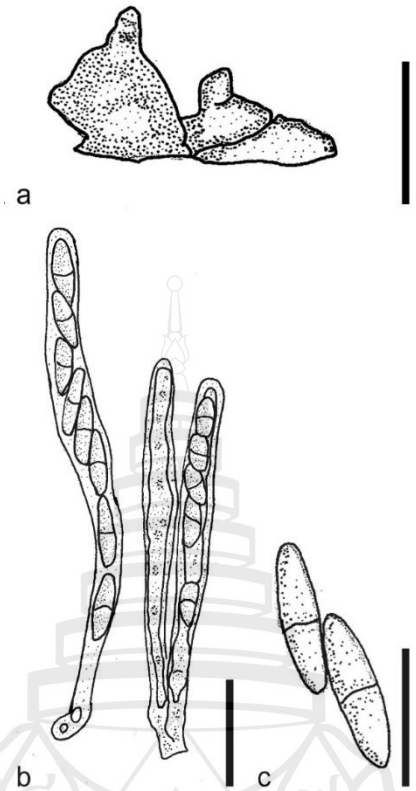

Note (a) Ascomata on host; (b) Asci; (c) Ascospores. Scale bars: (a) 20 µm; (b-c) 5 µm.
Source Redrawn from Réblová et al. (2020)

Figure 3.42 *Dendrophoma cytisporoides* (CBS 144107)

Family *Linocarpaceae*

Linocarpon Syd. & P. Syd

Citation when using this entry: Amuhenage et al., in prep – Fungalpedia, grass and wetland fungi.

Index Fungorum, Faceoffungi, MycoBank, GenBank, Figure 3.43

Classification: *Linocarpaceae*, *Chaetosphaeriales, Sordariomycetidae*, *Sordariomycetes*, *Pezizomycotina*, *Ascomycota*, Fungi

Genus *Linocarpon* was first proposed by Syd. & P. Syd in 1917 and typified to *Linocarpon pandani* (Wijayawardene et al., 2022; Hyde et al., 2024). Originally *Linocarpon* was placed under family *Chaetosphaeriaceae*. Morphological and multilocus phylogenetic investigations conducted by Konta et al. (2017) observed the members of genus *Linocarpon* form a sister clade distinct to *Chaetosphaeriaceae*. Based on those evidence they erected a new family *Linocarpaceae* to accommodate

genus *Linocarpon*. Sexual morph characterized by solitary, superficial, black, dome-shaped, subglobose, ascomata with flattened at the base and central ostiole. Peridium composed with multiple layers. The outer cells at the margin merge with the host epidermal cells and composed with dark brown to black cells of *textura angularis*. Hamathecium contain hyaline, septate paraphyses with are longer than asci which process wider bases, tapering towards the apexes (Konta et al., 2017). Paraphyses protects cylindrical to unitunicate, asci with rounded tips, with a small non amyloid apical ring. Asci develops from the base and periphery of the ascomata and each ascus bear eight ascospores. Ascospores in genus *Linocarpon* are hyaline, appear yellowish when clustered, filiform, arranged parallelly or spiral in the ascus, ends rounded, inflated, appendage or acute, containing numerous refringent septum-like bands (Konta et al., 2017). Appendages at the end of *Linocarpon* ascospores enable to distinguish *Linocarpon* from closely related *Neolinocarpon*. Asexual morphs tant observed in *Linocarpon* were similar in morphology to genus *Phialophora* (Konta et al., 2017). Members of this genus reported as saprobes on both monocotyledon and dicotyledon plant materials and show worldwide distribution. As an example, *Linocarpon stipae* was isolated from *Stipa* sp. in South Australia (Karunarathna et al., 2022) and *Linocarpon bambusinum* was found on Bamboo, Yunnan, China (Zhang et al., 2023). Zhang et al. (2023) added the most recent species to the genus as *Linocarpon bambusinum* and the utilized ITS, LSU and *tef1-α* for their phylogenetic analysis. According to that morphology and multilocus phylogeny are important to obtain robust view to genus *Linocarpon*.

Type species: ***Linocarpon pandani*** Syd. & P. Syd

Other accepted species: see Species Fungorum, search *Linocarpon* for names.

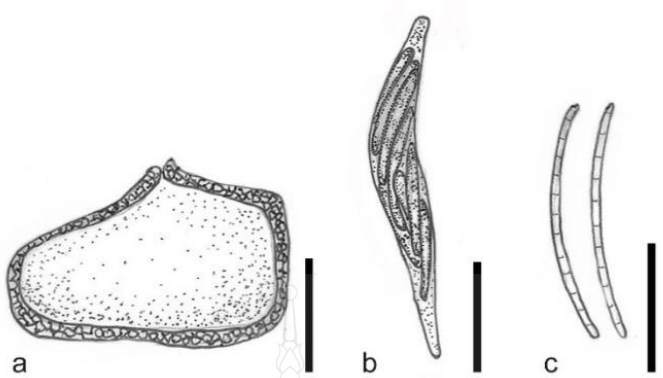

Note (a) Ascomata cross section; (b) Ascus; (c) Ascospores. Scale bars: (a) 200 µm; (b) 20 µm; (c) 50 µm.

Source Redrawn from Zhang et al. (2023)

Figure 3.43 *Linocarpon bambusina* (GMB1360, holotype)

Order *Magnaporthales*

Family *Ceratosphaeriaceae*

Ceratosphaeria Niessl

Citation when using this entry: Amuhenage et al., in prep – Fungalpedia, grass and wetland fungi.

Index Fungorum, Faceoffungi, MycoBank, GenBank, Figure 3.44

Classification: *Ceratosphaeriaceae, Magnaporthales*, *Sordariomycetidae*, *Sordariomycetes*, *Pezizomycotina*, *Ascomycota*, Fungi

Ceratosphaeria was erected by Niessl in 1876, and typified to *Ceratosphaeria lampadophora* (Wijayawardene et al., 2022; Hyde et al., 2024). *Ceratosphaeria* process both sexual and asexual life stages in the genus. The sexual morphs are characterized by brown to back, immersed to erumpent, globose to pyriform, aggregated perithecial ascomata with central and long rostrum, and multi-layered, peridium composed from *textura prismatica* cells (Huhndorf et al., 2008; Yang et al., 2023). Paraphyses are hyaline, smooth, filiform, unbranched, moniliform at the base, narrowing towered the apexes and longer than asci. Asci in *Ceratosphaeria* are unitunicate, clavate, inoperculate, apically conical to rounded short pedicelate an amyloid. Each ascus process 8 hyaline, smooth, thin-walled, fusoid, slightly curved, transversely septate ascospore that are tapering towards the ends. Asexual morphs develop hyaline, septate,

branched conidiophores or they are reduced to pale brown to sub-hyaline, smooth, subcylindrical, terminal, and collarette conidiogenous cells. Conidia that develop in genus *Ceratosphaeria* are hyaline, smooth, fusoid with obtuse, aseptate, and aggregated in mucoid masses (Huhndorf et al., 2008; Yang et al., 2023). Members of the genus exhibit worldwide distribution, and known as saprobic organisms win divers types of plant including members under order Poales. As an example, *Ceratosphaeria phyllostachydis* was isolated from *Phyllostachys edulis* in Lehaie, China (Karunarathna et al., 2022). *Ceratosphaeria* process 29 morphologically known species and only 6 species with molecular data (Yang et al., 2023). The most recent species to genus was added by Yang et al. (2023) as *Ceratosphaeria flava* from China. They utilized ITS, LSU, SSU, *rpb2* and *tef1-α* sequences in their analysis indicating the importance of those loci in species delineation in genus *Ceratosphaeria*.

Type species: ***Ceratosphaeria lampadophora*** (Berk. & Broome) Niessl 1876

Other accepted species: see Species Fungorum, search *Ceratosphaeria* for names.

Note (a) Ascomata cross section; (b) Ascus; (c) Ascospores. Scale bars: (a) 100 µm; (b-c) 10 µm.

Source Redrawn from Huhndorf et al. (2008)

Figure 3.44 *Ceratosphaeria lampadophora*

Family *Magnaporthaceae*

Deightoniella Hughes

Citation when using this entry: Amuhenage et al., in prep – Fungalpedia, grass and wetland fungi.

Index Fungorum, Faceoffungi, MycoBank, GenBank, Figure 3.45

Classification: *Magnaporthaceae*, *Magnaporthales, Sordariomycetidae, Sordariomycetes*, *Pezizomycotina*, *Ascomycota*, Fungi

Deightoniella was proposed by Hughes in 1952 to accommodate two species including *D. africana* as the type and *D. arundinacea* (Wijayawardene et al., 2022; Hyde et al., 2024). Members of the genus are known as plant pathogenic hypomycetees. They are characterized by brown, smooth solitary, erect conidiophores, which are broader at the base and hyaline towards the apexes. Conidiophores produce circular scar at the host and showcase swellings along the axis (Klaubauf et al., 2014). Conidiogenous cells are terminal, integrated with truncate and flattened scar. Conidia that originate are pale brown, 1-septate, thin-walled, ellipsoid to pyriform, guttulate to granular, finely verruculose, bluntly to acutely rounded at apex and obtusely at the base (Klaubauf et al., 2014). *Deightoniella* show worldwide distribution and show affinity towered wide variety of plants. As example *Deightoniella Africana* was isolated from *Imperato cylindrical* in Togo, Africa, *Deightoniella bhopalensi* on *Arthraxon lancifolius* in India and *Deightoniella fimbristylidis* found on *Fimbristylis miliacea* in Taiwan, China (Karunarathna et al., 2022). The genus process 15 morphological delineated species and Klaubauf et al. (2014) provided sequence data for *Deightoniella roumeguerei*. They utilized ITS, LSU, *rpb1*, *act* and *cal* loci for the investigation. *D. roumeguerei* clade sister to *Macgarvieomyces borealis* and established the phylogenetic placement in *Magnaporthaceae*. Fresh collections and in-depth phylogenetic analysis utilizing both morphology and multilocus phylogeny are recommended to obtain robust view to genus *Deightoniella*.

Type species: ***Deightoniella africana*** Hughes

Other accepted species: see Species Fungorum, search *Deightoniella* for names.

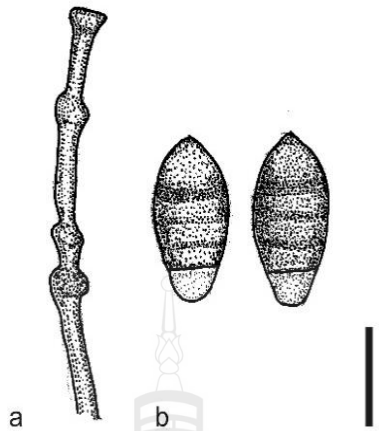

Note (a-b) Conidiophores with conidia; Scale bars: (a-b) 10 µm.

Source Redrawn from Barbosa et al. (2007)

Figure 3.45 *Deightoniella rugose*

Order *Phyllachorales*

Family *Incertae sedis*

Cyclodomus Höhn

Citation when using this entry: Amuhenage et al., in prep – Fungalpedia, grass and wetland fungi.

Index Fungorum, Faceoffungi, MycoBank, GenBank, Figure 3.46

Classification: *Incertae sedis*, *Phyllachorales*, *Sordariomycetidae*, *Sordariomycetes*, *Pezizomycotina*, *Ascomycota*, Fungi

Genus *Cyclodomus* introduced by Höhn in 1909.This mono phyletic genus resides in *Incertae sedis*, *Phyllachorales*, *Sordariomycetidae*, *Sordariomycetes* and typified to *Cyclodomus umbellulariae* (Wijayawardene et al., 2022; Hyde et al., 2024). This genus produces stromatic and pycnidial shaped dark conidiomata. They are loosely clustered or scatted on host tissue. Conidiomata are glabrous, immersed and multilocular. Outer layer of conidiomata wall consist from thick-walled cells of *textura angularis* and interior process thick-walled cells of *textura globosa* (Li et al., 2020). Conidiophores are reduced to enteroblastic, cylindrical, smooth walled and hyaline Conidiogenous cells. They are loosely aggregated on inner layer of the conidiomata wall. Conidia are hyaline, unicellular, subcylindrical in shape. They process blunt, rounded apex and slightly pointed base (Li et al., 2020). *Cyclodomus aequatoriensis*

was introduced to the genus by Hyde et al., 1996. Subcylindrical conidia formation and multilocular conidiomata in genus *Cyclodomus* were not observed in this new isolate. It produced unilocular conidiomata. Considering those morphological differences *Cyclodomus aequatoriensis* later excluded from the genus (Li et al., 2020). Use of multigene phylogeny with introduction of epitypes are necessary to get in depth view to taxonomic placement of genus *Cyclodomus*.

Type species ***Cyclodomus umbellulariae*** Höhn.

Other accepted species: see Species Fungorum, search *Cyclodomus* for names.

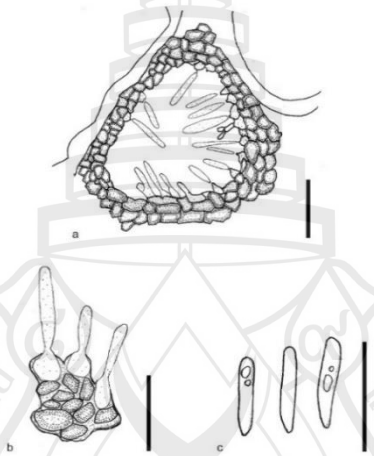

Note (a) Vertical section of conidioma; (b) conidiogenous cells with developing conidia; (c) Conidia. Scale bars: (a) 50 µm; (b-c) 20 µm.

Source Redrawn from Li et al. (2020)

Figure 3.46 *Cyclodomus umbellulariae* (holotype)

Order *Sordariales*

Family *Beltraniaceae*

Beltrania Penz

Citation when using this entry: Amuhenage et al., in prep – Fungalpedia, grass and wetland fungi.

Index Fungorum, Faceoffungi, MycoBank, GenBank, Figure 3.47

Classification: *Beltraniaceae*, *Sordariales*, *Sordariomycetidae*, *Sordariomycetes*, *Pezizomycotina*, *Ascomycota*, Fungi

Beltrania is a monophyletic genus under family *Beltraniaceae* in *Sordariales* (Wijayawardene et al., 2022; Hyde et al., 2024). The genus was proposed by Penz in 1882 and typified to *Beltrania rhombica*. Members under *Beltrania* are hyphomycetes and currently contain 30 entries in index Fungorum. They include 19 morphological species and 11 species with molecular data (Lin et al., 2017). *Beltrania* characterized by processing unbranched, septate, infertile setae with lobed basal cells, straight, hyaline to subhyaline conidiophores that originate from separate radially lobed basal cells at the base. Those conidiophores bear sympodial, denticulate conidiogenous cells at the apexes and connected with swollen separating cells. Conidia in genus *Beltrania* are hyaline to sub hyaline, biconic, spicate or apiculate with transverse band at the center and with or without apical appendage (Lin et al., 2017). Members of the genus showcase wide distribution. Majority of the isolates were found from Asia and Europe. They are known saprobes and inhabit submerged wood in aquatic environments, decomposing woody materials, leaf litter of both monocotyledonous and dicotyledonous plants (Lin et al., 2017). As example *Beltrania eremochloae* was introduced from *Eremochloa ciliaris* in China (Karunarathna et al., 2022). Species identification of the genus *Beltrania* requires morphological examination and multigene phylogenetic approaches utilizing at least ITS and LSU loci (Lin et al., 2017). More fresh collections and using protein coding loci are recommended to obtain clear in depth understanding of the genus.

Type species: ***Beltrania rhombica*** Penz

Other accepted species: see Species Fungorum, search *Beltrania* for names.

Note (a) Setae and conidiophores; (b) Conidiophores with connecting cells (c) Conidiam. Scale bars: (a-c) 20 µm.

Figure 3.47 *Beltrania pseudorhombica* (TB146)

Sub-Class *Xylariomycetidae*

Order *Amphisphaeriales*

Family *Apiosporaceae*

Apiospora Sacc

Citation when using this entry: Amuhenage et al., in prep – Fungalpedia, grass and wetland fungi.

Index Fungorum, Faceoffungi, MycoBank, GenBank, Figure 3.48

Classification: *Apiosporaceae*, *Amphisphaeriales*, *Xylariomycetidae*, *Sordariomycetes*, *Pezizomycotina*, *Ascomycota*, Fungi

Apiospora is a monophyletic genus that introduced by Sacc 1845 and typified by *Apiospora montagnei* (Wijayawardene et al., 2022; Hyde et al., 2024). The genus comprises with both sexual and asexual stages. Sexual morphs are characterized by

perithecial, ascomata that aggregated in to immersed or erumpent to superficial, elongated stromata. Asci in the genus *Apiospora* are unitunicate, clavate, with a rounded apex. Each ascus bears eight hyaline, smooth-walled, asscospores containing well developed gelatinous sheath (Manawasinghe et al., 2025). *Apiospora* develop asexual morphs characterized by, smooth-walled, hyaline to pale brown or brown, globose to ellipsoid conidiogenous cells, giving rice to lenticular conidia with a paler equatorial slit. Members of the genus *Apiospora* showcase cosmopolitan distribution, mainly reported as saprobic organisms and occasionally isolated as endophyte or opportunistic pathogens (Manawasinghe et al., 2025). There are significant number of *Apiospora* species were removed from host order Poales. *Apiospora bambusigena*, isolated from Bamboo was one of the most recent species added to the genus. Authors utilized ITS, LSU, *tef1-α*, and *tub2* sequences in their analysis, indicating the importance of using those loci for species delineation in the genus (Li et al., 2024).

Type species: ***Apiospora montagnei*** Sacc

Other accepted species: see Species Fungorum, search *Apiospora* for names.

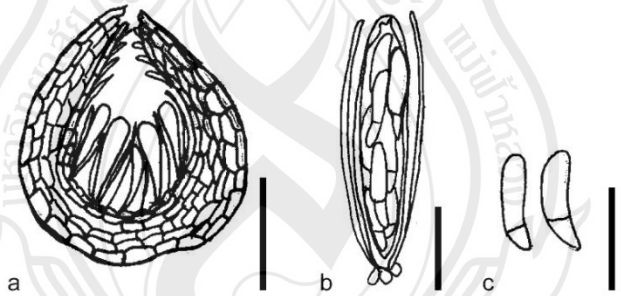

Note (a) Ascomata cross section; (b) Ascus with Paraphyses; (c) Ascospores. Scale bars: (a) 40 µm; (b-c) 10 µm.

Source Redrawn from Müller EMIL (1992)

Figure 3.48 *Apiospora deschampsiae*

Order *Xylariales*

Family *Cainiaceae*

Arecophila KD Hyde

Citation when using this entry: Amuhenage et al., in prep – Fungalpedia, grass and wetland fungi.

Index Fungorum, Faceoffungi, MycoBank, GenBank, Figure 3.49

Classification: *Cainiaceae*, *Xylariales*, *Xylariomycetidae, Sordariomycetes*, *Pezizomycotina*, *Ascomycota*, Fungi

Genus *Arecophila* was introduced by K.D. Hyde in 1996 to accommodate five species in *Xylariales* (*Sordariomycetes*) and typified to *Arecophila gulubiicola* (Wijayawardene et al., 2022; Hyde et al., 2024). Members of the genus characterized by sub-globose or lenticular ascomata that mostly immersed in host tissue, with peridium composed by dark cells in *textura angularis* and poorly developed clypeus. Asci are unitunicate, cylindrical, and bear wedge-shaped, J+ apical ring. Each ascus holds eight, 2-celled, brown ascospores with striations and mucilaginous sheath (Li et al., 2022). Initially genus *Arecophila* was introduced under *Amphisphaeriaceae*. Multigene phylogenetic studies utilizing LSU and ITS loci indicated that the genus *Arecophila* resides under *Cainiaceae*, *Xylariales* (Li et al., 2022). Members under *Arecophila* saprobic organisms on decomposing plat materials. They exhibit worldwide distribution and affinity towards monocotyledonous host materials (Li et al., 2022). As examples *Arecophila bambusae* was isolated on Bamboo in Philippines, *Arecophila muroiana* found saprobic on *Phyllostachys bambusoides var. marliacea* in Japan and *Arecophila striatispora* isolated from *Pseudosasa japonica* in France (Karunarathna et al., 2022). Index fungorum mention 21 entries under genus *Arecophila* but only four species process molecular data. According to that fresh collection and phylogenetic analysis beast on multilocus phylogeny are recommended to obtain robust view into the genus.

Type species: ***Arecophila gulubiicola*** KD Hyde

Other accepted species: see Species Fungorum, search *Arecophila* for names.

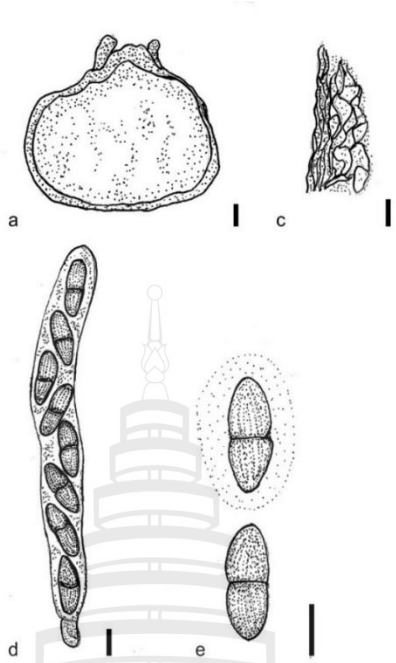

Note (a) Ascomata cross section; (b) Peridium; (c) Ascus; (d) Ascospores. Scale bars: (a) 50 µm; (b-d) 5 µm.

Source Redrawn from Li et al. (2022)

Figure 3.49 *Arecophila australis* (Holotype)

Atrotorquata Kohlm. & Volkm. -Kohlm

Citation when using this entry: Amuhenage et al., in prep – Fungalpedia, grass and wetland fungi.

Index Fungorum, Faceoffungi, MycoBank, GenBank, Figure 3.50

Classification: *Cainiaceae*, *Xylariales*, *Xylariomycetidae, Sordariomycetes*, *Pezizomycotina*, *Ascomycota*, Fungi

Atrotorquata is a monotypic genus introduced by Kohlmeyer and Volkmann-Kohlmeyer in 1993 and typified to *Atrotorquata lineata* (Liu et al., 2015; Wijayawardene et al., 2022; Hyde et al., 2024).This genus characterized by the ascomata that appear immersed below the clypeus, unitunicate, cylindrical J+ asci that bear brown, two-celled, ascospores which showcase 5–7 longitudinal striations at each apex and conspicuous mucilaginous sheath (Liu et al., 2015). Molecular data for the initial collection of *Atrotorquata lineata* are not publicly available. The second species of the genus *Atrotorquata spartii*, was introduced by Thambug in 2015 from *Spartium junceum*, Italy.

Multiclocus phylogenetic analysis conducted on that species indicated that genus *Atrotorquata* clade sister to *Monographella nivalis* (UPSC 3273) under *Cainiaceae*, thus verify the currant phylogenetic placement of the genus (Liu et al., 2015). *Atrotorquata* was isolated only from Italy as *Atrotorquata spartii* (Liu et al., 2015) and *Atrotorquata lineata* on *Juncus roemerianus* in North Carolina USA (Karunarathna et al., 2022). More collections and in depts phylogenetic analysis utilizing multilocus phylogeny are required to obtain clear view into the genus and understand correct evolutionary relationship of genus *Atrotorquata* to other related members.

Type species: ***Atrotorquata lineata*** Kohlm. & Volkm. -Kohlm

Other accepted species: *Atrotorquata spartii* Thambug (2015)

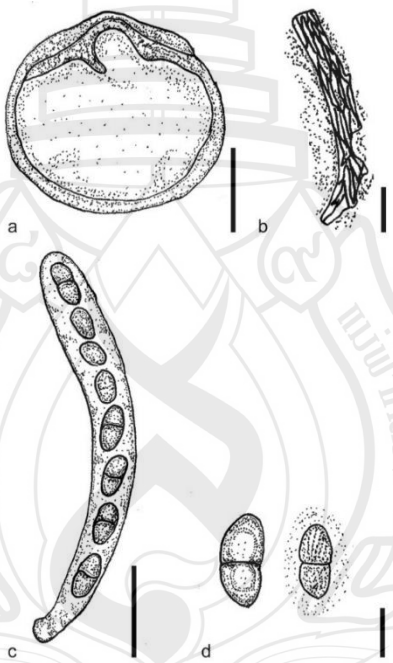

Note (a) Ascomata cross section; (b) Peridium; (c) Ascus; (d) Ascospores. Scale bars: (a) 150 µm; (b) 20 µm; (c-d) 10 µm.

Source Redrawn from Liu et al. (2015)

Figure 3.50 *Atrotorquata spartii* (Holotype)

Family *Zygosporiaceae*

Zygosporium Montin

Citation when using this entry: Amuhenage et al., in prep – Fungalpedia, grass and wetland fungi.

IndexFungorum; Facesoffungi; MycoBank; GenBank; Figure 3.51

Classification: *Zygosporiaceae*, *Xylariales*, *Xylariomycetidae*, *Sordariomycetes, Pezizomycotina Ascomycota*, Fungi

Genus *Zygosporium* was first introduced by Montin 1842 by typifying to *Zygosporium oscheoides*. (Wijayawardene et al., 2022; Hyde et al., 2024). Previously this genus was known to resides under family *Microdochiaceae*. After extensive multigene phylogenetic investigations and morphological identification genus *Zygosporium* now placed in family *Zygosporiaceae* under *Xylariales*, *Sordariomycetes* (Li et al., 2017). Members of this genus have been reported to be saprobes on monocotyledonous host species including *Cortaderia selloana* (Karunarathna et al., 2022). Colonies appear as dark ash to black color patches on the host tissue. Genus *Zygosporium* process to types of conidiophores. Setiform conidiophores are mostly pigmented with hyaline epical cell. They are narrowly clavate. Vesicular conidiophores erect from the sides of setiform conidiophores. They are brown in color and consists of two or three septa. Unicellular conidia of Genus *Zygosporium* are hyaline, smooth walled, spherical to ellipsoidal in shape (Taheriyan et al., 2014). Multigene phylogenetic analysis conducted for this genus utilized ITS, LSU, *actA* and *tbu2* loci (Crous et al., 2018). That indicates those gene regions are required to provide detailed insight to genus *Zygosporium*.

Type species: ***Zygosporium oscheoides*** Montin

Other accepted species: see Species Fungorum, search *Zygosporium* for names.

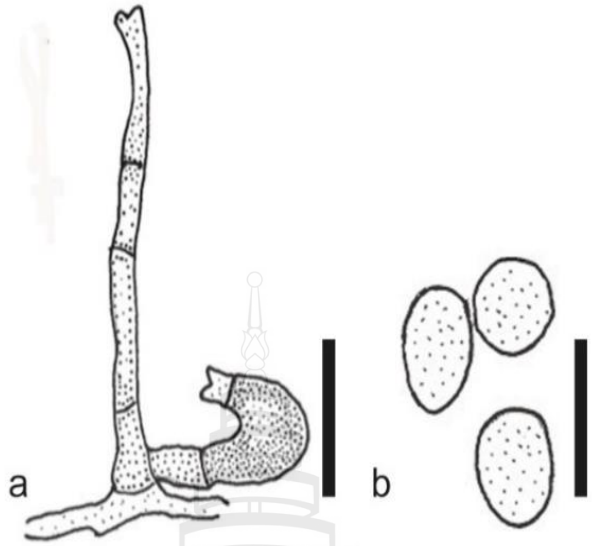

Note (a) Vesicular conidiophores; (b) Conidia; Scale bars: (a-b) 20 µm.

Source Redrawn from Taheriyan et al. (2014)

Figure 3.51 *Zygosporium oscheoides* (holotype)

3.4 Conclusion

This study examined microfungi associated with wetland-dwelling Poales across global wetland ecosystems. The dataset encompasses genera belonging to more than six fungal classes, *Dothideomycetes*, *Eurotiomycetes*, *Leotiomycetes*, *Orbiliomycetes*, *Saccharomycetes*, *Sordariomycetes***,** and *Incertae sedis*. *Dothideomycetes* was identified as the dominant class, with 117 genera distributed across three subclasses. Among these, *Pleosporomycetidae* and *Dothideomycetidae* accounted for 42 and 32 genera, respectively. Nineteen orders were represented within *Dothideomycetes*, with *Pleosporales* being the most frequently encountered. The class further included 53 families, with *Didymellaceae***,** *Didymosphaeriaceae*, and *Lentitheciaceae* comprising 5, 6, and 5 genera, respectively. The second most represented class was *Sordariomycetes*, which included five subclasses, with *Sordariomycetidae* being the most prevalent. The dataset recorded 16 orders under this class, with *Chaetosphaeriales* identified as the most dominant. In total, 37 families were documented within Sordariomycetes, of which *Chaetosphaeriaceae* was the most prominent, having nine genera associated with wetland-dwelling Poales.

This investigation also highlights the existing limitations and knowledge gaps concerning microfungi associated with wetland-dwelling Poales. Notably, 32 genera in the compiled list lack molecular data, and ten genera are monotypic, each known from a single collection. These factors hinder comprehensive taxonomic resolution and raise uncertainty over the current placement of several taxa. The present study not only documents the considerable diversity of microfungi inhabiting wetland-associated Poales, but also emphasizes the requirement of continued, integrative research. Such efforts are essential to improve our understanding of the taxonomy, ecology, and evolutionary relationships of fungi in these ecologically sensitive and vitally important wetland environments.

The fungal communities associated with wetland ecosystems are of considerable importance, as they play critical roles in decomposition processes, nutrient cycling, and maintaining overall ecosystem health. Documenting fungal diversity in these habitats holds both academic and conservation value, underscoring the requirement to prioritize the protection of wetland ecosystems. Future investigations should emphasize the use of advanced molecular systematics, and aim to uncover the deeper ecological functions and biogeographic patterns of microfungi associated with wetland Poales. Increased efforts are essential to ensure the conservation of these sensitive, dynamic, and ecologically significant habitats, consequently supporting the long-term sustainability of wetland ecosystems.

CHAPTER 4

TAXONOMY AND PHYLOGENY OF MICROFUNGI ASSOCIATED WITH FRESHWATER COASTAL WETLAND-DWELLING POALES IN THAILAND

4.1 Introduction

Wetlands are defined as ecosystems that encompass marshes, fens, peatlands, and aquatic habitats, whether natural or artificial, containing water that either stagnant or flowing, and with salinity levels ranging from freshwater to marine environments (RAMSAR Information Paper No. 1). The hydrological conditions and ecological characteristics of wetlands fluctuate with seasonal variations, geographical location, vegetation composition surrounding the wetland, soil properties, nutrient availability, pH, and salinity. Globally, wetlands occupy approximately 6% of the Earth's land surface and are categorized into six major types, including Marine, Estuarine, Lacustrine, Riverine, and Palustrine (marshes), based on water flow dynamics and hydrological regimes (RAMSAR Information Paper No. 1).

Thailand, located in the tropical zone, contains approximately 36,600 km² of wetlands, making up about 7.5% of the country's total land area. Major wetland systems include Thale Noi Non, Don Hoi Lot, the Mekong River, and coastal areas such as Khao Sam Roi Yot and the Pran Buri estuary (Trisurat, 2006). These wetlands cover a wide variety of habitats, such as floodplains, marine wetlands, and coastal wetlands linked to tidal freshwater marshes, estuaries, and mangrove swamps (Trisurat, 2006; Hempattarasuwan et al., 2021). Coastal freshwater wetlands in Thailand, like those in Khao Sam Roi Yot and Pran Buri, support highly diverse communities of plants and animals. These ecosystems are essential for supporting local economies, ecological stability, and community livelihoods. Therefore, conserving, maintaining ecological balance, and sustainably managing these coastal wetlands and their resources are

crucial for preserving both biodiversity and economic resilience in Thailand (Trisurat, 2006).

Fungal communities in these coastal freshwater wetlands represent an ecologically important group of organisms. They include a diverse array of taxa, including zoosporic fungi such as members of the *Chytridiomycota* and *Oomycota*, as well as representatives of the *Glomeromycota*, *Ascomycota*, and *Basidiomycota* (Cornwell et al., 2001; Stephenson et al., 2013; Calabon et al., 2022). These fungi exhibit different life modes as pathogens, endophytes, and saprobes in these environments. Saprobic fungi, in particular, play a crucial role as primary decomposers that facilitate nutrient cycling and improve nutrient availability in the ecosystem (Hyde & Jones, 2002; Calabon et al., 2023). As a result, they are a key component in maintaining the sustainability and ecological functions of coastal freshwater wetlands (Kuehn et al., 2011; Stephenson et al., 2013).

Among the decomposer communities of Thailand's coastal freshwater wetlands, ascomycetous fungi are a particularly important and abundant group. The primary organic substrates available for their colonization and decomposition originate from the dominant plant families of these wetlands, particularly the monocotyledonous order Poales, which currently makes up the majority of the coastal freshwater wetland flora (Trisurat, 2006; Thambugala et al., 2017; Jones & Pang, 2012; Hempattarasuwan et al., 2021). Poales is the largest order of monocotyledonous plants within the angiosperms, with an origin dating back to the Late Cretaceous period (approximately 66 million years ago) (Bouchenak-Khelladi et al., 2012). Members of this order exhibit diverse life forms, including epiphytes, hydrophytes, emergent-rooted aquatic plants, as well as annual and perennial species (Linder & Rudall, 2005). This study focuses on three main families within the order Poales, Cyperaceae, Poaceae, and Typhaceae, which represent the dominant vegetation in Khao Sam Roi Yot and Pran Buri wetlands.

Cyperaceae diverged from other members of Poales during the Late Cretaceous (100–66 million years ago) in North America and today exhibits a cosmopolitan distribution, occupying diverse habitats worldwide. Members of this family are characterized by typically triangular stems and 3-ranked leaves with closed sheaths (Spalink et al., 2016). In Thailand's wetlands, Cyperaceae species are commonly found in shallow areas near the banks (Bhagya et al., 2025). The largest family within the

order Poales is Poaceae, which originated, and diversified toward the end of the Oligocene Epoch (around 23 million years ago). Poaceae comprises more than 20,000 species and is characterized by caryopsis-type fruits and spikelets bearing a lemma and palea (Linder & Rudall, 2005; Bouchenak-Khelladi et al., 2012). *Phragmites* and members of the subfamily Bambusoideae represent the predominant Poaceae types occurring in the selected coastal freshwater wetlands of this study. Typhaceae is a relatively small family within the order Poales and comprises the genus *Typha*, which includes 13 scientifically described species. The genus diverged during the Late Paleogene period (66–23 million years ago) (Greb et al., 2022). Members of Typhaceae are characterized by dense, brown, unisexual flower spikes and long, flat, blade-like leaves. They have a worldwide distribution and are dominant components of wetland ecosystems in Asia, North America, and Australia (Zhou et al., 2018; Bhagya et al., 2024).

In Thailand's coastal freshwater wetlands, members of the families Cyperaceae, Poaceae, and Typhaceae serve as hosts for saprobic, endophytic, and pathogenic fungi. These plant groups are also important primary producers and contribute to maintaining optimal water quality (Quaedvlieg et al., 2013; Thambugala et al., 2017; Abbas et al., 2021). The majority of microfungal studies on wetland-associated Poales have focused primarily on arbuscular mycorrhizal fungi (AMF) and other soil microbial communities. For example, most fungal records associated with Typhaceae involve asexual morphs and AMF (Seerangan & Thangavelu, 2014; Zhang et al., 2024). Karunarathna et al. (2022) reported over 2,000 fungal isolates related to grasses and grass-like plants, however, these isolates were predominantly obtained from dryland or terrestrial ecosystems, leaving the fungal diversity of wetland-associated Poales largely underexplored. Calabon et al. (2022) documented significant fungal diversity in freshwater ecosystems in the world, including 49 genera of *Eurotiomycetes*, 82 genera of *Leotiomycetes*, 229 genera of *Dothideomycetes* (comprising 677 species), and 298 genera of *Sordariomycetes* (comprising 823 species). Despite this diversity richness, only around 20 species were found to be associated with wetland-inhabiting Poales, with bamboo (Poaceae) being the most frequently studied host group.

Recent studies on wetland ecosystems in central and southern Thailand have revealed a diverse and plentiful community of saprobic fungi, underscoring that

detailed taxonomic research on understudied host substrates can reveal previously unknown fungal diversity (Asghari et al., 2023; Apurillo et al., 2024; Aumentado et al., 2024; Bhagya et al., 2024; Karimi et al., 2024; Mukhopadhyay et al., 2024). In the present study, decomposing materials from Poales were collected from the wetlands of Khao Sam Roi Yot, Pran Buri, and Narathiwat in Thailand. Detailed photo plates, comprehensive morphological descriptions, and molecular data are provided for microfungi associated with members of Cyperaceae, Poaceae, and Typhaceae. Species identification was conducted using a polyphasic approach, combining morphological characteristics with multilocus phylogenetic analyses (Turner et al., 2013; Quaedvlieg et al., 2014; Jeewon & Hyde, 2016; Phukhamsakda et al., 2020). Cultures were deposited in the Mae Fah Luang University Culture Collection (MFLUCC), and specimens were deposited in the Mae Fah Luang University Herbarium (Herb. MFLU). Facesoffungi (FoF) and Index Fungorum (IF) numbers will be obtained following the guidelines outlined in Jayasiri et al., (2015), Index Fungorum (2016) and Kirk et al. (2015).

4.2 Materials and Methods

Sample collection, morphological studies, and isolation

Dead and decomposing plant materials, including leaves, stems, peduncles, and inflorescences, were collected from members of the families *Cyperaceae*, *Poaceae*, and *Typhaceae* in the Pranburi Wetland, Pranburi River in Prachuap Khiri Khan Province, Khao Sam Roi Yot Wetland in Kui Buri District, and Narathiwat Wetland in Tambon Sala Mai, Thailand. Samples were segregated based on host family and plant material type, packed into airtight zip-lock bags, and transferred to the laboratory. Required permissions for the above-mentioned collections were obtained from the relevant authorities (No. 0907.4/23579; Book No. 02/020; Book No. 02/001; and No. 0401/5816). Morphological observations were conducted following Senanayake et al. (2020), using an OLYMPUS SZX16 stereomicroscope (Olympus Corporation, Japan) and a Nikon ECLIPSE Ni compound microscope (Nikon Instruments Inc., Japan). Taxonomically important features were photographed with a Nikon DS-Ri2 digital

camera mounted on the microscope, and the morphological features of fungi were organized into detailed photo plates using Adobe Photoshop CS3 Extended version 10.0 (Adobe Inc., California, USA). Measurements were obtained using Image Framework software (Tarosoft, Nonthaburi, Thailand). The single spore isolation technique was employed to obtain pure cultures. Cultures were grown on selected media such as Malt Extract Agar (MEA), and Potato Dextrose Agar (PDA) for 2 to 8 weeks at room temperature (25 ± 5°C) before photographing culture characteristics or obtaining morphological features from the cultures. Selected holotype materials of the isolated fungi were deposited in the Mae Fah Luang University Herbarium (MFLU), and the ex-type living cultures were deposited in the Mae Fah Luang University Culture Collection (MFLUCC). Faces of Fungi and Index Fungorum numbers were obtained following Jayasiri et al., (2015) and Index Fungorum (2025). Data on the taxa will be deposited in the Greater Mekong Subregion database (Chaiwan et al., 2021).

DNA extraction, PCR amplification and sequencing

Seven to ten days old cultures, fruiting bodies, or separated spore clusters were used to extract genomic DNA using the E.Z.N.A. Fungal DNA Mini Kit (D3390-02; Omega Bio-Tek, USA), following the manufacturer's instructions. The purified DNA was stored at 4°C for short-term use and at −20 °C for long-term preservation. Polymerase chain reactions (PCR) were performed to amplify selected loci, depending on the fungal genus (Table 4.1). Each PCR mixture had a final volume of 25 µl, comprising 12.5 µl of 2× Power Taq PCR Master Mix, 9.5 µl of deionized H_2O, 1 µl of each primer (20 µM), and 1 µl of genomic DNA (15 ng/µl). Amplification of the selected loci was carried out using the primers and PCR conditions listed in Table 4.1. SafeView™ DNA stain (SOMBIO, Taiwan, China) was used to visualize the PCR products, which were separated using 1.7% agarose gel electrophoresis. Gel visualization was performed using an E-Box CX5 gel documentation system (Vilber Lourmat Deutschland GmbH, Eberhardzell, Germany), and sequencing was conducted by Solgent Corporation (Yuseong-gu, Daejeon, Korea).

Table 4.1 The amplified loci, primers, and PCR thermal cycle protocols used in the study

Gene	Primer		PCR protocol					Reference
	Forward	Reverse	Initial Denaturation	Denaturation	Annealing	Extension	Final extension	
Internal transcribed spacer (ITS)	ITS4	ITS5	95°C, 5 min 1 cycle	95°C, 30 sec 35 cycles	55°C, 50 sec	72°C, 30 sec	72°C, 10 min 1 cycle	White et al. (1990)
Large subunit ribosomal RNA (LSU)	LR0R	LR5	95°C, 3 min 1 cycle	95°C, 30 sec 35 cycles	55°C, 50 sec	72°C, 30 sec	72°C, 10 min 1 cycle	Rehner and Samuels (1994) Vilgalys and Hester (1990)
Small subunit ribosomal RNA (SSU)	NS1	NS4	95°C, 3 min 1 cycle	95°C, 30 sec 35 cycles	55°C, 50 sec	72°C, 30 sec	72°C, 10 min 1 cycle	White et al. (1990)
Translation elongation factor-1 alpha (*tef*1-α)	EF1-728F	EF1- 986R	94°C, 3 min 1 cycle	94°C, 30 sec 35 cycles	55°C, 50 sec	72°C, 1 min	72°C, 10 min 1 cycle	Carbone and Kohn (1999)
	EF1-688F/	EF1-1251R	95°C, 5 min 1 cycle	94°C, 30 sec 30 cycles	55°C, 45 sec	72°C, 90 sec	72°C, 10 min 1 cycle	Alves et al. (2008)
RNA polymerase II second largest subunit (*rpb*2)	fRPB2-5F	fRPB2-7cr	95°C, 5 min 1 cycle	95°C, 45 sec 35 cycles	55°C, 2 min	72°C, 90 sec	72°C, 10 min 1 cycle	Liu et al. (1999)
Beta tubulin (*tub*2)	Bt2a	Bt2b	95°C, 5 min 1 cycle	94°C, 30 sec 35 cycles	55°C, 45 sec	72°C, 90 sec	72°C, 10 min 1 cycle	Glass and Donaldson (1995)

Phylogenetic analyses

The quality of the raw sequence data was checked by BioEdit v 7.0.9.0 software (Hall, 1999) and Lasergene SeqMan Pro v.7 (DNASTAR, Inc, USA) was used to generate consensus sequences (Afshari et al., 2023). BLASTn searches at NCBI (https://blast.ncbi.nlm.nih.gov/Blast.cgi) and related published literature were utilized to find highly similar sequences (Cai et al., 2006; Phookamsak et al., 2019). All the sequences used in each phylogenetic analysis were aligned in MAFFT 6.864b online tool with the FFT-NS-i method (Katoh et al., 2019). The trimming was conducted manually by BioEdit v 7.0.9.0 software. Low quality sections, primer binding sites and ambiguous based were manually removed from the alignment. Each aligned dataset was individually subjected to maximum likelihood (ML) and Bayesian inference (BI) analyses. The IQ-Tree web server (http://iqtree.cibiv.univie.ac.at/) with 1,000 pseudo-replicates was used for ML tree construction and MrBayes v. 3.2.7a (Ronquist et al., 2012) on XSEDE in CIPRES Science Gateway (Miller et al., 2015) was used for BI analysis. The optimum models for each locus were selected by the use of jModelTest2 in CIPRESS. MEGA11 (version 11.0.13; HANSALOG GmbH & Co. KG, Germany) was used to calculate pairwise distance matrix values, based on the requirements of the phylogenetic analyses (Tamura et al., 2021). Figuretree version 1.4.4 (http://tree.bio.ed.ac.uk/software/Figuretree/) was used to visualize phylogenetic trees and edited in Microsoft PowerPoint (2019), Microsoft Corporation, Washington, United States.

4.3 Results

4.3.1 Taxonomy and Phylogeny

Ascomycota

Pezizomycotina

Dothideomycetes O.E. Erikss. & Winka

Dothideomycetidae P.M. Kirk, P.F. Cannon, J.C. David & Stalpers

Microthyriales G. Arnaud

Microthyriaceae Sacc

Heliocephala V. Rao, K.A. Reddy & de Hoog

Heliocephala V. Rao, K.A. Reddy & de Hoog

The genus *Heliocephala*, placed in the family *Microthyriaceae*, was established by Rao et al. (1984) and typified by *H. proliferans*. This genus comprises hyphomycetous members characterized by macronematous conidiophores that develop terminal aggregations of monoblastic conidiogenous cells. These conidiogenous cells produce hyaline to subhyaline, obclavate, rostrate, or hooked conidia (Iturrieta-González et al., 2020).

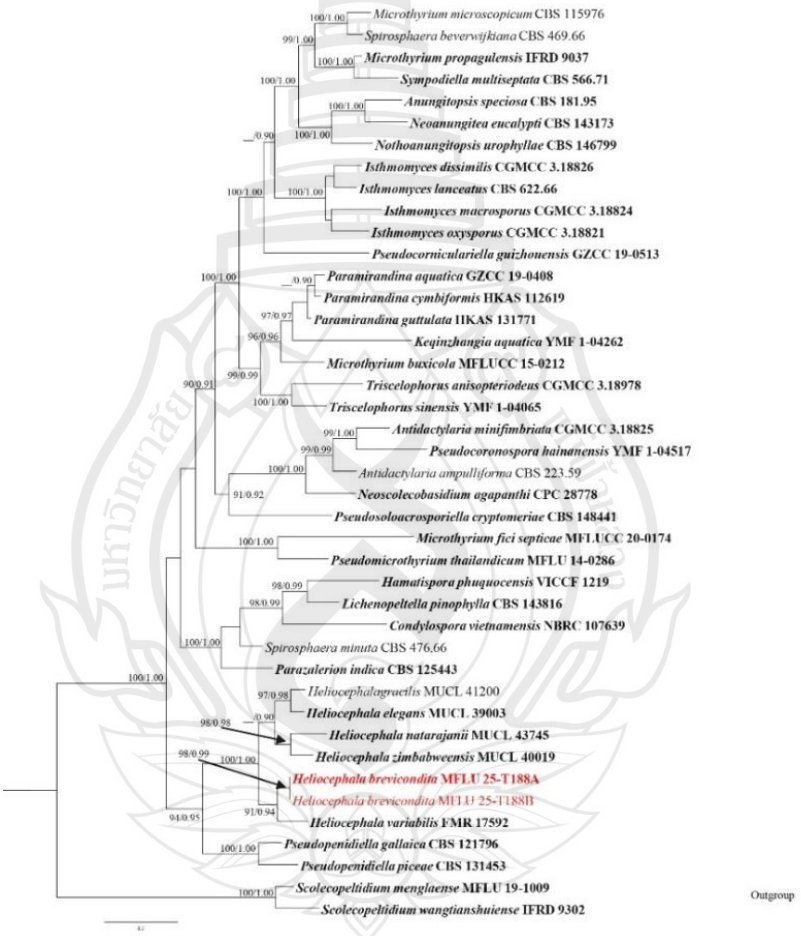

Note The data set comprises 1856 characters including gaps from of selected 42 strains were included in the phylogenetic analyses. Bootstrap support values for ML ≥ 90 % and Bayesian posterior probabilities (BPP) ≥ 0.9 are mentioned at the nodes.

Figure 4.1 Phylogram generated from Maximum Likelihood (ML) analysis based on combined ITS, and LSU sequence.

Heliocephala brevicondita Bhagya, Phukhams E.B.G. Jones & K.D. Hyde, sp. nov.

Index Fungorum number: IF; Facesoffungi number: FoF 18900

Etymology – The name refers to the short conidiophores characteristic of this species.

Holotype – MFLU 25-0413

Saprobic on dead decomposing stem of *Typha*, (Typhaceae), **Sexual morph**: Un-determined. **Asexual morph**: Hyphomycetous, tightly aggregated or occasionally fasciculate as dark brown to pale brown patchers. *Conidiophores* 15–42 × 2–4 µm ($\overline{x}$ = 32 × 2.5 µm, n = 15), macronematous, mononematous, erect, straight or flexuous, dark brown at the base, pale brown to subhyaline towards the apex, smooth, thick-walled, 3-4septate, unbranched or occasionally branched. *Conidiogenous cells* 3–6 × 1.5–2.5 µm ($\overline{x}$ = 4.5 × 1.8 µm, n = 15), pale brown to sub-hyaline, smooth-walled, discrete, monoblastic, subcylindrical or ampuliform, terminal. *Conidia* 20–32 × 3.5–6.0 µm ($\overline{x}$ = 28.5 × 4.5 µm, n = 20), hyaline to subhyaline, smooth, thick-walled, broadly ellipsoidal, subcylindrical or obclavate, tunicate at the ends, 4–6sepate, constricted at 3rd septum, with filiform epical rostrum.

Material examined: Thailand, Chang Wat Prachuap Khiri Khan Province, Pran Buri District, Pran Buri wetland, decomposing stem of *Typha* sp. (Typhaceae), 02 January 2025, Tharindu Bhagya TB188A, (MFLU 25-0413), *ibid.*, TB188B (MFLU 24-0414).

GenBank numbers – MFLU 25-0413: ITS = PX397512, LSU = PX397511

Distribution – decomposing stem of *Typha* sp. (Typhaceae), in Pran Buri wetland, Thailand.

Notes – The new strain MFLU 25-0143 formed a clade sister to *H. variabilis* (FMR 17592) with 91% ML and 0.94 BPP statistical support (Figure 4.1). Pairwise base pair comparisons revealed 6.83% difference in ITS sequences and 2.56% difference in LSU sequences between *H. brevicondita* (MFLU 25-xxxx) and *H. variabilis* (FMR 17592) (Iturrieta-González et al., 2020). Morphologically, *H. brevicondita* (MFLU 25-xxxx) is distinguishable from *H. variabilis* (FMR 17592) by the relatively shorter conidiophores, predominantly subcylindrical conidiogenous cells, and 4–6-septate conidia with a filiform apical rostrum. *Heliocephala triseptata* and *H. vietnamensis* in the lack molecular data, and

H. brevicondita (MFLU 25-0413) differs morphologically from these species by producing conidia with 4–6 septa and a constricted nature at the third septum (Figure 4.2) (Decock et al., 1998; Heredia-Abarca et al., 2011; Mel'nik et al., 2013). Based on the available morphological and phylogenetic evidence, I recognize *H. brevicondita* (MFLU 25-0413) as a new species in the genus *Heliocephala*, isolated from *Typha* sp., in freshwater coastal wetlands of Thailand.

Note a *Typha* sp. host material. b–c Conidiophores on the host surface. e–f Conideogenus cells at the end of conidiophores g–h Conidiophores with conidia. i–k Conidia development. l–n Mature conidia. Scale bars: b–c 250 µm, d 50 µm, e–n 10 µm.

Figure 4.2 *Heliocephala brevicondita* (MFLU 25-0413, holotype)

Incertae sedis

Botryosphaeriales C.L. Schoch, Crous & Shoemaker

Aplosporellaceae Slippers, Boissin & Crous

Aplosporella Speg

The genus *Aplosporella* was proposed by Speg. in 1880 and typified with *Aplosporella chlorostroma*. Members of this genus exhibit a worldwide distribution and various nutritional modes, such as saprobes, opportunistic pathogens, and endophytes. They have been recovered from a variety of host species, including both dicotyledonous and monocotyledonous plants (Zhu et al., 2018; Hyde et al., 2024). *Aplosporella* species are known from both sexual and asexual morphs. The sexual morphs are characterized by black or dark brown, pulvinate, multiloculate, erumpent ascomata, composed of thin-walled, black-pigmented cells arranged in a textura angularis. The asci developed in *Aplosporella* are bitunicate, cylindrical to clavate, with a short pedicel and a rounded apex featuring a well-developed apical chamber. Each ascus contains eight hyaline, smooth, thick-walled, ellipsoid to ovate, aseptate ascospores (Ekanayaka et al., 2016). The most common asexual morphs of the genus produce erumpent to immersed, multilocular pycnidial conidiomata, which are composed of hyaline, smooth-walled, predominantly phialidic conidiogenous cells. These give rise to aseptate, ellipsoid to subcylindrical conidia that are hyaline, smooth, and thin-walled when immature, becoming dark brown to black, thick-walled, and spinulose at maturity (Dissanayake et al., 2021; Hyde et al., 2024).

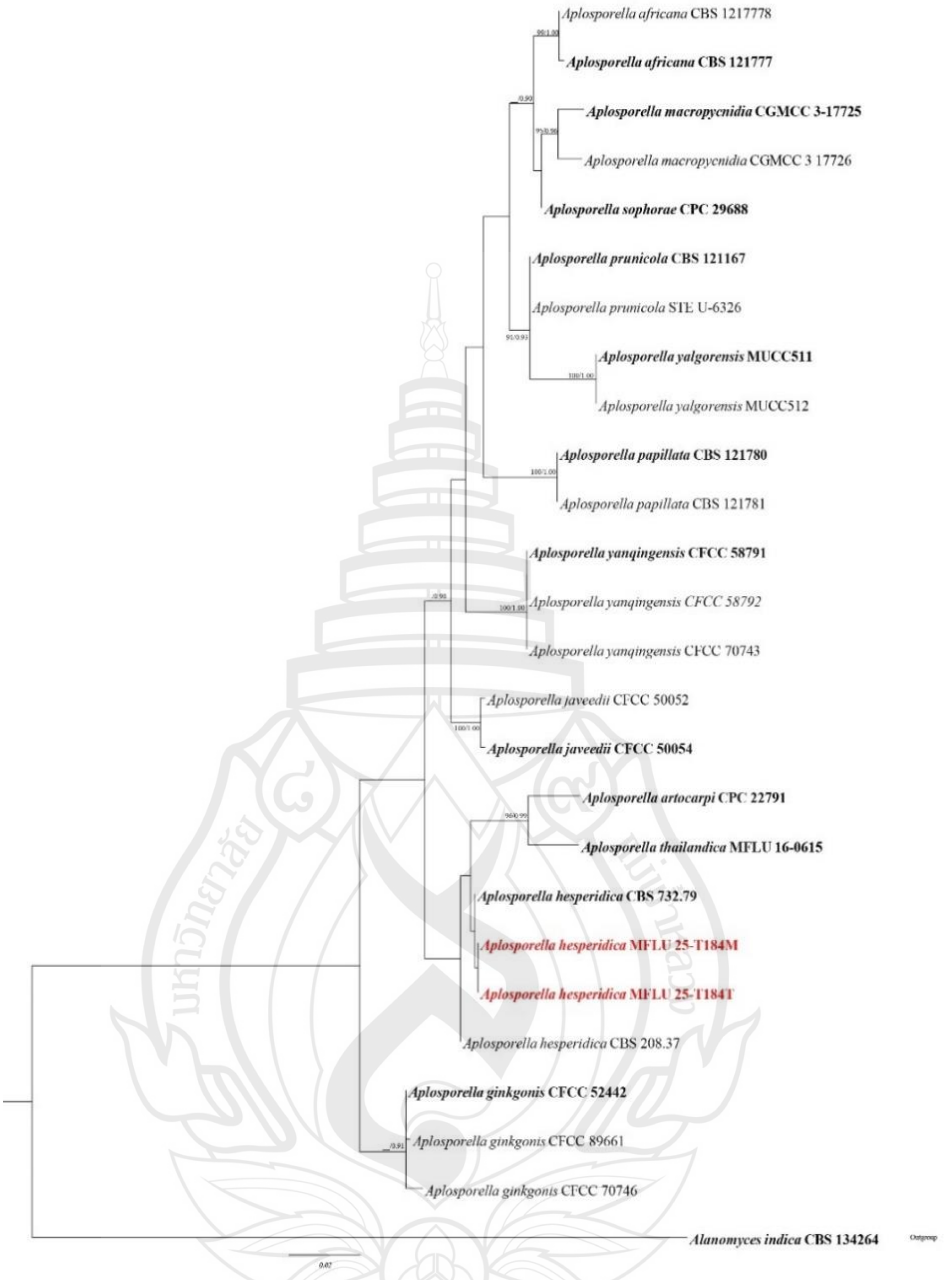

Note The data set comprises 938 characters including gaps from of selected 25 strains of *Aplosporella* were included in the phylogenetic analyses. Bootstrap support values for ML ≥ 90 % and Bayesian posterior probabilities (BPP) ≥ 0.9 are mentioned at the nodes.

Figure 4.3 Phylogram generated from Maximum Likelihood (ML) analysis based on combined ITS, and *tef1-α* sequence.

Aplosporella hesperidica Speg., Anal. Soc. cient. argent. 13(1): 18 (1882)

Saprobic on dead, moist, decaying stems of *Typha*, (Typhaceae), **Sexual morph**: Undetermined. **Asexual morph**: Coelomycetous, *Conidiomata* 170–220 × 150–190 µm ($\bar{x}$ = 210 × 180 µm, n = 5), solitary or gregarious, dark brown to black, immersed to semi-immersed to erumpent on host tissue, multiloculate with central ostiole. *Ostiole* 40–50 µm, central, narrowing to the apex. *Peridium* 60–170 µm ($\bar{x}$ = 85 µm, n = 5), consist with multiple layers outer layers process of dark brown to black, thick-walled cells in *textura angularis*, inner layer process hyaline to sub-hyaline, thin-walled cells in *textura angularis*. *Paraphyses* 20–40 × 4–6 µm ($\bar{x}$ = 45 × 4.5 µm, n = 10), hyaline, smooth-walled, septate, occasionally branched at wider base. *Conidiophores,* reduced to conidiogenous cells. *Conidiogenous cells* 5–13 × 2.5–3.5 µm ($\bar{x}$ = 8 × 3 µm, n = 10), holoblastic, hyaline, smooth-walled, cylindrical to doliiform, percurrently proliferating. *Conidia* 15–25 × 10–20 µm ($\bar{x}$ = 22 × 10 µm, n = 20), hyaline, and smooth thick-walled when immature, yellowish brown to black or dark brown with smooth to verruculose at maturity, aseptate, broadly ellipsoidal to subcylindrical with rounded ends.

Culture characteristics: Conidia germinating on MEA within 12 h. Germ tubes produced from the side of the conidia. Colonies growing on MEA, reaching 20–40 mm in 3 weeks at 25°C. Mycelia superficial, umbonate shape culture with erose edge, from above off white and cottony center with pale white at the edge, from reverse off white to cinereous at the center to the hyaline edge. Hypha become more pigmented and cinereous after 4 weeks of growth.

Material examined: Thailand, Chang Wat Prachuap Khiri Khan Province, Pran Buri District, Pran Buri river, on decaying stems of *Typha* sp. (Typhaceae). 02 December 2024, Tharindu Bhagya, TB190A (MFLU 25-0415), Chang Wat Prachuap Khiri Khan Province, Pran Buri District, Khao Sam Roi Yot Wetland, 02 December 2024, Tharindu Bhagya, TB190B, *Typha* sp. (Typhaceae) (MFLU 25-0146).

GenBank numbers – MFLU 25-0145: ITS = PX506100, LSU = PX506113

Distribution – leaves of *Citrus aurantium*, Buenos Aires (Spegazzini, 1882), on *Chromolaena odorata* (Mapook et al., 2020), decaying woody host, Guizhou province, China (Dissanayake et al., 2021), on *Asplenium nidus* (Hyde et al., 2024), and decaying submerged *Typha* sp. stem, in freshwater river, Thailand (This study).

Notes – The new isolates, strain strain MFLU 25-0415, form a sister clade to the type species *Aplosporella hesperidica* (strain CBS 732.79) with 80% maximum likelihood (ML) and 0.83 Bayesian posterior probability (BPP) statistical support (Figure 4.3). Strain MFLU 25-0415 shares 99.5% similarity in ITS sequences with *A. hesperidica* strain CBS 732.79, without gaps. Morphologically, the new isolates share significant similarities with *A. hesperidica*, including immersed to semi-immersed multiloculate conidiomata, hyaline, smooth-walled, septate paraphyses, cylindrical to doliiform, percurrently proliferating, holoblastic conidiogenous cells, and mature black to dark brown, aseptate, broadly ellipsoidal to subcylindrical, smooth to verruculose conidia (Figure 4.4) (Dissanayake et al., 2021; Hyde et al., 2024). Considering the available morphological and phylogenetic evidence, I recognize these new strains as *A. hesperidica* and document a new host record from *Typha* sp. collected from freshwater wetlands in Thailand.

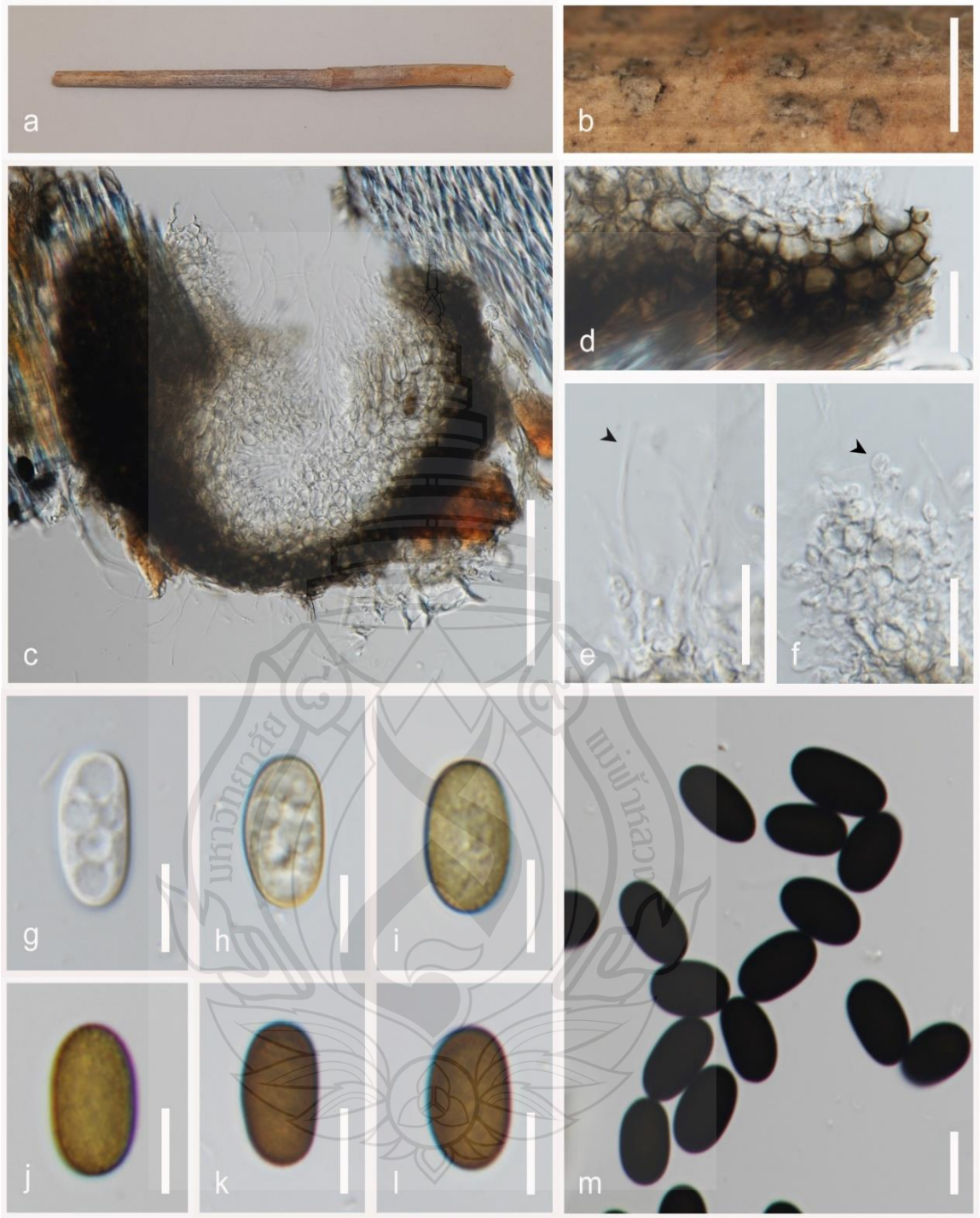

Note a *Typha* sp. host material. b Conidiomata on host surface. c Section of conidiomata. d Peridium. e Paraphysis (arrowed). f Conidiogenous cells with developing conidia (arrowed). g–l Conidia. q Mature conidia. Scale bars: b 750 µm, c 100 µm, d–f 20 µm, g-m 10 µm.

Figure 4.4 *Aplosporella hesperidica* (MFLU 25-0415)

Botryosphaeriaceae *Theiss. & Syd*

Lasiodiplodia Ellis & Everh

Lasiodiplodia was introduced by Ellis & Everhart in 1896 and typified by *Lasiodiplodia tubericola*. The genus exhibits a cosmopolitan distribution and is known to adapt saprobic, pathogenic, and endophytic lifestyles (Rathnayaka et al., 2023; Wu et al., 2023). The sexual morphs of *Lasiodiplodia* are characterized by dark brown to black, ascostromatic, uniloculate, ostiolate ascomata, which are either immersed or erumpent in host tissue. Pseudoparaphyses are hyaline, septate, and cellular. The asci are bitunicate, clavate, and stipitate, with a thickened endotunica forming a conspicuous apical chamber at the apex. Ascospores are aseptate, hyaline when immature, and become dark brown at maturity (Phillips et al., 2013; Rathnayaka et al., 2023; Wu et al., 2023). *Lasiodiplodia* develops coelomycetous asexual morphs, producing dark brown to black, unilocular or multilocular, stromatic, ostiolate conidiomata. These are either immersed or superficial on host tissue and possess a conidiomatal wall composed of dark brown to black, thick-walled cells arranged in a *textura angularis*. The wall becomes thinner and hyaline toward the fertile interior. Paraphyses are hyaline, smooth, cylindrical, and septate. Conidiophores are predominantly reduced to conidiogenous cells, when present, they are hyaline, smooth, septate, cylindrical, and rarely branched. Conidiogenous cells in *Lasiodiplodia* are holoblastic, hyaline, smooth, cylindrical to subobpyriform, determinate or indeterminate, and discrete. Depending on the species, proliferation occurs either through simple, same-level proliferation or percurrent proliferation with one or two distinct annellations. Conidia are hyaline when immature, becoming dark brown, thick-walled, oblong to ellipsoid, straight, and medianly 1-euseptate, with prominent longitudinal striations (Liu et al., 2012; Phillips et al., 2013; Rathnayaka et al., 2023; Wu et al., 2023).

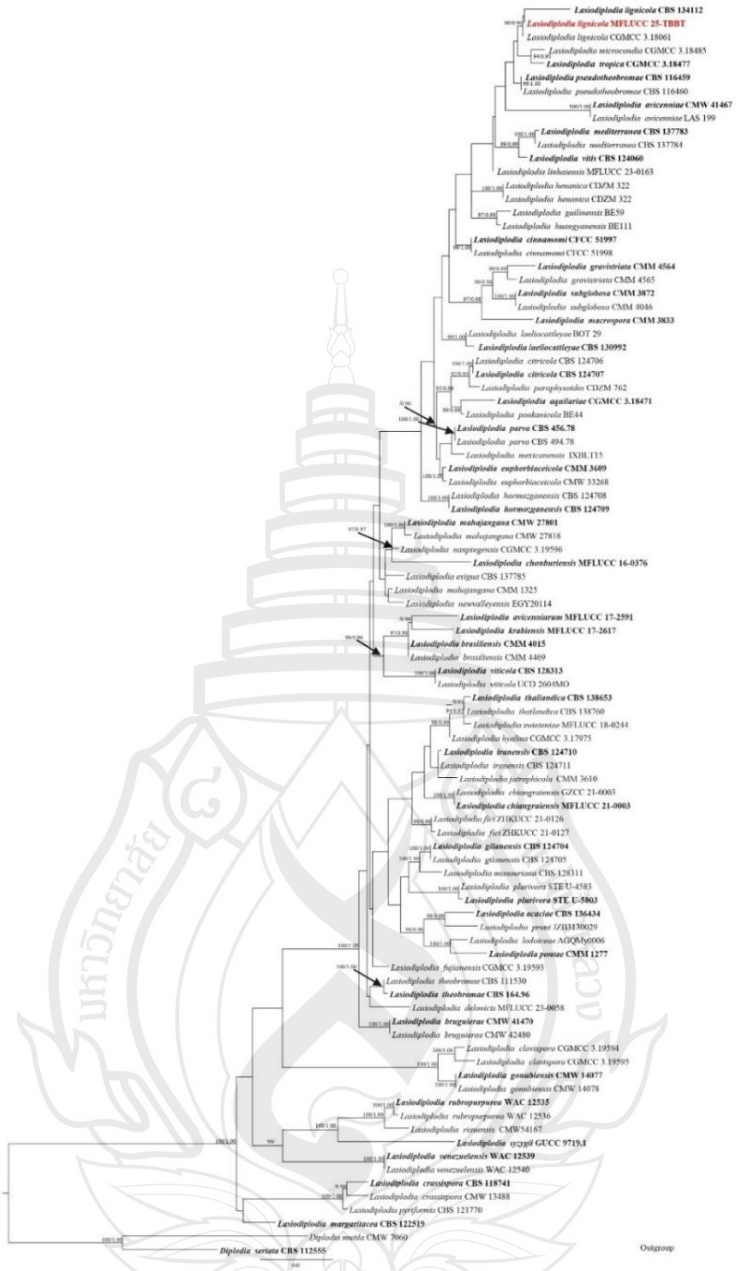

Note Bootstrap support values for ML ≥ 90 % and Bayesian posterior probabilities (BPP) ≥ 0.9 are mentioned at the nodes. The tree was rooted to *Diplodia mutila* (CMW 7060) and *D. seriata* (CBS 112555) combination. Newly generated sequence is in red and the type strains are in bold.

Figure 4.5 Phylogram generated from Maximum Likelihood (ML) analysis based on combined ITS, *tef1-α*, and *tub2* sequence data of 91 strains of genus *Lasiodiplodia*, that comprise 1608 characters including gaps, are included in the analyses.

Lasiodiplodia lignicola (H.A. Ariy., Jian K. Liu & K.D. Hyde) A.J.L. Phillips, A. Alves & Abdollahz., in Phillips, Alves, Abdollahzadeh, Slippers, Wingfield, Groenewald & Crous, Stud. Mycol. 76: 120 (2013)

Saprobic on dead, moist, decaying stems of Bamboo, (Poaceae), **Sexual morph**: Undetermined. **Asexual morph**: Coelomycetous, *Conidiomata* 130–110 × 120–105 µm ($\bar{x}$ = 124 × 116 µm, n = 5), pycnidial, tightly aggregated, superficial, semi-immersed or erupt from host tissue at maturity, dark brown to purplish black in color, globose to subglobose with numerous seate. *Setae* conspicuous, pale brown to purplish at the base and hyaline at tips, unbranched, septate, tapered toward apex. *Conidiomatal wall* 29–22 µm wide ($\bar{x}$ = 27 µm, n = 10), multi layered, thick-walled outer layer composed from brown to purplish cells of *textura angularis*, inner layer comprises from thinner, hyaline cells of *textura angularis* which turn in to *textura prismatica* close to conidial hymenium. *Paraphyses* 44–31 × 1.8–1.4 µm ($\bar{x}$ = 38.2 × 1.5 µm, n = 20), cylindrical, aseptate, hyaline with rounded apex. *Conidiogenous cells* 7.5–6.5 × 3.8–2.5 µm ($\bar{x}$ = 7.2 × 3.1 µm, n = 10), originates from the inner hyaline layer of conidiomata, proliferating in different levels, embedded in paraphyses, smooth-walled, hyaline, cylindrical and holoblastic. *Conidia* 24–19 × 13–10 µm ($\bar{x}$ = 21.7 × 12.3 µm; n = 20), hyaline, unicellular, ellipsoid to obovoid, thick-walled, granular on surface, rounded at apex, occasionally constricted at the middle.

Culture characteristics: Conidia germinating on MEA within 12 h. Germ tubes produced from the side of the conidia. Colonies growing on MEA, reaching 20–30 mm in 2 weeks at 25°C. Mycelia superficial, umbonate shape culture with erose edge, from above off-white cottony center with pale white at the edge, from reverse yellowish white at the center and off white at the edge.

Material examined: Thailand, Chang Wat Prachuap Khiri Khan Province, Pran Buri District, Pran Buri river, on decaying stems of Bamboo (Poaceae), 02 December 2024, Tharindu Bhagya, TB_BT (MFLU 25-0417).

GenBank numbers – MFLU 25-0417: ITS = PX518033

Distribution – Decomposing wood in Bamboo, Muang District, Chiang Rai, Thailand (Liu et al., 2012), and on decomposing bead submerged stem of Bamboo, (Poaceae), in Pran Buri river, Chang Wat. Thailand (This study).

Notes – The new isolate MCLU 25-0417, clade among *Lasiodiplodia lignicola* strains CBS 134112 and CGMCC 3.18061, with 75% maximum likelihood (ML) and 0.70 Bayesian posterior probability (BPP) support (Figure 4.5). Phylogenetically, MCLU 25-0417 shares 99.8% similarity in ITS sequences and 98.9% similarity in *tub2* sequences with *L. lignicola* strain CBS 134112, excluding gaps. Morphologically, the new strain MCLUCC 25-0417 resembles the asexual morph produced by the ex-type strain CBS 134112, characterized by superficial, semi-immersed or erumpent, globose to subglobose conidiomata, and hyaline, holoblastic, cylindrical conidiogenous cells. The paraphyses in both MCLu 25-0417 and CBS 134112 are hyaline, cylindrical, and aseptate. The conidia are ellipsoid to obovoid, hyaline, unicellular, and possess a granular surface (Figure 4.6) (Liu et al., 2012; Phillips et al., 2013). Based on the available phylogenetic and morphological evidence, I recognize strain MCLU 25-0417 as the asexual morph of *L. lignicola*, isolated from a decomposing bamboo stem (Poaceae) in a freshwater river in Thailand.

Note a Bamboo host material. b–c Conidiomata on host. d Vertical section conidiomata. e Peridium. f Seate developed on the conidiomata. g Paraphysis. h–j Conidiogenous cells. k–l Conidia. m A germinated conidium. n Culture on MEA above. o reverse. Scale bars: d 50 µm, e 80 µm, f 50 µm, g 25 µm, h 10 µm, i–j 25 µm, k 50 µm, l 25 µm, m 20 µm.

Figure 4.6 *Lasiodiplodia lignicola* (MFLU 25-0417)

Macrophomina *Petr*

Macrophomina was established by Petrak in 1923 and typified with *Macrophomina philippinensis*. This cosmopolitan genus contains members that are phytopathogenic and saprobic on a variety of host materials (Zhao et al., 2019). *Macrophomina* is characterized by solitary or gregarious, immersed, glabrous, ostiolate conidiomata, with a peridium composed of black or dark brown, thick-walled cells arranged in a textura angularis. The conidiogenous cells are hyaline, cylindrical to ellipsoidal, terminal, and produce hyaline, smooth-walled, oblong to cylindrical, aseptate conidia with a granular surface and mucilaginous appendages at the apex (Zhao et al., 2019; Wu et al., 2023).

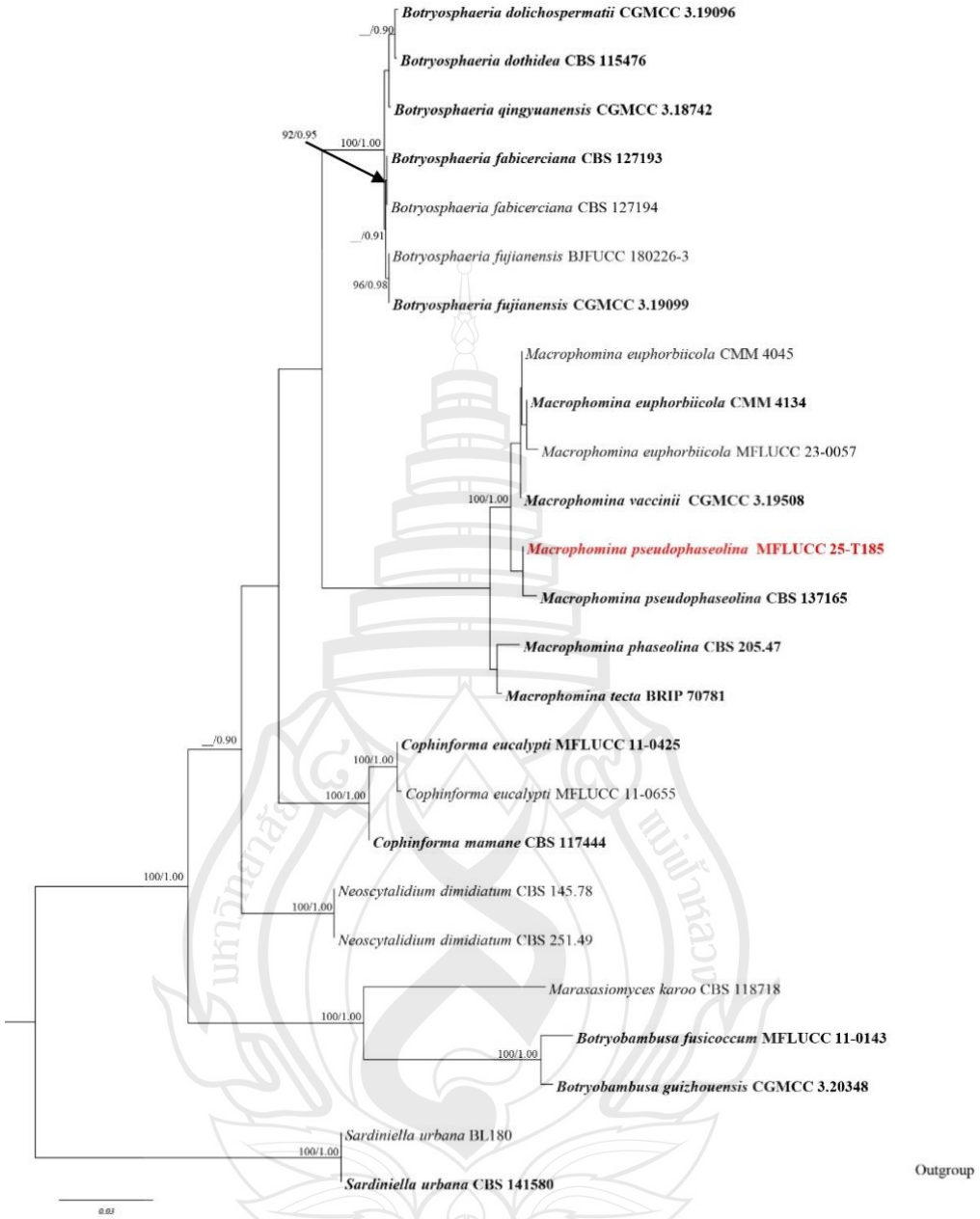

Note Bootstrap support values for ML ≥ 90 % and Bayesian posterior probabilities (BPP) ≥ 0.9 are mentioned at the nodes. The tree was rooted *Sardiniella urbana* (CBS 141580, and BL180) combination. Newly generated sequence is in red and the type strains are in bold.

Figure 4.7 Phylogram generated from Maximum Likelihood (ML) analysis based on combined ITS, LSU, *tef1-α,* and *tub2* sequence data of 25 strains in *Botryosphaeriaceae*, which comprise 2268 characters including gaps, are included in the analyses.

Macrophomina pseudophaseolina Crous, M.P. Sarr & M. Ndiaye, in Sarr, Ndiaye, Groenewald & Crous, Phytopath. Mediterr. 53(2): 265 (2014)

Saprobic on dead, moist, decaying stems of *Typha*, (Typhaceae), **Sexual morph**: Undetermined. **Asexual morph**: Coelomycetous, *Conidiomata* 110–170 × 170–230 µm ($\bar{x}$ = 150 × 210 µm, n = 5), solitary to gregarious, black to dark brown, globose to subglobose, glabrous, immersed to erupt on host tissue. *Peridium* 10–25 µm ($\bar{x}$ = 22 µm, n = 5), outer layer consists of dark brown to black thick-walled cells in *textura angularis*, inter thin layer process hyaline, smooth thin-walled cells in *textura angularis*. *Ostiole* 8–14 µm, short, central, cylindrical. *Paraphyses* absent. *Conidiophores,* reduced to conidiogenous cells. *Conidiogenous cells* 5–15 × 2–8 µm ($\bar{x}$ = 8.5 × 4.5 µm, n = 20), terminal, holoblastic, enteroblastic, hyaline, smooth-walled, cylindrical to ellipsoidal. *Conidia* 20–30 × 8–12 µm ($\bar{x}$ = 24 × 10 µm, n = 30), hyaline, smooth, thick-walled, aseptate, oblong to cylindrical, rounded at the apex, narrowed towered the base, straight, occasionally constricted in the middle with mucoid apical appendage.

Culture characteristics: Conidia germinating on MEA within 12 h. Germ tubes produced from the side of the conidia. Colonies growing on MEA, reaching 30–50 mm in 3 weeks at 25°C. Mycelia superficial, umbonate shape culture with erose edge, from above off white and cottony center with pale white at the edge, from reverse off white at the center to the hyaline edge.

Material examined: Thailand, Chang Wat Prachuap Khiri Khan Province, Pran Buri District, Sam Roi Yot, wetland on decaying stems of *Typha* sp. (Typhaceae), 07 May 2023, Tharindu Bhagya, TB185 (MFLU 25-0418).

GenBank numbers – MFLU 25-0418: ITS = PX506115, LSU = PX506121

Distribution – Stems and roots of *Hibiscus sabdariffa*, Senegal (Sarr et al., 2014), roots of *Lens culinaris*, Northwest Algeria (Kouadri et al., 2021), *Gossypium hirsutum*, Brazil (Brito et al., 2019), *Manihot esculenta*, Brazil (Brito et al., 2019), stems and roost of *Cucumis melo*, Northeastern Brazil (Negreiros et al., 2019), *Trianthema* sp., Brazil, semi-arid region (Negreiros et al., 2019), Maize, Sorghum, Mung bean, and Cowpea, Australia (Poudel et al., 2021), and decaying submerged *Typha* sp. leaf, in freshwater river, Thailand (This study).

Notes – The new strain, MFLU 25-0418, develop a clade with *M. pseudophaseolina* (CBS 137165) with 76% maximum likelihood (ML) and 0.78 Bayesian posterior probability (BPP) support (Figure 4.7). Phylogenetically, the pairwise comparison indicated the ITS sequence of the new strain shares 99.64% similarity, and 99.87% similarity in LSU sequences with strain CBS 137165, excluding gaps. Morphologically, strain MFLU 25-0418 resembles *M. pseudophaseolina* (CBS 137165) by possessing globose to subglobose, glabrous, and single ostiolate conidiomata; hyaline, cylindrical to ellipsoidal, terminal, holoblastic to enteroblastic conidiogenous cells, and hyaline, smooth, thick-walled, aseptate, oblong to cylindrical conidia with a mucoid apical appendage (Figure 4.8) (Sarr et al., 2014; Zhao et al., 2019; Kouadri et al., 2021; Wu et al., 2023). Considering the available morphological and phylogenetic evidence, I recognize the isolate, strain MFLU 25-0418, as new strain of *M. pseudophaseolina*, and report a new host record from *Typha* sp. in a freshwater coastal wetland in Thailand.

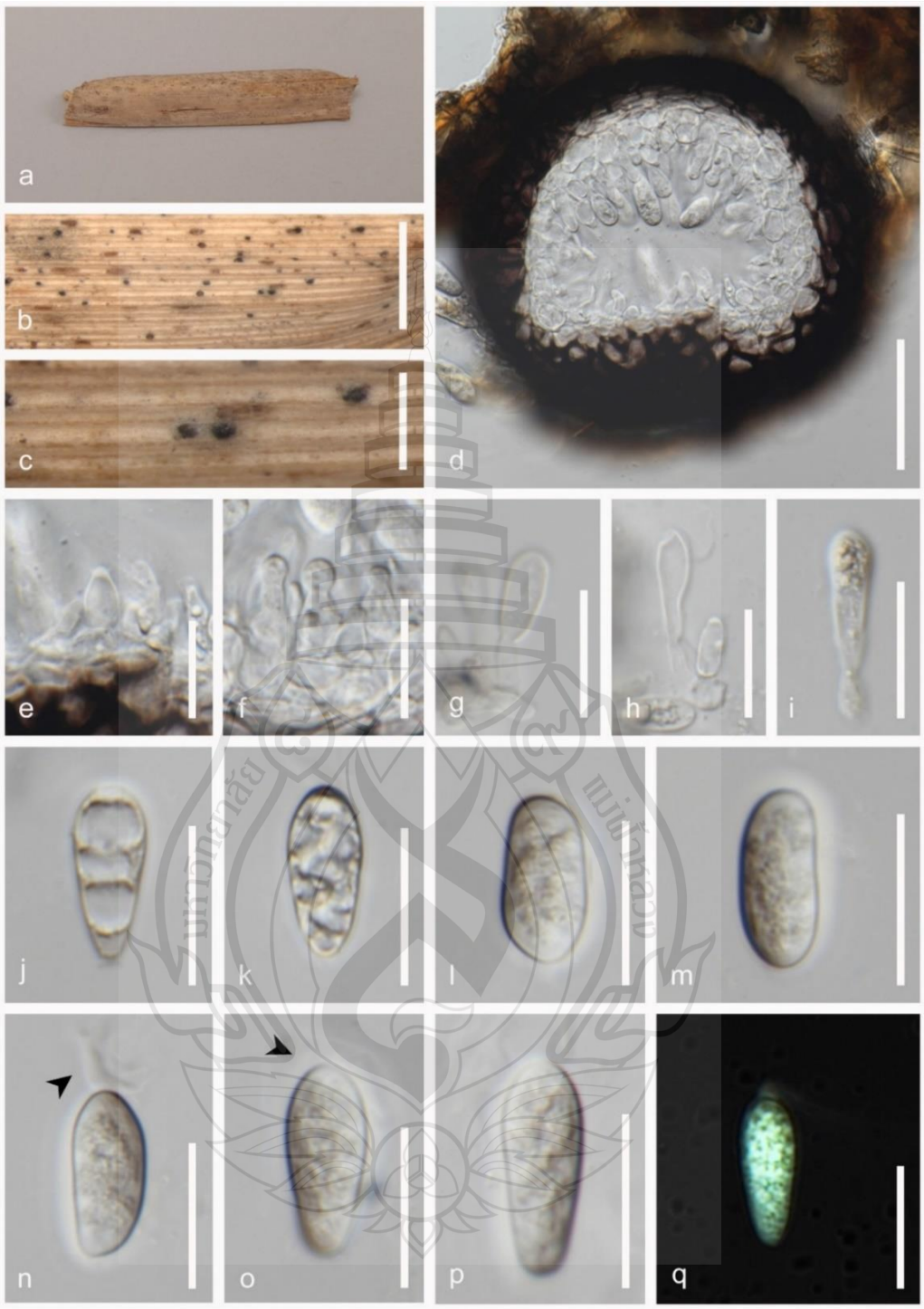

Note a *Typha* sp. host material. b–c Conidiomata on host. d Section of conidiomata. e–i Conidiogenous cells bearing conidia, j–p Conidia mounted on water with mucoid appendage (arrowed). q Conidium mounted in Indian Ink. Scale bars: b 2.5 mm, c 750 µm, d 50 µm, e–q 20 µm.

Figure 4.8 *Macrophomina euphorbiicola* (MFLU 25-0418)

Muyocopronales Mapook, Boonmee & K.D. Hyde

Muyocopronaceae K.D. Hyde

Muyocopron Speg

Spegazzini (1881) erected the genus *Muyocopron*, typified by *M. corrientinum* (Mapook et al., 2016). Members of *Muyocopron* exhibit a worldwide distribution and are predominantly saprobic on terrestrial substrates, although a few species have been reported as endophytic or pathogenic. *Muyocopron* is known from both sexual and asexual morphs (Mapook et al., 2016; Hongsanan et al., 2020; Chethana et al., 2021; Tennakoon et al., 2021). The sexual morph is characterized by black to dark brown, superficial, applanate, carbonaceous ascomata with a central ostiole. Pseudoparaphyses are hyaline, septate, and cylindrical to filiform. Asci are bitunicate, fissitunicate, and contain 4–8 hyaline, unicellular, oval to obovoid ascospores. The asexual morph produces irregular conidiomata resembling sporodochia. Conidiogenous cells are hyaline, smooth-walled, phialidic or annellidic, ampulliform to cylindrical, and give rise to hyaline to pale brown, smooth to roughened, globose, ellipsoidal to oblong, aseptate to occasionally septate conidia (Mapook et al., 2016; Hongsanan et al., 2020; Chethana et al., 2021; Tennakoon et al., 2021; Mapook & Hyde, 2023; Hongsanan et al., 2025; Manawasinghe et al., 2025).

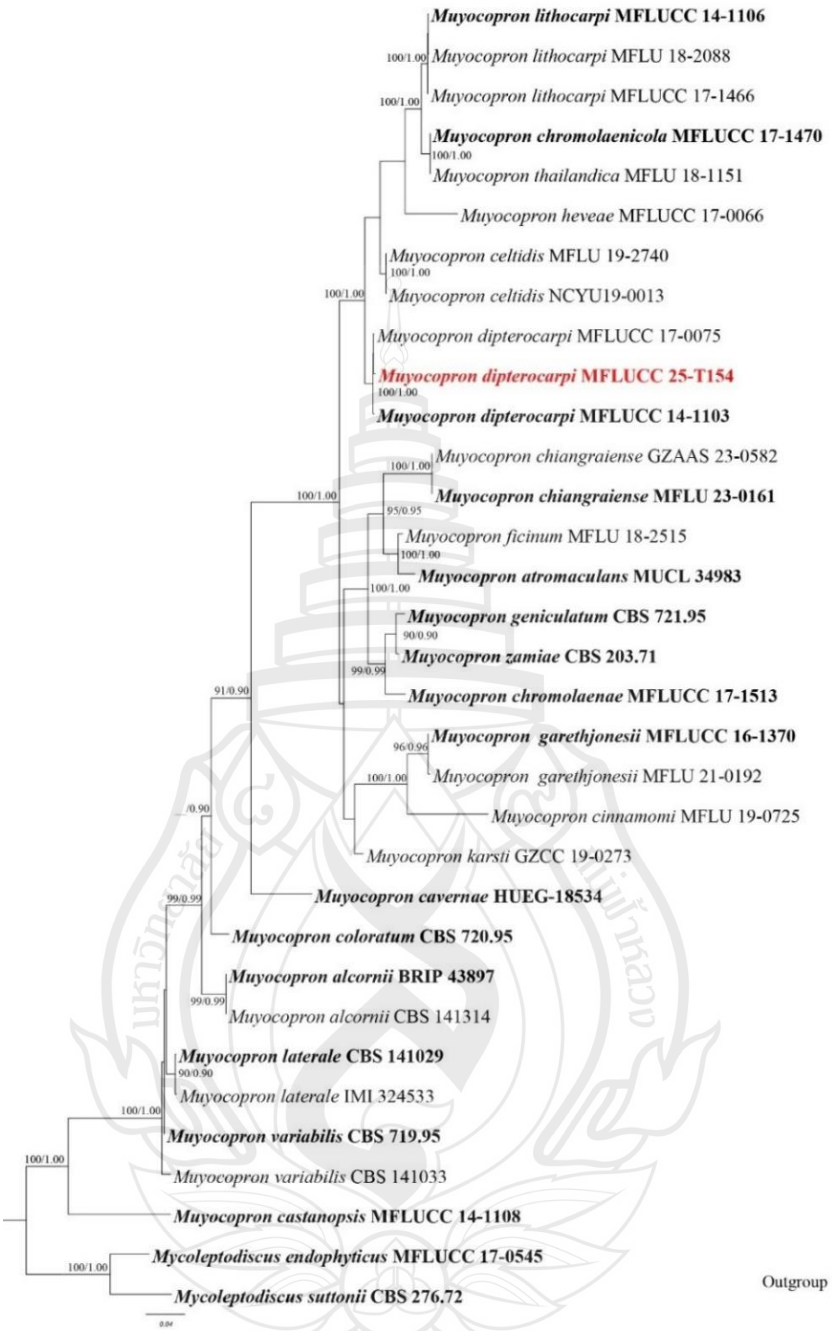

Note The data set comprises 2776 characters including gaps from of selected 33 strains which were included in the phylogenetic analyses. Bootstrap support values for ML ≥ 90 % and Bayesian posterior probabilities (BPP) ≥ 0.9 are mentioned at the nodes. The tree was rooted to *Mycoleptodiscus endophyticus* (MFLUCC 17-0545) and *M. suttonii* (CBS 276.72).

Figure 4.9 Phylogram generated from Maximum Likelihood (ML) analysis based on combined LSU, SSU, and ITS sequence.

Muyocopron dipterocarpi Mapook, Boonmee & K.D. Hyde, in Mapook, Hyde, Dai, Li, Gareth Jones, Bahkali & Boonmee, Phytotaxa 265(3): 232 (2016)

Saprobic on dead, decaying leaf of *Typha*, (Typhaceae). **Sexual morph**: *Ascomata* 90–150 × 250–350µm ($\bar{x}$ = 135× 280 µm, n = 5), black or dark brown, aggregated or occasionally scattered, superficial on host tissue, slightly raised, circular, coriaceous, glabrous, golobose to subglobose with central, short ostiole. *Peridium* 15–30 µm wide ($\bar{x}$ = 22 µm, n = 10), show different thickness, thick at the sides, outer layers composed of dark brown to black dark brown to black pseudoparenchymatous cells and, thick-walled cells in *textura angularis,* inner layer process light brown cells of *textura angularis*. *Pseudoparaphyses* 1–3 µm wide ($\bar{x}$ = 1.5 µm, n = 10), hyaline, trabeculae, septate to aseptate, smooth walled, and cylindrical. *Asci* 50–75 × 20–40 µm ($\bar{x}$ = 65 × 28 µm, n = 10), 8-spored, bitunicate, fissitunicate, saccate, broadly obpyriform, or obclavate, straight or slightly curved, short pediculate, with conspicuous, minute ocular chamber at the tip. *Ascospores* 15–22 × 7–12 µm ($\bar{x}$ = 17 × 10 µm, n = 20), overlapping or crowded, hyaline, aseptate, smooth to granular, oval or ellipsoid to obovoid, obtuse at ends. **Asexual morph**: undetermined.

Culture characteristics: Ascospores germinating on PDA within 72 h. Germ tubes produced from the tips of the ascospore. Colonies growing on PDA, reaching 30–40 mm in 2 weeks at 25°C. Mycelia superficial, cottony, culture umbonate with entire edge, from above off white with cinereous tinge concentric, thick white ring towards the hyaline edge, from below off white from the center to the hyaline edge. Mycelium turn more pale brown after 4 weeks.

Material examined: Thailand, Chang Wat Prachuap Khiri Khan Province, Pran Buri District, Pran Buri Wetland, on decaying stems of *Typha* sp. (Typhaceae), 16 January 2025, Tharindu Bhagya, T154, MFLU 25-0419.

GenBank numbers – MFLU 25-0419: ITS = PX518035, LSU = PX518036

Distribution – Dried twigs of *Dipterocarpus tuberculatus* (*Dipterocarpaceae*), Chiang Rai, Thailand (Mapook et al., 2016), on dried twig of *Hevea brasiliensis* (Euphorbiaceae), Phayao, Thailand (Senwanna et al., 2019), on dead twigs of *Mangifera indica* (Anacardiaceae), Sukhothai, Thailand (Jyasiri et al., 2019), on decaying pod septum of *Delonix regia* (*Fabaceae*), Phrae, Thailand (Huanraluek et al., 2020), on dead leaves and decaying twig of *Celtis formosana* (*Cannabaceae*), Taiwa,

China (Chethana et al., 2021; Tennakoon et al., 2021), on dead twigs of *Zanthoxylum fagara*, Phrae, Thailand (Mapook & Hyde, 2023), decomposing *Typha* sp. stem, Chang Wat Prachuap Khiri Khan Province, Thailand (This study).

Notes – The new strain MFLU 25-0419 forms a clade among *Muyocopron dipterocarpi* type strain MFLUCC 14-1103, with 100% maximum likelihood (ML) support and 1.00 Bayesian posterior probability (BPP) support (Figure 4.9). This strain resembles *Muyocopron* by possessing carbonaceous, flat, dark brown to black ascomata, bitunicate, fissitunicate, saccate asci bearing hyaline, unicellular, oval to obovoid ascospores (Mapook et al., 2016; Hongsanan et al., 2020; Chethana et al., 2021; Tennakoon et al., 2021; Hongsanan et al., 2025). Phylogenetically, pairwise comparison using strain shows 100% similarity in SSU and LSU sequences and 99.61% similarity in the ITS sequence with strain MFLUCC 14-1103, and 99.24% similarity in the ITS sequences with strain MFLUCC 17-0075. Morphologically, the saccate, broadly obpyriform to obclavate asci, and hyaline, aseptate, smooth to granular, oval to ellipsoid or obovoid ascospores with a similar length (L) to width (W) ratio support the similarity between strains MFLU 25-0419 and strain MFLUCC 17-0075 (MFLU 25-0419 = 1.70 vs MFLUCC 17-0075 = 1.78) (Figure 4.10) (Mapook et al., 2016; Hongsanan et al., 2020). Considering all available evidence, I identify the new strain as *Muyocopron dipterocarpi* and report a new host record from *Typha* sp., collected from a freshwater coastal wetland in Thailand.

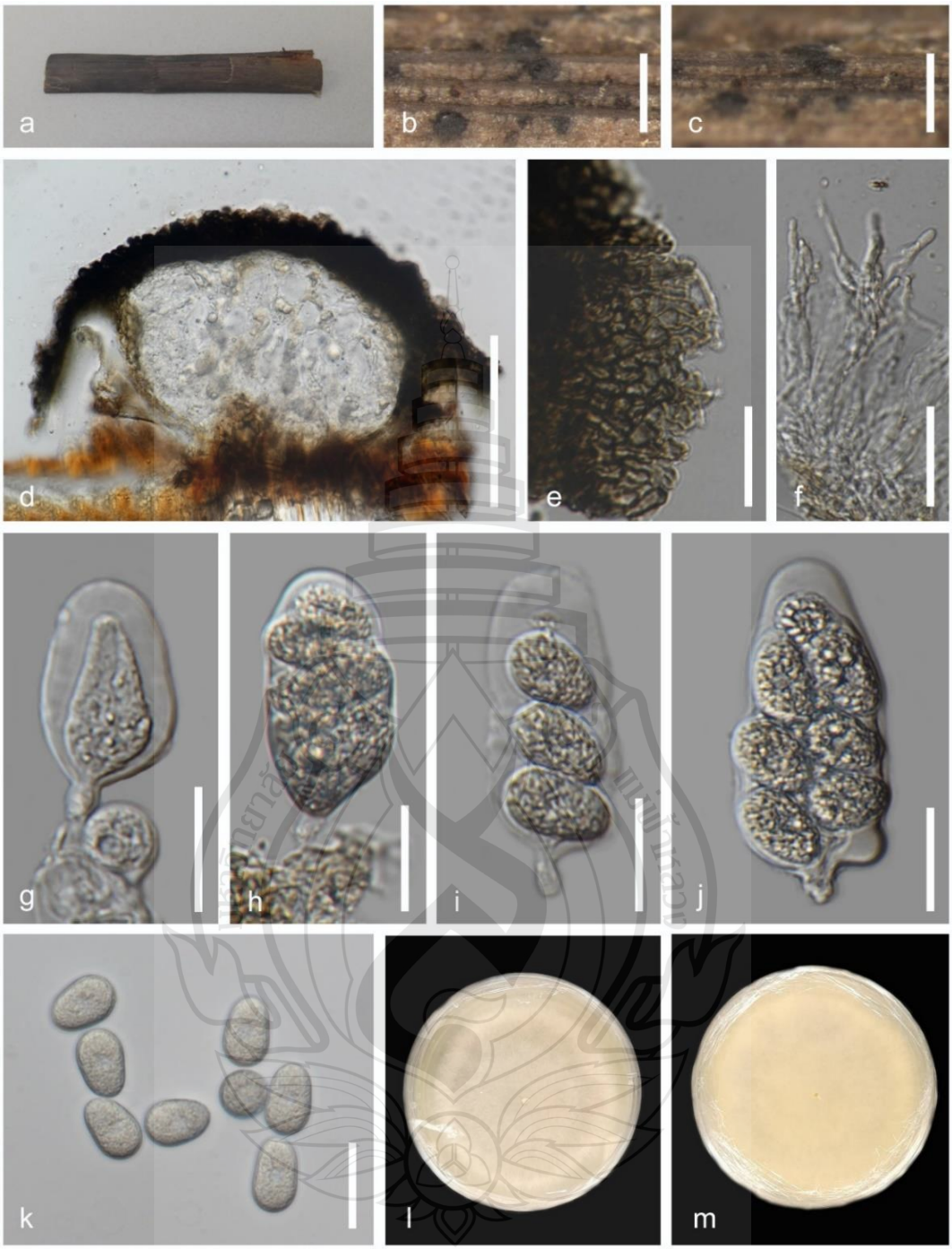

Note a *Typha* sp. host material. b–c Black immersed ascomata on the host. d Vertical section of ascomata exposing the peridium. e Squash mount showcasing surface view of peridium. f Pseudoparaphyses. g–j Asci with developing ascospores. k Ascospores. l Two weeks old culture on MEA above. m reverse. Scale bars: b–c 500 µm, d 100 µm, e–k 20 µm.

Figure 4.10 *Muyocopron dipterocarpi* (MFUL 25-0419)

Pleosporomycetidae C.L. Schoch, Spatafora, Crous & Shoemaker

Pleosporales Luttr. ex M.E. Barr

Acrocalymmaceae Crous & Trakun

Acrocalymma Alcorn & J.A.G. Irwin

Acrocalymma was proposed by Alcorn and Irwin in 1987, first isolated from the roots of *Medicago sativa*. The genus is typified by *Acrocalymma medicaginis* and is placed under the monotypic family Acrocalymmaceae (Das et al., 2020; Calabon et al., 2023). Members of the genus exhibit both sexual and asexual morphs. The sexual morphs of *Acrocalymma* are characterized by ascomata with a central ostiole, cylindrical bitunicate asci with eight spores, and hyaline, smooth-walled ascospores surrounded by a hyaline sheath (Liu & Zeng, 2022). The asexual morphs produce cylindrical, hyaline conidia with mucilaginous appendages. *Acrocalymma* species have been isolated from a wide variety of environments and substrates, including submerged wood and other plant litter in tropical water bodies (Das et al., 2020; Liu & Zeng, 2022; Calabon et al., 2023).

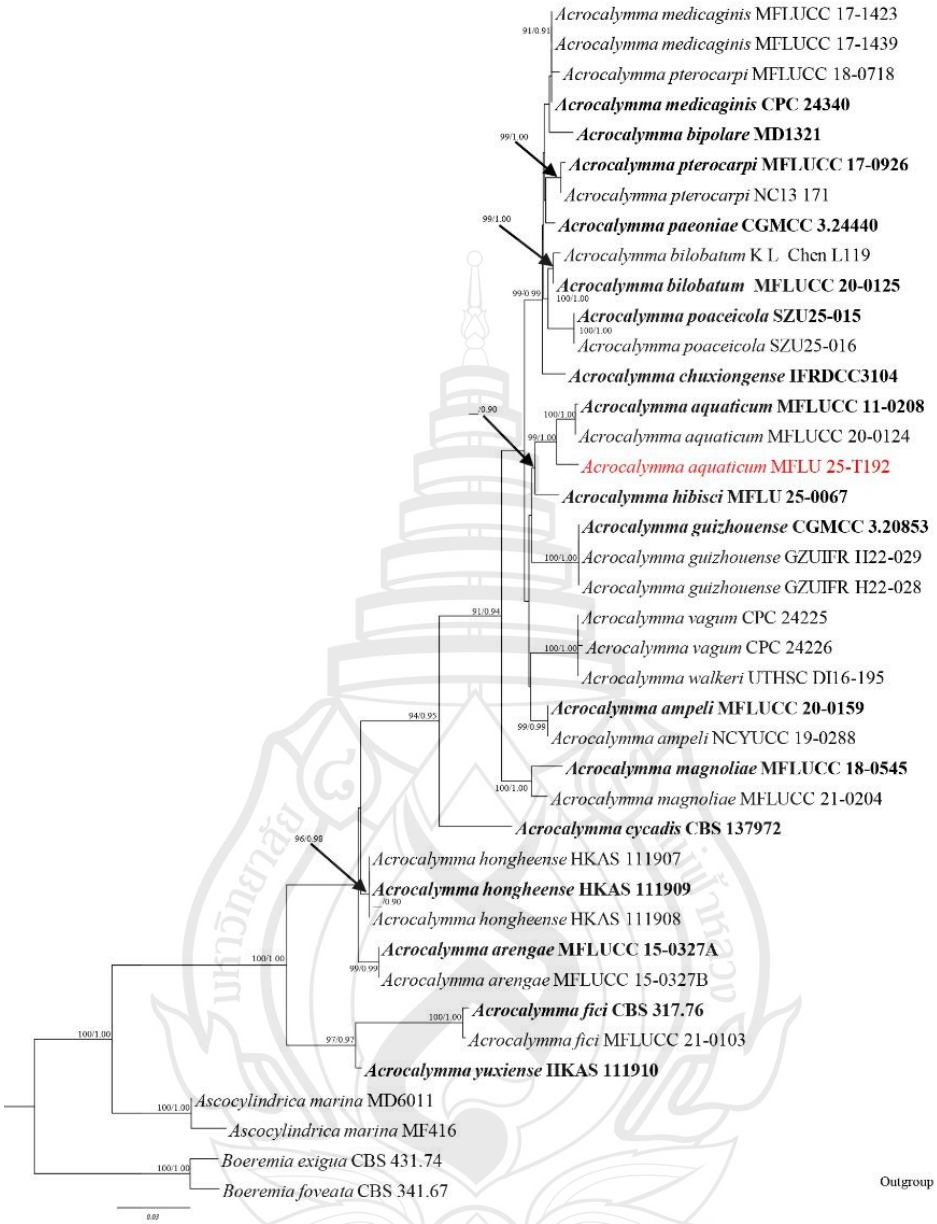

Note Bootstrap support values for ML ≥ 90 % and Bayesian posterior probabilities (BPP) ≥ 0.9 are mentioned at the nodes. The tree was rooted to Boeremia exigua (CBS 431.74) and *B. foveata* (CBS 341.67) combination. Newly generated sequence is in red and the type strains are in bold.

Figure 4.11 Phylogram generated from Maximum Likelihood (ML) analysis based on combined SSU, LSU, ITS, and *tef1-α* sequence data of 40 strains of genus *Acrocalymmaceae*, which comprise 3768 characters including gaps, are included in the analyses.

Acrocalymma aquaticum Huang Zhang & K.D. Hyde [as 'aquatica'], Cryptog. Mycol. 33(3): 337 (2012)

Saprobic on dead, decaying stems of *Carex*, (Cyperaceae), **Sexual morph:** Undetermined. **Asexual morph:** *Conidiomata* 150–210 × 130–190 μm ($\bar{x}$ =170 × 150 μm, n = 15), pycnidial, immersed to semi-immersed, solitary or loosely aggregated, glabrous, papillate, unilocular, dark brown to black, globose to subglobose, covered with dark brown to black setae. *Peridium* 10–22 μm ($\bar{x}$ =16 μm, n = 15), outer layer composed with thick-walled, dark brown to black cells of *textura angularis*, the inner layer, thin, thin-walled cells in *textura angularis*, converting to hyaline cells towards conidial hymenium. *Conidiophores* reduced to conidiogenous cells. *Conidiogenous cells* 5–14 × 3–5 μm ($\bar{x}$ =12 × 4.5 μm, n = 10), hyaline, enteroblastic, phialidic, ampulliform to lageniform, determinate, originate from inner most layers of peridium. *Conidia* 10–18 × 2–4 μm ($\bar{x}$ =15 × 3 μm, n = 30), hyaline, cylindrical, obtuse at apex and a narrow truncate towards base, straight, aseptate, thin and smooth walled, guttulate, bearing a mucilaginous flabellate appendage at both ends.

Culture characteristics: Conidia germinating on MEA within 12 h. Germ tube produced from the side of conidia. Colonies growing on MEA, reaching 30 mm in 2 weeks at 25°C. Mycelia superficial, effuse to flat or undulate, from above gray to off white at the center, hyaline to entire edge, from reverse off white to light brown at the center, hyaline to the edge.

Material examined: Thailand, Chang Prachuap Khiri Khan Province, Pran Buri District, Pran Buri river, on decaying submerged stems of *Carex* sp. (Cyperaceae), 04 January 2025, Tharindu Bhagya, T192 (MFLU 25-0420).

GenBank Numbers – MFLU 25-0420: ITS = PX518039

Distribution – On decomposing submerged wood, Chiang Mai Province, Thailand (Zhang et al., 2011), on decomposing submerged wood, Tak Province, Thailand (Calabon et al., 2023), and on decaying submerged stems of *Carex* sp. Chang Prachuap Khiri Khan Province, Thailand (This study).

Notes – The new isolate obtained from *Carex* sp. forms a clade sister to *Acrocalymma aquaticum* strains MFLUCC 20-0124 and MFLUCC 11-0208, with strong support (99% ML and 1.00 BPP) (Figure 4.11). Phylogenetically, strain MFLU 25-0420 exhibit 98.1% similarity in ITS sequences and 99.8% similarity in LSU

sequences (excluding gaps) with strain MFLUCC 11-0208. Morphologically, the new strain MFLU 25-0420 resembles the type strain of *A. aquaticum*, characterized by globose to subglobose, glabrous, papillate conidiomata, enteroblastic, phialidic, ampulliform to lageniform conidiogenous cells, and hyaline, aseptate, cylindrical conidia with obtuse apices, truncate bases, and flabellate appendages (Figure 4.12) (Zhang et al., 2011; Calabon et al., 2023). Based on the available evidence, I recognize MFLU 25-0420 as a new strain of *A. aquaticum*, isolated from a *Carex* sp. substrate in a freshwater river in Thailand.

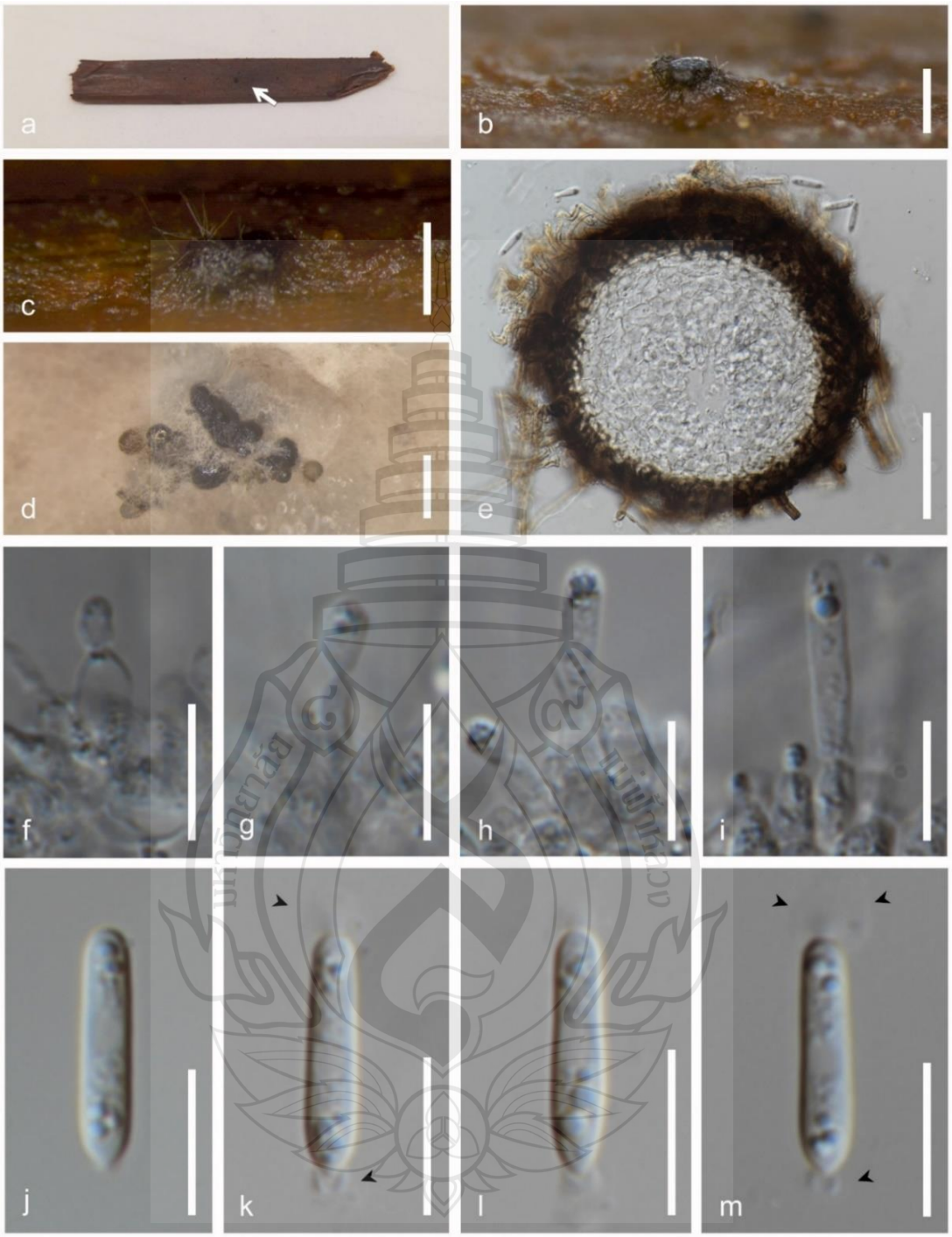

Note a *Carex* sp. host material. b–c Conidiomata on the host surface with setae. d Conidiomata, *in vitro.* e Cross section of conidiomata. f–i Conidiogenous cells and conidia development. j–m Conidia with flabellate mucilaginous appendage at both ends (arrowed). Scale bars: b–c 500 µm, d 1.00 mm, e 50 µm, f–m 10 µm.

Figure 4.12 *Acrocalymma aquaticum* (MFLU 25-0420)

***Bambusicolaceae* D.Q. Dai & K.D. Hyde**

***Bambusicola* D.Q. Dai & K.D. Hyde**

Bambusicola was erected by D.Q. Dai & K.D. Hyde in 2012 and typified by *Bambusicola massarinia* (Dai et al., 2012). Members of the genus are mainly reported as saprobic organisms and opportunistic pathogens associated with terrestrial bamboo plants. *Bambusicola aquatica* represents the first report of the genus from an aquatic, submerged environment (Brahmanage et al., 2020; Phookamsak et al., 2024). *Bambusicola* is a pleomorphic genus. The sexual morph is characterized by immersed, conical, ostiolate ascomata with a peridium composed of an outer layer of thick-walled cells in *textura angularis*, and an inner layer of hyaline cells. Pseudoparaphyses are longer than the asci and show anastomosing and branching nature. Asci in the genus *Bambusicola* are bitunicate, cylindrical, with short, furcate pedicels and shallow apical chambers. Each ascus bears eight, hyaline, smooth-walled, broadly fusiform, 1-septate ascospores with a gelatinous sheath. The asexual morphs of *Bambusicola* produce subglobose, immersed conidiomata that bear hyaline, smooth, holoblastic, annellidic, discrete, and cylindrical conidiogenous cells. These give rise to pale brown to dark brown, smooth, thick-walled, cylindrical, straight to slightly curved, 1–3-septate, multi-guttulate conidia with obtuse apices (Dai et al., 2012; Dai et al., 2017; Brahmanage et al., 2020).

Note Bootstrap support values for ML ≥ 90 % and Bayesian posterior probabilities (BPP) ≥ 0.9 are mentioned at the nodes. The tree was rooted to *Pseudotetraploa bambusicola* (CGMCC 3-20939), and *P. curviappendiculata* (JCM 12852). Newly generated sequence is in red and the type strains are in bold.

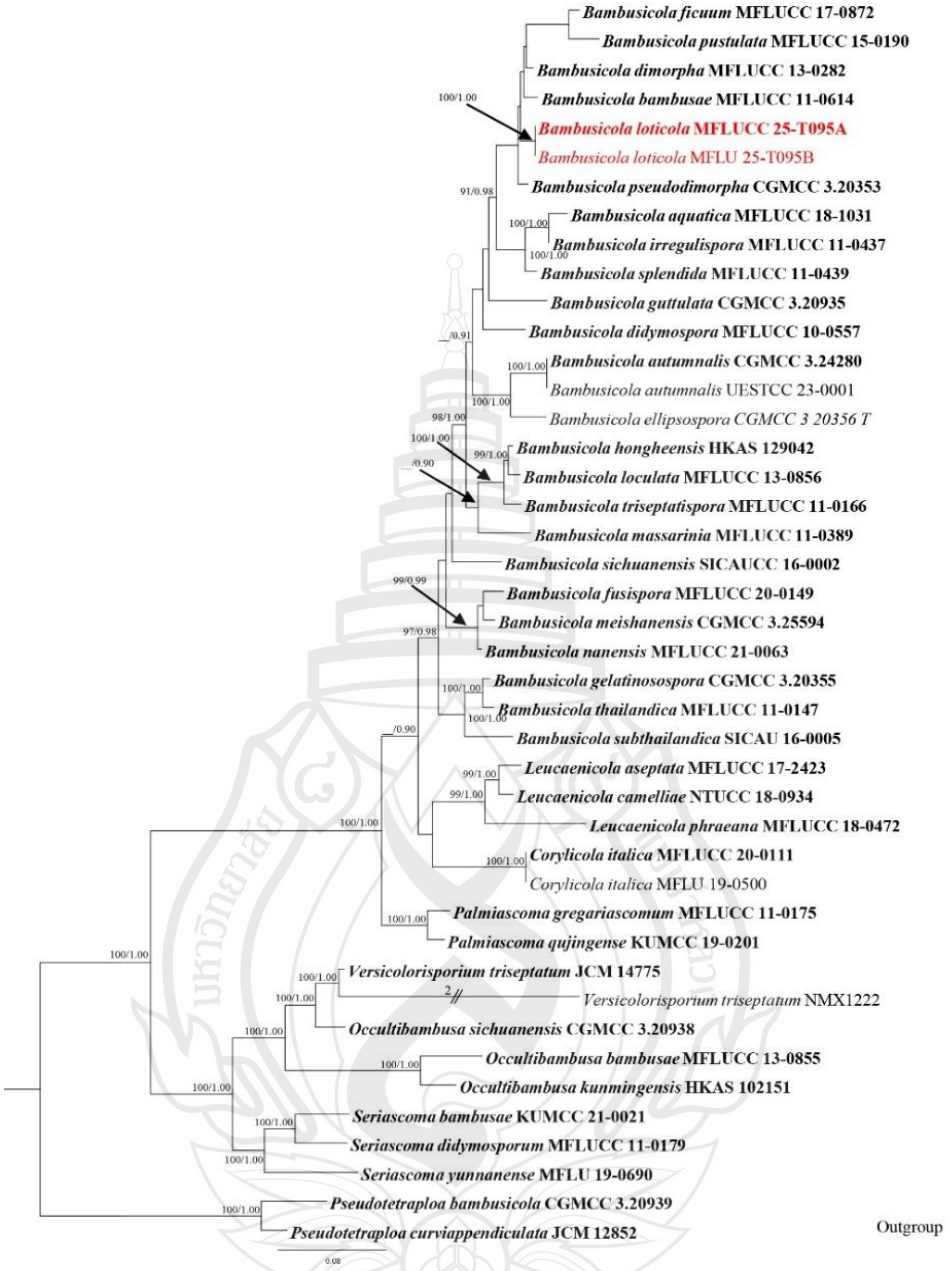

Note Bootstrap support values for ML ≥ 90 % and Bayesian posterior probabilities (BPP) ≥ 0.9 are mentioned at the nodes. The tree was rooted to *Pseudotetraploa bambusicola* (CGMCC 3-20939), and *P. curviappendiculata* (JCM 12852). Newly generated sequence is in red and the type strains are in bold.

Figure 4.13 Phylogram generated from Maximum Likelihood (ML) analysis based on combined LSU, ITS, *rpb2*, SSU, and *tef1-α* sequence. The data set comprises 5068 characters including gaps from of selected 32 strains which were included in the phylogenetic analyses.

Bambusicola loticola Bhagya, Phukhams E.B.G. Jones & K.D. Hyde, sp. nov.

Index Fungorum number: IF; Facesoffungi number: FoF 18901

Etymology – Named after its riverine habitat the species was removed.

Holotype – MFLU 25-0421

Saprobic on dead, moist, decaying stems of *Bambusa*, (Poaceae), **Sexual morph**: Undetermined. **Asexual morph**: Coelomycetous, *Conidiomata* 80–170 × 130–250 µm ($\bar{x}$ = 125 × 185 µm, n = 5), pycnidial, coriaceous, gregarious, semi-immersed or erupt from host epidermis, dark brown to black, globose to subglobose with single central ostiole. *Conidiomatal wall* 5–20 µm wide ($\bar{x}$ = 14 µm, n = 10), multi layered, thick outer layer composed from brown to black cells of *textura angularis*, inner most layer comprises from thinner, hyaline cells of *textura angularis*. *Conidiogenous cells* 4–10 × 1–2 µm ($\bar{x}$ = 7.5 × 1.5 µm, n = 10), originates from the inner hyaline layer of conidiomata, smooth-walled, hyaline, ampulliform to obpyriform or cylindrical and holoblastic, sachizolytic detachment of spores. *Conidia* 15–35 × 4–6 µm ($\bar{x}$ = 25.5 × 5.5 µm; n = 20), hyaline and unicellular at the origin, yellowish brown, cylindrical, straight to slightly curved thick-walled at maturity, 3-septate, slightly constricted at septa, process prominent guttules, obtuse at both ends, occasionally narrower at base.

Culture characteristics: Conidia germinating on MEA within 24 h. Germ tubes produced from each cell of conidia. Colonies growing on MEA, reaching 20–30 mm in 2 weeks at 25°C. Mycelia superficial, cottony, umbonate shape culture with erose edge, from above off-white cottony center with pale yellow ring, white to hyaline at the edge, from reverse yellowish brown at the center and off white at the edge. Mycelium rapidly radiates to the culture.

Material examined: Thailand, Chang Wat Prachuap Khiri Khan Province, Pran Buri District, Pran Buri River, on decaying stems of Bamboo (Poaceae). 05 Jan 2024, Tharindu Bhagya, T95 (MFLU 25-0421, holotype), *ibid.,* T95_2, Bamboo (Poaceae) (MFLU 25-0422, isotype).

GenBank numbers – MFLU 25-0421: ITS = PP572909

Distribution – Decaying submerged Bamboo, *Poaceae.* stem, in freshwater river, Thailand.

Notes – Multigene phylogenetic analysis placed the new isolates of *B. loticola* (MFLU 25-0421 and MFLU 25-0422), in an independent lineage within *Bambusicola*,

with strong statistical support (72% ML and 0.80 BPP) (Figure 4.13). The phylogenetically closest taxon to the new isolate, strain MFLU 25-0421, is *B. bambusae* strain MFLUCC 11-0614. Strain MFLU 25-0421 differs from MFLUCC 11-0614 by 1.4% in ITS sequences, 1.1% in LSU sequences, and 2.6% in *tef1-α* sequences (excluding gaps). Furthermore, the pairwise distance matrix value between MFLU 25-0421 and other related taxa was >0.05, indicating that the isolates belong to the same genus, *Bambusicola*, but represent a distinct species (Gostinčar, 2020; Maharachchkumbura et al., 2021). *Bambusicola irregulispora* strain MFLUCC 11-0437 and *B. splendida* strain MFLUCC 11-0439 share morphological similarities with strain MFLU 25-0421. However, the presence of two-layered conidiomata and predominantly ampulliform to obpyriform conidiogenous cells distinguishes strain MFLU 25-0421 from *B. irregulispora* and *B. splendida* (Figure 4.14) (Dai et al., 2012). These strains also form distinct clades separate from the newly isolated strains. Considering the available evidence, I recognize the isolate *B. loticola* (MFLU 25-0421 and MFLU 25-0422) as a new species of *Bambusicola*, collected from a submerged, decomposing bamboo stem in a freshwater river in Thailand.

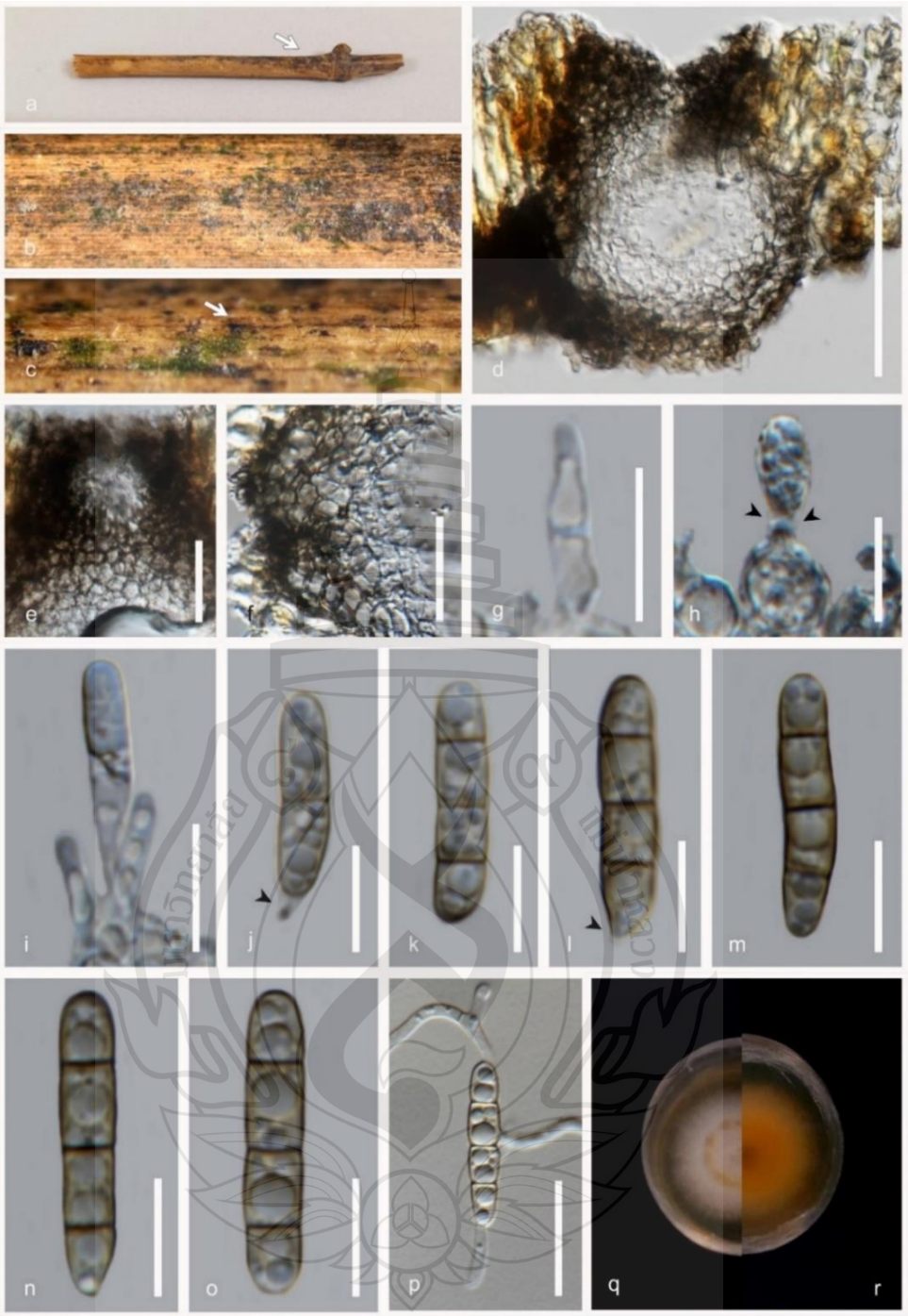

Note a Bamboo host material. b–c Conidiomata on host (arrowed). d Vertical section conidiomata. e Ostiole. f Peridium. g–h Holoblastic, and ampulliform conidiogenous cells (arrowed). j–o Conidia and occasional narrowed base (arrowed). p Germinated conidiospore. q Culture on MEA above. r reverse. Scale bars: d–e 50 µm, f 20 µm, g–o 10 µm, p 20 µm.

Figure 4.14 *Bambusicola loticola* (MFLU 25-0421, holotype)

Corynesporascaceae Sivan

Corynespora Güssow, J. Royal Agric. Soc. England 65: 272 (1905) [1904]

The genus *Corynespora* was introduced by Güssow in 1904 and typified with *C. mazei*, which was later synonymized with *C. cassiicola* by C.T. Wei in 1950 based on morphological evidence (Hyde et al., 2020; Du et al., 2024; Zhang et al., 2025). Members of the genus are known from both sexual and asexual morphs. The sexual morphs are characterized by dark brown to black, superficial or immersed, globose, subglobose, or pyriform carbonaceous ascomata, with walls composed of *textura angularis* and *textura prismatica*. The pseudoparaphyses are hyaline, smooth-walled, septate, and unbranched. Asci are bitunicate, fissitunicate, cylindrical to clavate, and bear eight hyaline to pale brown, smooth- to rough-walled, ellipsoid to fusiform, distoseptate ascospores (Li et al., 2023; Liu et al., 2023). The asexual morphs of *Corynespora* develop brown to dark brown conidiophores with integrated, terminal, conidiogenous cells that produce solitary to catenate, acrogenous, distoseptate conidia (Du et al., 2024; Zhang et al., 2025).

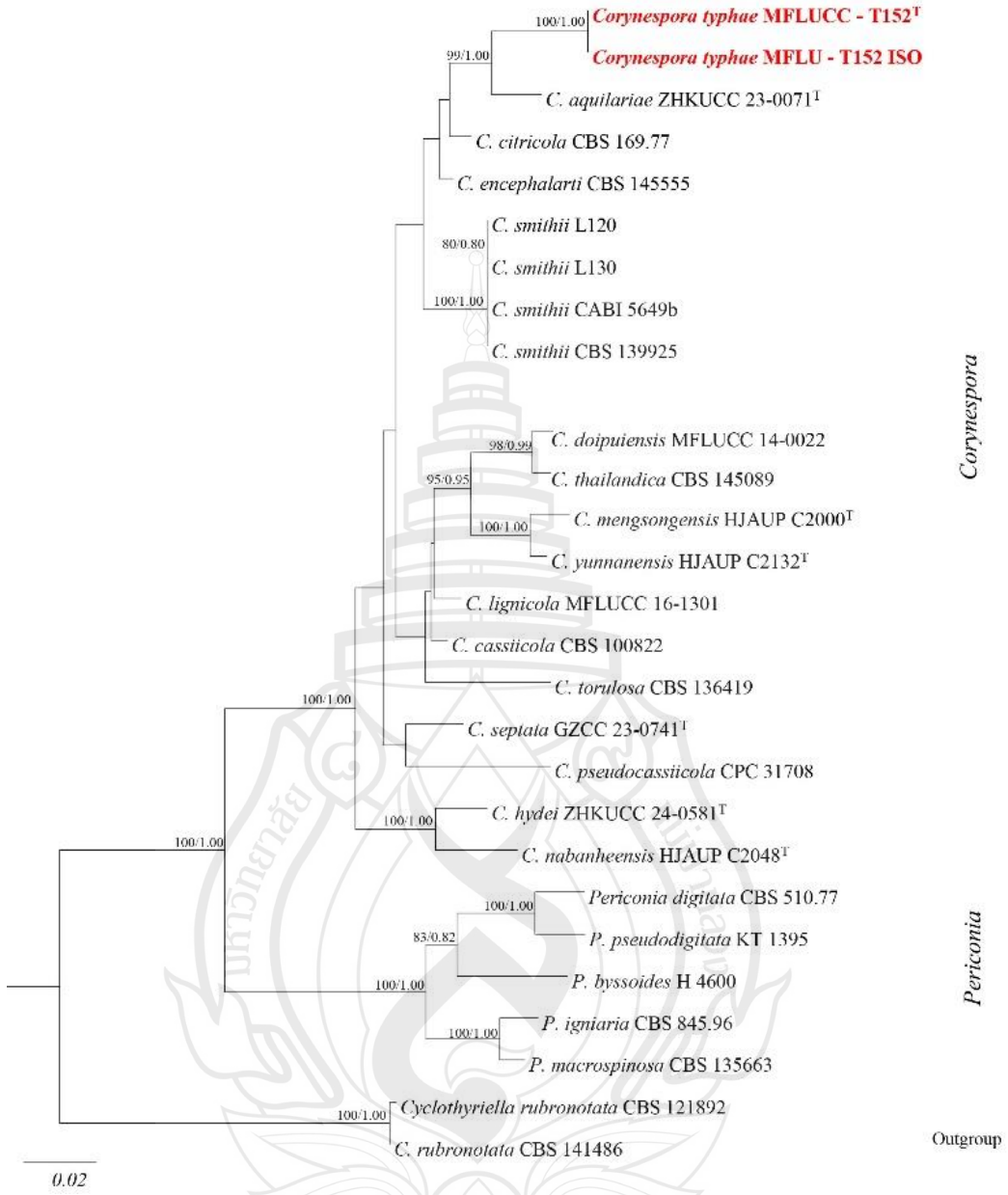

Note Bootstrap support values for maximum likelihood (ML, first value) equal to or greater than 80% and Bayesian posterior probabilities from MCMC analyses (BYPP, second value) equal to or greater than 0.80 are mentioned above the nodes. The scale bar indicates expected changes per site. The tree is rooted to *Cyclothyriella rubronotata* (CBS 121892 and CBS 141486). Ex-type strains are indicated with "T". The newly generated sequences are indicated in red.

Figure 4.15 Maximum likelihood consensus tree inferred from the combined ITS, SSU, LSU, and *tef1-α* multiple sequence alignments.

Corynespora typhae. Bhagya, Phukhams., K.D. Hyde & E.B.G. Jones, ***sp. nov.***

Index Fungorum number: IF; Facesoffungi number: FoF 18902

Etymology – in reference to the host genus the species was isolated.

Holotype – MFLU 25-0423

Saprobic on dead decomposing leaf of *Thypa*, (Typhaceae), **Sexual morph**: Undetermined. **Asexual morph**: *Hyphomycetous*, scattered to subfasciculate on host, dark brown and amphigenous hairy. *Mycelium* 1–3.5 μm ($\bar{x}$ = 2.5 μm, n = 10), immersed or partly superficial, pale-brown to dark brown, smooth, thick walled, septet, simple or branched. *Conidiophores* 110–190 × 4.5–7.5 μm ($\bar{x}$ = 172 × 5.5 μm, n = 10), macronematous, mononematous, dark brown to black at base, pale brown to olivaceous brown towards apex, thick-walled, 5–8-septate, smooth, flexuous or straight, unbranched. *Conidiogenous cells* 25–36 x 2–7 μm ($\bar{x}$ = 28 × 4.5 μm, n = 10), monotretic, monoblastic, integrated, terminal, determinate, olivaceous to pale-brown or brown, smooth, thick-walled, cylindrical to sub-cylindrical or clavate. *Conidia* 190–260 × 11–16 μm ($\bar{x}$ = 245 × 12.5 μm, n = 20), acrogenous, 20–28-distoseptate, constricted at 5th or 7th septum, smooth, thick walled, olivaceous brown to pale-brown, sub hyaline at the apexes, elongated, cylindrical or obclavate, straight to slightly curved with flexuous towards the pointed apex, truncate at the base with prominent dark basal scar.

Culture characteristics: Conidia germinating on malt extract agar (MEA) within 24 h. Germ tubes produced from the ends of the conidium. Colonies growing on MEA, reaching 30 mm in 8 weeks at 25°C. Mycelia superficial, dense, effuse to umbonate, with complete edges, from above off white to cinereous at center and olivaceous brown and hyaline to the edge, from reverse dark brown to black at the center and light brown to subcinereous at the edge.

Material examined: Thailand, Chang Wat Prachuap Khiri Khan Province, Pran Buri District, Pran Buri wetland, on decaying stems of *Typha* sp. (Typhaceae), 01 December 2023, Tharindu Bhagya, T152 (MFLU 25-0423, holotype), *ibid*., T152_ISO (MFLU 25-0424).

GenBank numbers – MFLU 25-0423: ITS = PX129558, LSU = PX129608, MFLU 25-0424 ITS = PX129556, LSU = PX129642

Notes –The new isolate *Corynespora typhae* (MFLU 25-0423) forms a sister clade to *C. aquilariae* (ZHKUCC 23-0071) with 99% maximum likelihood (ML) and 1.00

Bayesian posterior probability (BYPP) support (Figure 4.15). Pairwise sequence comparisons indicate that MFLU 25-0423 differs from *C. aquilariae* (ZHKUCC 23-0071) by 5.68% in ITS and 1.32% in LSU sequences, excluding gaps. Furthermore, the pairwise distance matrix values were >0.05 between MFLU 25-0423 and other closely related taxa (Gostinčar, 2020; Maharachchikumbura et al., 2021), indicating that the new isolate represents a congenic but distinct species within *Corynespora*. Morphologically, *Corynespora* (MFLU 25-0423) is distinguishable from *C. aquilariae* (ZHKUCC 23-0071) by the larger height-to-width ratio of conidiogenous cells (6.23 vs. 2.11) and the absence of percurrent proliferation (Du et al., 2024). The conidia of MFLU 25-0423 are 20–28-distoseptate, whereas those of *C. aquilariae* comprise 10–16 distosepta, further supporting the morphological distinction. The combination of conidiogenous cell structure, conidial morphology including 20–28 distosepta, and olivaceous-brown to pale brown conidia with subhyaline apices makes MFLUCC 25-xxxxa clearly distinguishable from other described *Corynespora* species (Figure 4.16) (Li et al., 2023; Du et al., 2024; Zhang et al., 2025). *Corynespora submersa* strain MFLUCC 16-1101 was excluded from the analysis due to its uncertain placement within the phylogenetic tree. Considering both molecular and morphological evidence, I recognize *C. typhae* (MFLU 25-0423) as a new species of *Corynespora*, isolated from decomposing *Typha* sp., in a freshwater coastal wetland in Thailand.

Note a *Typha* sp. host material. b–c Conidiophores on the host surface with erected conidia. d–e Conidiophores with conidiogenous cells at terminals. f–g Conidiogenous cells with developing conidia attached. h–j Conidia development. k–m Mature conidia. Scale bars: b–c 250 µm. d–m 20 µm.

Figure 4.16 *Corynespora typhae* (MFLU 25-0423, holotype)

Dictyosporiaceae Boonmee & K.D. Hyde

Dictyocheirospora *M.J. D'souza, Boonmee & K.D. Hyde*

Dictyocheirospora is a hyphomycetous genus established by M.J. D'Souza in 2016 and typified by *Dictyocheirospora rotunda* (Boonmee et al., 2016). Members of this genus have been isolated as saprobic organisms on decomposing plant materials in both terrestrial and aquatic environments, leading to the conclusion that *Dictyocheirospora* is an aero-aquatic, monophyletic genus. The sexual morphs of *Dictyocheirospora* are yet to be discovered, while the asexual morphs are characterized by sporodochial, punctiform conidiomata or aggregations of conidia on host materials. The mycelium is predominantly immersed, branched, septate, and hyaline to subhyaline or pale brown (Boonmee et al., 2016; Tibpromma et al., 2018; Liu et al., 2023). The conidiophores in *Dictyocheirospora* are hyaline to subhyaline or pale brown, septate, and either micronematous or semi-macronematous. These conidiophores bear integrated, holoblastic, determinate, and doliiform conidiogenous cells. *Dictyocheirospora* produces cheiroid, acrogenous, pale brown to dark brown, smooth-walled, euseptate or distoseptate conidia arranged in 6–8 rows of cells. The presence of appendages and hooked apices varies depending on the species (Boonmee et al., 2016; Tibpromma et al., 2018; Dong et al., 2020; Liu et al., 2023).

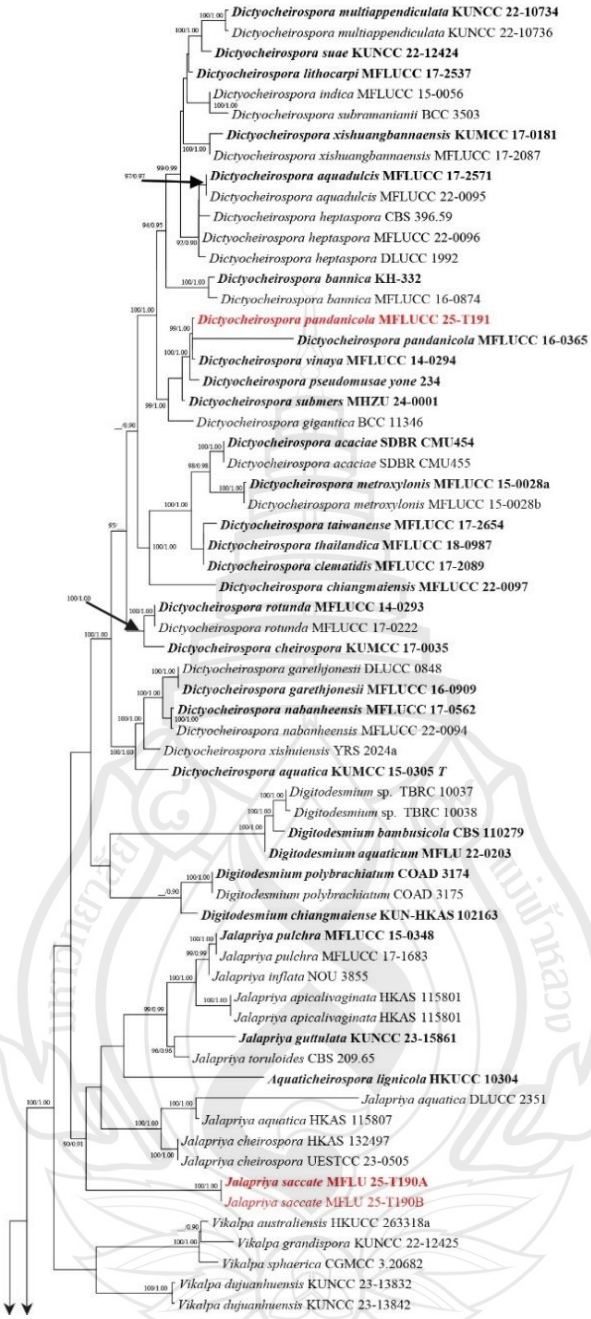

Note Bootstrap support values for ML ≥ 90 % and Bayesian posterior probabilities (BPP) ≥ 0.9 are mentioned at the nodes. The tree was rooted to *Periconia igniaria* (CBS 379.86 and CBS 845.96). Newly generated sequences are in red and the type strains are in bold.

Figure 4.17 Phylogram generated from Maximum Likelihood (ML) analysis based on combined SSU, ITS, LSU,and *tef1-α* sequence. The data set comprises 3938 characters including gaps from of selected 126 strains which were included in the phylogenetic analyses.

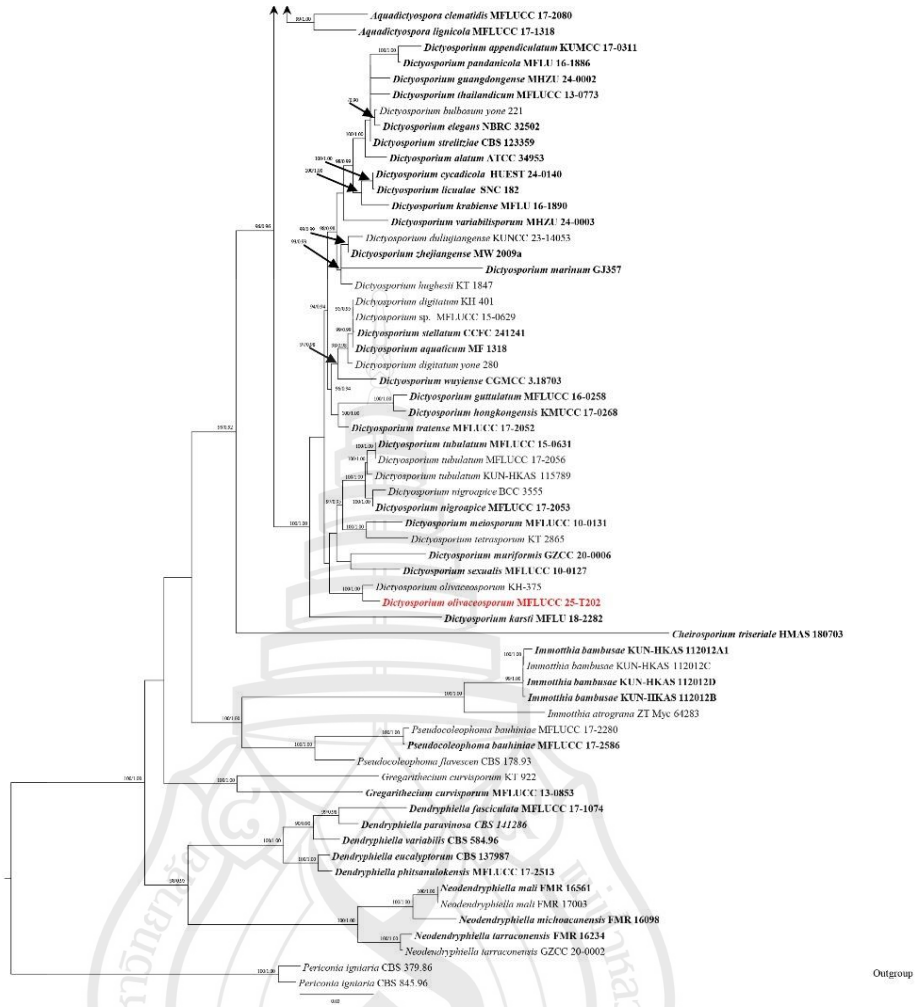

Figure 4.17 (continued)

Dictyocheirospora pandanicola Tibpromma & K.D. Hyde, in Tibpromma et al., Fungal Diversity 93: 10 (2018)

Saprobic on dead, decaying stems of *Typha,* (Typhaceae), **Sexual morph:** Undetermined. **Asexual morph:** *Hyphomycetous*, sporodochia on host, black to reddish brown or olivaceous, punctiform, scattered. *Conidiophores*, micronematous, abbreviated to conidiogenous cells. *Conidiogenous cells* 8–20 ×1–3 µm ($\bar{x}$ = 13 × 2.5 µm, n = 10), holoblastic, integrated, terminal, subcylindrical to cylindrical, determinate, doliiform, hyaline to sub-hyaline or pale brown. *Conidia* 55–80 ×15–35 µm ($\bar{x}$ = 65 × 25 µm, n = 20), ellipsoidal, subcylindrical, schizolytic, cheiroid, consisting of 90–120 cells, combined with 6–7 tightly appressed 6–18 euseptate, occasionally divergent or curved rows of cells, process cuneiform or rounded basal cell, brown to dark brown,

acrogenous, smooth, thick-walled, lack appendages or mucilaginous sheaths. **Sexual morph:** Undetermined.

Culture characteristics: Conidia germinating on MEA within 24 h. Germ tube produced multiple cells of conidia. Colonies growing on MEA, reaching 40 mm in 3 weeks at 25°C. Mycelia superficial, effuse to flat or undulate, from above gray to off white at the center, hyaline to the errors edge, from reverse yellowish brown, at the center, light brown to yellowish ring with off-white to hyaline tips at edge.

Material examined: Thailand, Chang Wat Prachuap Khiri Khan Province, Pran Buri District, Pran Buri Wetland, on decaying stems of *Typha* sp. (Typhaceae), 06 April 2024, Tharindu Bhagya, TB202 (MFLU 25-0425).

GenBank numbers – MFLU 25-0425: ITS = PX518040

Distribution – On decomposing Pandanus sp. Prachuap Khiri Khan Province, Thailand (Boonmee et al., 2016), decomposing *Typha*, stem, Chang Wat Prachuap Khiri Khan Province, Thailand (This study).

Notes – The new isolate clustered as a sister species to *Dictyocheirospora pandanicola* strain MFLUCC 16-0365, with 99% maximum likelihood (ML) and 1.00 Bayesian posterior probability (BPP) support (Figure 4.17). Strain MFLU 25-0425 agrees with the general description of *Dictyocheirospora*, exhibiting sporodochial, punctiform conidiomata and holoblastic, determinate, doliiform conidiogenous cells (Figure 4.18) (Boonmee et al., 2016; Tibpromma et al., 2018; Liu et al., 2023). Phylogenetically, the new isolates share 99.6% similarity in ITS sequences, 99.3% similarity in LSU sequences, and 97.8% similarity in *tef1-α* sequences (excluding gaps). Morphologically, our new isolate resembles *D. pandanicola* strain MFLUCC 16-0365 in producing reddish-brown sporodochia, holoblastic, cylindrical conidiogenous cells, and ellipsoidal to subcylindrical, cheiroid conidia with similar height-to-width ratios (2.60 vs 2.70) (Tibpromma et al., 2018). Considering the available evidence, I recognize MFLUCC 25-0425 as *D. pandanicola* and report a new host record for this species from *Typha* sp. in coastal freshwater wetlands in Thailand.

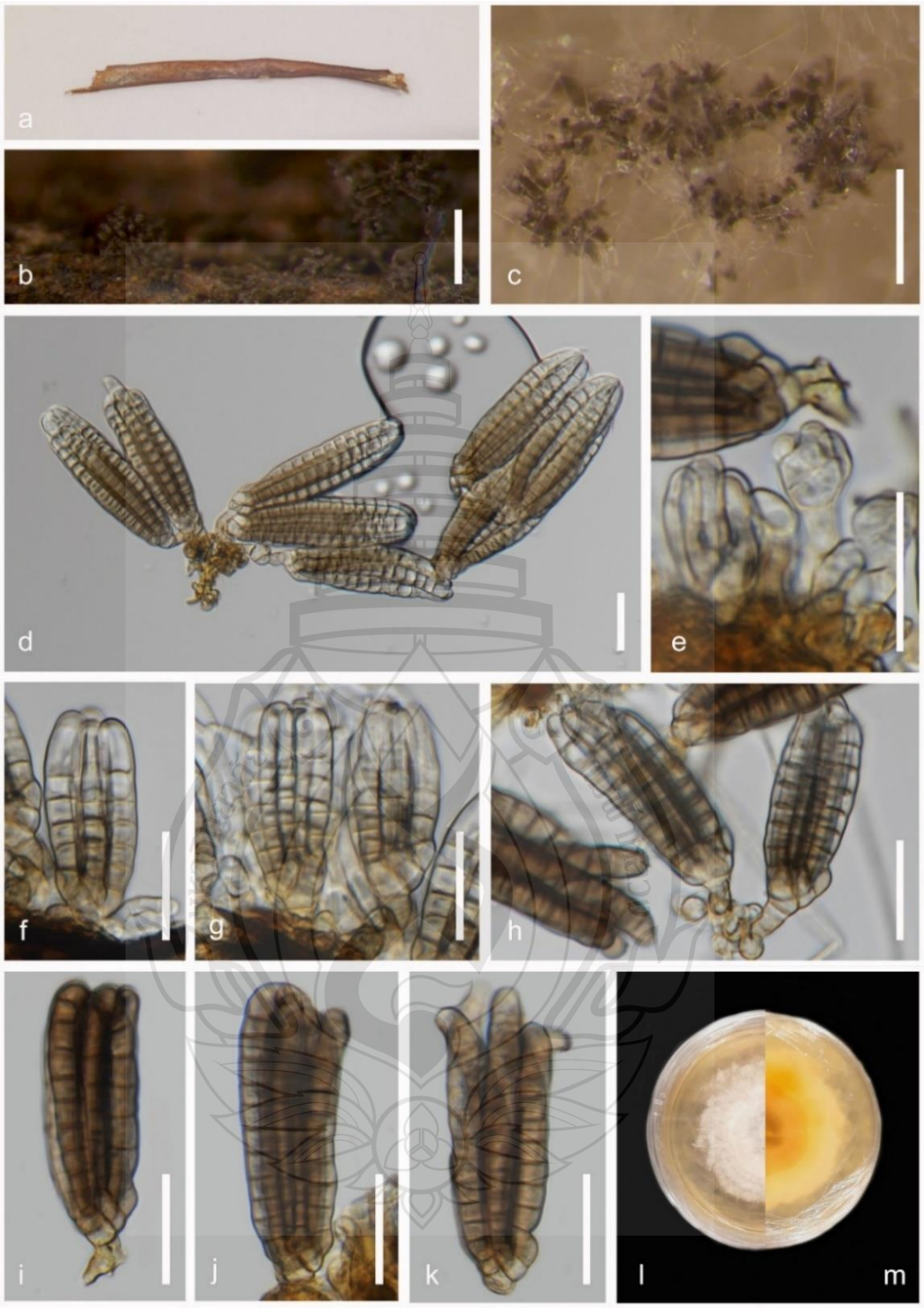

Note a *Typha* sp. host material. b Sporodochia on host surface. c Sporodochia, *in vitro*. d Squash mount of sporodochia in water. e–h Conidiogenous cells and conidia development. i–k Conidia. l Culture on MEA above. m reverse. Scale bars: b–c 250 µm, d–k 20 µm.

Figure 4.18 *Dictyocheirospora pandanicola* (MFLU 25-0425)

Dictyosporium Corda

Dictyosporium is a monophyletic genus in the family *Dictyosporiaceae*, introduced by Corda in 1837 and typified by *Dictyosporium elegans*. Members of *Dictyosporium* exhibit both sexual and asexual morphs. The sexual morphs are characterized by superficial, subglobose, black to dark brown perithecial ascomata with an apical ostiole. The peridium is composed of 2–3 layers of membranaceous cells arranged in a textura epidermoidea (Boonmee et al., 2016; Liu et al., 2023). Pseudoparaphyses in *Dictyosporium* are hyaline, cellular, and septate. Asci are bitunicate, fissitunicate, cylindrical, with well-developed ocular chambers and pedicellate bases. Each ascus bears eight, hyaline, fusiform, 1-septate ascospores that are constricted at the septum. Asexually, *Dictyosporium* forms hyphomycetous, effuse, brown to black, granular sporodochial colonies on the substrate. Conidiophores are micronematous, mononematous, hyaline to pale brown, and flexuous. These conidiophores develop monoblastic, integrated, determinate, cylindrical, doliiform to subsphaerical, terminal conidiogenous cells, which give rise to acrogenous, occasionally pleurogenous, olive to brown, smooth-walled, branched, cheiroid conidia composed of 4–7 rows of connected cells. *Dictyosporium* species have been isolated as saprobic organisms from both aquatic and terrestrial environments (Boonmee et al., 2016; Liu et al., 2023).

Dictyosporium olivaceosporum Kaz. Tanaka, K. Hiray., Boonmee & K.D. Hyde, in Boonmee et al., Fungal Diversity 80: 474 (2016)

Saprobic on dead, decaying stems of *Typha*, (Typhaceae). **Sexual morph:** Undetermined. **Asexual morph:** *Hyphomycetous*, sporodochia on host, tightly aggregated, black to olivaceous to brown. *Conidiophores*, micronematous, olivaceous to sub-hyaline, occasionally reduced to conidiogenous cells. *Conidiogenous cells* 6–8 ×2–5 μm ($\bar{x}$ = 6.5 × 3.5 μm, n = 10), holoblastic, integrated, terminal, olivaceous or hyaline to sub-hyaline. *Conidia* 30–50 ×18–30 μm ($\bar{x}$ = 40 × 24 μm, n = 20), solitary, ellipsoid to cylindrical, cheiroid, not complanate, olivaceous to brown, composed by 25–50 cells arranged in 5–6 rows with 6-9 euseptate, process light brown color basal connecting cell, occasionally bear globose to subglobose apical appendages from sides.

Culture characteristics: Conidia germinating on MEA within 72 h. Germ tube produced from the base of conidia. Colonies growing on MEA, reaching 40 mm in

2 weeks at 25°C. Mycelia superficial, effuse to flat or undulate, from above light yellow to off white at the center, white ring of mycelium surrounding the center and hyaline to the eros edge, from reverse orangish yellow at the center, with off-white to hyaline tips at edge.

Material examined: Thailand, Chang Wat Prachuap Khiri Khan Province, Pran Buri District, Pran Buri Wetland, on decaying stems of *Typha* sp. (Typhaceae), 06 April 202, Tharindu Bhagya, TB191 (MFLU 25-0426).

GenBank numbers – MFLU 25-0426: ITS = PX518043

Distribution – Submerged twigs of woody plant, Tropical Biosphere Research Center, Okinawa, Japan (Boonmee et al., 2016), and decomposing *Typha*, stem, Chang Wat Prachuap Khiri Khan Province, Thailand (This study).

Notes – The new strain, MFLU 25-0426, forms a clade with *Dictyosporium olivaceosporum* strain KH 375 with strong statistical support (100% ML and 1.00 BPP) (Figure 4.170. Our isolate resembles the genus *Dictyosporium* by producing sporodochial colonies on the substrate with cylindrical, doliiform to subsphaerical, terminal, monoblastic conidiogenous cells that give rise to olivaceous to brown, smooth-walled, branched, cheiroid conidia (Figure 4.19) (Boonmee et al., 2016). Phylogenetically, strain MFLU 25-0426 shares 98.2% similarity in ITS sequences, 99.6% similarity in LSU sequences, and 98.4% similarity in tef1-α sequences (excluding gaps). Morphologically, the new isolate shows significant similarities to *D. olivaceosporum* strain KH 375, including olivaceous, cylindrical, cheiroid conidia with 25–50 cells arranged in 5–6 rows, a similar height-to-width ratio on the substrate (1.66 vs. 1.57), and the presence of globose to subglobose apical appendages (Boonmee et al., 2016). Considering the available evidence, I recognize strain MFLU 25-0426 as *D. olivaceosporum*, isolated from decomposing *Typha* sp. substrate in a coastal freshwater wetland in Thailand.

Note a *Typha* sp. host material. b–c Sporodochia on host surface. d Squash mount of sporodochia in water. e–h Conidiophores bearing conidiogenous cells (arrowed) and conidia development with light brown color cells at edge (arrowed). i-m Conidia with occasional apical appendages (arrowed). n Culture on MEA above. o reverse. Scale bars: b–c 500 µm, d 50 µm, e–m 20 µm.

Figure 4.19 *Dictyosporium olivaceosporum* (MFLU 25-0426)

Jalapriya M.J. D'souza, Hong Y. Su, Z.L. Luo & K.D. Hyde

The genus *Jalapriya* was introduced by D'Souza in 2016 and is typified by *Jalapriya pulchra*. This is a hyphomycetous genus predominantly isolated from woody litter associated with aquatic environments (Boonmee et al., 2016). Members of *Jalapriya* are characterized by dark brown to pale brown effuse colonies, which develop micronematous, smooth, cylindrical conidiophores. These conidiophores bear holoblastic, integrated, determinate, and terminal conidiogenous cells. *Jalapriya* produces acrogenous, cheiroid, complanate or non-complanate, smooth-walled conidia with 5–7 rows of cells. These rows of cells may be convergent or non-convergent at the apex, depending on the species (Boonmee et al., 2016; Du et al., 2025).

Jalapriya saccate Bhagya, Phukhams E.B.G. Jones & K.D. Hyde, sp. nov.

Index Fungorum number: IF; Facesoffungi number: FoF 18903

Etymology – The name refers to the sac-shaped epical appendages observed in the species.

Holotype – MFLU 25-0427

Saprobic on dead, decaying stems of *Typha*, (Typhaceae), **Sexual morph:** Undetermined. **Asexual morph:** *Hyphomycetous*, appear as scatted sporodochia on host, off white to hyaline, punctiform. *Conidiophores*, reduced to conidiogenous cells. *Conidiogenous cells* 4–8 × 1–3 μm ($\bar{x}$ = 5.5 × 1.5 μm, n = 10), holoblastic, terminal, subcylindrical to cylindrical, hyaline to sub-hyaline or pale brown. *Conidia* 22–32 × 10–15 μm ($\bar{x}$ = 26 × 13 μm, n = 30), ellipsoidal, subcylindrical, schizolytic, combined with 2–4 tightly appressed 6–9 euseptate, rarely divergent rows of cells, process cuneiform or rounded basal cell, brown to dark brown, acrogenous, guttulate, smooth-walled, process two very prominent mucilaginous appendages at apexes.

Culture characteristics: Conidia germinating on MEA within 12 h. Germ tube produced multiple cells of conidia. Colonies growing on MEA, reaching 50 mm in 4 weeks at 25°C. Mycelia superficial, effuse to flat or undulate, from above yellowish gray to off white at the center followed by white, gray and anther wight ring towards bright yellow to sub-hyaline euros edge, from reverse yellowish brown, at the center, light brown to yellowish ring with off-white to hyaline tips at edge.

Material examined: Thailand, Chang Wat Prachuap Khiri Khan Province, Pran Buri District, Pran Buri wetland, on decaying stems of *Typha* sp. (Typhaceae), 06 April 2024, Tharindu Bhagya, TB190A (MFLU 25-0427, holotype), *ibid.*, TB190B, *Typha* sp. (Typhaceae) (MFLU 25-0428, isotype).

GenBank numbers – MFLU 25-0427: ITS = PX089563

Distribution – Decaying submerged *Typha* sp. stem, in freshwater river, Thailand.

Notes – The multi-locus phylogenetic analysis places our new isolates in an independent lineage, sister to the genus *Jalapriya* with 90% ML and 0.91 BPP support (Figure 4.17). Strains MFLU 25-0427 and MFLUCC 25-0428 morphologically resemble members of *Jalapriya* by exhibiting smooth, cylindrical conidiophores; holoblastic, integrated, determinate conidiogenous cells, and acrogenous, cheiroid conidia with multiple rows of cells (Figure 4.20) (Boonmee et al., 2016; Du et al., 2025). *Jalapriya cheirospora* was the most morphologically and phylogenetically closely related species to the new isolates. Phylogenetically, MFLU 25-0427 differs from *J. cheirospora* by 9.01% in ITS, 2.63% in LSU, and 8.32% in *tef1-α* sequences, excluding gaps. Furthermore, the pairwise distance matrix value was >0.05 between MFLU 25-0428 and other related taxa (Gostinčar, 2020; Maharachchkumbura et al., 2021). Morphologically, the new strains are distinguishable from other related taxa mainly by possessing cuneiform or rounded basal cells, 2–4 tightly packed, 6–9 euseptate, and rarely divergent rows of cells, as well as by bearing two conspicuous mucilaginous appendages at the apex. Considering the available phylogenetic and morphological evidence, I introduce strain MFLU 25-0427 as a new species in the genus *Jalapriya*, isolated from decomposing *Typha* sp. material in coastal freshwater wetlands of Thailand.

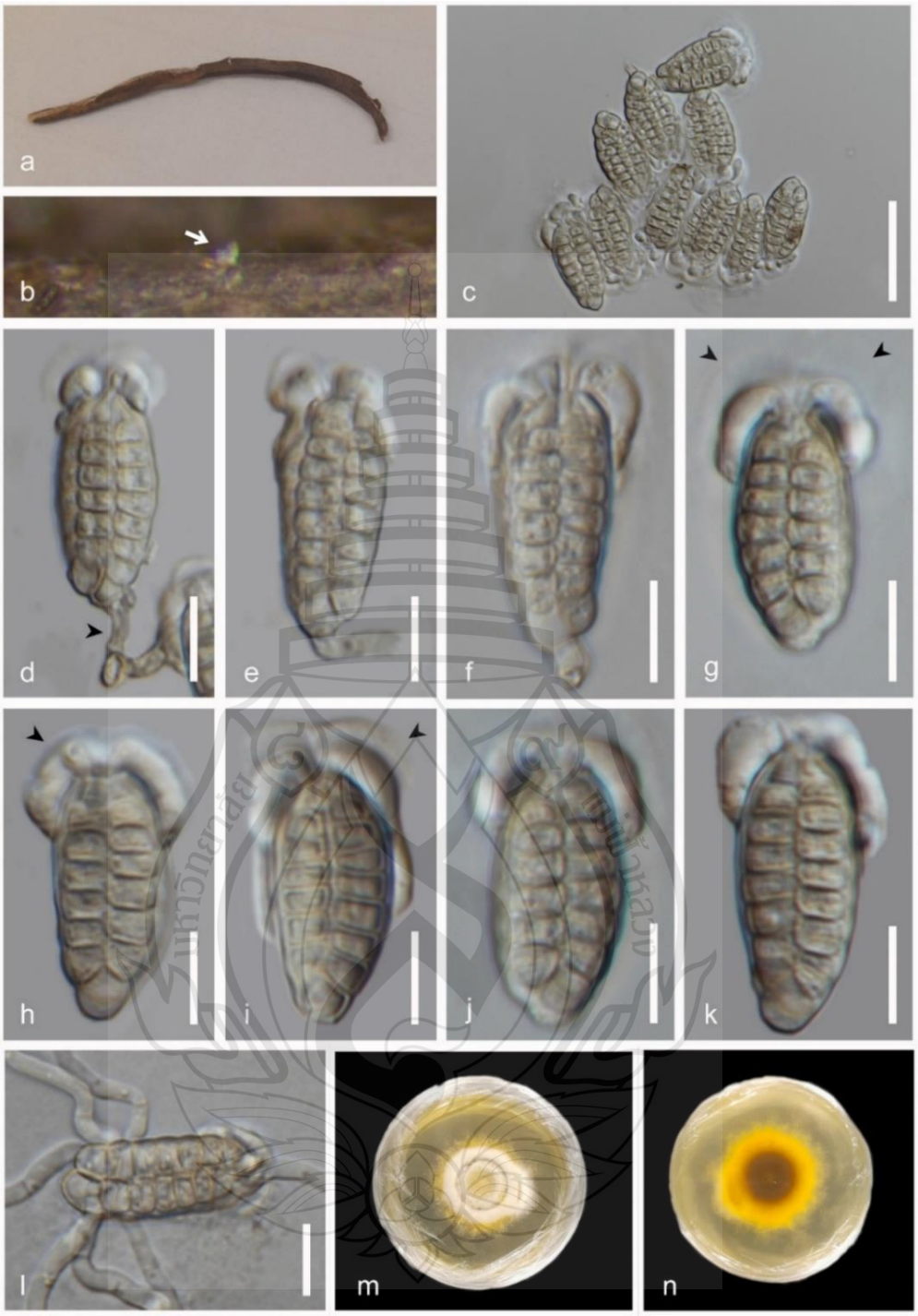

Note a *Typha* sp. host material. b Sporodochia on host surface. c Squash mount of sporodochia in water. d–f Conidiogenous cells (arrowed) and conidia development. g–k Conidia with prominent mucilaginous appendages (arrowed). l Germinating conidium. m Culture on MEA above. n reverse. Scale bars: b 250 µm, c 20 µm, d–l 10 µm.

Figure 4.20 *Jalapriya saccate* (MFLU 25-0427, holotype)

Didymosphaeriaceae Munk

Paraphaeosphaeria O.E. Erikss

Paraphaeosphaeria was proposed by O.E. Eriksson in 1967 and typified by *Paraphaeosphaeria michotii*. The sexual morphs of the genus are characterized by dark brown to black, globose to subglobose or ellipsoidal, single ostiolate, perithecial ascomata that are immersed to semi-erumpent in host tissue (Ariyawansa et al., 2014; Wanasinghe et al., 2018; Hongsanan et al., 2020). Pseudoparaphyses are abundant, hyaline, smooth-walled, filiform, septate, and unbranched. Asci in the genus *Paraphaeosphaeria* are bitunicate, fissitunicate, cylindrical to clavate, and possess short pedicels. Each ascus contains eight, oliveruse -brown to dark brown or pale brown, thick-walled, smooth to verrucose, ellipsoidal to fusiform, 1–3-septate ascospores, often constricted at the septa. The asexual morphs of *Paraphaeosphaeria* are recognized as *Paraconiothyrium*- or *Microsphaeropsis*-like. They are characterized by dark brown to black, immersed or erumpent, globose to subglobose, pycnidial conidiomata that produce hyaline, smooth-walled, ampulliform to lageniform, phialidic conidiogenous cells. The resulting conidia are pale brown to dark brown, thick-walled, smooth, ellipsoidal to ovoid, and 0–1-septate (Ariyawansa et al., 2014; Wanasinghe et al., 2018; Hongsanan et al., 2020; Tennakoon et al., 2022). *Paraphaeosphaeria* exhibits a worldwide distribution and shows a strong affinity toward monocotyledonous plants. Members of the genus are predominantly saprobic, occasionally act as opportunistic pathogens, and are rarely reported as endophytes (Ariyawansa et al., 2014; Wanasinghe et al., 2018; Hongsanan et al., 2020; Tennakoon et al., 2022; Absalan et al., 2024).

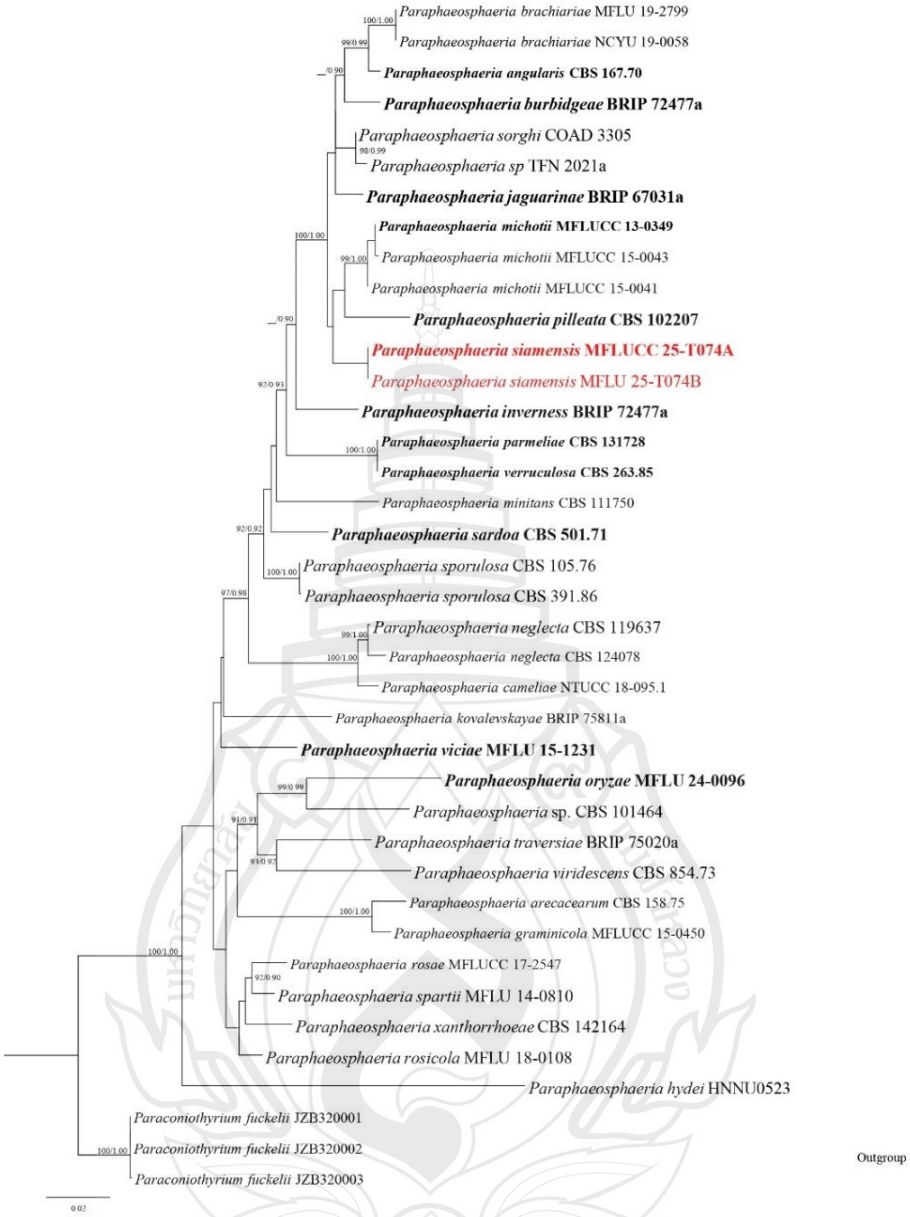

Note Bootstrap support values for ML ≥ 90 % and Bayesian posterior probabilities (BPP) ≥ 0.9 are mentioned at the nodes. The tree was rooted to *Paraconiothyrium fuckelii* (JZB320001, JZB320002, and JZB320003). Newly generated sequences are in red and the type strains are in bold.

Figure 4.21 Phylogram generated from Maximum Likelihood (ML) analysis based on combined ITS, LSU, SSU, and *tub2* sequence. The data set comprises 3358 characters including gaps from of selected 39 strains which were included in the phylogenetic analyses.

Paraphaeosphaeria siamensis Bhagya, Phukhams E.B.G. Jones & K.D. Hyde, sp. nov.

Index Fungorum number: IF; Facesoffungi number: FoF 18904

Etymology – The name refers to "Siam," the historical name of Thailand, where the species was collected.

Holotype – MFLU 25-0429

Saprobic on dead, areal, decaying inflorescence petiole of grass, (Poaceae), **Sexual morph**: *Ascomata* 150–180 × 120–140 µm ($\bar{x}$ =165 × 125 µm, n = 5), appear as dark light brown dots, solitary, scatted or loosely aggregated, globose, subglobose to ovoid, develop intra-epidermal in host tissue. *Peridium* 9–18 µm wide ($\bar{x}$ = 12 µm, n = 10), single layered, pigmented, thick-walled cells of *textura angularis*. *Hamathecium* 1–2.5 µm wide ($\bar{x}$ = 1.5 µm, n = 10), composed from numerous, densely packed, hyaline, smooth-walled, filiform pseudoparaphyses. *Asci* 60–85 × 12–18 µm ($\bar{x}$ = 77 × 14.5 µm, n = 10), 8-spored, bitunicate, fissitunicate, broadly-clavate to cylindrical, develop orbicular pedicel, rounded at apex with inconspicuous ocular chamber. *Ascospores* 18–25 × 4.5–7.5 µm ($\bar{x}$ = 22 × 5.5 µm, n = 20), overlapping bi-seriate or obliquely tri-seriate, di-septate, upper cell wider, constricted at the middle with blunt or flat apex. Base cell small and short, pointed towards the end, reddish brown in color with smooth thick walls. **Asexual morph**: Undetermined.

Culture characteristics: Ascospores germinating on MEA within 24 h. Germ tubes produced from the epical cell of the ascospore. Colonies growing on MEA, reaching 10–20 mm in 2 weeks at 25°C. Mycelia superficial, culture umbonate with erose edge, from above brownish gray with whitish cottony appearance from center, light color concentric rings close to edge, from reverse dark greenish brown at the center, light brown to yellowish white at the edge.

Material examined: Thailand, Chang Wat Narathiwat Province, Amphoe Tak Bai, District, Tambon Sala Mai on decaying petiole of grass (Poaceae). xx xx 2023, Tharindu Bhagya, T74_A (MFLU 25-0429, holotype), *ibid.*, T74_B, grass (Poaceae) (MFLU 25-0430, isotype).

GenBank numbers – MFLU 25-0429: ITS = PX068323, LSU = PX068320

Distribution – Decaying petiole of grass, (Poaceae). Narathiwat, Thailand.

Notes – The new isolates formed an independent lineage sister to the clade comprising *Paraphaeosphaeria michotii* (MFLUCC 13-0349, MFLUCC 15-0043, and MFLUCC 15-0041) and *P. pilleata* strain CBS 102207, with 57% maximum likelihood (ML) and 0.79 Bayesian posterior probability (BPP) support (Figure 4.21). Strain MFLU 25-0425 resembles other species in the genus *Paraphaeosphaeria* by producing globose to subglobose perithecial ascomata, hyaline, smooth-walled, filiform pseudoparaphyses, cylindrical to clavate asci, and dark brown to pale brown, thick-walled, ellipsoidal to fusiform, septate ascospores (Ariyawansa et al., 2014; Wanasinghe et al., 2018; Hongsanan et al., 2020; Tennakoon et al., 2022; Absalan et al., 2024). Strain MFLU 25-0429 is morphologically distinguishable from *P. michotii* (MFLUCC 13-0349, MFLUCC 15-0043, and MFLUCC 15-0041) and *P. pilleata* (CBS 102207) by possessing 1-septate ascospores with a relatively larger length-to-width (L/W) ratio (MFLU 25-0429 L/W = 4.00 vs *P. michotii* L/W = 3.08 and *P. pilleata* L/W = 3.85) (Figure 4.22) (Câmara et al., 2001; Soares et al., 2006; Garcia-Hermoso et al., 2019). The pairwise distance matrix values between MFLU 25-0429 and related strains were between 0.01–0.05, indicating that the new strain is congeneric with *Paraphaeosphaeria* but represents a distinct species (Gostinčar, 2020; Maharachchkumbura et al., 2021). The asexual morph was not observed for the new isolates, and *P. youngiae* strain BRIP 75896a was excluded from the analysis due to its segregation as an outgroup. Based on the available evidence, I introduce MFLU 25-0429 as a new species *P. siamensis* in the genus *Paraphaeosphaeria*, isolated from a dead, decomposing grass petiole in Narathiwat, Thailand.

Note a Decomposing grass petiole. b–c Black immersed ascomata on the host. d Vertical section of ascomata. e Peridim. f Pseudoparaphyses. g–k Asci. l–p Ascospore. q Germinates ascospore. r Culture on MEA above. s reverse. Scale bars: d 50 µm, e–f 10 µm, g–k 20 µm, 1–q 10 µm.

Figure 4.22 *Paraphaeosphaeria siamensis* (MFLU 25-0429, holotype)

Periconiaceae Nann

Periconia Tode

Periconia was introduced by Tode in 1791 and is typified by *Periconia lichenoides* in the family *Periconiaceae*. Members of the genus exhibit a wide distribution, with the majority of isolates originating from China, Thailand, France, India, and the United States (Hyde et al., 2018; Madagmmana et al., 2024; Sun et al., 2025). The sexual morphs of *Periconia* are characterized by globose, immersed or erumpent, ostiolate ascomata with a thin-walled peridium and a periphysate ostiolar neck. Asci in the genus *Periconia* are bitunicate, fissitunicate, oblong, and contain eight fusiform, 1-septate ascospores. *Periconia* develops hyphomycetous asexual morphs with macronematous, branched or unbranched, septate, smooth, thick-walled conidiophores that appear pale brown to brown. Conidia in the genus *Periconia* are globose or ellipsoidal, aseptate, pale brown to brown, and possess smooth or verruculose walls (Hyde et al., 2018; Madagmmana et al., 2024; Sun et al., 2025).

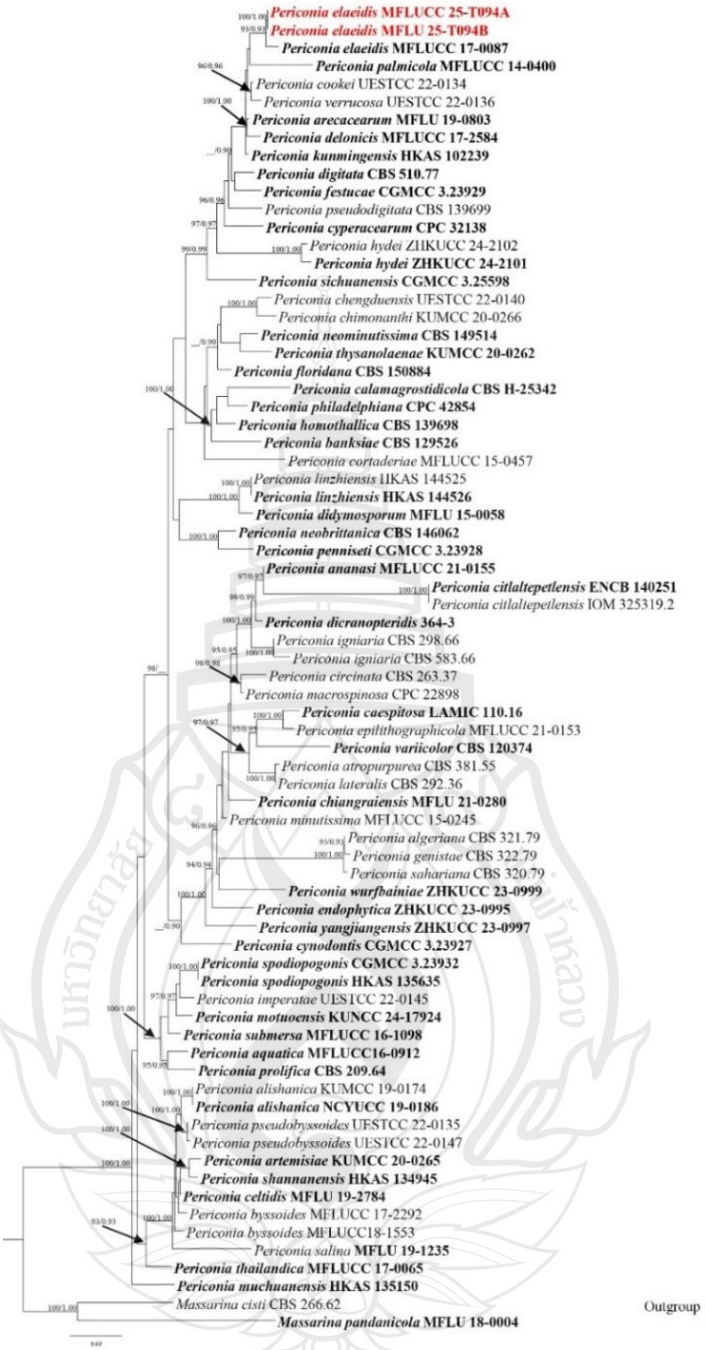

Note Bootstrap support values for ML ≥ 90 % and Bayesian posterior probabilities (BPP) ≥ 0.9 are mentioned at the nodesNewly generated sequences are in red and the type strains are in bold.

Figure 4.23 Phylogram generated from Maximum Likelihood (ML) analysis based on combined ITS, SSU, LSU, and *tef1-α* sequence data of 74 strains of genus *Periconia* with related taxa, which comprise 3786 characters including gaps, are included in the analyses.

Periconia elaeidis Sunpapao & K.D. Hyde, in Hyde et al., Mycosphere 9(2): 323 (2018)

Saprobic on decaying decaying petiole of *Thypa*, (Typhaceae), **Sexual morph**: Undetermined. **Asexual morph**: Hyphomycetous, numerous, effuse on host. *Conidiophores* 270–390 × 8–12 μm ($\bar{x}$ = 345 × 10 μm, n = 10), macronematous, mononematous, dark brown, straight to slightly flexuous, 5–7 septate, simple, unbranched, thick-walled, smooth or rarely verruculose with clusters conidiogenous cells and conidia at the apex. *Conidiogenous cells*, polyblastic, integrated, subglobose, proliferating pale brown to yellowish brown and verruculose. *Conidia* 7–3 × 6–4 μm ($\bar{x}$ = 5.8 × 3.5 μm, n = 20), solitary or catenate, subglobose to globose, brown to yellowish brown, aseptate, echinulate or verrucose with thick walled.

Culture characteristics: Conidia germinating on MEA within 12 h. Germ tubes produced from side. Colonies growing on MEA, reaching 25 mm in 2 weeks at 25°C. Mycelia superficial, effuse to umbonate, entire edges, from above pale white from center to the edge, from reverse yellowish white at the center and the white to hyaline at the edge.

Material examined: Thailand, Chang Wat Prachuap Khiri Khan Province, Pran Buri District, Pran Buri Wetland, on decaying stems of *Typha* sp. (Typhace*ae*). xx January 2023, Tharindu Bhagya, TB94P (MFLU 25-0431), Chang Wat Prachuap Khiri Khan Province, Khao Sam Roi Yot Wetland, 06 May 2024, Tharindu Bhagya, decaying peduncle of *Typha* sp. (Typhaceae) TB94M (MFLU 25-0432).

GenBank numbers – MFLU 25-0431: ITS = PP572906

Distribution – Decaying wood submerged in stream, Cangshan Mountain, Yunnan Province, China (Hyde et al., 2018). Decaying *Typha* sp. peduncle, and stem in freshwater wetland, Thailand (This study).

Notes – Our new isolates form a clade sister to *Periconia elaeidis* strain MFLUCC 17-0087, with strong statistical support (93% ML and 0.93 BPP) (Figure 4.23). Phylogenetically, MFLU 25-0431 aligns with *P. elaeidis* strain MFLUCC 17-0087, exhibiting 99.9% similarity in the ITS sequence and 99.8% in the LSU sequence (excluding gaps). The new isolates are morphologically similar to *P. elaeidis* strain MFLUCC 17-0087, featuring dark brown, straight, 5–7-septate, simple, unbranched conidiophores; polyblastic, integrated, proliferating conidiogenous cells, and catenate,

subglobose to globose, echinulate or verruculose, aseptate conidia (Figure 4.24) (Hyde et al., 2018). Based on the available morphological and phylogenetic evidence, I recognize the new isolates as *P. elaeidis*.

Note a *Typha* sp. host material. b Conidiophores. c–e Conidiophores with conidia. f–g Conidia aggregation. h–o Conidia with central conidia. p Culture on MEA above. q reverse. Scale bars: c–e 50 µm, f–g 20 µm, h–o 10 µm.

Figure 4.24 *Periconia elaeidis* (MFLU 25-0431)

Lentitheciaceae Y. Zhang, C.L. Schoch, J. Fourn, Crous & K.D. Hyde

Halobyssothecium Dayar., E.B.G. Jones & K.D. Hyde

Halobyssothecium was introduced by Dayar., E.B.G. Jones & K.D. Hyde, in 2018 from salt marsh environment in Thailand, and typified to *H. obiones* (Dayarathne et al., 2018). *Halobyssothecium* contain both sexual and asexual morphs. The sexual morphs are distinguishable from other related genera in Lentitheciaceae by processing versicolored ascospores (Dayarathne et al., 2018). Asexual morphs are characterized by pycnidial conidiomata, ampulliform to cylindrical, enteroblastic conidiogenous cells, and ovoid to cylindrical or subcylindrical, hyaline conidia (Calabon et al., 2023).

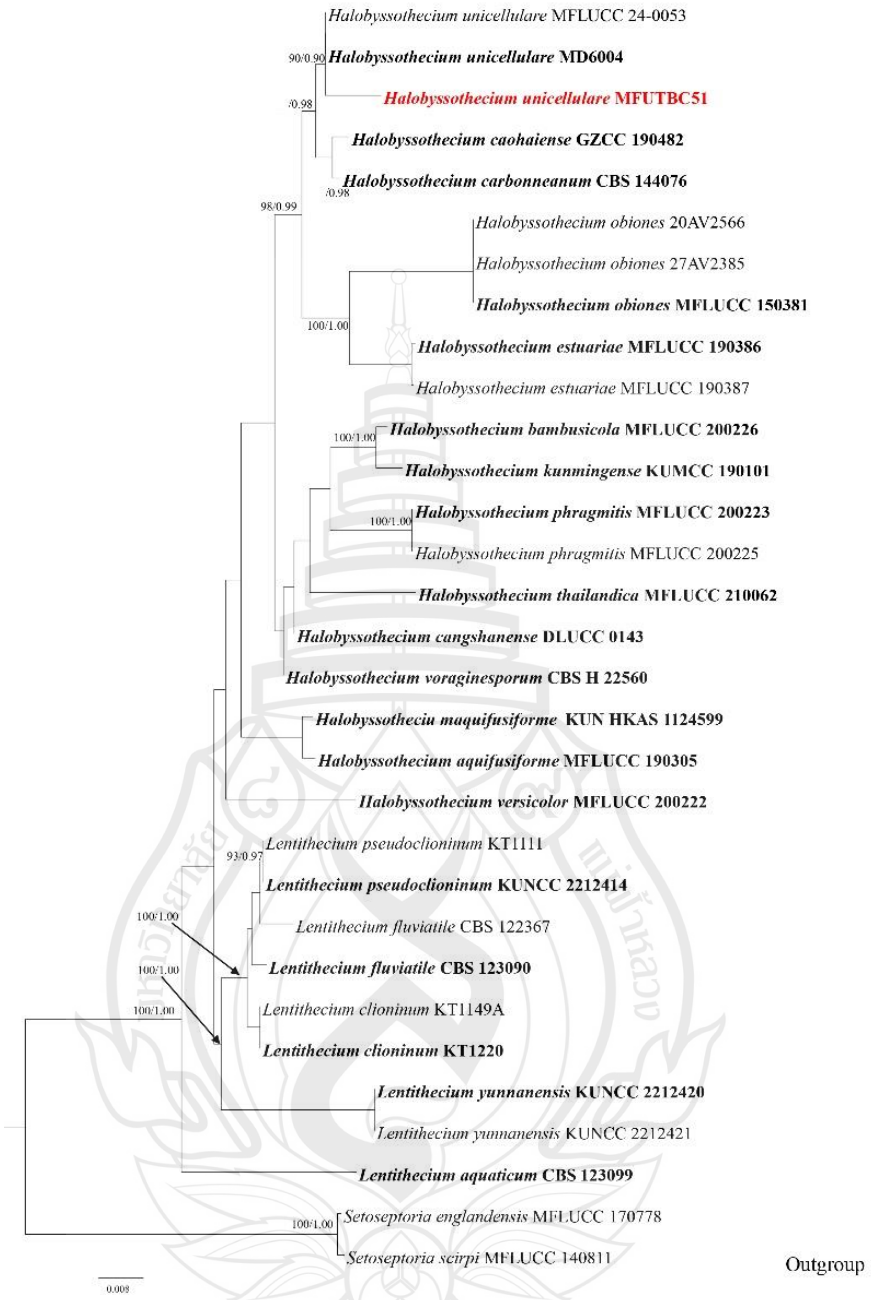

Note Bootstrap support values for ML ≥ 90 % and Bayesian posterior probabilities (BPP) ≥ 0.9 are mentioned at the nodes. The tree was rooted to *Setoseptoria phragmitis* (CBS 114802, and CBS 114966) combination. Newly generated sequence is in red and the type strains are in bold.

Figure 4.25 Phylogram generated from Maximum Likelihood (ML) analysis based on combined LSU, SSU, ITS and *tef1-α* sequence data of 31 strains, which comprise 3142 characters including gaps, are included in the analyses.

Halobyssothecium unicellulare (Abdel-Aziz) M.S. Calabon, K.D. Hyde & E.B.G. Jones Mycological. Progress, 20, 715 (2021)

Saprobic on dead, moist, decaying stems of Bamboo, (Poaceae), **Sexual morph**: Undetermined. **Asexual morph**: *Coelomycetous*, *Conidiomata* 135–210 × 110–140 μm ($\bar{x}$ = 160 × 125 μm, n = 5), pycnidial, loosely aggregated, semi-immersed, dark brown to black, globose to subglobose with setae, unilocular, ostiolate. *Ostiole,* circular, papillate, located at the center. *Setae* inconspicuous, pale brown at the base and hyaline at apex, unbranched, septate, narrowing toward apex. *Conidiomatal wall* 15–28 μm wide ($\bar{x}$ = 19 μm, n = 5), outer layer composed thick-walled from brown to black cells of *textura angularis*, inner layer consists with hyaline cells of *textura prismatica. Conidiophores* reduced to conidiogenous cells. *Conidiogenous cells* 8–14 × 3–4 μm ($\bar{x}$ = 12 × 3.5 μm, n = 10), develop inner hyaline layer of conidiomata, proliferating in different levels, smooth-walled, hyaline, ampulliform, holoblastic. *Conidia* 10–15 × 3–5 μm ($\bar{x}$ = 12 × 4.5 μm; n = 20), hyaline, smooth, thick-walled, unicellular, oval, oblong or ellipsoidal, rounded to the apex, obtuse at bases, occasionally constricted at the middle, guttulated.

Culture characteristics: Conidia germinating on MEA within 48 h. Germ tubes developed from the ends of the conidia. Colonies growing on MEA, reaching 10–30 mm in 10 weeks at 25°C. Mycelia superficial, umbonate, and produce fimbriate at edges, from above greenish ash at the center with conspicuous pale white at the edge; from reverse dark brown at the center, radiating orange yellow ring and turn white at the edge.

Material examined: Thailand, Chang Wat Prachuap Khiri Khan Province, Pran Buri District, Pran Buri river, on decaying stems of Bamboo (Poaceae), 07 May 2023, Tharindu Bhagya, TB121 (MFLU 25-0433).

GenBank numbers – MFLU 25-0433: ITS = PV775682

Distribution – On Unknown submerged wood, China (Shen et al., 2023), on unknown submerged wood, Egypt (Hyde et al., 2016), decomposing submerged Bog Grass clumps, Thailand (Hyde et al., 2024), submerged decaying Bamboo stem in freshwater river, Thailand (This study).

Notes – The multigene phylogenetic analysis placed the new isolate as a sister to *Halobyssothecium unicellulare* strain MD 6004, with less than 90% ML and 0.90

BPP bootstrap support (Figure 4.25). Phylogenetically, the new isolate shares 99.3% similarity in the ITS sequence, 99.7% similarity in the LSU sequence, 99.8% similarity in the SSU sequence, and 98.4% similarity in the *tef1-α* sequence (excluding gaps) with *H. unicellulare* strain MD 6004. Morphologically, the presence of pycnidial conidiomata, ampulliform holoblastic conidiogenous cells, and hyaline, oval to oblong-ellipsoidal conidia make strain MFLU 25-0433 morphologically resemble *H. unicellulare* strain MD 6004 (Figure 4.26) (Dayarathne et al., 2018; Shen et al., 2023). Based on the available morphological and phylogenetic evidence, I recognize our isolate as a new strain of *H. unicellulare*, and report it as a new host record from Bamboo in a freshwater wetland in Thailand.

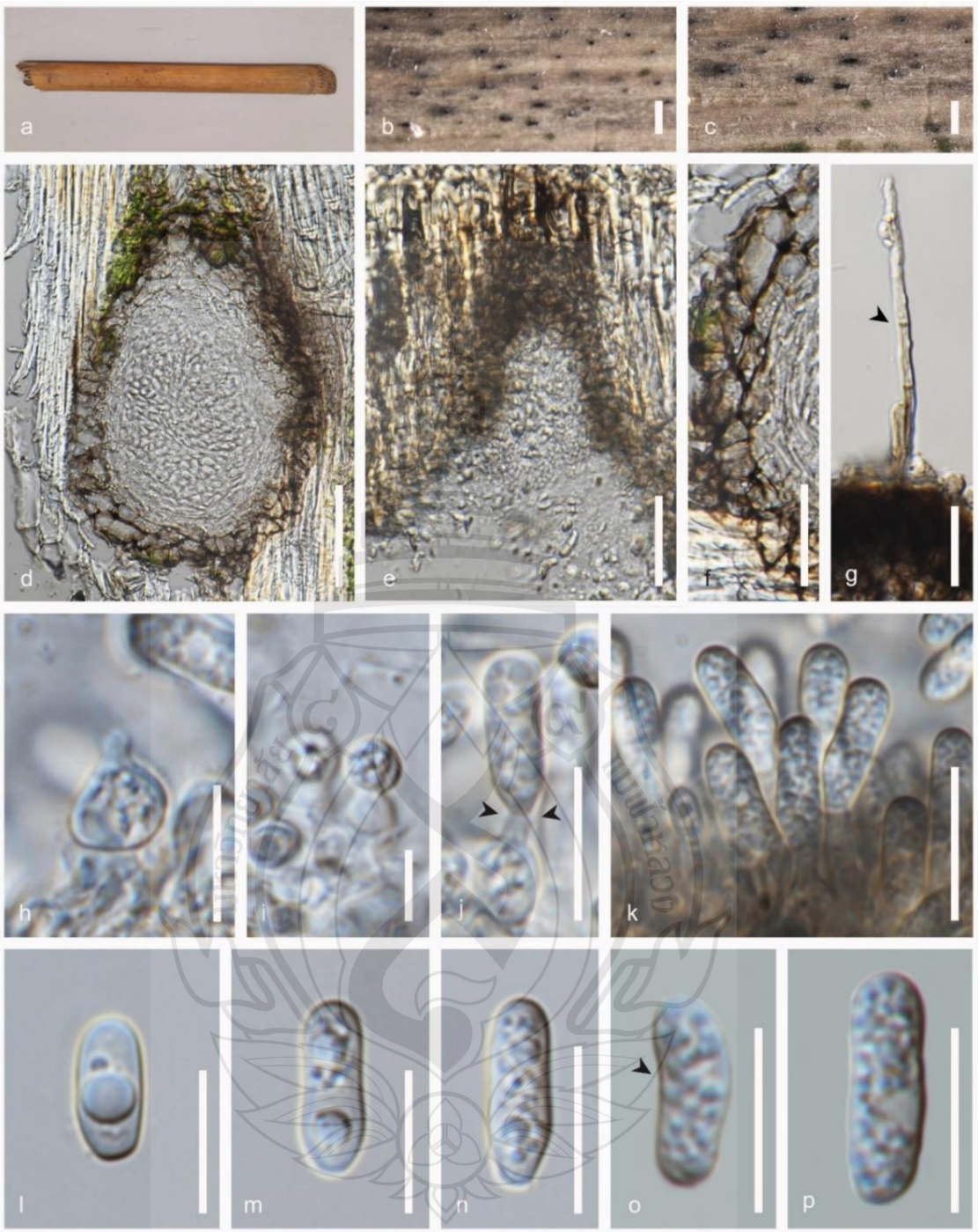

Note a Bamboo host material. b–c conidiomata on host. d vertical section conidiomata. e ostiole. f peridium. g septate setae developed on the conidiomata (arrowed). h–k Conidiogenous cells with conidia formation (arrowed). l–p conidia with constrictions at the middle (arrowed). Scale bars: b 1 mm, c 500 µm, d 50 µm, e–g 20 µm, h–p 10 µm.

Figure 4.26 *Halobyssothecium unicellulare* (MFLU 25-0433)

***Poaceascoma* Phookamsak & K.D. Hyde**

Poaceascoma is a monophyletic genus introduced by Phookamsak and K.D. Hyde in 2015. The genus is placed in the family *Lentitheciaceae* and is typified by *Po. helicoides* (Phookamsak et al., 2015). *Poaceascoma* is characterized by dark brown to black, globose to subglobose, uniloculate ascomata bearing bitunicate, fissitunicate, elongate to cylindrical asci. Each ascus contains eight hyaline, smooth, thick-walled, fasciculate, filiform ascospores, which are arranged in a spiral form within the ascus (Phookamsak et al., 2015; Zhang et al., 2023). Members of the genus have been recorded from both terrestrial and aquatic environments. They are predominantly saprobic, though occasionally reported as endophytic. The asexual morphs have not yet been observed either in nature or under in vitro conditions (Phookamsak et al., 2015; Zhang et al., 2023; Liu et al., 2025).

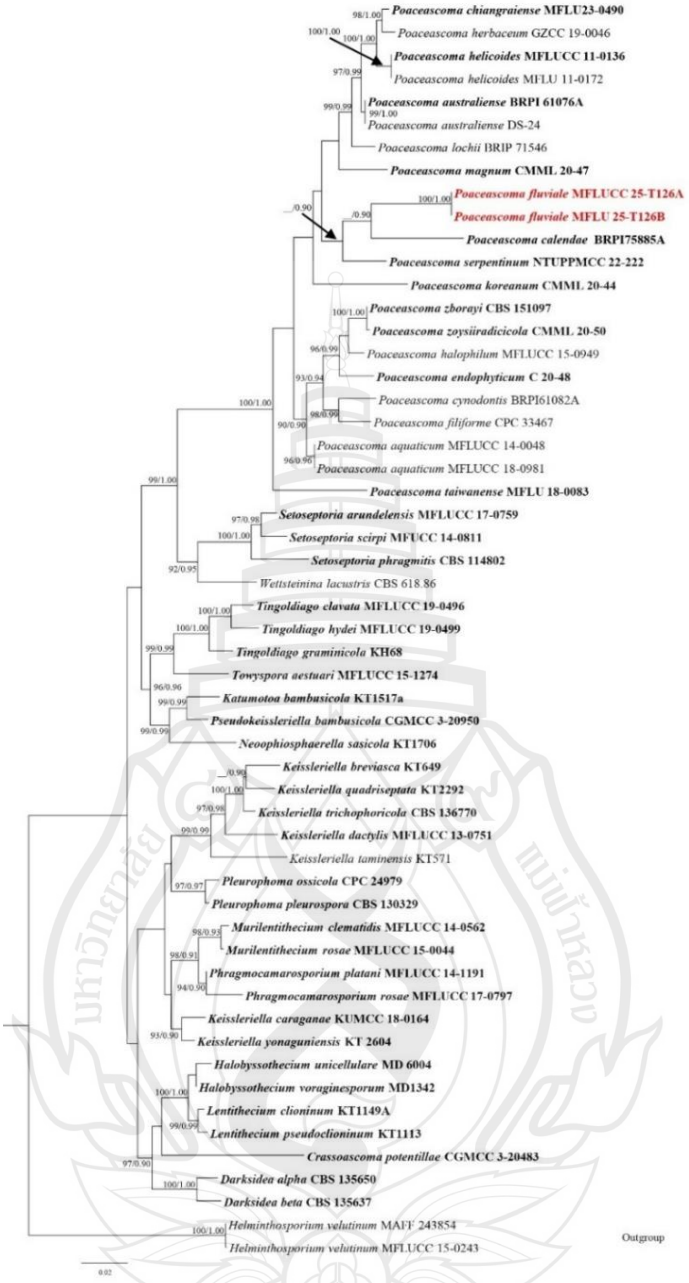

Note Bootstrap support values for ML ≥ 90 % and Bayesian posterior probabilities (BPP) ≥ 0.9 are mentioned at the nodes. The tree was rooted to *Helminthosporium velutinum* (MAFF 243854, and MFLUCC 15-0243). Newly generated sequences are in red and the type strains are in bold.

Figure 4.27 Phylogram generated from Maximum Likelihood (ML) analysis based on combined SSU, ITS, LSU, and *tef1-α* sequence. The data set comprises 4367 characters including gaps from of selected 55 strains which were included in the phylogenetic analyses.

Poaceascoma fluviale Bhagya, Phukhams E.B.G. Jones & K.D. Hyde, sp. nov

Index Fungorum number: IF; Facesoffungi number: FoF 18905

Etymology – Named after its riverine habitat the species was recovered.

Holotype – MFLU 25-0434

Saprobic on decaying stem of *Carex*, (Cyperaceae). **Sexual morph**: *Ascomata* 250–450 × 250–370µm ($\bar{x}$ = 420 × 290 µm, n = 5), black or dark brown, solitary, scattered or occasionally aggregated, immersed under host tissue, slightly raised, glabrous, ampulliform or golobose to subglobose with uni-loculate opening. *Peridium* 80–130 µm wide ($\bar{x}$ = 90 µm, n = 10), show different thickness, thick at the base, composed of multiple layers from brown thick-walled cells in *textura angularis*. *Pseudoparaphyses* 2–4 µm wide ($\bar{x}$ = 3.5 µm, n = 10), hyaline, cellular, trabeculae, septate, branched, smooth walled, and end taping towards blunt rounded apexes. *Asci* 130–180 × 15–22 µm ($\bar{x}$ = 162 × 17 µm, n = 10), 8-spored, bitunicate, fissitunicate, elongate-cylindrical, cylindrical to cylindric-clavate or obclavate, slightly curved, process short pediculate, with conspicuous, minute ocular chamber at the tip. *Ascospores* 350–480 × 2.5–5.5 µm ($\bar{x}$ = 420 × 3.5 µm, n = 20), hyaline, fasciculate, aggraded spirally in the ascus, scolecosporous, filiform to filamentous, smooth walled, guttiulated and multi-septate, not constricted at septum, narrowing towards apexes. **Asexual morph**: Undetermined.

Culture characteristics: Ascospore germinating on MEA within 48 h. Germ tubes produced from multiple locations of the ascospore. Colonies growing on MEA, reaching 30–40 mm in 4 weeks at 25°C. Mycelia superficial, cottony, umbonate shape culture with complete edge, from above cinereous at the center with pale yellow to off-white ring with, white to hyaline at the edge, from reverse yellowish brown to olivaceous at the center and off white at the edge.

Material examined: Thailand, Chang Wat Prachuap Khiri Khan Province, Pran Buri District, Pran Buri River, on decaying stems of *Carex* sp. (Cyperaceae), 05 April 2024, Tharindu Bhagya, T126_A (MFLU 25-0434, holotype), *ibid.*, T126_B, (MFLU 25-0435, isotype).

GenBank numbers – MFLU 25-0434: ITS = PX062145, LSU = PX062143

Distribution – Decaying submerged *Carex* sp. (Cyperaceae), stem, in freshwater river, Thailand.

Notes – The new isolate forms a sister clade associated with *Poaceascoma calendae* strain BRIP 75885a, with strong phylogenetic support (86% ML and 0.90 BPP) (Figure 4.27). Strain MFLU 25-0434 resembles other species in the genus by producing globose to subglobose, uniloculate ascomata, and cylindrical, bitunicate, fissitunicate asci containing spirally arranged, hyaline, fasciculate, filiform ascospores (Phookamsak et al., 2015; Zhang et al., 2023; Liu et al., 2025). Phylogenetically, strain MFLU 25-0434 differs from *Po. calendae* strain BRIP 75885a by 5.08% in ITS sequence data (without gaps). Further phylogenetic or morphological comparisons between the two strains are currently not possible due to the lack of SSU, LSU, *tef1-α* sequence data, and complete morphological description for *Po. calendae* strain BRIP 75885a (Tan & Wong, 2024). Morphologically, strain MFLU 25-0434 shares similarities with *Po. halophilum* strain MFLUCC 15-0949 (Figure 4.28). In contrast, the distinctly thicker *textura angularis* cells dominating the peridium (80–130 µm vs. 35–58 µm), shorter asci (130–180 µm, $\bar{x}$ = 162 vs. 248.5–300 µm, $\bar{x}$ = 205.5), and its placement in a distant clade distinguish MFLU 25-0434 from *Po. halophilum* strain MFLUCC 15-0949 (Abreu et al., 2017). In addition, the pairwise distance matrix value between MFLU 25-0434 and other related taxa within the genus was >0.05, indicating that the isolate belongs to the genus *Poaceascoma* and represents a distinct species (Gostinčar, 2020; Maharachchkumbura et al., 2021). Based on the available evidence, I introduce *Po. fluviale* (MFLUCC 25-0434) as a new species of *Poaceascoma*, collected from decomposing submerged *Carex* sp. material in a freshwater river in Thailand.

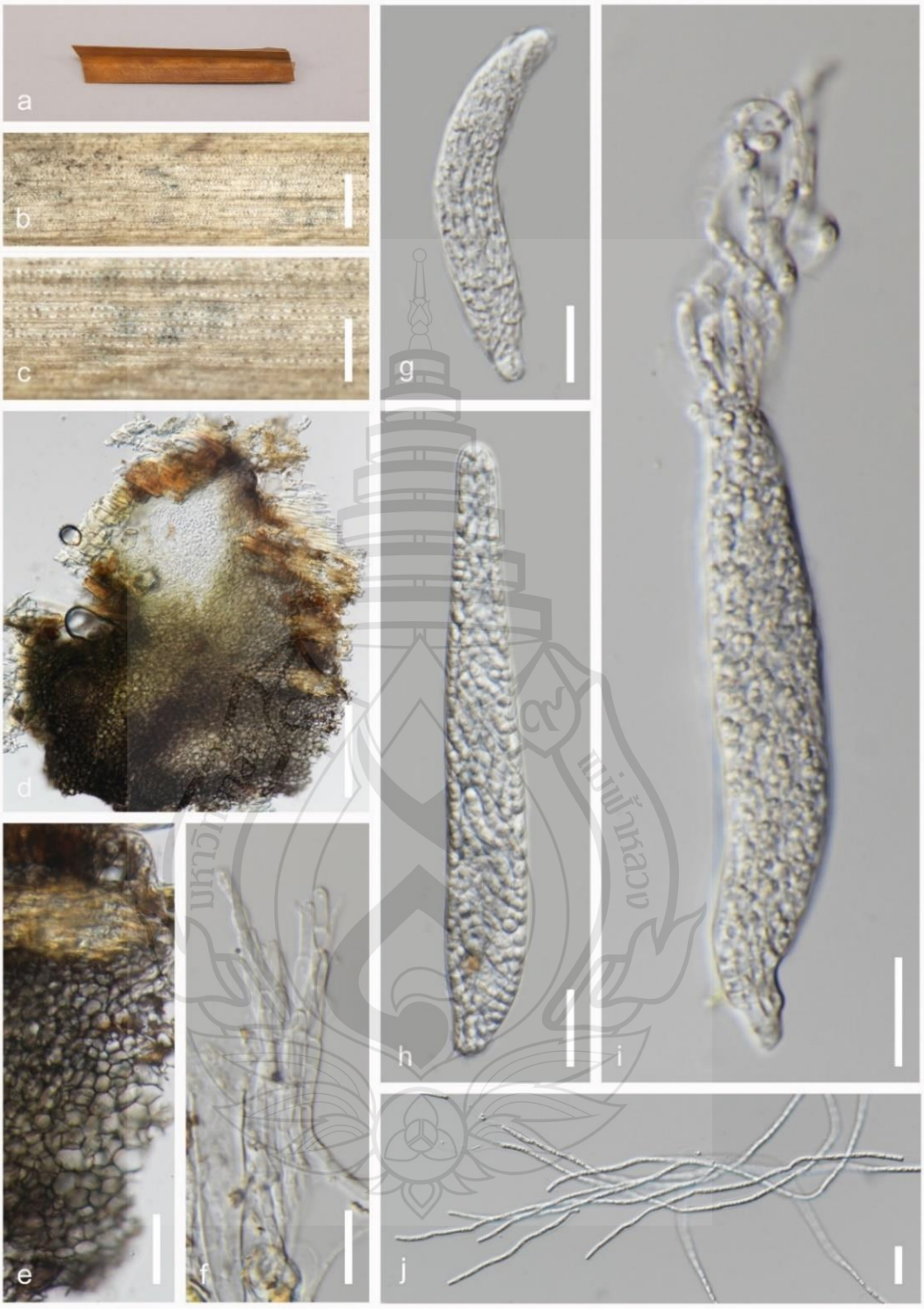

Note a *Carex* sp. host material. b–c Immersed ascomata in the host tissue. d Vertical section of ascomata. e Peridium. f Pseudoparaphyses; g–i Mature asci. j Ascospores. Scale bars: b 1 mm, c 500 µm, d 100 µm, e–j 20 µm.

Figure 4.28 *Poaceascoma fluviale* (MFLUC 25-0434, holotype)

Lindgomycetaceae K. Hiray., Kaz. Tanaka & Shearer

Hongkongmyces C.C.C. Tsang, J.F.W. Chan, Trend. -Sm., A.H.Y. Ngan, I.W.H. Ling, S.K.P. Lau & P.C.Y. Woo

Genus *Hongkongmyces* resides in the family *Lindgomycetaceae*, class *Dothideomycetes*. Tsang et al. (2014) introduced the genus *Hongkongmyces* typifying to *Hongkongmyces pedis* which was isolated from infected human feet (Dan-Feng et al., 2021). At present genus *Hongkongmyces* bears eight morphologically and phylogenetically confirmed species. Those isolated show the worldwide distribution and higher affinity towards aquatic environments (Yang et al., 2023). Among those isolated *Hongkongmyces aquaticus*, *H. kokensis*, and *H. snookiorum* are known from asexual morphs, and *Hongkongmyces brunneisporus* and *H. thailandica* were isolated and described as sexual morphs (Dan-Feng et al., 2021). Most recent discoveries of the genus *Hongkongmyces* came from Jilin Province and Guizhou Province China. Jayawardena et al. (2022) reported *Hongkongmyces changchunensis* Phukhams., W.X. Su, & Y. Li, from submerged *Betula* twigs in a freshwater stream, and Yang et al. (2023) published *Hongkongmyces aquisetosus* J. Yang Jian K. Liu & K.D. Hyde, from submerged wood in river Suoluo. As a finding of the ongoing investigation of fungal communities in Thailand wetlands, this study introduces a new species of *Hongkongmyces* from decaying *Typhaceae* substrate, submerged in lotic wetland waters.

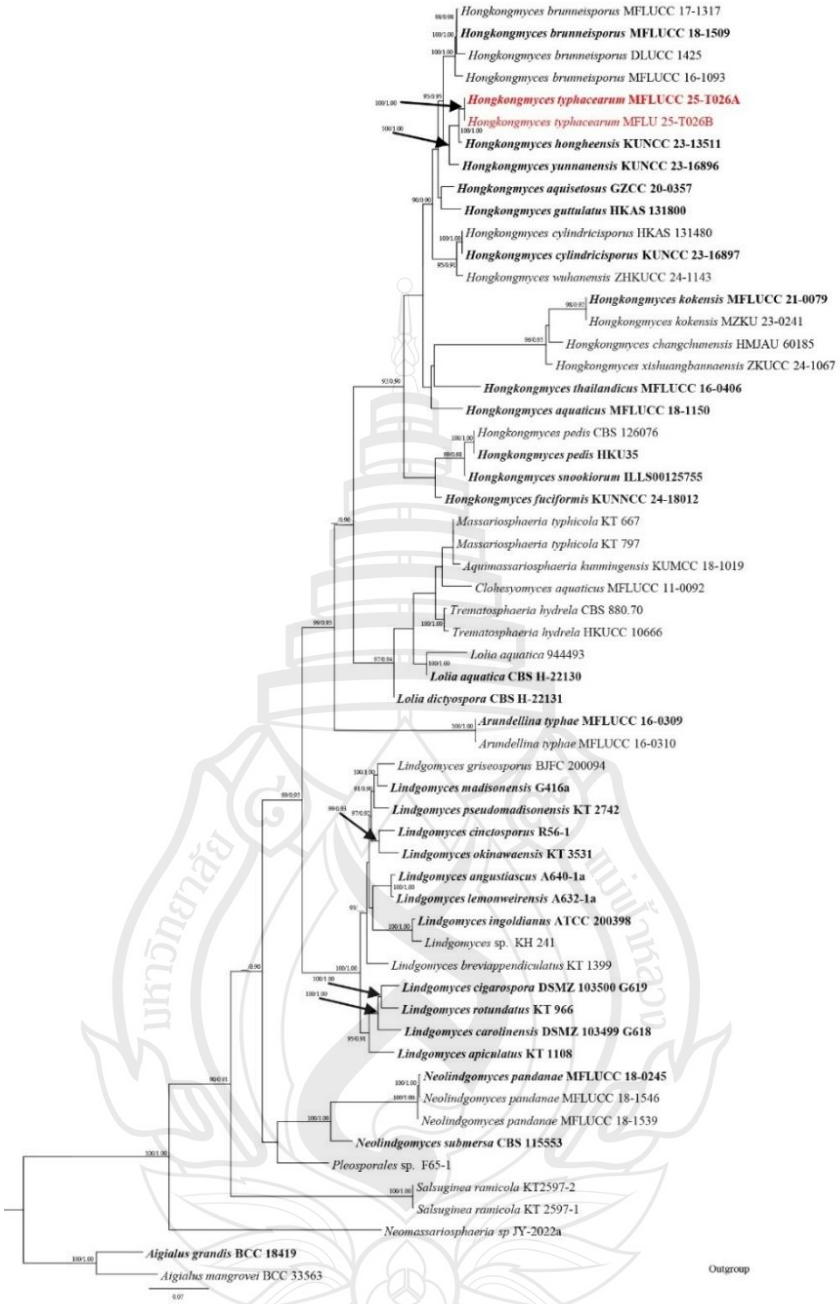

Note The data set comprises 5928 characters including gaps from of selected 58 strains which were included in the phylogenetic analyses. Bootstrap support values for ML ≥ 90 % and Bayesian posterior probabilities (BPP) ≥ 0.9 are mentioned at the nodes. The tree was rooted to *Aigialus grandis* strain BCC18419, and *A. mangrovei* STRAIN BCC33563.

Figure 4.29 Phylogram generated from Maximum Likelihood (ML) analysis based on combined LSU, SSU, ITS, *tef1-α* and *rpb2* sequence.

Hongkongmyces typhacearum Bhagya, Phukhams E.B.G. Jones & K.D. Hyde, sp. nov.

Index Fungorum number: IF; Facesoffungi number: FoF 18906

Etymology – The "typhacearum" refers to the host family Typhaceae, that the fungus was isolated.

Holotype – MFLU 25-0436

Saprobic on dead, decaying leaf of *Typha*, (Typhaceae), **Sexual morph**: fruiting structures appearing as black spherical to semi-spherical gelatinous dots adhere to the surface**.** *Ascomata* 134–138 × 140–142 µm ($\bar{x}$ =136 × 142 µm, n = 5), scattered or slightly gregarious, semi-immersed, ellipsoidal and papillated. *Peridium* 25–29 µm wide ($\bar{x}$ = 28 µm, n = 10)*,* comprising several layers of light brown to dark brown cells in *textura globulosa* and *textura angularis*. *Pseudoparaphyses* 2–4 µm wide ($\bar{x}$ = 2.5 µm, n = 10), numerous, tubercular with uneven width, hyaline, septate and hype like. *Asci* 80–125 × 12–14µm ($\bar{x}$ = 95 × 13.5 µm, n = 10), 8-spored, bitunicate, fissitunicate, short pedicel, broadly clavate, elongate while dehisces for spore discharge, apically rounded with ocular chamber at the end. *Ascospores* 27–30 × 5–6 µm ($\bar{x}$ = 30 × 5.5 µm, n = 20), biseriate, 5–6-septate, constricted at the septa, narrowly to broadly fusoid, third cell from the apex get enlarged, minutely verruculose with rounded ends, narrow to thick-walled, straight or slightly curved, yellowish brown to reddish brown, mature spores with a thin, broadly fusoid or irregular, gelatinous sheath. **Asexual morph:** *Conidiomata* 110–170 × 90–140 µm ($\bar{x}$ =140 × 115 µm, n = 5), pycnidia scattered, semi-immersed to immersed, dark brown to black, uniloculate, globose to subglobose or ellipsoidal, coriaceous, ostiolate. *Peridium* 12–30 µm ($\bar{x}$ =18 µm, n = 15), composed with large, dark brown to black, thick-walled cell in textura angularis, converting to hyaline cells towards conidial hymenium. *Conidiophores,* reduced to conidiogenous cells. *Conidiogenous cells* 9–15 × 2–5 µm ($\bar{x}$ =7.5 × 3.5 µm, n = 10), enteroblastic, phialidic, determinate, hyaline, smooth, thin-walled, cylindrical to subcylindrical or obpyriform. *Conidia* 10–16 × 9–12 µm ($\bar{x}$ =14.5 × 10.5 µm, n = 30), hyaline or occasionally pale yellow, thin-walled, ellipsoidal to obovoid, aseptate, accommodate large single guttule and smooth when immature, malty guttulate, and faintly ornamented at maturity, lacking mucilaginous sheath.

Culture characteristics: Ascospores germinating on PDA within 72 h. Germ tubes produced from the tips of the ascospore. Colonies growing on PDA, reaching 20–30 mm in 6 weeks at 25°C. Mycelia superficial, culture umbonate with entire edge, from above brownish gray from center to the edge with some light color concentric rings close to edge, from below dark brown at the center, yellowish brown at the edge.

Material examined: Thailand, Chang Wat Prachuap Khiri Khan Province, Pran Buri District, Pran Buri Wetland, on decaying stems of *Typha* sp. (Typhaceae), 08 May 2023, Tharindu Bhagya, TB25A (MFLU 25-0436), and Chang Wat Prachuap Khiri Khan Province, Pran Buri District, Pran Buri Wetland, on decaying stems of *Typha* sp. (Typhaceae), 04 August 2023, Tharindu Bhagya TB25B (MFLU 25-0437).

GenBank numbers – MFLU 25-0436, LSU = PV775681

Distribution – Decomposing *Typha* sp. (Typhaceae) stem, Chang Wat Prachuap Khiri Khan Province, Khao Sam Roi Yot Wetland, Thailand.

Notes – Multigene phylogenetic analysis using LSU, SSU, ITS, *tef1-α,* and *RPB2* sequences placed our isolate *H.* typhacearum (MFLU 25-0436) in a clade sister to *Hongkongmyces hongheensis* strain KUNCC 23-13511, with strong support (100% ML and 1.00 BPP) (Figure 4.29). The papillate, dark ascomata, fissitunicate, clavate asci with short pedestals and an ocular chamber, and fusoid, multi-septate, yellow to brown ascospores with a mucilaginous sheath render our isolate morphologically similar to other members of the genus (Yang et al., 2023; Shu et al., 2025). The sexual morph of the new isolate exhibit significant morphological resemblance to *H. hongheensis* strain KUNCC 23-13511, including similar ascus dimensions (95 × 12 μm vs. 95 × 13.5 μm), 5–6-septate ascospores, and overall ascomatal morphology. However, the difference in the length-to-width ratio of the ascospores between *H. hongheensis* strain KUNCC 23-13511 and strain MFLU 25-0436 (3.66 vs. 5.45), along with the presence of relatively wider, cellular pseudoparaphyses in MFLU 25-0436, makes our isolate morphologically distinguishable from *H. hongheensis* and other related taxa, including *H. yunnanensis* strain KUNCC 23-16896 (Figure 4.30 & 4.31) (Shen et al., 2024). Phylogenetically, strain MFLU 25-0436 differs from *H. hongheensis* strain KUNCC 23-13511 by 0.6% in LSU, 0.2% in SSU, and 1.9% in *tef1-α* sequences (excluding gaps). The pairwise distance matrix value between strains KUNCC 23-13511 and MFLU 25-0436 is 0.024, indicating that the two strains are

congeners but represent two distinct species (Gostinčar, 2020; Maharachchkumbura et al., 2021). Considering the available morphological and phylogenetic evidence, I recognize isolates *H. typhacearum* MFLU 25-0436 (sexual morph) and MFLU 25-0437 (asexual morph) as representing a new species in the genus *Hongkongmyces*, isolated from a coastal freshwater wetland in central Thailand.

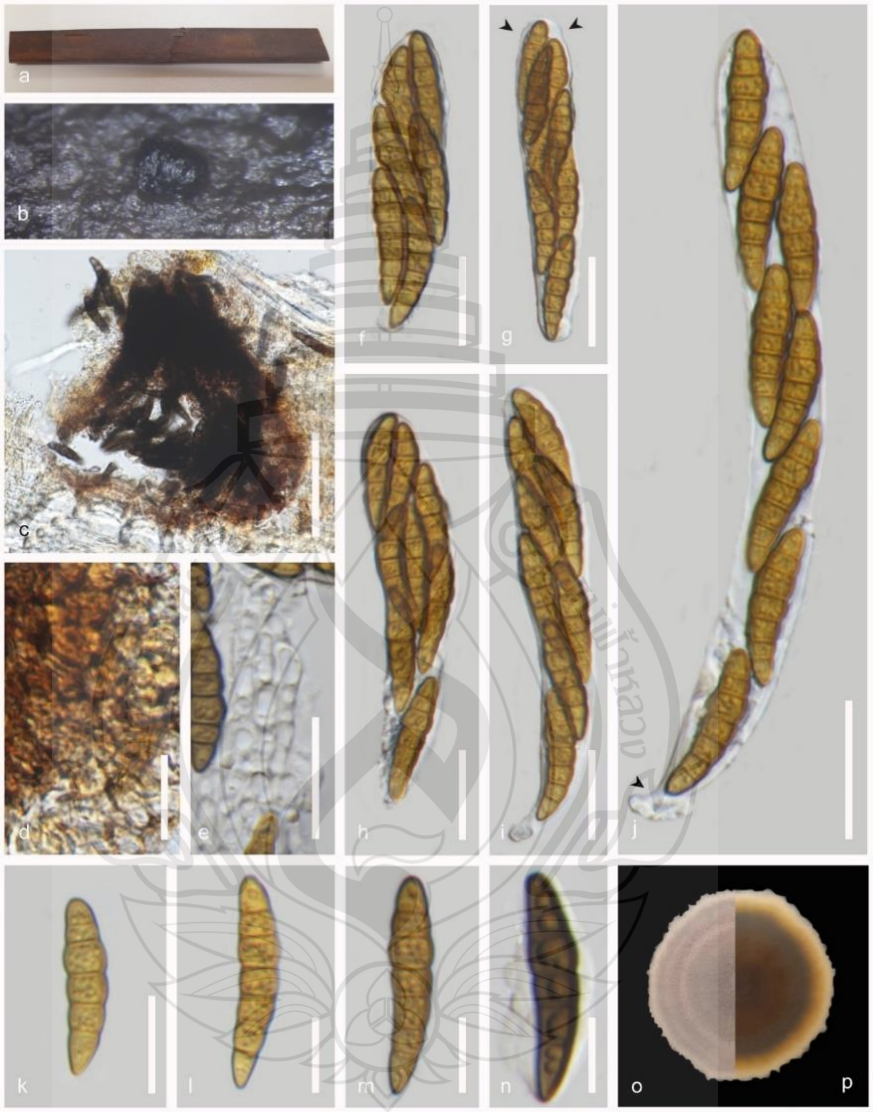

Note a *Typha* sp. host material. b Black semi-immersed ascomata on the host. c Vertical section of ascomata. d Surface view of peridium. e Pseudoparaphyses. f–j Asci with an ocular chamber (arrowed) and short pedestal (arrowed). k–m Ascospores. n Ascospore with gelatinous sheath. o Culture on PDA above. p reverse. Scale bars: c 50 µm, d–j 20 µm, k–n 10 µm.

Figure 4.30 Sexual morph of *Hongkongmyces typhacearum* (MFUL 25-0436, holotype)

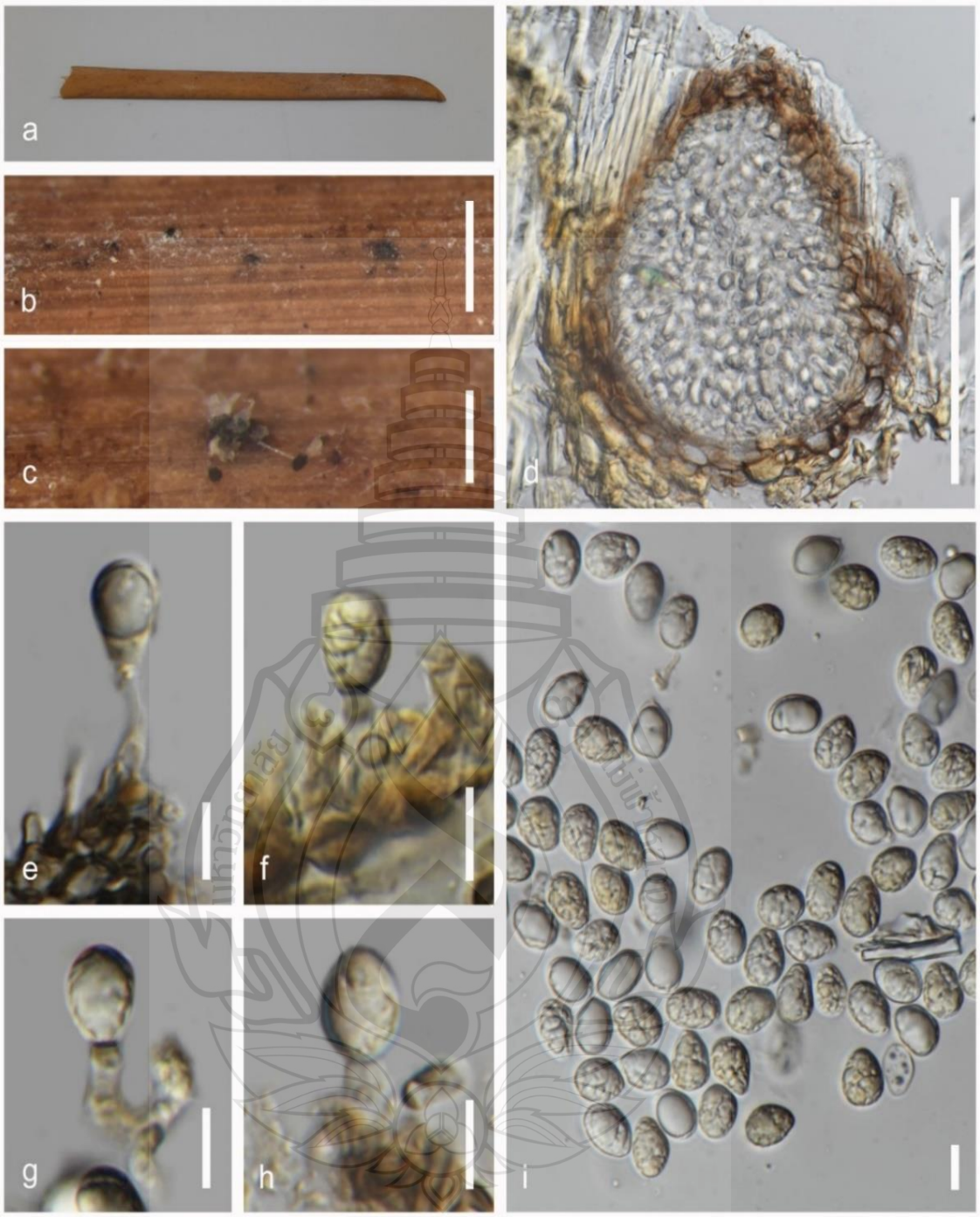

Note a *Typha* sp. host material. b–c Conidiomata on the host surface. d Conidiomata cross section. e–h Conidiogenous cells and conidia development. i Conidia. Scale bars: b 1.00 mm, c 500 µm, d 100 µm. e–i 10 µm.

Figure 4.31 Asexual morph of *Hongkongmyces typhacearum* (MFUL 25-0437, holotype)

Massarinaceae Munk

Neottiosporina Subram

Neottiosporina ***i***s a monophyletic genus, established by Subramanian in 1962, and typified by *Neottiosporina apoda* (Sutton & Alcorn, 1974). The genus is only known from asexual morphs and is characterized by dark brown to black, immersed or semi-immersed, globose to subglobose pycnidial conidiomata, bearing hyaline, smooth-walled, holoblastic, doliiform, determinate, and discrete conidiogenous cells. Conidia in the genus *Neottiosporina* are hyaline, smooth, thick-walled, cylindrical to ellipsoidal, often 1–3-septate, and possess gelatinous appendages or sheaths. Members of the genus are distributed worldwide and have been reported from both terrestrial and aquatic environments. They are predominantly saprobic organisms, but have also been reported as opportunistic pathogens and endophytes (Sutton & Alcorn, 1974; Thambugala et al., 2017; Tsai et al., 2019; Wimalasena et al., 2025).

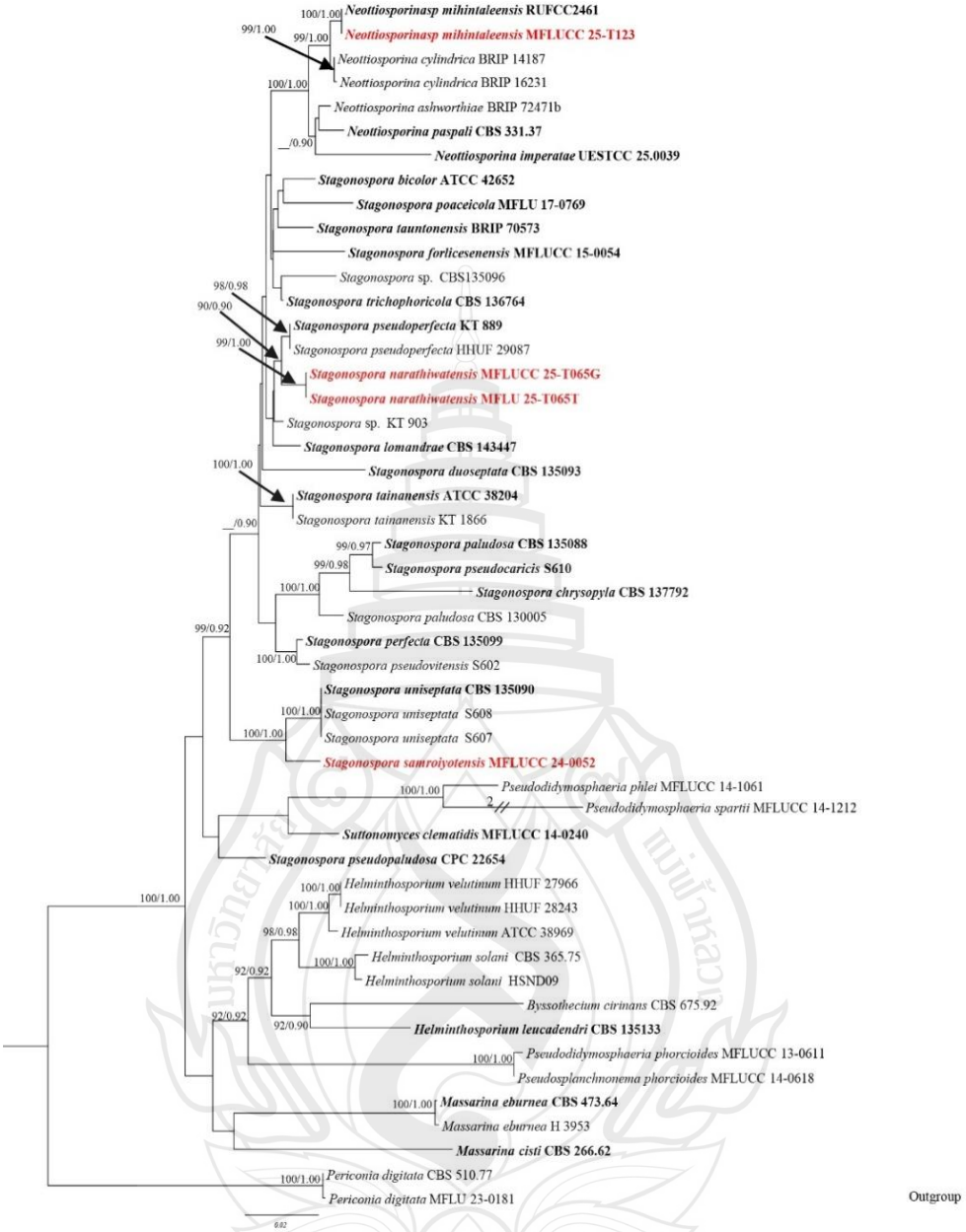

Note Bootstrap support values for ML ≥ 90 % and Bayesian posterior probabilities (BPP) ≥ 0.9 are mentioned at the nodes. The tree was rooted to *Periconia digitata* (MFLU 23-0181 and CBS 510.77). Newly generated sequences are in red and the type strains are in bold.

Figure 4.32 Phylogram generated from Maximum Likelihood (ML) analysis based on combined ITS, LSU, SSU, and *tef1-α* sequence. The data set comprises 4032 characters including gaps from of selected 50 strains which were included in the phylogenetic analyses.

Neottiosporina mihintaleensis Wimalasena, Wijayaw. & Bamunuarachchige, in Wimalasena, Wijayawardene, Bamunuarachchige, Zhang, Jayalal, Dawoud, de Zoysa & Dai, Front. Cell. Infect. Microbiol. 14(1475114).

Saprobic on dead, moist, decaying stems of *Carex*, Cyperaceae, **Sexual morph**: Undetermined. **Asexual morph**: Coelomycetous. *Conidiomata* 210-320 × 200-260 µm ($\bar{x}$ = 290 × 240 µm, n = 5), pycnidia, mostly solitary or scatterd on shot tissue, unilocular, superficial or semi-immersed, globose to subglobose, carbonaceous, septate setae protruding from outer layer, ostiolate, dark brown to black in color. *Ostiole* inconspicuous, circular, papillate, located towerds the center. *Setae* inconspicuous, pale brown at the base and hyaline at tips, unbranched, septate, tapered toward apex. *Conidiomatal wall* 15–25 µm wide ($\bar{x}$ = 21.5 µm, n = 5), composed of thick-walled brown to black cells of *textura angularis*, hyaline towards conidial hymenium. *Conidiophores* reduced to singles cells and each conidiophore bear single unicellular conidiogenous cell. *Conidiogenous cells* 4–5 × 2–6 µm ($\bar{x}$ = 5.5 × 3.5 µm, n = 10), formed in the inner layer of conidiomata wall, proliferating in different levels, ampulliform, holoblastic, determinate, hyaline, smooth-walled. *Conidia* 12–17 × 4–8 µm ($\bar{x}$ = 15.5 × 5.2 µm, n = 20), oval, oblong or ellipsoidal, rounded to the apex, 1-septate, sometimes constricted at the septum, unicellular, hyaline, thick, guttulate, smooth walled and gelatinous appendage originating from the base.

Culture characteristics: Conidia germinating on MEA within 24 h. Germ tubes produced from the sides of the conidium. Colonies growing on MEA, reaching 40 mm in 6 weeks. Mycelia superficial, umbonate with erose edge, from above off-white cottony hype with dark ash to pale brown ring developing at the middle after 4 weeks, from reverse pale brown to dark brown at the center, off-white with hyaline towards the edge.

Material examined: Thailand, Chang Wat Narathiwat Province, Amphoe Tak Bai, District, Tambon Sala Mai on decaying petiole of *Carex* sp. (Cyperaceae), 05 April 2024, Tharindu Bhagya, TB123 (MFLU 25-0438).

GenBank numbers – MFLU 25-0438: ITS = PX518046

Distribution – Endophytic in *Salvinia molesta* leaves, freshwater tank, Sri Lanka, and decaying petiole of *Carex* sp. (Cyperaceae). Narathiwat, Thailand (This study).

Notes – The new isolate forms a sister clade to *Neottiosporina mihintaleensis* strain RUFCC2461 with 100% ML and 1.00 BPP support (Figure 4.32). Strain MFLU 25-0438 resembles members of *Neottiosporina* by producing globose to subglobose conidiomata; holoblastic, hyaline, smooth-walled, determinate conidiogenous cells; and hyaline, smooth-walled, oblong to ellipsoidal, 1-septate conidia (Figure 4.33) (Sutton & Alcorn, 1974; Thambugala et al., 2017; Tsai et al., 2019). Phylogenetically, strain MFLU 25-0438 is 99.61% identical in ITS, 99.96% in LSU, and 100% in SSU sequences to *N. mihintaleensis* strain RUFCC2461 (Wimalasena et al., 2025). Based on the available evidence, I identify strain MFLU 25-0438 as *N. mihintaleensis* and provide the first detailed morphological description of *N. mihintaleensis* from *Carex* sp. in Narathiwat, Thailand.

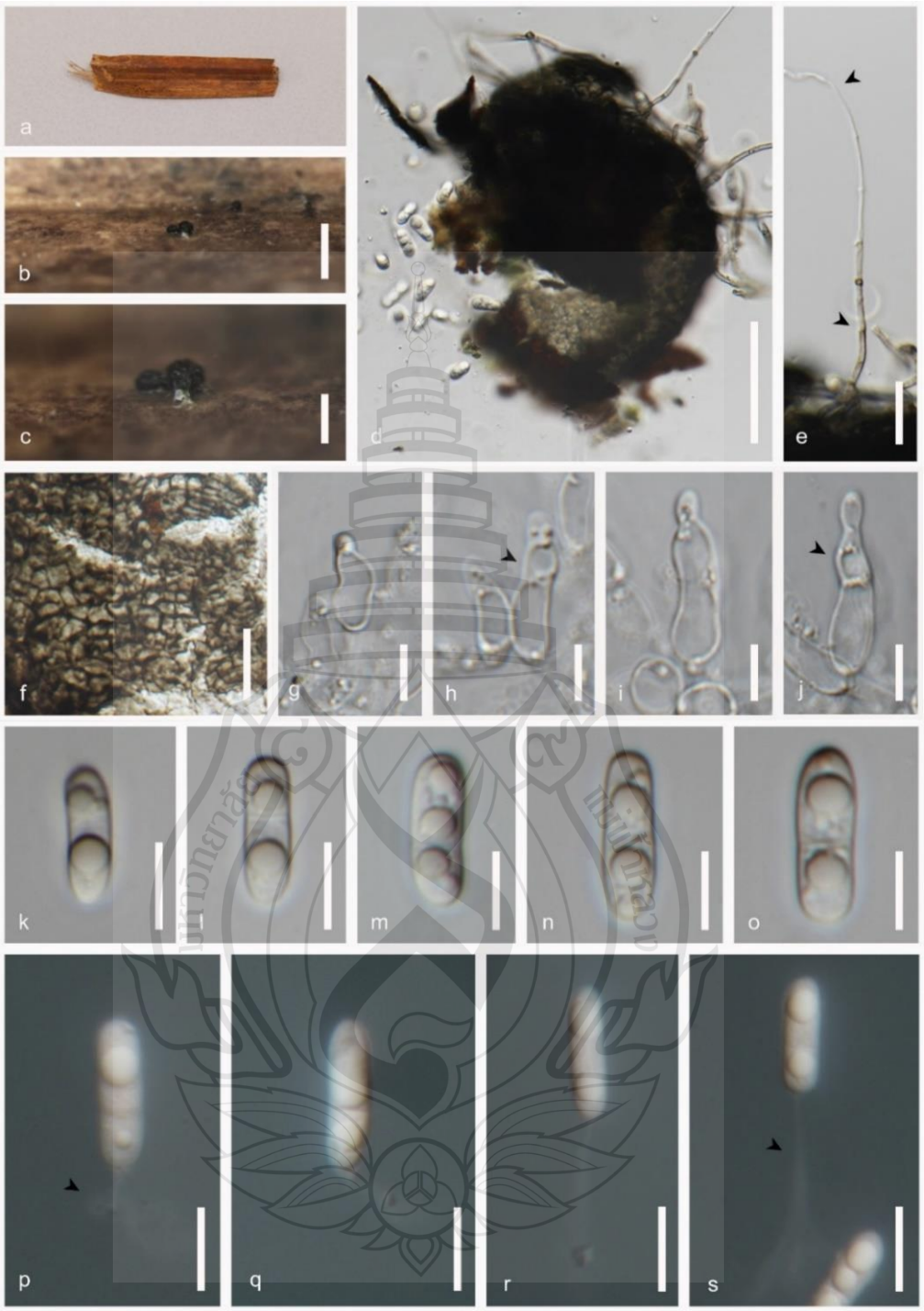

Note a Decomposing *Carex* sp. host. b–c Black spherical cleistothecial ascomata on the host. d Squashed mount of ascomata. e Septate setae. f Surface of peridium. g–j Conidiophores with unicellular conidiogenous cells (arrowed). k–o Conidia in water. k–o Conidia with gelatinous basal appendage. Scale bars: b 750 µm, c 250 µm, (d) 100 µm, e–f 20 µm, g–s 10 µm.

Figure 4.33 *Neottiosporina mihintaleensis* (MFLU 25-0438)

Stagonospora (Sacc.) Sacc

The genus *Stagonospora* was erected by Saccardo and Spegazzini (1884) (Wijayawardene et al., 2022) and is typified by *Stagonospora paludosa*. Members of Stagonospora exhibit a worldwide distribution and are known to be endophytic, saprobic, pathogenic, or endophytic. The asexual morphs of *Stagonospora* are characterized by immersed, globose, black pycnidia with walls comprised of textura angularis cells. Conidiogenous cells are phialidic and hyaline, and conidia are guttulate, subcylindrical, (6–)7–8-septate, becoming constricted at the septa upon maturity (Quaedvlieg et al., 2013; Jayasiri et al., 2015; Bhagya et al., 2024). Sexual morphs of *Stagonospora* develop globose, brown ascomata with a short ostiole, and the peridium is composed of textura angularis cells. The pseudoparaphyses are dense, hyaline, and septate, surrounding bitunicate, clavate asci containing eight ascospores. The ascospores are ellipsoidal, 1-septate, with guttules in each cell (Quaedvlieg et al., 2013; Crous et al., 2019).

Stagonospora narathiwatensis Bhagya, Phukhams E.B.G. Jones & K.D. Hyde, sp. nov.

Index Fungorum number: IF; Facesoffungi number: FoF 18907

Etymology – The name refers to Narathiwat a southern coastal province in Thailand, where this species was first collected.

Holotype – MFLU 25-0439

Saprobic on dead, decaying stems of Grass, (Poaceae), **Sexual morph**: Undetermined. **Asexual morph**: Coelomycetous. *Conidiomata* 70–100 ×30–50 μm ($\bar{x}$ = 85 × 42 μm, n = 5), pycnidial, loosely aggregated, occasionally clustered, immersed under host epidermis or partially erupt on the host, dark brown to black in color, globose to subglobose, uni-loculate. *Conidiomatal wall* 5–15 μm wide ($\bar{x}$ = 7.5 μm, n = 10), consist with two layers, outer layer light brown, thick-walled cells in *textura angularis*, inner layer thin, hyaline to brown cells of *textura pseudoparenchyma*. *Conidiophores* reduced to conidiogenous cells. *Conidiogenous cells* 5–10 × 2–4 μm ($\bar{x}$ = 6 × 3.5 μm, n = 10), proliferating from inner hyaline layer of conidiomata, smooth-walled, hyaline, ampulliform to subglobose or obovid, enteroblastic, determinate, annellidic, show rhexolytic detachment of conidia. *Conidia* 12–20 × 3–6 μm ($\bar{x}$ = 15.5 × 4.5 μm; n = 20), hyaline, 3-euseptate, smooth thick-walled, each cell bears a prominent large guttulate,

sub-cylindrical, occasionally irregularly concaved, obtuse and rounded at apex, tapering to narrow base with flatten scar from conidiogenesis, bear gelatinous cap when immature, disappear with maturity.

Culture characteristics: Conidia germinating on MEA within 72 h. Germ tubes produced from several cells of the conidia. Colonies growing on MEA, reaching 5–10 mm in 6 weeks at 25°C. Mycelia superficial, umbonate with papillated culture with entire edge, from above greenish black from center to the edge with cottony white areal mycelium on surface, from reverse greenish brown to black from the center and ash to the edge

Material examined: Thailand, Chang Wat Narathiwat Province, Amphoe Tak Bai, District, Tambon Sala Mai on decaying petiole of grass (Poaceae), 10 August2023, Tharindu Bhagya, T65_A (MFLU 25-0439, holotype), Chang Wat Narathiwat Province, Amphoe Tak Bai, District, Tambon Sala Mai on *Typha* sp. (Typhaceae), 10 August 2023, Tharindu Bhagya T65_B, (MFLU 25-0440, isotype).

GenBank numbers – MFLU 25-0439, ITS = PX062274, LSU = PX062273

Distribution – Decaying stem of grass, (Poaceae), and *Typha* sp. (Typhaceae) in Narathiwat, Thailand.

Notes – The new isolate *Stagonospora narathiwatensis* (MFLU 25-0439), forms a sister clade to *S. pseudoperfecta* (KT 889 and HHUF 29087), with 90% ML and 0.90 BPP support (Figure 4.32). Strain MFLU 25-0439 agrees with the general characteristics of *Stagonospora*, by producing globose to subglobose, uniloculate conidiomata, smooth-walled, hyaline, subglobose conidiogenous cells, and hyaline, smooth, thick-walled, 3-euseptate, cylindrical conidia (Quaedvlieg et al., 2013; Crous et al., 2019; Bhagya et al., 2024). The presence of thin, hyaline to brown cells of textura pseudoparenchyma inner cell layer and annellidic conidiogenesis process make strain MFLU 25-0439 distinguishable from *S. pseudoperfecta* (KT 889 and HHUF 29087) (Figure 4.34) (Crous et al., 2019). The pairwise distance matrix values between MFLU 25-0439 and related strains range from 0.01 to 0.05, indicating that the new strain belongs to the genus *Stagonospora* but represents a distinct species (Gostinčar 2020; Maharachchkumbura et al., 2021). Based on the available evidence, I introduce *S. narathiwatensis* (MFLU 25-0439) as a new species in the genus *Stagonospora*, isolated from a decomposing grass stem and Typha sp. stem in Narathiwat, Thailand.

Note a Stem of decomposing grass. b-c Conidiomata on host. d Vertical section of conidiomata. e Peridium. f–j Conidiogenous cells and annellidic conidiogenesis. (arrowed). k–n Conidia with flatten scar (arrowed). o Germinated condiospore. p Culture on MEA above. q reverse. Scale bars: d–e 20 µm, f–o 10 µm.

Figure 4.34 *Stagonospora narathiwatensis* (MFLU 25-0439, holotype)

Stagonospora samroiyotensis Bhagya. & Phukhams *sp. nov.*

Index Fungorum number: IF901771; Facesofungi number: FoF 15567

Etymology – Name reflects the forest park, Khao Sam Roi Yot where the fungus was collected.

Holotype – MFLU 24-0020

Saprobic on decaying leaves of *Typha* (Typhaceae). **Sexual morph:** Undetermined. **Asexual morph**: Coelomycetous. *Conidiomata* 240–315 × 170–250 μm, pycnidial, solitary, scattered, semi-immersed to immersed, subglobose to globose, brown to black, central ostiole. *Conidiomatal wall* 11–18 μm wide, outer layer composed of thick-walled, dark brown cells of *textura angularis*, internal wall composed with cells of *textura angularis*, light brown with a hyaline layer of cells of *textura prismatica*, bearing the conidiogenous cell layer. *Conidiophores* reduced to conidiogenous cells. *Conidiogenous cells* 10– 11 × 4–6 μm, pyriform to truncate in shape, thin-walled, hyaline, smooth. *Conidia* 25–32 × 3–4 μm ($\bar{x}$ = 28.5 × 3.5 μm, n = 30), oblong, cylindrical, 1-septate, constricted at the septa, rounded at the apex and tapered toward the base, guttulate, hyaline, smooth-walled.

Culture characteristics: Conidia germinated on PDA within 12 hours. Germ tubes produced from the basal cell of the conidia. Colonies growing on PDA, reaching 20–25 mm in 6 weeks at 25°C. Mycelia superficial, raised with papillate surface, lobate shape with smooth ending at edges, from above pale white from center to the edge; reverse dark brown at the center, orangey at the edge. Light yellow to light orange pigment diffusing in the agar.

Material examined: Thailand, Prachuap Khiri Khan Province: Pran Buri District, Khao Sam Roi Yot Wetland on decaying and submerged stem of *Typha* sp. (Typhaceae) in lotic waters, 25 Feb 2023, Amuhenage T. Bhagya, TBC11C16 (MFLU 24-0020, holotype); ex-type living culture, MFLUCC 24-0052.

GenBank numbers – ITS = PP463951, LSU = PP463950, SSU = PP463952, *tef1-α* = PP526741

Distribution – Decomposing *Typha* sp. stem, Chang Wat Prachuap Khiri Khan Province, Thailand.

Notes – In the phylogenetic analyses, *Stagonospora samroiyotensis* (MFLUCC 24-0052) formed a separate lineage sister to three isolates of *S. uniseptata* (CBS

135090) with 100% ML and 1.00 BYPP statistic support (Figure 4.32). *Stagonospora samroiyotensis* matches with the general concept of *Stagonospora*. Our isolate is characterized by having globose pycnidial conidiomata, thick peridial wall composed of *textura angularis* and *textura prismatica* cell types, conidiophores reduced to conidiogenous cells with percurrent proliferation from the inner layer of the pycnidial wall. Conidiogenous cells are doliiform, terminal, and holoblastic producing hyaline, cylindrical to ellipsoidal, straight or slightly curved and guttulate conidia (Li et al., 2016; Quaedvlieg et al., 2013; Tanaka et al., 2015). The conidiomata diameter of *S. samroiyotensis* is larger (170–250 μm) than *S. uniseptata* (150 μm), and *S. samroiyotensis* has a higher L/ W ratio for the conidia (*S. samroiyotensis* = 8.25, *S. uniseptata* = 3.67). The conidiomata wall of *S. uniseptata* consists only of red-brown cells of *textura angularis* (Quaedvlieg et al., 2013), but *S. samroiyotensis* has inner hyaline cell layers in *textura angularis* and *textura prismatica*. *Stagonospora samroiyotensis* has pyriform to truncate holoblastic conidiogenous cells while those of *S. uniseptata* are phialidic. *Stagonospora uniseptata* conidia are blunt, obtuse, and tapering towards the base with rounded ends (Quaedvlieg et al., 2013), while *S. samroiyotensis* has more clavate conidia that are tapered and narrow towards the base (Figure 4.35). *Stagonospora macropycnidia*, *S. typhoidearum*, *S. pseudoperfecta* and *S. typhae* have been reported from the same host plant family while *S. uniseptata* was reported from *Carex acutiformis* (Quaedvlieg et al., 2013). Based on morph-molecular evidence I introduce *S. samroiyotensis* as a novel species. No sexual stage has been observed.

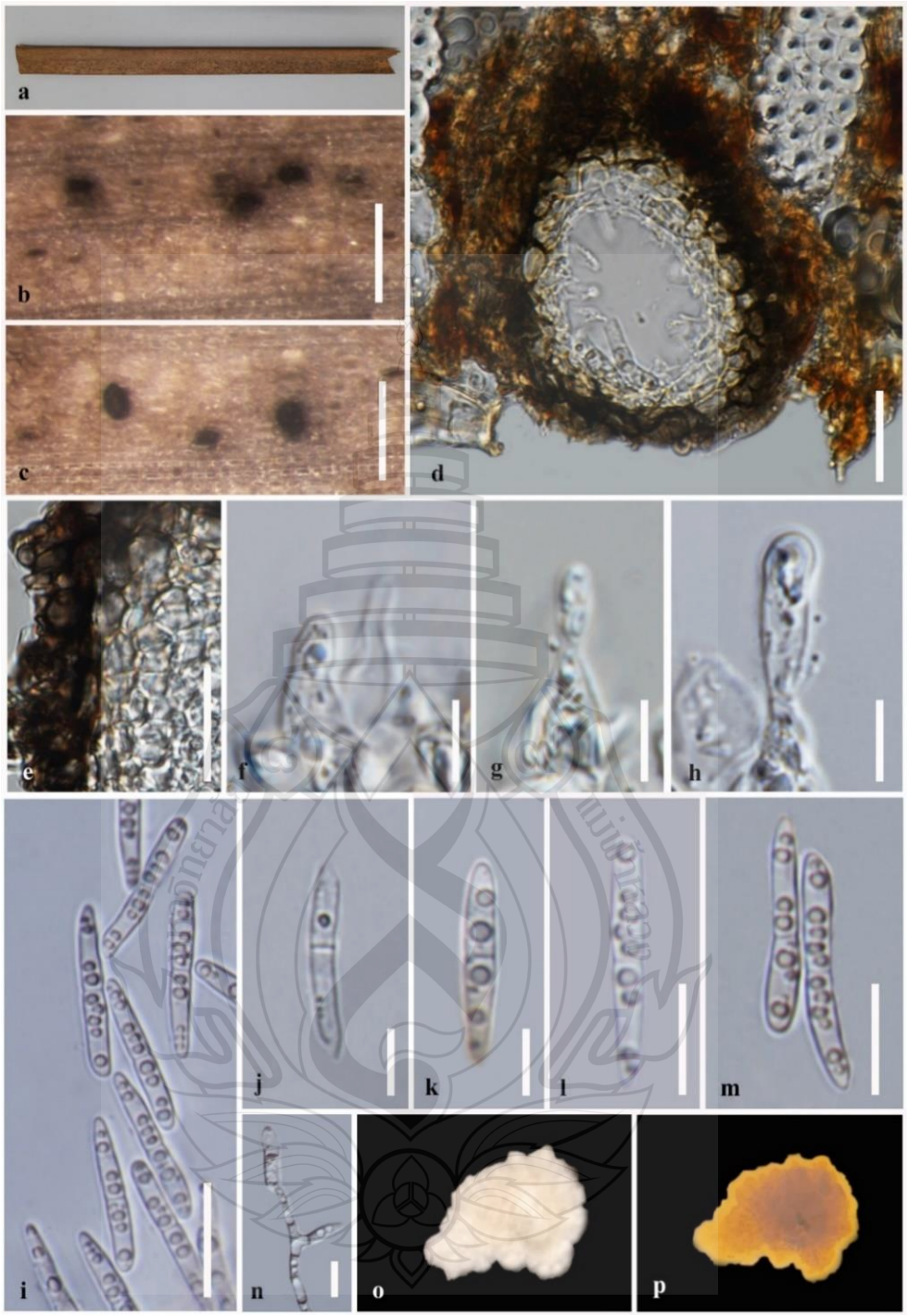

Note a. Decaying stem of *Typha* species from a lotic wetland. b, c. Close up of conidiomata on the host surface. d. Vertical section of conidioma. e. Vertical section of partial conidiomatal wall. f–h. Developing conidia and conidiogenous cells. i–m. Conidia. n. Germinated conidium. o. Colonies on PDA from above; p reverse. Scale bars: b–c = 1 mm, d =50 µm, e–h, j–n = 10 µm, i= 20 µm.

Figure 4.35 *Stagonospora samroiyotensis* (MFLU 24-0020, Holotype)

Phaeosphaeriaceae M.E. Barr

Ophiosphaerella Speg

Ophiosphaerella was erected by Speg. in 1909 and typified by *Ophiosphaerella graminicola*. Members of this genus are often reported as saprobic organisms or pathogens and show an affinity toward host species in the Poaceae and Cyperaceae families (Câmara et al., 2000). The phylogenetic placement of this genus within *Phaeosphaeriaceae* was confirmed by multi-locus phylogenetic analyses (Hyde et al., 2013). *Ophiosphaerella* is characterized by papillate ascomata containing bitunicate, fissitunicate, cylindrical, narrow asci with short, furcate pedicels, and pale brown, smooth, filamentous, multi-septate ascospores that lack swollen cells or division into part-spores (Tennakoon et al., 2020; Zhang et al., 2023).

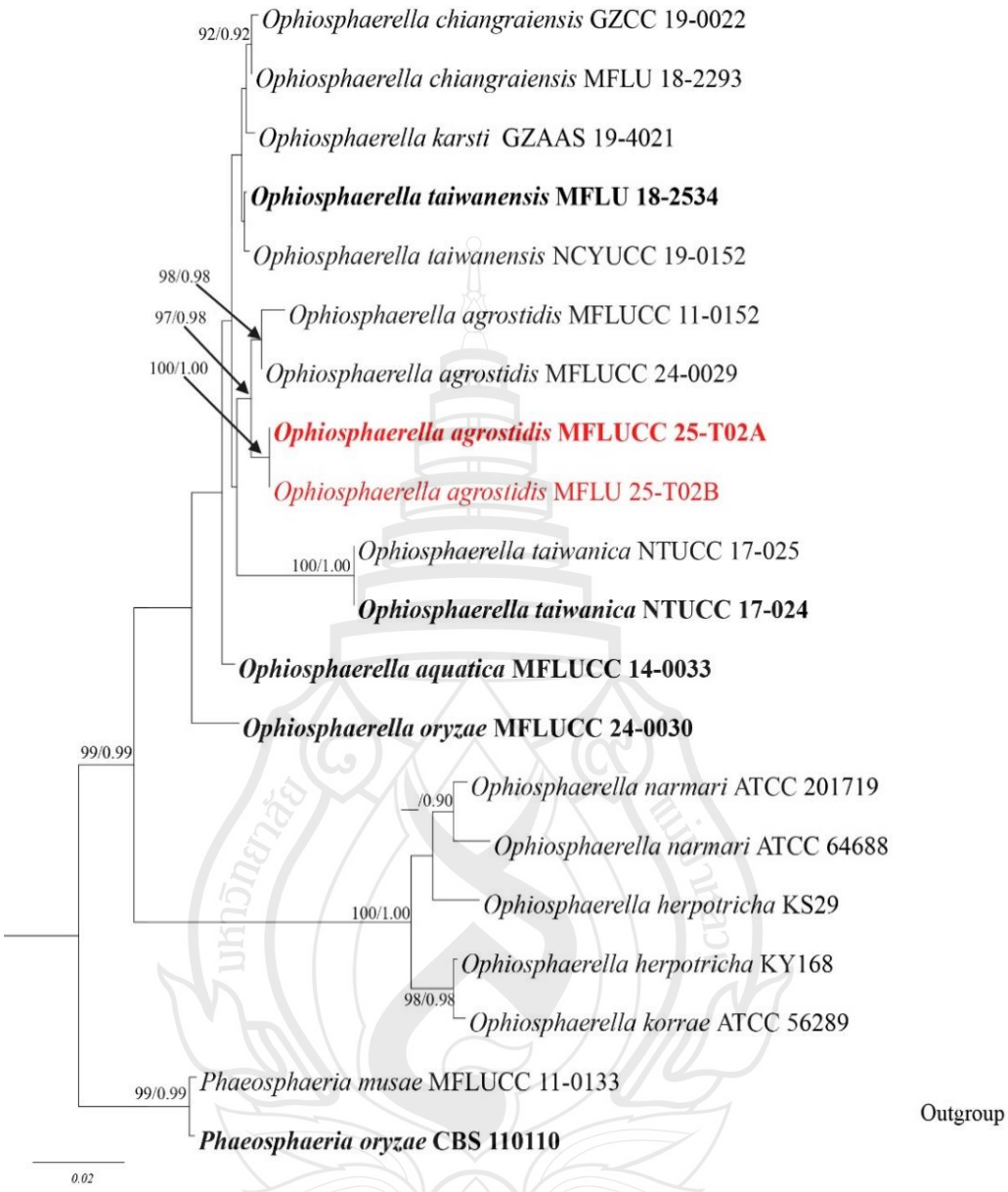

Note Bootstrap support values for ML ≥ 90 % and Bayesian posterior probabilities (BPP) ≥ 0.9 are mentioned at the nodes. The tree was rooted to *Phaeosphaeria musae* strain MFLUCC 11-0133, and *P. oryzae* strain CBS 110110. Newly generated sequences are in red and the type strains are in bold.

Figure 4.36 Phylogram generated from Maximum Likelihood (ML) analysis based on combined ITS, LSU, SSU and *tef1* sequence. The data set comprises 3516 characters including gaps from of selected 20 strains which were included in the phylogenetic analyses.

Ophiosphaerella agrostidis Dern., M.P.S. Câmara, N.R. O'Neill, Berkum & M.E. Palm [as 'agrostis'], in Câmara, O'Neill, Berkum, Dernoeden & Palm, Mycologia 92(2): 320 (2000)

Saprobic on decaying stem of grass (Poaceae). **Sexual morph**: *Ascomata* 150–360 × 140–330 µm ($\bar{x}$ = 320 × 290 µm, n = 5), black or dark brown, solitary, scattered or occasionally clustered, immersed under host tissue or erumpent, short black short ostiole erupt from host tissue, slightly raised, glabrous, ampulliform or golobose to subglobose with uni-loculate opening. *Ostiole*, black, erect, rounded or obtuse and compose by dark, black cells in *textura angularis. Peridium* 30–60 µm wide ($\bar{x}$ = 48 µm, n = 10), show unequal thickness, thick at the base, composed of multiple layers from brown thick-walled cells in *textura angularis*. *Pseudoparaphyses* 1–2 µm wide ($\bar{x}$ = 1.5 µm, n = 10), hyaline, septate, branched, smooth walled, filamentous, anastomosing, and end taping towards blunt rounded apexes, embedded in to a viscus looking metrix. *Asci* 130–190 × 10–15 µm ($\bar{x}$ = 170 × 12 µm, n = 10), 8-spored, bitunicate, fissitunicate, cylindrical to cylindric-clavate or obclavate, slightly curved, process short furcate pediculate, with conspicuous, well developed ocular chamber at the apexes. *Ascospores* 110–160 × 7.5–4.5 µm ($\bar{x}$ = 125 × 6.5 µm, n = 20), hyaline, fasciculate, aggraded in parallel or spiral manner, scolecosporous, filiform to filamentous, smooth walled, guttiulate and multi-septate, narrowing towards apexes. **Asexual morph**: Undetermined.

Culture characteristics: Conidia germinating on MEA within 12 h. Germ tubes produced from multiple cells of the ascospore. Colonies growing on MEA, reaching 20 mm in 2 weeks at 25°C. Mycelia superficial, cottony, umbonate shape culture with erose edge, from above light gray at the center and hyaline at the edge, from reverse light brown from the center, off white at the middle and surrounded with reddish brown conspicuous ring, from the far edge hyaline mycelia radiate to the Metrix.

Material examined: Thailand, Chang Wat Prachuap Khiri Khan Province, Pran Buri District, Pran Buri wetland, on decaying leaves of submerged grass (Poaceae), 02 December 2023, Tharindu Bhagya, T2_A (MFLU 25-0441,), Chang Wat Prachuap Khiri Khan Province, Pran Buri District, Pran Buri wetland, on decaying leaves of submerged grass (Poaceae), 06 April 2024, Tharindu Bhagya T2_B, submerged grass (Poaceae) (MFLU 25-0442).

GenBank numbers – MFLU 25-0441: ITS = PX518049, LSU = PX518047

Distribution – Saprobic or pathogenic on *Agrostis palustris*, Virginia (Câmara et al., 2000), dead culms of grass, Maejo University Phrae Campus, Rongkwang District. Thailand (Phookamsak et al., 2014), brown rot of leaf sheaths of *Zingiber mioga*, Kochi, Japan (Oki et al., 2022), dead culm of unidentified herbaceous plant, Guizhou Province, China (Zhang et al., 2023), dead, submerged, decomposing leaves of grass, Pran Buri wetland, Thailand (This study).

Notes – The multi-locus phylogenetic analysis placed the newly isolated strains in a clade sister to *Ophiosphaerella agrostidis* (MFLUCC 11-0152) and strain MFLUCC 24-0029, with 97% ML and 0.98 BPP statistical support (Figure 4.36). This phylogenetic placement was further supported by 99.2% similarity in ITS sequences, 99.8% similarity in LSU sequences, and 98.1% similarity in tef1 sequences between MFLU 25-0441 and MFLUCC 24-0029 (excluding gaps). The pairwise distance matrix value was <0.01 between MFLU 25-0442 and MFLUCC 24-0029, indicating that both strains belong to the same species (Gostinčar, 2020; Maharachchkumbura et al., 2021). Considering the available evidence, I recognize the strain as *O. agrostidis* and document the first report of this species from completely submerged, decomposing grass leaves in a freshwater coastal wetland.

Note a Ascomata on *Poaceae* host (arrowed). b–c Immersed ascomata in the host tissue. d Vertical section of ascomata. e Ostiole. f Peridium with septa (arrowed). g Pseudoparaphyses. h–j Mature asci with ocular chamber (arrowed). k–m Ascospores. n Culture on MEA above. o reverse. Scale bars: d–e 50 µm, f–m 20 µm.

Figure 4.37 *Ophiosphaerella agrostidis* (MFLU 25-0441)

Pleosporaceae Nitschke

Curvularia Boedijn

Boedijn (1933) introduced the genus *Curvularia* and designated *Curvularia lunata* as the type species. This species-rich genus exhibits a cosmopolitan distribution and includes a variety of life modes, such as saprobic organisms, endophytes, edaphic fungi, and pathogens of both plants and animals. The genus *Cochliobolus* has been considered the sexual morph of *Curvularia*, but *Curvularia* is predominantly known and isolated in its asexual hyphomycetous stage. The asexual morph is characterized by pale to dark brown, smooth to slightly roughened, thick-walled, erect, septate, simple or occasionally branched, straight to flexuous conidiophores. These bear polyblastic, integrated, and sympodially proliferating terminal conidiogenous cells. The conidia of *Curvularia* are pale to dark brown, smooth-walled to verrucose, curved, ellipsoid to fusiform, 3–4-septate, with an enlarged central cell (Manamgoda et al., 2012; Zhou et al., 2015; Marin-Felix, 2020; Yasanthika et al., 2023; Zibani et al., 2024).

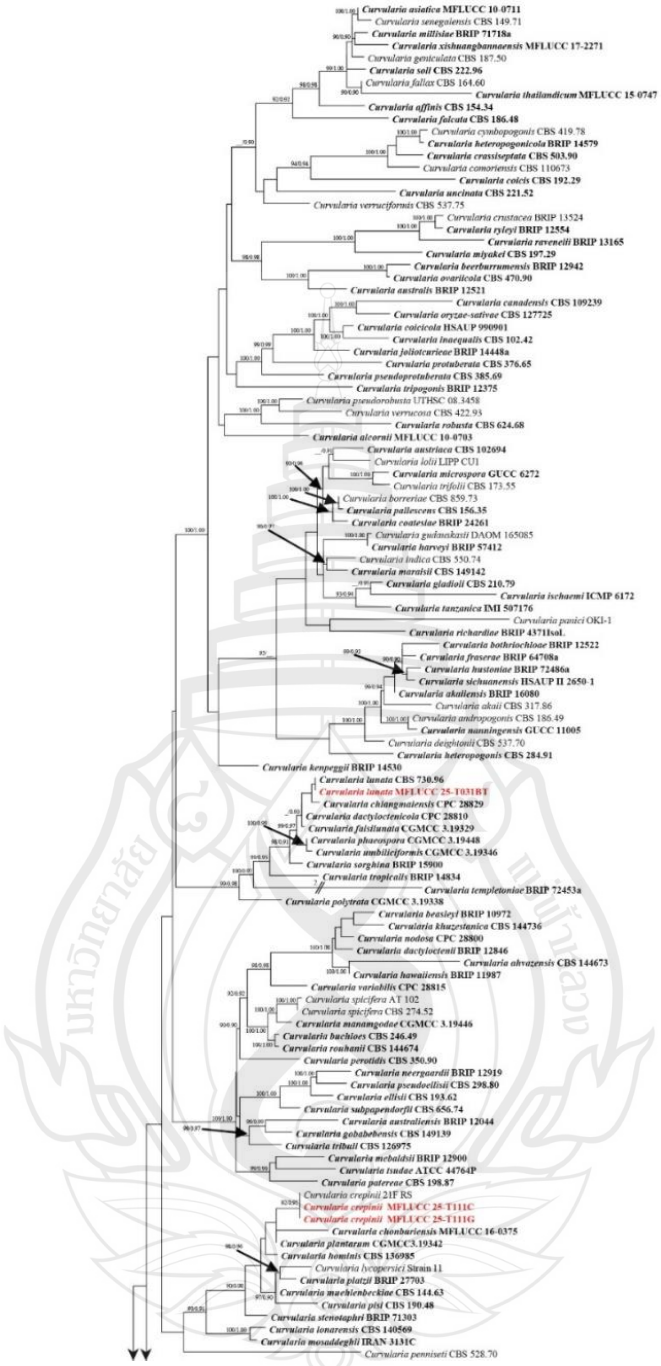

Note The data set comprises 2301 characters including gaps from of selected 186 strains which were included in the phylogenetic analyses. Bootstrap support values for ML ≥ 90 % and Bayesian posterior probabilities (BPP) ≥ 0.9 are mentioned at the nodes. The tree was rooted to Bipolaris maydis (CBS 136.29) and Exserohilum turcicum (CBS 690.71) Newly generated sequences are in red and the type strains are in bold.

Figure 4.38 Phylogram generated from Maximum Likelihood (ML) analysis based on combined ITS, *gap1*, and *tef1-α* sequence.

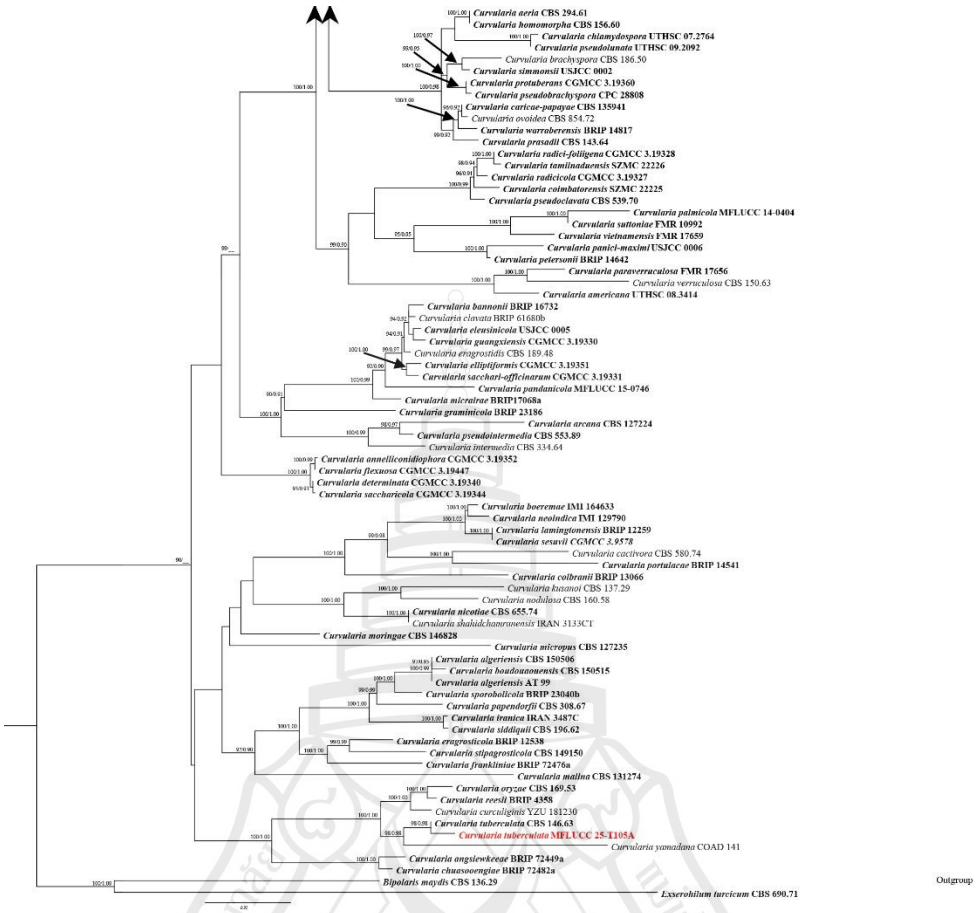

Figure 4.38 (continued)

Curvularia crepinii (Westend.) Boedijn, Bull. Jard. bot. Buitenz, 3 Sér. 13(1): 128 (1933)

Saprobic on dead decomposing leaf of *Carex*, (Cyperaceae), **Sexual morph**: Undetermined. **Asexual morph**: *Hyphomycetous*, numerous, dark brown and amphigenous on host. *Conidiophores in-situ* 190–320 × 1–4.5 µm ($\bar{x}$ = 285 × 3.5 µm, n = 10), *in-vitro* 70–180 × 1–4.5 µm ($\bar{x}$ = 92 × 3.5 µm, n = 10), macronematous, mononematous, pale-brown to dark brown to light brown at base, pale brown to sub-hyaline towards apex, thick-walled, septate, smooth or verruculose flexuous or straight, to simple or occasionally branched. *Conidiogenous cells*, 3–5 x 2–8 µm ($\bar{x}$ = 4.5 × 5.5 µm, n = 10), monoblastic or polyblastic, polytretic, integrated, terminal or intercalary, sympodial, pale-brown to sub-hyaline or hyaline, smooth, thick-walled, cylindrical to sub-cylindrical. *Conidia in-vitro* 15–30 × 8–12 µm ($\bar{x}$ = 22 × 9.5 µm, n = 20), 3- septate or 2-4 septate, straight or curved, cylindrical to ellipsoidal or clavate, process thickened hilum, terminal cells hyaline to sub-hyaline,

smooth, thick-walled, central cells large, pale-brown to brown, 3rd cells larger, verruculose, basal cell with darker, protruding, thick hilum.

Culture characteristics: Conidia germinating on MEA within 24 h. Germ tubes produced from ends of conidium. Colonies growing on MEA, reaching 40 mm in 2 weeks at 25°C. Mycelia superficial, effuse to umbonate, erose edges, from above yellowish brown to off white from center to the edge with ash color cottony patchers, from reverse greenish black at the center and yellowish brown at the edge with light yellow ring leading to hyaline tips. Culture sporulates after 6 weeks at 25°C.

Material examined: Thailand, Chang Wat Prachuap Khiri Khan Province, Pran Buri District, Pran Buri wetland, decomposing stem of *Carex* sp. (Cyperaceae), 02 December 2023 T111A (MFLU 25-0443), Thailand, Chang Wat Prachuap Khiri Khan Province, Pran Buri District, Pran Buri wetland, decomposing leaf of Grass (Poaceae), 02 December 2023, T111B (MFLU 25-0444).

GenBank numbers – MFLU 25-0443: ITS = PX518058

Distribution – *Ophioglossum vulgatum* (adder's-tongue fern), Rochefort, France (Saccardo, 1883); *Ophioglossum vulgatum*, Franklin & Delaware Counties, Ohio, USA (Ellett, 1980); *Ophioglossum vulgatum*, Outer Hebrides, Scotland, United Kingdom (Watling, 2010); *Hedyotis diffusa*, Zhejiang, China (Zhou et al., 2015); *Pantala flavescens* larvae gut, Jinhua, Zhejiang, China (Li et al., 2018), decomposing *Carex* sp., and grass stems, in Parn Buri, Thailand (This study).

Notes – Multi-locus phylogenetic analysis placed the new isolates in a sister clade to *Curvularia crepinii* strain 21FRS, with 92% ML and 0.95 BPP support (Figure 4.38). Phylogenetically, strain MFLU 25-0443 exhibited 99.14% similarity in ITS and 99.22% similarity in *gap1* sequences (excluding gaps) with *C. crepinii* strain 21FRS (Zhou et al., 2015; Vasikasin et al., 2019; Dhar et al., 2023). Morphologically, the isolates produce monoblastic or polyblastic, integrated, intercalary and terminal, sympodial conidiogenous cells, predominantly forming 3-septate, fusiform conidia with a wider and darker median cell, resembling the general description of *C. crepinii* (Figure 4.39) (Gusmão et al., 2005). Based on the available evidence, I identify the new strains as *C. crepinii* and report new host records from grasses and *Carex* sp. in freshwater coastal wetlands of Thailand.

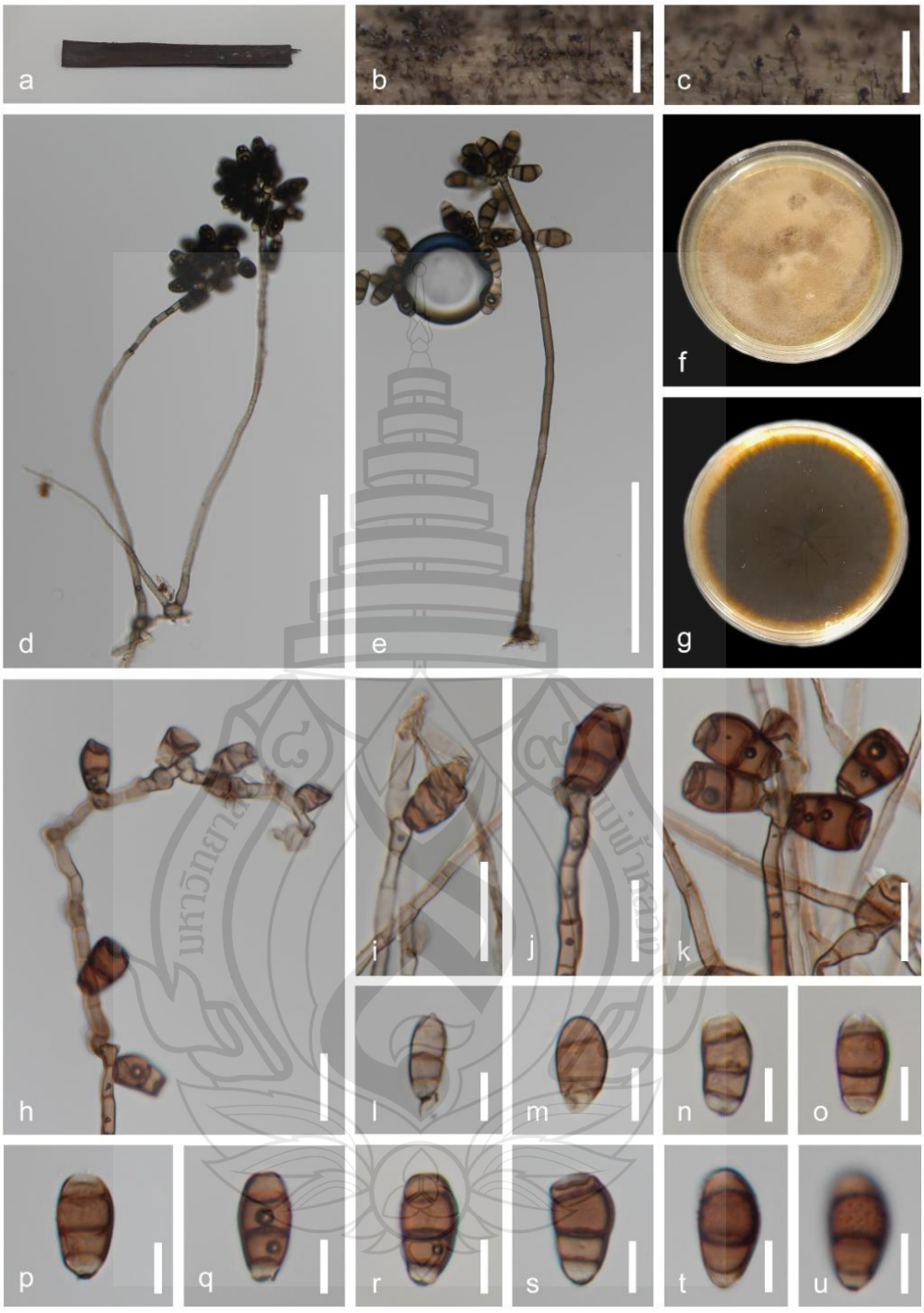

Note a *Carex* sp. host material. b–c Colonies on host surface. d–e Squash mount of conidiophores from host. f Culture on MEA above. g Reverse. h Conidiophores *in-vitro*. i–k Conidiogenous cells bearing developing conidia *in-vitro*. l–o Conidial development. p–t Mature conidia. u Conidium in different focused showcasing verruculose third cell. Scale bars: b–c 250 µm, d–e 100 µm, h–k 20 µm, l–u 10 µm.

Figure 4.39 *Curvularia crepinii* (MFLU 25-0443)

Curvularia lunata (Wakker) Boedijn, Bull. Jard. bot. Buitenz, 3 Sér. 13(1): 127 (1933)

Saprobic on dead decomposing leaf of *Thypa*, (Typhaceae), **Sexual morph**: Undetermined. **Asexual morph**: *Hyphomycetous*, numerous, dark brown and amphigenous on host. *Conidiophores in-situ* 110–270 × 4.5–7.5 μm ($\bar{x}$ = 125 × 5.5 μm, n = 10), *in-vitro* 70–130 × 2.5–6.5 μm ($\bar{x}$ = 95 × 4.5 μm, n = 10), macronematous, mononematous, dark brown to pale-brown at base, pale brown to sub-hyaline towards apex, thick-walled, septate, smooth, flexuous or straight, to simple or branched. *Conidiogenous cells*, 3–8 x 2–6 μm ($\bar{x}$ = 6.5 × 4.5 μm, n = 10), monoblastic or polyblastic, sympodial, integrated, terminal, intercalary, pale-brown to sub-hyaline or hyaline, smooth, thick-walled, cylindrical to sub-cylindrical. *Conidia in-vitro* 15–30 × 8–18 μm ($\bar{x}$ = 26 × 12.5 μm, n = 20), 3-septate, straight or curved, clavate, ellipsoid, fusiform, thickened non-protuberant hilum, terminal cells sub-hyaline to pale brown, smooth, thick-walled, occasionally atypical and bifurcate from apex, central cells large, pale-brown to brown, unequally asymmetrical.

Culture characteristics: Conidia germinating on MEA within 24 h. Germ tubes produced from ends of conidium. Colonies growing on MEA, reaching 40 mm in 4 weeks at 25°C. Mycelia superficial, effuse to umbonate, erose edges, from above dark brown to black from center to the edge with ash color to brown cottony patchers, from reverse greenish black at the center leading to hyaline edge. Culture sporulates after 8 weeks at 25°C.

Material examined: Thailand, Chang Wat Prachuap Khiri Khan Province, Pran Buri District, Pran Buri wetland, decomposing stem of *Thypa* sp. (Typhaceae), 30 November 2023, T31B (MFLU 25-0445).

GenBank numbers – MFLU 25-0445, ITS = PX518057

Distribution – *Acrothecium lunatum*, Netherlands (Wakker & Went, 1898); *Curvularia lunata*, Java, Indonesia (Boedijn, 1933); *Hymenachne amplexicaulis*, Pantanal do Mato Grosso, Brazil (Evans & Reeder, 2001); *Cynodon dactylon*, Brazil (Evans & Reeder, 2001); *Cymbopogon citratus*, Brazil (Evans & Reeder, 2001); *Gladiolus* sp., Brazil (Evans & Reeder, 2001); *Jatropha curcas*, Tamaulipas, Mexico (Arellano et al., 2010); *Fragaria* × *ananassa*, Jammu & Kashmir, India (Verma & Gupta, 2010); *Nelumbo nucifera*, Jiangxi Province, China (Cui & Sun, 2012); *Zea mays*,

Shandong Province, China (Zhang et al., 2014); *Triticum aestivum*, Northern China (Zhang et al., 2014); *Hordeum vulgare*, Northern China (Zhang et al., 2014); *Morus* sp., Chiang Mai Province, Thailand (Phutthacharoen et al., 2017); *Mallotus oblongifolius*, Hainan Province, China (Liu et al., 2018); *Brassica rapa* subsp. *pekinensis*, Thailand (Wonglom et al., 2018); *Hylocereus polyrhizus*, Peninsular Malaysia (Chai et al., 2019); *Dracaena fragrans*, Kanchanaburi Province, Thailand (Phukhamsakda et al., 2020); *Zea mays*, North Carolina, USA (Nischwitz et al., 2023); *Oryza sativa*, Sabah, Malaysia (Roslan et al., 2023); *Citrus reticulata*, Guangdong Province, China (Cui et al., 2023); *Sorghum bicolor*, Giza, Egypt (Soliman et al., 2024); *Cucumis melo*, Tamil Nadu, India (Vanitha et al., 2024); *Vigna unguiculata*, Nigeria (Onuh & Ayodele, 2024); *Arachis hypogaea*, Nigeria (Onuh & Ayodele, 2024); *Glycine max*, Nigeria (Onuh & Ayodele, 2024); *Vigna subterranea*, Nigeria (Onuh & Ayodele, 2024), decomposing *Typha* sp., in Parn Buri, Thailand (This study).

Notes – The phylogenetic analysis places the new isolate, strain MFLU 25-0445, as sister to *Curvularia lunata* strain CBS 730.96 with 85% maximum likelihood (ML) and 0.86 Bayesian posterior probability (BPP) statistical support (Figure 4.38). The ITS sequence of strain MFLU 25-0445 showed 99.45% similarity, and the *gap1* sequence 98.76% similarity, to respective loci in *C. lunata* strain CBS 730.96 (Vu et al., 2019). Morphologically, the presence of polyblastic, sympodial, integrated, terminal, and intercalary conidiogenous cells, along with 3-septate, straight to curved, clavate, ellipsoid, fusiform, atypical, and bifurcate conidia, makes strain MFLU 25-0445 resemble the general disruption patterns typical of *C. lunata* (Figure 4.40) (Gusmão et al., 2005). Considering the available evidence, I recognize the new strain as *C. lunata* and document a new host record from *Typha* sp. in freshwater coastal wetlands in Thailand.

Note a *Typha* sp. host material. b–c Colonies on host surface. d–f Squash mount of conidiophores from host. g Culture on MEA above. h Reverse. i–j Conidiophores *in-vitro*. k–n Conidiogenous cells bearing developing conidia *in-vitro*. o–s Conidial development. t–u Atypical and bifurcate conidia. v–x Mature conidia with expanded central call. Scale bars: b 500 µm, c 250 µm, d–f 50 µm, n–k 20 µm, o–x 10 µm.

Figure 4.40 *Curvularia lunata* (MFLU 25-0445)

Curvularia tuberculata B.L. Jain, Trans. Br. mycol. Soc. 45(4): 539 (1962)

Saprobic on dead decomposing leaf of *Thypa*, (Typhaceae), **Sexual morph**: Undetermined. **Asexual morph**: *Hyphomycetous*, numerous, dark brown and amphigenous on host. *Conidiophores in-vitro* 90–210 × 1–4.5 µm ($\bar{x}$ = 175 × 3.5 µm, n = 10), macronematous, dark brown to light brown at base, hyaline at the apex, flexuous straight to simple or branched, septets, thick-walled, smooth or rarely verruculose. *Conidiogenous cells*, 2–4 × 1–2 µm ($\bar{x}$ = 2.5 × 1.5 µm, n = 10), monoblastic, terminal or intercalary, geniculate, show echinulate nature close to developing conidia. *Conidia* 20–60 × 10–18 µm ($\bar{x}$ = 42 × 16 µm, n = 10), straight or curved, cylindrical to ellipsoidal or clavate, tuberculate or ornamented, process thickened hilum, olivaceous brown, 2-4 septate.

Culture characteristics: Conidia germinating on MEA within 12 h. Germ tubes produced from side. Colonies growing on MEA, reaching 30 mm in 1 week at 25°C. Mycelia superficial, effuse to umbonate, erose edges, from above yellowish brown to off white from center to the edge, from reverse greenish black at the center and yellowish brown at the edge. Culture sporulates after 4 weeks at 25°C.

Material examined: Thailand, Chang Wat Prachuap Khiri Khan Province, Pran Buri District, Pran Buri wetland, on decaying petiole of *Typha* sp. (Typhaceae), 08 May 2023, T105 (MFLU 25-0446).

GenBank numbers – MFLU 25-0446, ITS = PX518059

Distribution – *Zea mays*, Rajastha, Inida (Jain, 1962), *Vigna aconitifolia* (moth bean), Rajasthan, South Asia, India (Majumdar, 2002),*Fimbristylis miliacea* (rice flat sedge), Southeast Asia, India (Karuppiah & Seetharaman, 2004), Human tissue (disseminated infection), Unknown origin, Thailand or India (Vasikasin et al., 2019), *Archontophoenix alexandrae* (Alexandra palm), Australia (Queensland), Pakistan (Haq et al., 2020), *Rhododendron ferrugineum* (alpine rose), Central Europe origin, Himachal Pradesh, Uttarakhand, India (Dhar et al., 2023), *Saccharum officinarum* (sugarcane), Tropical Asia, Kiribati (Biota of NZ, 2025), *Fimbristylis cymosa* (sedge), Pantropical, Samoa and Tuvalu (Biota of NZ, 2025) and decaying stem of *Typha* sp. (Typhaceae) in Parn Buri, Thailand (This study).

Notes – The new isolate, strain MFLU 25-0446, forms a sister clade to *Curvularia tuberculata* strain CBS 146.63 with 98% ML and 0.98 BPP support (Figure

4.38). Phylogenetically, strain MFLU 25-0446 exhibit 99.16% similarity in ITS and 98.72% similarity in *gap1* sequences to *C. tuberculata* strain CBS 146.63 (Dhar et al., 2024). The cylindrical, ellipsoidal, and clavate conidia with tuberculate ornamentation make strain MFLU 25-0446 morphologically resemble *C. tuberculata* (Figure 4.41) (Jain, 1962, Dhar et al., 2024). Based on the available morphological and phylogenetic evidence, I identify the new isolate as *C. tuberculata*, and report it as a new host record from *Typha* sp., collected from coastal freshwater wetlands in Thailand.

Note a *Typha* sp. host material. b–c Colonies on host surface. d Culture on MEA above. e reverse. f–k Conidiophores with developing conidia in culture. i Proliferation of conidia on conidiophore. m–o Conidia. Scale bars: b 2.5 mm, c 500 µm, f–o 20 µm.

Figure 4.41 *Curvularia tuberculata* (MFLU 25-0446)

Exserohilum K.J. Leonard & Suggs

The genus *Exserohilum* was introduced by Leonard and Suggs (1974) to accommodate species previously classified under *Bipolaris*. The segregation was based on the presence of a prominent conidial hilum, a distinguishing feature of *Exserohilum* species (Leonard & Suggs, 1974). Initially, *Setosphaeria* was recognized as the sexual morph of the genus, however, the name *Exserohilum* was retained over *Setosphaeria*. Members of *Exserohilum* exhibit a cosmopolitan distribution and diverse nutritional modes, including pathogenic, saprobic, and endophytic lifestyles (Hernández-Restrepo et al., 2018; Ferdinandez et al., 2020; Absalan et al., 2024; Tian et al., 2024).

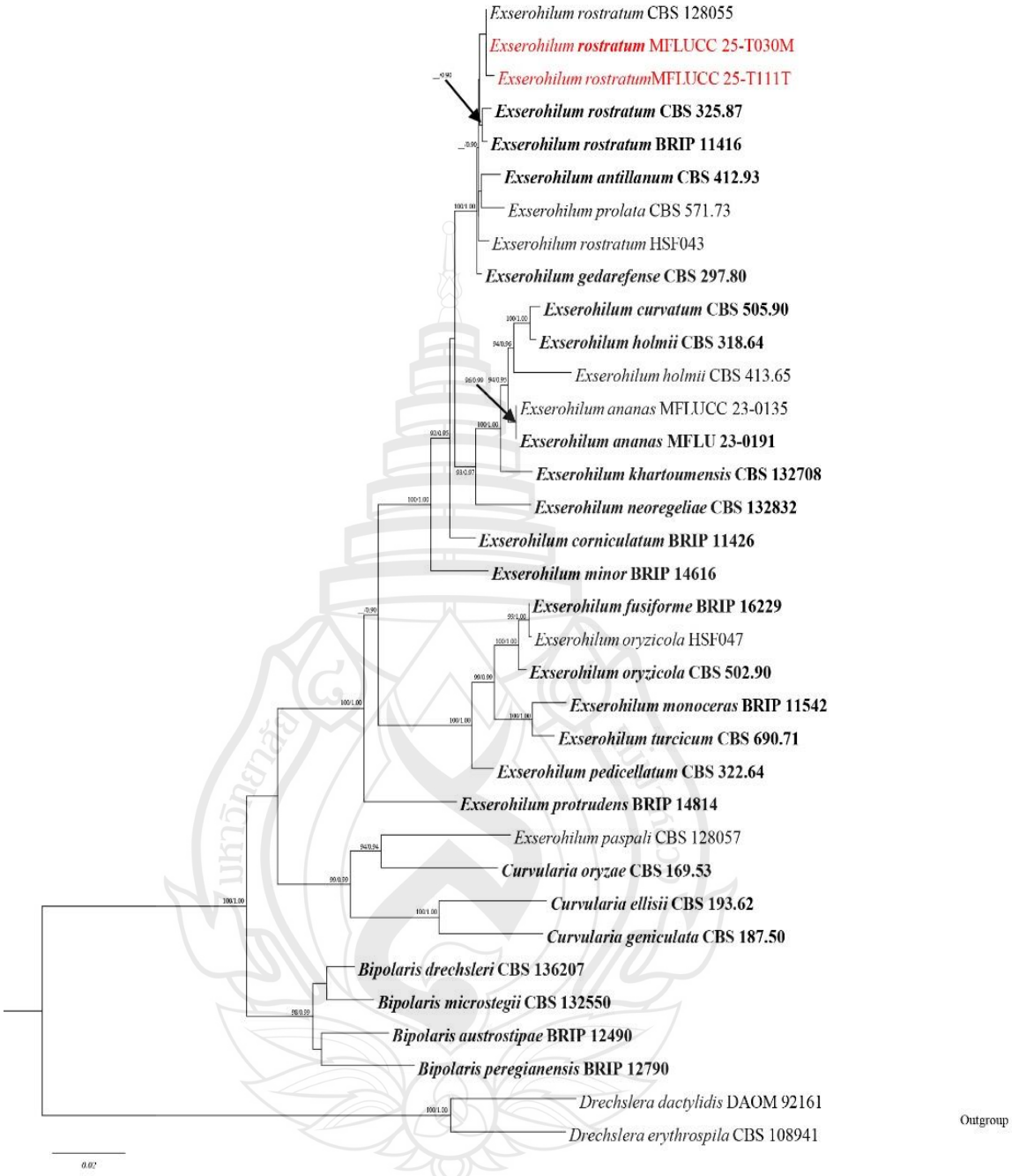

Note The data set comprises 3088 characters including gaps from of selected 35 strains which were included in the phylogenetic analyses. Bootstrap support values for ML ≥ 90 % and Bayesian posterior probabilities (BPP) ≥ 0.9 are mentioned at the nodes. The tree was rooted to *Drechslera dactylidis* (DAOM 92161) and *D. erythrospila* (CBS 108941).

Figure 4.42 Phylogram generated from Maximum Likelihood (ML) analysis based on combined ITS, LSU, *tef1-α*, and *GAPDH* sequence.

Exserohilum rostratum (Drechsler) K.J. Leonard & Suggs, Mycologia 66(2): 290 (1974)

Saprobic on dead decomposing leaf of *Thypa*, *Typhaceae*, **Sexual morph**: Undetermined. **Asexual morph**: Hyphomycetous, numerous, aggregated or occasionally fasciculate as dark brown to black patchers. *Conidiophores* 210–310 × 9–14 µm ($\overline{x}$ = 275 × 11.5 µm, n = 15), macronematous, mononematous, erect, straight or flexuous, dark brown at the base, pale brown towards the apex, smooth, thick-walled, septate, unbranched. *Conidiogenous cells*18–32 × 4.5–6 µm ($\overline{x}$ = 26 × 5.5 µm, n = 15), pale brown to sub-hyaline, smooth-walled, integrated, subcylindrical or cylindrical, terminal and intercalary, mono-to polyblastic, sympodial, cicatrized. *Conidia* 52–90 × 10–20 µm ($\overline{x}$ = 78 × 14 µm, n = 30), dark brown, olivaceous brown to pale brown at the middle with pale brown to hyaline terminal cells, smooth, thick walled, subcylindrical to obclavate rostrate, 5–14- distoseptate, straight to flexuous with protruding hilum.

Culture characteristics: Conidia germinating on MEA within 12 h. Germ tubes produced from base of conidium. Colonies growing on MEA, reaching 40 mm in 2 weeks at 25°C. Mycelia superficial, effuse to umbonate, erose edges, from above dark brown to black from center to the edge with ash color to brown cottony patchers, from reverse greenish black at the center leading to hyaline edge. Culture sporulates after 6 weeks at 25°C.

Material examined: Thailand, Chang Wat Prachuap Khiri Khan Province, Pran Buri District, Pran Buri wetland, decomposing stem of *Thypa* sp. (Typhaceae), 02 December 2023, Tharindu Bhagya, T30M, (MFLU 25-0447), Chang Wat Prachuap Khiri Khan Province, Pran Buri District, Pran Buri wetland, decomposing stem of *Carex* sp. (Cyperaceae), 02 December 2023, Tharindu Bhagya, T111T, (MFLU 25-448).

GenBank numbers – MFLU 25-0447, ITS = PX518060

Distribution – Decomposing plant debris, India (Subramanian, 1957), corneal ulcer (human), India (Bouchon et al., 1994), barnyard grass (*Echinochloa crus-galli*), and rice (*Oryza sativa*), Malaysia (Ng et al., 2011), sugarcane (Saccharum officinarum), Iran (Ahmadpour et al., 2012), invasive infection in immunocompromised patient, USA (da Cunha et al., 2012), clinical and environmental isolates, multi-country collection

(Chowdhary et al., 2015), Egypt (Walsh Medical Media, 2020), *Caryota* palm (*Caryota mitis*), Argentina (Loureiro, 2020), maize (Zea mays), China (Sharma et al., 2014), pineapple (*Ananas comosus*), Malaysia (Ibrahim et al., 2017), rice (*Oryza sativa*), Thailand (Pramesh et al., 2025), decomposing stem of *Thypa* sp. (Typhaceae), and decomposing stem of *Carex* sp. (Cyperaceae) in Pran Buri wetland, Thailand (This study).

Notes – The new isolates, strains MFLU 25-0437 and MFLU 25-0438, cluster within the *E. rostratum* clade (BRIP 11416, CBS 325.87, and CBS 128055) with 0.69 ML and 0.72 BPP support (Figure 4.42). Morphologically, the new strains resemble *E. rostratum* (CBS 128055), producing fusoid to obclavate, straight or curved, septate conidia with conspicuous protruding, truncate hilum at the base (Figure 4.43) (Boonkorn et al., 2024). Based on the available evidence, I report two new host records for *E. rostratum* from *Typha* sp. (Typhaceae) and *Carex* sp. (Cyperaceae) in freshwater coastal wetlands of Thailand.

Note (a) *Typha* sp. host material; (b) Colonies; (c–e) Conidiophores; (h–f) Conidiogenous cells bearing developing conidia *in-vitro*; (i–k) Conidia development; (l–m) Mature conidia. Scale bars: (b) 250 µm; (c–e) 50 µm; (f–m) 20 µm.

Figure 4.43 *Exserohilum rostratum* (MFLU 25-0447)

Sporormiaceae Munk

Westerdykella Stolk

The genus *Westerdykella* was introduced by Stolk in 1955, typified by *Westerdykella ornata*, and named in honor of Johanna Westerdijk, the first female professor in the Netherlands (Crous et al., 2017). Members of this genus exhibit a cosmopolitan distribution, occurring in both aquatic and terrestrial habitats. The sexual morphs are characterized by dark brown to black, discrete, globose, glabrous, cleistothecioid ascomata bearing globose to subglobose, occasionally clavate asci with short pedicels. Ascospores in the genus *Westerdykella* are prominently unicellular, pale brown to brown or olivaceous, and typically reniform in shape. Species such as *W. aquatica* possess ascospores that break into four individual cells and produce 32 ascospores per ascus (Song et al., 2020). The asexual morphs form pycnidial conidiomata, which produce cylindrical to sub-cylindrical, aseptate, hyaline conidia (Ebead et al., 2012; Crous et al., 2017).

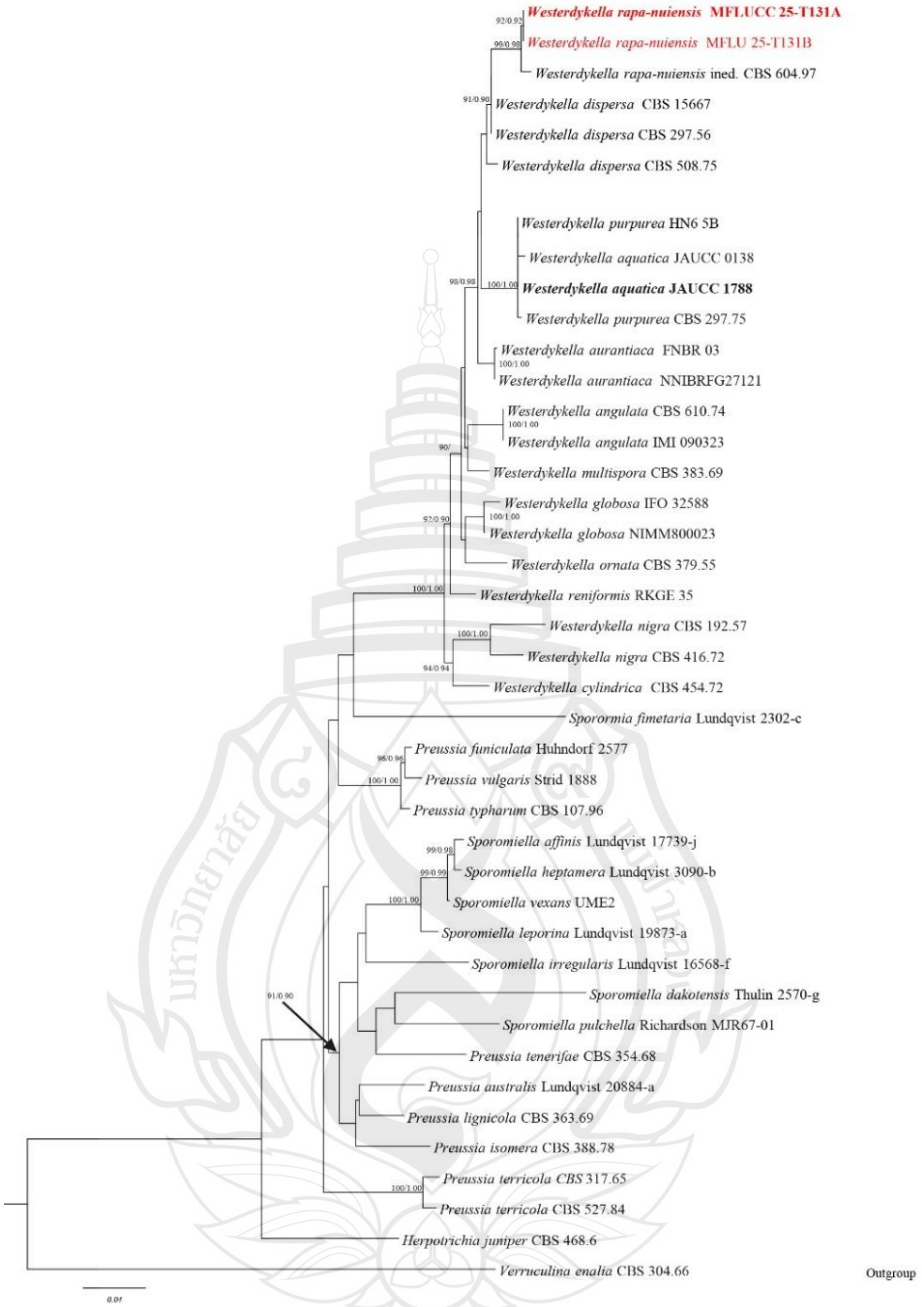

Note The data set comprises 2868 characters including gaps from of selected 41 strains which were included in the phylogenetic analyses. Bootstrap support values for ML ≥ 90 % and Bayesian posterior probabilities (BPP) ≥ 0.9 are mentioned at the nodes. The tree was rooted to *Verruculina enalia* strain CBS 304.6. Newly generated sequences are in red and the type strains are in bold.

Figure 4.44 Phylogram generated from Maximum Likelihood (ML) analysis based on combined LSU, ITS, *tub2* sequence.

Westerdykella rapa-nuiensis ined. (CBS 604.97)

Saprobic on decaying stem of *Carex*, (Cyperaceae), **Sexual morph**: *Ascomata* 220–300 × 230–320 ($\bar{x}$ = 240 × 250 μm, n = 5), cleistothecia, black or greenish brown, solitary, scattered or loosely aggregated, superficial, glabrous, ampulliform or golobose to subglobose with hyphae surrounding ascomata. *Peridium*, thin, membranous, composed of single layer of brown thick-walled cells in *textura angularis*. *Pseudoparaphyses* 1–2 μm wide ($\bar{x}$ = 1.5 μm, n = 10), hyaline, aseptate, branched, smooth walled, end taping towards blunt rounded apexes, and mixed with ascogenous hyphae. *Asci* 10–14 × 12–18μm ($\bar{x}$ = 12 × 14 μm, n = 20), multi-spored, bitunicate, ovoid when immature, becoming globose to subglobose at maturity. *Ascospores* 2.5–4.5 × 2.5–3.5 μm ($\bar{x}$ = 3.5 × 2.0 μm, n = 20), hyaline, or subhyaline ellipsoidal, smooth walled, aseptate, with two prominent guttules at each end. **Asexual morph**: Undetermined.

Culture characteristics: Conidia germinating on MEA within 12 h. Germ tubes produced from side. Colonies growing on MEA, reaching 30 mm in weeks at 25°C. Mycelia superficial, effuse to flat, undulate edges, from above pale white from center to the edge and zonate, from reverse olive greenish brown at the center, process melanized zones, yellowish white to hyaline edge. Produce ascomata in vitro after 4 weeks.

Material examined: Thailand, Chang Wat Prachuap Khiri Khan Province, Pran Buri District, Pran Buri River, on decaying stems of *Carex* sp. (Cyperaceae), 05 April 2024, Tharindu Bhagya, T131_T (MFLU 25-0449), *ibid.,* T131_I, *Carex* sp. (Cyperaceae) (MFLU 25-0450).

GenBank numbers – MFLU 25-0449, ITS = PX308845

Distribution – From soil in Chile (Ebead et al., 2012), decaying submerged *Carex* sp. stem, in freshwater river, Thailand (This study).

Notes – Phylogenetic analysis placed our isolates in a clade sister to *Westerdykella rapa-nuiensis* ined. strain CBS 604.9, with strong statistical support (99% ML and 0.98 BPP) (Figure 4.44). Strain MFLU 25-0449 agrees with the general description of *Westerdykella*, producing globose to subglobose cleistothecia (ascomata), bitunicate, globose to subglobose asci, and ellipsoidal, smooth-walled, aseptate ascospores (Figure 4.45) (Ebead et al., 2012; Crous et al., 2017).

Phylogenetically, strain MFLUCC 25-0449 shares 98.9% similarity in ITS sequences and 99.2% similarity in LSU sequences with *W. rapa-nuiensis* ined. (CBS 604.9). The limitations of available detailed morphological data for strain CBS 604.9 hinders morphological comparison between *W. rapa-nuiensis* ined. and our new isolates (Ebead et al., 2012). Morphologically, strain MFLU 25-0449 most closely resembles *W. aquatica* strain JAUCC 1788, but the characteristic four-celled ascospores of *W. aquatica* were not observed in our isolates. Furthermore, *W. aquatica* (JAUCC 1788) and MFLU 25-0449 form distinct phylogenetic clades (Song et al., 2020). Considering the available evidence, I recognize the new isolates from aquatic habitat as novel strains of *W. rapa-nuiensis* ined. This study provides the first complete morphological description of the species, along with a new host and a new geographic record from a freshwater river in central Thailand.

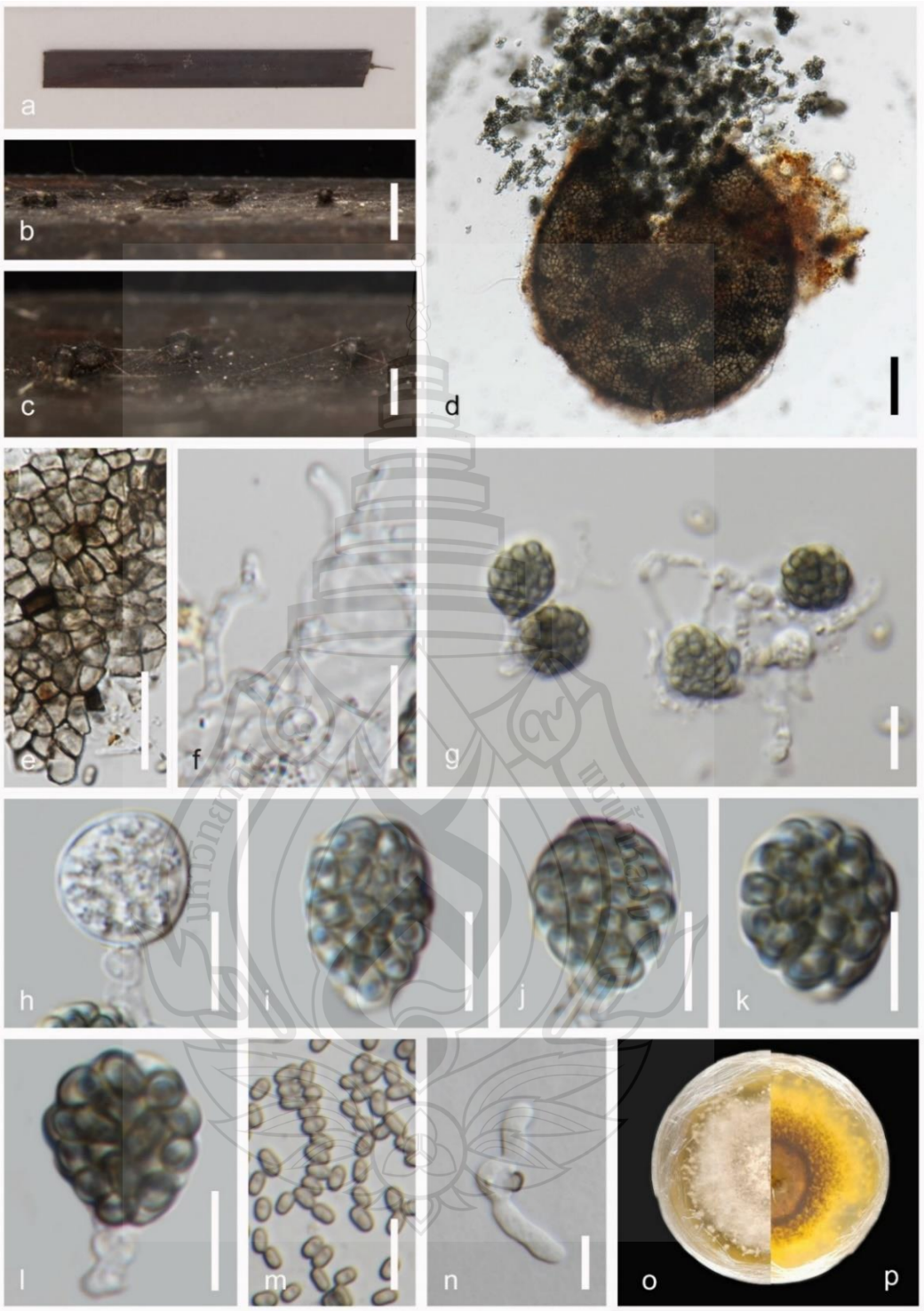

Note a *Carex* sp. host material. b–c Ascomata in the host tissue. d Squash mount of ascomata. e Peridium. f Pseudoparaphyses. g–l Asci. m Ascospores. n Germinated ascospores. o Culture on MEA above. p reverse. Scale bars: b–c 250 µm, d 50 µm, e 20 µm, f–n 10 µm.

Figure 4.45 *Westerdykella rapa-nuiensis* (MFLU 25-0449)

Tetraplosphaeriaceae Kaz. Tanaka & K. Hiray

Tetraploa Berk. & Broome

Tetraploa was erected by Berk. & Broome in 1850 and typified by *Tetraploa aristata* (Berkeley & Broome, 1850). Members of the genus are predominantly saprobic organisms and are occasionally reported as endophytes. They are known to exhibit a worldwide distribution and have been reported from both aquatic and terrestrial habitats (Wang et al., 2024; He et al., 2025). *Tetraploa* is represented by both sexual and asexual morphs. Sexual morphs are characterized by globose to subglobose, immersed to erumpent, dark brown to black, glabrous ascomata; bitunicate, fissitunicate, cylindrical to clavate, shortly pedicellate asci, bearing eight, hyaline, smooth, narrowly fusiform, uniseptate ascospores with a mucilaginous, appendage-like sheath. Asexual morphs dominate the sexual morphs in the genus *Tetraploa*. They are characterized by monoblastic conidiogenous cells and pale brown to dark brown (or olive), verrucose, euseptate conidia with setose appendages at the apex (Tanaka et al., 2009; Zhang et al., 2023; Wang et al., 2024; Asghari et al., 2025; He et al., 2025).

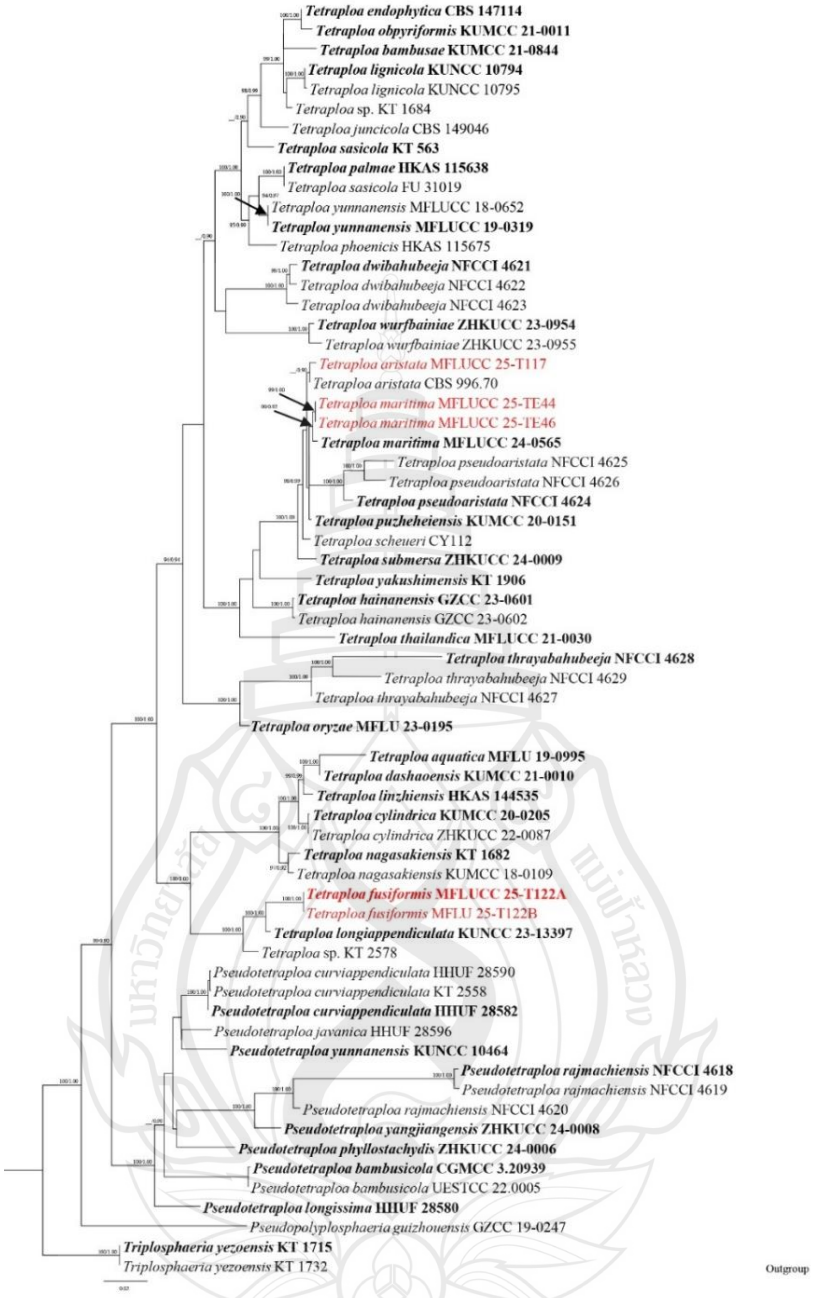

Note Bootstrap support values for ML ≥ 90 % and Bayesian posterior probabilities (BPP) ≥ 0.9 are mentioned at the nodes. The tree was rooted to *Triplosphaeria yezoensis* (KT 1715 and KT 1732). Newly generated sequences are in red and the type strains are in bold.

Figure 4.46 Phylogram generated from Maximum Likelihood (ML) analysis based on combined LSU, SSU, ITS, and *tub2* sequence. The data set comprises 3633 characters including gaps from of selected 63 strains which were included in the phylogenetic analyses.

Tetraploa fusiformis Bhagya, Phukhams E.B.G. Jones & K.D. Hyde, sp. nov

Index Fungorum number: IF; Facesoffungi number: FoF 18908

Etymology – The name refers to the fusiform (spindle-shaped) ascospores characteristic of this species.

Holotype – MFLU 25-0451

Saprobic on dead, decaying leaf of *Carex,* (Cyperaceae), **Sexual morph**: *Ascomata* 130–190 × 110–140 µm ($\bar{x}$ =158 × 115 µm, n = 5), scattered or gregarious on host, immersed to semi-immersed, glabrous, globose to ellipsoidal or pyriform, papillated, ostiolate. *Ostiole* 40–70 × 30–55 µm ($\bar{x}$ =60 × 42 µm, n = 5), central, cylindrical, comprises with pigmented, dark brown to pale brown, thick-walled cells in *textura angularis*. *Peridium* 20–32 µm ($\bar{x}$ =25 µm, n = 10), composed of 2–3 layers, outer layers process dark brown to pale brown, thick-walled cells in *textura angularis*, inner layers consist with, pale brown to hyaline, thin-walled cells in *textura angularis*. *Pseudoparaphyses* 50–90 × 1.5–3.5 µm ($\bar{x}$ =65 × 2.5 µm, n = 10), hyaline smooth walled, aseptate, tubular, unbranched, anastomosed. *Asci* 50–85 × 10–22 µm ($\bar{x}$ =70 × 14 µm, n = 20), 8-spored, bitunicate, fissitunicate, cylindrical to broadly clavate, short pedicellate, apically rounded with ocular chamber. *Ascospores* 18–25 × 4–6 µm ($\bar{x}$ =22 × 5 µm, n = 20), overlapping biseriate, hyaline, smooth, thick-walled, fusiform to slightly curved with acute ends, 1-septate, constricted at the septum, upper cells wider than lower cell, bear one prominent guttule at each cell, gelatinous sheath absent. **Asexual Morph:** Undetermined.

Culture characteristics: Ascospores germinating on MEA within 24 h. Germ tube produced from the base of the spores. Colonies growing on MEA, reaching 30 mm in 8 weeks at 25°C. Mycelia superficial, effuse to flat or undulate, from above olivaceous to cinereous canter to the off-white irregular edge, from reverse greenish-black at the canter, light brown to black to hyaline edge. Brown colour, thick-walled, mycelium radiate to the culture to the growth media.

Material examined: Thailand, Chang Wat Narathiwat Province, Amphoe Tak Bai, District, Tambon Sala Mai, Narathiwat peat swamp, on decaying leaf of *Carex* sp. (Cyperaceae) 25 August 2023, Tharindu Bhagya, TB122 (MFLU 25-0451, holotype); *ibid*., TB122B (MFLU 25-0452, isotype).

GenBank numbers – MFLU 25-0451, ITS = PX089565, LSU = PX089566

Distribution – Decaying *Carex* sp. leaf in freshwater wetland, Thailand.

Notes – The multi-locus phylogenetic analysis placed the new isolates in a clade sister to *Tetraploa longiappendiculata* strain KUNCC 2313397, with 100% ML and 1.00 BPP statistical support (Figure 4.46). Strain MFLU 25-0451 differs phylogenetically from *T. longiappendiculata* strain KUNCC 2313397 by 3.68% in ITS and 1.02% in LSU sequences, excluding gaps. The new isolate, MFLU 25-0451, represents a sexual morph, whereas *T. longiappendiculata* strain KUNCC 2313397 is only known from its asexual morph, limiting direct morphological comparison between the sister strains (Wang et al., 2024). Strain MFLU 25-0451 is morphologically similar to the sexual morph of *T. scheueri* strain CY112. However, the presence of a peridium composed of cells in *textura angularis*, aseptate tubular unbranched pseudoparaphyses, and the absence of a gelatinous sheath in the ascospores distinguish MFLU 25-0451 from *T. scheueri* strain CY112 (Figure 4.47) (Scheuer, 1991; Dong et al., 2020). Furthermore, *T. scheueri* strain CY112 forms a distinct clade from MFLU 25-0451, and the pairwise distance matrix value between the two strains is 0.037, indicating that they are congeners but represent separate species (Gostinčar, 2020; Maharachchkumbura et al., 2021). Considering the available morphological and phylogenetic evidence, I introduce *T. fusiformis* (MFLU 25-0451) as a new species of *Tetraploa*, collected from Narathiwat, Thailand.

Note a *Carex* sp. host material. b Black semi-immersed ascomata on the host. d Vertical section of ascomata. e Pseudoparaphyses. f–i Asci with an ocular chamber and short pedestal. j–m Ascospores. n Culture on MEA above. o reverse. Scale bars: b 1 mm, c 200 µm, d 100 µm, e–m 20 µm.

Figure 4.47 *Tetraploa fusiformis* (MFUL 25-0451, holotype)

Tetraploa aristata Berk. & Broome, Ann. Mag. nat. Hist., Ser. 2 5: 459 (1850)

Saprobic on submerged decayed stem of genus *Carex,* (Cyperaceae). **Sexual morph**: undetermined. **Asexual morph**: *Hyphomycetous*, colonies placed host, sporodochial, solitary or loosely aggregated, dry, brown or dark greyish brown cells. *Mycelium* 1–3 ($\bar{x}$ = 1.5 µm, n = 10), partially immersed, septate, branched, hyphae subhyaline to hyaline. *Conidiophores* are indistinct, micronematous, hype like, sepatae, hyaline or light brown. *Conidiogenous cells in-vitro* 1–6 × 1–2.5 µm ($\bar{x}$ = 2.5 × 2.0 µm, n = 10), indistinct hyaline when present. *Conidia* body *in-vitro* 22–30 × 12–22 µm ($\bar{x}$ = 26 × 19 µm, n = 20), brown or dark greyish brown in color, septate, setose, verrucose at senescence, conidial body composed of four closely-adhered vertical lobs, ovate to semi-ovate at young and oblong at maturity, olive brown to light brown with apical appendages. *Appendages in-vitro* height 25–50 µm ($\bar{x}$ = 42 µm, n = 20), width at base 2–4 µm ($\bar{x}$ = 2.2 µm, n = 30) greenish brown at wide base and taping towards almost hyaline tip.

Culture characteristics: Conidia germinating on MEA within 12 h. Germ tube erupted from the base of the conidiospore. Colonies growing on MEA, reaching 15-20 mm in 2 weeks at 25°C. Mycelia superficial, dense, cottony, flat or effuse with fimbriate or erose at the edge, from above dark greenish brown from center and fading to pale white towards the edge, from reverse dark brown at the center, followed by greenish black ring and off white to the edge.

Material examined: Thailand, Chang Wat Prachuap Khiri Khan Province, Pran Buri District, Pran Buri Wetland, on decaying stems of *Carex* sp. (Cyperaceae), 23 August 2023, Tharindu Bhagya, T117 (MFLU 25-0453).

GenBank numbers – MFLU 25-0453, ITS = PX518073

Distribution – On Poaceae host in Great Britain (Berkeley & Broome, 1850), On dead culms and sheaths of *Saccharum spontaneum*, Madhya Pradesh, India (Sharma, 1978), on decomposing *Carex* sp. material, United Kingdom (Scheuer, 1991). leaf litter submerged in pond in Maharashtra, India (Shinde & Pawar, 2009), decaying *Carex* sp. leaf in freshwater wetland, Thailand (This study).

Notes – The new isolate formed a clade sister to *Tetraploa aristata* strain CBS 996.70 with 76% ML and 0.90 BPP statistical support (Figure 4.46). The new strain shares 99.98% similarity in ITS and 98.99% similarity in LSU sequences, excluding gaps with

strain CBS 996.70, indicating a close phylogenetic relationship. Morphologically, the pale brown, verrucose conidia with four columns of thick-walled cells and a similar length-to-width ratio (MFLU 25-0453: 1.37 vs. CBS 996.70: 1.32) further support this resemblance (Figure 4.48) (Tanaka et al., 2009). Considering the available morphological and phylogenetic evidence, I recognize the new isolate as a new strain of *T. aristata* and report it as a new geographical record for the species, with detailed morphological documentation from a freshwater coastal wetland in Thailand.

Note a *Carex* sp. host material. b–c Colonies on host surface. d Culture on MEA above. e reverse. f Conidia formation on culture. g-l Conidiogenous with developing conidia in culture. m–p Immature conidia. q–r Mature conidia. Scale bars: b 2.5 mm, c 500 µm, f–h 20 µm, i–r 10 µm.

Figure 4.48 *Tetraploa aristata* (MFLU 25-0453)

Tetraploa maritima R. Asghari, Phukhams. & K.D. Hyde, in Asghari, Phukhamsakda, Jones, Bahkali, Apurillo, Karimi, Kakumyan & Hyde, MycoKeys 118: 184 (2025)

Saprobic on submerged decayed stem of genus *Thypha,* (Typhaceae). **Sexual morph**: Undetermined. **Asexual morph**: **Emergent colonies**, *Hyphomycetous*. Colonies effuse on the host, sporodochial, loosely aggregated, dry, brown or dark greyish brown collections of conidia. *Mycelium* 1–2.5 µm ($\bar{x}$ = 1.5 µm, n = 5), partially immersed, septate, branched, hyphae hyaline. *Conidiophores* are indistinct, micronematous. *Conidiogenous cells* 1–3 × 1–2.5 µm ($\bar{x}$ = 2.5 × 2.0 µm, n = 5), indistinct hyaline and unicellular when present. Conidia body 23–30 × 16–25 µm ($\bar{x}$ = 26 × 18 µm, n = 20), brown or dark greyish brown, septate, setose, verrucose at senescence, conidial body composed of four closely-adhered vertical lobs, oblong, olive brown to light brown. **Submerged colonies**, *Hyphomycetous*. Colonies effuse on the host, sporodochial, solitary or loosely aggregated, dry, brown or dark greyish brown cells. *Mycelium* 1–2.5 µm ($\bar{x}$ = 2.0 µm, n = 5), partially immersed, septate, branched, hyphae subhyaline to hyaline. *Conidiophores* are indistinct, micronematous. *Conidiogenous cells* indistinct hyaline when present. Conidia body 30–40 × 22–30 µm ($\bar{x}$ = 34 × 23 µm, n = 20), brown or dark greyish brown in color, septate, setose, verrucose at senescence, conidial body composed of four closely-adhered vertical lobs, semi ovate at young and oblong at senescence, olive brown to light brown with apical appendages. *Appendages* height 30–60 µm ($\bar{x}$ = 35 µm, n = 20), width at the base 2–7 µm ($\bar{x}$ = 4.5 µm, n = 20) greenish brown at wide base and taping towards almost hyaline tip.

Culture characteristics: Conidia germinating on MEA within 24 h. Germ tube erupted from the base of the conidia. Colonies growing on MEA, reaching 20-25 mm in 4 weeks at 25°C. Mycelia superficial, dense, cottony, flat or effuse with fimbriate or complete at the edge, from above dark ash from center and produces distinctive white concentric circle at the middle and at the edge, from reverse yellowish white at the center, greenish brown at the middle and distinctive of white concentric circle to the edge. After 6 weeks, culture changes the MEA color from light amber yellow to orangey yellow.

Material examined: Thailand, Chang Wat Prachuap Khiri Khan Province, Pran Buri District, Pran Buri wetland, on decaying stems of *Typha* sp. (Typhaceae), 02 December 2023, Tharindu Bhagya, TB44 (MFLU 25-0454), Chang Wat Prachuap Khiri Khan Province, Pran Buri District, Pran Buri wetland, on decaying stems of *Typha* sp. (Typhaceae), 02 December 2023, Tharindu Bhagya, TB46 (MFLU 25-0455).

GenBank numbers – MFLU 25-0455, ITS = PX518069, LSU = PX518068

Distribution – On decomposing *Carex acutiformis* material, United Kingdom (Scheuer.1991, Dong et al., 2020), decaying *Typha* sp. stem in freshwater wetland, Thailand (This study).

Notes – The new isolates formed a clade sister to *Tetraploa maritima* (MFLUCC 24-0565) with 90% ML and 0.92 BPP statistical support (Figure 4.46). Pairwise comparison mentioned that strain MFLU 25-0454 shares 98.21% ITS sequence similarity, 99.64% LSU similarity, and 98.61% *tub2* similarity (excluding gaps) with strain MFLUCC 24-0565. Both the submerged (MFLU 25-0454) and emergent (MFLU 25-0455) strains share morphological similarities with *T. maritima* (MFLUCC 24-0565), producing verrucose, oblong conidia with four closely adherent vertical lobes forming the conidial body (Asghari et al., 2025). *Tetraploa maritima* (MFLUCC 24-0565) was originally isolated from a marine environment (Asghari et al., 2025). Therefore, unavoidable morphological differences are observed between the newly isolated freshwater strains (MFLU 25-0454 and MFLU 25-0455) and the type strain of *T. maritima* (Figure 4.49 & 4.50) (MFLUCC 24-0565). These differences include the absence of a pale brown hilum in our isolates, as well as variations in overall conidial body size, shape, and the number of cells comprising the conidia. Considering the available morphological and phylogenetic evidence, we identify the new strains as *T. maritima*. Accordingly, I report a new host and habitat record for the species, provide detailed morphological observations, and highlight the phenotypic plasticity exhibited under different environmental conditions.

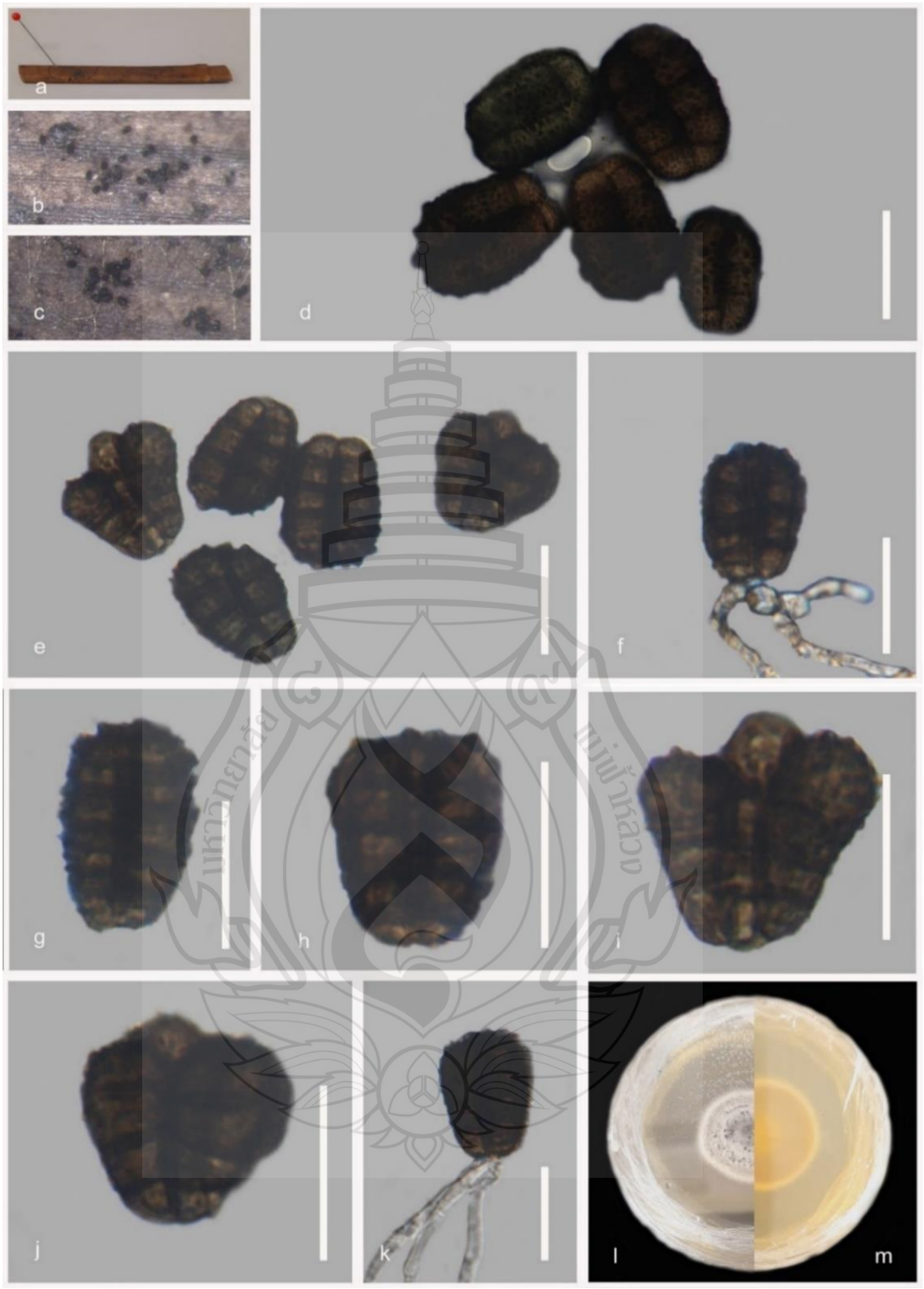

Note a *Typha* sp. host. b–c Conidia aggregation on the host. d–e Conidia aggregation under microscope. f Conidia with conidiogenous cell. g–j Conidia. k Germinating conidium. l Two weeks old culture on MEA above. m Reverse. Scale bars: d–k 20 µm.

Figure 4.49 Emergent *Tetraploa maritima* (MFLU 25-0454)

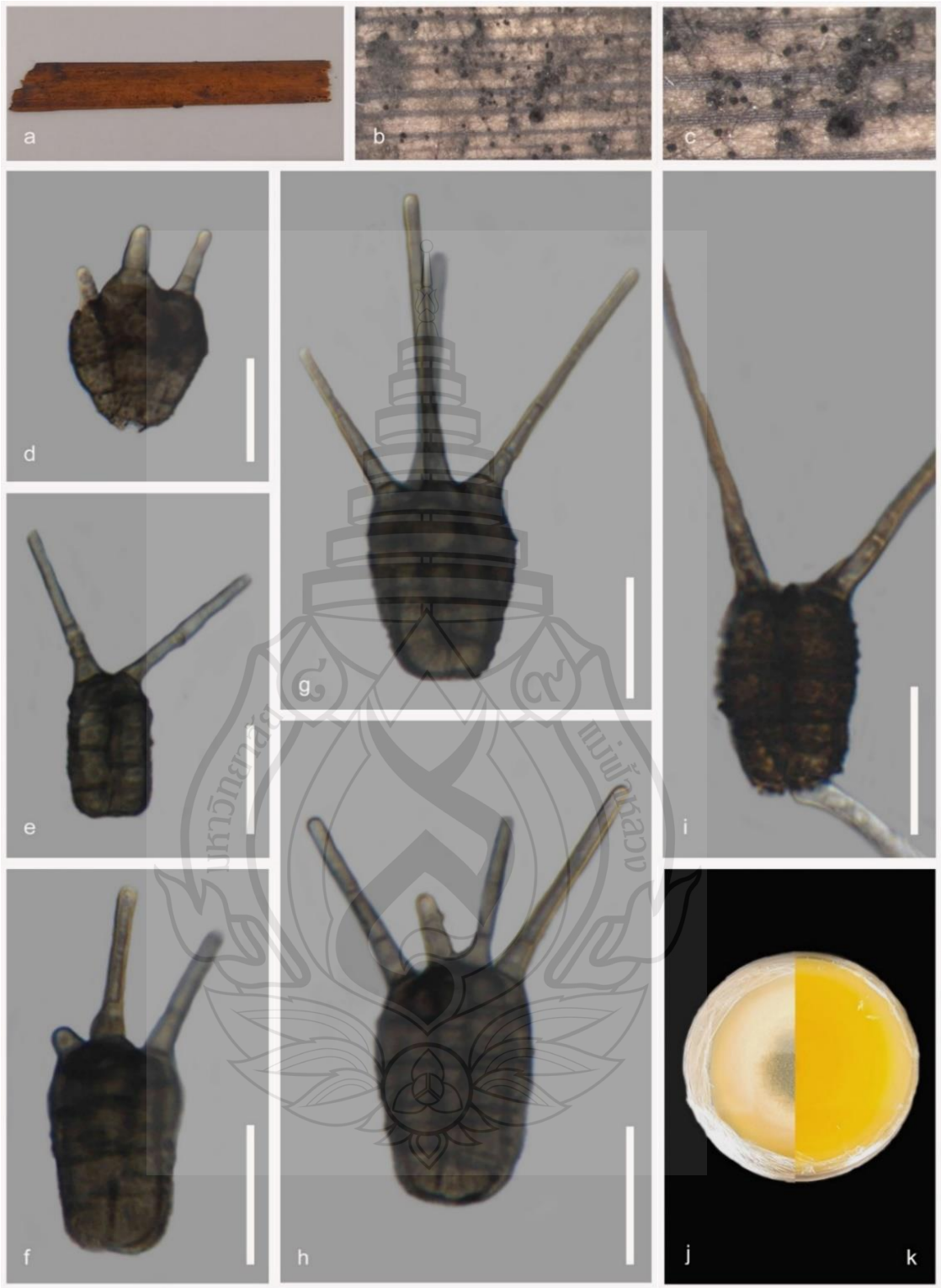

Note a *Typha* sp. host. b–c Conidia aggregation on the host. d–e Young conidia. f–h Developed conidia. i Germinating conidium. j Six weeks old culture on MEA above. k Reverse. Scale bars: d–i 20 µm.

Figure 4.50 Submerged *Tetraploa maritima* (MFLU 25-0455)

Torulaceae Corda

Torula Pers

Torula is a species-rich genus in the family *Torulaceae*, introduced by Pers. in 1795 and typified by *Torula monilis*. Species are predominantly reported as saprobic organisms and exhibit a cosmopolitan distribution. *Torula* is an asexual genus characterized by monoblastic or polyblastic, terminal or lateral, melanized conidiogenous cells with thickened bases, and hyaline to pale brown conidia. The majority of *Torula* species has limited molecular data or are known from single collections. Therefore, the genus requires relocation of several species currently placed under *Torula* (Tian et al., 2023; Wang et al., 2023).

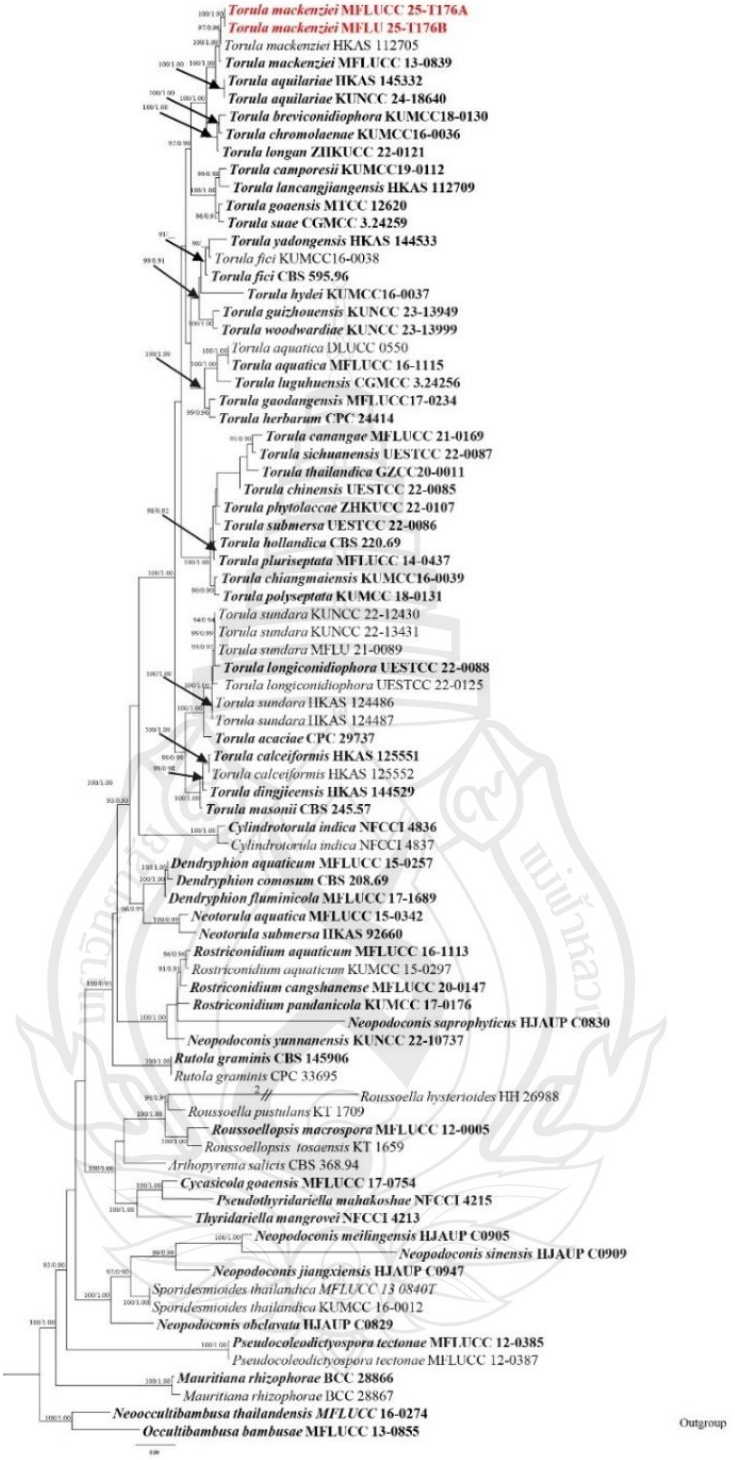

Note The data set comprises 5128 characters including gaps from of 81 strains which were included in the analyses. Bootstrap support values for ML ≥ 90 % and Bayesian posterior probabilities (BPP) ≥ 0.9 are mentioned at the nodes.

Figure 4.51 Phylogram generated from Maximum Likelihood (ML) analysis based on combined ITS, LSU, SSU, *tef1-α*, and *rpb2* sequence.

Torula mackenziei Jun F. Li, Phookamsak & K.D. Hyde, in Li, Phookamsak, Jeewon, Bhat, Mapook, Camporesi, Shang, Chukeatirote, Bakhali & Hyde, Mycol. Progr. 16(4): 455 (2017)

Saprobic on dead, decaying stems of *Typha*, (Typhaceae), **Sexual morph:** Undetermined. **Asexual morph:** *Hyphomycetous*. *Colonies* pale brown to cinereous or black, superficial, hairy, effuse, tightly aggregated. *Mycelium* 1.5–3.5 µm ($\bar{x}$ = 2.5 µm, n = 10), immersed, to superficial, pale brown to hyaline, smooth, often branched, septate. *Conidiophores* 3–6 × 2–4 µm ($\bar{x}$ = 4 × 3.5 µm, n = 10), macronematous, mononematous, erect, often comprise with two pale brown to dark brown, smooth, thick-walled, ellipsoid to subglobose cells. *Conidiogenous cells* 3–6 × 3–5 µm ($\bar{x}$ = 4 × 4.5 µm, n = 10), terminal, polyblastic, pale brown or brown with paler apexes, smooth or verruculose, thick-walled, globose to ellipsoid with schizolytic secession. *Conidia* 8–20 × 3–6.5 µm ($\bar{x}$ = 15 × 5.5 µm, n = 30), acrogenous, phragmosporous, catenated, pale brown to olivaceous brown with lighter rounded ends, smooth to minutely verruculose, moniliform, septate, constricted at septa.

Culture characteristics: Conidia germinating on MEA within 12 h. Germ tubes produced from ends of the conidium. Colonies growing on MEA, reaching 50 mm in 8 weeks at 25°C. Mycelia superficial, dense, cottony effuse, with erose edges, from above pale to off white from center to the edge, from reverse light yellowish brown at the center, followed by brown to olivaceous ring, leading to pale brown and olivaceous rings accordingly and ending with white to hyaline edge. Brown to black color hype aggregation was observed after 4 weeks of incubation under 25°C.

Material examined: Thailand, Chang Wat Prachuap Khiri Khan Province, Pran Buri District, Pran Buri Wetland, on decaying stems of *Typha* sp. (Typhaceae), 25 January 2023, Tharindu Bhagya, TB176A (MFLU 25-0456), Thailand, Chang Wat Prachuap Khiri Khan Province, Pran Buri District, Pran Buri Wetland, on decaying peduncle of *Typha* sp. (Typhaceae), 08 March 2023, Tharindu Bhagya, TB176B (MFLU 25-0457).

GenBank numbers – MFLU 25-0456, ITS = PP463952

Distribution – Dead branch of Bidens pilosa, Doi Mae Salong, Chiang Rai, Thailand (Li et al., 2017), decaying *Typha* sp. stem and leaf in freshwater wetland, Thailand (This study).

Notes – The new isolates formed a clade sister to *Torula mackenziei* strains MFLUCC 13-0839 and HKAS 112705, with 97% ML and 0.96 BPP support (Figure 4.51). Phylogenetically, strain MFLUCC 25-xxxxa is similar to strain MFLUCC 13-0839, exhibiting 99.1% identity in the ITS region, 99.7% in the LSU sequence, and 98.6% in the *tef1-α* sequence (excluding gaps). Morphologically, the presence of thick-walled, globose to ellipsoid polyblastic conidiogenous cells with schizolytic conidial secession, and moniliform, olivaceous to cinereous conidia, makes the new strains resemble *T. mackenziei* strain MFLUCC 13-0839 (Figure 4.52) (Li et al., 2017). Based on the available evidence, I recognize the new strains as *T. mackenziei* and report a new host record from *Typha* sp. in freshwater coastal wetlands of Thailand.

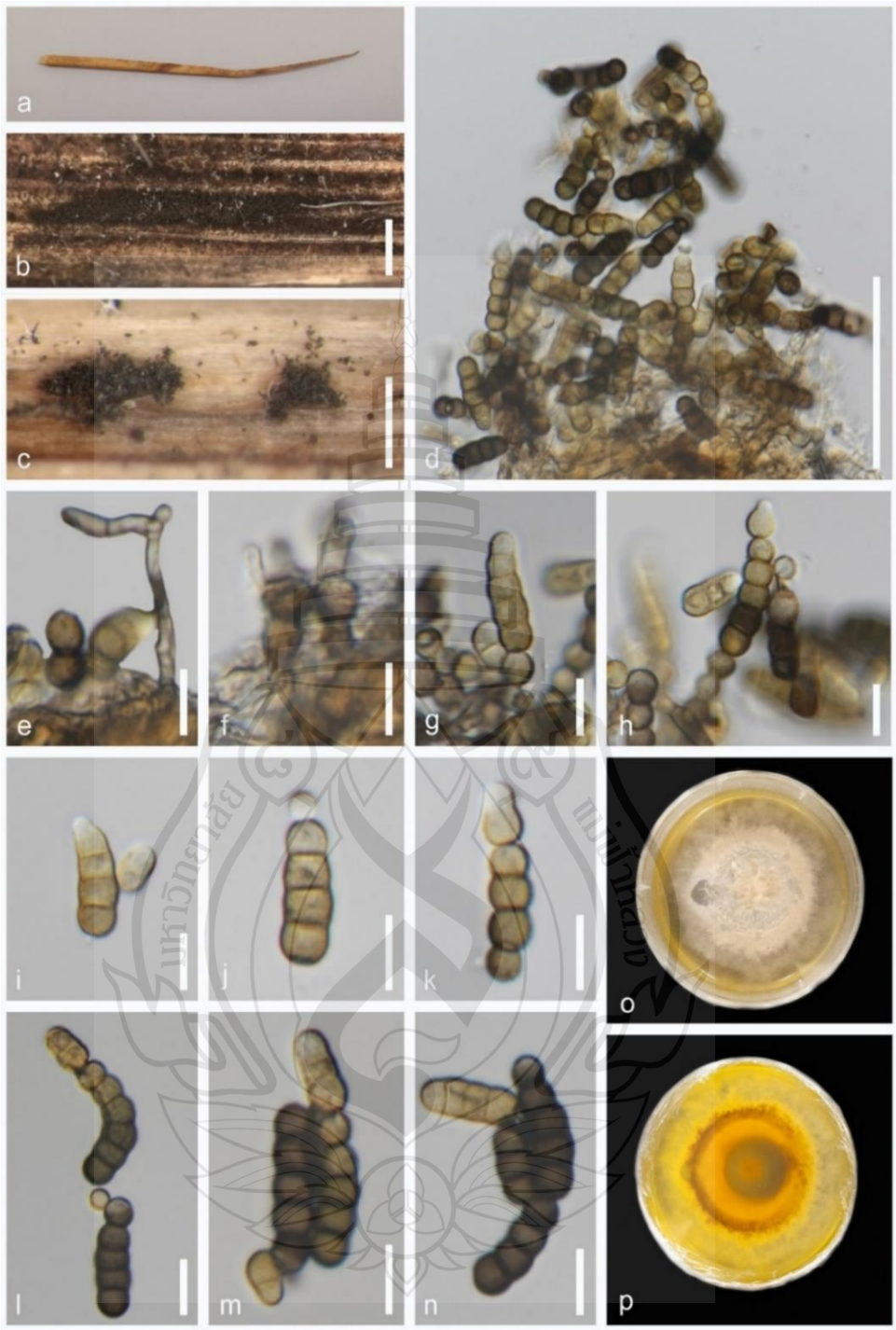

Note a *Typha* sp. host material. b–c Colonies on the host surface with setae and conidia. d Squash mount of the colony. e–f Conidiophores attached to substrate. g–h Conidiophores with developing conidia. i–k Conidia development. l–n Conidia bearing moniliform, and olivaceous cells. o culture on MEA above. p reverse. Scale bars: b 500 µm, c 250 µm, d 50 µm, e–n 10 µm.

Figure 4.52 *Torula mackenziei* (MFLUC 25-0456)

Tubeufiales Boonmee, Rossman & K.D. Hyde

Tubeufiaceae M.E. Barr

Helicosporium Nees

Helicosporium is a monophyletic genus residing in *Tubeufiaceae*, within the class *Dothideomycetes*. The genus was introduced by Nees in 1816 and is typified by *Helicosporium vegetum* (Peng et al., 2025). Members of *Helicosporium* are predominantly saprobic organisms, exhibit a cosmopolitan distribution, and are known by both sexual and asexual morphs. The sexual morph is characterized by globose to subglobose, yellow to orange, superficial, single ostiolate ascomata, which appear individually or scattered on the host surface. The ascomata darken around the ostiole. The peridium comprises several layers, the outer layers consist of bright yellow cells of textura angularis, while the inner layers are made up of yellow cells of textura prismatica. Pseudoparaphyses are filiform, septate, and branched. Asci in *Helicosporium* are bitunicate, cylindric-clavate, with thickened apices possessing an ocular chamber. Each ascus contains eight hyaline, smooth-walled, multi-septate, fusiform ascospores, tapering toward subacute ends (Lu et al., 2018; Peng et al., 2025). The asexual morph is hyphomycetous, characterized by macronematous, mononematous, erect, brown to dark brown, smooth, thick-walled, setiferous, septate conidiophores. These conidiophores produce holoblastic, monoblastic to polyblastic, mostly discrete, determinate, denticulate, hyaline to pale brown, smooth-walled conidiogenous cells. The resulting conidia are helicoid, pleurogenous, hyaline to yellowish green (flavovirens), smooth, thin-walled, multi-septate, and guttulate (Lu et al., 2018; Ma et al., 2024; Peng et al., 2025).

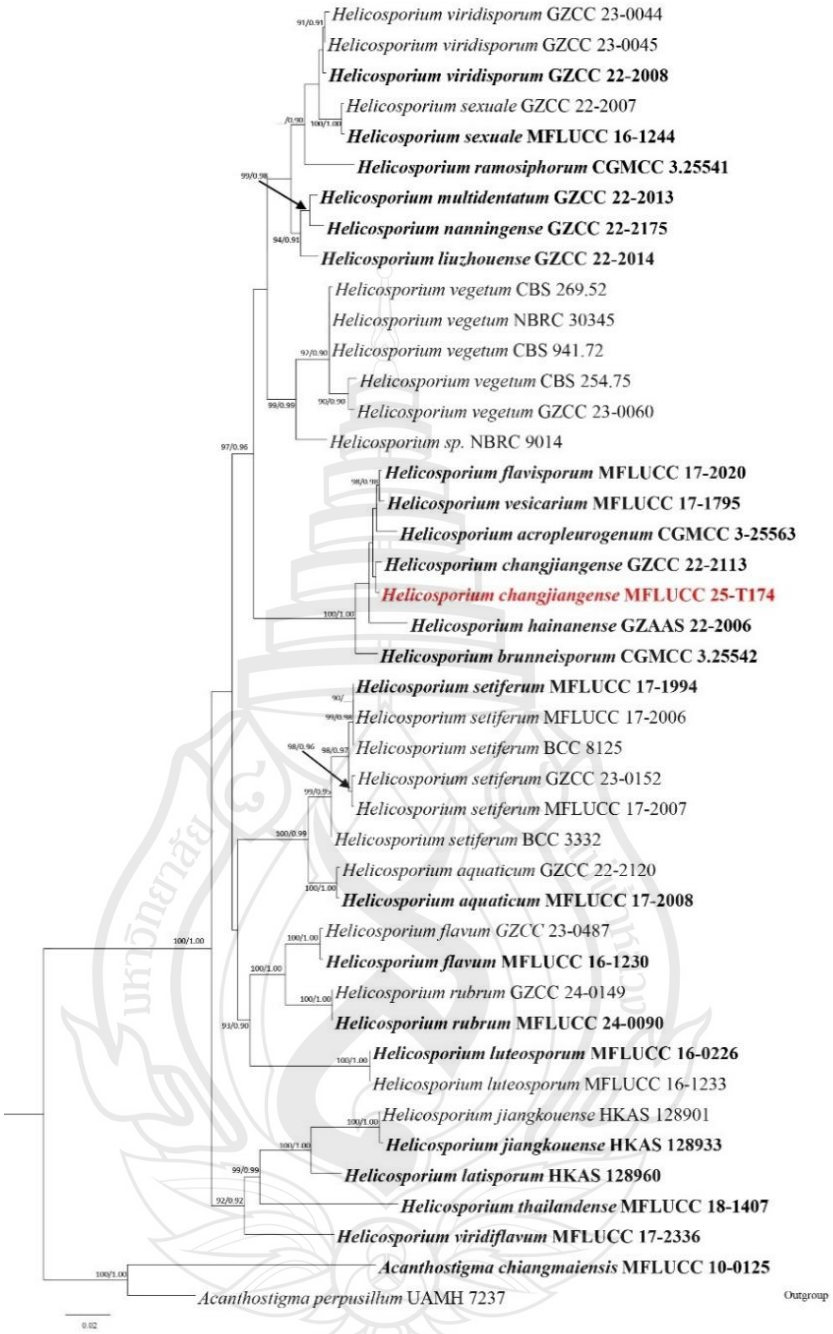

Note The data set comprises 3572 characters including gaps from of 43 strains which were included in the analyses. Bootstrap support values for ML ≥ 90 % and Bayesian posterior probabilities (BPP) ≥ 0.9 are mentioned at the nodes. The tree was rooted to *Acanthostigma chiangmaiensis* (MFLUCC 10-0125), and *A. perpusillum* (UAMH 7237).

Figure 4.53 Phylogram generated from Maximum Likelihood (ML) analysis based on combined LSU, ITS, *tef1-α*, and *rpb2* sequence.

Helicosporium changjiangense Jian Ma, K.D. Hyde & Y.Z. Lu, in Ma, Hyde, Tibpromma, Gomdola, Liu, Norphanphoun, Bao, Boonmee, Xiao, Zhang, Luo, Zhao, Suwannarach, Karunarathna, Liu & Lu, Fungal Diversity 129: 429 (2024)

Saprobic on dead, decaying stems of *Typha*, (Typhaceae), **Sexual morph:** Undetermined. **Asexual morph:** *Hyphomycetous*. *Colonies* pale brown to glistening yellow, superficial, hairy, effuse, gregarious or tightly aggregated on host tissue. *Mycelium* 1.5–3.5 μm ($\bar{x}$ = 2.5 μm, n = 5), partly immersed or superficial, composed of hyaline to pale brown or brown, branched, smooth-walled, septate, and guttulate hyphae. *Conidiophores* 100–190 × 5–6 μm ($\bar{x}$ = 130 × 5.5 μm, n = 10), macronematous, mononematous, erect, swollen at base, pale brown to dark brown with sub-hyaline to pale brown apexes, smooth, thick-walled, septate, straight or slightly curved, simple, unbranched. *Conidiogenous cells* 8–22 × 4–6.5 μm ($\bar{x}$ = 12 × 5.5 μm, n = 5), holoblastic, monoblastic to polyblastic, discrete, intercalary, pale brown to hyaline, ampulliform, pyriform to rostrate or cylindrical, denticulate, dense at subterminal region of conidiophores. *Conidia* 12–28 μm ($\bar{x}$ = 22 μm, n = 30) in diameter, 1.5–3 μm ($\bar{x}$ = 2.5 μm, n = 30) in conidial filament, solitary, pleurogenous, helicoid with narrowing towards the rounded ends, hyaline to subhyaline, smooth, thin-walled, aseptate, guttulate at maturity.

Culture characteristics: Conidia germinating on MEA within 24 h. Germ tubes produced from sides of the conidium. Colonies growing on MEA, reaching 40 mm in 4 weeks at 25°C. Mycelia superficial, dense, effuse, with erose to entire edges, from above light brown to dark brown or cinereous, and pale brown to hyaline to the edge, from reverse dark brown to olivaceous at the center and the pale brown to hyaline at the edge.

Material examined: Thailand, Chang Wat Prachuap Khiri Khan Province, Pran Buri District, Sam Roi Yot wetland, on decaying stems of *Typha* sp. (Typhaceae), 02 January 2025, Tharindu Bhagya, TB174 (MFLU 25-0458).

GenBank numbers – MFLU 25-0458, ITS = PX518096

Distribution – Decaying wood in a terrestrial habitat, Hainan Province, Changjiang, Baomeiling, China (Ma et al., 2024), decaying *Typha* sp. stem in freshwater wetland, Thailand (This study).

Notes – The new strain MFLU 25-0458 forms a clade sister to *Helicosporium changjiangense* strain GZCC 22-2113, with 46% ML and 0.51 BPP support (Figure 4.53). Phylogenetically, the new isolate shares 99.7% similarity in ITS, 99.9% in LSU, and 98.2% in *tef1-α* sequences (excluding gaps). Morphologically, strain MFLU 25-0458 resembles *H. changjiangense* strain GZCC 22-2113, producing monoblastic to polyblastic, ampulliform to pyriform, intercalary, denticulate conidiogenous cells, and pleurogenous, helicoid conidia that appear as glistening yellow clusters on the host (Figure 4.54) (Ma et al., 2024). Based on the combined evidence, I identify the new isolate as a new strain of *H. changjiangense*, and report the species from a decomposing submerged stem of *Typha* sp. in a freshwater coastal wetland in Thailand.

Note a *Typha* sp. host material. b Conidiophores on the host surface with yellowish conidia masses. c–e Conidiophores with conidiogenous cells and developing conidia. f–h Conidiogenous cells, i–l Conidia development. Scale bars: b 250 µm, c–e 20 µm, f–l 10 µm.

Figure 4.54 *Helicosporium changjiangense* (MFLU 25-0458)

Tubeufia Penz. & Sacc

Tubeufia was proposed by Penz. & Sacc. in 1897 and is typified by *Tubeufia javanica* (Lu et al., 2018). Members of the genus have been isolated from both aquatic and terrestrial habitats. They exhibit a cosmopolitan distribution and are known from both sexual and asexual morphs. The sexual morphs are characterized by globose to subglobose, light brown to black, superficial pseudothecial ascomata bearing setae or ascomatal hairs. The asci are bitunicate, fissitunicate, cylindrical to broadly clavate, and each ascus contains eight, hyaline to pale brown, fusiform to cylindrical, multi-septate or occasionally muriform ascospores. The majority of species in the genus are reported only in their asexual morphs. Asexual morphs are characterized by pale brown to dark brown, smooth, thick-walled, mononematous, occasionally branched, septate conidiophores. These give rise to holoblastic, hyaline to pale brown, smooth, thin-walled, cylindrical to ampulliform conidiogenous cells, which are monoblastic or polyblastic, and positioned terminally or intercalarily. Conidia in the genus *Tubeufia* are helicosporous, hyaline to subhyaline or pale brown, smooth, thin-walled, and either aseptate or septate (Boonmee et al., 2014; Lu et al., 2017; Ma et al., 2023a; Ma et al., 2023b; Ma et al., 2024).

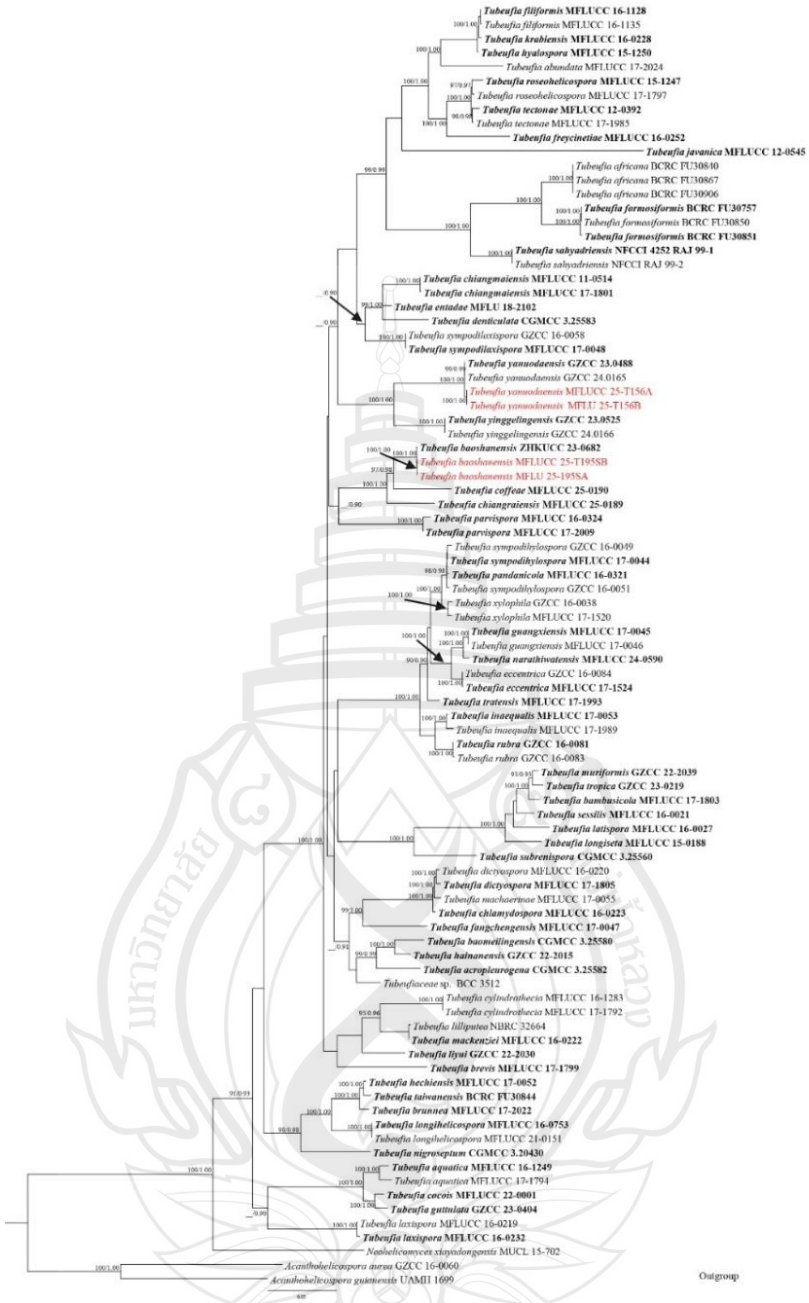

Note The data set comprises 4366 characters including gaps from of 91 strains which were included in the analyses. Bootstrap support values for ML ≥ 90 % and Bayesian posterior probabilities (BPP) ≥ 0.9 are mentioned at the nodes. The tree was rooted to *Acanthohelicospora aurea* (GZCC 16-0060), and *A. guianensis* (UAMH, 1699). *Sordaria fimicola* (CBS 508.50 and CBS 723.96). Newly generated sequences are in red and the type strains are in bold.

Figure 4.55 Phygenetic tree generated from Maximum Likelihood (ML) analysis based on combined LSU, ITS, *tef1-α*, and *rpb2* sequence.

Tubeufia yanuodaensis X.Y. Ma, J. Ma & Y.Z. Lu, in Ma, Tian, Feng, Wang, Shi & Ma, MycoKeys 121: 95 (2025)

Saprobic on dead, decaying stems of *Typha*, (Typhaceae), **Sexual morph**: Undetermined. **Asexual morph:** Hyphomycetous, helicosporous with effuse, white colonies, gregarious or closely aggregated. *Mycelium* 2.0–3.5 μm ($\bar{x}$ = 2.5 μm, n = 10), immersed, consist with branched, septate, smooth, hyaline to sub-hyaline hyphae. *Conidiophores* 35–55 × 2.5–5.5 μm ($\bar{x}$ = 46 × 3.0 μm, n = 10), macronematous, mononematous, hyaline to light brown, erect, cylindrical, unbranched, septate, straight, smooth and thick walled. *Conidiogenous cells* 10–16 × 1.5–3.5 μm ($\bar{x}$ = 13 × 2.5 μm, n = 10), holoblastic, monoblastic to occasionally polyblastic, hyaline to light brown, subcylindrical, smooth, thin-walled, integrated, sympodial, terminal or occasionally intercalary, with apical thickening. *Conidia* 20–50 μm ($\bar{x}$ = 32 μm, n = 30) in diameter, 1.5–4.5 μm ($\bar{x}$ = 2.0 μm, n = 30) in conidial filament, hyaline, helicoid, uncoiled in water, multi-septate, guttulate, acrogenous or acropleurogenous, appear individually and process smooth walls.

Culture characteristics: Conidia germinating on MEA within 24 h. Germ tubes produced from sides of the conidium. Colonies growing on MEA, reaching 30 mm in 6 weeks at 25°C. Mycelia superficial, dense, effuse, with erose edges, from above light brown to dark brown with olivaceous ring at the middle, and pale brown to hyaline to the edge, from reverse dark brown to olivaceous at the center, and the pale brown to hyaline towards edge.

Material examined: Thailand, Chang Wat Prachuap Khiri Khan Province, Pran Buri District, Sam Roi Yot wetland, on decaying stems of *Typha* sp. (Typhaceae), 02 December 2023, Tharindu Bhagya, TB156A (MFLU 25-0449), Chang Wat Prachuap Khiri Khan Province, Pran Buri District, Sam Roi Yot wetland, on decaying leaf of *Typha* sp. (Typhaceae), 08 April 2024, Tharindu Bhagya, TB156B (MFLU 25-0460).

GenBank numbers – MFLU 25-0459, ITS = PX062190

Distribution – On submerged decaying wood in a freshwater stream in Yanuoda Rainforest Cultural Tourist District, China (Ma et al., 2025), and decaying submerge stem, and immerse leaf of *Typha* sp. in freshwater wetland, Thailand (This study.

Notes – The newly isolated strains (MLFU 25-0459 and MFLU 25-0460) formed a clade sister to *T. yanuodaensis* (GZCC 23-0488 and GZCC 24-0165), with

100% maximum likelihood (ML) bootstrap support and a Bayesian posterior probability (BPP) of 1.00 (Figure 4.55). Phylogenetically, pairwise comparisons between the new isolate (MFLU 25-0459) and the type strain of *T. yanuodaensis* (GZCC 23-0488) revealed sequence similarities of 1.61% in ITS, 1.04% in LSU, 1.17% in *rpb2*, and 2.21% in *tef1-α*. Morphologically, the new strains resemble *T. yanuodaensis* (GZCC 23-0488 and GZCC 24-0165) by producing holoblastic, monoblastic, integrated, subcylindrical, terminal conidiogenous cells, and guttulate, hyaline, smooth-walled conidia with multiple septa (Figure 4.56) (Ma et al., 2025). According to the available evidences I recognize the sew strains as *T. yanuodaensis* and report new host and geographical record for the species from *Typha* sp. in freshwater costal wetland, in Thailand. However, the new isolates (MLFU 25-0459 and MFLU 25-0460) differ morphologically from *T. yanuodaensis* (GZCC 23-0488 and GZCC 24-0165) in having conidiogenous cells that exhibit percurrent proliferation with apical thickening and by producing acropleurogenous conidia (Lu et al., 2018; Ma et al., 2023; Ma et al., 2024; Ma et al., 2025). These differences demonstrate the morphological plasticity and adaptive strategies of *Tubeufia* species in response to environmental conditions (Boonmee et al., 2014).

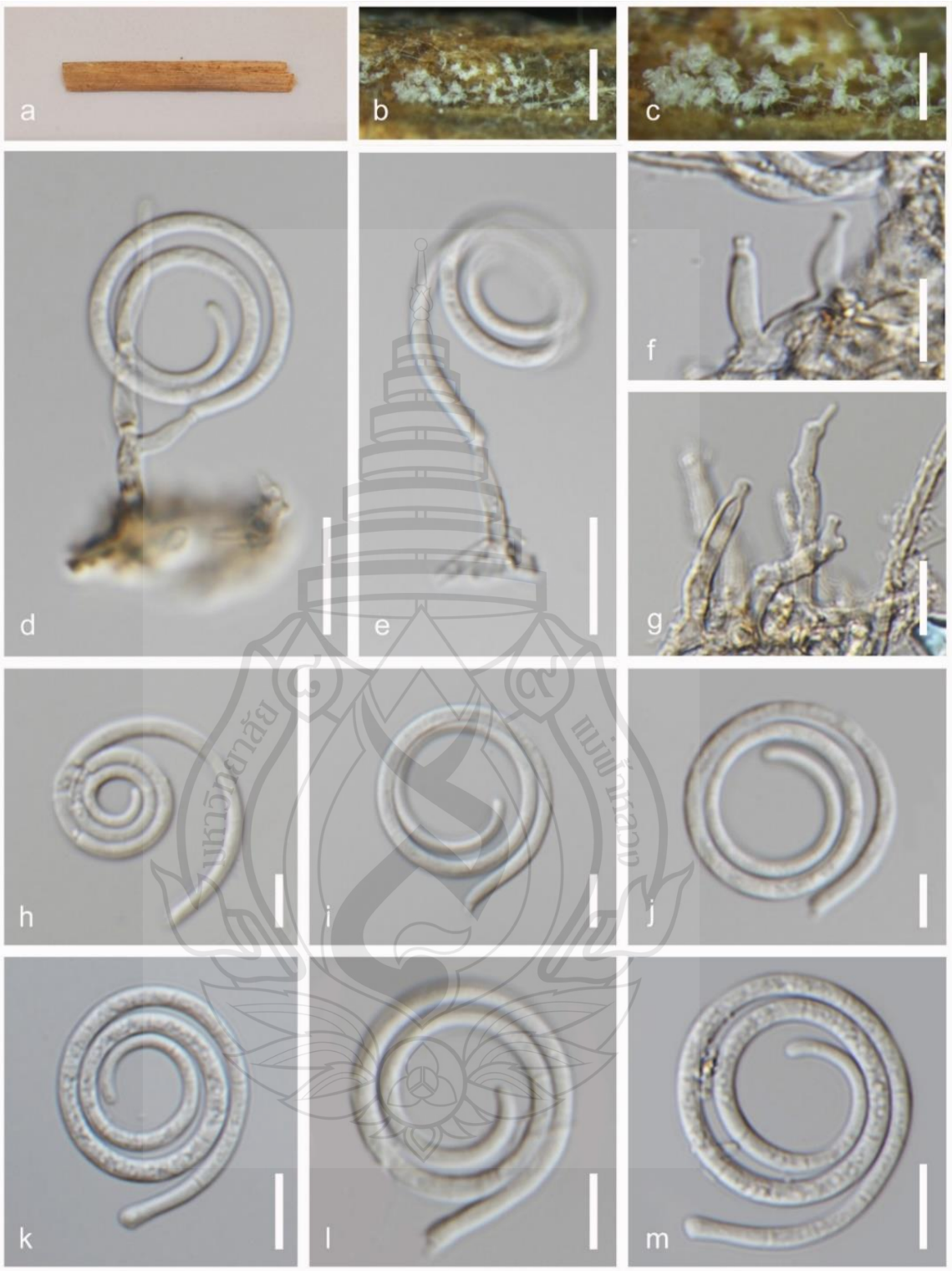

Note a *Typha* sp. host material. b–c Conidiophores on the host surface with white conidia. d–e Conidiophores with conidia. f–g Conidiophores and conidiogenous cells. h–m Conidia. Scale bars: b 500 µm, c 250 µm, d–e 20 µm, f–m 10 µm.

Figure 4.56 *Tubeufia yanuodaensis* (MFLUC 25-0459)

Tubeufia baoshanensis L. Lu & Karun., in Liu, Zhao, Cai, Shen, Wei, Na, Han, Wei, Ge, Ma, Karunarathna, Perprint, 2025

Saprobic on dead, decaying stems of *Typha*, (Typhaceae), **Sexual morph**: *Ascomata* 130–190 × 110–160 µm ($\bar{x}$ = 170 × 155 µm, n = 5), perithecial, superficial, gregarious in aggregation, scattered on the host, globose to subglobose to oval with short ostiole, light orange to yellowish orange with surface smooth not distinctly warted, collapsing with slight pressure. *Peridium* 12–22 µm ($\bar{x}$ = 18 µm, n = 5), thin, leathery, comprise with brownish yellow cells of *textura angularis* to *textura globose* and *textura epidermodiea*. *Paraphyses* not observed. *Asci* 62–84 × 12–20 µm ($\bar{x}$ = 72 × 16.5 µm, n = 15), 8-spored, bitunicate, cylindrical to subcylindrical or clavate, short pedicellate with conspicuous ocular chamber. *Ascospores* 35–48 × 2.5–6 µm ($\bar{x}$ = 41 × 4.5 µm, n = 10), 2–3-seriate or variably arranged, hyaline, fusiform, 4–7-pseudoseptate, tapering towards rounded ends, occasionally slightly curved, guttulate with smooth-walled. **Asexual morph**: *Hyphomycetous*, helicosporous, developed *in vitro*, *Conidiogenous cells*, indistintive on culture, *Conidia* 25–38 µm ($\bar{x}$ = 30 µm, n = 5) in diameter, 1.5–4.5 µm ($\bar{x}$ = 2.5 µm, n = 5), solitary, helicoid, hyaline, smooth walled.

Culture characteristics: Ascospores germinating on MEA within 24 h. Germ tubes produced from both ends of the spores. Colonies growing on MEA, reaching 40 mm in 6 weeks and sporulation in 8 weeks at 25°C. Mycelia superficial, umbonate with erose edge that fungal filaments radiate to the culture, from above off-white cottony hype aggregation at center with ash to back, olivaceous green, leading to black edge with hyaline tips, concentric ring like statures are prominent, from reverse olivaceous green to black at the center and leading to black edge with hyaline tips off white at the edge. Mycelium melts the culture media from underneath and produces a cavity that visible from reverse.

Material examined: Thailand, Chang Wat Prachuap Khiri Khan Province, Pran Buri District, Pran Buri wetland, on decaying stems of *Typha* sp. (Typhaceae), 06 April 2024, Tharindu Bhagya, TB195A (MFLU 25-0461), Chang Wat Prachuap Khiri Khan Province, Pran Buri District, Pran Buri river, decaying leaf of Grass (Poaceae)**,** 06 April 2024, Tharindu Bhagya**,** TB195B (MFLU 25-0462).

GenBank numbers – MFLU 25-0461, ITS = PV775680

Distribution – Decaying branch of *Coffea* sp., Yunnan Province, China, and decaying submerge stem, and immerse leaf of *Typha* sp. and decomposing stem of Grass, (Poaceae), in freshwater wetland, Thailand (This study).

Notes – The new isolates (MLFU 25-0461 and MFLU 25-0462) formed a sister lineage to *T. baoshanensis* (ZHKUCC 23-0682), with 100% ML bootstrap support and a Bayesian posterior probability (BPP) of 1.00 (Figure 4.55). Based on pairwise comparisons, strain MFLU 25-0461 was phylogenetically similar to *T. baoshanensis* (ZHKUCC 23-0682), showing sequence differences of 1.56% in ITS, 1.11% in LSU, and 2.09% in tef1-α (Lu et al., 2025). Morphologically, the new strains (MLFU 25-0461 and MFLU 25-0462) resemble *T. baoshanensis* (ZHKUCC 23-0682) by having a yellowish to pale-brown outer peridial layer composed of textura angularis cells, bitunicate cylindrical asci, and hyaline fusiform ascospores (Figure 4.57) (Lu et al., 2025). Considering available evidences, I recognize the strains (MLFU 25-0461 and MFLU 25-0462) as *T. baoshanensis*, isolated from *Typha* sp. and Grass, (Poaceae) in freshwater coastal wetlands in Thailand, and report new host and geographical record to the species. However, strain MFLU 25-0461 displays unique features that distinguish it from the type strain ZHKUCC 23-0682, including light orange to yellowish-orange ascomata, a peridium dominated by *textura epidermoidea* cells, absence of pseudoparaphyses, and short-pedicellate asci bearing 4–7-pseudoseptate ascospores (Lu et al., 2025). These distinctive morphological features may be attributed to environmental variation and differences in host material (Boonmee et al., 2014).

Note a *Typha* sp. host material. b–c Ascomata on the host. d Squashed mount of ascomata. e Surface of peridium. f–h Asci. i–j Ascospores; k Germinating ascospore. l Culture on MEA above. m Reverse. n Hyaline fungal mycelium. o Hyaline chlamydospores. p Conidia development, *in vitro*. Scale bars: b–c 250 µm, d 100 µm, e–p 20 µm.

Figure 4.57 *Tubeufia baoshanensis* (MFLUC 25-0461)

Eurotiomycetes O.E. Erikss. & Winka

Eurotiomycetidae Tehler

Eurotiales *G.W. Martin ex Benny & Kimbr*

Aspergillaceae *Link*

Aspergillus *P. Micheli ex Haller*

Aspergillus is a filamentous fungal genus proposed by P. Micheli ex Haller in 1769 and typified by *Aspergillus glaucus*. This genus is one of the most widespread in the kingdom Fungi and has been recovered from diverse habitats and substrates, including decomposing plant materials, as phytopathogens, animal pathogens, and also from soil (Sklenář et al., 2017; Glässnerová et al., 2022; Sklenář et al., 2022). The asexual morphs of members of this genus are characterized by a specialized basal cell at the base of the conidiophore, a vesicle at the tip of the conidiophore giving rise to metulae and phialides. The sexual morphs of *Aspergillus* are characterized by hyaline to pale brown ascomata with globose to subglobose asci (Sklenář et al., 2017; Sklenář et al., 2022). Based on morphological and phylogenetic complexity, environmental affinities, and the large number of species, the genus *Aspergillus* is divided into several sections such as *Flavi*, *Nigri*, and *Restricti*. For example, members of section *Restricti*, such as *A. halophilicus*, are relatively slow-growing and prefer environments with low water activity (Sklenář et al., 2017; Sklenář et al., 2022).

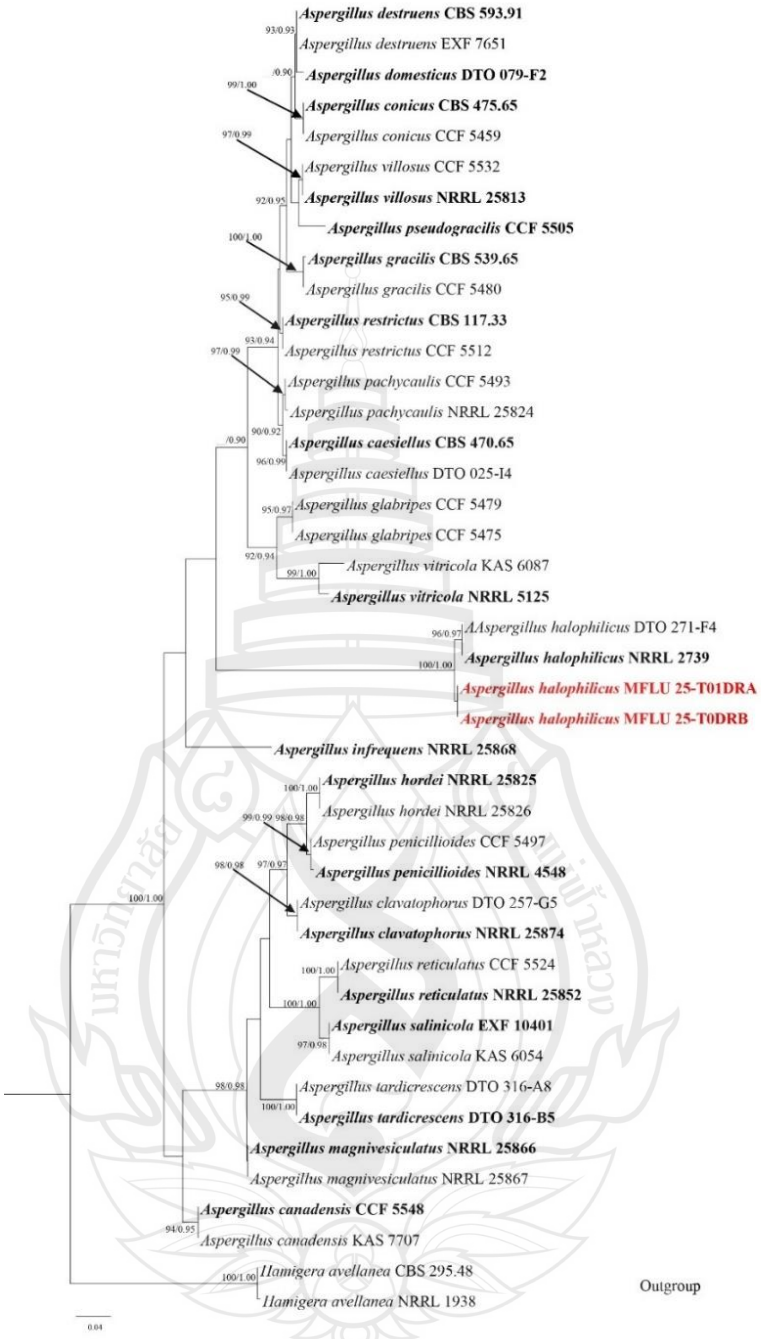

Note The data set comprises 642 characters including gaps from of selected 43 strains which were included in the phylogenetic analyses. Bootstrap support values for ML ≥ 90 % and Bayesian posterior probabilities (BPP) ≥ 0.90 are mentioned at the nodes. The tree was rooted to Hamigera avellanea (NRRL 1938, and CBS 295.48). Newly generated sequences are in red and the type strains are in bold.

Figure 4.58 Phylogram generated from Maximum Likelihood (ML) analysis based on ITS, sequence.

Aspergillus halophilicus M. Chr., Papav. & C.R. Benj., Mycologia 51(5): 638 (1961) [1959]

Saprobic on decaying of stem of *Typha,* (Typhaceae). **Sexual morph**: *Ascomata* 100–170 × 100–150 ($\bar{x}$ = 155 ×135 µm, n = 5), cleistothecial, hyaline or light pale brown, solitary to scattered, superficial on host tissue, globose to subglobose and fragile or slightly coriaceous when immature. *Peridium*, thin, slightly coriaceous, composed of hyaline thick-walled cells in *textura angularis*. *Paraphyses* absent. *Asci* 8–12 × 4–6.5 ($\bar{x}$ = 10.5 × 5.5 µm, n = 10), 8-spored, unitunicate, globose to subglobose or subcylindrical, sessile. *Ascospores* 4.5–7 x 3.5–6.5 ($\bar{x}$ = 5.5 × 4.5 µm, n = 30), crowded, hyaline, aseptate, smooth, ellipsoidal to lenticular with convex surfaces, process equatorial depression. **Asexual morph**: Undetermined.

Material examined: Thailand, Chang Wat Prachuap Khiri Khan Province, Pran Buri District, Pran Buri Wetland on decaying stems of *Typha* sp. (Typhaceae), 06 April 2024, Tharindu Bhagya, TB_dr_A (MFLU 25-0463), Chang Wat Prachuap Khiri Khan Province, Pran Buri District, Pran Buri river TB_dr_B, Bamboo (Poaceae), 06 April 2024, Tharindu Bhagya (MFLU 25-0464).

GenBank numbers – MFLUC 25-0463: ITS = PX518100

Distribution – On dried corn, Minnesota, St. Paul, USA (Sklenář et al., 2017), decaying submerged *Typha* sp. leaf in freshwater wetland, and decaying submerged Bamboo stem, in freshwater river, Thailand (This study).

Notes – The new isolate forms a clade sister to *Aspergillus halophilicus* strains NRRL 2739 and DTO 271.F4, with strong statistical support (100% ML and 1.00 BPP) (Figure 4.58). Strain MFLU 25-0463 shares 99.2% similarity with strain NRRL 2739 in ITS sequences, excluding gaps. The new isolates also share similar morphological characteristics with *A. halophilicus* strain NRRL 2739, producing hyaline to pale brown ascomata, globose asci, and hyaline, aseptate, lenticular ascospores with convex surfaces (Figure 4.59) (Sklenář et al., 2017; Sklenář et al., 2022). The absence of an ex-type culture for strain MFLU 25-0463 limits a full morphological comparison with the asexual morph of type strain NRRL 2739. Based on the available phylogenetic and morphological evidence, I recognize strains MFLU 25-0463 and MFLU 25-0464 as *Aspergillus halophilicus*, and report them as new host records from wetland-dwelling Bamboo and Typhaceae in Thailand.

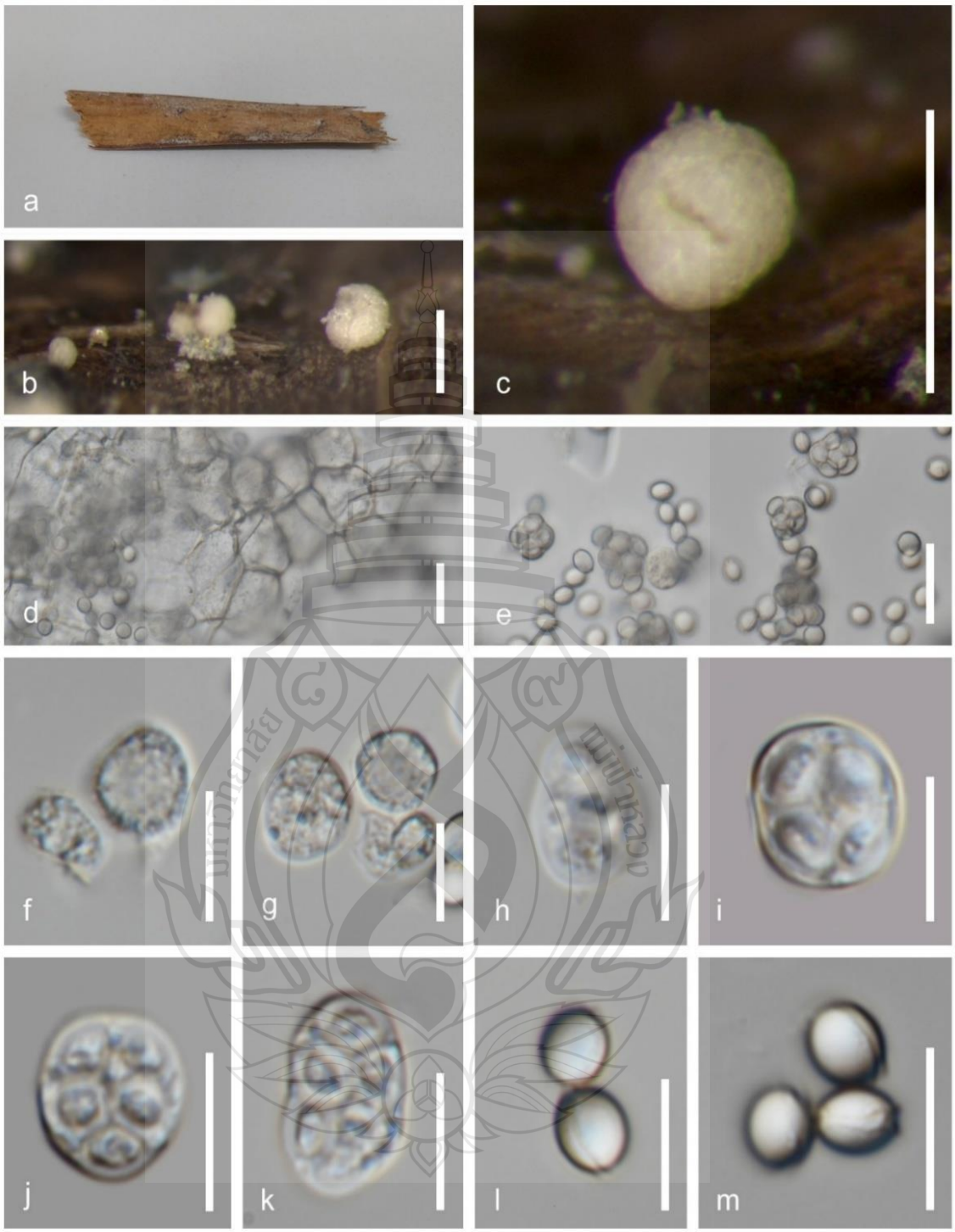

Note a *Typha* sp. host material. b–c Ascomata on the host tissue. d Surface of the peridium. e Asci and ascospores. f–k Asci; l–m Ascospores. Scale bars: b 250 µm, c 500 µm, d–e 20 µm, f–m 10 µm.

Figure 4.59 *Aspergillus halophilicus* (MFLU 25-0463)

Chaetothyriomycetidae Doweld

Chaetothyriales M.E. Barr

Herpotrichiellaceae Munk

Veronaea Cif. & Montemart

The genus *Veronaea* was introduced by Cif. & Montemart in 1957 and typified by *Veronaea botryosa*. Members of the genus are characterized by pale brown, sympodial, polyblastic conidiogenous cells, and hyaline to pale brown, smooth-walled, septate, cylindrical to pyriform conidia with truncate bases or bearing scars at the base. *Veronaea* exhibits a wide distribution and is frequently isolated from decomposing wood in aquatic habitats, other decaying plant materials, and animal tissues (Dong et al., 2018; Chandrasiri et al., 2021; Su et al., 2023).

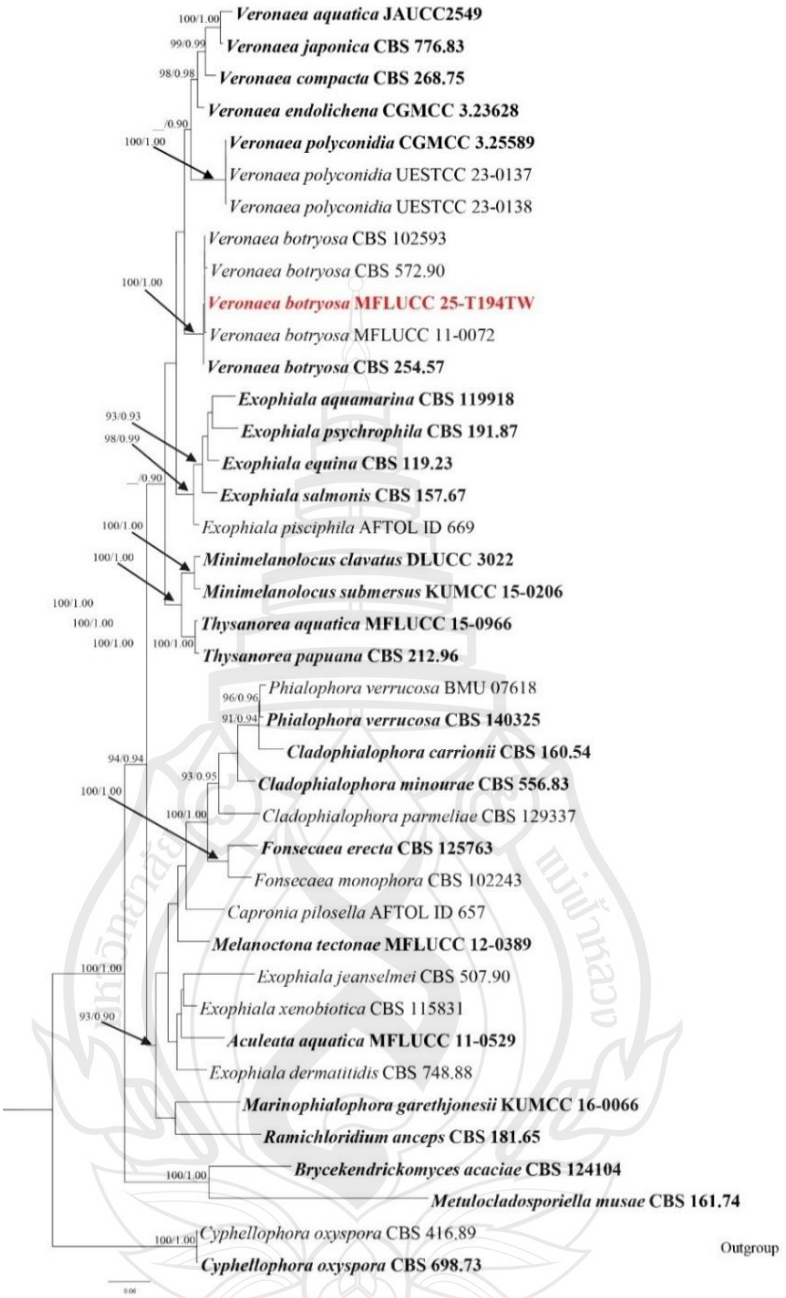

Note Bootstrap support values for ML ≥ 90 % and Bayesian posterior probabilities (BPP) ≥ 0.9 are mentioned at the nodes. The tree was rooted to *Cyphellophora oxyspora* (CBS 416. 89 and CBS 698.73). Newly generated sequence is indicated in red and the type strains are in bold.

Figure 4.60 Phylogentic tree generated from Maximum Likelihood (ML) analysis based on combined LSU, SSU, ITS, and *tub2* sequence from *Veronaea* and related taxa, compressing 3198 characters including gaps from of 40 strains which were included in the analyses.

Veronaea botryosa Cif. & Montemart., Atti Ist. bot. Univ. Lab. crittog. Pavia, sér. 5 15: 68 (1957)

Saprobic on dead, decaying stems of *Typha*, (Typhaceae), **Sexual morph:** Undetermined. **Asexual morph:** *Hyphomycetous*. *Colonies* on the natural substrate numerous, hairy, effuse, appear as dark brown to black patchers. *Mycelium,* 1.5–2.5 µm ($\bar{x}$ = 2 µm, n = 10), immersed in the substrate, consisting of hyaline or subhyaline to pale brown, smooth hyphae. *Conidiophores*, 140–210 × 3.5–6.5 µm ($\bar{x}$ = 180 × 4.5 µm, n = 10), macronematous, mononematous, brown to dark brown with hyaline to subhyaline apexes, straight or slightly flexuous, unbranched, solitary or loosely aggregated, smooth, thick-walled. *Conidiogenous cells*, 6–8 × 3–5 µm ($\bar{x}$ = 6. 5 × 4.5 µm, n = 10), polyblastic, terminal, cylindrical, hyaline to pale brown to olivaceous-brown and process slightly prominent denticles. *Conidia*, 5–12 × 3.5–5.5 µm ($\bar{x}$ = 10.5 × 4 µm, n = 30), acropleurogenous, schizolytic, solitary and smooth, cylindrical to pyriform, pale brown to light brown, 1–3-septate process rounded apex and truncate at base. **Sexual morph:** Undetermined.

Culture characteristics: Conidia germinating on MEA within 12 h. Germ tube produced from the side of conidia. Colonies growing on MEA, reaching 20 mm in 6 weeks at 25°C. Mycelia superficial, effuse to flat or undulate, from above gray to off white at the center, olivaceous to greyish to the euros white edge, from reverse greenish black at the center, light brown to white ring and hyaline tips at edge.

Material examined: Thailand, Chang Wat Prachuap Khiri Khan Province, Sam Roi Yot Wetland, on decaying stems of *Typha* sp. (Typhaceae), 08 April 2024, Tharindu Bhagya, TB145A (MFLU 25-0465).

GenBank numbers – MFLU 25-0465: ITS =PX518098, LSU = PX518101

Distribution – Olive slag, Italy (Ciferri & Montemartini, 1957), decomposed rachis of a palm (*Arecaceae*), Italy (Arzanlou et al., 2007), Human infection in skin, China (Zhu et al., 2015), submerged wood, Huai Kang Pla, Chiang Rai, Thailand (Dong et al., 2018), on decaying *Typha* sp. leaf in freshwater wetland, Thailand (This study).

Notes – The strain MFLU 25-0465 forms a sister clade to *Veronaea botryosa* strain MFLUCC 11-0072 with 59% ML and 0.62 BPP support (Figure 4.60). The isolate exhibits characteristics typical of the genus *Veronaea*, including sympodial, polyblastic conidiogenous cells and septate, cylindrical to pyriform conidia with scars at the base

(Figure 4.61) (Dong et al., 2018; Chandrasiri et al., 2021; Su et al., 2023). Phylogenetically, MFLU 25-0465 shares 98.6% similarity in ITS sequences and 99.4% similarity in LSU sequences (excluding gaps) with *V. botryosa* strain MFLUCC 11-0072. Strain MFLU 25-0465 resembles *V. botryosa* strain MFLUCC 11-0072 by exhibiting similar lengths of conidiophores ($\bar{x}$ = 180 μm vs $\bar{x}$ = 182 μm), acropleurogenous, schizolytic conidiogenesis, and a comparable conidial height-to-width ratio (2.63 vs 2.53). Furthermore, the pairwise distance matrix value between MFLU 25-0465 and *V. botryosa* strain MFLUCC 11-0072 was <0.01 (Gostinčar, 2020; Maharachchkumbura et al., 2021). Based on the available phylogenetic and morphological evidence, I recognize the new strain MFLU 25-0465 as a strain of *V. botryosa*, isolated from *Typha* (Typhaceae) in freshwater coastal wetlands in Thailand.

Note a *Typha* sp. host material. b–c Conidiophores on the host surface. d–f Conidiophores. g–h Fertile tips of conidiophores with conidiogenous loci (arrowed) and attached conidia. g–j Denticulate conidiophores. i Conidia. j Culture on MEA above. k Reverse. Scale bars: b 500 µm, c 250 µm, d–f 20 µm, g–i 10 µm.

Figure 4.61 *Veronaea botryosa* (MFLU 25-0465)

Sordariomycetes O.E. Erikss. & Winka

Diaporthomycetidae Senan., Maharachch. & K.D. Hyde

Diaporthales Nannf.

Schizoparmaceae Rossman, D.F. Farr & Castl.

Coniella Höhn., Ber. dt. bot. Ges. 36(7): 316 (1918)

Coniella was first described by Höhnel in 1918 and is typified with *Coniella pulchella*. The genus includes both pathogenic and saprobic species that exhibit worldwide distribution and affinity toward diverse host species. *Coniella* comprises both sexual and asexual morphs. The sexual morph is characterized by brown to black, globose, papillate, erumpent to superficial ascomata bearing eight-spored, clavate to subcylindrical asci with a distinct apical ring. Ascospores in the genus *Coniella* are ellipsoid, aseptate, hyaline when immature, and pale yellow at maturity (Alvarez et al., 2016; Li et al., 2025). The asexual morph often produces immersed to semi-immersed pycnidia, containing discrete, cylindrical, subcylindrical, obclavate to lageniform, hyaline, and smooth-walled conidiogenous cells. Conidia are hyaline or pale yellow, smooth, ellipsoid, globose, napiform, or fusiform (Alvarez et al., 2016; Wang et al., 2022; Li et al., 2025).

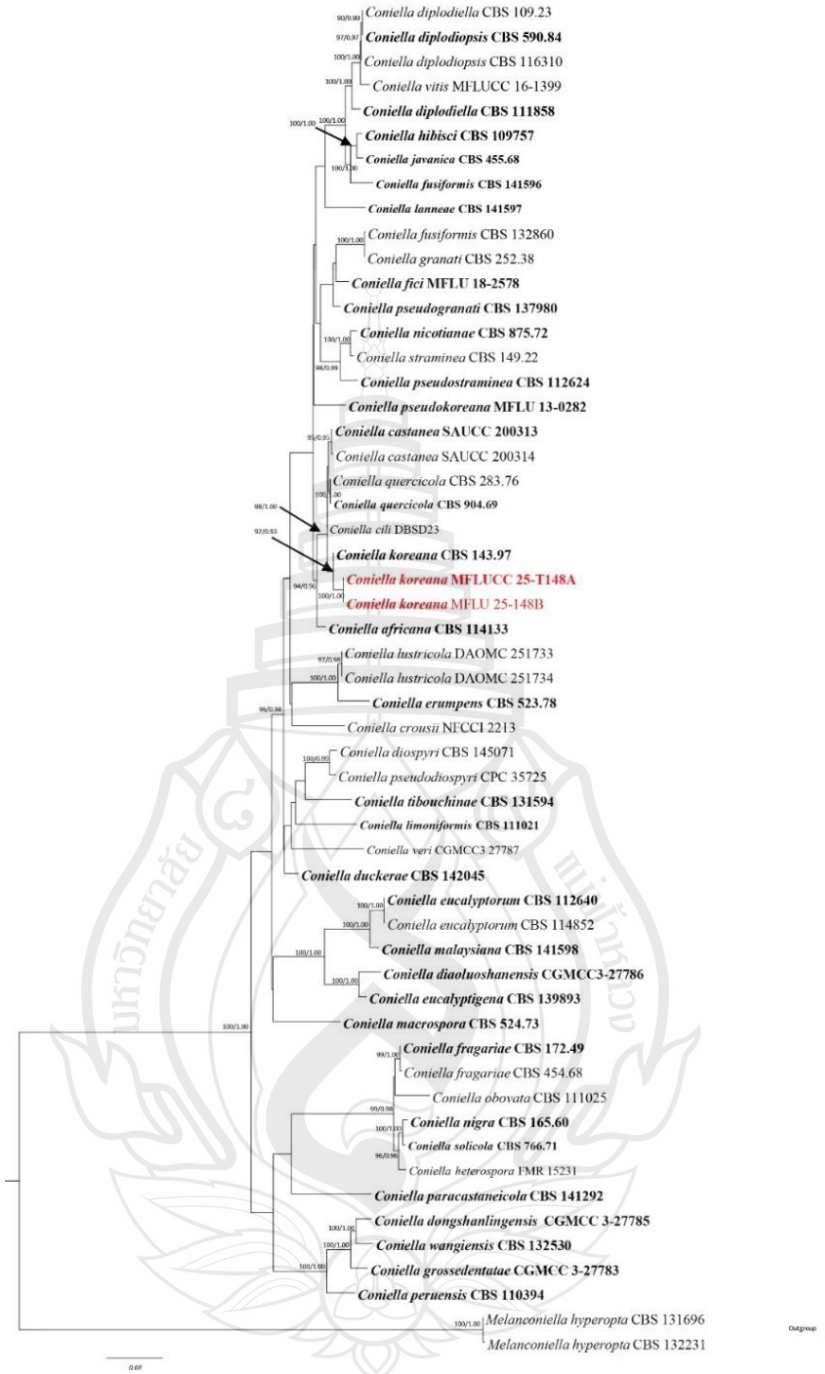

Note Compressing 3263 characters including gaps from of 55 strains which were included in the analyses. Bootstrap support values for ML ≥ 90% and Bayesian posterior probabilities (BPP) ≥ 0.9 are mentioned at the nodes. The tree was rooted to *Melanconiella hyperopta* (CBS 131696 and CBS 132231). Newly generated sequences are indicated in red and the type strains are in bold.

Figure 4.62 Phylogenetic tree generated from Maximum Likelihood (ML) analysis based on combined ITS, LSU, *rpb2* and *tef1-α* sequence.

Coniella koreana L.V. Alvarez & Crous, in Alvarez, Groenewald & Crous, Stud. Mycol. 85: 18 (2016)

Saprobic on dead, decaying stems of *Typha*, (Typhaceae). **Sexual morph**: Undetermined. **Asexual morph**: Coelomycetous. *Conidiomata* immersed to erumpent, gregarious on host. *Conidiomata in vitro*,140–250 × 110–230 µm ($\bar{x}$ = 190 × 145 µm, n = 5), cespitose to subfasciculate, superficial, semi-immersed to erupt in mycelium, hyaline when immature, dark brown to black at maturity, glabrous, globose to subglobose with short central ostiole. *Conidiomatal wall*, 15–22 µm wide ($\bar{x}$ = 18 µm, n = 5), 2-3 layered composed from dark brown to black, thick-walled of cells *textura angularis*. *Ostiole*, 35–52 × 28–50 µm ($\bar{x}$ = 45 × 48 µm, n = 5), central, wider at base and narrowing to the opening, composed with dark brown to black cells of *textura angularis*. *Conidiophores,* 7–14 × 2–3 µm ($\bar{x}$ =12.5 × 2.5 µm, n = 20), dance, hyaline, smooth walled, reduced to 1-2 cells or absent, subulate to cylindrical or sub cylindrical, breached or occasionally simple, submerged in gelatinous metrix. *Conidiogenous cells*, 9–16 × 1.5–3.5 µm ($\bar{x}$ =13.5 × 2.5 µm, n = 20), proliferating in different levels, hyaline, smooth-walled, holoblastic, cylindrical, attenuate to acuminate or subulate with prominent periclinal thickening. *Conidia*, 12–17 × 1.5–4.5 µm ($\bar{x}$ = 15.5 × 3.5 µm, n = 30), hyaline or pale yellowish, unicellular, straight to falcate, ellipsoid to obovoid, smooth thick-walled, rounded at apex, with truncated base.

Culture characteristics: Conidia germinating on MEA within 12 h. Germ tubes produced from both ends of the conidium. Colonies growing on MEA, reaching 50 mm in 2 weeks. Mycelia superficial, umbonate with complete edge, from above off-white cottony hype with imbricated concentric zones and conidiomata aggravations developing after 6 weeks, from reverse off white with dance concentric zones bearing dark spots scatted on mycelium.

Material examined: Thailand, Chang Wat Prachuap Khiri Khan Province, Pran Buri District, Pran Buri Wetland, on decaying stems of *Typha* sp. (Typhaceae), 02 January 2024, Tharindu Bhagya, TB148A (MFLU 25-0466), Chang Wat Prachuap Khiri Khan Province, Khao Sam Roi Yot Wetland, On decaying peduncle of Grass (Poaceae), 02 January 2024, Tharindu Bhagya, TB148B (MFLU 25-0467).

GenBank numbers – MFLU 25-0466: ITS =PX518103, LSU = PX518104

Distribution – Unknown host, South Korea (Alvarez et al., 2016), *Loropetalum chinense* var. *rubrum*, Sichuan, China (Chen et al., 2023), decaying *Typha* sp. stem and grass stem in freshwater wetland, Thailand (This study).

Notes – The new isolates formed a sister clade to *Coniella koreana* strain CBS 143.97 with 100% ML and 1.00 BPP support (Figure 4.62). MFLU 25-0466 and MFLU 25-0467 resemble other members of *Coniella* by producing unilocular, glabrous, ostiolate conidiomata, cylindrical to subcylindrical conidiogenous cells with periclinal thickening, and hyaline, fusiform, smooth-walled conidia (Alvarez et al., 2016). The new isolates shear morphologically similarities to *C. koreana* strain CBS 143.97 due to the presence of subulate to cylindrical conidiophores, cylindrical to attenuate or subulate conidiogenous cells, and hyaline to pale yellowish, unicellular, straight to falcate conidia with rounded apices and truncated bases (Figure 4.63) (Alvarez et al., 2016). Based on the available phylogenetic and morphological evidence, I recognize MFLUCC 25-0466 and MFLU 25-0467 as new strains of *C. koreana*, isolated from *Typha,* (Typhaceae) and grass, (Poaceae), respectively.

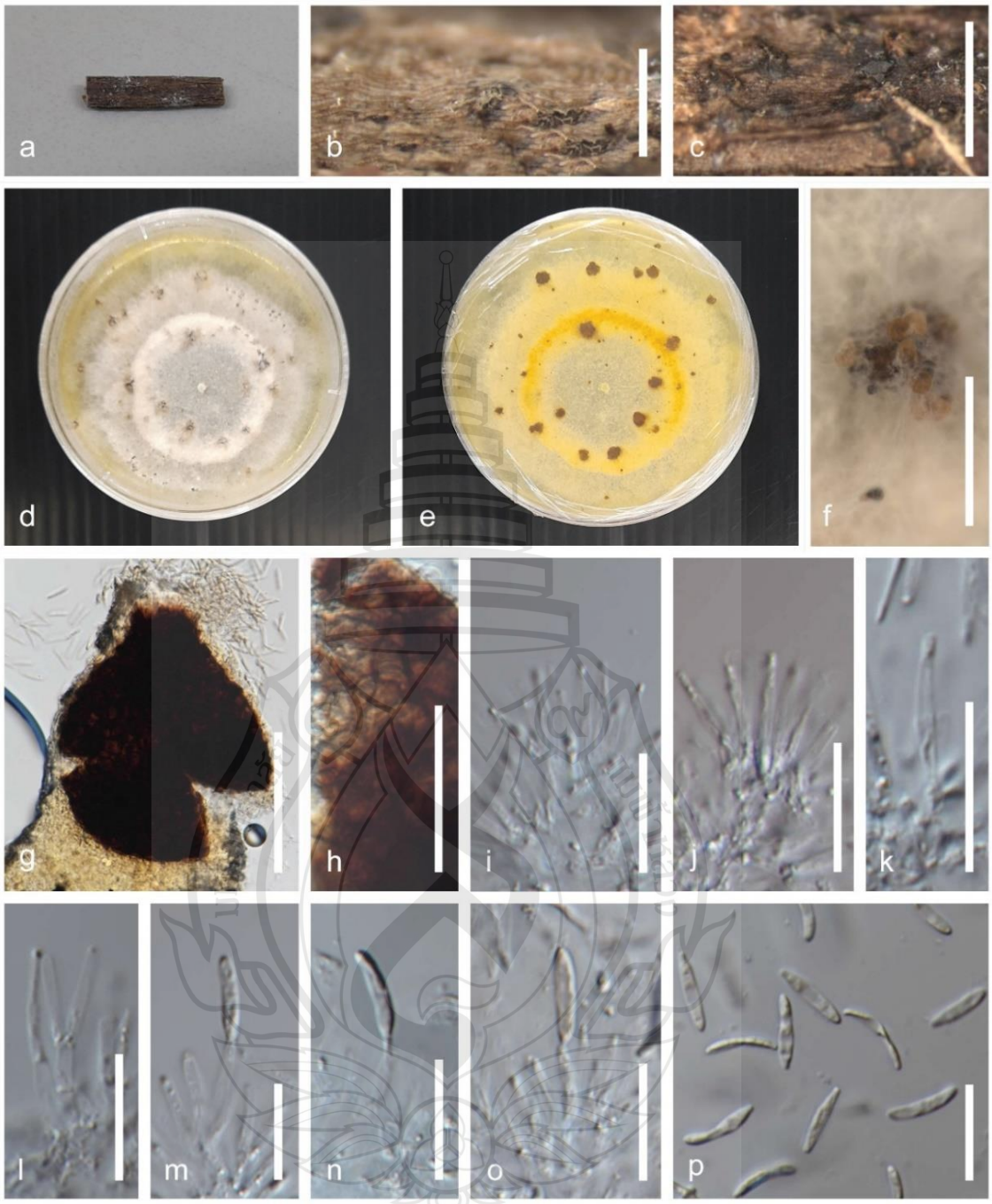

Note a *Typha* sp. host. b-c Conidia aggregation on the host. d Culture on MEA above. e Reverse. f Conidia aggregation *in vitro*. g Squash mount of conidiomata developed *in vitro*. f Conidiomata wall. i–k Conidiophores with conidogenous cells. l–o Conidia development with conidiogenous cells. p Conidia. Scale bars: b–c 500 µm, f 1 mm, g 100 µm, h 50 µm, i–p 20 µm.

Figure 4.63 *Coniella koreana* (MFLU 25-0466)

Togniniales Senan., Maharachch. & K.D. Hyde

Togniniaceae Réblová, L. Mostert, W. Gams & Crous

Phaeoacremonium W. Gams, Crous & M.J. Wingf., Mycologia 88(5): 789 (1996)

The genus *Phaeoacremonium* was established by W. Gams, Crous, and M.J. Wingfield in 1996, with *P. parasiticum* as the type species, and was classified in the monotypic order *Togniniales* (Maharachchikumbura et al., 2015). Initially, *Phaeoacremonium* was known only from its sexual morphs. *Togninia*, typified by *T. minima*, was recognized as the genus representing the sexual morphs of *Phaeoacremonium*. This connection was confirmed through mating experiments (Mostert et al., 2003). Based on these findings, *Togninia* was synonymized with *Phaeoacremonium*, and the name *Phaeoacremonium* was preserved (Réblová et al., 2016). Members of this genus are characterized in their sexual morphs by astromatic, papillate or long-necked perithecial ascomata, clavate asci with broadly rounded to obtuse apices, and hyaline, smooth, aseptate, cylindrical to allantoid ascospores (Maharachchikumbura et al., 2015; Dayarathne et al., 2019). *Phaeoacremonium* comprises asexual morphs which are characterized by unbranched conidiophores that end with a single terminal collaretted phialide. Conidia are hyaline, smooth walled, ellipsoidal to oblong or allantoid (Maharachchikumbura et al., 2015; Dayarathne et al., 2019; Calabon et al., 2024). Members of *Phaeoacremonium* have been reported from woody substrates, stems, and branches, and are known to cause pathogenic infections in animals (Dayarathne et al., 2019; Calabon et al., 2024).

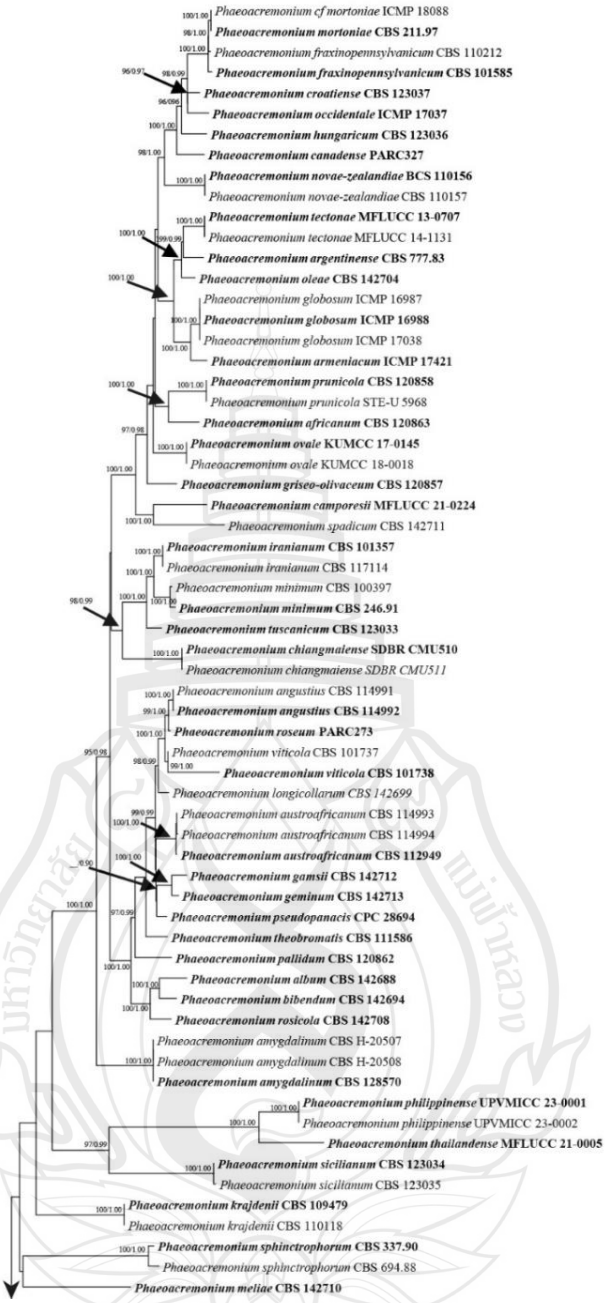

Note The data set comprises 3398 characters including gaps from of selected 113 strains which were included in the phylogenetic analyses. Bootstrap support values for ML ≥ 90 % and Bayesian posterior probabilities (BPP) ≥ 0.9 are mentioned at the nodes. The tree was rooted to *Flabellascus tenuirostris* (CBS 138680) and *Jattaea algeriensis* (STE-U 6201). Newly generated sequences are in red and the type strains are in bold.

Figure 4.64 Phylogram generated from Maximum Likelihood (ML) analysis based on combined ITS, *tub*, *act*, *tef1-α* and LSU sequence.

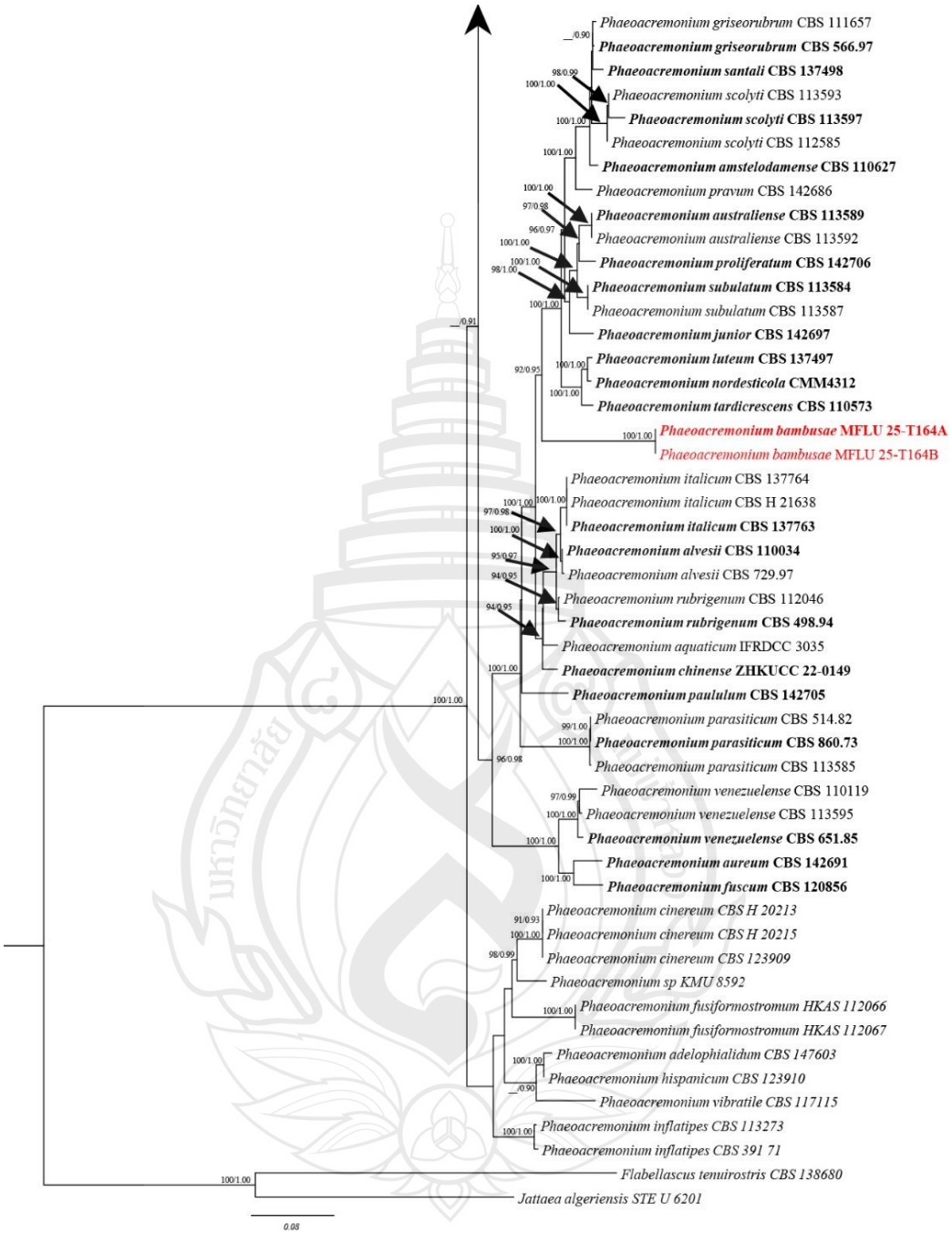

Figure 4.64 (continued)

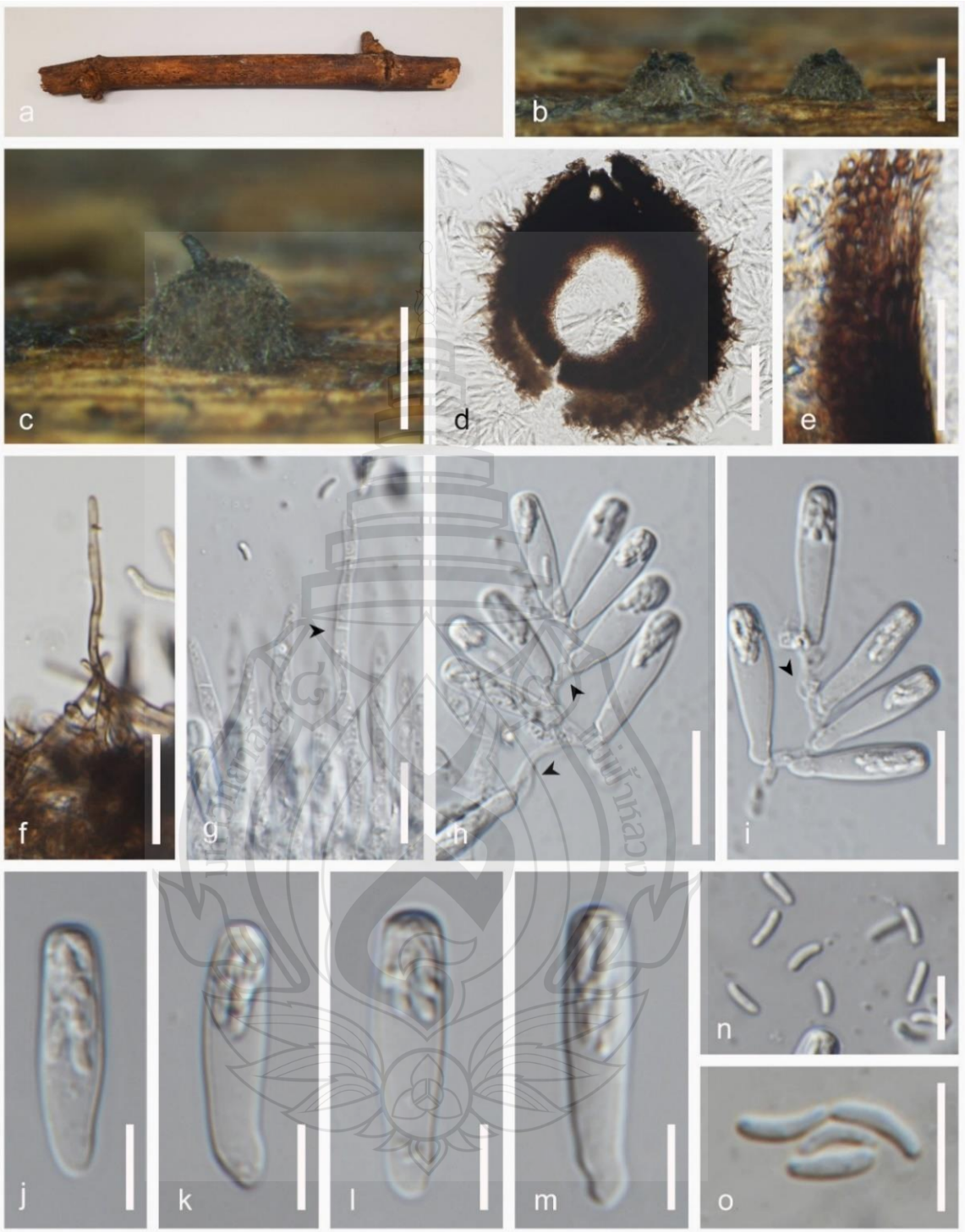

Note a Bamboo host. b–c Ascomata on the host tissue. d Section of ascomata with tomentum of mycelium. e Peridium. f Hyphae on ascomata. g Septate paraphyses (arrowed). h–i Ascogenous hyphae producing asci (arrowed). j–m Asci. n-o Ascospores. Scale bars: b-c 500 µm, d 100 µm, e–i 20 µm. j–o 10 µm.

Figure 4.65 *Phaeoacremonium bambusae* (MFLU 25-0468, holotype)

Phaeoacremonium bambusae Bhagya, Phukhams E.B.G. Jones & K.D. Hyde, sp. nov

Index Fungorum number: IF; Facesoffungi number: FoF 18909

Etymology – Based on the host material from which the species originates.

Holotype – MFLU 25-0468

Saprobic on decaying of stem of Bamboo (Poaceae). **Sexual morph**: *Ascomata* 150–210 × 150–190 ($\bar{x}$ = 178 ×175 μm, n = 5), dark brown or black, clustered, solitary to scattered, superficial on host tissue, obpyriform, subglobose or ellipsoidal, single ostiolate, coriaceous, covered with tomentum of brown septate hyphae 30–55 ($\bar{x}$ = × 45 μm, n = 5), turn hyaline towards the end. *Ostiole* 55–70 × 35–50 ($\bar{x}$ = 62 × 45 μm, n = 5), periphysate, relatively short, central. *Peridium* 25–55 ($\bar{x}$ = 35 μm, n = 5), thick, carbonaceous, composed of two layers, outer layer brown thick-walled cells in *textura angularis*, inner layer consists with cells in *textura angularis* or *textura prismatica*. *Paraphyses* hyaline, septate, cylindrical, narrowing towards the apex. *Ascogenous hyphae* 1.5–3.5 ($\bar{x}$ = 2.5 μm, n = 20), hyaline, branched, smooth-walled, remnant bases of asci. *Asci* 20–32 × 4–7.5 ($\bar{x}$ = 28 × 5.5 μm, n = 20), 8-spored, show acropetal succession, unitunicate, clavate to obclavate or subcylindrical, tapering towards the truncate or bluntly obtuse bases, spicate, sessile, bluntly rounded at apices with non-amyloid apical ring. *Ascospores* 3.5–7.5 x 1–2.5 ($\bar{x}$ = × 5.5 x 1.5 μm, n = 30), biseriate, hyaline, aseptate, reniform to oblong-ellipsoidal with blunt ends, process small guttules at the ends, **Asexual morph**: Undetermined.

Material examined: Thailand, Chang Wat Prachuap Khiri Khan Province, Pran Buri District, Pran Buri river, on decaying stems of Bamboo (Poaceae), 06 May 2024, Tharindu Bhagya, TB164A (MFLU 25-0468, holotype), *ibid.,* TB164B, Bamboo, (Poaceae) (MFLU 25-0469, isotype).

GenBank numbers – MFLU 25-0468, ITS = PX062272

Distribution – Decaying submerged Bamboo stem, in freshwater river, Thailand.

Notes – The multi-locus phylogenetic analysis identified new isolates forming an independent lineage, supported by 92% ML and 0.96 BPP among *Phaeoacremonium* species (Figure 4.64). These isolates match the typical features of *Phaeoacremonium* sexual morphs, which include a two-layered peridium, acropetal succession of asci, and

oblong ascospores. (Dayarathne et al., 2019; Jamali et al., 2012). Based on the molecular data, *ACT* and *tub* sequences of strain MFLU 25-0468 were statistically most similar to *P. rubrigenum* strain CBS 498.94 (ACT = 86.35% and tub = 86.00%). The ITS sequence of the new isolate showed greater affinity towards *P. parasiticum* (≡*Togninia parasitica*) with a 94.06% similarity in BLAST, and the *tef1-α* locus shared a 96.68% match with *P. minimum* (≡*Togninia minima*). Furthermore, pairwise distance matrix value was >0.05 between MFLU 25-0468, and other lactated taxa (Gostinčar 2020, Maharachchkumbura et al., 2021). *Phaeoacremonium rubrigenum* and *P. parasiticum* are known only by their asexual morphs, and the lack of ex-type culture for MFLU 25-0468 renders a morphological comparison between the strains difficult (Jamali et al., 2012; Kubátová et al., 2004). Although *P. minimum* exhibits sexual morphs, MFLU 25-0468 differs by having a relatively shorter ostiole (250–285 μm vs. 55–70 μm) and a thick hyphal tomentum connected to the peridium (Figure 4.65) (Mostert et al., 2003). Considering the morphology of the asci, ascospores, and paraphyses, strain MFLU 25-0468 shares similarities with *P. aureum* strain MFLU 17-1581. However, the ostiole in MFLU 25-0468 is shorter compared to *P. aureum* strain MFLU 17-1581 (55–70 μm vs. 300–380 μm), and the tomentum consists of brown septate hyphae, distinguishing MFLU 25-0468 from *P. aureum*. Additionally, the distinct clustering in the phylogenetic tree further differentiates it from *P. aureum* strain MFLU 17-1581(Dayarathne et al., 2019). The development of an independent lineage, along with distinctive morphological features, enables the recognition of *P. bambusae* (MFLU 25-0468) as a new species.

Hypocreomycetidae O.E. Erikss. & Winka

Coronophorales Nannf

Ceratostomataceae G. Winter [as 'Ceratostomeae'], Rabenh

Melanospora Corda, Icon. fung. (Prague) 1: 24 (1837)

Melanospora belongs to the family *Ceratostomataceae*, proposed by Corda in 1837, with *M. zamiae* as the type species. Members of *Melanospora* are characterized by translucent ascomata with an ostiole made of intermingled hyphae, which develop into an apical crown of setae. The asci are obovoid to broadly clavate and highly evanescent. Ascospores in this genus have apiculate germ pores, and their surfaces are either smooth or ornamented (Maharachchikumbura et al., 2016; Marin-Felix et al., 2018; Huang et al., 2021). Asexual stages have also been observed in *Melanospora*. They exhibit cylindrical, straight to flexuous conidiophores that produce hyaline to brown, globose, aseptate to 1-septate conidia (Huang et al., 2021). Species within *Melanospora* display a variety of nutritional modes and are found to be saprobic, pathogenic, fungicolous, and biotrophic. This ecological versatility has allowed *Melanospora* to thrive in diverse habitats (Maharachchikumbura et al., 2016; Marin-Felix et al., 2018; Huang et al., 2021).

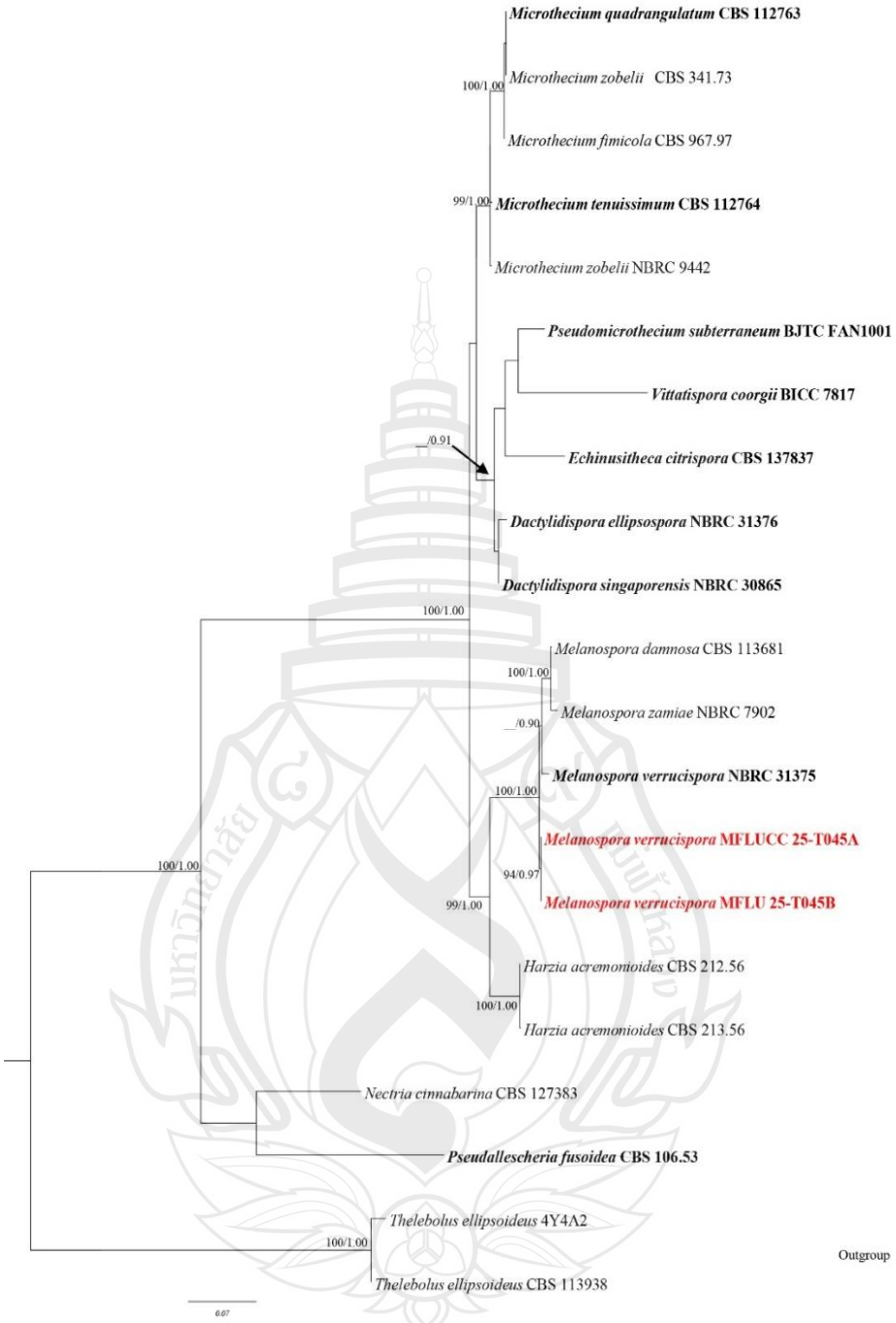

Note The data set comprises 2178 characters including gaps from of 21 strains which were included in the analyses. Bootstrap support values for ML ≥ 90 % and Bayesian posterior probabilities (BPP) ≥ 0.9 are mentioned at the nodes. The tree was rooted *Thelebolus ellipsoideus* (CBS 113938 and 4Y4A2). Newly generated sequence is in red and the type strains are in bold.

Figure 4.66 Phylogram generated from Maximum Likelihood (ML) analysis based on combined ITS, and LSU sequence.

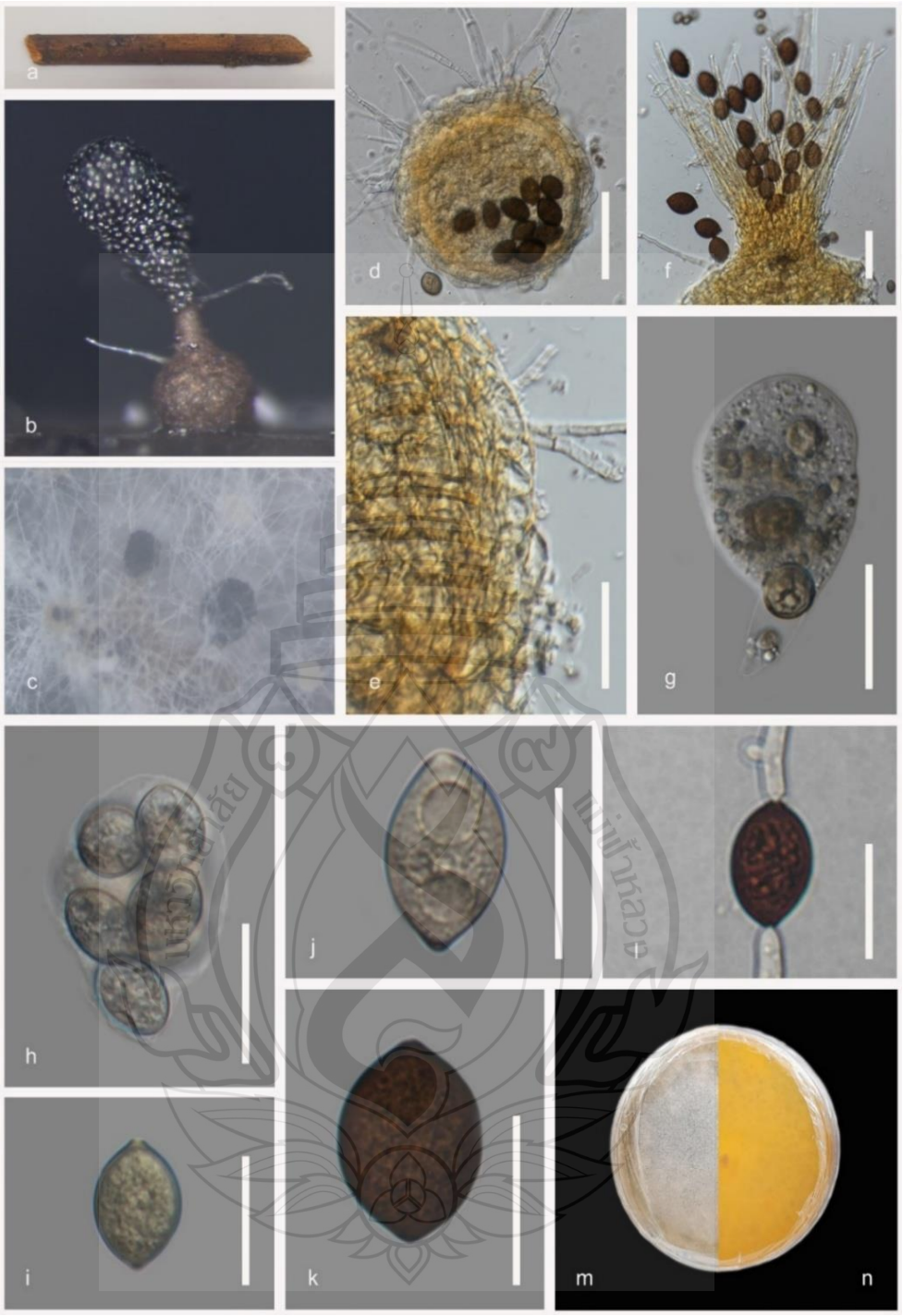

Note a *Typha* sp. host. b Ascomata on host with spore mass at ostiole opening. c Ascomata developed on the culture. d Squash mount of ascomata. e Peridium. f Hyphal neck of ascomata. g–h Asci. i–k Ascospores. l Germinated ascospore. m Culture on MEA above. n Reverse. Scale bars: d 50 µm, e 20 µm, f 100 µm, g 50 µm, h–I 25 µm, j–l 20 µm.

Figure 4.67 *Melanospora verrucispora* (MFLU 25-0470)

Melanospora verrucispora Takada, in Kobayasi et al., Bull. natn. Sci. Mus., Tokyo 16(3): 525 (1973)

Saprobic on dead, moist, decaying peduncle of aquatic macrophyte *Typha*, (Typhaceae), **Sexual morph**: fruiting structures appear superficial on the host surfaces. Light brown to amber in color. *Ascomata* 225–235 × 250–270 µm ($\bar{x}$ =228 × 260 µm, n = 5) globose to ovoid, gregarious, ostiolate, *ostiole setae* dark yellow at the base, tapering to hyaline tip and hold dark brown spore mass. *Peridium* 20–28 µm wide ($\bar{x}$ = 25 µm, n = 10), membranaceous, yellowish brown and compose from cells in *textura globulosa*. *Asci* 45–55 × 20–30µm ($\bar{x}$ = 48 × 25 µm, n = 10) 8-spored, unitunicate, clavate to obovate, fasciculate, apex rounded, broad, short pedicel, highly evanescent. *Ascospores* 20–25 × 15–20 µm ($\bar{x}$ = 23 × 16.5 µm, n = 30) irregularly biseriate or variably arranged, single celled, thick walled, hyaline at immature stage and turning brown at maturity, rough to labyrinthine on surface, irregularly verrucose, and apiculate. **Asexual morph**: Undetermined.

Culture characteristics: Ascospores germinating on MEA within 12 h. Germ tubes produced from both tip of the Ascospore. Colonies growing on MEA, reaching 20-25 mm in 3 weeks at 25°C. Mycelia superficial, dense, cottony, flat or effuse with fimbriate nature at the edge, from above pale white from center to the edge, from reverse orangey yellow at the center, fading towered the edge. Culture developed ascomata within 6 weeks and turned MEA color to yellowing amber color.

Material examined: Thailand, Chang Wat Prachuap Khiri Khan Province, Pran Buri District, Pran Buri wetland, on decaying stems of *Typha* sp. (Typhaceae), 23 December 2023, Tharindu Bhagya, TB45A (MFLU 25-0470), Chang Wat Prachuap Khiri Khan Province, Pran Buri District, Pran Buri River, 04 January 2025, Tharindu Bhagya, TB45B, Bamboo (Poaceae) (MFLU 25-0471).

GenBank numbers – MFLU 25-0471, ITS = PV764278

Distribution – Forest soil in Papua New Guinea (Takada, 1973), woodland soil in Singapore (Eberhardt et al., 2021), decaying submerged *Typha* sp. stem in freshwater coastal wetland, and Bamboo stem in a freshwater river, Thailand (This study).

Notes – New isolates obtained from *Typha* sp. and bamboo cluster as a sister group to *Melanospora verrucispora* strain NBRC 31375, with 81% ML and 0.90 BPP statistical support (Figure 4.66). Morphologically, our isolates resemble *M. verrucispora*

by possessing globose to ovoid, gregarious ascomata with pale yellow ostiolar setae that trap irregularly verrucose, apiculate ascospores (Figure 4.67) (Maharachchikumbura et al., 2016; Marin-Felix et al., 2018). Phylogenetically, *Melanospora* strain MFLU 25-0470 is similar to *M. verrucispora* strain NBRC 31375, showing 99.37% similarity in ITS and 98.69% in LSU regions, without gaps. Considering the available morphological and phylogenetic evidence, I recognize our isolates (MFLU 25-0470 and MFLU 25-0471) as *M. verrucispora*.

Fuscosporellales Jing Yang, Bhat & K.D. Hyde

Incertae sedis

Vanakripa Bhat, W.B. Kendr. & Nag Raj, Mycotaxon 49: 76 (1993)

Vanakripa is a polyphyletic genus introduced by Bhat, W.B. Kendr., and Nag Raj in 1993, with *V. gigaspora* as the type species (Goh et al., 2023; Liu et al., 2024). This genus is characterized by sporodochial, black conidiomata that develop micronematous, mononematous, erect, hyaline conidiophores, which are mainly simple and occasionally branched. The conidiogenous cells, originating from these conidiophores, are hyaline, smooth, pyriform, clavate to vermiform, ellipsoidal to broadly fusiform, and give rise to light brown to dark brown or black, 0–1-septate conidia that are clavate, pyriform, ovoid, ellipsoidal, or broadly fusiform (Castan˜eda-Ruiz et al., 2005; Goh et al., 2023; Liu et al., 2024).

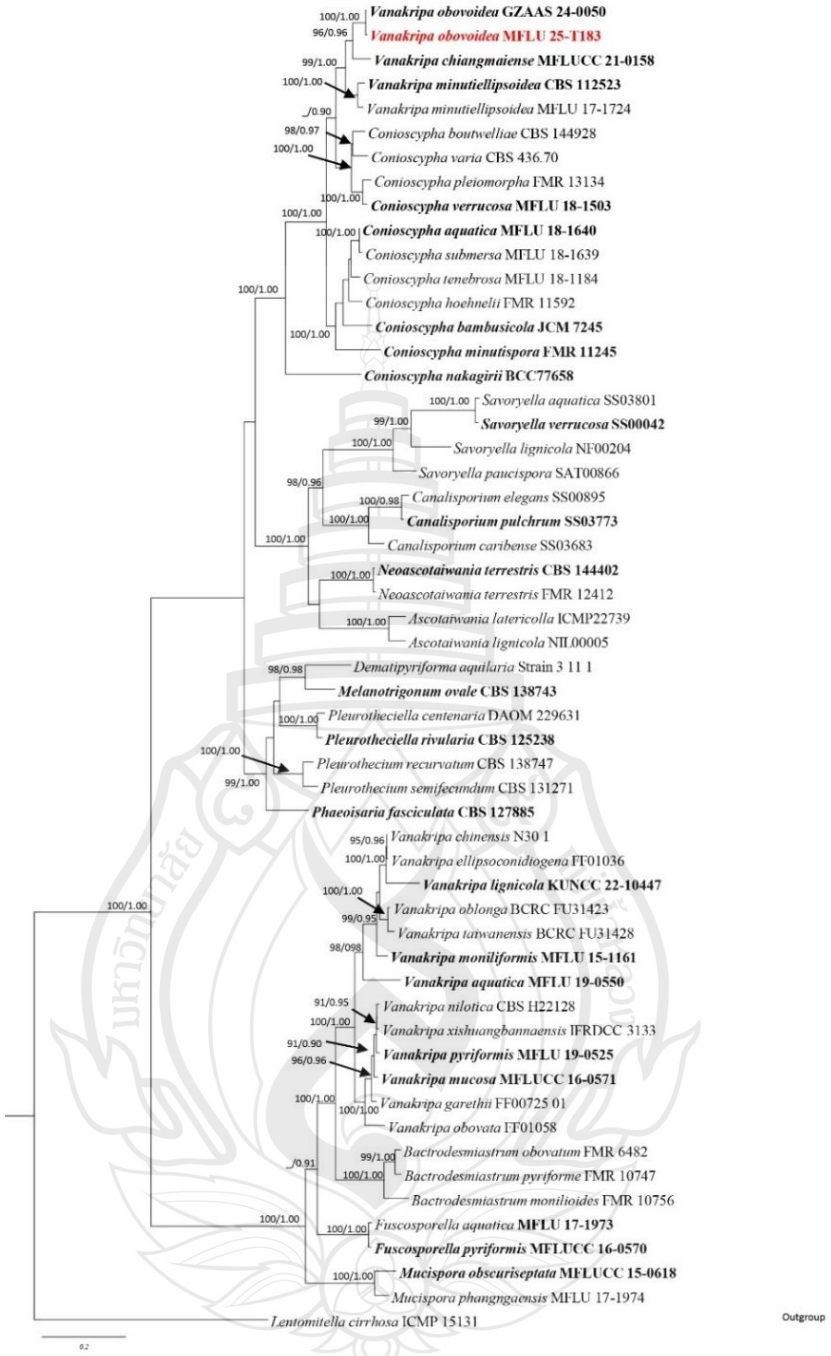

Note The data set comprises 3612 characters including gaps from of 55 fungal strains which were included in the analyses. Bootstrap support values for ML ≥ 90 % and Bayesian posterior probabilities (BPP) ≥ 0.9 are mentioned at the nodes. The tree was rooted to *Lentomitella cirrhosa* (ICMP 15131). Newly generated sequence is indicated in red and the type strains are in bold.

Figure 4.68 Phylogram generated from Maximum Likelihood (ML) analysis based on combined LSU, ITS, and SSU sequence.

Vanakripa obovoidea N.G. Liu, Jian K. Liu & K.D. Hyde, in Liu, Hyde, Sun, Bhat, Gareth Jones, Jumpathong, Lin, Lu, Yang, Liu, Liu & Liu, Fungal Diversity 129: 224 (2024)

Saprobic on dead, decaying stems of *Typha*, (Typhaceae), **Sexual morph:** Undetermined. **Asexual morph*:*** *Hyphomycetous*. *Colonies* on substrate are sporodochial, gregarious to fasciculate, punctate to maculiform or occasionally lenticulate, effuse, black to dark brown. *Mycelium*, immersed, hyaline, smooth branched, septate. *Conidiophores*, macronematous, mononematous, hyaline, smooth, thin-walled. *Conidiogenous cells* 20–45 × 6–18 µm ($\bar{x}$ = 32 × 9.5 µm, n = 20), monoblastic, holoblastic, hyaline, smooth, integrated, terminal, clavate, cylindrical to vermiform or pyriform. *Conidia* 15–24 × 8–14 µm ($\bar{x}$ = 18 × 10.5 µm, n = 20), solitary, brown to reddish brown or dark brown, smooth walled, ellipsoidal to obovoid or reniform, rounded at the apex with truncate base, brown to blackish brown, septate, aseptate, and found attached to conidiogenous cells.

Material examined: Thailand, Chang Wat Prachuap Khiri Khan Province, Pran Buri District, Pran Buri Wetland, on decaying stems of *Typha* sp. (Typhaceae), 05 January 2025, Tharindu Bhagya, TB183 (MFLU 25-0472).

GenBank numbers – MFLU 25-0472: ITS = PX518112

Distribution – Decaying wood in terrestrial habitat, Chiang Rai Thailand, decaying *Typha* sp. stem in freshwater wetland, Pran Buri, Thailand (This study).

Notes – Our isolate did not produce a culture, so direct DNA extraction was used to obtain genomic DNA from the colonies. The phylogenetic analysis showed that the MFLU 25-xxxxx clade is related to *V. obovoidea* (GZAAS 24-0050) with 100% ML and 0.98 BPP support (Figure 4.68). The new isolate resembles the morphology of *V. obovoidea* (GZAAS 24-0050), displaying cylindrical, clavate, or vermiform conidiogenous cells and brown to dark brown, ellipsoidal to obovoid conidia (Liu et al., 2024). Additionally, the new isolate (MFLU 25-0472) and *V. obovoidea* (GZAAS 24-0050) share the same height-to-width (H/W) ratio for conidiogenous cells (3.36 vs. 3.32) (Figure 4.69) (Liu et al., 2024). Based on the phylogenetic and morphological evidence, I identify the strain MFLU 25-0472 as a new strain of *V. obovoidea* from *Typha* sp. (Typhaceae).

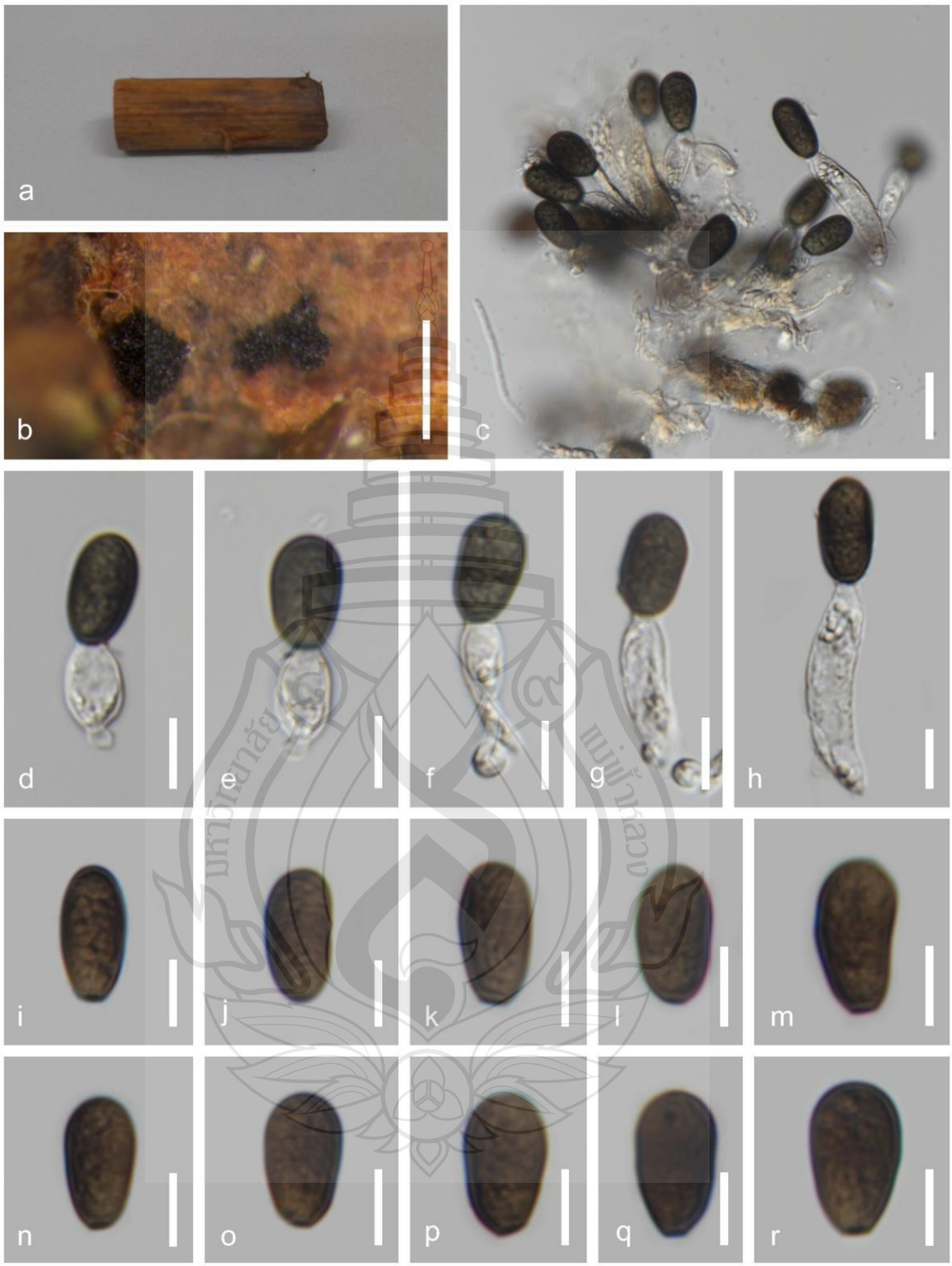

Note a *Typha* sp. host. b–c Sporodochial aggregation on the host. c Squash mount of conidia in sporodochial. d–h Developing conidia attached to conidiogenous cells. i–r Conidia. Scale bars: b 250 µm, c 50 µm, d–r)10 µm.

Figure 4.69 *Vanakripa obovoidea* (MFLU 25-0472)

Hypocreales Lindau, (1897)

Stachybotryaceae L. Lombard & Crous 283 (2014)

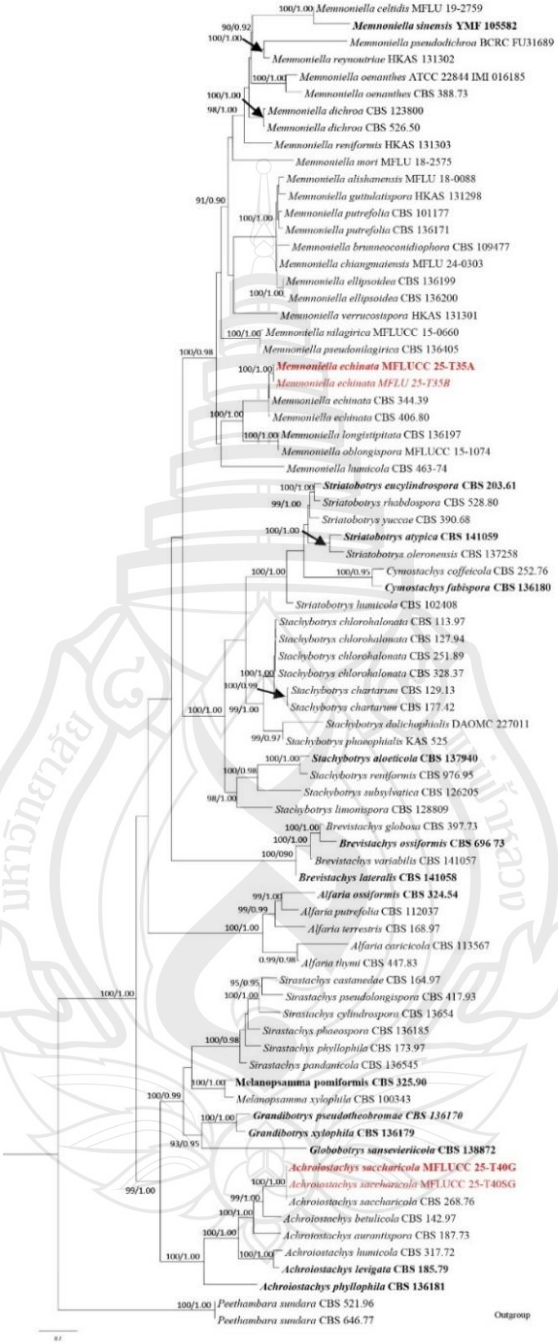

Note The data set contains 3346 characters including gaps from of 78 strains which were included in the analyses. Bootstrap support values for ML ≥ 90 % and Bayesian posterior probabilities (BPP) ≥ 0.9 are mentioned at the nodes.

Figure 4.70 Phylogenetic tree generated from Maximum Likelihood (ML) analysis based on combined cam, SSU, ITS, *rpb2, tef1-α*, and *tub2* sequence.

Achroiostachys L. Lombard & Crous, in Lombard, Houbraken, Decock, Samson, Meijer, Réblová, Groenewald & Crous, Persoonia 36: 172 (2016)

Achroiostachys is a monophyletic genus introduced by Lombard & Crous in 2016, with *A. humicola* serving as the type species. Members of this genus are characterized by macronematous, mononematous, erect, unbranched or occasionally branched conidiophores that develop phialidic, elongate ampulliform, and ventricose conidiogenous cells with raised apical openings. *Achroiostachys* produces ellipsoidal to limoniform or subglobose, hyaline, aseptate conidia. The genus is distributed from Canada and Europe to Asia, with most members being saprobic organisms (Lombard et al., 2016).

Achroiostachys saccharicola L. Lombard & Crous, in Lombard, Houbraken, Decock, Samson, Meijer, Réblová, Groenewald & Crous, Persoonia 36: 175 (2016)

Saprobic on decaying stem of submerged Greass, (Poaceae) **Sexual morph**: Undetermined. **Asexual morph**: *Hyphomycetous*. *Colonies* on host surface, orangey amber, irregular, caespitose to fasciculate. *Conidiophores* 80–140 × 3–5 µm ($\bar{x}$ = 125 × 4.0 µm, n = 20), macronematous, fasciculate, hyaline, simple, unbranched, with clusters of several ampulliform to inverted pyriform phialides at the apex. *Conidiogenous cells* 9–11 µm × 3–4 µm ($\bar{x}$ = 10 x 3.5 µm, n = 20), terminal, hyaline, smooth, ampulliform, ventricose to subcylindrical or obpyriform with raised apical opening. *Conidia* 6–9 × 3–4 µm ($\bar{x}$ = 8.0 × 3.5 µm, n = 30), acrogenous, aseptate, single celled, limoniform to subglobose or ellipsoidal to fusiform with slightly blunt ends, smooth-walled, hyaline with two guttules.

Culture characteristics: Conidia germinating on PDA within 12 h. Germ tubes produced from both ends of the conidia. Colonies growing on PDA, reaching 20–25 mm in 2 weeks at 25°C. Mycelia superficial, effuse to umbonate, dentate at edges, from above pale orangey white from center and the white to hyaline at the edge, from reverse light orangey white from center and the white to hyaline at the edge.

Material examined: Thailand, Chang Prachuap Khiri Khan Province, Pran Buri District, Pran Buri wetland, on decaying submerged stems of grass (Poaceae), 25 May 2023, Tharindu Bhagya, TB35A (MFLU 25-0473), Chang Prachuap Khiri Khan

Province, Pran Buri District, Pran Buri wetland, on decaying submerged stems of *Carex* sp. (Cyperaceae), 12 January 2025, Tharindu Bhagya, TB35B (MFLU 25-0474).

GenBank Numbers – MFLU 25-0473, ITS = PQ120587

Distribution – Dead twig, Narayani, Nepal (Lombard et al., 2016), dead decomposing, submerged stems of grass, (Poaceae) and *Carex*, (Cyperaceae), Thailand (This study).

Notes – The newly obtained isolates (MFLU 25-473 and MFLU 25-474) form a sister clade to *A. saccharicola* CBS 268.76 with 100% ML and 1.00 BPP support (Figure 4.70). MFLU 25-0473 and MFLU 25-474 exhibit the defining characteristics of the genus *Achroiostachys*, including hyaline, simple, unbranched conidiophores and ampulliform to ventricose conidiogenous cells that produce ellipsoidal, limoniform, globose, or subglobose conidia (Lombard et al., 2016). The obpyriform conidiogenous cells with raised apical openings, and relatively longer conidiophores than other members in the genus *Achroiostachys*, make strains were morphologically similar to *A. saccharicola* (Figure 4.71) (Lombard et al., 2016). Considering available evidences, I introduce two new host records of *A. saccharicola* from grass, (Poaceae), and *Carex* sp. (Cyperaceae) in wetland ecosystems of Thailand.

Note a Grass host material. b–c Conidiophores on the host surface. d–e Conidiophores and conidiogenous cells. f–h Phialides with conidia formation. i–l Conidia. m Germinated conidium. n Culture on PDA above. o reverse. Scale bars: c–d 80 µm, e 100 µm, f 20 µm, g 10 µm, h 15 µm, j–l 10 µm, m 50 µm.

Figure 4.71 *Achroiostachys saccharicola* (MFLU 25-0473)

Memnoniella Höhn., Zentralbl. Bakt. ParasitKde, Abt. II, 60, 16 (1923)

Memnoniella was proposed by Höhn in 1923 and typified by *M. aterrima*. The genus is characterized by macronematous, mononematous, septate conidiophores that produce monophialidic, terminal, determinate conidiogenous cells. *Memnoniella* develops globose or subglobose, olivaceous to dark brown or black, verrucose conidia. Members of this genus predominantly exhibit a saprobic lifestyle and have a worldwide, cosmopolitan distribution (Bao et al., 2023; Hyde et al., 2024).

Memnoniella echinata (Rivolta) Galloway Trans. Brit. Mycol. Soc. 18, 165 (1933)

Saprobic on decaying stem of *Typha*, (Typhaceae). **Sexual morph**: Undetermined. **Asexual morph**: *Hyphomycetous*. *Colonies* on the surface, caespitose to floccose, black to dark brown. *Conidiophores* 70–130 × 2–4 μm ($\bar{x}$ = 115 × 3.0 μm, n = 20), macronematous, mononematous, fasciculate, solitary or gregarious, erect, unbranched, 2-3 septate, smooth, thick walled, light brown at the base, dark brown to olivaceous brown towards the apex, end with clusters of several ampulliform, phialides at the apex. *Conidiogenous cells* 6–9 × 3–6 μm ($\bar{x}$ = 7.5 × 4.5 μm, n = 20), monophialidic, terminal, ampulliform, obovoid to obpyriform, smooth walled, pale brown to light yellow. *Conidia* 4–7 × 4–7 μm ($\bar{x}$ = 5.0 × 5.5 μm, n = 30) single celled, globose or subglobose with muricate to verrucose exterior, light brown when immature, olivaceous brown at maturity, arranged in columnar chains synchronously formed from the apex.

Culture characteristics: Conidia germinating on PDA within 24 h. Germ tubes produced from both sides of the conidia. Colonies growing on PDA, reaching 20–25 mm in 4 weeks at 25°C. Mycelia superficial, effuse to semi umbonate, dentate or erose at edges, from above pale pinkish white from center and the pale white to hyaline at the edge, from reverse light orangey white from center and the light yellow to hyaline at the edge. Culture change PDA color from light yellow to dark orangey yellow with time.

Material examined: Thailand, Chang Prachuap Khiri Khan Province, Pran Buri District, Pran Buri wetland, on decaying areal stems of *Typha* sp. (Typhaceae). 12 January 2023, Tharindu Bhagya, TB35AA (MFLU 25-0475), Chang Prachuap Khiri

Khan Province, Pran Buri District, Pran Buri wetland, on grass (Poaceae), 22 May 2023, Tharindu Bhagya, TB35BB (MFLU 25-476).

GenBank Numbers – MFLU 25-0475, ITS = PP463952

Distribution – Soil in Cleveland, Ohio (Jarvis et al., 1998), *Triticum saltivum*, Netherland (Lombard et al., 2016), leaf of *Macaranga tanarius* Taiwan, Chian (Tennakoon et al., 2021), submerged decaying wood in Chenghai Lake, China (Bao et al., 2023), dead leaf of Panda*nus* sp. (Hyde et al., 2024), decaying areal *Typha* sp. stem and decaying submerged grass, (Poaceae) stem in freshwater wetland, Thailand (This study).

Notes – The newly isolated strains (MFLU 25-0475 and MFLU 25-0476) form a clade with *M. echinata* (CBS 344.39 and CBS 406.80). This grouping is supported by 90% ML and 0.90 BPP statistics (Figure 4.70). The new isolates show key features of the genus *Memnoniella*, including macronematous, mononematous, septate conidiophores; monophialidic, terminal, determinate conidiogenous cells; and olivaceous to black, verrucose conidia (Figure 4.72) (Tennakoon et al., 2021; Bao et al., 2023; Hyde et al., 2024). MFLU 25-0475 and MFLU 25-0476 closely resemble *M. echinata* morphologically, characterized by 2–3-septate, smooth conidiophores bearing ampulliform phialides, conidiogenous cells, and globose to subglobose, verrucose conidia that develop in columnar phialidic chains (Tennakoon et al., 2021; Bao et al., 2023; Hyde et al., 2024). Based on available morphological and phylogenetic data, we identify these new isolates as strains of *M. echinata*. Therefore, I report two new host records of *M. echinata* from wetland-dweller *Typha* sp. (Typhaceae), and bog grass (Poaceae), in wetland ecosystems of Thailand.

Note a *Typha* sp. host. b–c Conidiophores on the host surface. d–f Conidiophores with strings of conidia. g Phialides with conidia formation. h Synchronously formed Phialoconidia. i–j Conidia. k Germinated conidium. l Culture on PDA above. m Reverse. Scale bars: d 120 µm, e 100 µm, f 50 µm, g 20 µm, h 50 µm, i–k 20 µm.

Figure 4.72 *Memnoniella echinata* (MFLU 25-0475)

Microascales Luttr. ex-Benny & R.K. Benj

Microascaceae **Luttr.** ex-Malloch

Scedosporium Sacc. ex Castell. & Chalm

Scedosporium was introduced by Sacc. ex Castell. & Chalm. in 1919 and is typified by *Scedosporium apiospermum*. This filamentous fungus has a worldwide distribution and is isolated from various habitats and substrates (Jayawardena et al., 2022; Wang et al., 2024). These habitats include soil, decaying plant material, sewage, herbivore dung, and polluted water caused by human activity (Abrantes et al., 2021). The sexual forms of *Scedosporium* are characterized by cleistothecial ascomata with a peridium made of cells in *textura epidermoidea*. The asci are unitunicate, clavate or spherical, and contain ellipsoidal to fusiform ascospores (Jayawardena et al., 2022; Wang et al., 2024). *Scedosporium* produces asexual morphs consisting of erect hyphal bundles bearing terminal, hyaline, cylindrical, densely packed conidiogenous cells. These cells produce hyaline, smooth, obovoidal to subcylindrical conidia (Jayawardena et al., 2022; Wang et al., 2024).

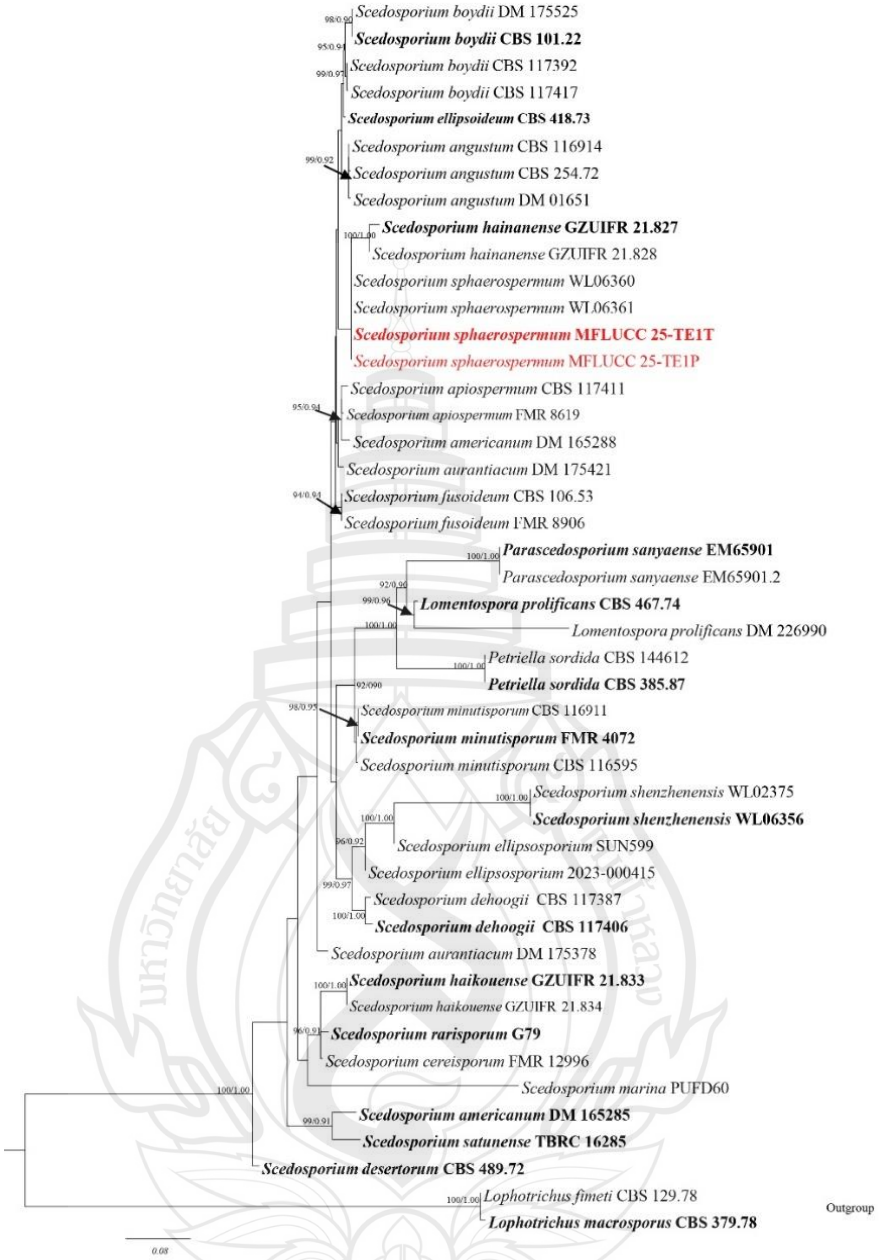

Note Bootstrap support values for ML ≥ 90 % and Bayesian posterior probabilities (BPP) ≥ 0.9 are mentioned at the nodes. The tree was rooted to *Lophotrichus fimeti* (CBS 129. 78), and *L. macrosporus* (CBS 379.78). Newly generated sequences are in red indicated in red and the type strains are in bold.

Figure 4.73 Phylogenetic tree generated from Maximum Likelihood (ML) analysis based on combined ITS, and *tub2* sequence from *Scedosporium* and related taxa, compressing 1286 characters including gaps from of 46 strains which were included in the analyses.

Scedosporium sphaerospermum M.M. Wang, W. Li & L. Cai, in Wang, Yang, Li, Zheng, Ma, Tu, Li & Cai, J. Fungi 10(1, no. 45): 19 (2024)

Saprobic on decaying submerged stem of genus *Thypa*, (Typhaceae). **Sexual morph**: Undetermined. **Asexual morph**: Hyphomycetous, synnematous. *Conidiophores* 139–142 × 6–8 μm ($\bar{x}$ = 140.6 × 7.2 μm, n = 20) macronematous, synnematous, dark brown, septate, simple or unbranched, with clusters of several cylindrical conidiogenous cells at the apex. *Conidiogenous cells* 6–9 μm × 2–3 μm ($\bar{x}$ = 8.6 x 7.3 μm, n = 10) hyaline, parallel, smooth-walled, cylindrical and taping towards the tip. *Conidia* 4–7 × 1.5–2.5 μm ($\bar{x}$ = 5.5 × 1.8 μm, n = 30), single celled, cylindrical with blunt ends, smooth-walled, hyaline.

Culture characteristics: Conidia germinating on MEA within 12 h. Germ tubes produced from both ends of the conidia. Colonies growing on MEA, reaching 20–25 mm in 2 weeks at 25°C. Mycelia superficial, effuse to umbonate, dentate at edges, from above pale white with ash brown patches from center and the white to hyaline at the edge, from reverse light orangey white from center and the white to hyaline at the edge.

Material examined: Thailand, Chang Wat Prachuap Khiri Khan Province, Pran Buri District, Pran Buri wetland, on decaying stems of *Typha* sp. (Typhaceae), 12 January 2024, Tharindu Bhagya, TE1T (MFLU 25-0477), Chang Wat Prachuap Khiri Khan Province, Pran Buri District, Pran Buri wetland, on Grass (Poaceae), 12 January 2024, Tharindu Bhagya, TE1P, (MFLU 25-0478).

GenBank numbers – MFLU 25-0477: ITS = PX518118

Distribution – Intertidal sediment, Shandong Province, Qingdao city, China (Wong et al., 2024), decaying submerged *Typha* sp. stem in freshwater coastal wetland, and Grass leaf blade, in freshwater river, Thailand (This study).

Notes – The new isolates in this study form a clade sister to *Scedosporium sphaerospermum* (WL06360 and WL06361), with 70% ML and 0.84 BPP statistical support (Figure 4.73). They conform to the general morphological characteristics of the genus *Scedosporium*, exhibiting synnemata, hyaline cylindrical conidiogenous cells, and hyaline subcylindrical conidia (Jayawardena et al., 2022; Wang et al., 2024). Phylogenetically, the new isolates (Figure 4.74) (MFLU 25-0477 and MFLU 25-0478) share 99.6% similarity in ITS sequences and 99.1% similarity in *tub2* with *S. sphaerospermum* strain WL06360. Furthermore, pairwise distance matrix value was

<0.01 between MFLU 25-0477, and *S. sphaerospermum* strain WL06360 (Gostinčar, 2020; Maharachchkumbura et al., 2021). Considering the available morphological and phylogenetic evidence, I identify these isolates as new strains of *S. sphaerospermum* and report two new host records from *Typha* sp. and grass from freshwater coastal wetlands in Thailand.

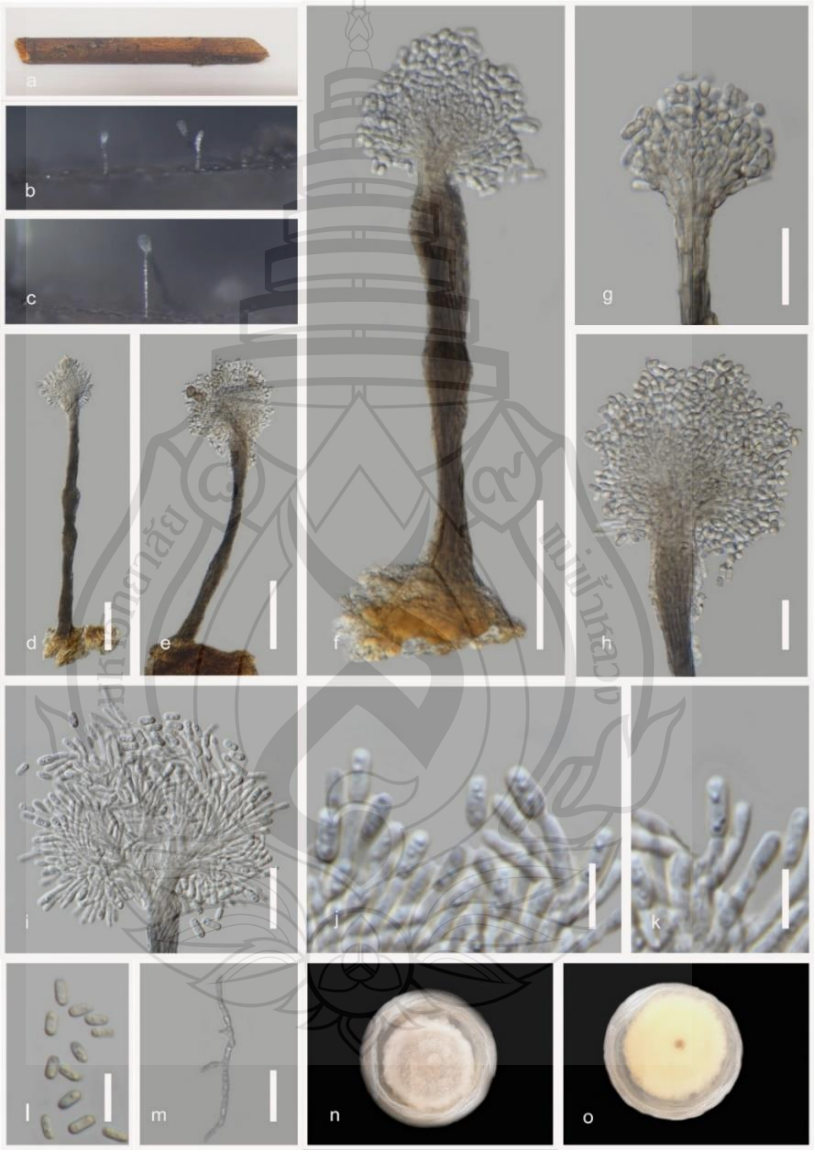

Note a *Typha* sp. host material. b–c Conidiophores. d–f Conidiogenous cells. g–i conidiophore head. j–k Conidia formation. m Conidia. n Germinated conidium. o Culture on MEA above. p Reverse. Scale bars: d 80 µm, e–f 50 µm, g–i 20 µm, j–k 5 µm, h 15 µm, l–m 10 µm, n 15 µm.

Figure 4.74 *Scedosporium sphaerospermum* (MFLU 25-0477)

Triadelphiaceae Y.Z. Lu, J.K. Liu, Z.L. Luo & K.D. Hyde

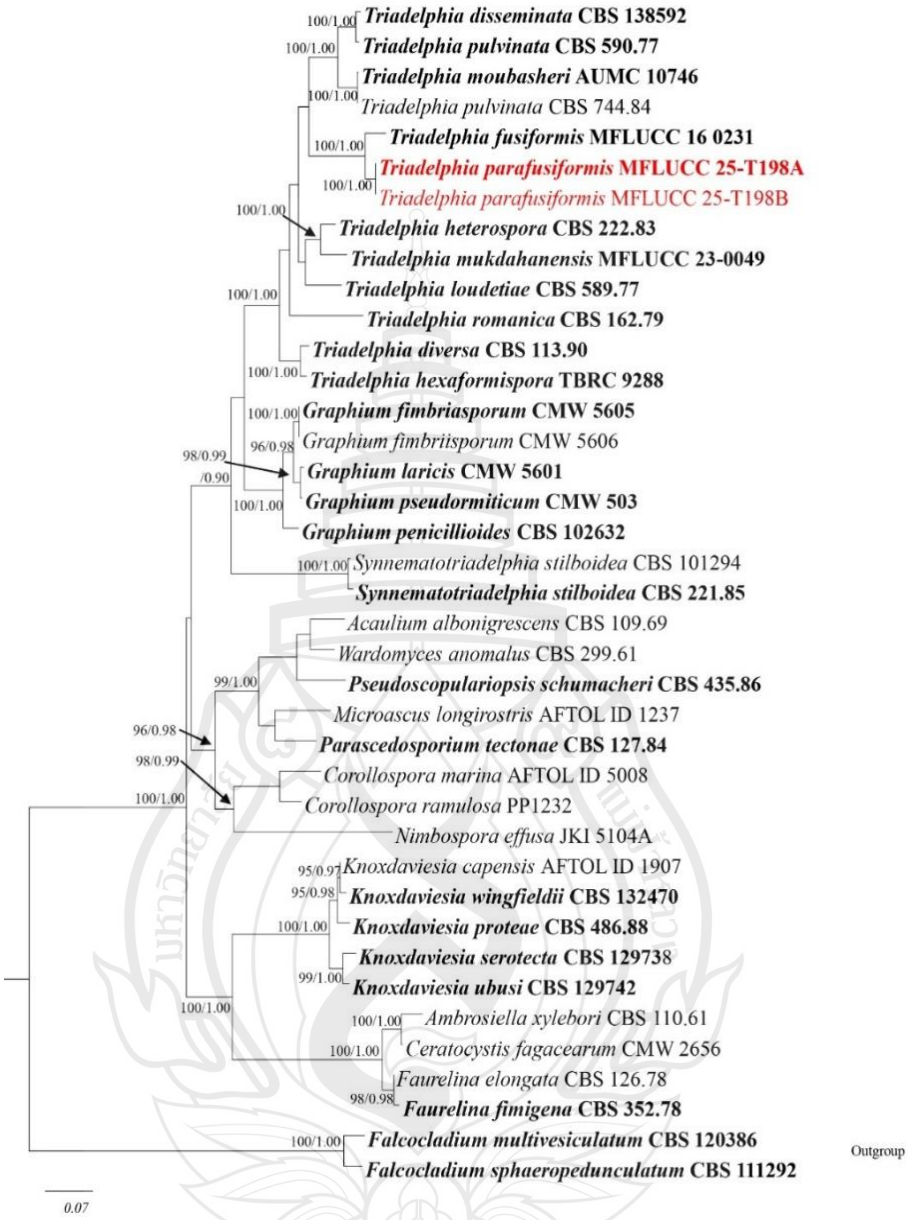

Note The data set comprises 3728 characters including gaps from of 39 strains which were included in the analyses. Bootstrap support values for ML ≥ 90 % and Bayesian posterior probabilities (BPP) ≥ 0.9 are mentioned at the nodes. The tree was rooted to *Falcocladium multivesiculatum* CBS 120386 and *F. sphaeropedunculatum* CBS 111292. Newly generated sequences are indicated in red and the type strains are in bold.

Figure 4.75 Phylogram generated from Maximum Likelihood (ML) analysis based on combined ITS, LSU, SSU and *rpb2* sequence.

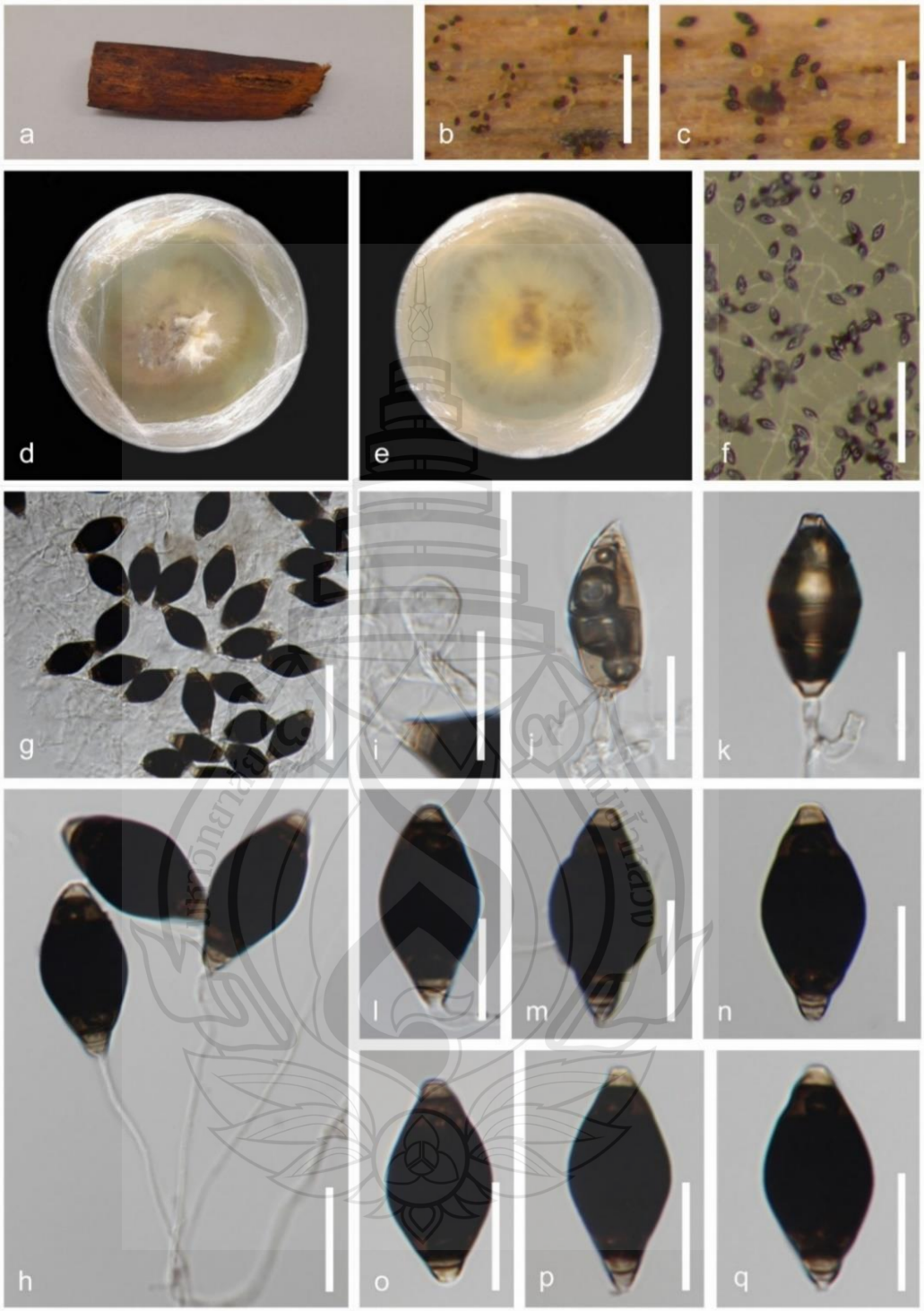

Note a Typha sp. host. b–c Conidia aggregation on the host. d Culture on MEA above. e Reverse. f Conidia aggregation in vitro. g–h Squash mount of conidia developed in vitro. i–k Conidia development with conidiogenous cells. l–m Conidia with depression at hilum. n–q Conidia. Scale bars: b, c & f 250 µm, g 50 µm, h–q 20 µm.

Figure 4.76 *Triadelphia parafusiformis* (MFLU 25-479, holotype)

Triadelphia Shearer & J.L. Crane

Triadelphia was introduced by Shearer & J.L. Crane from the USA and typified by *Triadelphia heterospora*. Members of this genus have been isolated from both aquatic and terrestrial environments. *Triadelphia* is a pleomorphic and synasexual genus, characterized by holoblastic, unilocular conidiogenous cells that give rise to individual, pigmented conidia (Chuaseeharonnachai et al., 2020; Mapook et al., 2023).

Triadelphia parafusiformis Bhagya, Phukham, E.B.G. Jones & K.D. Hyde, sp. nov

Index Fungorum number: IF; Facesoffungi number: FoF 18910

Etymology – Reflecting the resemblance to the most closely related species.

Holotype – MFLU 25-0479

Saprobic on submerged decayed stem of genus *Thypha,* (Typhaceae), in tropical wetland habitats. **Sexual morph**: Undetermined. **Asexual morph**: Hyphomycetous. *Colonies* effuse on the host, sporodochial, loosely aggregated, dry, brown or dark brown collections of conidia. *Mycelium* 1.5–2.0 μm ($\bar{x}$ = 1.8 μm, n = 20), partially immersed, smooth, septate, branched, hyaline. *Conidiophores* are indistinct, micronematous. *Conidiogenous cells* 3–4 × 1.5–2.5 μm ($\bar{x}$ = 3.5 × 2.0 μm, n = 10), indistinct hyaline and unicellular, holoblastic when present. *Conidia* 40–50 × 16–22 μm ($\bar{x}$ = 44 × 18 μm, n = 30), 5-6 distoseptate, oblong ellipsoidal or doliform, light or dark yellowish brown when immature, center cells expand, turns dark brown to opaque black at maturity, terminal cells shrink, bear lunate or falcate depression at hilum, turn olive brown to light brown or hyaline at maturity.

Culture characteristics: Conidia germinating on MEA within 72 h. Germ tube erupted from the base of the conidia. Colonies growing on MEA, reaching 20-25 mm in 6 weeks at 25°C. Mycelia superficial, cottony, flat or effuse with complete at the edge, from above off-white to hyaline from center and produces distinctive white cottony mycelium agitations at the center, from reverse light yellowish white at the center to hyaline edge. Culture sporulates after 4 weeks in drake conditions and make ash color conidia aggregations close to the edge, changing the culture color from off white to ash.

Material examined: Thailand, Chang Prachuap Khiri Khan Province, Pran Buri District, Pran Buri wetland, on decaying submerged stems of *Typha* sp. (Typhaceae). 12 January 2023, Tharindu Bhagya, TB198A (MFLU 25-479, holotype), Chang Prachuap

Khiri Khan Province, Pran Buri District, Pran Buri River, 15 January 2023, Tharindu Bhagya, Bamboo (Poaceae), TB198B (MFLU 25-480).

GenBank Numbers – MFLU 25-0479, ITS = PX062290, LSU = PX062277

Distribution – Decaying *Typha* sp. stem and decaying Bamboo stem in freshwater wetland, Thailand.

Notes – The new isolate *T. parafusiformis* (MFLU 25-479) forms a sister clade to the type strain of *T. fusiformis* MFLUCC 16-0231 with 100% ML and 1.00 BPP support (Figure 4.45). *T. parafusiformis* MFLU 25-479 aligns with the general description of *Triadelphia*, possessing sporodochial aggregations with dematiaceous and sympodial conidia (Mapook et al., 2023). *T. parafusiformis* (MFLU 25-0479) is similar to *T. fusiformis* MFLUCC 16-0231 in producing only one type of conidia with 5–6 septa (Figure 4.76) (Lu et al., 2018). However, the type strain MFLU 25-0479 differs by 10.14% in ITS sequences and 4.11% in LSU sequences, with gaps. Morphologically, *T. parafusiformis* (MFLU 25-0479) is distinguishable from *T. fusiformis* MFLUCC 16-0231 by producing darker, more opaque conidia with lunate or falcate depressions at the hilum. Considering the evidences, I propose *T. parafusiformis* (MFLU 25-0479) as a new species in the genus *Triadelphia*, isolated from the wetland-dwelling plant *Typha* sp. (Typhaceae).

Incertae sedis

Distoseptisporales Z.L. Luo, K.D. Hyde & H.Y. Su

Distoseptisporaceae K.D. Hyde & McKenzie

Distoseptispora K.D. Hyde, McKenzie & Maharachch., Fungal Diversity 80: 402 (2016)

The genus *Distoseptispora* was first introduced in 2016 by Su et al. (2016) and is typified by *Distoseptispora fluminicola*. Members of this genus are saprobic organisms, mainly found in aquatic environments. Most *Distoseptispora* species reproduce asexually, and Yang et al. (2021) described the first sexual species of the genus. *Distoseptispora* is characterized by macronematous, mononematous, solitary, or fasciculate conidiophores that bear blastic, terminal, mostly cylindrical conidiogenous cells. These conidiogenous cells produce obclavate, ellipsoidal, obovoid, or fusiform, euseptate, distoseptate, or rarely muriform conidia (Zhang et al., 2022; Karimi et al., 2024; Shean et al., 2024).

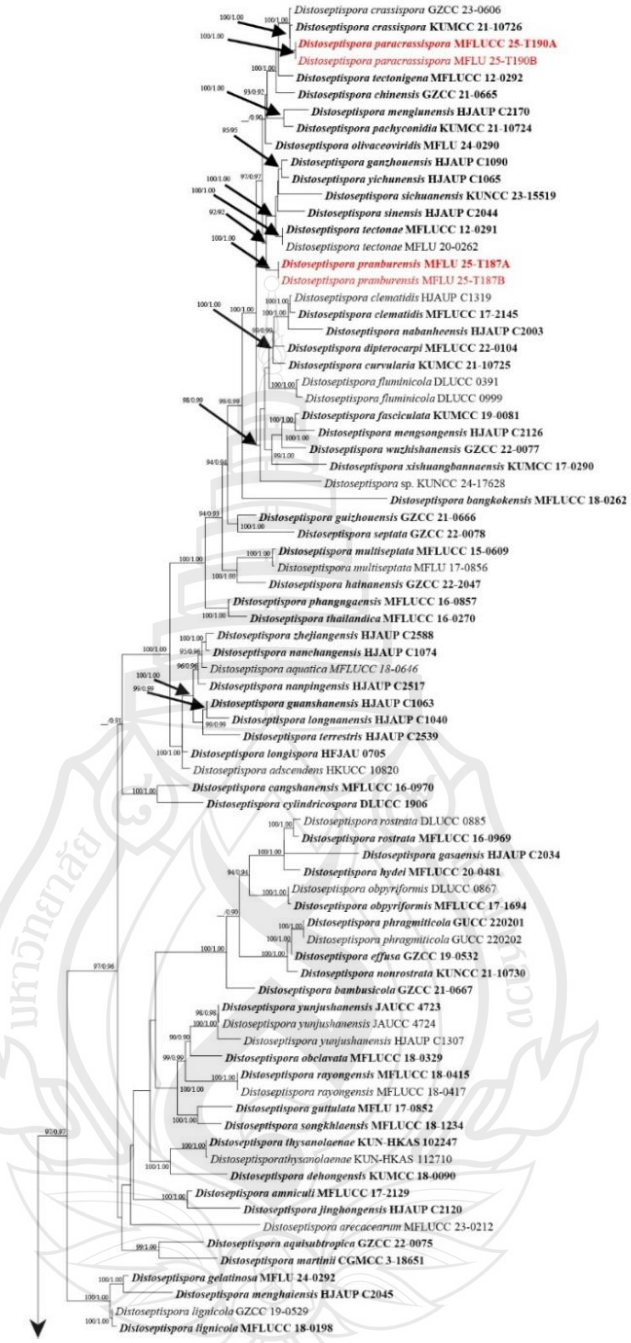

Note Bootstrap support values for ML ≥ 90 % and Bayesian posterior probabilities (BPP) ≥ 0.9 are mentioned at the nodes. The tree was rooted to *Aquapteridospora aquatic* (MFLUCC 17-2371) and *A. fusiformis* (MFLU 18-1601) combination. Newly generated sequences are indicated in red and the type strains are in bold.

Figure 4.77 Phylogram generated from Maximum Likelihood (ML) analysis based on combined ITS, LSU, *rpb2* and *tef1-α* sequence data of 125 strains, which comprise 3888 characters including gaps, are included in the analyses.

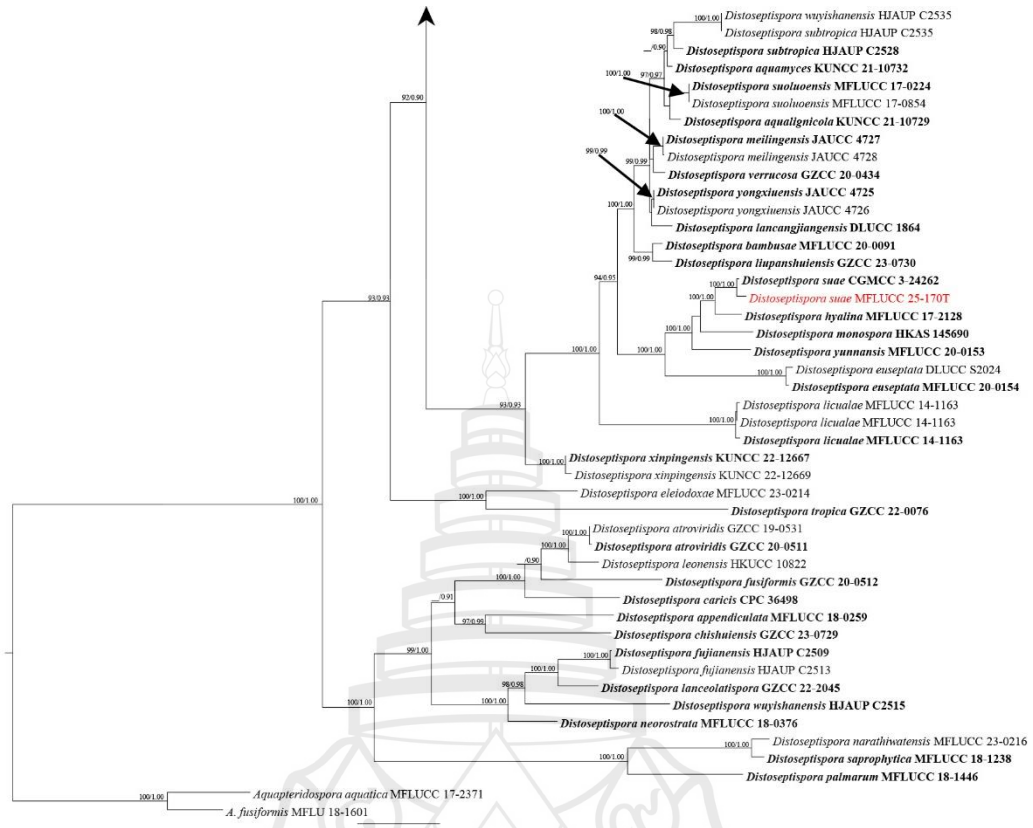

Figure 4.77 (continued)

Distoseptispora paracrassispora, Bhagya, Phukham E.B.G. Jones & K.D. Hyde, sp. nov

Index Fungorum number: IF; Facesoffungi number: FoF 18911

Etymology – Reflecting the phylogenetic affinity towered *D. crassispora.*

Holotype – MFLU 25-0499

Saprobic on dead, decaying stems of *Typha*, (Typhaceae), **Sexual morph:** Undetermined. **Asexual morph:** *Hyphomycetous*. *Colonies* effuse, erect, brown to olivaceous or black, solitary or gregariously fasciculate on host. *Mycelium* 2.5–3.5 µm ($\bar{x}$ = 2.5 µm, n = 10), superficial, occasionally immerse, septate, branched, thick-walled, dark brown to pale brown. *Conidiophores*, 16–25 × 3.5–5.0 µm ($\bar{x}$ = 22 × 4.5 µm, n = 10), macronematous, mononematous, erect, straight to slightly flexuous, smooth, thick-walled, dark brown or black, single to seriated or fasciculate, 2–5-septate, unbranched. *Conidiogenous cells* 10–15 × 3.5–5.5 µm ($\bar{x}$ = 13 × 4.0 µm, n = 10), monoblastic, terminal, determinate, cylindrical with wider apex or amphora-shaped, smooth, light brown to dark brown. *Conidia* 110–290 × 8–15 (at wider base) µm, 3–5 (at narrow apex) ($\bar{x}$ = 260 × 11.5

(base) µm, 3.5 (apex) µm, n = 20), acrogenous, solitary or aggregated, 15–38-septate, smooth, thick walled, brown to olivaceous brown, sub hyaline at the apexes, cylindrical or obclavate, elongated, straight or slightly curved with flexuous towards the apex, truncate at the base, rounded to pointed at the apex.

Culture characteristics: Conidia germinate on MEA within 24 h. Germ tubes produced from side of the conidium. Colonies growing on MEA, reaching 40 mm in 4 weeks at 25°C. Mycelia superficial, dense, effuse to umbonate, with complete edges, from above black at center and olivaceous brown to black to the edge, from reverse dark brown to black at the center and light brown to ash at the edge.

Material examined: Thailand, Chang Wat Prachuap Khiri Khan Province, Pran Buri District, Sam Roi Yot wetland, on decaying stems of *Typha* sp. (Typhaceae), 06 April 2024, Tharindu Bhagya, TB190A (MFLU 25-0499, holotype), Chang Wat Prachuap Khiri Khan Province, Pran Buri District, Sam Roi Yot wetland, decaying peduncle of Nymphaeaceae**,** 06 April 2024, Tharindu Bhagya TB190B (MFLU 25-0500).

GenBank numbers – MFLU 25-0499, ITS = PV263323

Distribution – Decaying stem of *Typha* sp. (Typhaceae), and Nymphaeaceae peduncle in freshwater wetland, Thailand.

Notes – *Distoseptispora paracrassispora* (MFLU 25-0499) forms a sister clade to *D. crassispora* (HKAS 122181 and GZCC 23-0606) with 100% ML and 1.00 BPP support (Figure 4.77). *Distoseptispora* (MFLU 25-0499) differs from *D. crassispora* (HKAS 122181) based on molecular sequences data by 2.19% (12/547) in ITS, 4.83% (46/984) in *rpb2*, and 2.73% (28/1023) in *tef1-α*, including gaps. The new isolate is morphologically distinguishable from strain HKAS 122181 and other related taxa by having cylindrical, by processing wider apex or amphora-shaped conidiogenous cells, longer (110–290 µm vs. 95–197 µm), and narrower conidia (Figure 4.48) (8–15 µm vs. 13–24 µm) (Zhang et al., 2022). Based on the available morphological and phylogenetic evidence, I introduce *D. paracrassispora* (MFLU 25-0499) as a new species from freshwater wetlands in Thailand.

Note a *Typha* sp. host. b–c Conidiophores on the host surface with conidia aggregation. d–e Conidiophores with developing conidia. f Distoseptation of developing conidia. g–h Immature conidia. j–l Mature conidia with flexuous nature. Scale bars: b–c 250 µm, d–k 20 µm.

Figure 4.78 *Distoseptispora paracrassispora* (MFLU 25-0499, holotype)

Distoseptispora pranburensis Bhagya, Phukhams E.B.G. Jones & K.D. Hyde, sp. nov. Figure xx

Index Fungorum number: IF; Facesoffungi number: FoF 18912

Etymology – Name reflects the forest park, Khao Sam Roi Yot where the species was collected.

Holotype – MFLU 25-0497

Saprobic on dead, decaying stems of *Typha*, (Typhaceae), **Sexual morph:** Undetermined. **Asexual morph:** *Hyphomycetous*. *Colonies* are superficial, effuse, gregarious, hairy, erect, dark brown to black. *Mycelium* 2.5–4.0 µm ($\bar{x}$ = 3.5 µm, n = 10), superficial occasionally immerse, septate, branched, dark brown, thick-walled. *Conidiophores* 5–9 × 2.5–6.5 µm ($\bar{x}$ = 6.5 × 3.5 µm, n = 10), macronematous, mononematous, erect, straight, or slightly flexuous, dark brown to black, relatively short, 2–3-septate, unbranched, single, or fasciculate in groups, thick-walled with robust, bulbous base. *Conidiogenous cells* 2.5–5.0 × 2.5–4.5 µm ($\bar{x}$ = 4.5 × 3.0 µm, n = 10), monoblastic, terminal, determinate, cylindrical, light brown to dark brown. *Conidia* 60–210 × 9.5–14.5 µm (at wider base) µm, 4–7 (at narrow apex) ($\bar{x}$ = 260 × 12.5 (base) µm, 5.5 (apex) µm, n = 20), solitary, 12–40-distoseptate, smooth, thick walled, cylindrical or obclavate, elongated, straight or slightly curved, truncate at the base, rounded at the apex, olivaceous when young, brown to reddish brown when mature, and scars or disjunction present, and bear enteroblastic percurrent extensions of conidia.

Culture characteristics: Conidia germinating on MEA within 48 h. Germ tubes produced from ends of the conidium. Colonies growing on MEA, reaching 20 mm in 5 weeks at 25°C. Mycelia superficial, dense, effuse to umbonate, with complete edges, from above white floccos mycelium at center and olivaceous brown to ash to the edge, from reverse dark yellowish brown at the center leading to black or olivaceous brown ring next to the edge and light yellowish brown at the edge.

Material examined: Thailand, Chang Wat Prachuap Khiri Khan Province, Pran Buri District, Pran Buri Wetland, on decaying stems of *Typha* sp. (Typhaceae), 06 April 2024, Tharindu Bhagya, TB187A (MFLU 25-0497, holotype), *ibid.*, TB187B (MFLU 25-0498).

GenBank numbers – MFLU 25-0497, ITS = PP463952

Distribution – Decaying submerged *Typha* sp. stem, and peduncle in freshwater wetland, Thailand.

Notes – *Distoseptispora pranburensis* (MFLU 25-0497) forms an independent clade and clusters with D. *ganzhouensis* (HJAUP C1090), *D. yichunensis* (HJAUP C1065), *D. sinensis* (HJAUP C2044), *D. tectonae* (MFLUCC 12-0291 and MFLU 20-0262), and *D. sichuanensis* (KUNCC 23-15519). The segregation is statistically supported by 98% ML and 0.95 BPP values, indicating that the newly isolated strain is phylogenetically distinct from the sister taxa (Figure 4.77). Morphologically, the newly isolated strain is most similar to *D. yichunensis* (HJAUP C1065) and *D. tectonae* (MFLUCC 12-0291) by comprising brown to reddish brown when mature conidia with enteroblastic percurrent extensions (Hu et al., 2023; Chen et al., 2024). In contrast, the conidiophore morphology distinguishes *D. pranburensis* (MFLU 25-0497) from *D. yichunensis* (HJAUP C1065), *D. tectonae* (MFLUCC 12-0291), and other related taxa, as new isolate (MFLU 25-0497) characterized by shorter conidiophores (5–9 µm vs. 35–80 µm in *D. tectonae* and 17.9–52.7 µm in *D. yichunensis*) with a bulbous or expanded base (Figure 4.49) (Hu et al., 2023; Chen et al., 2024). Considering the available morphological and phylogenetic evidence, I identify the new strain MFLU 25-0497 as a novel species in genus *Distoseptispora* isolated from *Typha* sp. in freshwater wetlands of Thailand.

Note a *Typha* sp. host. b Conidiophores on the host surface with conidia. c Conidiophores. d–f Conidiophores with attached conidia. e Immature conidium. f Conidium with enteroblastic percurrent extensions. h–i Mature conidia. j culture on MEA above. k Reverse. Scale bars: b 250 µm, c–i 10 µm.

Figure 4.79 *Distoseptispora pranburensis* (MFLU 25-0497, holotype)

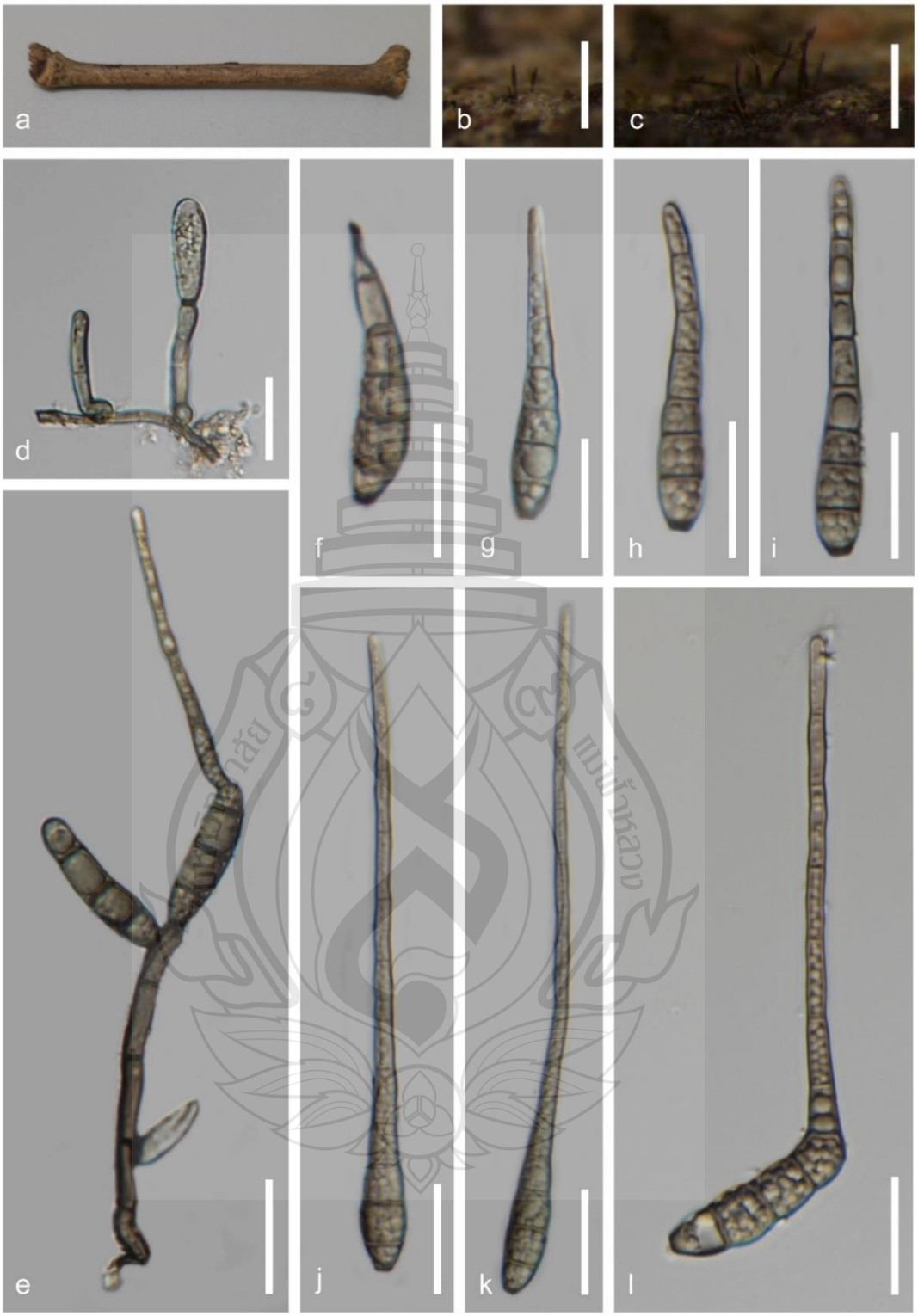

Note a Bamboo host material. b–c Conidiophores on the host surface with conidia. d–e Conidiophores with developing conidia. f–i Immature conidia. j–l Mature conidia. Scale bars: b–c 250 µm, d–l 20 µm.

Figure 4.80 *Distoseptispora suae* (MFLU 25-0501)

Distoseptispora suae H.W. Shen & Z.L. Luo, in Shen, Bao, Boonmee, Lu, Su, Li & Luo, MycoKeys 102: 16 (2024)

Saprobic on dead, decaying stems of Bamboo, Poaceae, **Sexual morph:** Undetermined. **Asexual morph:** *Hyphomycetous*. *Colonies* effuse, erect, brown to olivaceous, solitary or subfasciculate on host. *Mycelium* 2.0–3.5 µm ($\bar{x}$ = 2.5 µm, n = 10), superficial or immerse, septate, branched, dark brown to pale brown, thick-walled. *Conidiophores*, 20–70 × 3.5–5.5 µm ($\bar{x}$ = 28 × 4.0 µm, n = 10), macronematous, mononematous, erect, straight to slightly flexuous with geniculate base, smooth, thick walled, olivaceous to dark brown or black, single or gregariously fasciculate, relatively short or occasionally longer, 2–6-septate, unbranched. *Conidiogenous cells* 10–15 × 3.5–5.5 µm ($\bar{x}$ = 13 × 4.0 µm, n = 10), monoblastic, terminal, determinate, cylindrical, light brown to olivaceous brown. *Conidia* 105–125 × 6–9 µm ($\bar{x}$ = 117 × 7.5 µm, n = 20), acrogenous or pleurogenous, solitary or caespitose, 3–15-septate, smooth, thick walled, olivaceous to light brown to dark brown, cylindrical or obclavate, elongated, straight or slightly curved with a tight bend at 4th to 6th septate, truncate at the base or rostrate, rounded to pointed at the apex.

Culture characteristics: Conidia germinating on MEA within 48 h. Germ tubes produced from side of the conidium. Colonies growing on MEA, reaching 40 mm in 6 weeks at 25°C. Mycelia superficial, dense, effuse to umbonate, with erose edges, from above dark brown to black at center and olivaceous brown to the edge, from reverse dark brown to black at the center and light brown to olivaceous at the edge.

Material examined: Thailand, Chang Wat Prachuap Khiri Khan Province, Pran Buri District, Pran Buri river, on decaying stems of Bamboo (Poaceae), 06 April 2024, Tharindu Bhagya, TB170A (MFLU 25-0501).

GenBank numbers – MFLU 25-0501: ITS = PX518122

Distribution – Submerged decaying branches in a freshwater stream, Yunnan Province China (Shean et al., 2024) and submerged decaying Bamboo stem in freshwater river wetland, Thailand (This study).

Notes – The new isolate clades with the *D. suae* type strain CGMCC 3.24262, with 100% ML and 1.00 BPP support (Figure 4.77). The new strain isolated in the study (MFLU 25-0501) morphologically is similar to *D. suae* (CGMCC 3.24262), showcasing 3–15-septate conidia that truncate or rostrate at the base and tightly bending

at the 4th to 6th septa (Figure 4.80) (Shean et al., 2024). Phylogenetically the pairwise comparison between strain MFLU 25-0501 and strain CGMCC 3.24262 showcased 99.58% similarity in ITS, and 99.35% similarity in *tef1-α* sequences. Considering the available evidence, I recognize MFLU 25-0501 as a new strain of *D. suae*, isolated from a submerged decaying Bamboo (Poaceae) stem, and report the findings as a new geographical record from freshwater coastal wetlands in Thailand.

Pleurotheciales Réblová & Seifert

Pleurotheciaceae Réblová & Seifert

Phaeoisaria Höhn., Sber. Akad. Wiss. Wien, Math. -naturw. Kl., Abt. 1 118: 330 (1909)

Phaeoisaria belongs to the family *Pleurotheciaceae*, which was introduced by Höhnel in 1909, and is typified by *Phaeoisaria bambusae*. Members of this genus are predominantly saprobic, hyaline-spored hyphomycetes with a cosmopolitan distribution. *Phaeoisaria* is characterized by erect synnemata that produce parallelly arranged, polyblastic, sympodially developing, denticulate conidiogenous cells, which give rise to hyaline, aseptate, ellipsoidal, fusiform to cylindrical, or obovoidal conidia (Luo et al., 2019; Yang et al., 2023; Wang et al., 2024; Xu et al., 2025).

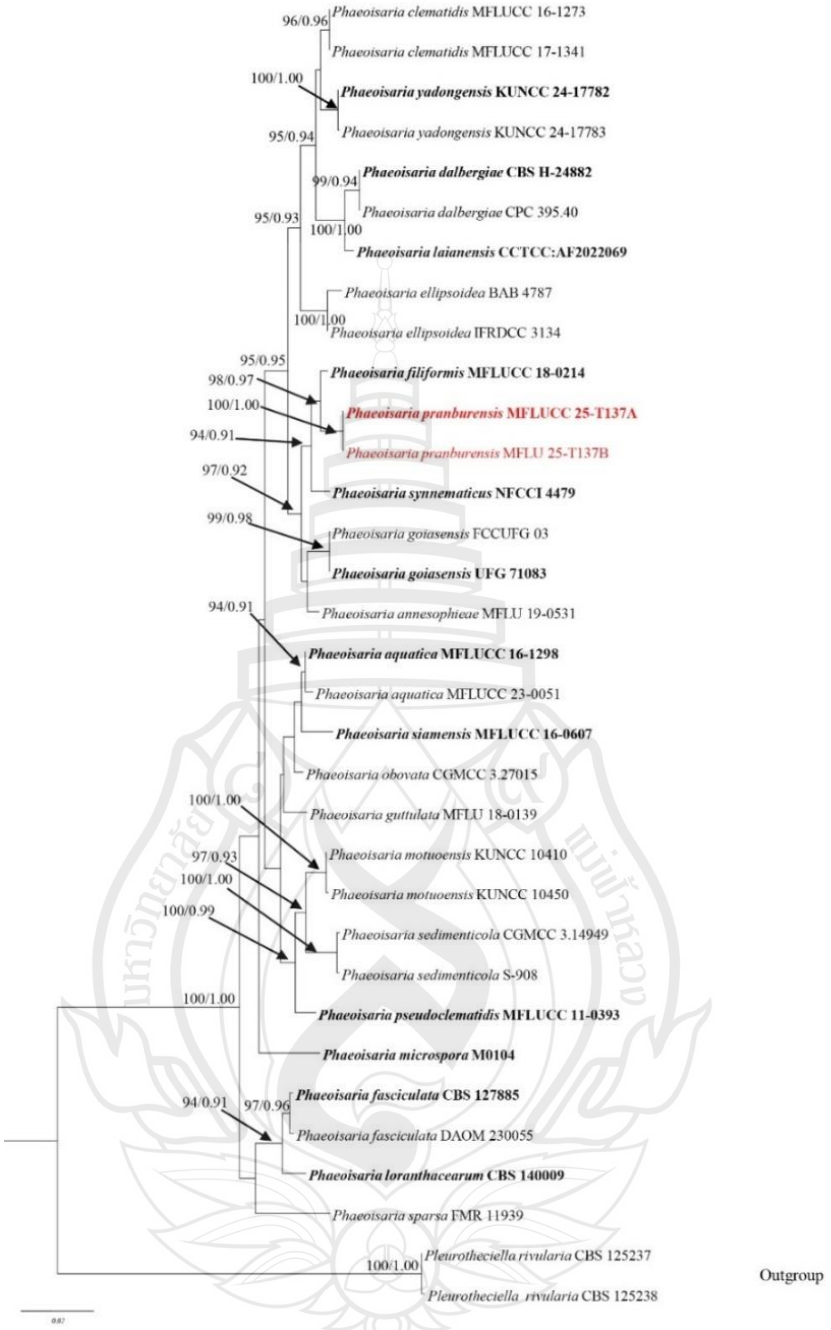

Note Bootstrap support values for ML ≥ 90 % and Bayesian posterior probabilities (BPP) ≥ 0.9 are mentioned at the nodes. The tree was rooted the combination of *Pleurotheciella rivularia* (CBS 125237 and CBS 125238). Newly generated sequences are in red and the type strains are in bold.

Figure 4.81 Phylogram generated from Maximum Likelihood (ML) analysis based on combined ITS, LSU, and SSU, sequence comprising 3446 characters including gaps from of 34 strains which were included in the analyses.

Phaeoisaria pranburensis Bhagya, Phukham E.B.G. Jones & K.D. Hyde, sp. nov

Index Fungorum number: IF; Facesoffungi number: FoF 18913

Etymology – Name reflects the wetland, Parn Buri, where the fungus was collected.

Holotype – MFLU 25-0481

Saprobic on dead, decaying stems of Bamboo, (Poaceae), **Sexual morph:** Undetermined. **Asexual morph:** *Hyphomycetous*, gregariose or gregariosely fasciculate on host. *Synnemata* 235–450 × 15–32 μm ($\bar{x}$ = 360 × 24 μm, n = 10), erect, rigid, dark brown to black, smooth, septate, composed of compactly and parallelly arranged conidiophores, flared conidiogenous cells at the apexes. *Conidiophores* 1.5–3.5 μm ($\bar{x}$ = 2.8 μm, n = 20), macronematous, synnematous, smooth, brown to black, straight, simple or occasionally branched, with hyaline to sub-hyaline apexes. *Conidiogenous cells* 11–17 × 1.5–4.5 μm ($\bar{x}$ = 13.5 × 2.5 μm, n = 20), cylindrical, subcylindrical, ampulliform to pyriform, clavate, or lageniform, urceolate, hyaline to sub-hyaline or light brown, polyblastic, smooth, terminal, discrete, recurved, sympodial, denticulate with 4–6 denticulate conidiogenous loci. *Conidia* 3.5–6.5 × 1–2.5 μm ($\bar{x}$ = 4.5 × 1.8 μm, n = 20), ellipsoidal to obovoid, hyaline, smooth, aseptate, obpyriform with rounded apex and with slightly pointed or subacute at base, aguttulate.

Culture characteristics: Conidia germinating on MEA within 24 h. Germ tube produced from the side of conidia. Colonies growing on MEA, reaching 40 mm in 6 weeks at 25°C. Mycelia superficial, effuse to flat or undulate, from above gray to off white at the center, olivaceous to greyish center to the euros edge, from reverse greenish black at the center, light brown to orangeries tinge with hyaline tips at edge.

Material examined: Thailand, Chang Wat Prachuap Khiri Khan Province, Pran Buri District, Pran Buri river, on decaying submerged stems of Bamboo (Poaceae), 08 May 2023, Tharindu Bhagya, TB137A (MFLU 25-0481, holotype), *ibid*., TB137B (MFLU 25-0482, isotype).

GenBank numbers – MFLU 25-0481, ITS = PX062148

Distribution – Decaying submerged stem of Bamboo in freshwater river, Thailand.

Notes – Multi-locus phylogenetic analysis positioned the new isolates in a distinct lineage sister to *Phaeoisaria filiformis* strain MFLUCC 18-0214, with strong

statistical support (98% ML and 0.97 BPP) (Figure 4.81). The new isolates, strains MFLU 25-0481 and MFLU 25-0482, match the general description of *Phaeoisaria* morphologically, showing erect, dark brown to black synnemata lined with parallel, adpressed conidiophores, polyblastic, sympodially arranged, denticulate conidiogenous cells, and aseptate conidia (Luo et al., 2019; Yang et al., 2023; Wang et al., 2024). They differ from *Ph. filiformis* strain MFLUCC 18-0214 at the molecular level by 3.81% in ITS and 1.86% in LSU, including gaps. Morphologically, strains MFLU 25-0481 and MFLU 25-0482 can be distinguished from *Ph. filiformis* by producing shorter synnemata (360 μm vs. 447 μm) and by having ampulliform, pyriform, clavate to lageniform conidiogenous cells (Figure 4.82) (Wang et al., 2024; Xu et al., 2025). Based on both phylogenetic and morphological evidence, I describe *Ph. pranburensis* (MFLU 25-0481 and MFLU 25-0482) as a new species in the genus *Phaeoisaria*, isolated from freshwater coastal wetlands in Thailand.

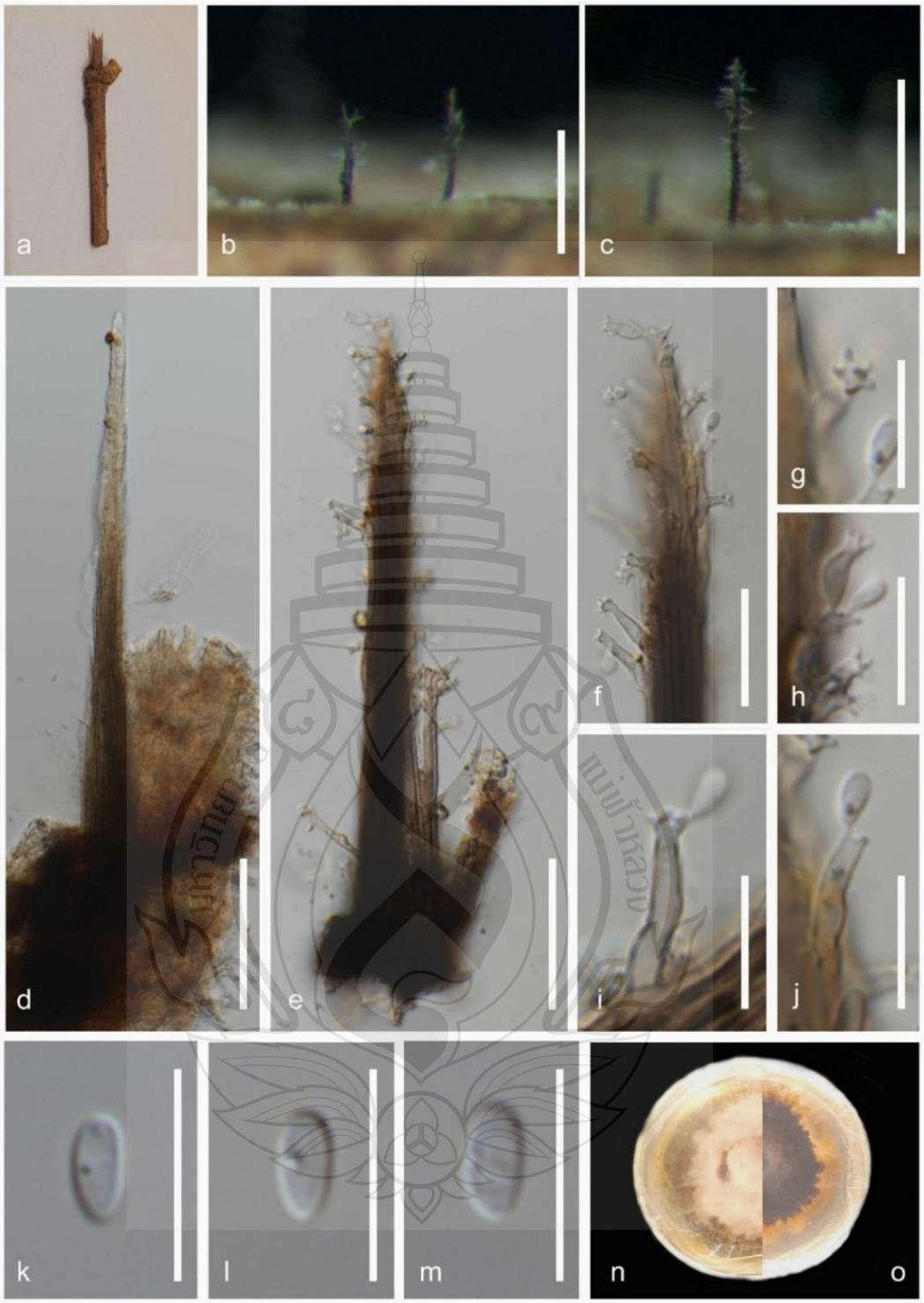

Note a Bamboo host material. b–c Conidiophores on the host surface with conidia. d–e Conidiophore. f Apex of conidiophore. g–j Denticulate conidiophores with attached conidia. k–m Conidia. n Culture on MEA above. o Reverse. Scale bars: b–c 250 µm, d–e 50 µm, f 20 µm, g–m 10 µm.

Figure 4.82 *Phaeoisaria pranburensis* (MFLU 25-0481, holotype)

Dematipyriforma L. Y. Sun, Hai-Yan Li, Xiang Sun & L.D. Guo

Dematipyriforma was introduced by Sun et al. (2017), under *Pleurotheciaceae*, *Pleurotheciales* in *Sordariomycetes*, and typified by *Dematipyriforma aquilariae*. The species have been reported from both aquatic and terrestrial environments (Sun et al., 2017; Bao et al., 2022). Endophytic and saprobic nutritional modes were reported from *Dematipyriforma* isolates from Asia (Bao et al., 2022). *Dematipyriforma* is characterized by immersed thick, light brown hyphae, monoblastic, intercalary, determinate, light brown and cylindrical conidiogenous cells. Conidiogenous cells give rise to pyriform, smooth, thin-walled, transverse or longitudinal septate conidia. Conidia often possess single small basal cells connected to conidiogenous cells or to the hyphae (Sun et al., 2017; Bao et al., 2022).

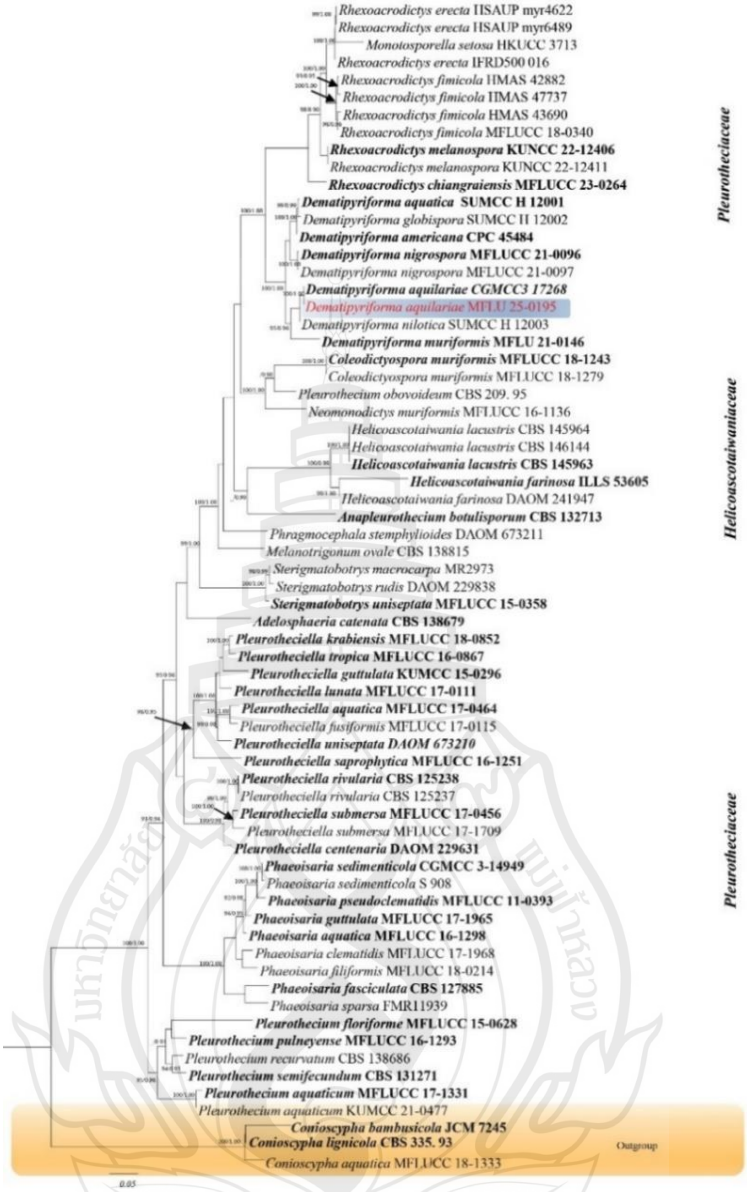

Note The tree topology of the maximum likelihood analysis is similar to the Bayesian analysis. Bootstrap support values for ML equal or greater than 75% and Bayesian posterior probabilities greater than 0.90 are given near nodes respectively. The tree is rooted with *Conioscypha lignicola* (CBS 335.93), *C. bambusicola* (JMC 7245), and *C. aquatica* (MFLUCC 18-1333).

Figure 4.83 The best maximum likelihood tree for *Dematipyriforma* is presented. The phylogenetic tree constructed from maximum likelihood analysis based on the combined ITS, LSU, SSU and *rpb*2 sequence 67 strains are included in the combined sequence analysis, which comprised 4519 characters with gaps.

Dematipyriforma aquilariae L.Y. Sun, Hai Y. Li, Xiang Sun & L.D. Guo.

Saprobic on dead, decaying stems of *Typha* (Typhaceae). **Sexual morph:** Undetermined. **Asexual morph:** Hyphomycetous. *Colonies* black, effuse, sporodochial. *Mycelium*, 1.2–2.5 μm ($\bar{x}$ = 2 μm, n = 30), immersed, smooth, subhyaline to pale brown, branched, septate, thin-walled. *Chlamydospores*, 4–5 × 6.5–8.5 μm ($\bar{x}$ = 4.5 × 7 μm, n = 30), intercalary or terminal, solitary, catenated, straight, or curved, brown to dark brown with a pale intermediate cell, smooth walls thickened with axial performative canals 1–8 transverse and occasionally 1 or more oblique or longitudinal septa, constricted at the septa. *Conidiophores* 2–6 μm wide ($\bar{x}$ = 4.5 μm, n = 10), micronematous, mononematous, subhyaline to pale brown, smooth, straight to flexuous, septate. *Conidiogenous cells*, 4.5–6× 5.5–8μm ($\bar{x}$ = 5.5 × 7.8 μm, n = 30), holoblastic, integrated, intercalary, determinate, cylindrical, pale brown to brown with thin walls, conidial secession rhexolytic. *Conidia* 24–30 × 15–20 μm ($\bar{x}$ = 26.5 × 17.5 μm, n = 30), pyriform or elongated pyriform, solitary, intercalary, smooth, thin-walled, muriform, rounded at the apex, pale grey olivaceous to pale brown, acropetal pigmentation during conidium formation.

Culture characteristics: Conidia germinating on malt extract agar (MEA) within 24 h. Germ tube produced from the base of conidia. Colonies growing on MEA, reaching 40 mm in 4 weeks at 25°C. Mycelia superficial, effuse to flat or undulate, from above olivaceous to greyish canter to the complete edge, from reverse greenish-black at the canter, light brown to black to hyaline edge.

Material examined: Thailand, Chang Wat Prachuap Khiri Khan Province, Pran Buri District, Pran Buri Wetland, on decaying stems of *Typha* sp. (Typhaceae), 25 August 2023, Tharindu Bhagya, TB113 (MFLU 25-0195), ex-type living culture (MFLUCC 25-0242).

GenBank numbers – MFLU 25-0195: ITS = PV759789, LSU = PV759788, SSU = PV759791, *rpb2* = PV779202

Notes – *Dematipyriforma aquilariae* (MFLU 25-0195) has a phylogenetic affinity with *D aquilariae* (CGMCC 3.17268) and clusters with 100% ML and 1.00 BYPP support (Figure 4.83). The new isolate agrees with the general description of *Dematipyriforma* by possessing monoblastic integrated conidiogenous cells and pyriform conidia with transverse, oblique or longitudinal septation (Sun et al., 2017;

Bao et al., 2022). *Dematipyriforma aquilariae* (MFLU 25-0195) and *D. aquilariae* (CGMCC 3.17268) have rhexolytic conidial secession, smooth and thin-walled, pyriform or elongated pyriform, dark brown to black conidia with acropetal pigmentation environments (Figure 4.84) (Sun et al., 2017; Bao et al., 2022). Considering both phylogenetic and morphological evidence, I identify MFLU 25-0195 as a new isolate of *D aquilariae*, and report this as a new host record for *Typha* sp., from freshwater coastal wetlands of Thailand.

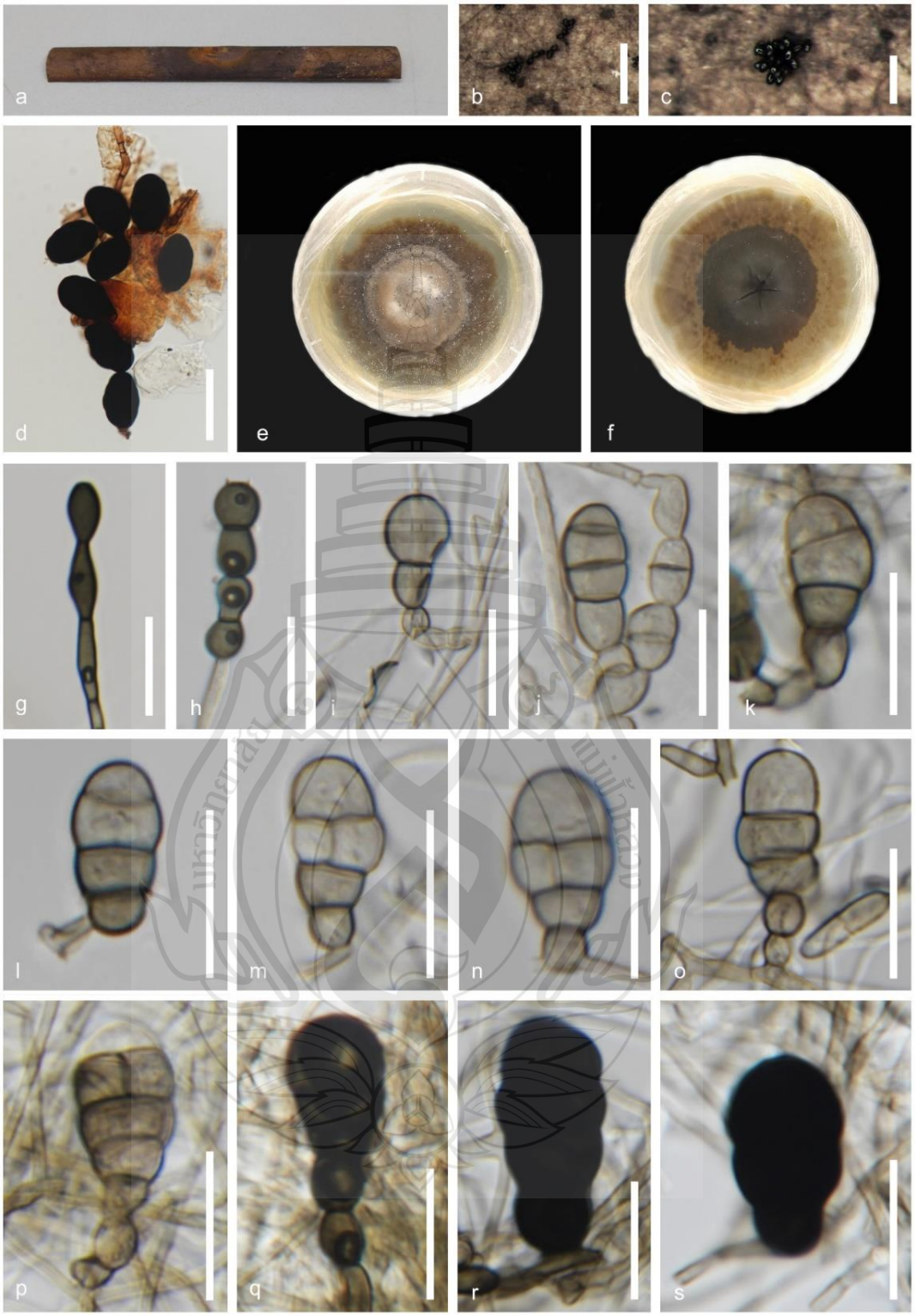

Note a *Typha* sp. host material. b–c. Colonies on host surface. d Squash mount of conidia. e Culture on MEA above. f Reverse. g–h Chlamydospores. i–s Conidial development. Scale bars: b 500 µm, c 250 µm, d 50 µm, g–s 20 µm.

Figure 4.84 *Dematipyriforma aquilaria* (MFLU 25-0195)

Sordariomycetidae O.E. Erikss. & Winka

Chaetosphaeriales Huhndorf, A.N. Mill. & F.A. Fernández

Chaetosphaeriaceae Réblová, M.E. Barr & Samuels

Chloridium Link, Mag. Gesell. naturf. Freunde, Berlin 3(1-2): 13 (1809)

The genus *Chloridium*, introduced by Link in 1809, is classified within the family *Chaetosphaeriaceae* and the order *Chaetosphaeriales*, with *C. viride* serving as the type species. Members of this genus are saprobic organisms found worldwide, including in aquatic environments (Luo et al., 2016). They show a preference for various substrates, such as decomposing plant material and organic matter in soil. *Chloridium* produces both sexual and asexual forms. The sexual morph is characterized by ovoid to globose, dark brown ascomata bearing conspicuous, multi-septate setae. The peridium consists of *textura angularis* cells on the surface and pseudoparenchymatous cells internally. In *Chloridium*, asci are cylindrical to clavate and short-stalked, each containing eight ellipsoid, septate, hyaline ascospores. The asexual form is hyphomycetous, producing unbranched, pigmented, and erect conidiophores. Conidiogenous cells develop on these conidiophores are phialidic, with a collarette, and produce unicellular, hyaline to subhyaline conidia that are globose, subglobose, or ellipsoidal in shape (Luo et al., 2016; Réblová et al., 2016; Bao et al., 2021; Yasanthika et al., 2022).

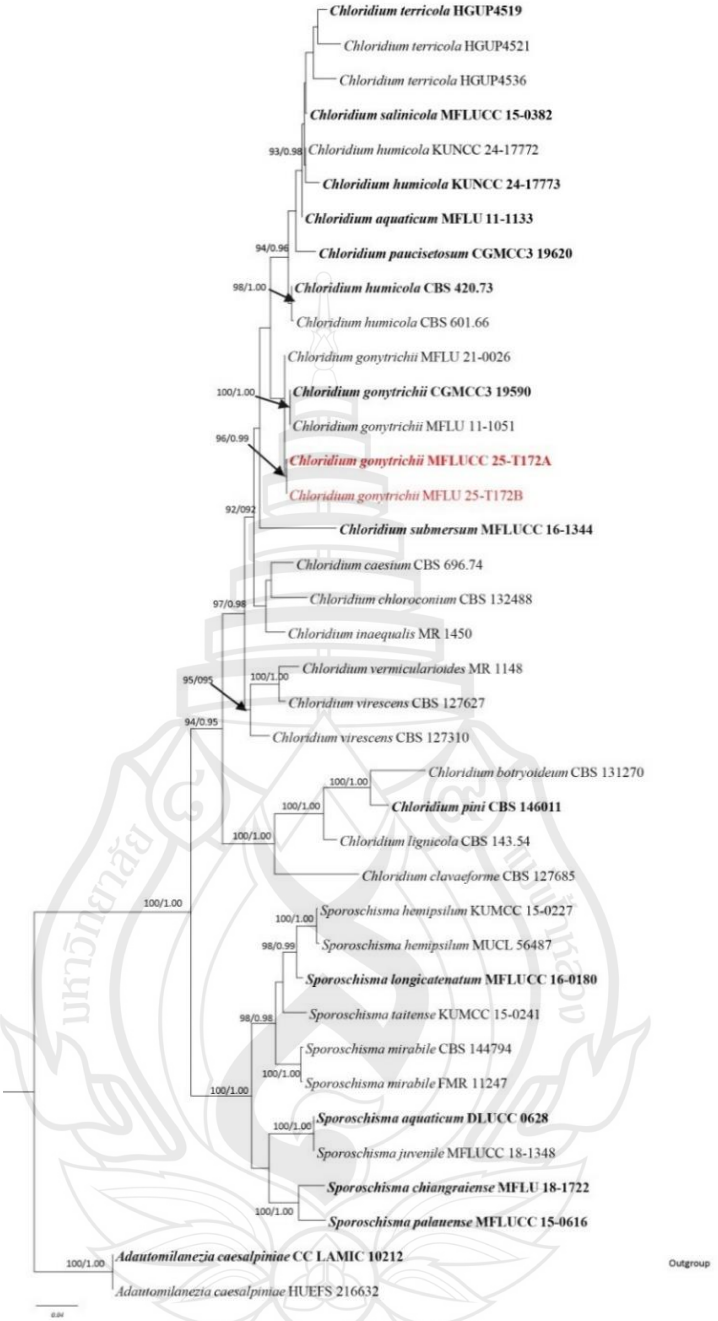

Note Bootstrap support values for ML ≥ 90 % and Bayesian posterior probabilities (BPP) ≥ 0.9 are mentioned at the nodes. The tree was rooted to *Adautomilanezia caesalpiniae* strain LAMIC 10212 and HUEFS 216632 combination. Newly generated sequences are indicated in red and the type strains are in bold.

Figure 4.85 Phylogram generated from Maximum Likelihood (ML) analysis based on combined ITS, and LSU sequence data of 38 fungal strains, which comprise 1528 characters including gaps, are included in the analyses.

Chloridium gonytrichii (F.A. Fernández & Huhndorf) Réblová & Seifert, in Réblová et al., IMA Fungus 7(1): 134 (2016)

Saprobic on dead, decaying submerged stems of Bamboo, (Poaceae), **Sexual morph:** Undetermined. **Asexual morph:** *Hyphomycetous*, effuse, erect, olivaceous to cinereous or light brown, fasciculate to caespitose or gregariosely fasciculate on host. *Mycelium*, immerse rarely superficial, septate, branched, hyaline to pale brown, thick-walled. *Conidiophores* 190–350 × 2.5–5.5 μm ($\bar{x}$ = 255 × 3.5 μm, n = 10), macronematous, mononematous, erect, 6–12 septate, simple or occasionally branched, smooth, thick walled, straight to slightly flexuous towards apexes, robust, bulbous at dark brown or black base, pale brown to olivaceous at middle with whorls of phialides, tapering towards hyaline to subhyaline apexes baring single phialidie. *Conidiogenous cells*, monoblastic to occasional polyblastic, terminal, determinate, cylindrical, light brown to olivaceous brown or subhyaline, at middle 11–18 × 2.5–5.5 μm ($\bar{x}$ = 13 × 3.5 μm, n = 10), arranged in 4-6 whorls, monophialidic, occasionally percurrent, apiculate to subulate and collarette, at apexes 14–35 × 2.5–3.5 μm ($\bar{x}$ = 26 × 3.0 μm, n = 10), monophialidic, enteroblastic, smooth, hyaline to subhyaline. *Conidia* 3.5–4.5 × 2–4 μm ($\bar{x}$ = 4.0 × 3.5 μm, n = 30), acrogenous, solitary or caespitose, aseptate, smooth, smooth, thick walled, olivaceous to subhyaline, ellipsoidal to subglobose occasionally tunicate at the base. Aggregated into slimy, imbricate clusters or occasionally into oblong cirrhus.

Culture characteristics: Conidia germinating on MEA within 12 h. Germ tubes produced from side of the conidium. Colonies growing on MEA, reaching 40 mm in 4 weeks at 25°C. Mycelia superficial, dense, effuse to umbonate, with erose edges, from above dark brown to olivaceous brown at center and off-white ring at the edge, from reverse yellowish brown to bark brown at the center, followed by light brown to olivaceous brown section lading to yellowish brown ring ending with off white edge. Hyaline cottony mycelium development observed after 4 weeks and produced whit color hyphal matts at the edges.

Material examined: Thailand, Chang Wat Prachuap Khiri Khan Province, Pran Buri District, Pran Buri river, on decaying stems of Bamboo (Poaceae), 02 December 2023, Tharindu Bhagya, TB172A (MFLU 25-0483), Pran Buri District, Sam Roi Yot

wetland, decaying stem of *Typha* sp. (Typhaceae), 02 December 2023, Tharindu Bhagya TB172B (MFLU 25-0484).

GenBank numbers – MFLUC 25-0483: ITS =PX518132, LSU = PX518138

Distribution – Decomposing branch, Puerto Rico (Réblová et al., 2016), submerged decaying wood, Thailand (Bao et al., 2021), tropical forest soil, Thailand (Yasanthika et al., 2022), decomposing submerged Bamboo stem and decomposing stem of *Typha* sp., Thailand (This study).

Notes – The new isolates form a clade with *Corynascus gonytrichii* strains MFLU 11-1051 and MFLU 21-0026, with moderate statistical support (55% ML and 0.72 BPP) (Figure 4.85). They share similar morphological characteristics with *C. gonytrichii*, including macronematous, mononematous, erect, 6–12-septate conidiophores with bulbous bases and whorls of phialidic, subulate, collared, enteroblastic conidiogenous cells (Figure 4.86) (Réblová et al., 2016; Bao et al., 2021; Yasanthika et al., 2022). Based on the available morphological and phylogenetic evidence, we identify our isolates MFLU 25-0483 and MFLU 25-0484 as new strains of *C. gonytrichii*. Consequently, I report two new host records for *C. gonytrichii*, Bamboo and *Typha* sp., from freshwater coastal wetlands of central Thailand.

Note a Bamboo host material. b Conidiophore aggregation on the host surface. c–e Conidiophores with whorls of phialides at the middle and terminal phialides. f Central philide. g–i Terminal phialides with attached. j Mass of conidia. k culture on MEA above. l Reverse. Scale bars: b 500 µm, c–j 20 µm.

Figure 4.86 *Chloridium gonytrichii* (MFLU 25-0483)

Savoryellales Boonyuen, Suetrong, Sivichai, K.L. Pang & E.B.G. Jones

Savoryellaceae Jaklitsch & Réblová

Ascolacicola Ranghoo & K.D. Hyde, Mycologia 90(6): 1055 (1998)

The genus *Ascolacicola* was introduced by Ranghoo & Hyde in 1998 to accommodate *A. aquatic* as the type species. Initially, the genus was monotypic and contained only the type species. Wang et al. (2024) used phylogenetic and morphological data to synonymize members from *Ascotaiwania* and added *A. coffeae*, *A. mitriformis*, *A. minispora*, *A. sawadae*, and *A. uniseptata* to the genus. *Ascolacicola* comprises both sexual and asexual species. The sexual morphs are characterized by subglobose, superficial, coriaceous ascomata with periphysate ostioles and filamentous, flexuous, narrow, thread-like paraphyses. Asci in *Ascolacicola* are unitunicate, cylindrical, with short pedicels at the base and an apical ring at the apex. Each ascus bears eight ellipsoidal to fusiform, brown to pale brown ascospores with hyaline cells at each end. The asexual morphs produce obovoid to pyriform, 1–3-septate conidia that are light brown to dark brown in color (Ranghoo & Hyde, 1998; Wang et al., 2024).

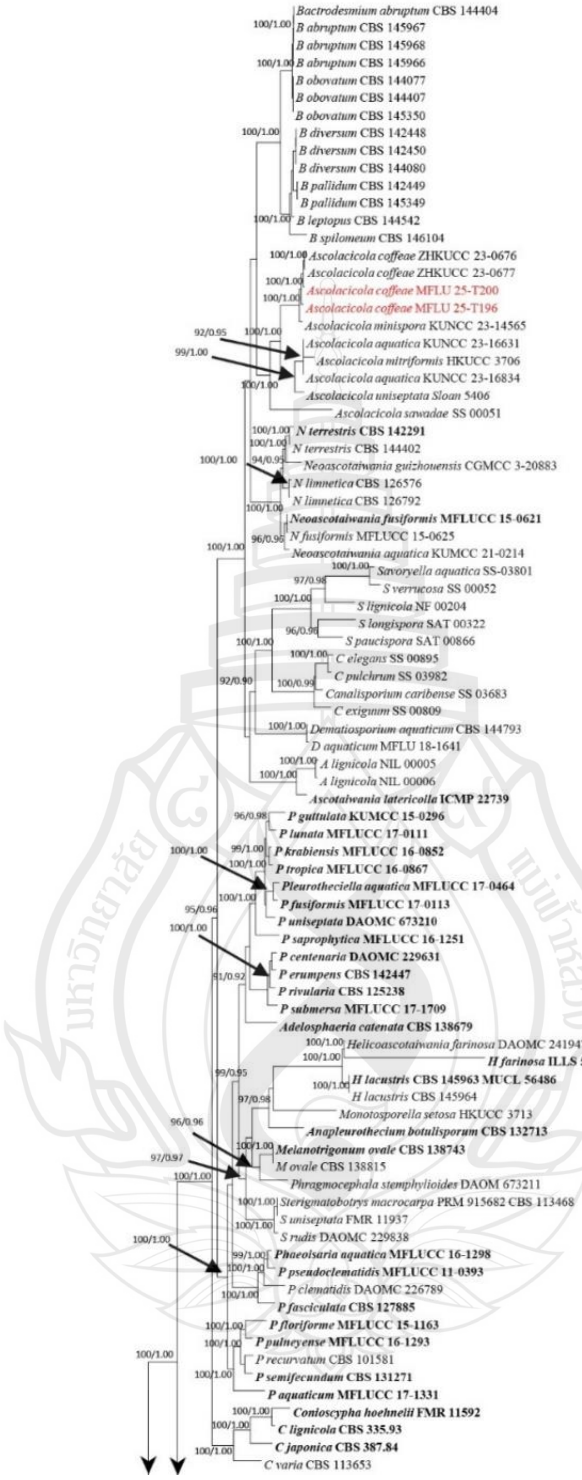

Note Compressing 6876 characters including gaps from of 112 strains which were included in the analyses. Bootstrap support values for ML ≥ 90% and Bayesian posterior probabilities (BPP) ≥ 0.9 are mentioned at the nodes.

Figure 4.87 Phylogentic tree generated from Maximum Likelihood (ML) analysis based on combined ITS, LSU, SSU, *rpb2* and *tef1-α* sequence.

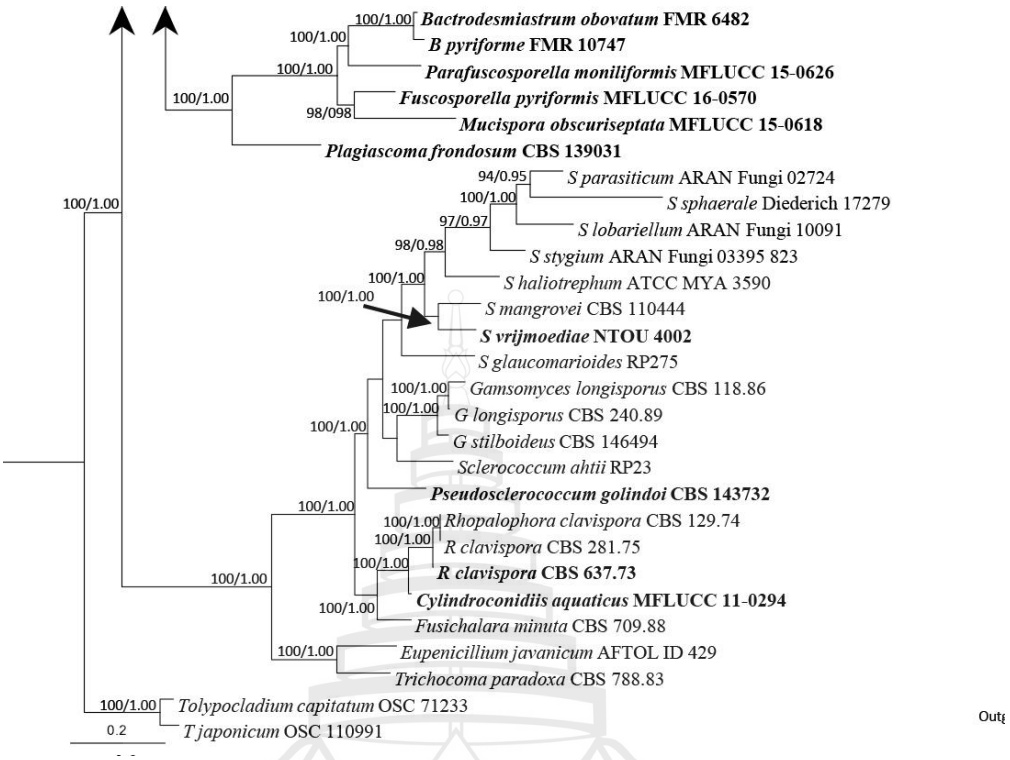

Figure 4.87 (continued)

Ascolacicola coffeae (L. Lu & Karunarathna) W.P. Wang, H.W. Shen & Z.L. Luo, in Wang, Hyde, Bao, Wanasinghe, Lin, Shen, Lu, Zhang, Su, Li, Al-Otibi, Yang & Luo, Mycosphere 15(1): 6611 (2024)

Saprobic on dead, moist, decaying leaf of a *Typha* sp. (Typhaceae), **Sexual morph**: *Ascomata* 190–270 × 140–210 µm ($\bar{x}$ = 245 × 190 µm, n = 5) scattered on the host, superficial, perithecial, carbonaceous subglobose or ampulliform, papillated, black, with short ostiole. *Peridium,* outer layer comprising with black carbonaceous black to greenish brown polyhedralc ells of *textura prismatica*, outer layer brittle, breaking apart into angular, cuboid or polygonal fragments, inner layer process thin walled, pigmented cells in *textura angularis*. *Paraphyses* 1.5–2.5 ($\bar{x}$ = 2.0 µm n = 5) smooth walled, hyphae like and aseptate. *Asci* 45–75 × 5–8 µm ($\bar{x}$ = 68 × 7.5 µm n = 10), 8-spored, fasciculate, unitunicate, cylindrical to subcylindrical or clavate, short pedicellate with nonamyloid (J-) apexes. *Ascospores*, 11–17 × 4–7 µm ($\bar{x}$ = 14.5 × 5.5 µm, n = 20) ellipsoidal, cylindrical to subcylindrical, 3-septate, slightly constricted at the septa, hyaline wen immature, wider middle cells olivaceous brown to pale brown at maturity, process two hyaline to subhyaline polar cells. **Asexual morph:** *Hyphomycetous*. *Colonies* are black to brown, effuse,

punctiform, sporodochia. *Mycelium* immersed, smooth, septate, hyphae subhyaline to pale brown, branched, thin walled. *Conidiophores*, inconspicuous, when present micronematous, and mononematous, *Conidiogenous cells*, 3–5 × 2–4 µm (x– = 3.5 × 3.0 µm, n = 10), holoblastic, integrated, intercalary, determinate, subglobose or ampulliform. *Conidia* 8–14 × 5–9 µm (x– = 10.5 × 6.5 µm, n = 30), solitary, smooth, thick-walled, obovoid, broadly rounded or elongated, 1-septate, rounded at the apex, upper large cell pale grey olivaceous to pale brown, small basal cell hyaline to sub hyaline.

Culture characteristics: Conidia germinating on MEA within 48 h. Germ tubes produced from side of the conidium. Colonies growing on MEA, reaching 10 mm in 6 weeks at 25°C. Mycelia superficial, dense, effuse irregular with erose edges, from above dark brown to black at the center, olivaceous black to cinereous from center to the edge, from reverse dark brown or black at the center and olivaceous black to pale brown towerds the hyaline edge. White color vegetative mycelium started to develop from the edges after 4 weeks.

Material examined: Thailand, Chang Wat Prachuap Khiri Khan Province, Pran Buri District, Sam Roi Yot Wetland, on decaying stems of *Typha* sp. (Typhaceae). xx January 2023, Tharindu Bhagya, TBA (MFLU 25-0495, Asexual Morph), *ibid*., TBA2, (MFLU 25-0496, Sexual Morph).

GenBank numbers – MFLU 25-0495: ITS = PX518139

Distribution – Decaying branch of *Coffea arabica*, China (Liu et al., 2025), decaying *Typha* sp. peduncle in freshwater wetland, Thailand (This study).

Notes – Newly isolated taxa clade sister to *Ascolacicola coffeae* (ZHKUCC 23-0676 and ZHKUCC 23-0677), and *A. minispora* (KUNCC 23-14565) with 100 ML and 1.00 BPP support (Figure 4.87). MFLU 25-0495, the asexual isolate morphologically resembles the *A. coffeae* (ZHKUCC 23-0676) by producing subglobose or ampulliform conidiogenous cells, and thick-walled, obovoid, broadly rounded or elongated conidia (Liu et al., 2025). Furthermore, MFLU 25-0495 and strain ZHKUCC 23-0676 shear similar height to width ratio for the conidia (MFLU 25-0495 1.6 vs ZHKUCC 23-0676). MFLU 25-0496, the newly isolated sexual morph phylogenetically similar to the *A. coffeae* (ZHKUCC 23-0676) by 98.9% in ITS, 99.4% in LSU, and 99.8% in *rpb2* without gaps. Considering available phylogenetic and morphological evidences I recognize MFLU 25-0495 as anew isolate of *A. coffeae* asexual morph and MFLU 25-0496 as the sexual morph

of *A. coffeae* strain ZHKUCC 23-0676 (Figure 4.88). According this study introduces a new host and geographical record for *A. coffeae*, as well as the sexual morph for the species from central coastal freshwater wetlands of Thailand.

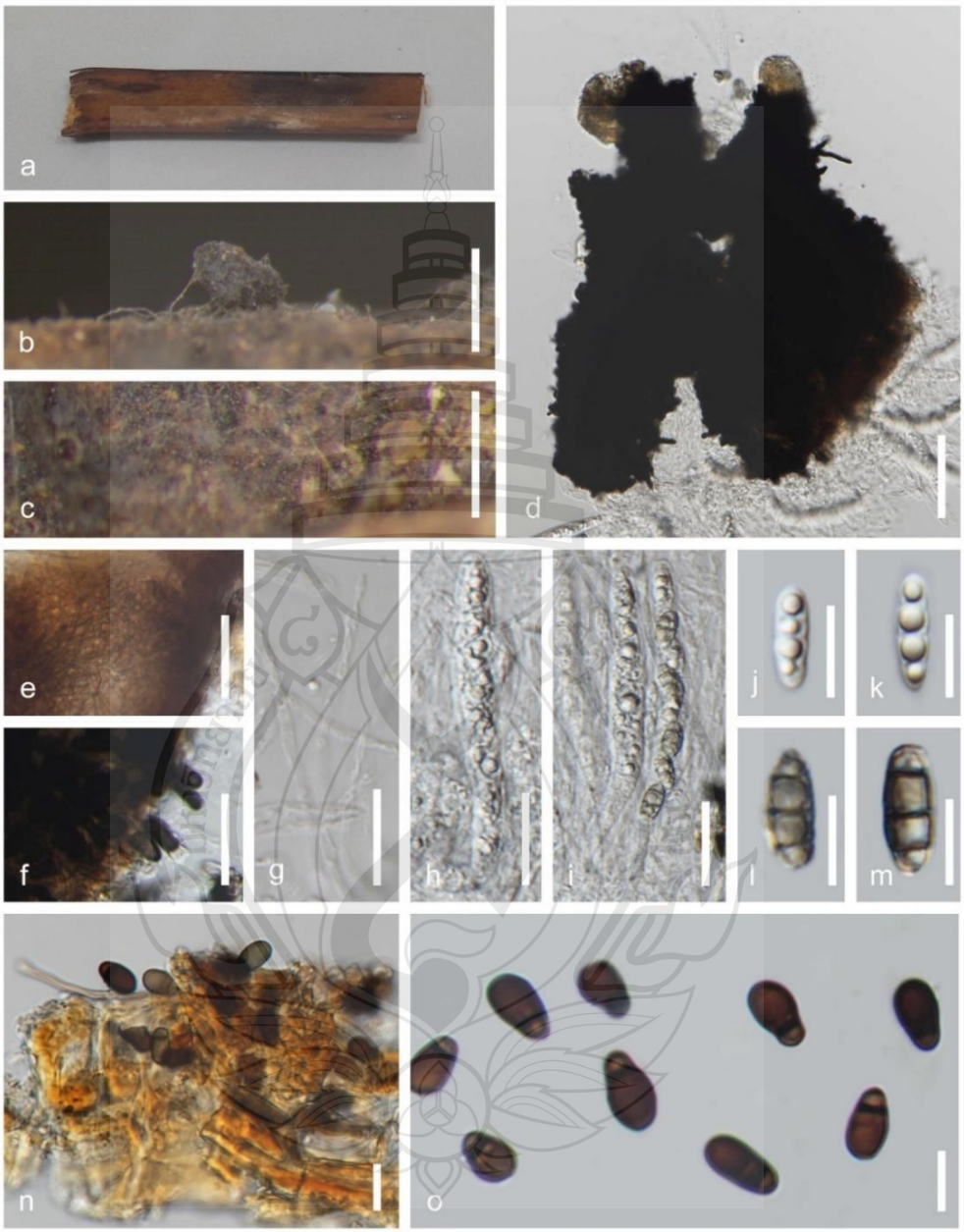

Note a *Typha* sp. host. b Ascomata. c Sporodochia. d Squashed mount of ascomata. e Peridium. f Outer surface of peridium. g Paraphyses. h–I Asci; j–m Ascospores. n Squashed mount of sporodochia. o Conidia. Scale bars: b 500 µm, c 250 µm, d 50 µm, e–i 20 µm, j–o 10 µm.

Figure 4.88 *Ascolacicola coffeae* (MFLU 25-0495 Asexual morph, MFLU 25-0496 sexual morph)

Amphisphaeriales D. Hawksw. & O.E. Erikss

Beltraniaceae Nann

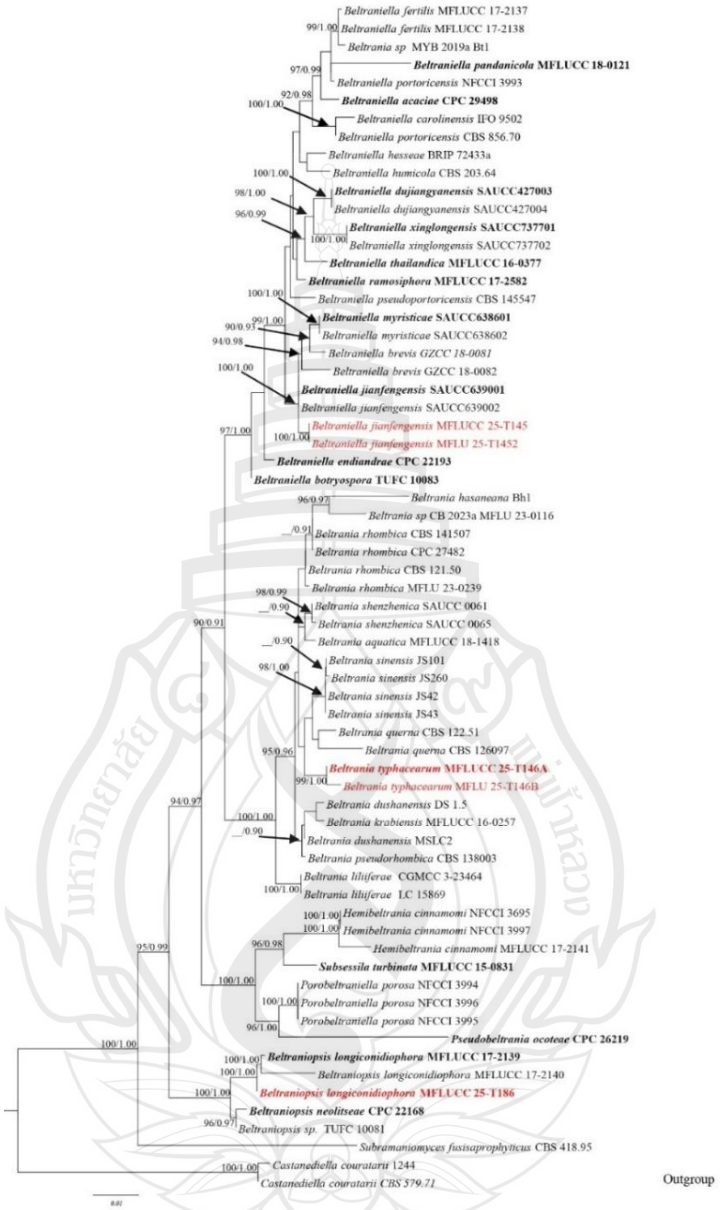

Note Bootstrap support values for ML ≥ 90 % and Bayesian posterior probabilities (BPP) ≥ 0.9 are mentioned at the nodes. The tree was rooted *Castanediella couratarii* (1244 and CBS 579.71) Newly generated sequences are in red and the type strains are in bold.

Figure 4.89 Phylogram generated from Maximum Likelihood (ML) analysis based on combined ITS, and LSU sequence. The data set comprises 1563 characters including gaps from of 66 strains which were included in the analyses.

Beltrania Penz., Nuovo G. bot. ital. 14(2): 72 (1882)

Beltrania is the type genus of the family *Beltraniaceae* and was erected by Penz in 1882. The genus is typified by *B. rhombica* and is characterized by dark, mostly unbranched setae that originate from lobed basal cells. Conidiophores develop from the basal cells of the setae or arise directly from the basal cells. They give rise to polyblastic, sympodial, denticulate conidiogenous cells that produce separating cells. Conidia in the genus *Beltrania* are apiculate and hyaline to subhyaline, with transverse bands (Hyde et al., 2020; Perera et al., 2020; Lin et al., 2024).

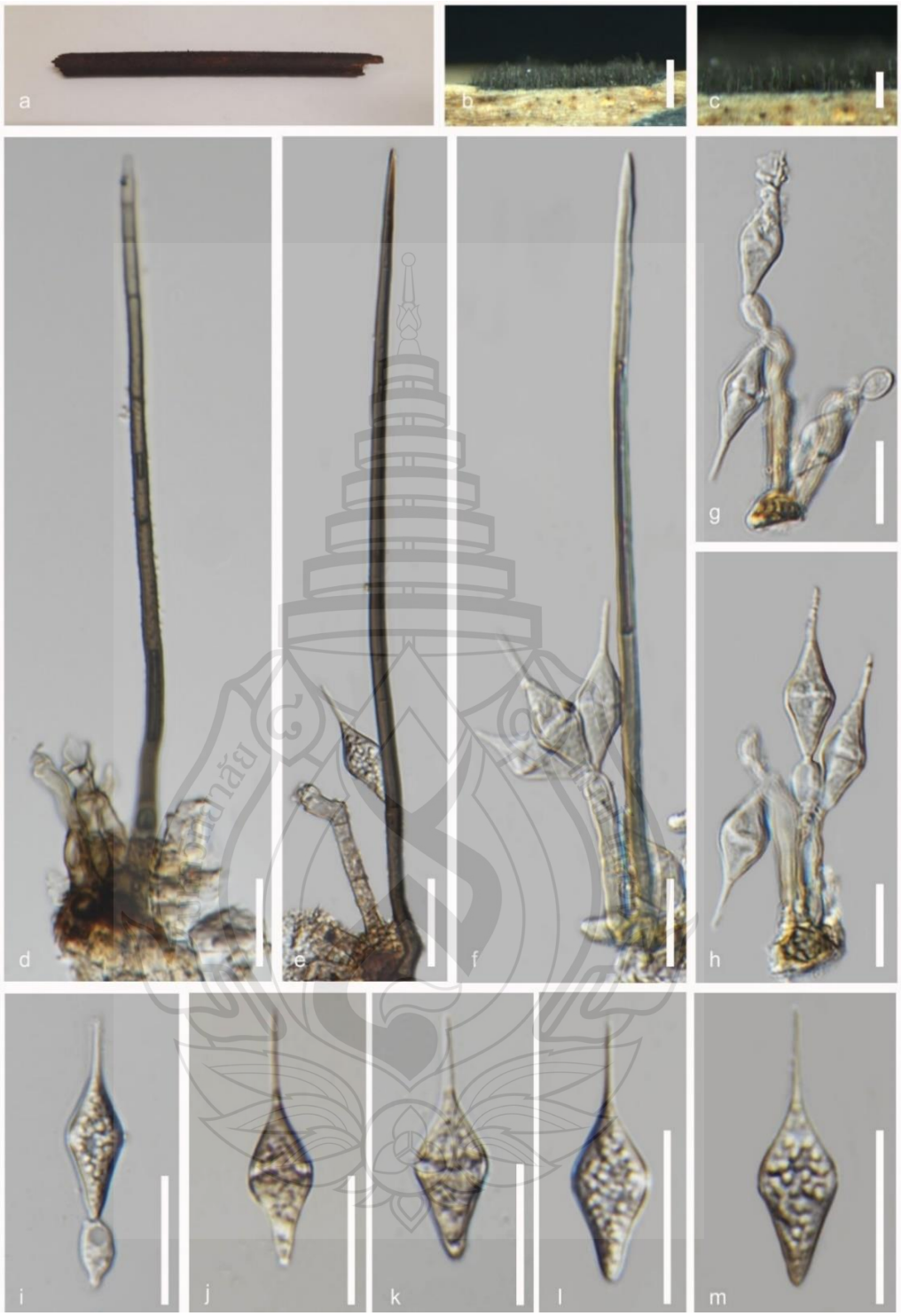

Note a *Typha* sp. host. b–c Conidiophores on the host surface with setae and conidia. d–f Conidiophores with setae and conidia. g–h Conidiophores with attached conidia. i Conidia attached to a separating cell. j–m Conidia development. Scale bars: b 750 µm, c 250 µm, d–m 20 µm.

Figure 4.90 *Beltrania typhacearum* (MFLU 25-0493, holotype)

Beltrania typhacearum Bhagya, Phukhams E.B.G. Jones & K.D. Hyde, sp. nov

Index Fungorum number: IF; Facesoffungi number: FoF 18914

Etymology – Epithet indicates the fungal origin from the host family Typhaceae.

Holotype – MFLU 25-0493

Saprobic on dead, decaying stems of *Typha* sp. (Typhaceae), **Sexual morph**: Undetermined. **Asexual morph:** *Hyphomycetous*, *Colonies* effuse, gregarious, dark brown to olivaceus brown or black. *Mycelium* immersed, branched or straight, septate, smooth, hyaline. *Setae* 140–220 × 2.5–3.5 µm ($\bar{x}$ = 190 × 3.0 µm), numerous, erect, unbranched, straight or slightly flexuous, tapering to acute apex, thick-walled, light to dark brown. *Conidiophores* 50–70 × 6.5–3.5 µm ($\bar{x}$ = 55 × 4.5 µm, n = 10), macronematous, mononematous, erect, pale brown, to subhyaline, thin-walled, smooth, subcylindrical, predominately fexuous, aseptate or occasionally 1-2 septate, unbranched. *Conidiogenous cells* 12.5–15.5 × 6.5–4.5 µm ($\overline{x}$=13.5 × 5 µm, n=10), polyblastic, integrated, terminal, pale brown, smooth, subcylindrical, denticulate and show sympodial proliferations. *Separating cells* 8.5–11.5 × 5.5–6.5 µm ($\overline{x}$=8.5×6 µm, n=10), smooth, thin-walled, pale brown to hyaline or sub-hyaline, clavate, bear 1–2 apical, fat-tipped denticles and hilum. *Conidia* 18–30×6–8 µm ($\overline{x}$=25×7.5 µm, n=20), pale brown to sub-hyaline with wider transverse band and spicate with pointed appendage, develop from separating cells, acrogenous, solitary, dry, thin walled, smooth, biconic.

Culture characteristics: Conidia germinating on MEA within 12 h. Germ tubes produced from the side of the conidium. Colonies growing on MEA, reaching 40 mm in 2 weeks. Mycelia superficial, umbonate with erose edge that fungal filaments radiate to the culture, from above off-white cottony hype with dark color aggregation developing after 4 weeks, from reverse off white with dark spots scatted on mycelium with hyaline tips off white at the edge.

Material examined: Thailand, Chang Wat Prachuap Khiri Khan Province, Pran Buri District, Pran Buri Wetland, on decaying stems of *Typha* sp. (Typhaceae), 06 April 2024, Tharindu Bhagya, TB146A (MFLU 25-0493, holotype), decaying stem of Bamboo (Poaceae), 06 April 2024, PranBuri river, Thailand, Tharindu Bhagya, TB208B (MFLU 25-0494).

GenBank numbers – MFLU 25-0493, ITS = PX062182, LSU = PX062183

Distribution – Decaying *Typha* sp. stem in freshwater wetland, Thailand and decaying stem of Bamboo (Poaceae), in freshwater river, Thailand.

Notes – MFLU 24-0493 and MFLU 25-0494 form an independent clade within *Beltrania*, sister to the isolates *B. sinensis* (JS101, JS260, JS42, and JS43) and *B. querna* (CBS 122.51 and CBS 126097), with 63% ML and 0.78 BPP support (Figure 4.89). The new isolates share similar characteristics with other members of *Beltrania*, possessing unbranched setae and conidiophores originating from basal cells, as well as polyblastic, sympodial, denticulate conidiogenous cells and apiculate conidia with hyaline transverse bands (Hyde et al., 2020; Perera et al., 2020). The type strain of the new isolates differs by 3.07% and 2.61% in ITS sequences and 1.68% and 1.72% in LSU sequences from *B. sinensis* strain JS260 and *B. querna* strain CBS 122.51, respectively. The pairwise distance matrix value was >0.05 between MFLU 25-0493 and other related taxa (Gostinčar, 2020; Maharachchikumbura et al., 2021). The aseptate, or occasionally 1–2-septate, pale brown to subhyaline conidiophores make the new strain MFLU 24-0494 morphologically distinguishable from *B. sinensis* (JS260) and *B. querna* (CBS 122.51) (Figure 4.90) (Elkhateeb et al., 2019; Zheng et al., 2020). MFLU 24-0493 and MFLU 25-0494 morphologically resemble *B. pseudorhombica* (CBS 138003) by possessing geniculate conidiophores and similar conidial dimensions, but they are phylogenetically distinct (Lichtemberg et al., 2019). Considering the available morphological and phylogenetic evidence, I introduce *Beltrania typhacearum* (MFLU 24-0493 and MFLU 25-0494) as a new species in the genus *Beltrania* from freshwater coastal wetlands of Thailand.

Beltraniella Subram., Proc. Indian Acad. Sci., Sect. B 36: 227 (1952)

Beltraniella was introduced by Subram (1952) from India and is typified by *B. odinae*. The distinctive features of the genus include sterile setae and branched conidiophores that develop from lobed basal cells, ending in setiform apexes. Conidiogenous cells in *Beltraniella* are polyblastic and sympodial, producing acropleurogenous, biconic, turbinate, hyaline to pale brown conidia with prominent hyaline transverse bands. Most Beltraniella species have been isolated from decomposing herbaceous materials, such as leaves, seeds, and fruits (Hyde et al., 2020; Perera et al., 2020; Lin et al., 2024).

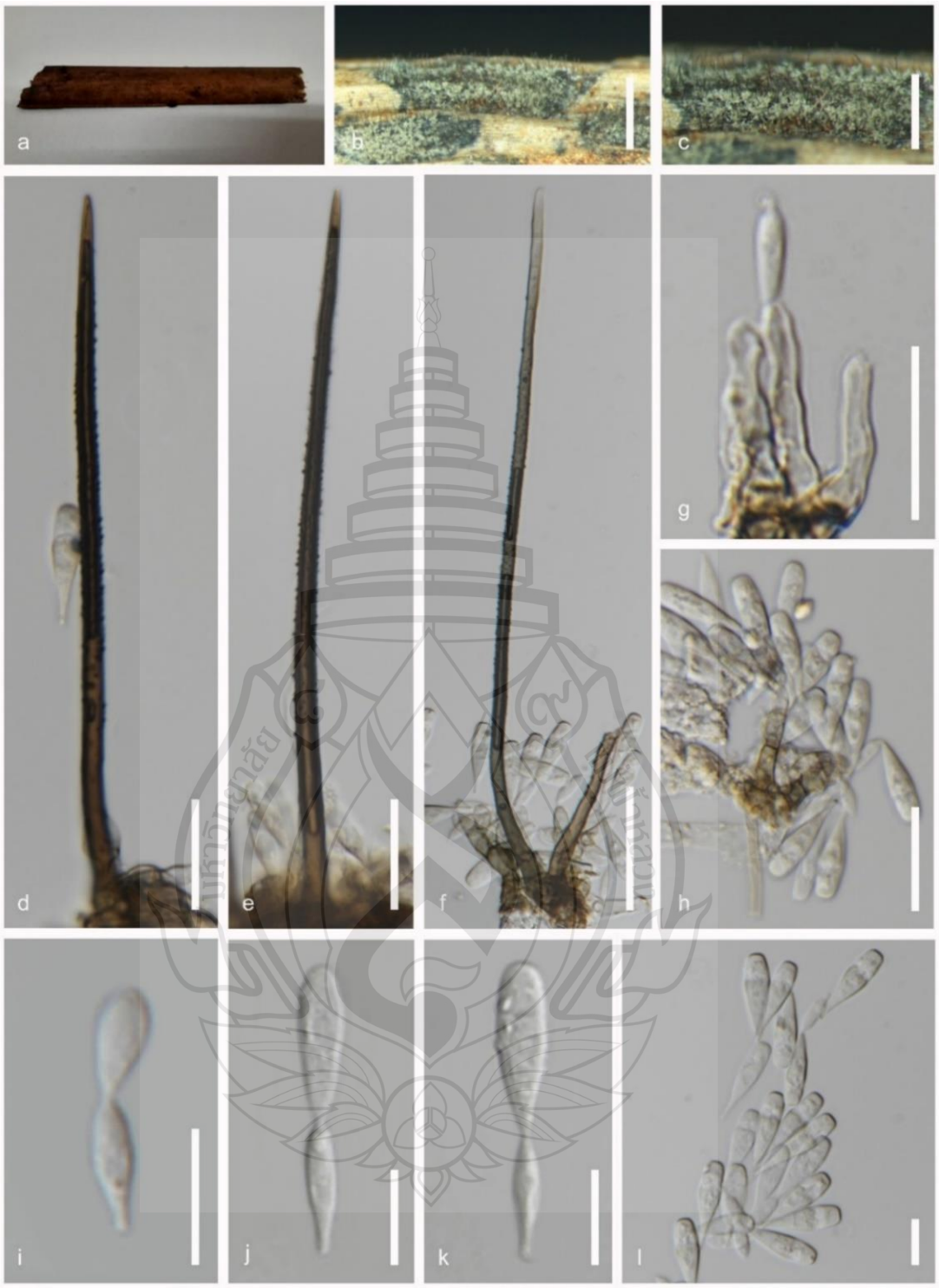

Note a *Thypa* sp. host. b–c Conidiophores on the host surface with setae and conidia. d–f Conidiophores, setae and conidia. g–h Conidiophores with attached conidia. i–k Conidia attached to a separating cell. l Conidia development. Scale bars: b 1 mm, c 500 µm, d–h 20 µm, i–l 10 µm.

Figure 4.91 *Beltraniella jianfengensis* (MFLU 25-0491)

Beltraniella jianfengensis W.W. Liu, C.Z. Yin, Zhao X. Zhang & X.G. Zhang, in Liu, Yin, Zhang, Wang, Meng, Zhang & Wang, MycoKeys 116: 132 (2025)

Saprobic on dead, decaying stems of *Typha*, (Typhaceae), **Sexual morph:** Undetermined. **Asexual morph:** *Hyphomycetous*. *Colonies* light brown to ash or light black, superficial, hairy, effuse, tightly aggregated on host tissue. *Setae* 140–220 × 3.5–6.5 μm ($\bar{x}$ = 155 × 4.5 μm, n = 10), erect, originate from basal cells. dark brown to olivaceous brown, thick-walled, straight or flexuous, unbranched, tapering to an acute apex, indistinctly septate, and verrucose. *Conidiophores* 32–45 × 7.0–11 μm ($\bar{x}$ = 42 × 8.5 μm, n = 10), macronematous, mononematous, erect, hyaline or pale brown, single or sympodial around the setae, straight or slightly curved, simple or branched, septate, thin and smooth-walled, *Setiform conidiophores* are absent. *Conidiogenous cells* 15–19 × 4.5–6.5 μm ($\bar{x}$ = 17 × 5.5 μm, n = 5), terminal, intercalary, cylindrical or subcylindrical, polyblastic, flat-tipped denticles at apex, hyaline to pale brown, smooth-walled. *Separating cells* 12–18 × 2.5–4.5 μm ($\bar{x}$ = 14.5 × 3.5 μm, n = 30), hyaline to pale brown, ovoid or obovoid, fusiform, thin and smooth walled, with a single flat-tipped denticle at the base. *Conidia* 22–28 × 4.0–7.0 μm ($\bar{x}$ = 24.5 × 5.5 μm, n = 30), solitary, turbinate to pyriform, distal with truncate end, hyaline, smooth, aseptate, base tapering to an acutely pointed tip with rounded apex.

Culture characteristics: Conidia germinating on MEA within 12 h. Germ tubes produced from side of the conidium. Colonies growing on MEA, reaching 30 mm in 2 weeks at 25°C. Mycelia superficial, dense, effuse to umbonate, with erose edges, from above pale white from center to the edge, from reverse light yellowish white at the center and the white to hyaline at the edge. Brown color hype aggregation was observed after 4 weeks of incubation under 25°C.

Material examined: Thailand, Chang Wat Prachuap Khiri Khan Province, Pran Buri District, Pran Buri Wetland, on decaying stems of *Typha* sp. (Typhaceae), 08 April 2024, Tharindu Bhagya, TB145A (MFLU 25-0491), *ibid.*, decaying peduncle of *Typha* sp. (Typhaceae) TB145B (MFLU 25-0492).

GenBank numbers – MFLU 25-0492, ITS = PX062187, LSU = PX062185

Distribution – Decomposing leaves in Hainan, China (Liu et al., 2025), and on decaying *Typha* sp. stem and peduncle in freshwater wetland, Thailand (This study).

Notes – The new isolates form a sister clade to *B. jianfengensis* (SAUCC639001 and SAUCC639002) with 100% ML and 1.00 BPP statistical support (Figure 4.89). They share characteristic features of the genus *Beltraniella*, including sterile setae developing from lobed cells, polyblastic, sympodial conidiogenous cells, and acropleurogenous, turbinate conidia with hyaline transverse bands (Lin et al., 2024). Phylogenetically, MFLU 25-0491 shows 98.78% similarity in ITS and 99.16% in LSU sequences with *B. jianfengensis* strain SAUCC639001 (Liu et al., 2025). Morphologically, the new strains MFLU 25-0491 and MFLU 25-0492 resemble *B. jianfengensis* strain SAUCC639001 by comprising cylindrical or subcylindrical, polyblastic conidiogenous cells with flat-tipped denticles at the apex, and turbinate to pyriform conidia with truncate ends (Figure 4.91) (Liu et al., 2025). Based on morphological and phylogenetic evidence, I recognize the new strains, MFLU 25-0491 and MFLU 25-0492, as *B. jianfengensis*, isolated from coastal freshwater wetlands of Thailand.

Beltraniopsis Bat. & J.L. Bezerra, Publicações Inst. Micol. Recife 296: 4 (1960)

Beltraniopsis is a hyphomycetous genus in the family Beltraniaceae, proposed by Bezerra (1960) and typified by *Beltraniopsis esenbeckiae*. This genus is characterized by setiform conidiophores, along with polyblastic, discrete, sympodial, denticulate conidiogenous cells. Conidia originating from the conidiogenous cells are hyaline to subhyaline, aseptate, and biconic, with a prominent transverse band (Lin et al., 2017; Xiao et al., 2019).

Note a *Typha* sp. host. b–c Colonies. d–f Conidiophores with conidiogenous cells. g Bace of the conidiophore with dislodge separating cells. h–i Conidiogenous cells. j–m Conidia. Scale bars: b–c 250 µm, d–f 100 µm, g–m 20 µm.

Figure 4.92 *Beltraniopsis longiconidiophoras* (MFLU 25-0490)

Beltraniopsis longiconidiophora C.G. Lin & K.D. Hyde, in Lin, Hyde, Lumyong & Mckenzie, Cryptog. Mycol. 38(3): 306 (2017)

Saprobic on dead, decaying stems of *Typha*, (Typhaceae), **Sexual morph**: Undetermined. **Asexual morph:** *Hyphomycetous*. *Colonies* with effuse, velutinous, colonies, gregarious, dark brown. *Mycelium* immersed, branched or straight, septate, smooth, hyaline. *Conidiophores* 280–340 × 6.5–3.5 µm ($\bar{x}$ = 310 × 4.5 µm, n = 10), macronematous, mononematous, erect, pale brown, thin-walled, smooth, fexuous, septate, unbranched, tapering to acute apex, originate from dark brown, swollen, radially lobed cell or thick stalk. *Conidiogenous cells* 8.5–5.5 × 4.5–6.5 µm ($\bar{x}$=6.5 × 5 µm, n=10), holoblastic, polyblastic, integrated, terminal, pale brown, smooth, ampulliform to subcylindrical, denticulate. *Separating cells*, smooth, thin-walled, pale brown to hyaline or sub-hyaline. *Conidia* 28–20 × 6–4 µm ($\bar{x}$=25 × 4.5 µm, n=20), pale brown to sub-hyaline with transverse band, develop from separating cells, acrogenous, biconic, turbinate, dry, thin walled, smooth.

Culture characteristics: Conidia germinating on MEA within 12 h. Germ tubes produced from side of the conidium. Colonies growing on MEA, reaching 50 mm in 3 weeks at 25°C. Mycelia superficial, dense, effuse to umbonate, with complete edges, from above pale white from center to the edge, from reverse light yellowish white at the center and the off white to hyaline at the edge.

Material examined: Thailand, Chang Wat Prachuap Khiri Khan Province, Pran Buri District, Pran Buri Wetland, on decaying stems of *Typha* sp. (Typhaceae), 08 April 2024, Tharindu Bhagya, TB186 (MFLU 25-0490),

GenBank numbers – MFLU 25-0490: ITS = PX518141, LSU = PX518142

Distribution – Decaying leaf Chiang Mai, Thailand (Lin et al., 2017), and Decaying *Typha* sp. stem in freshwater wetland, Thailand (This study).

Notes – MFLU 25-0490 forms a sister clade to *Beltraniopsis longiconidiophora* (MFLUCC 17-2139 and MFLUCC 17-2140) with 100% ML and 1.00 BPP support (Figure 4.89). The newly isolated strain aligns with the general description of *Beltraniopsis*, possessing setiform conidiophores emerging from lobed basal cells and biconic conidia with hyaline to subhyaline transverse bands (Lin et al., 2017). Our isolate closely resembles *B. longiconidiophora* (MFLUCC 17-2139) due to the presence of setiform conidiophores that lack a fertile apex, ampulliform to

subcylindrical conidiogenous cells, and relatively longer conidia (28–20 μm, $\bar{x}$ = 25 μm, n = 20), compared to other close relatives (Figure 4.92) (Lin et al., 2017). Based on the available morphological and phylogenetic evidence, I identify MFLU 25-0490 as a new collection of *B. longiconidiophora* from T*ypha* sp. (Typhaceae).

Chaetomiaceae G. Winter

Corynascus Arx

Corynascus was introduced by Arx (1973) and typified by *C. sepedonium*. It is characterized by sexual morphs that produce cleistothecial, soft, dark brown to black ascomata, comprising a peridium made of cells in textura epidermoidea, evanescent asci that bear eight ellipsoidal to fusiform ascospores in each ascus. Asexual morphs of the genus produce globose to subglobose, hyaline, thick-walled conidia (Marin-Felix et al., 2015; Crous et al., 2016). Members of the genus have a wide distribution including Asian, African continents, and European. *Corynascus* species are primarily saprobic and have been isolated from both terrestrial and aquatic habitats, particularly from decomposing plant material, as well as from soil. There is limited information of the evanescent nature of the asci and paraphyses in *Corynascus* species (Marin-Felix et al., 2015; Crous et al., 2016). Our investigation provides a detailed description of asci from the new isolate and reports the presence of paraphyses for the genus.

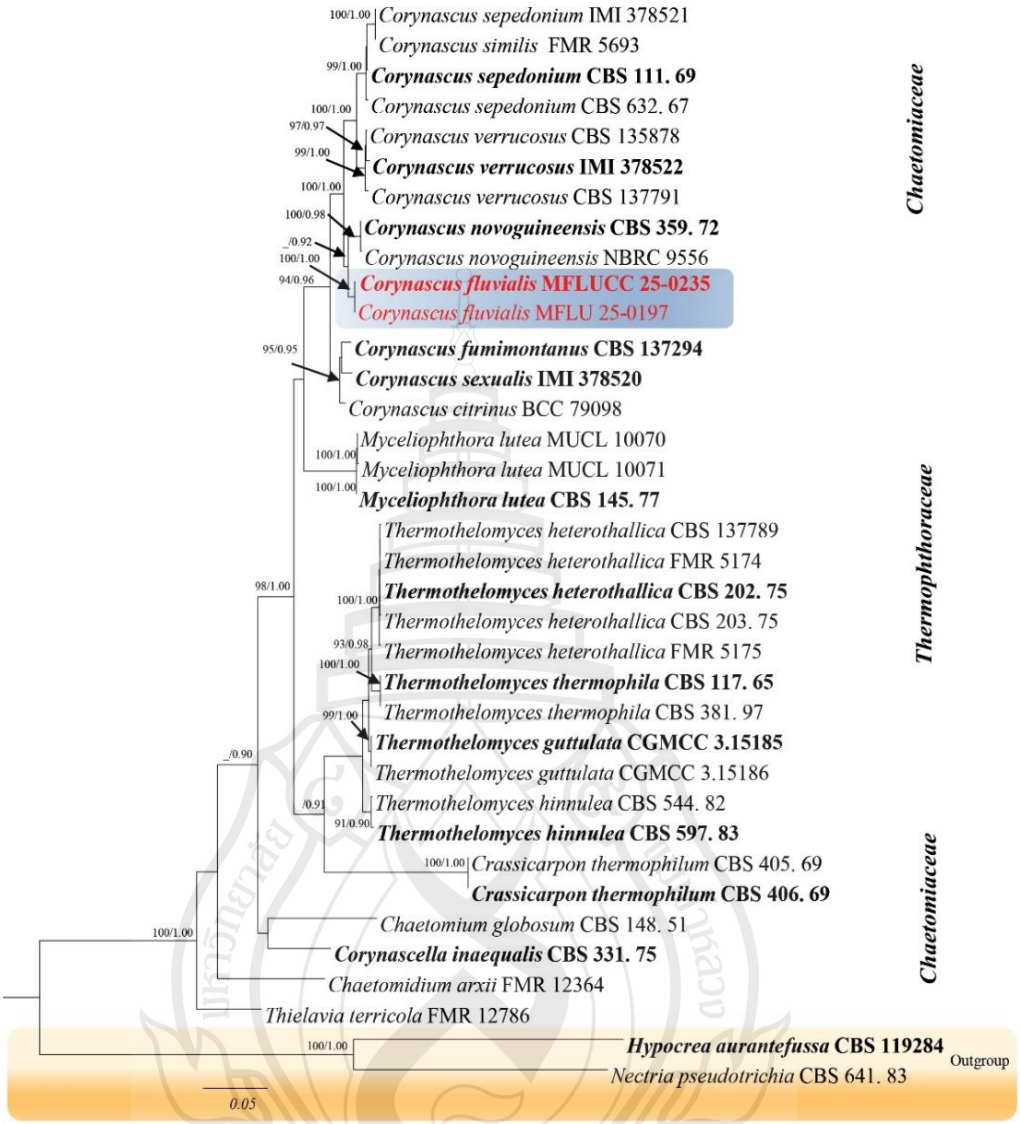

Note The tree topology of the maximum likelihood analysis is resembling to the Bayesian analysis. Bootstrap support values for ML equal or greater than 90% and Bayesian posterior probabilities greater than 0.90 are given near nodes respectively. The tree is rooted with *Hypocrea aurantefussa* (CBS 119284) and *Nectria pseudotrichia* (CBS 641.83). Newly generated sequences are in red and the type strains are in bold.

Figure 4.93 The best maximum likelihood tree for *Corynascus* is presented. The phylogenetic tree constructed from maximum likelihood analysis based on the combined ITS, *tef1-α* and *rpb*2 sequence 35 strains are included in the combined sequence analysis, which comprised 2616 characters with gaps.

Corynascus fluvialis Bhagya, Phukhams., K.D. Hyde & E.B.G. Jones, sp. nov

Index Fungorum number: IF 903990; Facesoffungi number: FoF 17785

Etymology – Based on the habitat of the host.

Holotype – MFLU 25-0196

Saprobic on dead, moist, decaying stems of *Carex* (Cyperaceae). **Sexual morph**: *Ascomata* 110–150 ($\bar{x}$ = 124 μm, n = 5), cleistothecial, scattered, loosely aggregated or gregarious, superficial on host surface, dark brown, to black or olivaceous, globose to subglobose, smooth, and coriaceous. *Peridium* 1–3 μm ($\bar{x}$ = 1.5 μm, n = 5) composed of olivaceous brown cells in *textura epidermoidea*. *Paraphyses* 12–25 ×1–2.5 μm ($\bar{x}$ = 18.5 ×1.5 μm, n = 5), filiform, aseptate, hyaline, shorter than the asci. *Asci* 25–38 × 22–35 μm ($\bar{x}$ = 35 × 28 μm, n = 10), 8-spored, unitunicate, globose, subglobose to pyriform or broadly clavate, thin-walled, caudate with short cylindrical to angular pedicel, evanescent. *Ascospores* 12–18 × 6–10 μm ($\bar{x}$ = 14.5 × 8.5 μm, n = 30), overlapping, biseriate to tri-seriate or variably arranged, ellipsoidal or broadly fusiform, straight, aseptate, hyaline when immature, olivaceous-green when mature, thick, smooth-walled, pointed towered end, with one germ pore at apex. **Asexual morph**: Undetermined.

Culture characteristics: Ascospore germinating on MEA within 72 h. Germ tubes are produced from the apical ends of the ascospores. Colonies growing on MEA, reaching 20 mm in 4 weeks at 25°C. Mycelia superficial, umbonate with a complete edge, from above light grey at the canter, off white to hyaline towards edge, from reverse dark greenish ash from the canter surrounded with off-white ring at the edge.

Material examined: Thailand, Prachuap Khiri Khan Province, Pran Buri District, Pranburi river, on decaying leaf of *Carex* sp. (Cyperaceae), 25 August 2023, Tharindu Bhagya, TB130 (MFLU25-0196, holotype); ex-type living culture (MFLUCC 25-0235); *ibid.*, TB130B (MFLU25-0197, isotype).

GenBank numbers – MFLU 25-0196: - ITS = PV764283, *rpb2* = PV799940, *tef1α* = PV799942, MFLU 25-0197: ITS = PV764282, *rpb2* = PV799941

Distribution – Decaying leaf of *Carex* sp. (Cyperaceae), Prachuap Khiri Khan Province, Pran Buri District, Pranburi river, Thailand.

Notes – The newly isolated strain clustered with *Corynascus novoguineensis* (CBS 359.72 and NBRC 9556) with 89% ML and 0.90 BYPP support (Figure 4.93).

Strain MFLUCC 25-0235 shares common characteristics with *Corynascus*, including cleistothecial ascomata, a peridium composed of cells in *textura epidermoidea*, and fusiform ascospores (Marin-Felix et al., 2015; Crous et al., 2016). Phylogenetically, the new strain differs from the *C. novoguineensis* type strain (CBS 359.72) by 2.8% in ITS, 3.2% in *tef1-α*, and 4.4% in *rpb2*, base pairs excluding gaps. Morphologically, the new isolate is distinguishable from *C. novoguineensis* (CBS 359.72 and NBRC 9556) by possessing a smooth ascomatal wall, asci with cylindrical to angular pedicel and hyaline immature ascospores that change to olivaceous-green at maturity. In comparison, *C. novoguineensis* (CBS 359.72 and NBRC 9556) develops a verrucous ascomatal wall and pinkish immature ascospores. The presence of hyaline, filiform paraphyses makes the new isolate unique among related taxa in the genus *Corynascus* (Figure 4.94) (Marin-Felix et al., 2015; Crous et al., 2016). Considering the available morphological and phylogenetic evidence, I introduce *C. fluvialis* (MFLUCC 25-0235) as a new species from freshwater wetlands in Thailand.

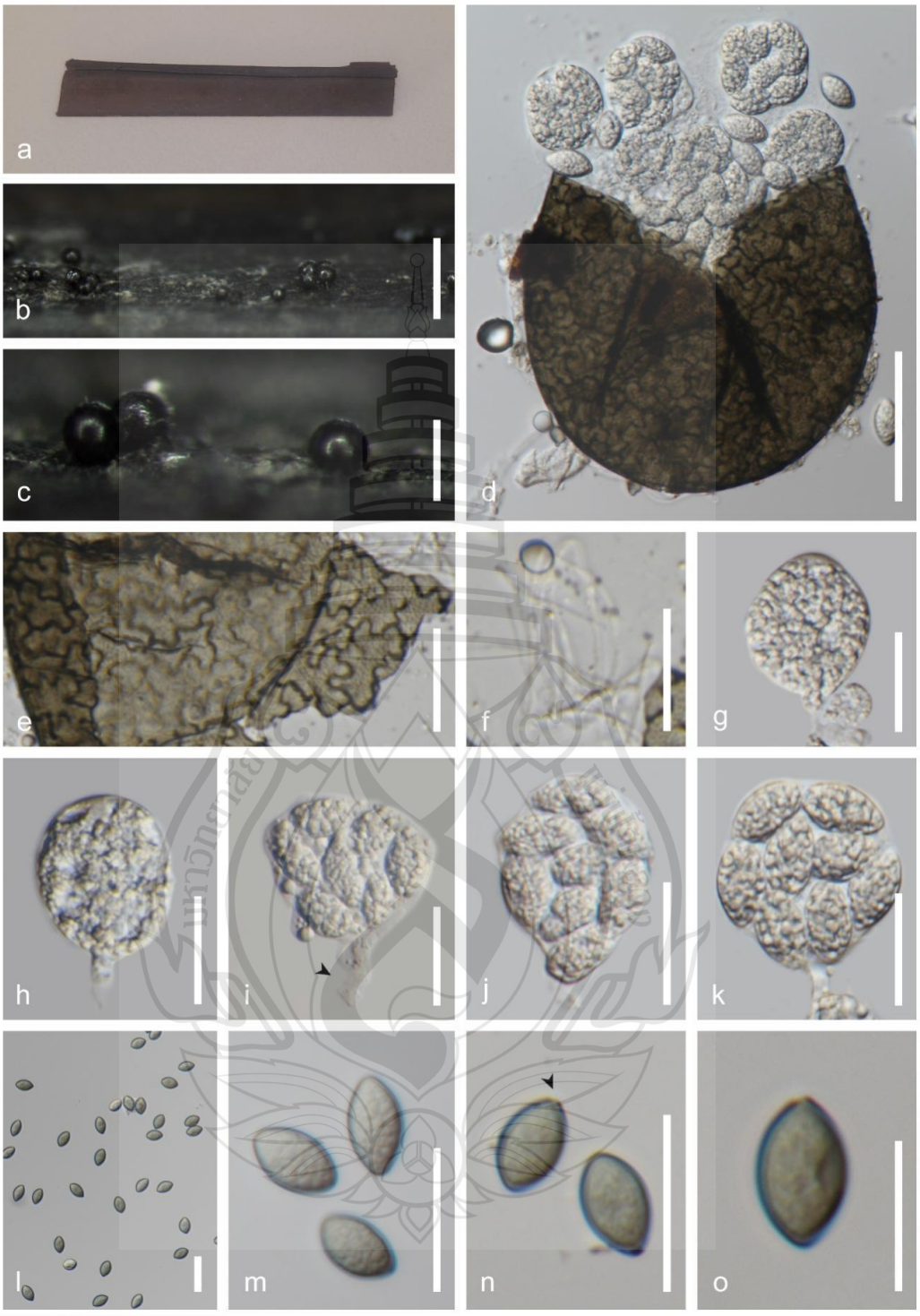

Note a *Carex* sp. host material. b–c Superficial ascomata. d Squash mount of ascoma. e Peridium. f Paraphysis mounted in lactoglycerol. g–k Ascus development with angular pedicel (arrowed). l–o Ascospores with single apical germ pore (arrowed). Scale bars: d 250 µm, c 100 µm, d 50 µm, e–n 20 µm, o 10 µm.

Figure 4.94 *Corynascus fluvialis* (MFLU 25-0196, holotype)

Lasiosphaeriaceae Nannf

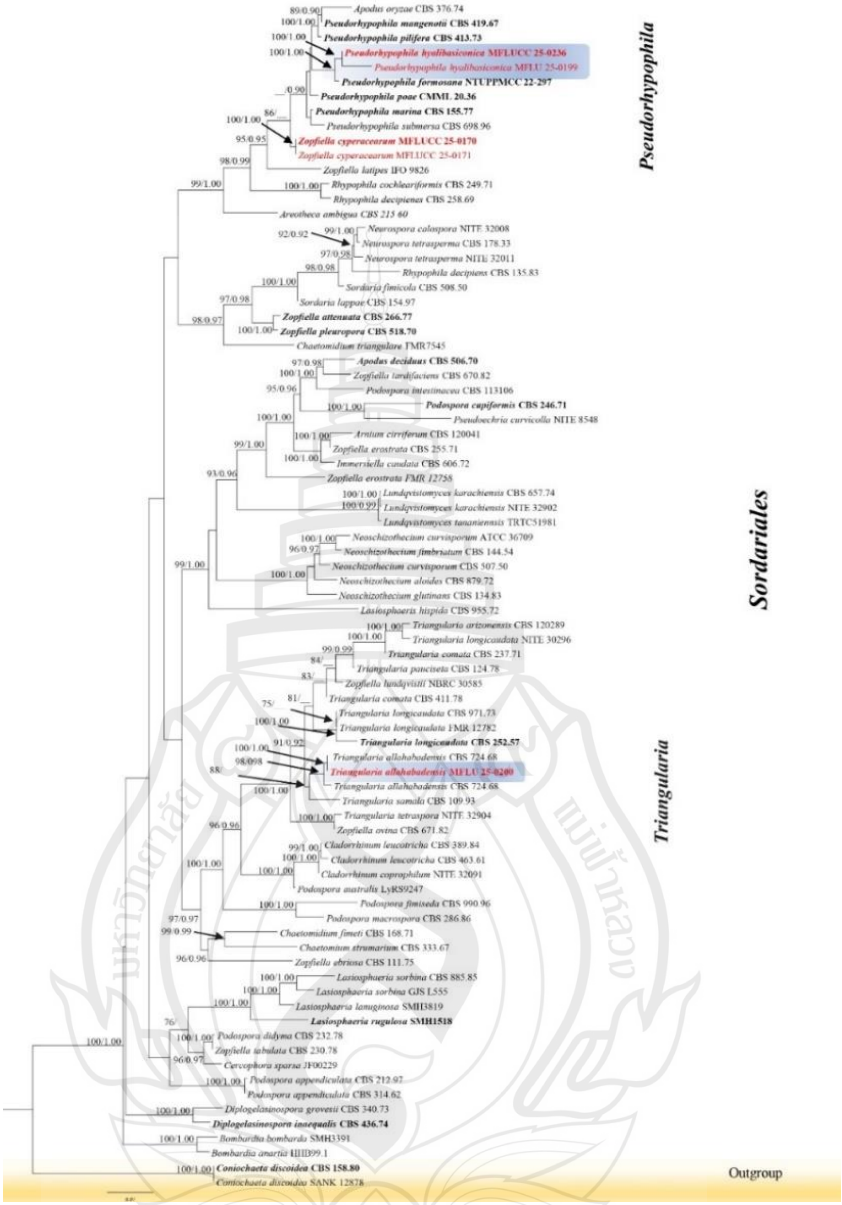

Note The phylogenetic tree constructed from maximum likelihood analysis based on the combined LSU, ITS, *tub2* and *rpb2* sequence 81 strains are included in the combined sequence analysis, which comprised 3578 characters with gaps. The tree topology of the maximum likelihood analysis is similar to the Bayesian analysis. Bootstrap support values for ML equal or greater than 75% and Bayesian posterior probabilities greater than 0.90 are given near nodes respectively.

Figure 4.95 The best maximum likelihood tree tree represents for *Triangularia allahabadensis*, *Pseudorhypophila hyalibasiconica* and *Zopfiella cyperacearum.*

Zopfiella G. Winter

Zopfiella was introduced by Winter in 1884 (Rabenhorst 1889) and typified by *Zopfiella tabulata* (Maharachchikumbura et al., 2015; Wijayawardene et al., 2022). *Zopfiella* was initially placed in the family *Chaetomiaceae* and later transferred to *Lasiosphaeriaceae* (Cai et al., 2006; Morgenstern et al., 2012). The characteristics of *Zopfiella* align with the concept of *Lasiosphaeriaceae*. Species in this genus produce cleistothecial ascomata, evanescent, cylindrical or clavate asci, and 8 ellipsoidal, guttulate ascospores with germ pores, with a hyaline base cell that may deliquesce at ascospore maturity, and a dark apical cell (Cai et al., 2006; Marin-Felix et al., 2020). Guarro et al., (1997) observed the asexual morph of *Z. latipes* which produced a humicola-like anamorph under sterile conditions.

Zopfiella cyperacearum Bhagya, Phukhams., K.D. Hyde & E. B. Gareth Jones, sp. nov.

Index Fungorum number: IF 903321; Facesoffungi number: FoF 16315

Etymology – Based on the host family, Cyperaceae

Holotype – MFLU 24–0130

Saprobic on dead, moist, decaying leaf of a sedge appearing as black spherical globules loosely adhering to the host tissue. **Sexual morph**: *Ascomata* 160–250 μm in diameter ($\bar{x}$ = 220 μm, n = 5), cleistothecial, solitary or gregarious, scattered, superficial, globose, black, smooth-walled, lacking an ostiole. Peridium 7–8 μm wide ($\bar{x}$ =7.6 μm, n = 10), relatively thin, single-layer comprising dark brown to light browncells of *textura angularis* and *textura intricata*. *Paraphyses* 2–5 μm wide ($\bar{x}$ = 3.5 μm, n = 20), tube-like, cellular paraphyses, hyaline, aseptate. *Asci* 100–120 × 15–20 μm ($\bar{x}$ = 112 × 16 μm), 8-spored, unitunicate, evanescent, cylindrical to subcylindrical or clavate, short pedicellate with nonamyloid (J-) apices. *Ascospores* upper cell, 18–24 × 11–14 μm ($\bar{x}$ = 21.5 × 12.5 μm, n = 20), fusiform or narrowing towards apex, apiculate, hyaline when young, greenish-brown to dark brown at maturity, aseptate, smooth-walled; basal cell 2–3.5 × 3–4 μm ($\bar{x}$ = 2.5 × 3.2 μm, n = 10), semi-curricular, deliquescing, pedicel-like, hyaline, narrowing to blunt base. **Asexual morph**: Undetermined.

Culture characteristics: Ascospores germinating on malt extract agar (MEA) within 24 h. Germ tube produced from the tip of the ascospore. Colonies growing on

MEA, reaching 20–25 mm in 4 weeks at 25°C. Mycelia superficial, dense, cotton surfaces, flat or effuse with fimbriate nature at the edge, from above pale white from centre to the edge, from reverse orangey yellow at the centre, fading towered the edge.

Material examined: Thailand, Prachuap Khiri Khan Province, Pran Buri District, Pran Buri Wetland, on leaf of aquatic *Cyperus* sp. (Cyperaceae), 25 January 2023, Tharindu Bhagya, TB42 (MFLU 24-0130, holotype), ex-type living culture, MFLUCC 25– 0170; same location and collection details, TB42B (MFLU 24-0131, isotype), ex-isotype living culture, MFLUCC 25–0171.

GenBank numbers – MFLUCC 25-0170: ITS = PQ120587, LSU = PQ120588, *rpb2* = PQ351350, *tub2* = PV170919, MFLUCC 25-0171: ITS = PQ120590, LSU = PQ120589, *rpb2* = PQ351351

Distribution – Decaying leaf of *Carex* sp. (Cyperaceae), Prachuap Khiri Khan Province, Pran Buri District, Pranburi wetland, Thailand.

Notes – The multi-locus phylogenetic analysis illustrates the separation of *Zopfiella cyperacearum* as a distinct taxon, forming a sister clade to *Z. latipes* (IFO 9826) with strong support (100% ML and 1.00 PP) (Figure 4.95). The base pair similarity between *Z. cyperacearum* MFLUCC 25–0170 and *Z. latipes* IFO 9826 was 92.06% for the ITS locus, 97.27% for the LSU locus, and 77.73% for the *tub2* locus (Jeewon & Hyde, 2016). *Zopfiella cyperacearum* aligns with the general description of *Zopfiella*. The strain *Z. cyperacearum* MFLU 24–0130 has cleistothecial ascomata with evanescent asci that are clavate to cylindrical, lacking an apical apparatus. Ascospores are ellipsoidal with hyaline, deliquescing, basal cell (Cai et al., 2006; Phookamsak et al., 2019). *Zopfiella cyperacearum* differs from *Z. latipes* (IFO 9826) in lacking the hyaline, flexuous, ascomatal hairs on cleistothecial ascomata. *Zopfiella latipes* (IFO 9826) produces larger ascomata (diameter range 0.5–1.0 mm) compared to *Z. cyperacearum* (MFLUCC 25–0170) (diameter range 160–250 μm) (Malloch & Cain, 1971; Calaça and Xavier-Santos, 2016). Additionally, *Z. latipes* IFO 9826 has relatively larger hyaline cells in its ascospores (length (L)/width (W) ratio = 1.14) than *Z. cyperacearum* MFULUCC 24-0170 (L/W) ratio = 0.88). *Zopfiella cyperacearum* shares some morphological features with *Z. submersa* (CBS 698.96) but differs in lacking pale brown setae on the ascomata. *Zopfiella submersa* (CBS 698.96) produce relatively larger ascomata (maximum 470 μm diameter) than *Z. cyperacearum*

(maximum 250 μm diameter) (Figure 4.96) (Guarro et al., 1997). Paraphyses in *Z. submersa* (CBS 698.96) were not reported in the original description, whereas *Z. cyperacearum* MFLUCC 25–0170 has hyaline, aseptate paraphyses. In our analysis, *Z. indica* (NFCCI-4217) was due to its uncertain placement within the phylogenetic tree (Phookamsak et al., 2019). Based on both morphological and phylogenetic evidence, I introduce *Zopfiella cyperacearum* as a new species of *Zopfiella*, following the guidelines of Maharachchikumbura et al. (2021).

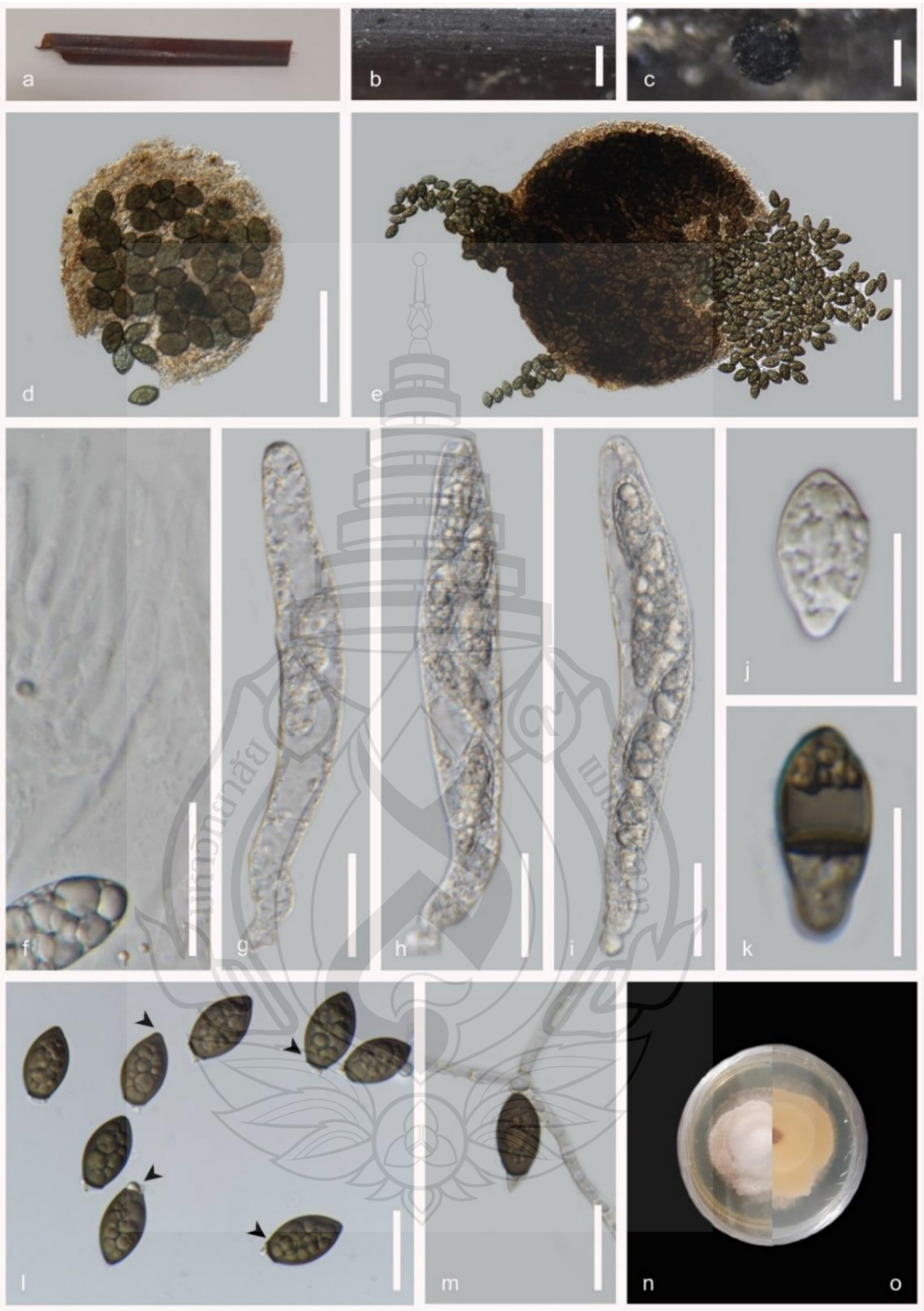

Note a Host. b–c, Black ascomata on the surface. d–e Ascomata in water. f Paraphyses. g–i Asci. j–l Ascospores with a pedicel-like hyaline cell and dark septum at the base cells (arrowed). m Germinating ascospore. n Culture on MEA above. o Reverse. Scale bars: b 200 µm, c–e 100 µm, d 50 µm, f–m 20 µm.

Figure 4.96 *Zopfiella cyperacearum* (MFLU 24–0130, holotype)

Naviculisporaceae Y. Marin & Stchigel

Pseudorhypophila Y. Marín & Stchigel

Pseudorhypophila was proposed by Y. Marín (2021) by synonymising *Triangularia mangenotii* under *Pseudorhypophila* as *P. mangenotii* (CBS 419.97). Members of *Pseudorhypophila* are characterized by superficial or immersed, globose, subglobose, ovate to pyriform, black or dark brown ascomata covered with flexuous hairs, clavate to cylindrical asci that bear either 4 or 8 ascospores and occasionally possess inconspicuous apical ring at each ascus. Ascospores are predominantly 2-celled, upper cells are usually larger, olivaceous brown to dark brown, ovoid to limoniform and truncate at the base. Some species have subapical germ pores or with distinct apical appendages. Lower cells of the ascospores are hyaline, pale olivaceous brown or pale brown, cylindrical and straight or curved, or hemispherical. Asexual morphs of *Pseudorhypophila* exhibit spherical to ovate to elongate, hyaline conidia that originate directly from the vegetative hyphae (Harms et al., 2021).

Pseudorhypophila hyalibasiconica Bhagya, Phukhams., K.D. Hyde & E.B.G. Jones, sp. nov.

Index Fungorum number: IF 903989; Facesoffungi number: FoF 17786

Etymology – Based on the ascospore morphology

Holotype – MFLU 25-0198

Saprobic on dead and decaying leaf of a *Carex* sp., appearing as black spherical globes loosely attached to the host tissue. **Sexual morph**: *Ascomata* 300–450 μm ($\bar{x}$ = 320 μm, n = 5) cleistothecial, gregarious in aggregation, scattered on the host, superficial on host surface, globose, black, smooth-walled, non-ostiolate, covered with hyaline to light brown flexuous ascomatal hairs. *Peridium* 15–20 μm wide ($\bar{x}$ = 18 μm, n = 10), relatively thin, single–layer comprising black to light brown cells of *textura angularis* and *textura intricata*. *Paraphyses* not observed. *Asci* 90–150 × 20–28 μm ($\bar{x}$ = 112 × 24 μm), 8-spored, unitunicate, highly evanescent, cylindrical to subcylindrical or clavate, long pedicellate with nonamyloid (J-) apices. *Ascospores* 24–30 × 12–14 μm ($\bar{x}$ = 25.5 × 13.5 μm, n = 20), uniseriate or overlapping biseriate, upper cell, 17–22 × 11–14 μm ($\bar{x}$ = 19.5 × 12.5 μm, n = 20), fusiform, narrowing towards apex, apiculate, ovoid to limoniform, hyaline when young, greenish-brown to dark brown at maturity, aseptate, smooth-walled; basal cell 5–7 × 4–6 μm ($\bar{x}$ = 5.5 × 5.2 μm,

n = 10), limoniform when young, conical when maturity, deliquescing, pedicel-like, hyaline, originating at the base, narrowing to blunt base. **Asexual morph**: Undetermined.

Material examined: Thailand, Chang Wat Prachuap Khiri Khan Province, Pran Buri District, Pranburi river, on decaying leaf of *Carex* sp. (Cyperaceae), 25 August 2023, Tharindu Bhagya, TB125 (MFLU 25-0198, holotype); ex-type living culture, MFLUCC 25-0236; *ibid.*, TB125B (MFLU 25-0199, isotype).

GenBank numbers: MFLU 25-0198: ITS = PV764279, LSU = PV764280, *rpb2* = PV786267, *tub2* = PV799943, MFLU 25-0199: ITS = PV764278, LSU = PV764281, *rpb2* = PV786268

Distribution – Decaying leaf of *Carex* sp. (Cyperaceae), Prachuap Khiri Khan Province, Pran Buri District, Pranburi river, Thailand.

Notes – *Pseudorhypophila hyalibasiconica* (MFLUCC 25-0236) clustered with *Ps. formosana* (NTUPPMCC 22-297) with 100% ML and 1.00 BYPP statistical support (Figure 4.95). The new isolate agrees with the general description of *Pseudorhypophila* by possessing globose, subglobose ascomata with flexuous ascomata hairs, unitunicate asci with inconspicuous apical rings and 2-celled ascospore with olivaceous brown to dark brown, ovoid to limoniform upper cells and hyaline, pale olivaceous smaller lower cell (Figure 4.97) (Harms et al., 2021). *Pseudorhypophila hyalibasiconica* (MFLUCC 25-0236) is phylogenetically different from *Ps. formosana* (NTUPPMCC 22-297) with 3.28% in ITS, 1.01% in LSU, 7.32% in *tub2* and 8.19% for the *rpb2* in base pairs with gaps. *Pseudorhypophila mangenotii* is separated from other species based on the presence of an ostiole in the ascomata, while *P. pilifera* and *P. marina* are distinguishable from each other based on the shape of the basal cell of the ascospore (Harms et al., 2021). *Pseudorhypophila hyalibasiconica* (MFLUCC 25-0236) is distinguishable from closely related *Ps. formosana* (NTUPPMCC 22-297), and *Ps. mangenotii* (CBS 419.97) by possessing non-ostiolate, cleistothecial ascomata and *Ps. pilifera* (CBS 413.73) by ovoid to limoniform upper cells and conical lower cell at maturity. *Pseudorhypophila* currently comprises five species, with this study introducing *Ps. hyalibasiconica a*s the sixth species from Thailand (Harms et al., 2021; Cheng et al., 2025).

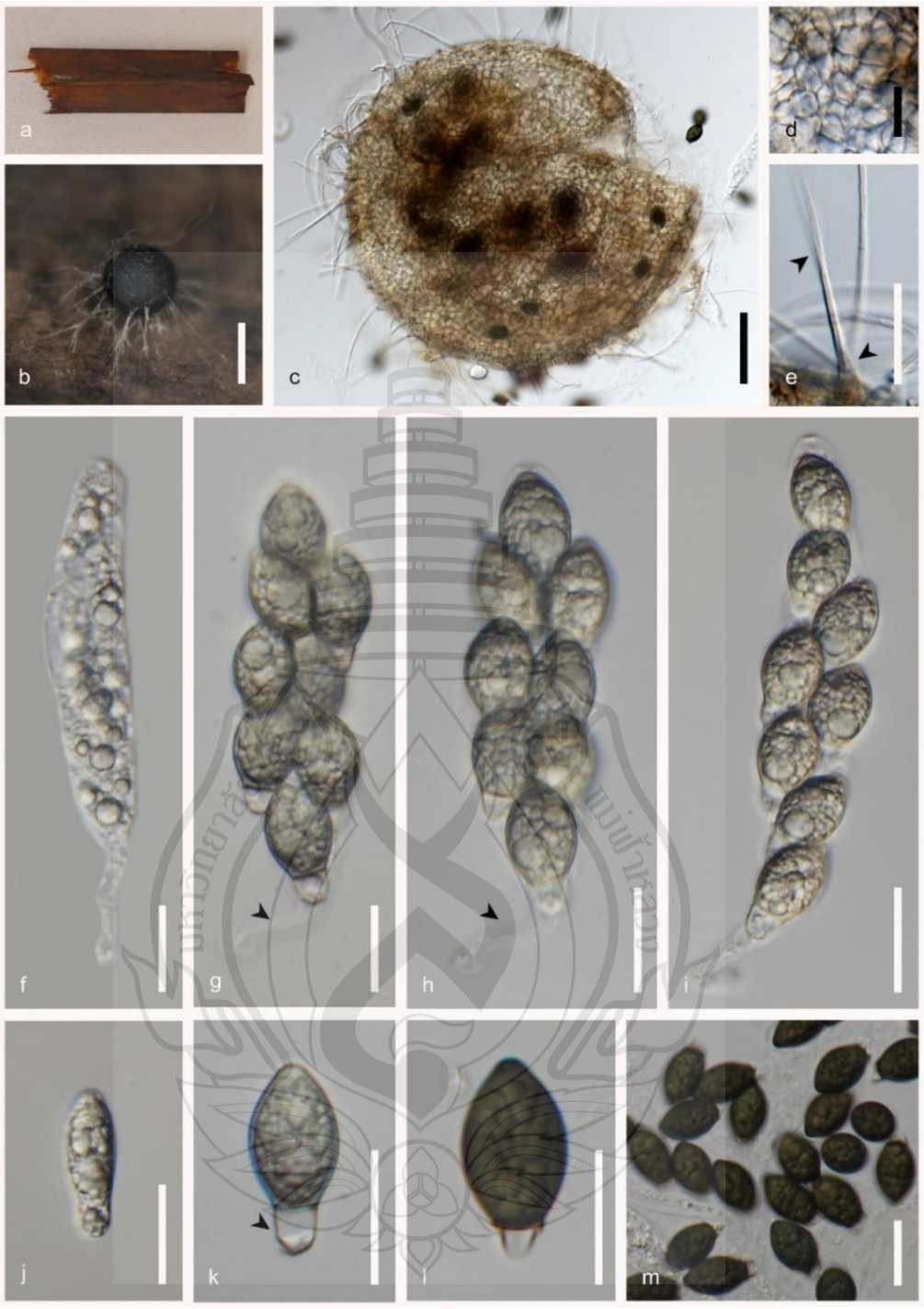

Note a *Carex* sp. host material. b Black spherical cleistothecial ascoma on the host. c Squashed mount of ascoma. d Surface of peridium. e Ascomatal hairs originating directly from peridium cells (arrowed). f–i Asci with long curved pedicel (arrowed). j–m Ascospores with hyaline basal cell (arrowed). Scale bars: b 500 µm, c 50 µm, d–m 20 µm.

Figure 4.97 *Pseudorhypophila hyalibasiconica* (MFLU 25-0198, holotype)

Schizotheciaceae Y. Marin & Stchigel

Triangularia Boedijn, Ann.

Triangularia was introduced by Boedijn (1934), typified by *T. bambusae*. According to the current classification, the genus resides under *Schizotheciaceae*, *Sordariales*, *Sordariomycetidae* (Wang et al., 2019; Marin-Felix et al., 2020; Hyde et al., 2024). Members of the genus *Triangularia* are distinguishable from closely related taxa by possessing cylindrical to clavate asci with a prominent apical ring, predominately 1-sepate or aseptate, smooth ascospores, which consist of relatively large pigmented, conical or triangular upper cell and hyaline to sub-hyaline and triangular to hemispherical lower cell. The gelatinous appendages are yet to be observed in the genus (Wang et al., 2019; Marin-Felix et al., 2020).

Triangularia allahabadensis (M.P. Srivast., Tandon, Bhargava & A.K. Ghosh) X. Wei Wang & Houbraken.

Saprobic on dead and decaying leaf of a *Carex* sp. (Cyperaceae), appearing as black spherical globes loosely attached to the host tissue. **Sexual morph**: *Ascomata* 380–520 μm ($\bar{x}$ = 410 μm, n = 5) scattered on the host, superficial, perithecial, subglobose or ampulliform, carbonaceous, papillated, black, smooth-walled, with short ostiole, covered with hyaline to light brown ascomatal hairs. *Peridium* carbonaceous, black to greenish-brown cells of *textura angularis*. *Paraphyses* 120–180 × 2–4 μm ($\bar{x}$ = 142 × 2.5 μm) smooth-walled, hyphae-like and septate. *Asci* 90–160 × 15–22 μm ($\bar{x}$ = 135 × 19 μm), 8-spored, fasciculate, unitunicate, evanescent, cylindrical to subcylindrical or clavate, short pedicellate with a nonamyloid apex. *Ascospores* upper cell, 24–32 × 8–12 μm ($\bar{x}$ = 28.5 × 9.5 μm, n = 20), fusiform or semi-spheroid, narrowing towards the apices, apiculate, hyaline when young, greenish-brown to dark brown at maturity, aseptate, coarse at maturity; immature spores process a basal cell that is evanescent and disappears at spore maturity; basal cell 9–16 × 2–4 μm ($\bar{x}$ = 13.2 × 3.5 μm, n = 10), semi-curricular, pedicel-like, hyaline, originating at the base, narrowing to the pointed base. **Asexual morph**: Undetermined.

Material examined: Thailand, Chang Wat Prachuap Khiri Khan Province, Pran Buri District, Pranburi river, on decaying leaf of *Carex* sp. (Cyperaceae), 25 August 2023, Tharindu Bhagya, TB127 (MFLU 25-0200).

GenBank numbers: MFLU 25-0200: ITS = PV759786, LSU = PV759787, *rpb2* = PV779203, *tub2* = PV786266

Distribution – Decaying leaf of *Carex* sp. (Cyperaceae), Prachuap Khiri Khan Province, Pran Buri District, Pranburi river, Thailand.

Notes – The isolate MFLU 25-0200, clusters sister to *Triangularia allahabadensis* CBS 724.68 with 100% ML and 1.00 BYPP bootstrap support (Figure 4.95). MFLU 25-0200 has general morphological characters of *Triangularia* in producing ostiolate and ovoid, obpyriform to ampulliform, globose ascomata, cylindrical to elongated or clavate asci, septate ascospores with larger pigmented, conical or triangular upper cell and triangular to hemispherical, paler lower cell (Wang et al., 2019; Marin-Felix et al., 2020). The new isolate collected from *Carex* species, shares significant morphological similarities with the sister taxon, *T. allahabadensis* (CBS 724.68) including fasciculate, cylindrical, subcylindrical or clavate asci that lack a conspicuous apical ring, and fusiform, dark to greenish-brown ascospores with evanescent smaller basal cells (Figure 4.98) (Wang et al., 2019; Marin-Felix et al., 2020). Considering available morphological and phylogenetic evidence I recognize MFLU 25-0200 as a new strain of *Triangularia allahabadensis*. Therefore, we document the first report of *T. allahabadensis* from *Carex* sp. (Cyperaceae) collected in Thailand.

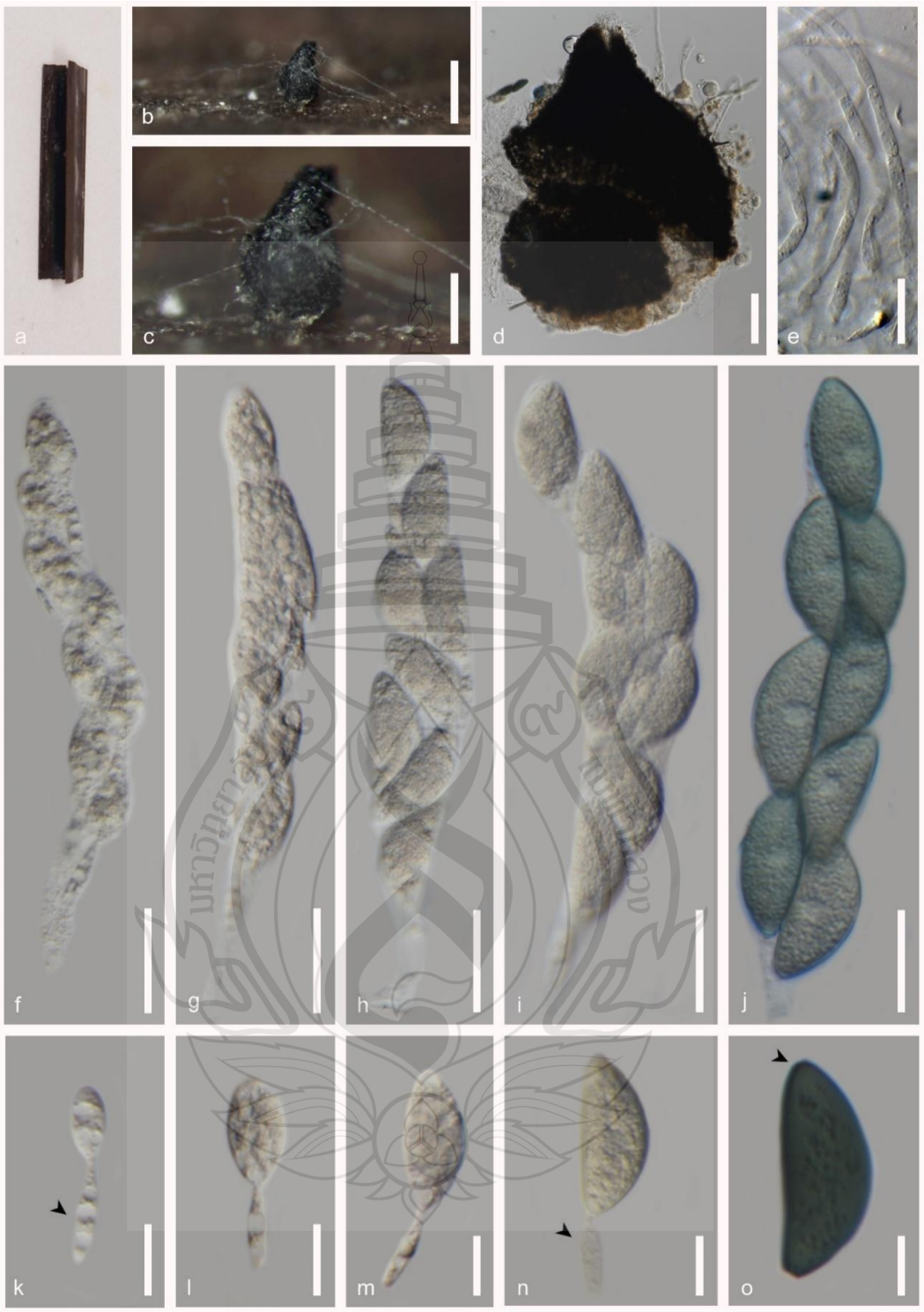

Note a *Carex* sp. host material. b–c Black ascoma. d Squashed mount of ascoma. e Hyphae-like paraphyses. f–j, immature and mature asci. j–m Ascospores with hyaline base cell disappearing at spore maturity (arrowed). Scale bars: b 500 µm, c 250 µm, d 50 µm, e–j 20 µm, k–o 10 µm.

Figure 4.98 *Triangularia allahabadensis* (MFLU 25-0200)

Sporidesmiales Crous, Persoonia 40: 377 (2018)

Sporidesmiaceae Fr. [as ‘Sporidemsiacei’], Summa veg. Scand., Sectio Post. (Stockholm): 504 (1849)

Sporidesmium Link, Mag. Gesell. naturf. Freunde, Berlin 3(1-2): 41 (1809)

Sporidesmium is a genus introduced by Link in 1809 and typified by *Sporidesmium ehrenbergii*. Members of the genus are saprobic organisms, primarily recovered from aquatic environments or associated with aquatic ecosystems (Hyde et al., 2016; Liu et al., 2019; Calabon et al., 2023). Members of the genus *Sporidesmium* are characterized by dark brown to pale brown colonies that develop either solitarily or loosely on the host. The monoblastic conidiogenous cells produce conidia that are pale brown to dark brown, occasionally olivaceous, and may be cylindrical, fusiform, obclavate, obpyriform, or rarely rostrate. The conidia typically have truncate bases and are sometimes ornamented or hyaline at the apex. (Hyde et al., 2016; Su et al., 2016; Liu et al., 2019; Dong et al., 2024).

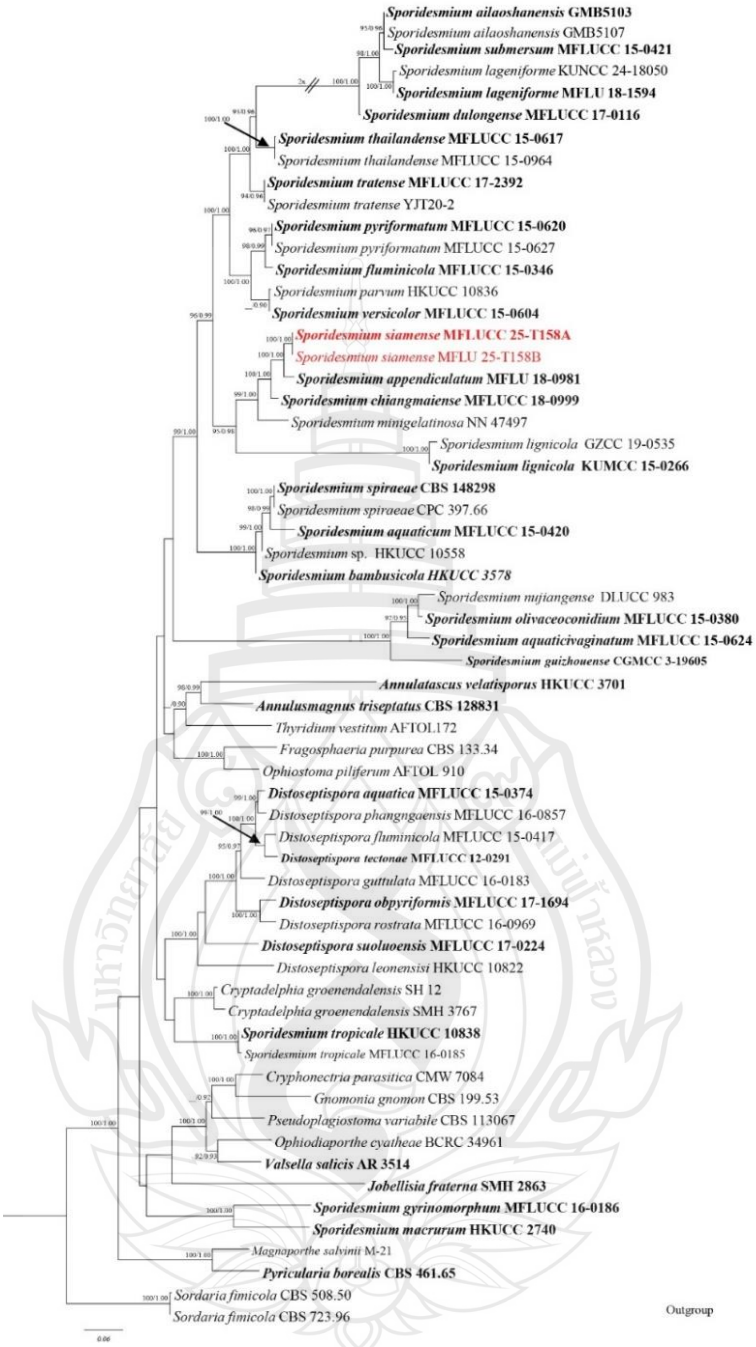

Note The data set comprises 5022 characters including gaps from of 61strains which were included in the analyses. Bootstrap support values for ML ≥ 90 % and Bayesian posterior probabilities (BPP) ≥ 0.9 are mentioned at the nodes. The tree was rooted *Sordaria fimicola* (CBS 508.50 and CBS 723.96). Newly generated sequences are in red and the type strains are in bold.

Figure 4.99 Phygenetic tree generated from Maximum Likelihood (ML) analysis based on combined LSU, SSU, ITS, *tef1-α*, and *rpb2* sequence.

Sporidesmium siamense, Bhagya, Phukhams E.B.G. Jones & K.D. Hyde, sp. nov.

Index Fungorum number: IF; Facesoffungi number: FoF 18915

Etymology – The name reflects the nation of Thailand (Siyam), from which the species was isolated.

Holotype – MFLU 25-0488

Saprobic on dead, decaying stems of *Typha* sp. (Typhaceae), **Sexual morph:** Undetermined. **Asexual morph*:*** *Hyphomycetous*. *Colonies* black, superficial, hairy, effuse, gregarious on host tissue. *Mycelium* 2–3 × 1.5–2.5 µm ($\bar{x}$ = 2.5 × 2.0 µm, n = 10), partly immersed, composed of septate, thin-walled, brown to light brown, hyphae. *Conidiophores* 50–80 × 3–5 µm ($\bar{x}$ = 72 × 4.0 µm, n = 10), macronematous, mononematous, erect, smooth walled, unbranched, brown to dark brown, septate, constricted at the septate close to apex, cylindrical with narrowed apex, straight or slightly flexuous, with robust wide base. *Conidiogenous cells* 7–9 × 4–6 µm ($\bar{x}$ = 8.5 × 5.0 µm, n = 10), holoblastic, monoblastic, integrated, determinate, terminal, brown to dark brown, smooth walled, cylindrical with narrow apex or obclavate to aphelform. *Conidia* 45–55 × 12–18 µm ($\bar{x}$ = 48 × 15 µm, n = 10), acrogenous, solitary, thin-walled, smooth-walled, straight or curved, hyaline to olivaceous when immature, pale brown to brown at maturity, 8–10-distoseptate, with or without guttules, obclavate with truncate darker base, tapering towards apex, process hyaline cuneiform apical cells 12–16 × 4–5 µm ($\bar{x}$ = 14.5 × 4.5 µm, n = 10) with hyaline gelatinous sheath at terminus.

Culture characteristics: Conidia germinating on MEA within 48 h. Germ tubes produced from side. Colonies growing on MEA, reaching 20 mm in 3 weeks at 25°C. Mycelia superficial, effuse to flat or undulate, from above pale white from center to the complete edge, from reverse light brown to brownish yellow at the center, yellowish white to hyaline edge.

Material examined: Thailand, Chang Wat Prachuap Khiri Khan Province, Pran Buri District, Pran Buri Wetland, on decaying stems of *Typha* sp. (Typhaceae), 06 April 2024, Tharindu Bhagya, T145A (MFLU 25-0488, holotype). *ibid.,* T145B (MFLU 25-0489)

GenBank numbers – MFLU 25-0488: ITS = PX062191, LSU = PX062192

Distribution – Decaying *Typha* sp. stem and peduncle in freshwater wetland, Thailand.

Notes – The new cluster sister to *Sporidesmium appendiculatum* strain MFLU 18-0981, with 100% ML and 0.98 BPP support (Figure 4.99). *poridesmium siamense* (MFLU 25-0488) differs from *S. appendiculatum* (MFLU 18-0981) by 3.58% in the ITS sequence, without gaps. Morphologically, the new isolate is distinguishable from *S. appendiculatum* strain MFLU 18-0981 by possessing a hyaline cuneiform apical cell and lacking hyaline hypha-like appendages at the apexes (Figure 4.100) (Liu et al., 2019; Dong et al., 2024). *Sporidesmium aquaticivaginatum* (MFLUCC 15-624), *S. guizhouense* (CGMCC 3.19605), *S. olivaceoconidium* (MFLUCC 15-380), and *S. minigelatinosum* share similar morphological characteristics with the newly isolated *S. siamense* (MFLU 25-0488). *Sporidesmium aquaticivaginatum* (MFLUCC 15-624), *S. guizhouense* (CGMCC 3.19605), and *S. olivaceoconidium* (MFLUCC 15-380) cluster in a distinct clade from *S. siamense* (MFLU 25-0488), indicating that new isolate (MFLU 25-0488) is phylogenetically distinct from them (Hyde et al., 2016; Su et al., 2016; Liu et al., 2019; Dong et al., 2024). *Sporidesmium siamense* (MFLU 25-0488) develops longer and wider conidia than *S. minigelatinosum* (45–55 × 12–18 μm vs. 36–50 × 6–8 μm). Additionally, *S. minigelatinosum* lacks hyaline cuneiform apical cells, making the new strain distinguishable (Matsushima 1971). Considering the available phylogenetic and morphological evidence, I recognize *S. siamense* (MFLU 25-0488) as a new species within the genus *Sporidesmium*, from Thailand's freshwater wetlands.

Note a *Typha* sp. host. b–c Conidiophores on the host surface with conidia. d–e Conidiophores. f–g Conidiophores with attached conidia. h–j Conidia development with cuneiform apical cells. k Culture on MEA above. l Reverse. Scale bars: b–c) 250 µm, d–j 20 µm.

Figure 4.100 *Sporidesmium siamense* (MFLU 25-0488, holotype)

Xylariomycetidae O.E. Erikss. & Winka

Amphisphaeriales D. Hawksw. & O.E. Erikss

Sporocadaceae Corda

Pestalotiopsis Steyaert, Bull. Jard. bot. État Brux.

Pestalotiopsis is a large genus in the family *Sporocadaceae*, class *Sordariomycetes*, and exhibits a cosmopolitan distribution. This asexual morph-dominated genus was introduced by Steyaert (1949) and has been reported as comprising endophytes, opportunistic pathogens, and saprobes on a variety of host plants (Maharachchikumbura et al., 2011, 2012, 2014; Tibpromma et al., 2018; Luo et al., 2024). The sexual morphs of *Pestalotiopsis* are characterized by immersed, subglobose to globose ascomata, bearing unitunicate, cylindrical, J+ asci with a short pedicel. Ascospores in *Pestalotiopsis* are yellowish-brown, unicellular, and oblong to ellipsoidal or fusiform (Maharachchikumbura et al., 2016). Conidiomata produced by members of the genus *Pestalotiopsis* are acervular to pycnidial and subglobose to globose in shape. Conidiophores are hyaline, smooth, predominantly branched and septate, or reduced to conidiogenous cells. The conidiogenous cells are hyaline, smooth, discrete, ampulliform to lageniform or cylindrical, holoblastic, and exhibit percurrent proliferation. Conidia in *Pestalotiopsis* species are fusoid, ellipsoid, or subcylindrical, 4–5-septate, bearing apical appendages, with hyaline to subhyaline cells at the apexes (Maharachchikumbura et al., 2011, 2012, 2014, 2016; Tibpromma et al., 2018; Luo et al., 2024).

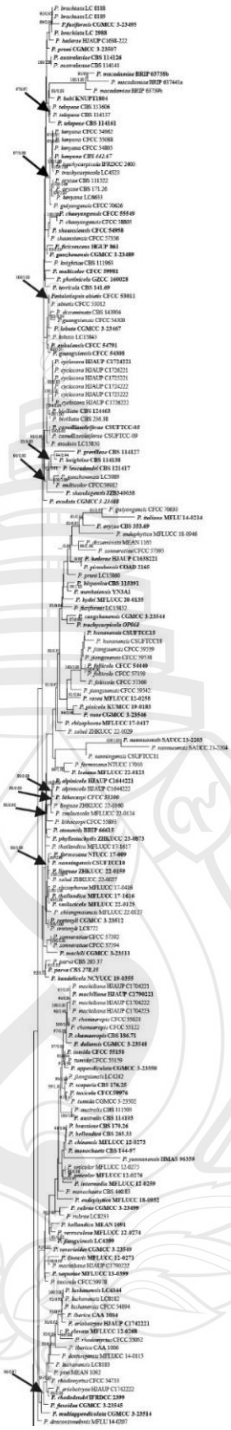

Note Bootstrap support values for ML ≥ 90 % and Bayesian posterior probabilities (BPP) ≥ 0.9 are mentioned at the nodes.

Figure 4.101 Phylogram generated from Maximum Likelihood (ML) analysis based on combined ITS, *tef1-α*, and *tub2* sequence data of 268 strains of genus *Pestalotiopsis*, which comprise 2538 characters including gaps, are included in the analyses.

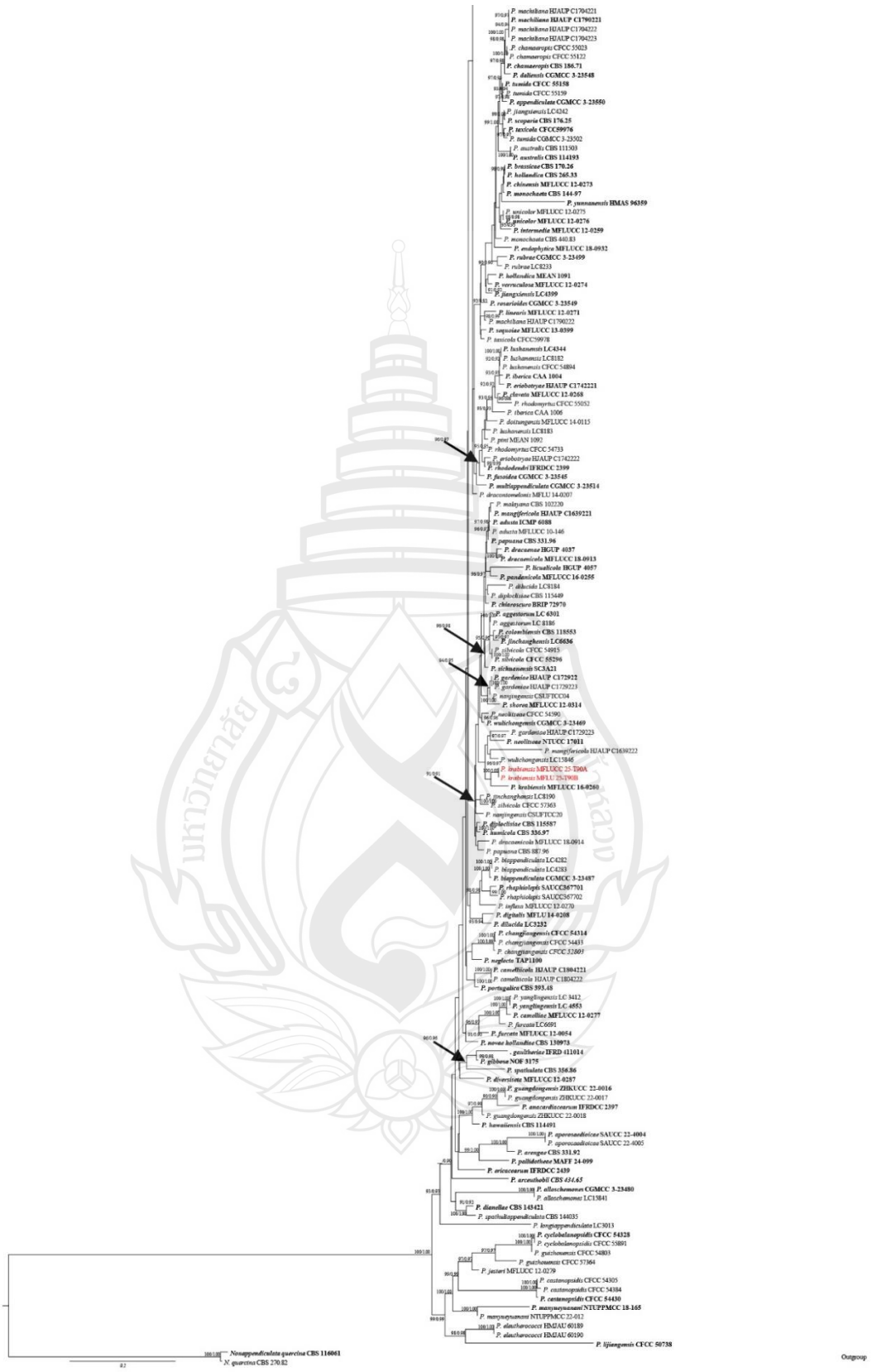

Figure 4.101 (continued)

Pestalotiopsis krabiensis Tibpromma & K.D. Hyde, in Tibpromma et al., Fungal Diversity 93: 143 (2018)

Saprobic or pathogenic on dead, decaying stems of *Carex*, (Cyperaceae), **Sexual morph**: Undetermined. **Asexual morph**: Coelomycetous, *Conidiomata* 130–140 × 110–114 µm ($\bar{x}$ = 136 × 111 µm, n = 5), acervular, loosely aggregated or rarely solitary on host surface, superficial or erumpent, dark brown to black in color, globose to subglobose in shape, unilocular or pluri-loculate. *Conidiomatal wall* 24–27 µm wide ($\bar{x}$ = 25 µm, n = 5), integrated with host tissue and consist of thick-walled hyaline cells of *textura angularis*. *Conidiophores,* occasionally breached and reduced into hyaline, septate structures with few cells. *Conidiogenous cells* 7–12 × 2–3 µm ($\bar{x}$ =11.3 × 2.2 µm, n = 15), cylindrical, ampulliform or lageniform, hyaline with smooth and thin walls, holoblastic and proliferate in different levels. *Conidia* 19–24 × 5–6 µm ($\bar{x}$ = 22 × 4.5 µm, n = 30), ellipsoid, fusoid, slightly curved and 4-septate, cells at the tips are hyaline, basal cell obconic, thin smooth walled with short hyaline appendage, apical cell subcylindrical, thin smooth walled with 3–4 tubular apical appendages, cells at the middle doliiform, concolourous, verruculose and thick walled.

Culture characteristics: Conidia germinating on MEA within 48 h. Colonies growing on MEA, reaching 20–30 mm in 4 weeks at 25°C. Mycelia superficial, umbonate shape floccose culture with frimbriat ending at edges, from above off-white color at the center to the edge, from reverse yellowish white from the center to the edge. After 6 weeks of growth culture generated black color conidia masses in plates.

Material examined: Thailand, Chang Prachuap Khiri Khan Province, Pran Buri District, Pran Buri wetland, on decaying submerged stems of *Carex* sp. (Cyperaceae), 12 January 2024, Tharindu Bhagya, T90A (MFLU 25-0486), 12 January 2024, Tharindu Bhagya, Chang Prachuap Khiri Khan Province, Pran Buri District, Pran Buri wetland, on decaying submerged stem of *Typha* sp. (Typhaceae), T90B (MFLU 25-0487).

GenBank Numbers – MFLU 25-0486: ITS =PX518143, MFLU 25-0487: ITS = PX518144

Distribution – Leaves of *Pandanus* sp. Krabi Province, Thailand (Tibpromma et al., 2018), decomposing dry leaves of *Carex* sp. (Cyperaceae), and *Typha* sp. (Typhaceae) in freshwater wetland, Thailand (This study).

Notes – The new isolates obtained from *Carex*, (Cyperaceae), and *Typha*, (Typhaceae) forms a clade sister to *Pestalotiopsis krabiensis* (MFLUCC 16-0260), with 80% maximum likelihood (ML) and 0.91 Bayesian posterior probability (BPP) statistical support (Figure 4.101). Phylogenetically, strain MFLU 25-0486 shows 99.1% sequence similarity to *P. krabiensis* strain MFLUCC 16-0260. The shorter *tub* sequences in MFLUCC 16-0260 limit the comparison of this gene between the two isolates. Morphologically, strain MFLU 25-0486 exhibits significant similarities to *P. krabiensis* MFLUCC 16-0260, including fusoid to ellipsoid conidia of similar dimensions (length: 19–25 μm in MFLUCC 16-0260 vs. 19–24 μm in MFLU 25-0486; width: 4–6 μm in MFLUCC 16-0260 vs. 5–6 μm in MFLU 25-0486), with conic to obconic basal cells (Figure 4.102) (Tibpromma et al., 2018). Considering the available phylogenetic and morphological evidence, I conclude that the new isolates represent new strains of *P. krabiensis* from freshwater coastal wetlands in Thailand.

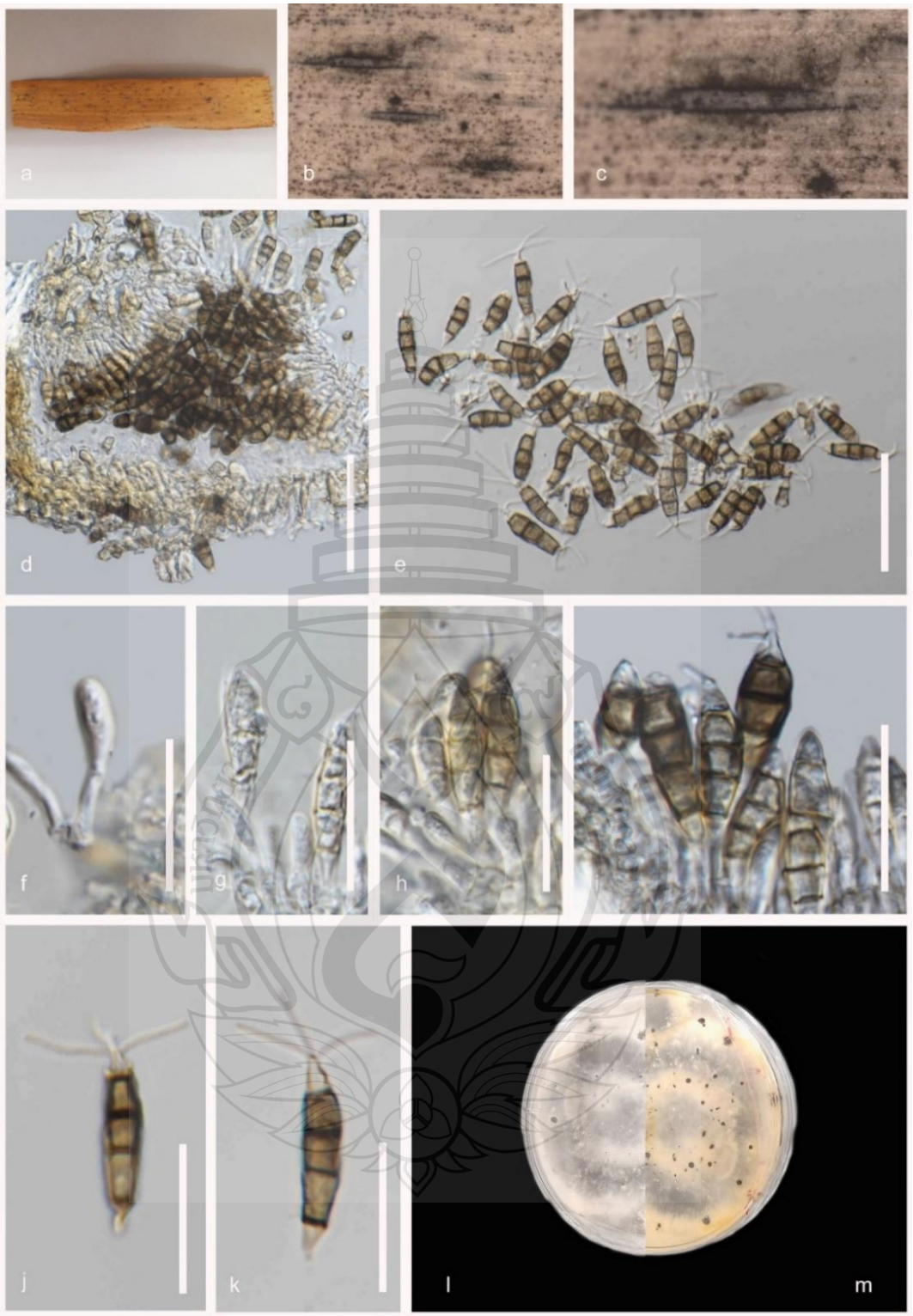

Note a Decomposing *Carex* sp. host material. b–c Conidiomata on host. d Vertical section conidiomata. e Conidia aggregation on host. f–i Conidiogenous cells. i–k Conidia. l Culture on MEA above. m Reverse. Scale bars: d–e 50 µm, f–k 20 µm.

Figure 4.102 *Pestalotiopsis krabiensis* (MFLUCC 25-0486)

Xylariales Nannf

Zygosporiaceae J.F. Li, Phookamsak & K.D. Hyde

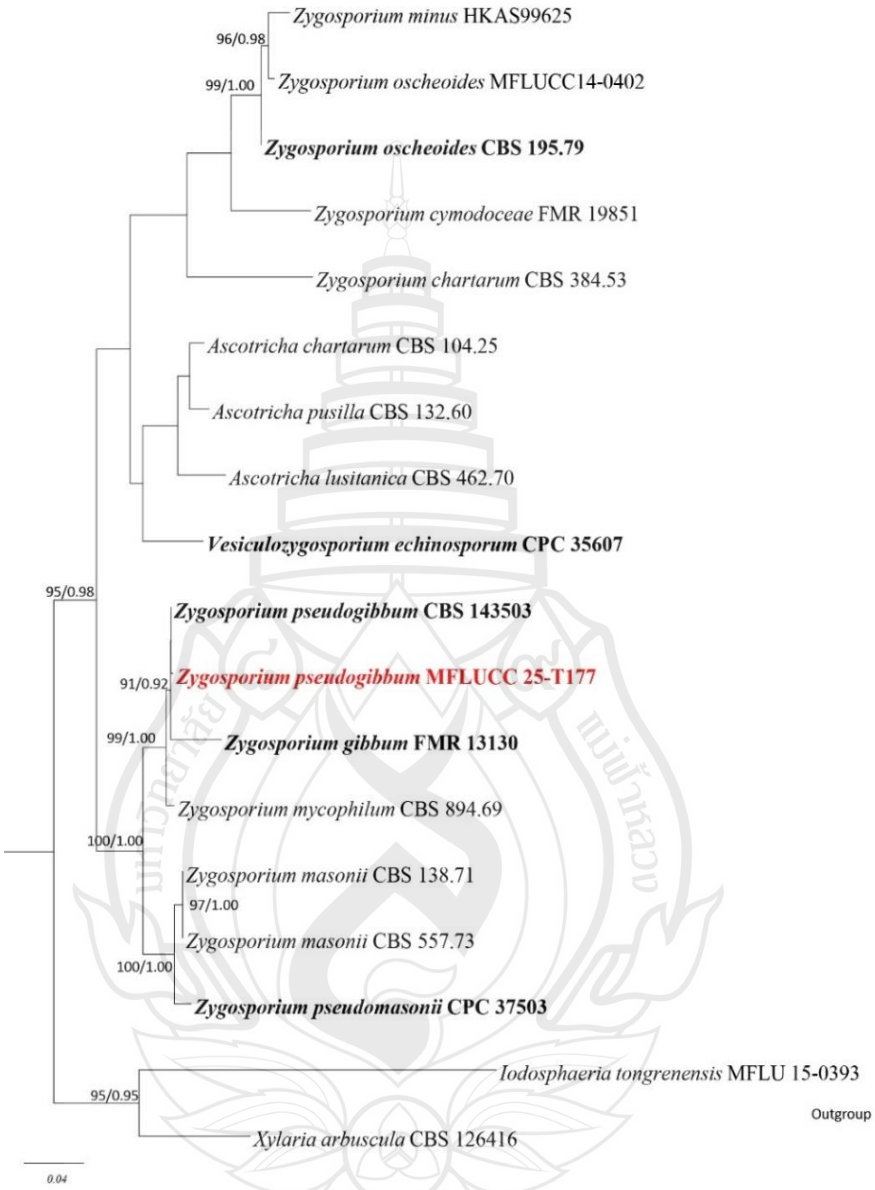

Note Bootstrap support values for ML ≥ 90 % and Bayesian posterior probabilities (BPP) ≥ 0.9 are mentioned at the nodes. The tree was rooted to *Xylaria arbuscula* CBS 126416 and *Iodosphaeria tongrenensis* MFLU 15-0393 combination. Newly generated sequence is indicated in red and the type strains are in bold.

Figure 4.103 Phylogram generated from Maximum Likelihood (ML) analysis based on combined ITS and LSU sequence data of 18 strains, which comprise 1516 characters including gaps, are included in the analyses.

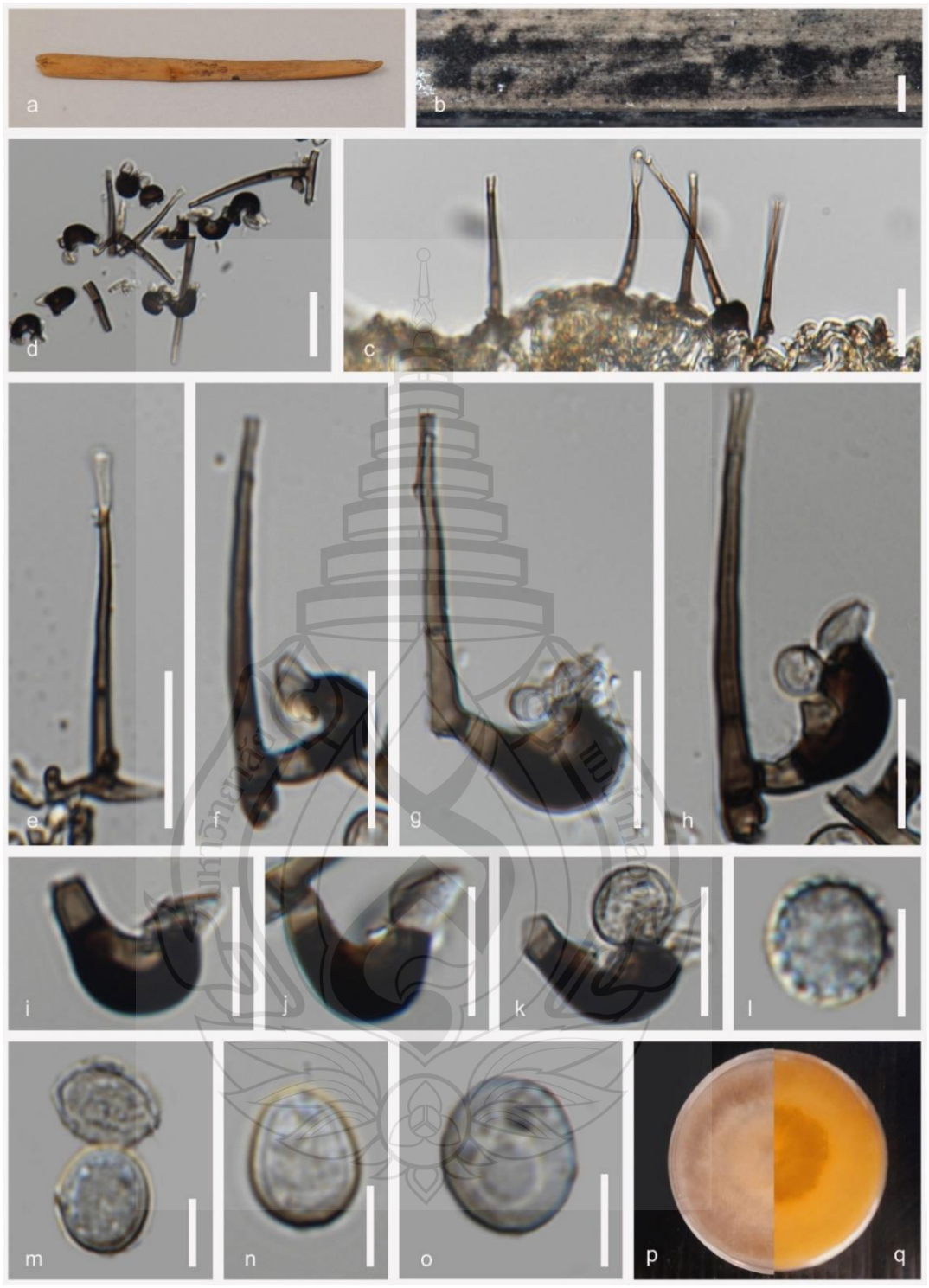

Note a *Typha* sp. host. b Colonies on host surface. c Conidiophores on the host surface. d Colony under microscope. e–h Conidiophores with collarette vesicles. i–k Vesicles with conideogenus cells. i–o Conidia. p Culture on MEA above. q Reverse. Scale bars: b 1 mm, c–f 20 µm, g–k 10 µm, 1–o 05 µm.

Figure 4.104 *Zygosporium pseudogibbum* (MFLU 25-0485)

Zygosporium Mont

This hyphomycetous genus was introduced by Mont. in 1842 and is typified by *Zygosporium oscheoides*. *Zygosporium* has a worldwide distribution and includes detailed fossil species such as *Z. palaeogibbum* from the Middle Miocene era (Mahato et al., 2024). Members of this genus are characterized by pigmented, incurved vesicular cells. Vesicles originate from the side of the setiform conidiophore. *Zygosporium* develops ampulliform conidiogenous cells that produce hyaline, aseptate, smooth or variously textured, ellipsoid or globose conidia (Whitton et al., 2002; Crous et al., 2018).

Zygosporium pseudogibbum Crous, Persoonia 43: 321 (2019)

Saprobic on decaying decaying leaf of *Thypa*, (Typhaceae), **Sexual morph**: Undetermined. **Asexual morph**: Hyphomycetous, numerous, dark brown and amphigenous on host. *Conidiophores* 30–45 × 1.5–2.5 µm ($\bar{x}$ = 35 × 1.8 µm, n = 20), macronematous, setiform and vesicular, dark brown at base and hyaline at the apex, straight to slightly flexuous, 2–3-septats, simple, unbranched, thick-walled, smooth or rarely verruculose or tuberculate with vesicles irrupting from base. *Vesicles* 15–22 × 4–6 µm ($\bar{x}$ = 17 × 4.5 µm, n = 10), uncinated, black to dark brown, reniform, collarette, inflated and process conidiogenous cells at the terminal form a whorl. *Conidiogenous cells*, 4–7 × 2–4 µm ($\bar{x}$ = 5.5 × 2.5 µm, n = 10) monoblastic, discrete, determinate, ampulliform to lageniform or subglobose, pale brown to hyaline. *Conidia* 6–8 × 4–7 µm ($\bar{x}$ = 7.5 × 5.5 µm, n = 10), subglobose or globose, unicellular, verruculose or smooth, and hyaline

Culture characteristics: Conidia germinating on MEA within 24 h. Germ tubes produced from side. Colonies growing on MEA, reaching 25 mm in 3 weeks at 25°C. Mycelia superficial, effuse to umbonate, erose edges, from above pale white from center to the edge, from reverse yellowish white at the center and the white to hyaline at the edge.

Material examined: Thailand, Chang Wat Prachuap Khiri Khan Province, Pran Buri District, Khao Sam Roi Yot wetland, on decaying petiole of *Typha* sp. (Typhaceae). 14 January 2023, Tharindu Bhagya, T25AZ (MFLU 25-0485).

GenBank numbers – MFLU 25-0485: ITS =PX518145, LSU = PX518150

Distribution – Leaves of *Eucalyptus pellit*, Sabah, Malaysia (Crous et al., 2018) and Decaying *Typha* sp. stem and decaying Bamboo stem in freshwater wetland, Thailand (This study).

Notes – Our isolate MFLUCC 25-0485, associated with *Zygosporium pseudogibbum* strain CBS 143503, has moderate statistical support (91% ML & 0.92 BPP) (Figure 4.103). MFLU 25-0485 shares common characteristics of the genus *Zygosporium* by producing dark pigmented, incurved vesicular cells at the base and ampulliform conidiogenous cells (Whitton et al., 2002). Morphologically, MFLU 25-0485 resembles the type strain *Z. pseudogibbum* CBS 143503, featuring pigmented reniform, collarette vesicles that produce terminal, ampulliform conidiogenous cells arranged in a whorl (Figure 4.104) (Crous et al., 2018). Based on phylogenetic and morphological evidence, I report *Z. pseudogibbum* MFLUCC 25-0485 from Typha, (Typhaceae), in Thailand as a new host and geographic location record.

4.4 Discussion

The present study focused on microfungi associated with Poales hosts in freshwater coastal wetlands of central and southern Thailand. The selected sampling sites include Khao Sam Roi Yot, Pran Buri Wetland, and Narathiwat Wetlands. Three dominant Poales families, viz. Cyperaceae, Poaceae, and Typhaceae, were selected as major hosts in these wetlands. Dead and decomposing plant substrates, excluding roots, were collected for investigation. Fungal identification was carried out using a polyphasic taxonomic approach (Turner et al., 2013; Quaedvlieg et al., 2014; Jeewon & Hyde, 2016; Phukhamsakda et al., 2020).

Fungal identification revealed *Dothideomycetes* as the most dominant class, comprising 30 species (51.72%), with *Pleosporales* being the most abundant order. This was followed by *Sordariomycetes*, represented by 26 species (44.82%), predominantly within the orders *Sordariales* and *Distoseptisporales*. *Eurotiomycetes* accounted for 3.46% of the total results, represented by one species each from the genera *Aspergillus* and *Veronaea*. Cumulatively, the investigation documented 58 species distributed across 47 genera, 35 families, 21 orders, and eight sub-classes.

The distribution of fungal genera isolated across different host families was uneven. Typhaceae supported the highest number of genera, with 36 recorded, including 17 found only on Typhaceae. Poaceae yielded 23 genera, with 6 specifically associated with grasses, including submerged decomposing bamboo. In contrast, Cyperaceae supported the fewest genera among the three host families, with only 11 genera, of which just 5 were unique to sedges. *Alternaria*, *Curvularia* and *Tetraploa* were present in all three host families, while several genera such as *Achroiostachys*, *Distoseptispora*, *Pestalotiopsis*, and *Tubeufia* were found associated with two of the wetland Poales members. The distribution of isolated genera across the three plant families is illustrated in Figure 4.105.

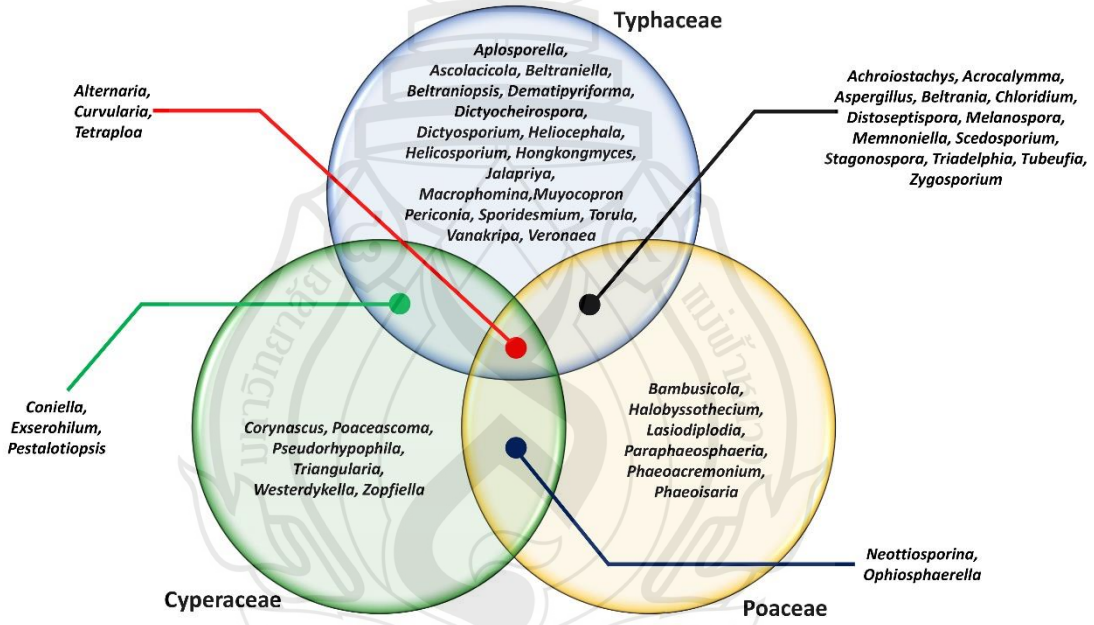

Note Venn diagram related to each host family.

Figure 4.105 Distribution of fungal genera reported in the study across three host families

Most fungal genera were isolated in association with Typhaceae. The abundance of this host in wetland ecosystems positively correlates with the observed segregation of fungal species. Typhaceae was the most dominant host family in the selected freshwater wetlands and was found throughout the ecosystem, from shallow banks to deeper middle sections. The dense meadows formed by these plants efficiently trap

organic debris. Compared to most wetland-dwelling members of Cyperaceae and Poaceae (excluding bamboo), species of Typhaceae tend to be larger and more robust, providing a greater surface area for fungal colonization and increased organic material to support saprobic fungal communities (Somrithipol & Jones, 2003; Zhou et al., 2018). The larger surface area of Typhaceae leaf blades can accumulate more airborne fungal spores, while their relatively robust stems, often grouped in dense meadows, are more effective at trapping spores dispersed through water (Wong et al., 1998; Kuehn et al., 2011; Stephenson et al., 2013; Golan & Pringle, 2017). This results in a higher initial inoculum of fungal propagules on the more abundant Typhaceae host material, potentially accelerating colonization and providing a mechanistic explanation for the high abundance of saprobic microfungi in wetland Typhaceae.

The Poaceae hosted the second-highest number of saprobic fungal genera, following the Typhaceae. Among the recorded genera, 54.56% were recovered from bamboo, highlighting it as the most preferred substrate for saprobic fungi within this study's environmental context. The high lignin and cellulose content in bamboo tissues, along with the presence of silicates, contribute to their durability, allowing fungal colonization to persist over time. Additionally, the hollow anatomy of bamboo culms creates specialized niches for fungal growth, while the increased surface area supports greater host–fungus interactions (Hyde et al., 2002; Wei, 2014; Jiang et al., 2022; Tennakoon et al., 2022; An et al., 2023; Yu et al., 2024). These features may explain the relatively high abundance of saprobic fungi associated with bamboo observed in the current investigation.

The current study utilized both submerged and aerial portions of host materials to isolate fungal species, resulting in the recovery of both aquatic and terrestrial fungal genera. Submerged samples yielded isolates from genera typically associated with aquatic habitats. For example, *Acrocalymma*, *Jalapriya*, *Halobyssothecium*, and *Hongkongmyces* were predominantly found in submerged portions. In contrast, aerial host materials yielded well-known terrestrial genera such as *Curvularia*, *Melanospora*, *Periconia*, and *Torula*. These findings are consistent with those of Wong and Hyde (2002), Cai et al. (2006), and Hu et al. (2010), who reported that terrestrial portions of host materials, especially those of monocotyledonous plants such as *Phragmites australis* and *Schoenoplectus litoralis*, were colonized by fungi more adapted to

terrestrial conditions. In contrast, the submerged parts were dominated by aquatic-adapted saprobic fungi, reflecting a significant difference in fungal community composition and diversity between the two habitats.

There are some exceptions to this general pattern, as observed in the current study. For example, *Helicosporium changjiangense* (GZCC 22-2113) was originally reported from a terrestrial habitat on decomposing wood in Hainan, China, and *Dictyocheirospora pandanicola* (MFLU 16-1933) was previously isolated from decomposing *Pandanus* leaves in Thailand (Tibpromma et al., 2018; Ma et al., 2024). In our investigation, both *H. changjiangense* and D. *pandanicola* were recovered from submerged host materials, without significant morphological deviations from their holotype specimens. This highlights the adaptability and ecological plasticity of fungal taxa inhabiting coastal freshwater wetlands in Thailand (Calabon et al., 2023).

Several genera isolated as saprobic organisms in this study include exact species or closely related taxa, that have also been reported as endophytes or edaphic (soil-dwelling) fungi. In the present investigation, *Poaceascoma* sp. and *Neottiosporina mihintaleensis* were isolated as saprobes from Cyperaceae substrates. Liu et al. (2025), *introduced Poaceascoma magnum*, *Poaceascoma endophyticum*, and *Poaceascoma zoysiiradicicola* as root endophytes from *Zoysia japonica*, and *N. mihintaleensis*, originally described as an endophyte from *Salvinia molesta* leaves in freshwater habitats, was observed in the study as a saprobe (Wimalasena, et al., 2025). Other genera identified in this study, including *Coniella*, *Curvularia*, *Lasiodiplodia*, and *Pestalotiopsis*, also contain species that are known to function as endophytes (Chaiwan et al., 2020; Salvatore et al., 2020; Nwobodo et al., 2022; Rathnayaka et al., 2023; Monkai et al., 2025).

This study reported genera that exhibit an edaphic lifestyle, including the previously mentioned *Poaceascoma* and *Chloridium gonytrichii*, belonging to the genus *Chloridium*. Cheng et al. (2025) introduced a new species, *Poaceascoma serpentinum*, isolated from rice field soil, while Yasanthika et al. (2022) reported *Chloridium gonytrichii* from forest soil in Thailand. These findings indicate the ability of some saprobic fungi recorded in this study to adopt different nutritional strategies depending on environmental conditions, further supporting their ecological versatility.

Based on available reports and observations, it is reasonable to suggest that many of the saprobic fungi isolated during this study were originally endophytes living within plant tissues and later shifted to a saprobic lifestyle after the host plant died (Bhunjun et al., 2024; Rathnayaka et al., 2023). Initial inoculation may have occurred through water or soil, as fungal spores from both soil and non-soil sources can reach freshwater wetlands via wind dispersal and water influx (Calabon et al., 2023). These observations and interpretations further support the ecological adaptability of the fungal lineages associated with Poales inhabiting coastal freshwater wetlands.

Freshwater coastal wetlands are diverse, dynamic, and challenging environments that require organisms to adapt for survival, and fungi are no exception. The microfungi isolated in this study exhibit various adaptations that enable them to survive, reproduce, and disperse efficiently within wetland ecosystems (Trisurat, 2006; Hempattarasuwan et al., 2021). Most of these adaptations appear to be closely linked to spore dispersal mechanisms, which are particularly important in the environmental conditions typical of wetlands. Ascospores and conidia in our collection often have features such as mucilaginous sheaths and polar or bipolar appendages. For example, ascospores of *Hongkongmyces* sp. are surrounded by mucilaginous sheaths, while *Acrocalymma aquaticum* bears bipolar, mucilaginous, flabellate appendages. Additionally, species such as *Jalapriya* sp. and *Dictyosporium olivaceosporum* exhibit globose to subglobose apical appendages.

The mucilaginous sheaths observed in ascospores are hypothesized to play important roles in spore dispersal and adhesion. Ascospores with sheaths enclosed by a delimiting membrane has potential serve several functional purposes, they can help seal the ascus opening, conserving hydrostatic pressure to facilitate effective spore discharge, retain moisture, aiding germination under unfavorable or drier conditions, such as during the dry season in wetland habitats, and they likely act as adhesive structures that enable spores to firmly attach to potential substrates, reducing the likelihood of dislodgement by natural forces (Hyde et al., 1986a; Hyde et al., 1986b; Canon & Minter, 1986; Jones, 1995, 2006).

These anatomical structures, including mucilaginous sheaths and appendages, enable fungal spores to stay buoyant, float on or within water columns, and attach to various substrates (Hyde et al., 1986a, 1986b; Nag, 1993; Jones, 1995). According to

Jones (1995), successful spore germination often relies on a firm attachment to a suitable substrate. Adaptations like the development of mucilaginous sheaths and polar or bipolar appendages facilitate this process. These traits allow microfungi associated with Poales in wetland environments to effectively colonize and utilize decomposing organic matter, ensuring their survival in the physically dynamic and ecologically challenging conditions of freshwater wetlands (Hyde et al., 1986a, 1986b; Nag, 1993; Jones, 1995, 2006; Descals, 2005; Crous et al., 2012; Calabon, 2023).

The current study reports 50 species of saprobic microfungi belonging to 42 genera, isolated from Poales host materials in freshwater coastal wetlands, with Typhaceae emerging as the most dominant host family for fungal associations. These findings highlight the importance of studying largely underexplored habitats and ecosystems to gain a clearer understanding of fungal diversity and to reveal the elaborate adaptations fungi exhibit to survive in challenging environments. The main limitations in comprehensively understanding wetland-associated fungi lies with the limited sequence data, incomplete descriptions of fungal taxa, and the difficulty of inducing germination in many taxa. This study addresses these gaps by providing sequence data for all described isolates, updated phylogenetic trees, detailed descriptions with photo plates, thereby strengthening the molecular database for future research. To further uncover the hidden diversity of these ecosystems, I recommend the use of culture-independent techniques and tissue-based isolations, especially for taxa that are recalcitrant to germination under standard laboratory conditions.

CHAPTER 5

VERTICAL STRATIFICATION OF SAPROBIC FUNGI ON TYPHA ANGUSTIFOLIA IN THAILAND'S FRESHWATER COASTAL WETLANDS

5.1 Introduction

Thailand is a tropical country where wetlands are abundant and play a vital role in both ecological and economic contexts. Covering approximately 36,600 km², or about 7.5% of the country's land area, Thailand's wetlands include diverse categories such as marine wetlands, marshes, estuarine zones, peat and mangrove swamps. Among these, freshwater coastal wetlands, especially marshes are important for supporting national biodiversity, purifying water, serving as breeding grounds for fish, supplying irrigation water, and contributing to ecotourism (Hempattarasuwan et al., 2021). According to these valuable functions, the longevity and ecological balance of freshwater coastal wetlands are of paramount importance. These wetlands consist of rich biodiversity, providing habitats to a diverse variety of plants (Trisurat, 2006). The majority of these plants belong to the order Poales, under Cyperaceae, Poaceae, and Typhaceae as the dominant families. They co-exist with other aquatic families such as Acanthaceae, Nelumbonaceae, Nymphaeaceae, and Salviniaceae (Hempattarasuwan et al., 2021; Trisurat, 2006).

The most dominant plant family in coastal freshwater wetlands of central Thailand is Typhaceae. Typhaceae is the most recently derived family within the order Poales, originating during the Late Paleogene period (approximately 66–23 million years ago), and comprises around 13 species under the genus *Typha* (Zhou et al., 2016; Greb et al., 2022). Members of *Typha* are well-adapted to both semi-aquatic and terrestrial habitats, enabling them to thrive throughout freshwater wetland ecosystems. With characteristic heights exceeding 180 cm, relatively wide and thick pseudostems, robust flower peduncles, dense brown unisexual flower spikes, and long, flat, blade-

like leaves, *Typha* species generate biomass that spans three vertical layers of the wetland: (1) the completely submerged zone, (2) the zone near the water-air interface influenced by tidal fluctuations, and (3) the fully aerial portion exposed to air. These structural zones, defined by water level and plant height, establish distinct ecological niches that can be occupied by saprobic microfungi, thereby enhancing fungal colonization and biodiversity within the wetland environments (Zhou et al., 2016; Bhagya et al., 2024).

Although dead *Typha* stems standing in wetlands offer varied niches with different challenges and opportunities for colonization and utilization by saprobic fungi, studies investigating the vertical distribution of these fungi in wetland ecosystems are scarce. Studies of vertical distribution of marine fungi have been undertaken by Cumo et al. (1985) with *Poidoniae oceanica* in Italy; Sadaba et al. (1995) on *Acanthus ilicifolius* stems at Mai Po mangrove, Hong Kong; Kohlmeyer and Volkman-Kohlmeyer (1995) on *Juncus roemerianus*, North Carolina, USA. One of the most detailed studies was conducted by Alias and Jones (2000) in Selangor, Malaysia. Their study, initiated in 1993 and concluded in 1997, examined the vertical distribution of saprobic fungi on *Rhizophora apiculata* collected from different tidal levels. The results showed that the highest fungal diversity occurred at the mid-tidal level, where carbonaceous and superficial ascomata were predominantly found above the mean tidal level, while microfungi with more membranous-walled ascomata occurred below the mean tidal level. These findings suggest that water level significantly influences the diversity and distribution of saprobic fungi in wetland ecosystems.

A related study on the decomposition of *Phyllostachys bambusoides* in freshwater streams and adjacent terrestrial habitats was conducted in Xiao Bai Long Mountain, Yiliang, Yunnan, China. This investigation revealed a significant difference in the structure of saprobic fungal communities between aquatic and terrestrial environments (Cai, 2003). These findings further emphasize the importance of studying the vertical distribution of saprobic fungal fauna associated with dynamic environments such as freshwater coastal wetlands.

Calabon et al. (2022) reported 49 genera of *Eurotiomycetes*, 82 genera of *Leotiomycetes*, 229 genera of *Dothideomycetes*, and 298 genera of *Sordariomycetes* from freshwater ecosystems worldwide. Karunarathna et al. (2022) documented over

2,500 fungal species associated with the order Poales across the globe. These studies highlight the potential of freshwater coastal wetland-inhabiting Poales to harbor a rich diversity of fungi, justifying the need of further in-depth investigation. My study focuses on understanding the fungal genera associated with the most widespread and dominant coastal wetland-inhabiting order Poales in Thailand's wetlands, *T. angustifolia.* Specifically, I examine the vertical distribution of saprobic microfungi across the submerged to emergent niches formed by this macrophyte.

The Pranburi Wetland in Prachuap Khiri Khan Province and the Khao Sam Roi Yot Wetland in Kui Buri District were selected as study sites. Decomposing *T. angustifolia* samples were collected from three vertical zones: (1) leaf segments near the tip, (2) portions between the tip and the water interface, and (3) tissues located below the water surface. Fungal identification was conducted using a polyphasic taxonomic approach or, when applicable, based on morphological characteristics to the genus level. Statistical analyses were performed using the R software package. The Shannon–Wiener Index (H'), Sørensen's Index of Similarity (S'), and the Bray–Curtis Dissimilarity Index (BC) were calculated to assess fungal diversity and community similarity. Comparative analyses across niches and detailed interpretations of the results are discussed.

5.2 Methodology

5.2.1 Sample Collection, Morphological Studies, and Isolation

The family Typhaceae, and in particular *T. angustifolia* was identified as a suitable host due to its dominant distribution, tissue composition, and plant size, which provide both submerged and emergent decomposing substrates simultaneously. Necessary permissions were obtained from the relevant authorities to conduct the study (Permit No. 0907.4/23579; Book No. 02/020 and Book No. 02/001). Three plots were selected from each location, and 30 plants were randomly collected from each plot to obtain three categories of samples from dead and decomposing *T. angustifolia* plants, with 30 cm of plant material collected per category per plant: (1) leaves close to the tip, (2) the portion from above the tip to the water interface, and (3) tissues below the water

surface. Morphological characters were documented following Senanayake et al. (2020), using an OLYMPUS SZX16 stereomicroscope (Olympus Corporation, Japan) and a Nikon ECLIPSE Ni compound microscope (Nikon Instruments Inc., Japan), coupled with a Nikon DS-Ri2 digital camera. Adobe Photoshop CS3 Extended version 10.0 (Adobe Inc., California, USA) was used to construct detailed photo plates for fungal identification, and measurements were taken using Image Framework software (Tarosoft, Nonthaburi, Thailand). The single-spore isolation technique was employed to obtain pure cultures, using culture media such as Malt Extract Agar (MEA) and Potato Dextrose Agar (PDA). For fungi identified through polyphasic approaches, holotype materials were deposited in the Mae Fah Luang University Herbarium (MFLU), and ex-type living cultures were deposited in the Mae Fah Luang University Culture Collection (MFLUCC).

5.2.2 DNA Extraction, PCR Amplification and Sequencing

Genomic DNA was extracted using the E.Z.N.A. Fungal DNA Mini Kit (D3390-02; Omega Bio-Tek, USA), following the manufacturer's instructions. Samples were stored at 4°C for short-term use and at −20°C for long-term preservation. Polymerase chain reactions (PCR) were performed to amplify selected loci depending on each fungal genus. Each PCR mixture had a final volume of 25 µl, consisting of 12.5 µl of 2× Power Taq PCR Master Mix, 9.5 µl of deionized H_2O, 1 µl of each primer (20 µM), and 1 µl of genomic DNA (15 ng/µl). Amplification was carried out using the primers and PCR conditions in published literature. SafeView™ DNA stain (SOMBIO, Taiwan, China) was used to visualize the PCR products, which were separated using 1.7% agarose gel electrophoresis. Gel visualization was performed using an E-Box CX5 gel documentation system (Vilber Lourmat Deutschland GmbH, Eberhardzell, Germany), and sequencing was conducted by Solgent Corporation (Yuseong-gu, Daejeon, Korea).

5.2.3 Fungal Identification: Polyphasic Approach

Fungal identification from pure cultures or fruiting bodies was conducted using a combination of morphological examination and multilocus phylogenetic analysis. Newly generated sequences were processed using BioEdit v.7.0.9.0 (Hall, 1999) and Lasergene SeqMan Pro v.7 (DNASTAR, Inc., USA). Evolutionarily related published

sequences were obtained from the literature and GenBank (National Center for Biotechnology Information, USA), and were aligned using the MAFFT v.6.864b online tool with the FFT-NS-i method (Katoh et al., 2019). Sequence trimming was performed manually in BioEdit v.7.0.9.0 to remove low-quality regions, primer binding sites, and ambiguous bases.

Maximum Likelihood (ML) phylogenetic trees were constructed using the IQ-TREE web server (http://iqtree.cibiv.univie.ac.at/) with 1,000 pseudoreplicates. Bayesian Inference (BI) analyses were conducted using MrBayes v.3.2.7a (Ronquist et al., 2012) on XSEDE via the CIPRES Science Gateway (Miller et al., 2015). The best-fit evolutionary models for each locus were selected using jModelTest2 on CIPRES. Pairwise distance matrix values were calculated using MEGA11 (version 11.0.13; HANSALOG GmbH & Co. KG, Germany), based on the requirements of the phylogenetic analyses (Tamura et al., 2021). Phylogenetic trees were visualized using FigureTree version 1.4.4 (http://tree.bio.ed.ac.uk/software/Figuretree/) and edited in Microsoft PowerPoint (2019), Microsoft Corporation, Washington, United States

5.2.4 Fungal Identification: Morphological Approach

Fungal isolates that failed to germinate under laboratory conditions to yield pure cultures, or those observed with relatively few fruiting bodies or clusters, were identified to the genus level based on morphological characteristics. Published literature that containing detailed morphological keys and detailed descriptions was used to facilitate the identification process.

5.2.5 Statistical Analysis

In both the polyphasic and morphology-based approaches, a single fungal species was isolated from one 30 cm plant segment, was counted as one occurrence. Each fungal genus and its number of occurrences across three different selected niches at two locations were recorded for statistical analysis. R software, with the “vegan” and “betapart” packages, was used to evaluate the diversity of each selected niche. The Shannon–Wiener index (H’) was applied to assess the diversity of identified fungal genera, including richness. The normality of the dataset was tested using the Shapiro–Wilk test, variance homogeneity was examined using Levene’s test, and the overall statistical significance of the Shannon–Wiener index (H) was evaluated by ANOVA (Zheng et al., 2021; Gurarie, 2025).

Sørensen dissimilarity (S) and the Bray–Curtis dissimilarity index (BC) were calculated to compare different niches based on the presence/absence and abundance of fungal genera. The respective equations are provided below. Permutational Multivariate Analysis of Variance (PERMANOVA) and Permutational Analysis of Multivariate Dispersion (PERMDISP) were applied to assess the significance of Bray–Curtis and Sørensen index values, as well as to analyze the dispersion of the data (Goldmann et al., 2016; Marion et al., 2021; Zheng et al., 2021; Xing et al., 2024; Gurarie 2025).

Shannon–Wiener index (H'),

$$H = -\sum_{j=1}^{S} p_i \ln p_i$$

H = Shannon–Wiener diversity index

S = Total number of species (or genera)

p_i = Proportion of individuals of species

i = ($p_i = n_i / N$)

n_i = Number of individuals of species i

N = Total number of individuals across all species

ln = Natural logarithm (log base *e*)

Sørensen's index of similarity (S'),

$$\text{Sørensen Dissimilarity Index (S)} = 1 - \frac{2C}{A + B}$$

S' = Sørensen's similarity index

A = Number of species in community A

B = Number of species in community B

C = Number of species common to both communities A and B

Bray-Curtis Dissimilarity Index (BC),

$$BC_{ij} = \sum \frac{|n_{ik} - n_{jk}|}{(n_{ik} + n_{jk})}$$

BC_{ij} = Bray–Curtis dissimilarity between site i and site j

Σ = Summation across all species or genera k

n_{ik} = Abundance (or frequency) of species k in site i

n_{jk} = Abundance (or frequency) of species k in site j

$(n_{ik} - n_{jk})$ = Absolute difference in abundance of species k between sites

5.3 Results

A total of 360 specimens were collected according to the experimental design, yielding 487 fungal taxa across 73 genera. The most abundant genera were *Chaetomium* (9.7%), *Pestalotiopsis* (6.9%), *Aspergillus* (6.2%), aniptodera-like *Halosphaeriaceae* genera (5.1%), and *Distoseptispora* (5.1%). The aerial portion contained 34 genera, with 9 genera exclusive to this section; *Chaetomium* and *Pestalotiopsis* were the most abundant. In the middle section, 48 genera were identified, including 9 unique genera, with *Pestalotiopsis* as the dominant genus. The submerged section, below the water surface, included 45 genera, 15 of which were unique, with aniptodera-like *Halosphaeriaceae* genera being most abundant (Figure 5.1). α-Diversity across the three sampling levels was assessed using the Shannon–Wiener index (H') and species richness (Table 5.1).

Table 5.1 Analysis of α-Diversity and statistical significance analysis

Sampling Level	Richness	Shannon Index	Normality Test (Shapiro–Wilk)		Variance Homogeneity (Levene's Test)		Distribution	Overall Test	Overall Pr (>F)
			W_Stat	p - value	F	p			
Aerial	34	3.0412	0.9497	0.7143	0.4737	0.6374	Normal	ANOVA	0.224
Middle	48	3.4452	0.9714	0.8499					
Submerged	45	3.3143	0.9929	0.9718					

5.3.1 α-Diversity Analysis

The Shannon–Wiener index (H') values for the sampling categories were 3.0412 (Aerial), 3.4452 (Middle), and 3.3143 (Submerged). The Shapiro–Wilk test was performed to assess normality, and the W-statistics were close to 1 with $p > 0.05$, indicating that the data followed a normal distribution (Wang et al., 2015; Zheng et al., 2021). Homogeneity of variance was examined using Levene's test, which yielded $F < 1$ and $p > 0.05$, confirming that group variances were similar and the assumption of homogeneity was satisfied (Table 5.1) (Chen et al., 2016; Mohammed et al., 2018). Based on these results, ANOVA was selected as the appropriate overall test to determine differences in α-diversity among the groups. The ANOVA yielded Pr(>F) = 0.224, which is greater than 0.05, indicating that there were no statistically significant differences in α-diversity among the three sampling categories (Table 5.1) (Legendre & Legendre, 2012; Wang et al., 2015; Zheng et al., 2021; Gurarie, 2025).

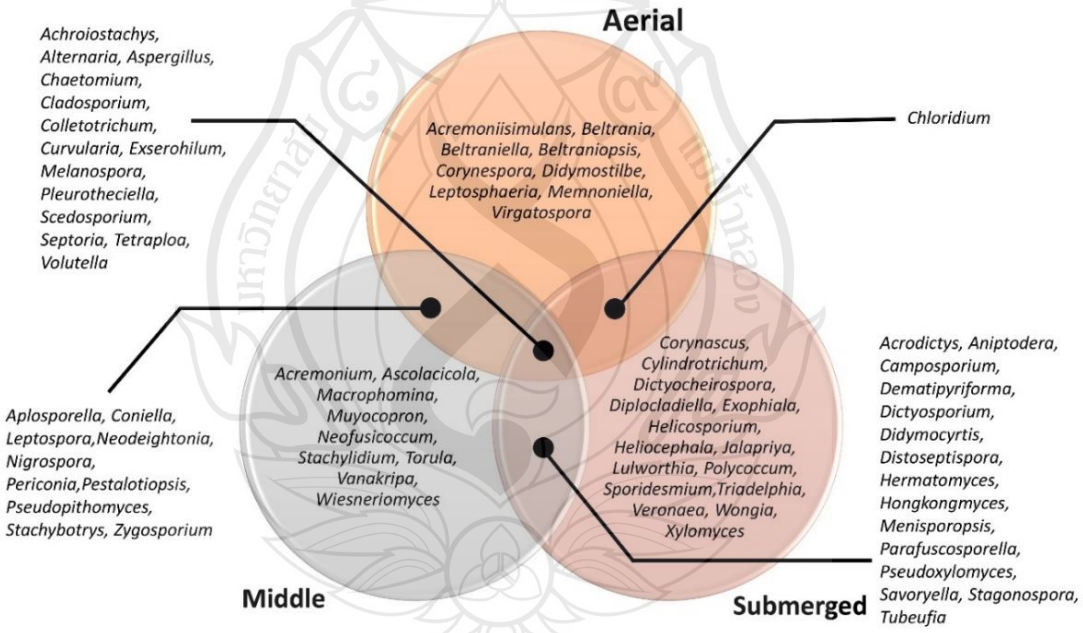

Note Venn diagram showcasing txa distribution.

Figure 5.1 Distribution of micro fungal genera over three different habitat levels

5.3.2 β-Diversity Analysis

The β-diversity of the selected sampling categories was examined using both the Bray–Curtis and Sørensen dissimilarity indices (Table 5.2). The Bray–Curtis dissimilarity index, introduced by Bray and Curtis (1957), is based on the relative

abundances of taxa within a given sampling category. This index emphasizes differences in abundance between sample sets and is insensitive to joint absences or shared absences (Shi et al., 2014; Zhou et al., 2020). In contrast, the Sørensen dissimilarity index considers only the presence and absence of taxa across two sampling categories, thus, making the index more sensitive to shared species rather than abundance differences among the categories (Sørensen, 1948; Hao et al., 2019; Yang et al., 2025). Assess the statistical significance of the observed differences, a PERMANOVA test was performed on both dissimilarity indices. The PERMANOVA analysis was further complemented by a PERMDISP test to evaluate whether the groups exhibited homogeneous dispersions or unequal spread (Table 5.3) (Hao et al., 2019; Marion et al., 2021; Zhou et al., 2020; Xing et al., 2024; Yang et al., 2025).

Table 5.2 Results of Bray–Curtis dissimilarity index and Sørensen dissimilarity index

Bray–Curtis Dissimilarity				**Sørensen Dissimilarity**			
	Aerial	**Middle**	**Submerged**		**Aerial**	**Middle**	**Submerged**
Aerial	0.0000	0.4037	0.7028	Aerial	0.0000	0.4146	0.6203
Middle	0.4037	0.0000	0.4529	Middle	0.4146	0.0000	0.3763
Submerged	0.7028	0.4529	0.0000	Submerged	0.6203	0.3763	0.0000

Based on the Bray–Curtis dissimilarity index, the aerial and middle categories were the most similar in species abundance, whereas the middle and submerged categories were moderately dissimilar. The greatest dissimilarity in abundance was observed between the aerial and submerged categories. According to the Sørensen dissimilarity index, the lowest dissimilarity occurred between the middle and submerged categories, while the highest dissimilarity was observed between the aerial and submerged categories (Table 5.3) (Goldmann et al., 2016; Marion et al., 2021; Xing et al., 2024).

Table 5.3 PERMANOVA and PERMDISP results for Bray–Curtis and Sørensen dissimilarity indexes

Bray–Curtis Dissimilarity					Sørensen Dissimilarity				
PERMANOVA			PERMDISP		PERMANOVA			PERMDISP	
R^2	F	Pr(>F)	F	Pr(>F)	R^2	F	Pr(>F)	F	Pr(>F)
0.3925	2.907	0.001	2.5445	0.148	0.3547	2.4735	0.005	0.8539	0.444

The PERMANOVA analyses based on Bray–Curtis and Sørensen dissimilarity indices revealed significant differences in fungal community composition among the sampling categories. Approximately 39% and 35% of the variation in community structure were explained by habitat level, as indicated by the Bray–Curtis and Sørensen indices, respectively (Table 5.3). The PERMDISP tests were not significant for either index, indicating that the observed differences were due to true compositional variation of fungal communities among habitats rather than unequal dispersion (Table 5.3) (Wang et al., 2015; Zheng et al., 2021; Xing et al., 2024).

The NMDS (Non-metric multidimensional scaling) plots revealed clear clustering of samples according to habitat level, consistent with the PERMANOVA results in both Bray–Curtis and Sørensen indices, with low stress values indicating good representation of community relationships (Figure 5.2) (Legendre & Legendre, 2012; Marion et al., 2021; Xing et al., 2024; Gurarie, 2025).

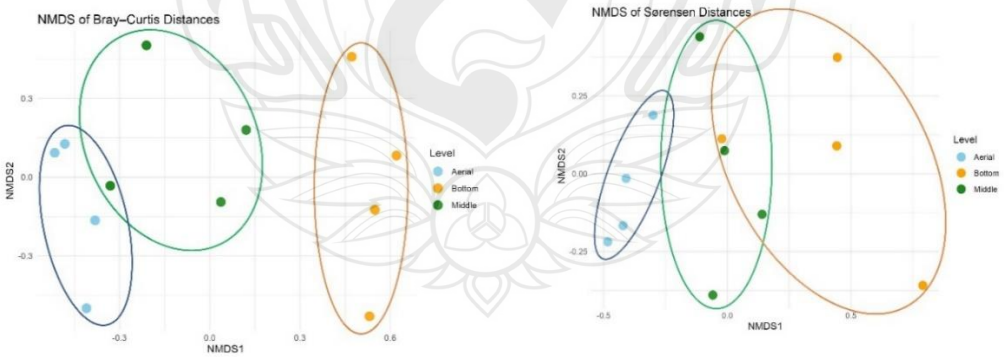

(a) (b)

Note Non-metric multidimensional scaling plots.

Figure 5.2 PERMANOVA NMDS plots of (a), Bray–Curtis, and (b), Sørensen dissimilarities

Boxplots of Bray–Curtis and Sørensen dissimilarities displayed habitat level highlighted the within-group variation, illustrating similar dispersion across groups and supporting the non-significant PERMDISP results originated by the analysis (Figure 5.3) (Xing et al., 2024; Gurarie, 2025).

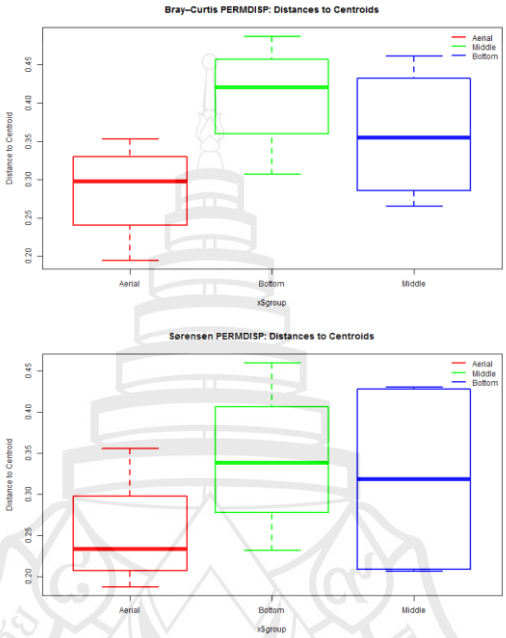

Note Boxpolts bsed on Permutational analysis of multivariate dispersions.

Figure 5.3 PERMDISP Boxplots of Bray–Curtis and Sørensen dissimilarities

Heatmaps of pairwise dissimilarities of both Bray–Curtis and Sørensen indices further confirmed these patterns, illustrating higher dissimilarity between microfungal communities from different habitats and greater similarity within the same habitat (Figure 5.4). Collectively, these visualizations provide a comprehensive representation of fungal community structure and variation across the three selected habitat levels in the study (Legendre & Legendre, 2012; Xing et al., 2024; Gurarie, 2025).

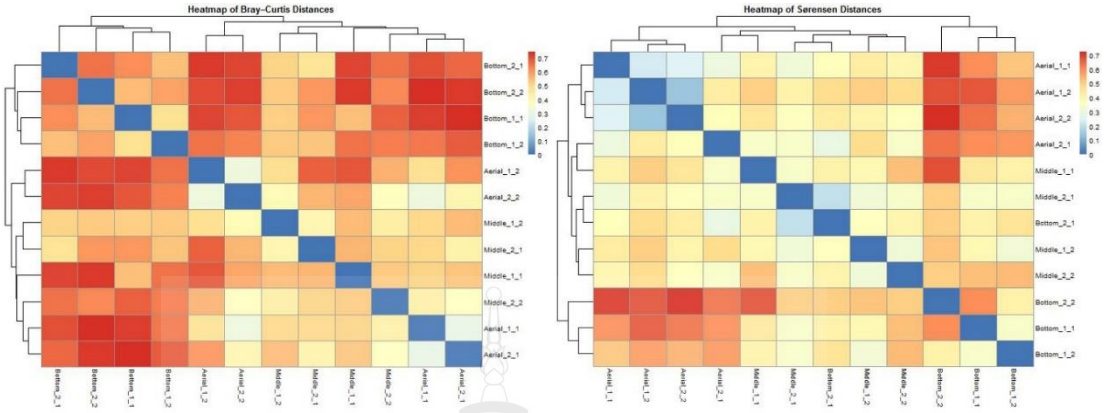

(a) (b)

Note Heatmaps showcasing the β diversity differences.

Figure 5.4 Heatmaps of pairwise dissimilarities for (a), Boxplots of Bray–Curtis, and (b), Sørensen dissimilarities

5.4 Discussion

5.4.1 α- and β- Diversity Interpretation

The investigation was conducted in a freshwater coastal wetland in central Thailand, focusing on the wetland-dwelling Poales species, *T. angustifolia*. A total of 360 samples were collected under three categories, (1) Aerial, leaf segments near the tip, (2) Middle, portions between the tip and the water interface, and (3) Submerged, tissues located below the water surface (Figure 5.1). Saprobic fungal identification yielded 487 fungal colonies, reflecting high microfungal diversity in freshwater coastal wetlands of central Thailand and extensive fungal colonization on decomposing *T. angustifolia* substrates across the three selected sampling zones (Table 5.1) (Vijaykrishna & Hyde, 2006; Bhagya et al., 2024). The dominant genera varied across the vertical levels. *Chaetomium* and *Pestalotiopsis* were most abundant and dominant in aerial and middle sections, whereas *Halosphaeriaceae* members and *Distoseptispora* were prevalent in submerged (bottom) samples. *Chaetomium* was observed in all three vertical levels, *Pestalotiopsis* was restricted to aerial and middle categories, and *Distoseptispora* together with *Halosphaeriaceae* members were confined to the middle and submerged (bottom) sections of decomposing *T. angustifolia* host substrates (Figure 5.1).

The Shannon α-diversity index was not statistically significant across the three sampling categories, indicating comparable levels of diversity among three vertical levels. However, the different vertical niches displayed variation in richness levels and the overall number of unique fungal genera (Table 5.1, Figure 5.1). For example, the aerial segment exhibited the lowest richness, with nine unique genera. The submerged (bottom) section ranked second in fungal richness (45) but harbored the highest number of unique genera (15). The middle section recorded the highest fungal richness (48), with nine unique genera (Table 5.1, Figure 5.1). The occurrence of unique taxa in relation to each vertical level highlights adaptations that enable successful occupation and persistence within specific niches.

According to the Bray–Curtis index, the aerial and middle categories were the most similar in species abundance (0.4037), while the middle and bottom categories showcased moderate dissimilarity (0.4529). The greatest dissimilarity in abundance was recorded between the aerial and bottom categories (0.7028). Based on the Sørensen index, the lowest dissimilarity was observed between the middle and bottom categories (0.3763), whereas the highest dissimilarity was again recorded between the aerial and bottom categories (0.6203) (Table 5.2). The PERMANOVA analysis on the Bray–Curtis dissimilarity index revealed significant differences in fungal community composition among the sampling categories ($R^2 = 0.3925$, $F = 2.907$, $p = 0.001$), indicating that approximately 39% of the variation in community structure was explained by habitat level (Shi et al., 2014; Zhou et al., 2020; Yang et al., 2025). The PERMANOVA results for the Sørensen index followed a similar pattern ($R^2 = 0.3547$, $F = 2.4735$, $p = 0.005$), demonstrating that 35% of the variation in community structure was attributable to vertical habitat differences (Table 5.3). The corresponding PERMDISP tests for both indices were not significant (Bray–Curtis: $F = 2.545$, $p = 0.148$; Sørensen: $F = 0.8539$, $p = 0.444$), confirming that the observed differences were due to genuine compositional variation rather than unequal dispersion among groups (Table 5.3) (Hao et al., 2019; Zhou et al., 2020; Yang et al., 2025).

The PERMDISP boxplots constructed from the cumulative data of each category (Figure 5.3) and the heatmaps of pairwise dissimilarities based on Bray–Curtis and Sørensen indices (Figure 5.4) visually illustrate the relationships among the three

sampling categories. The PERMDISP boxplots for the Bray–Curtis dissimilarity index exhibited that the aerial and bottom categories had approximate median distances of 0.30 and 0.42, respectively, with relatively homogeneous spread of data. The middle category of samples indicated the widest spread, with a median distance of approximately 0.35. PERMDISP boxplots for the Sørensen index displayed a similar median distribution across the sampling categories (Figure 5.3) (Legendre & Legendre, 2012; Zhou et al., 2020; Xing et al., 2024; Yang et al., 2025). The heatmaps represent higher dissimilarity with darker red colors, lower dissimilarity with lighter colors, and identical samples with blue. For both Bray–Curtis and Sørensen indices, stronger red tones were observed between bottom and aerial samples, indicating these categories were the most distinct from each other. Middle samples displayed intermediate color intensities, reflecting a transitional composition of taxa consistent with their ecological position between the bottom and aerial levels (Figure 5.4).

5.4.2 Ecology and Habitat Filtering

The fungal distribution patterns observed in both α- and β-diversity analyses indicate that fungi with specific adaptations to each microenvironment occupy distinct sampling categories. This segregation can be referred to as the habitat filtering phenomenon, where habitat attributes dictate which organisms can colonize the environment (Glassman et al., 2017). Accordingly, these results support the phenomenon, showing that different fungal community structures occur across the three sampling levels of saprobic microfungi associated with decomposing. *T angustifolia* host material in freshwater coastal wetlands of central Thailand (Table 5.1 and 5.2) (Glassman et al., 2017; Yang et al., 2019).

Some genera identified from the submerged section in this study (particularly within the *Halosphaeriaceae*) are known to produce lignicolous enzymes that facilitate the breakdown of lignocellulosic material in substrates, thereby making nutrients available for aquatic detritivores (Jones, 1971; Jones et al., 1988). The lignin-rich bottom sections of the *T. angustifolia* plant, included in the submerged sampling category of this study, likely provides a favorable substrate together with microenvironmental conditions, such as optimal water content, that promote the higher abundance of these fungi in the submerged category (Jones, 1971; Cuomo et al., 1985; Sabada et al., 1995).

The adaptations exhibited by fungal taxa in relation to their occupied vertical levels further support the habitat filtering argument. Fungal genera associated with submerged sections are adapted to occupy niches with higher moisture content, low temperature, and possess traits that enhance survival and dispersal in aquatic environments (Figure 5.1). For example, *Halosphaeriaceae* members and *Corynascus* produce membranous, soft ascomata and deliquescent asci, enabling efficient and effective ascospore release and passive spore dispersal under aquatic or submerged conditions (Figure 5.5) (Jones et al., 1980; Jones et al., 1986; Sakayaroj et al., 2011; Jones et al., 2017). The bitunicate asci capable of active ascospore dispersal, predominantly recorded in *Dothideomycetes*, are believed as an adaptation of terrestrial Ascomycota (Figure 5.7) (Jones & Kuthubutheen, 1989; Kohlmeyer & Kohlmeyer, 1979). Genera with those adaptations were mainly recovered from the aerial and middle segments of the study, as in examples, the sexual morphs of *Hongkongmyces* and *Tetraploa* (Figure 5.1).

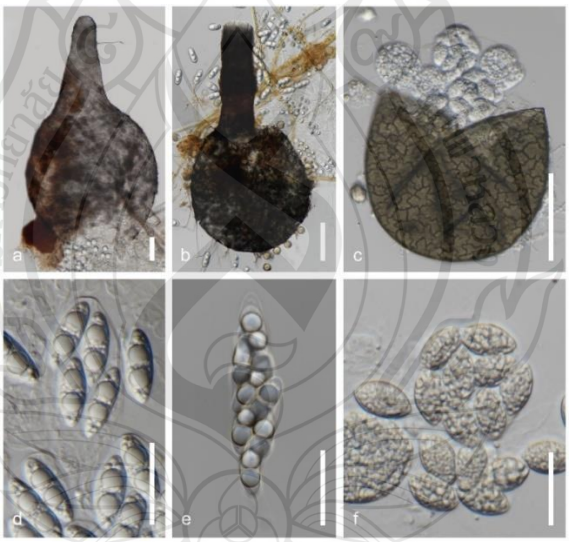

Note (a) *Aniptodera*; (b) *Lignincola*; (c) *Corynascus* and deliquescent asci (d) *Aniptodera*; (e) Lignincola; (f) *Corynascus* found in submerged portion of decomposing *Typha angustifolia* substrates. Scale Bars: (a-c) 50 µm; (d-f) 20 50 µm.

Figure 5.5 Membranous, soft ascomata

The ascospores of *Halosphaeriaceae* members, as well as the conidia of *Diplocladiella*, *Jalapriya*, and *Sporidesmium*, develop appendages that facilitate dispersal, entrapment and adherence to substrates in aquatic habitats (Jones, 1995;

Hyde, 1986; Calabon et al., 2022; Calabon et al., 2023). Additionally, genera such as *Helicosporium* and *Tubeufia* produce helicoid, light-weight spores adapted for dispersal through water with the ability to entangle with substrates, ensuring colonization and persistence in submerged niches (Figure 5.6) (Boonmee et al., 2014; Ma et al., 2024). These observations agree with Hyde (1990), who noted that aquatic fungi are adapted to fully exploit aquatic environmental conditions by evolving unique morphological features, Alias and Jones (2000), Barata (2002) and Hyde and Sarma (2006).

The aerial and middle segments of the study exhibit a similar pattern of habitat filtering as observed in the bottom or submerged segment. The most prominent or shared taxa in the aerial and middle sections are either generalists, cosmopolitan fungi with diverse nutritional modes (*Chaetomium*), or fungi that preferentially disperse via wind. For example, *Pestalotiopsis* spores develop appendages that facilitate wind-assisted dispersal and inoculation onto aerial segments of host exposed to wind (Figure 5.6) (Watanabe et al., 2000; EFSA Panel on Plant Health [PLH] et al., 2023). Those fungal genera inhabiting both aerial and middle sections are more resilient to drying out, tolerate relatively lower moisture contents are higher exposed to ultraviolet radiation (Walker & Campbell, 2010; Lyons et al., 2010; Al-Nasrawi & Hughes, 2012; Calado et al., 2015). Considering the reported fungal genera in this investigation, 40 genera (54.79%) were shared by at least two vertical sampling categories. This indicates the presence of a strong and stable core fungal community associated with the decomposition of *T. angustifolia* in the study locations. This ecological stability demonstrates the presence of resilient fungal communities across the three sampling categories (Calado et al., 2015).

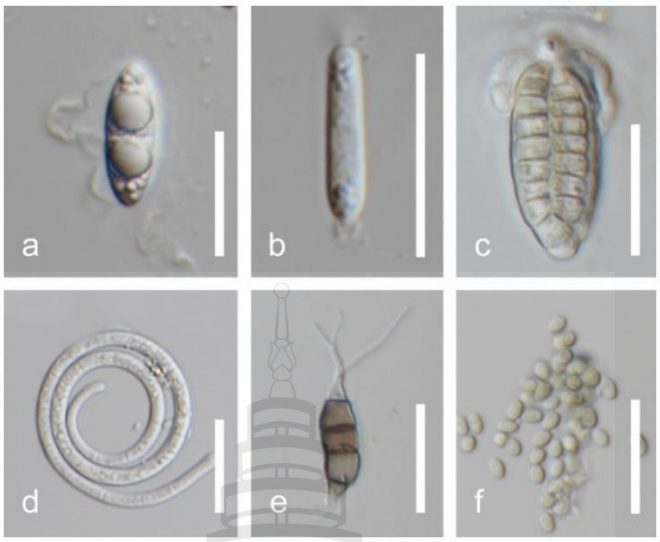

Note (a) *Aniptodera* ascospore with mucilaginous appendages; (b) *Acrocalymma* conidia with bipolar mucilaginous appendages; (c) *Jalapriya* conidia with apical mucilaginous appendages; (d) Helical conidia of genus *Tubeufia*. Adapted to water-born dispersal, (e) *Pestalotiopsis* conidia with filamentous appendages; (f) Smaller light conidia of *Chloridium*. Scale Bars: (a-f) 20 µm.

Figure 5.6 Fungal propagules adapted to ensure dispersal and colonization of decomposing *Typha angustifolia* substrates in wetland ecosystems. Adapted to water-born dispersal

5.4.3 Vertical Distribution of Fungi, and Ecotone

The tissue structure and microenvironmental conditions that expose the plant segments vary with the vertical level in *T. angustifolia* substrates in the studied wetland ecosystems (Ágoston-Szabó & Dinka, 2008; Oliveira et al., 2016; Wasko et al., 2022; Nedukha, 2025). The submerged portion was completely under water, experiencing relatively stable conditions with lower temperatures and higher water content compared to the middle and aerial segments. In contrast, the aerial and middle segments were exposed to air and subjected to more variable environmental conditions than the stable abiotic conditions of the submerged segments. This creates distinct microenvironments for saprobic fungi, with a moisture gradient decreasing from the submerged sections to the aerial portions (Zhou & Hyde,2001; Lyons et al., 2010; Al-Nasrawi & Hughes, 2012; Calado, 2015).

The available moisture, tissue structure, and temperature conditions determine the types of fungi that can occupy each segment of decomposing *T. angustifolia* substrates. The availability and number of reproductive structures were used as indicators of the presence of fungal taxa in each category, based on the assumption that a high density of reproductive structures reflects a well-established, substantial mycelial network (Newell & Wasowski, 1995; Newell & Porter, 2000). The ability to generate numerous fruiting structures in a given segment indicates the capacity of the respective taxa to develop under the specific microenvironmental conditions that each vertical level, host material composition of that segment of *T. angustifolia* substrates provide and, as a result playing a major role as decomposers at that vertical level (Newell, 2001; Walker & Campbell, 2010; Lyons et al., 2010; Al-Nasrawi & Hughes, 2012; Calado, 2015).

Alias and Jones (2000) studied the vertical distribution of marine fungi on *Rhizophora apiculata* in Malaysia. Their investigation reported that fungi, particularly ascomycetes with ascomata inhabiting sections exposed to salinity and water level fluctuations, exhibit special adaptations such as mucilaginous matrices surrounding the asci to prevent desiccation, or the development of immersed ascomata. The findings are consistent with these observations, as evidenced by the presence of different life stages of certain genera across vertical levels of decomposing *T. angustifolia* substrates. For instance, the asexual morphs of both *Hongkongmyces* and *Tubeufia* were isolated from the submerged sections, whereas their respective sexual stages were recorded only from the middle level. Furthermore, the asexual morphs of *Tetraploa* were observed in both aerial and submerged categories, while its sexual morph was restricted to the middle section, reflecting the influence of water-level fluctuations and harsh conditions over time (Figure 5.1). The ascomata of all three genera, *Hongkongmyces*, *Tetraploa*, and *Tubeufia*, recorded from the middle section comprised mucilaginous matrices surrounding the asci (Figure 5.7).

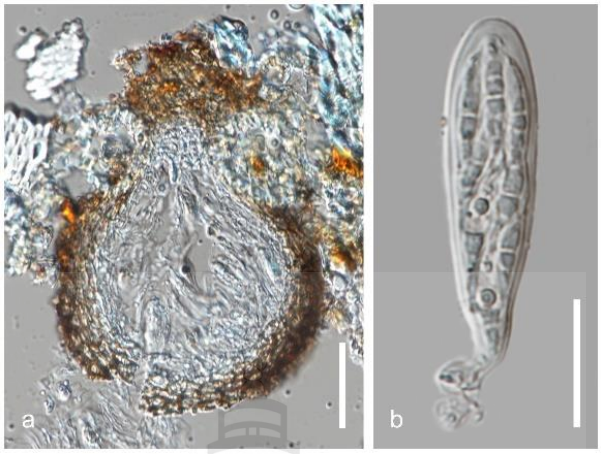

Note (a) Cross-section of *Tetraploa* ascomata showing mucilaginous matrices, (b) bitunicate ascus of *Tetraploa* isolated from the middle section. Scale Bars: (a) 50 µm; (b) 20 µm.

Figure 5.7 *Tetraploa* sexual morph

The ecological conditions of the middle section share characteristics of both the drier aerial and the moist submerged segments, depending on water level and surrounding environmental factors. The overall richness of the middle section (Richness = 48) and its α-diversity (H' = 3.4452) were higher than those of the adjacent aerial and bottom niches (Table 5.1). Considering these characteristics, together with the occurrence of fungal genera in different life stages, it is reasonable to deduce that the middle segment of decomposing *T. angustifolia* functions as a miniature ecotone, exhibiting features of both bordering niches. This transitional middle zone may act as a buffer section for microfungi inhabiting decomposing *T. angustifolia* and serve as a bridge facilitating species interactions across the water–air interface (Attrill et al., 2002; Heegaard et al., 2006; Dai et al., 2023; Qiu et al., 2023). Further in-depth investigations on this specific niche are therefore recommended.

The visual ordination plots constructed from PERMANOVA analyses using Bray–Curtis and Sørensen indices support the argument that species segregate across vertical levels of decomposing *T. angustifolia* substrates, as indicated by diversity metrics, PERMDISP boxplots, and heatmaps (Figure 5.2, 5.3, and Table 5.3). The plots illustrate clear clustering of the data, and the low stress values indicate that the NMDS

plots are reliable, reflecting true compositional changes in saprobic microfungal taxa associated with each vertical level.

Although both ordination plots broadly agree on the overall patterns, the Bray–Curtis and Sørensen NMDS plots reveal different perspectives. The Bray–Curtis NMDS plot expresses the aerial and middle sections as most similar and the aerial and submerge sections as most distinct, indicating that the aerial and middle segments share dominant taxa in terms of abundance (Figure 5.2). In contrast, the Sørensen NMDS plot shows the middle and bottom segments as most similar and the aerial and bottom segments as most dissimilar (Figure 5.2). The middle and aerial segments share dominant genera such as *Chaetomium* and *Pestalotiopsis* (Figure 5.1), which explains the higher abundance-based similarity observed in the Bray–Curtis index. Meanwhile, the greater number of shared genera between the middle and bottom segments leads the presence/absence-based Sørensen index to classify these sections as ecologically most resemble in saprobic microfungal association with *T. angustifolia* (Figure 5.1, and 5.2) (Legendre & Legendre, 2012; Xing et al., 2024; Gurarie, 2025). These observations statistically support the argument that vertical stratification and habitat filtering shape the saprobic microfungal communities in decomposing *T. angustifolia*, with the middle section acting as a transitional ecotone for saprobic microfungal populations in coastal freshwater wetlands of central Thailand (Legendre & Legendre, 2012; Wang et al., 2015; Marion et al., 2021; Zheng et al., 2021; Xing et al., 2024).

5.5 Conclusion

The decomposing *T. angustifolia* substrates from freshwater coastal wetlands of Thailand supported a diverse assemblage of saprobic microfungi, with 73 genera recorded from 360 samples. The aerial and middle segments each contained nine unique genera, while the submerged segment harbored 15 unique genera, and 14 genera were shared across all vertical levels (Figure 5.1). The middle segment showed the highest richness (48 genera, $H' = 3.4452$), whereas the aerial segment was the least diverse (34 genera, $H' = 3.0412$). The β-diversity analyses revealed significant differences in community composition, with aerial and middle segments most similar by Bray–Curtis,

middle and bottom segments most similar by Sørensen, and aerial and bottom segments consistently the most dissimilar in saprobic fungal occupation.

These findings highlight distinct saprobic microfungal community structures across vertical levels of decomposing *T. angustifolia* substrates. Generalist, cosmopolitan fungi accounted for the shared genera across all categories, while unique taxa such as *Halosphaeriaceae*, *Diplocladiella*, and *Jalapriya*, restricted to the submerged segment, illustrate the role of habitat filtering and vertical stratification (Alias & Jones, 2000; Legendre & Legendre, 2012). The higher richness, elevated α-diversity, and overlap between neighboring segments, together with specialized morphological adaptations to fluctuating environmental conditions, suggest that the middle section functions as a transitional zone or ecotone for saprobic microfungi in freshwater coastal wetlands of central Thailand (Marion et al., 2021; Zheng et al., 2021; Xing et al., 2024). This study promotes further investigation in understanding vertical distribution of fungi on plant substrates in wetlands around the world.

CHAPTER 6

CONCLUSIONS

6.1 Overall Conclusion

The current study provides an updated account on taxonomy, phylogeny, and vertical distribution of saprobic microfungal community associated with Poales hosts in freshwater coastal wetlands of southern Thailand. In the initial phase of this research, it was significant to recognize and strategically select the study sites, focusing on understudied geographical locations for microfungi and predominant hosts in coastal wetlands in Thailand. To understand these gaps, a well-arranged review is required. In Chapter 2, I integrated historical and contemporary fungal studies on wetland-dwelling fungi into a comprehensive review. It facilitated the identification of existing research gaps and future research directions.

The review highlights the origin and evolution of wetlands and the colonization and adaptation of fungi and fungi-like taxa within these ecosystems. Emphasis is placed on ecological and biological adaptations that allow fungi to survive in challenging conditions, underscoring the importance of studying underexplored habitats to better understand fungal distribution and diversity. Dead or decaying Poales substrates, primarily Cyperaceae, Poaceae, and Typhaceae, were targeted as dominant hosts, with Typhaceae showing the highest fungal associations, followed by Poaceae and Cyperaceae. Despite the rich diversity of these host plants, comprehensive mycological studies remain limited, and existing data are often scattered, incomplete, or lacking sequence information.

Chapter 3 compiles 50 Poales-associated fungal genera in Dothideomycetes and Sordariomycetes from wetlands, including illustrations, taxonomic notes, ecological roles, geographical distribution, and nutritional modes. Chapter 4 presents a detailed taxonomic study of 59 saprobic microfungi from wetland-dwelling Cyperaceae, Poaceae, and Typhaceae in Thai freshwater coastal wetlands, including 31 *Dothideomycetes*, 2 *Eurotiomycetes*, 26 *Sordariomycetes*, and 20 new species.

Sequence data, phylogenetic trees, complete morphological plates, and comprehensive descriptions are provided to fill gaps in current knowledge and support global molecular databases. Future studies should employ culture-independent and tissue-based isolation methods to capture taxa that are difficult to germinate under standard laboratory conditions, further revealing hidden fungal diversity in these ecosystems.

Chapter 5 investigates the vertical diversity of saprobic microfungi associated with Typha angustifolia (Typhaceae, Poales) in Thai freshwater coastal wetlands, using statistical analyses and graphical visualizations. A total of 73 genera were recorded from 360 decomposing samples. The aerial and middle segments each contained nine unique genera, the submerged segment had 15, and 14 genera were shared across all levels. Richness was highest in the middle segment (48 genera, $H' = 3.4452$) and lowest in the aerial segment (34 genera, $H' = 3.0412$). β-diversity analyses revealed distinct community compositions: Bray–Curtis showed aerial and middle segments as most similar, Sørensen indicated middle and submerged segments as most similar, and aerial and submerged segments were consistently most dissimilar. Generalist fungi accounted for shared genera, while taxa such as Halosphaeriaceae, Diplocladiella, and Jalapriya were restricted to submerged parts, highlighting vertical stratification and habitat filtering. The middle segment, with higher richness, elevated α-diversity, and overlap with neighboring segments, functions as a transitional zone or ecotone for saprobic microfungi in these wetlands.

6.2 Research Advantages

Poales constitute the most dominant monocotyledonous plant order globally, occupying diverse habitats and exhibiting a cosmopolitan distribution. As fungi richly colonized with plants, they are frequently reported as hosts for different fungal communites. Families Cyperaceae, Poaceae and Typhaceae in Poales, have been most extensively studied for their associations with saprobic fungi. However, the majority of available studies are focused on terrestrial ecosystems, with only limited attention given to aquatic environments. Therefore, research on saprobic microfungi associated with

Cyperaceae, Poaceae, and Typhaceae in freshwater coastal wetlands remains particularly scarce.

My study presents a comprehensive review of the current understanding of saprobic microfungi on Poales, supported by detailed illustrations and taxonomic notes, and phylogeny. Also, I discovered 20 novel fungal taxa as well as new host and habitat records to understand the fungal taxonomy and distribution. In this study, I addressed the ecological significance, threats, and conservation importance of wetland-associated microfungi, together with relevant management strategies. By consolidating and synthesizing the available knowledge, this work addresses a notable research gap concerning saprobic microfungi associated with wetland-dwelling Poales.

In-depth taxonomic studies on microfungi associated with wetland-dwelling Poales are limited. This investigation employed both polyphasic and morphology-based identification methods. Typhaceae supported the highest number of genera (36), including 17 unique to this family. Poaceae yielded 23 genera, six of which were specific to grasses, including submerged bamboo, while Cyperaceae had the lowest diversity with 11 genera, five unique to sedges. *Curvularia* and *Tetraploa* were found across all three families, whereas genera such as *Achroiostachys*, *Distoseptispora*, *Pestalotiopsis*, and *Tubeufia* occurred in two host families. Detailed photoplates, comprehensive morphological descriptions, and updated phylogenetic trees were provided, and all molecular data were deposited in GenBank, enhancing global fungal taxonomy and accurate species identification.

The vertical distribution of fungi across environmental gradients has been of interest since the 1950s, with several studies in aquatic environments like intertidal mangrove swamps. However, vertical diversity in coastal freshwater wetlands, particularly on *Typha angustifolia*, had not been examined, revealing a clear research gap in understanding fungal stratification on Poales hosts in these habitats.

To address this, microfungi were systematically sampled from three *T. angustifolia* segments: (1) aerial leaves near the tip, (2) the portion between tip and water interface, and (3) submerged leaves. α-diversity was calculated using the Shannon–Wiener index (H′), while β-diversity was assessed with Bray–Curtis and Sørensen dissimilarity indices, supported by PERMANOVA and PERMDISP. From 360 samples, 73 saprobic genera were recorded. The middle segment had the highest

richness (48 genera; H′ = 3.4452) and the aerial segment the lowest (34 genera; H′ = 3.0412). ANOVA (Pr(>F) = 0.224) showed no significant α-diversity differences, but β-diversity analyses revealed distinct community compositions: Bray–Curtis indicated greatest similarity between aerial and middle segments, while Sørensen showed the lowest dissimilarity between middle and submerged segments. PERMANOVA confirmed significant compositional variation (39% and 35% explained by Bray–Curtis and Sørensen), and PERMDISP verified that these differences were not due to dispersion.

6.3 Future Directions

The present investigation focused on saprobic microfungi associated with Cyperaceae, Poaceae, and Typhaceae (Poales) in freshwater coastal wetlands of Thailand. Several taxa encountered in this study have the potential to occur as pathogenic, necrotrophic, epiphytic, or endophytic organisms within the investigated host families. Accordingly, future research on endophytic fungi and wetland-dwelling Poales-associated fungal pathogens holds promising potential as an extension of the current work, in Thailand as well as worldwide. Such data could also be incorporated into studies of vertical distribution that include saprobic, endophytic, and pathogenic taxa, thereby contributing to a more comprehensive understanding of fungal ecology in these environments.

The study areas examined in this research also support other potential host species, including members of Nymphaeaceae, Lythraceae, Cabombaceae, Acanthaceae, Fabaceae (e.g., the water mimosa genus *Neptunia*), and Plantaginaceae. However, these host families were not examined in detail for their saprobic fungal communities. Future studies targeting these plant families could broaden knowledge of the microfungal community structure in coastal freshwater wetlands of Thailand.

Our study focused primarily on coastal freshwater wetlands. The host plant families investigated in detail are distributed across habitats ranging from freshwater to brackish water estuaries. Therefore, future taxonomic studies on fungi associated with Cyperaceae, Poaceae, and Typhaceae along salinity gradients would be of particular

interest. Such investigations have the potential to reveal the salt tolerance levels of microfungi and their adaptive flexibility in response to osmotic pressure in the environments they inhabit.

Furthermore, the continental rifts of the Gulf of Thailand and the coastal regions of China support high biodiversity and extensive seagrass habitats. Comparative studies of microfungal communities associated with Poales across freshwater, brackish water, and marine environments would provide valuable taxonomic insights. Such investigations hold strong potential for the discovery of novel species, new host records, and previously unrecognized adaptive strategies of fungi.

Freshwater wetlands in Thailand are not limited to coastal regions. Numerous inland wetlands are associated with major river systems such as the Chao Phraya, Mae Klong, and Mekong, as well as a variety of floodplains. Future investigations on Poales-associated fungi could be extended to these inland wetlands, while vertical diversity studies could also be applied to other host families in both coastal and inland freshwater habitats. Such studies would contribute to a better understanding of fungal colonization patterns and the mechanisms of long-distance fungal dispersal through water and wind.

This investigation was conducted using culture-dependent methods. Fungal identification at the species level was achieved through a combination of morphological characterization and multilocus phylogeny-based taxonomic approaches. Direct DNA extractions from fruiting structures were carried out for specimens that failed to germinate under laboratory conditions. Consequently, this study was limited to reporting fungi that were observable from the selected materials. Fungi present in the samples only at the vegetative stage, or those that failed to develop reproductive structures during incubation, were not captured. Therefore, future studies are recommended to employ culture-independent approaches, as well as chemotaxonomic methods, to improve the accuracy of species delimitation and to provide a more comprehensive understanding of fungal diversity.

REFERENCES

Abdullah, S. K., Cano, J., Descals, E., & Guarro, J. (2000). The aero-aquatic *Helicodendron microsporum* n. sp. from Mallorca, Spain. *Mycological Research, 104*(3), 375–377. https://doi.org/10.1017/S0953756200001725

Ágoston-Szabó, E., & Dinka, M. (2008). Decomposition of *Typha angustifolia* and *Phragmites australis* in the littoral zone of a shallow lake. *Biologia, 63*(6), 1104–1110.

Alfonzo, A., Francesca, N., Sannino, C., Settanni, L., & Moschetti, G. (2013). Filamentous fungi transported by birds during migration across the Mediterranean Sea. *Current Microbiology, 66*, 236–242. https://doi.org/10.1007/s00284-012-0276-8

Alias, S. A., & Jones, E. B. G. (2000). Vertical distribution of marine fungi on *Rhizophora apiculata* at Morib mangrove, Selangor, Malaysia. *Mycoscience, 41*(5), 431–436. https://doi.org/10.1007/BF02461661

Al-Nasrawi, H. G., & Hughes, A. R. (2012). Fungal diversity associated with salt marsh plants *Spartina alterniflora* and *Juncus roemerianus* in Florida. *Jordan Journal of Biological Sciences, 5*, 247–254.

An, X., Han, S., Ren, X., Sichone, J., Fan, Z., Wu, X., . . . Sun, F. (2023). Succession of fungal community during outdoor deterioration of round bamboo. *Journal of Fungi, 9*(6), 691. https://doi.org/10.3390/jof9060691

Apurillo, C. C. S., Phukhamsakda, C., Mukhopadhyay, S., & Gunarathne, A., & Jones, E. B. G. (2023). *Nemania hydei* sp. nov. (Xylariaceae) from *Avicennia marina* in Central Thailand. *New Zealand Journal of Botany, 62*(1), 103–118. https://doi.org/10.1080/0028825X.2023.2289420

Asghari, R., Phukhamsakda, C., Jones, E. G., Bahkali, A., Apurillo, C. C. S., Karimi, O., . . . Hyde, K. D. (2025). Morphology and phylogeny reveal two new species and host records of hyphomycetous fungi on *Areca* species from marine habitats in Thailand. *MycoKeys, 118*, 179. https://doi.org/10.3897/mycokeys.118.10489

Asghari, R., Phukhamsakda, C., Karimi, O., Apurillo, C. C. S., & Jones, E. B. G. (2023). *Myrmecridium hydei*, a novel marine species from Thailand. *Phytotaxa, 625*(3), 265–279. https://doi.org/10.11646/phytotaxa.625.3.3

Attrill, M. J., & Rundle, S. D. (2002). Ecotone or ecocline: Ecological boundaries in estuaries. *Estuarine, Coastal and Shelf Science, 55*(6), 929–936. https://doi.org/10.1006/ecss.2002.1032

Aumentado, H. D. R., Armand, A., Chethana, K. T., Phukhamsakda, C., Norphanphoun, C., Hyde, K. D., . . . Jayawardena, R. S. (2024). Novel species, morpho-molecular identification and pathogenicity of *Allophoma* (Didymellacaeae) causing leaf spots of true mangroves and mangrove associates in Thailand. *Plant Pathology, 73*(7), 1730–1748. https://doi.org/10.1111/ppa.14024

Bai, Y., Wang, Q., Liao, K., Jian, Z., Zhao, C., & Qu, J. (2018). Fungal community as a bioindicator to reflect anthropogenic activities in a river ecosystem. *Frontiers in Microbiology, 9*, 3152. https://doi.org/10.3389/fmicb.2018.03152

Baltussen, T. J., Zoll, J., Verweij, P. E., & Melchers, W. J. (2020). Molecular mechanisms of conidial germination in *Aspergillus* sp. *Microbiology and Molecular Biology Reviews, 84*(1), 10-1128. https://doi.org/10.1128/MMBR.00004-19

Bao, D. F., Bhat, D. J., Boonmee, S., Hyde, K. D., Luo, Z. L., & Nalumpang, S. (2022). Lignicolous freshwater ascomycetes from Thailand: Introducing *Dematipyriforma muriformis* sp. nov., one new combination and two new records in Pleurotheciaceae. *MycoKeys, 93*, 57–80. https://doi.org/10.3897/mycokeys.93.87797

Bao, D. F., Hyde, K. D., Maharachchikumbura, S. S., Perera, R. H., Thiyagaraja, V., Hongsanan, S., . . . Luo, Z. L. (2023). Taxonomy, phylogeny and evolution of freshwater Hypocreomycetidae (Sordariomycetes). *Fungal Diversity, 121*, 1–94. https://doi.org/10.1007/s13225-023-00521-8

Barata, M. (2002). Fungi on the halophyte *Spartina maritima* in salt marshes. In K. D. Hyde (Ed.), *Fungi in marine environments* (pp. 179–193). Fungal Diversity Press.

Barbier, E. B. (2011). Wetlands as natural assets. *Hydrological Sciences Journal, 56*(8), 1360–1373. https://doi.org/10.1080/02626667.2011.630035

Bärlocher, F., & Boddy, L. (2016). Aquatic fungal ecology–How does it differ from terrestrial?. *Fungal Ecology, 19*, 5–13. https://doi.org/10.1016/j.funeco.2015.08.005

Barrett, D. M. (2007). Maximizing the nutritional value of fruits & vegetables. *Food Technology (Chicago), 61*(4), 40–44.

Barros, J., & Seena, S. (2022). Fungi in freshwaters: Prioritising aquatic hyphomycetes in conservation goals. *Water, 14*(4), 605. https://doi.org/10.3390/w14040605

Barros, J., Ben Tanfous, S., & Seena, S. (2024). Aquatic fungi as bioindicators of freshwater ecosystems. *Water, 16*(23), 3404. https://doi.org/10.3390/w16233404

Bhagya, A. T., Phukhamsakda, C., Jones, E. B. G., & Hyde, K. D. (2025). Unveiling a novel *Zopfiella* species (Lasiosphaeriaceae, Sordariales): Morphological characteristics and multigene phylogeny from *Carex* sp. (Cyperaceae) in Thailand. *New Zealand Journal of Botany*. https://doi.org/10.1080/0028825X.2025.2488389

Bhagya, A. T., Phukhamsakda, C., Tanaka, K., & Jones, E. B. G. (2024). Morphology and multigene phylogeny reveal a novel *Stagonospora* species (*Massarinaceae, Dothideomycetes*) from Thailand. *Phytotaxa, 644*(4), 281–293. https://doi.org/10.11646/phytotaxa.644.4.4

Bhunjun, C. S., Phukhamsakda, C., Hyde, K. D., McKenzie, E. H. C., Ramesh, K. S., & Li, Q. (2024). Do all fungi have ancestors with endophytic lifestyles?. *Fungal Diversity, 125*, 73–98. https://doi.org/10.1007/s13225-023-00516-5

Blackwell, M. (2010). Fungal evolution and taxonomy. In *The ecology of fungal entomopathogens* (pp. 7–16). Springer.

Bohrer, K. E., Friese, C. F., & Amon, J. P. (2004). Seasonal dynamics of arbuscular mycorrhizal fungi in differing wetland habitats. *Mycorrhiza, 14*, 329–337. https://doi.org/10.1007/s00572-004-0303-0

Boonmee, S., Rossman, A. Y., Liu, J. K., Li, W. J., Dai, D. Q., Bhat, J. D., . . . Hyde, K. D. (2014). *Tubeufiales*, ord. nov., integrating sexual and asexual generic names. *Fungal Diversity, 68*(1), 239–298. https://doi.org/10.1007/s13225-014-0294-x

Bouchenak-Khelladi, Y., Muasya, A. M., & Linder, H. P. (2014). A revised evolutionary history of Poales: Origins and diversification. *Botanical Journal of the Linnean Society, 175*(1), 4–16. https://doi.org/10.1111/boj.12119

Bray, J. R., & Curtis, J. T. (1957). An ordination of the upland forest communities of southern Wisconsin. *Ecological Monographs, 27*(4), 326–349. https://doi.org/10.2307/1942268

Brito, A. C. Q., de Mello, J. F., Michereff, S. J., Souza-Motta, C. M., & Machado, A. R. (2019). First report of *Macrophomina pseudophaseolina* causing stem dry rot in cassava in Brazil. *Journal of Plant Pathology, 101,* 1245. https://doi.org/10.1007/s42161-019-00309-3

Cai, L., Ji, K. F., & Hyde, K. D. (2006). Variation between freshwater and terrestrial fungal communities on decaying bamboo culms. *Antonie van Leeuwenhoek, 89*(2), 293–301. https://doi.org/10.1007/s10482-005-9004-5

Cai, L., Zhang, K., McKenzie, E. H., & Hyde, K. D. (2003). Freshwater fungi from bamboo and wood submerged in the Liput River in the Philippines. *Fungal Diversity*, 1–12.

Cai, L., Zhang, K., McKenzie, E. H., & Hyde, K. D. (2003). Freshwater fungi from bamboo and wood submerged in the Liput River in the Philippines. *Fungal Diversity, 13*, 1-12.

Calabon, M. S., Hyde, K. D., Jones, E. B. G., Luo, Z. L., Dong, W., Hurdeal, V. G., . . . Zeng, M. (2022). Freshwater fungal numbers. *Fungal Diversity, 114*(1), 3–235. https://doi.org/10.1007/s13225-022-00551-w

Calabon, M. S., Hyde, K. D., Jones, E. B. G., Bao, D. F., Bhunjun, C. S., Phukhamsakda, C., Shen, H. W., . . . Zeng, M. (2023). Freshwater fungal biology. *Mycosphere, 14*(1), 195–413. https://doi.org/10.5943/mycosphere/14/1/10

Canon, P. F., & Minter, D. W. (1986). The Rhytismataceae of the Indian subcontinent. *Mycol Pap No. 155*. C.A.B. International Mycological Institute, Slough.

Cerri, M., Sapkota, R., Coppi, A., Ferri, V., Foggi, B., Gigante, D., . . . Reale, L. (2017). Oomycete communities associated with reed die-back syndrome. *Frontiers in Plant Science, 8*, 1550. https://doi.org/10.3389/fpls.2017.01550

Chaiwan, N., Wanasinghe, D. N., Mapook, A., Jayawardena, R. S., Norphanphoun, C., & Hyde, K. D. (2020). Novel species of *Pestalotiopsis* fungi on *Dracaena* from Thailand. *Mycology, 11*(4), 306–315. https://doi.org/10.1080/21501203.2020.1821322

Chandrashekar, K. R., & Kaveriappa, K. M. (1989). Effect of pesticides on the growth of aquatic hyphomycetes. *Toxicology Letters, 48*(3), 311–315. https://doi.org/10.1016/0378-4274(89)90082-1

Chaturvedi, A. D., Pal, D., Penta, S., & Kumar, A. (2015). Ecotoxic heavy metals transformation by bacteria and fungi in aquatic ecosystem. *World Journal of Microbiology and Biotechnology, 31*(10), 1595–1603. https://doi.org/10.1007/s11274-015-1915-3

Chen, W., Xu, R., Wu, Y., Chen, J., Zhang, Y., Hu, T., . . . Fan, J. (2018). Plant diversity is coupled with beta not alpha diversity of soil fungal communities following N enrichment in a semi-arid grassland. *Soil Biology and Biochemistry, 116*, 388–398. https://doi.org/10.1016/j.soilbio.2017.10.025

Clarkson, B., & Peters, M. O. N. I. C. A. (2010). Wetland types. In *Wetland restoration: A handbook for New Zealand freshwater systems* (pp. 26–38). Bioeconomy Science Institute.

Cornwell, W. K., Bedford, B. L., & Chapin, C. T. (2001). Occurrence of arbuscular mycorrhizal fungi in a phosphorus-poor wetland and mycorrhizal response to phosphorus fertilization. *American Journal of Botany, 88*(10), 1824–1829. https://doi.org/10.2307/3558365

Crous, P. W., Schumacher, R. K., Akulov, A., Thangavel, R., Hernández-Restrepo, M., Carnegie, A. J., . . . Groenewald, J. Z. (2019). New and interesting fungi. 2. *Fungal Systematics and Evolution, 3*, 57. https://doi.org/10.3114/fuse.2019.03.06

Crous, P. W., Verkley, G. J. M., Christensen, M., Castañeda-Ruiz, R. F., & Groenewald, J. Z. (2012). How important are conidial appendages?. *Persoonia-Molecular Phylogeny and Evolution of Fungi, 28*(1), 126–137. https://doi.org/10.3767/003158512X630193

Cuomo, V., Vanzanella, F., Fresi, E., Cinelli, F., & Mazzella, L. (1985). Fungal flora of *Posidonia oceanica* and its ecological significance. *Transactions of the British Mycological Society, 84*(1), 35-40. https://doi.org/10.1016/S0007-1536(85)80217-5

Dai, T., Liu, R., Zhou, X., Zhang, J., Song, M., Zou, P., . . . Li, S. (2023). Role of lake aquatic–terrestrial ecotones in the ecological restoration of eutrophic water bodies. *Toxics, 11*(7), 560. https://doi.org/10.3390/toxics11070560

Delwiche, C. F., & Cooper, E. D. (2015). The evolutionary origin of a terrestrial flora. *Current Biology, 25*(19), R899–R910. https://doi.org/10.1016/j.cub.2015.08.037

Descals, E. (2005). Diagnostic characters of propagules of Ingoldian fungi. *Mycological Research, 109*, 545–555. https://doi.org/10.1017/S0953756205003284

Dias, A. A., Sampaio, A., & Bezerra, R. M. (2007). Environmental applications of fungal and plant systems: Decolourisation of textile wastewater and related dyestuffs. In *Environmental Bioremediation Technologies* (pp. 445–463). Springer. https://doi.org/10.1007/978-3-540-68896-6_21

Döll, P., & Zhang, J. (2010). Impact of climate change on freshwater ecosystems: A global-scale analysis of ecologically relevant river flow alterations. *Hydrology and Earth System Sciences, 14*(5), 783–799. https://doi.org/10.5194/hess-14-783-2010

Dong, W., Wang, B., Hyde, K. D., McKenzie, E. H. C., Raja, H. A., Tanaka, K., . . . Zhang, H. (2020). Freshwater *Dothideomycetes*. *Fungal Diversity, 105*(1), 319–575. https://doi.org/10.1007/s13225-020-00443-9

Eb, G. J. (2006). Form and function of fungal spore appendages. *Mycoscience, 47*(4), 167–183. https://doi.org/10.1007/s10267-006-0290-2

EFSA Panel on Plant Health (PLH), Bragard, C., Baptista, P., Chatzivassiliou, E., Di Serio, F., Gonthier, P., . . . Reignault, P. L. (2023). Pest categorisation of *Pestalotiopsis microspora*. *EFSA Journal, 21*(12), e08493. https://doi.org/10.2903/j.efsa.2023.8493

Ferreira, V., Elosegi, A., Gulis, V., Pozo, J., & Graça, M. A. (2006). Eucalyptus plantations affect fungal communities associated with leaf-litter decomposition in Iberian streams. *Archiv für Hydrobiologie, 166*(4), 467–490. https://doi.org/10.1127/0003-9136/2006/0166-0467

Figueroa, A., Contreras, M., Saavedra, B., & Espoz, C. (2016). Wetlands of Chile: Biodiversity, endemism and conservation challenges. In C. M. Finlayson, G. R. Milton, R. C. Prentice & N. C. Davidson (Eds.), *The wetland book* (pp. 1–17). Springer. https://doi.org/10.1007/978-94-007-6173-5_305-1

Freitas, E. S., Rujirawan, A., Ampai, N., Puanprapai, P., Yodthong, S., Termprayoon, K., . . . Aowphol, A. (2019). Amphibian surveys reveal no instances of *Batrachochytrium dendrobatidis* and suggest low prevalence of chytrid fungus in Thailand. *Herpetological Review, 50*(2), 290–298.

Fukasawa, Y., & Kaga, K. (2022). Surface area of wood influences the effects of fungal interspecific interaction on wood decomposition: A case study based on *Pinus densiflora* and selected white rot fungi. *Journal of Fungi, 8*(5), 517. https://doi.org/10.3390/jof8050517

Geiser, D. M., Gueidan, C., Miadlikowska, J., Lutzoni, F., Kauff, F., Hofstetter, V., . . . Aptroot, A. (2006). *Eurotiomycetes*: *Eurotiomycetidae* and *Chaetothyriomycetidae*. *Mycologia, 98*(6), 1053–1064. https://doi.org/10.1080/15572536.2006.11832636

Glassman, S. I., Wang, I. J., & Bruns, T. D. (2017). Environmental filtering by pH and soil nutrients drives community assembly in fungi at fine spatial scales. *Molecular Ecology, 26*(24), 6960–6973. https://doi.org/10.1111/mec.14414

Gleason, F. H., Daynes, C. N., & McGee, P. A. (2010). Some zoosporic fungi can grow and survive within a wide pH range. *Fungal Ecology, 3*(1), 31–37. https://doi.org/10.1016/j.funeco.2009.07.001

Goh, T. K., & Hyde, K. D. (1999). Fungi on submerged wood and bamboo in the Plover Cove Reservoir, Hong Kong. *Fungal Diversity, 2*, 1–10.

Golan, J. J., & Pringle, A. (2017). Long-distance dispersal of fungi. *Microbiology Spectrum, 5*(4), 5–29. https://doi.org/10.1128/microbiolspec.FUNK-0047-2016

Goldmann, K., Schröter, K., Peña, R., Schöning, I., Schrumpf, M., Buscot, F., . . . Wubet, T. (2016). Divergent habitat filtering of root and soil fungal communities in temperate beech forests. *Scientific Reports, 6*(1), 31439. https://doi.org/10.1038/srep31439

Greb, S. F., DiMichele, W. A., & Gastaldo, R. A. (2006). Evolution and importance of wetlands in earth history. In S. F. Greb & W. A. DiMichele (Eds.), *Wetlands through Time* (pp. 1–41). Springer. https://doi.org/10.1130/2006.2399(01)

Greb, S. F., DiMichele, W. A., Gastaldo, R. A., Eble, C. F., Wing, S. L., Mehner, T., . . . Kockner, K. (2022). Prehistoric wetlands. In G. E. Likens (Ed.), *Encyclopedia of Inland Waters* (2nd ed., vol. 3, pp. 23–32). Elsevier. https://doi.org/10.1016/B978-0-12-822550-5.00006-1

Grossart, H. P., Wurzbacher, C., James, T. Y., & Kagami, M. (2016). Discovery of dark matter fungi in aquatic ecosystems demands a reappraisal of the phylogeny and ecology of zoosporic fungi. *Fungal Ecology, 19*, 28–38. https://doi.org/10.1016/j.funeco.2015.06.008

Gulis, V. (2001). Are there any substrate preferences in aquatic hyphomycetes?. *Mycological Research, 105*(9), 1088–1093. https://doi.org/10.1017/S0953756201004729

Gulis, V., Ferreira, V., & Graça, M. A. (2006). Stimulation of leaf litter decomposition and associated fungi and invertebrates by moderate eutrophication: Implications for stream assessment. *Freshwater Biology, 51*(9), 1655–1669. https://doi.org/10.1111/j.1365-2427.2006.01596.x

Gurarie, E. (2025). Bray–Curtis similarity. University of Maryland. https://terpconnect.umd.edu/~egurarie/research/skinmicrobiome/TransectAnalysis/Step4_Similarity.html

Hall, T. A. (1999). BioEdit: A user-friendly biological sequence alignment editor and analysis program for Windows 95/98/NT. *Nucleic Acids Symposium Series, 41*, 95–98.

Hao, M., Corral-Rivas, J. J., González-Elizondo, M. S., Ganeshaiah, K. N., Nava-Miranda, M. G., Zhang, C., . . . Von Gadow, K. (2019). Assessing biological dissimilarities between five forest communities. *Forest Ecosystems, 6*(1), 30. https://doi.org/10.1186/s40663-019-0192-2

Harrison, J. G., Forister, M. L., Parchman, T. L., & Koch, G. W. (2016). Vertical stratification of the foliar fungal community in the world's tallest trees. *American Journal of Botany, 103*(12), 2087–2095. https://doi.org/10.3732/ajb.1600277

Hassett, B. T., Thines, M., Buaya, A., Ploch, S., & Gradinger, R. (2019). A glimpse into the biogeography, seasonality, and ecological functions of Arctic marine Oomycota. *IMA Fungus, 10*, 1–10. https://doi.org/10.1186/s43008-019-0014-y

Hawksworth, D. L., & Grube, M. (2020). Lichens redefined as complex ecosystems. *New Phytologist, 227*(5), 1281–1283. https://doi.org/10.1111/nph.16514

Hayward, J., & Hynson, N. A. (2014). New evidence of ectomycorrhizal fungi in the Hawaiian Islands associated with the endemic host *Pisonia sandwicensis* (Nyctaginaceae). *Fungal Ecology, 12*, 62–69. https://doi.org/10.1016/j.funeco.2014.09.001

He, Q., Li, Z. A., Daleo, P., Lefcheck, J. S., Thomsen, M. S., Adams, J. B., & Bouma, T. J. (2025). Coastal wetland resilience through local, regional and global conservation. *Nature Reviews Biodiversity, 1*(1), 50–67. https://doi.org/10.1038/s44358-024-00004-x

Heegaard, E., Lotter, A. F., & Birks, H. J. B. (2006). Aquatic biota and the detection of climate change: Are there consistent aquatic ecotones?. *Journal of Paleolimnology, 35*(3), 507–518. https://doi.org/10.1007/s10933-005-3239-x

Hellmann, L., Tegel, W., Eggertsson, Ó., Schweingruber, F. H., Blanchette, R., Kirdyanov, A., . . . Büntgen, U. (2013). Tracing the origin of Arctic driftwood. *Journal of Geophysical Research: Biogeosciences, 118*(1), 68–76. https://doi.org/10.1002/jgrg.20022

Hempattarasuwan, N., Untong, A., Christakos, G., & Wu, J. (2021). Wetland changes and their impacts on livelihoods in Chiang Saen Valley, Chiang Rai Province, Thailand. *Regional Environmental Change, 21*(4), 115. https://doi.org/10.1007/s10113-021-01842-7

Ho, W. H., Hyde, K. D., Hodgkiss, I. J., & Yanna. (2001). Fungal communities on submerged wood from streams in Brunei, Hong Kong and Malaysia. *Mycological Research, 105*(12), 1492–1501. https://doi.org/10.1017/S0953756201005090

Ho, W. H., Yanna, Hyde, K. D., & Hodgkiss, I. J. (2002). Seasonality and sequential occurrence of fungi on wood submerged in a forest stream at Tai Po, Hong Kong. *Fungal Diversity, 10*, 21–43.

Hongsanan, S., Hyde, K. D., Phookamsak, R., Wanasinghe, D. N., McKenzie, E. H., Sarma, V. V., . . . Xie, N. (2020). Refined families of Dothideomycetes: Orders and families incertae sedis in Dothideomycetes. *Fungal Diversity, 105*, 17–318. https://doi.org/10.1007/s13225-020-00462-6

Hopkinson, C. S., Wolanski, E., Cahoon, D. R., Perillo, G. M., & Brinson, M. M. (2019). Coastal wetlands: A synthesis. In G. M. E. Perillo, E. Wolanski, D. R. Cahoon & C. S. Hopkinson (Eds.), *Coastal Wetlands: An integrated ecosystem approach* (pp. 1–75). Elsevier.

Hu, D., Cai, L., Chen, H., Bahkali, A. H., & Hyde, K. D. (2010). Fungal diversity on submerged wood in a tropical stream and an artificial lake. *Biodiversity and Conservation, 19*(13), 3799–3808. https://doi.org/10.1007/s10531-010-9927-5

Huang, S. K., Hyde, K. D., Mapook, A., Maharachchikumbura, N. S. S., Bhat, D. J., McKenzie, E. H. C., . . . Wen, T. (2021). Taxonomic studies of some often overlooked *Diaporthomycetidae* and *Sordariomycetidae*. *Fungal Diversity, 111*, 443–572. https://doi.org/10.1007/s13225-021-00488-4

Hurdeal, V. G., Longcore, J. E., Jones, E. G., Simmons, D. R., Hyde, K. D., & Gentekaki, E. (2023). Integrative approach to species delimitation in Rhizophydiales: Novel species of *Angulomyces*, *Gorgonomyces*, and *Terramyces* from northern Thailand. *Molecular Phylogenetics and Evolution, 180*, 107706. https://doi.org/10.1016/j.ympev.2023.107706

Hyde, K. D., de Silva, N., Jeewon, R., Bhat, J. D., Phookamsak, R., Doilom, M., Boonmee, S., . . . Sarma, V. V. (2020a). AJOM new records and collections of fungi: 1–100. Asian Journal of Mycology, 3(1), 22–294. https://doi.org/10.5943/ajom/3/1/3

Hyde, K. D., Jones, E. B., & Moss, S. T. (1986b). How do fungal spores attach to surfaces?. In S. Barr, D. R. Houghton, G. C. Llewellyn, & C. E. O'Rear (Eds.), *Biodeterioration 6* (pp. 584–589). CAB International Mycological Institute and The Biodeterioration Society.

Hyde, K. D., Jones, E. B. G., & Moss, S. T. (1986a). Mycelial adhesion to surfaces. In S. T. Moss (Ed.), *The biology of marine fungi* (pp. 331–341). Cambridge University Press.

Hyde, K. D., & Sarma, V. V. (2006). Biodiversity and ecological observations on filamentous fungi of mangrove palm *Nypa fruticans* Wurumb (Liliopsida-Arecales) along the Tutong river, Brunei. *Indian Journal of Marine Sciences, 35*, 297–307.

Hyde, K. D. (1990). A comparison of the intertidal mycota of five mangrove tree species. *Asian Marine Biology, 7*, 93–107.

Hyde, K. D., & Jones, E. B. G. (2002). Introduction to fungal succession. *Fungal Diversity, 10*, 1–4.

Hyde, K. D., Hongsanan, S., Jeewon, R., Bhat, D. J., McKenzie, E. H., Jones, E. G., . . . & Zhu, L. (2016). Fungal diversity notes 367–490: Taxonomic and phylogenetic contributions to fungal taxa. *Fungal Diversity, 80*, 1–270. https://doi.org/10.1007/s13225-016-0357-0

Hyde, K. D., Jones, E. G., Liu, J. K., Ariyawansa, H., Boehm, E., Boonmee, S., . . . Zhang, M. (2013). Families of Dothideomycetes. *Fungal Diversity, 63*, 1–313. https://doi.org/10.1007/s13225-013-0263-4

Hyde, K. D., Tennakoon, D. S., Jeewon, R., Bhat, D. J., Maharachchikumbura, S. S., Rossi, W., . . . Doilom, M. (2019). Fungal diversity notes 1036–1150: Taxonomic and phylogenetic contributions on genera and species of fungal taxa. *Fungal Diversity, 96*, 1–242. https://doi.org/10.1007/s13225-019-00454-x

Hyde, K. D., Zhou, D., & Dalisay, T. (2002). Bambusicolous fungi: A review. *Fungal Diversity, 10*, 1–20.

Jayaram, S., Biswas, S., Philip, I., Umesh, M., & Sarojini, S. (2023). Differential laccase production among diverse fungal endophytes in aquatic plants of Hulimavu Lake in Bangalore, India. *Journal of Pure & Applied Microbiology, 17*(1), 298-308. https://doi.org/10.22207/JPAM.17.1.19

Jayasiri, S. C., Hyde, K. D., Ariyawansa, H. A., Bhat, J., Buyck, B., Cai, L., . . . Xu, J. (2022). A review of bambusicolous Ascomycota in China with an emphasis on species richness in southwest China. *Studies in Fungi, 7*(1), 1–33.

Jones, E. B. G. (1995). Ultrastructure and taxonomy of the aquatic ascomycetous order Halosphaeriales. *Canadian Journal of Botany, 73*(Suppl 1), S790–S801.

Jones, E. B. G., & Kuthubutheen, A. J. (1989). Malaysian mangrove fungi. *Sydowia, 41*, 160–169.

Jones, E. B. G. (1971). The ecology and rotting ability of marine fungi. In E. B. G. Jones & S. K. Eltringham (Eds.), *Marine borers, fungi and fouling organisms of wood* (pp. 237–258). Organisation for Economic Cooperation and Development.

Jones, E. B. G., Johnson, R. G., & Moss, S. T. (1986). Taxonomic studies of the Halosphaeriaceae. In C. Raghukumar (Ed.), *The biology of marine fungi* (pp. 211–230). Cambridge University Press.

Jones, E. B. G., Uyenco, R., & Follosco, P. (1988). Fungi on driftwood collected in the intertidal zone from the Philippines. *Asian Marine Biology, 5*, 103–106.

Jones, E. G., & Moss, S. T. (1980). Further observations on the taxonomy of the Halosphaeriaceae. *Botanica Marina, 23*(8), 483–500.

Jones, E. G., & Pang, K. L. (2012). Tropical aquatic fungi. *Biodiversity and Conservation, 21*, 2403–2423. https://doi.org/10.1007/s10531-011-0198-6

Jones, E. G., Ju, W. T., Lu, C. L., Guo, S. Y., & Pang, K. L. (2017). The Halosphaeriaceae revisited. *Botanica Marina, 60*(4), 453–468.

Karimi, O., Chethana, K. W. T., de Farias, A. R. G., Asghari, R., Kaewchai, S., Hyde, K. D., . . . Li, Q. (2024). Morphology and multigene phylogeny reveal three new species of *Distoseptispora*. *MycoKeys, 102*, 55–81. https://doi.org/10.3897/mycokeys.102.112815

Karunarathna, A., Withee, P., Pakdeeniti, P., Haituk, S., Tanakaew, N., Senwanna, C., . . . Cheewangkoon, R. (2022). Worldwide checklist on Grass Fungi: What do we know so far in Ascomycota. *Chiang Mai Journal of Science, 49*, 742–984.

Katoh, K., Rozewicki, J., & Yamada, K. D. (2019). MAFFT online service: Multiple sequence alignment, interactive sequence choice and visualization. *Briefings in Bioinformatics, 20*, 1160–1166. https://doi.org/10.1093/bib/bbx108

Kohlmeyer, J., & Kohlmeyer, E. (1979). Marine mycology—the higher fungi. Academic Press.

Kohlmeyer, J., Volkmann-Kohlmeyer, B., & Eriksson, O. E. (1995). Fungi on *Juncus roemerianus*. 4. New marine ascomycetes. *Mycologia, 87*(4), 532–542. https://doi.org/10.1080/00275514.1995.12026565

Kouadri, M. E. A., Zaim, S., & Bekkar, A. A. (2021). First report of *Macrophomina pseudophaseolina* infecting *Lens culinaris*. *Australasian Plant Disease Notes, 16*, 26. https://doi.org/10.1007/s13314-021-00440-0

Luo, Z. L., Bahkali, A. H., Liu, X. Y., Phookamsak, R., Zhao, Y. C., Zhou, D. Q., . . . Hyde, K. D. (2016). *Poaceascoma aquaticum* sp. nov. (Lentitheciaceae), a new species from submerged bamboo in freshwater. *Phytotaxa, 253*(1), 71–80.

Luo, Z. L., Hyde, K. D., Liu, J. K., Maharachchikumbura, S. S., Jeewon, R., Bao, D. F., . . . Su, H. Y. (2019). Freshwater Sordariomycetes. *Fungal Diversity, 99*, 451–660. https://doi.org/10.1007/s13225-019-00438-1

Lyons, J. I., Alber, M., & Hollibaugh, J. T. (2010). Ascomycete fungal communities associated with early decaying leaves of *Spartina* spp. from central California estuaries. *Oecologia, 162*, 435–442.

Ma, J., Hyde, K. D., Tibpromma, S., Gomdola, D., Liu, N. G., Norphanphoun, C., . . . Lu, Y. Z. (2024). Taxonomy and systematics of lignicolous helicosporous hyphomycetes. *Fungal Diversity, 129*(1), 365–653.

Ma, X. Y., Tian, F., Feng, J. F., Wang, M. M., Shi, H. H., & Ma, J. (2025). Morphological and phylogenetic analyses reveal two new species of *Tubeufia* (Tubeufiales, Tubeufiaceae) from freshwater habitats in China. *MycoKeys, 121*, 93.

Magaña-Dueñas, V., Cano-Lira, J. F., & Stchigel, A. M. (2021). New Dothideomycetes from freshwater habitats in Spain. *Journal of Fungi, 7*(12), 1102.

Maharachchikumbura, S. S., Hyde, K. D., Jones, E. G., McKenzie, E. H. C., Bhat, J. D., Dayarathne, M. C., . . . Wijayawardene, N. N. (2016). Families of Sordariomycetes. *Fungal Diversity, 79*, 1–317.

Marion, Z. H., Orwin, K. H., Wood, J. R., Holdaway, R. J., & Dickie, I. A. (2021). Land use, but not distance, drives fungal beta diversity. *Ecology, 102*(11), e03487.

Mayer, T., Moskaluk, A. E., Kolby, J. E., Russell, M., Schaffer, P., & Fagre, A. C. (2022). First recorded outbreak of *Veronaea botryosa* in North American amphibians: Clinicopathologic features of a rare cause of phaeohyphomycosis in captive White's tree frogs (*Litoria caerulea*). *Medical Mycology Case Reports, 38*, 13–17.

Miller, M. A., Pfeiffer, W., & Schwartz, T. (2010). Creating the CIPRES science gateway for inference of large phylogenetic trees. In *2010 Gateway Computing Environments Workshop (GCE)* (pp. 1–8). IEEE.

Mohammed, W. S., Ziganshina, E. E., Shagimardanova, E. I., Gogoleva, N. E., & Ziganshin, A. M. (2018). Comparison of intestinal bacterial and fungal communities across various xylophagous beetle larvae (Coleoptera: Cerambycidae). *Scientific Reports*, *8*(1), 10073. https://doi.org/10.1038/s41598-018-27342-z

Monkai, J., Phookamsak, R., Bhat, D. J., Ei, T. S. Z., Xu, J., & Lumyong, S. (2025). Novel endophytic pestalotioid species associated with *Itea* in Thailand. *Frontiers in Cellular and Infection Microbiology, 15*, 1532712. https://doi.org/10.3389/fcimb.2025.1532712

Mukhopadhyay, S., Bhunjun, C. S., Phukhamsakda, C., Apurillo, C. C. S., Al Otibi, F., Hyde, K. D., . . . Jones, E. B. G. (2024). Introducing a new species, *Vaginatispora acrostichi* (*Lophiostomataceae*), based on morphology and multigene phylogeny. *Botanica Marina, 67*(4), 401–410. https://doi.org/10.1515/bot-2024-0008

Mustafa, A., Azim, M. K., Laraib, Q., & Rehman, Q. M. U. (2024). Hybrid constructed wetlands and filamentous fungi for treatment of mixed sewage and industrial effluents. *Environmental Science and Pollution Research, 31*(31), 44230–44243.

Nag Raj, T. R. (1993). *Coelomycetes: Anamorphs with appendaged bearing conidia*. Mycologue Publishing.

Nam, B., & Choi, Y. J. (2019). Phytopythium and *Pythium* species (Oomycota) isolated from freshwater environments of Korea. *Mycobiology, 47*, 261–272.

Nedukha, O. (2025). Structural-functional signs of *Typha angustifolia* leaves plasticity depending on the growth conditions. *Plant Introduction, (105/106)*, 3–14.

Negreiros, A. M. P., Sales Júnior, R., León, M., de Assis Melo, N. J., Michereff, S. J., de Queiroz Ambrósio, M. M., . . . Armengol, J. (2019). Identification and pathogenicity of *Macrophomina* species collected from weeds in melon fields in Northeastern Brazil. *Journal of Phytopathology, 167*(6), 326–337. https://doi.org/10.1111/jph.12801

Newell, S. Y. (2001). Multiyear patterns of fungal biomass dynamics and productivity within naturally decaying smooth cordgrass shoots. *Limnology and Oceanography, 46*, 573–583.

Newell, S. Y., & Porter, D. (2000). Microbial secondary production from saltmarsh-grass shoots, and its known and potential fates. In M. P. Weinstein & D. A. Kreeger (Eds.), *Concepts and controversies in tidal marsh ecology* (pp. 159–185). Kluwer Academic Publishers.

Newell, S. Y., & Wasowski, J. (1995). Sexual productivity and spring intramarsh distribution of a key salt-marsh microbial secondary producer. *Estuaries, 18*, 241–249.

Nwobodo, D. C., Eze, P. M., Okezie, U. M., Okafoanyali, J. O., Okoye, F. B., & Esimone, C. O. (2022). Bioactive compounds characterization and antimicrobial potentials of crude extract of *Curvularia lunata*, a fungal endophyte from *Elaeis guineensis*. *Tropical Journal of Natural Product Research, 6*(3), 395-402.

Oliveira, C. S., Alcantara, G. B., Lião, L. M., Mesquita, G. M., Freitas, S. S., & Petacci, F. (2016). Decomposition dynamics of *Typha angustifolia* under aerobic conditions. *Journal of the Brazilian Chemical Society, 27*(9), 1687–1693.

Pang, K. L., Vrijmoed, L. L., & Gareth Jones, E. B. (2013). Genetic variation within the cosmopolitan aquatic fungus *Lignincola laevis* (Microascales, Ascomycota). *Organisms Diversity & Evolution, 13*, 301–309.

Peay, K. G., Garbelotto, M., & Bruns, T. D. (2010). Evidence of dispersal limitation in soil microorganisms: Isolation reduces species richness on mycorrhizal tree islands. *Ecology, 91*(12), 3631–3640.

Pereira, A., & Ferreira, V. (2021). Invasion of native riparian forests by acacia species affects in-stream litter decomposition and associated microbial decomposers. *Microbial Ecology, 81*(1), 14–25.

Pérez, J., Martínez, A., Descals, E., & Pozo, J. (2018). Responses of aquatic hyphomycetes to temperature and nutrient availability: A cross-transplantation experiment. *Microbial Ecology, 76*, 328–339. https://doi.org/10.1007/s00248-018-1211-6

Phookamsak, R., Norphanphoun, C., Tanaka, K., Dai, D. Q., Luo, Z. L., Liu, J. K., . . . Hyde, K. D. (2015). Towards a natural classification of *Astrosphaeriella*-like species; introducing Astrosphaeriellaceae and Pseudoastrosphaeriellaceae fam. nov. and *Astrosphaeriellopsis*, gen. nov. *Fungal Diversity, 74*, 143–197. https://doi.org/10.1007/s13225-015-0320-4

Phukhamsakda, C., McKenzie, E. H. C., Phillips, A. J. L., Jones, E. B. G., Bhat, D. J., Stadler, M., Bhunjun, C. S., . . . Hyde, K. D. (2020). Microfungi associated with *Clematis* (Ranunculaceae) with an integrated approach to delimiting species boundaries. *Fungal Diversity, 102*(1), 1–203. https://doi.org/10.1007/s13225-020-00448-4

Pinruan, U., Pinnoi, A., Hyde, K. D., & Jones, E. G. (2014). 17 Tropical peat swamp fungi with special reference to palms. In E. B. G. Jones, K. D Hyde & K.-L. Pang (Eds.), *Freshwater fungi: And fungal-like organisms* (pp.371-388). Walter de Gruyter GmbH & Co KG.

Poudel, B., Shivas, R. G., Adorada, D. L., Barbetti, M. J., Bithell, S. L., Kelly, L. A., . . . Vaghefi, N. (2021). Hidden diversity of *Macrophomina* associated with broadacre and horticultural crops in Australia. *European Journal of Plant Pathology, 161*, 169–188. https://doi.org/10.1007/s10658-021-02300-0

Qiu, M., Wang, Y., Sun, C., Gao, X., & Lu, X. (2023). Plant communities regulated by water-level gradient in Caohai aquatic–terrestrial ecotones affect bacterial and fungal structures and co-occurrence networks. *Rhizosphere, 25*, 100674. https://doi.org/10.1016/j.rhisph.2023.100674

Quaedvlieg, W. G. J. M., Verkley, G. J. M., Shin, H. D., Barreto, R. W., Alfenas, A. C., Swart, W. J., . . . Crous, P. W. (2013). Sizing up *Septoria*. *Studies in Mycology, 75*, 307–390. https://doi.org/10.3114/sim0017

R. L., Zhao, Q., Kang, J. C., & Promputtha, I. (2015). The Faces of Fungi database: Fungal names linked with morphology, phylogeny and human impacts. *Fungal Diversity, 74*, 3–18. https://doi.org/10.1007/s13225-015-0333-9

Raja, H. A., Shearer, C. A., & Tsui, C. K. (2018). Freshwater fungi. *eLS*, 1–13. https://doi.org/10.1002/9780470015902.a0026386

Ramsar Convention Secretariat. (2010). *Designating Ramsar sites: Strategic framework and guidelines for the future development of the List of Wetlands of International Importance* (Ramsar Handbooks for the Wise Use of Wetlands, 4th ed., vol. 18). Ramsar Convention Secretariat. https://www.ramsar.org/sites/default/files/documents/library/hbk4-18.pdf

Rathnayaka, A. R., Chethana, K. T., Phillips, A. J., Liu, J. K., Samarakoon, M. C., Jones, E. G., . . . Zhao, C. L. (2023). Re-evaluating Botryosphaeriales: Ancestral state reconstructions of selected characters and evolution of nutritional modes. *Journal of Fungi, 9*(2), 184. https://doi.org/10.3390/jof9020184

Ray, A. M., & Inouye, R. S. (2006). Effects of water-level fluctuations on the arbuscular mycorrhizal colonization of *Typha latifolia* L. *Aquatic Botany, 84*(3), 210–216. https://doi.org/10.1016/j.aquabot.2005.12.001

Rodríguez-Couto, S. (2017). Industrial and environmental applications of white-rot fungi. *Mycosphere, 8*(3), 456–466. https://doi.org/10.5943/mycosphere/8/3/7

Ronquist, F., Teslenko, M., Van Der Mark, P., Ayres, D. L., Darling, A., Höhna, S., . . . Huelsenbeck, J. P. (2012). 3.2: Efficient Bayesian phylogenetic inference and model choice across a large model space. *Systematic Biology, 61*, 539–542. https://doi.org/10.1093/sysbio/sys029

Rossman, A. Y., & Palm, M. E. (2006). Why are *Phytophthora* and other Oomycota not true fungi?. *Outlooks on Pest Management, 17*(5), 217–220.

Sadaba, R. B., Vrijmoed, L. L. P., Jones, E. B. G., & Hodgkiss, I. J. (1995). Observations on vertical distribution of fungi associated with standing senescent *Acanthus ilicifolius* stems at Mai Po Mangrove, Hong Kong. *Hydrobiologia, 295*(1), 119–126. https://doi.org/10.1007/BF00027093

Saelee, R., Busarakam, K., & Koohakan, P. (2021). Morphological characterization and phylogeny of *Pythium* and related genera in Rayong province, Thailand. *Current Applied Science and Technology, 21*(1), 132–153.

Sakayaroj, J., Pang, K. L., & Jones, E. G. (2011). Multi-gene phylogeny of the Halosphaeriaceae: Its ordinal status, relationships between genera and morphological character evolution. *Fungal Diversity, 46*(1), 87–109. https://doi.org/10.1007/s13225-010-0085-7

Salvatore, M. M., Andolfi, A., & Nicoletti, R. (2020). The thin line between pathogenicity and endophytism: The case of *Lasiodiplodia theobromae*. *Agriculture, 10*(10), 488. https://doi.org/10.3390/agriculture10100488

Sandberg, D. C., Battista, L. J., & Arnold, A. E. (2014). Fungal endophytes of aquatic macrophytes: Diverse host-generalists characterized by tissue preferences and geographic structure. *Microbial Ecology, 67*, 735–747. https://doi.org/10.1007/s00248-014-0427-0

Santillán-Manjarrez, J., Solís-Hernández, A. P., Castilla-Hernández, P., Maldonado-Mendoza, I. E., Vela-Correa, G., Chimal-Hernández, A., . . . Rivera-Becerril, F. (2019). Explorando interacciones raíz-hongo en un humedal neotropical de agua dulce. *Botanical Sciences, 97*(4), 661–674.

Sarr, M. P., Ndiaye, M., Groenewald, J. Z., & Crous, P. W. (2014). Genetic diversity in *Macrophomina phaseolina*, the causal agent of charcoal rot. *Phytopathologia Mediterranea, 53*(2), 250–268. https://doi.org/10.14601/Phytopathol_Mediterr-13736

Seekles, S. J. (2023). The breaking of fungal spore dormancy: A coordinated transition. *PLoS Biology, 21*(4), e3002077. https://doi.org/10.1371/journal.pbio.3002077

Selosse, M. A., Vohník, M., & Chauvet, E. (2008). Out of the rivers: Are some aquatic hyphomycetes plant endophytes? *New Phytologist, 178*(1), 3–7. https://doi.org/10.1111/j.1469-8137.2007.02321.x

Senanayake, I. C., Rathnayaka, A. R., Marasinghe, D. S., Calabon, M. S., Gentekaki, E., Lee, H. B., . . . Wijesinghe, S. N. (2020). Morphological approaches in studying fungi: Collection, examination, isolation, sporulation and preservation. *Mycosphere, 11*, 2678–2754. https://doi.org/10.5943/mycosphere/11/1/14

Shearer, C. A. (1993). The freshwater ascomycetes. *Nova Hedwigia, 56*(1-2), 1–33. https://doi.org/10.1127/nh/56/1993/1

Shen, H. W., Bao, D. F., Bhat, D. J., Su, H. Y., & Luo, Z. L. (2022). Lignicolous freshwater fungi in Yunnan Province, China: An overview. *Mycology, 13*(2), 119–132. https://doi.org/10.1080/21501203.2021.1979704

Shi, L. L., Mortimer, P. E., Ferry Slik, J. W., Zou, X. M., Xu, J., Feng, W. T., . . . Qiao, L. (2014). Variation in forest soil fungal diversity along a latitudinal gradient. *Fungal Diversity, 64*(1), 305–315. https://doi.org/10.1007/s13225-014-0276-8

Silvani, V. A., Colombo, R. P., Scorza, M. V., Fernandez Bidondo, L., Rothen, C. P., Scotti, A., . . . Godeas, A. (2017). Arbuscular mycorrhizal fungal diversity in high-altitude hypersaline Andean wetlands studied by 454-sequencing and morphological approaches. *Symbiosis, 72*, 143–152. https://doi.org/10.1007/s13199-017-0480-6

Simonis, J. L., Raja, H. A., & Shearer, C. A. (2008). Extracellular enzymes and soft rot decay: Are ascomycetes important degraders in fresh water?. *Fungal Diversity, 31*(1), 135–146. https://doi.org/10.1007/s13225-008-0011-0

Siriarchawatana, P., Harnpicharnchai, P., Phithakrotchanakoon, C., Kitikhun, S., Mayteeworakoon, S., Chunhametha, S., . . . Ingsriswang, S. (2024). Fungal communities as dual indicators of river biodiversity and water quality assessment. *Water Research, 253*, 121252. https://doi.org/10.1016/j.watres.2024.121252

Solé, M., Fetzer, I., Wennrich, R., Sridhar, K. R., Harms, H., & Krauss, G. (2008). Aquatic hyphomycete communities as potential bioindicators for assessing anthropogenic stress. *Science of the Total Environment, 389*(2-3), 557–565. https://doi.org/10.1016/j.scitotenv.2008.07.027

Somrithipol, S., & Jones, E. B. G. (2003). *Berkleasmium typhae* sp. nov., a new hyphomycete on narrow-leaved cattail (*Typha angustifolia*) from Thailand. *Fungal Diversity, 12*, 169–172. https://doi.org/10.1007/s13225-003-0008-0

Sorensen, T. (1948). A method of establishing groups of equal amplitude in plant sociology based on similarity of species content and its application to analyses of the vegetation on Danish commons. *Biologiske skrifter, 5*, 1–34.

Steiner, F. M., Schlick-Steiner, B. C., VanDerWal, J., Reuther, K. D., Christian, E., Stauffer, C., . . . Crozier, R. H. (2008). Combined modelling of distribution and niche in invasion biology: A case study of two invasive *Tetramorium* ant species. *Diversity and Distributions, 14*(3), 538–545. https://doi.org/10.1111/j.1472-4642.2007.00456.x

Stephenson, S. L., Tsui, C., & Rollins, A. W. (2013). Methods for sampling and analyzing wetland fungi. In J. T. Anderson & C. A. Davis (Eds.), *Wetland techniques: Volume 2: Organisms* (pp. 93–121). Springer.

Tamura, K., Stecher, G., & Kumar, S. (2021). MEGA11: Molecular evolutionary genetics analysis version 11. *Molecular Biology and Evolution, 38*(7), 3022–3027. https://doi.org/10.1093/molbev/msab120

Tennakoon, D. S., Kuo, C. H., Purahong, W., Gentekaki, E., Pumas, C., Promputtha, I., . . . Hyde, K. D. (2022). Fungal community succession on decomposing leaf litter across five phylogenetically related tree species in a subtropical forest. *Fungal Diversity, 115*(1), 73–103. https://doi.org/10.1007/s13225-022-00526-5

Thambugala, K. M., Wanasinghe, D. N., Phillips, A. J. L., Camporesi, E., Bulgakov, T. S., Phukhamsakda, C., . . . Hyde, K. D. (2017). Mycosphere notes 1–50: Grass (*Poaceae*) inhabiting Dothideomycetes. *Mycosphere, 8*(4), 697–796. https://doi.org/10.5943/mycosphere/8/4/5

Thormann, M. N. (2006). Diversity and function of fungi in peatlands: A carbon cycling perspective. *Canadian Journal of Soil Science, 86*(Special Issue), 281–293. https://doi.org/10.4141/S05-059

Tibpromma, S., Hyde, K. D., McKenzie, E. H., Bhat, D. J., Phillips, A. J., Wanasinghe, D. N., . . . Karunarathna, S. C. (2018). Fungal diversity notes 840–928: Micro-fungi associated with Pandanaceae. *Fungal Diversity, 93*(1), 1–160. https://doi.org/10.1007/s13225-018-0419-7

Tickner, D., Opperman, J. J., Abell, R., Acreman, M., Arthington, A. H., Bunn, S. E., . . . Young, L. (2020). Bending the curve of global freshwater biodiversity loss: An emergency recovery plan. *BioScience, 70*(4), 330–342. https://doi.org/10.1093/biosci/biaa002

Tittensor, D. P., Walpole, M., Hill, S. L., Boyce, D. G., Britten, G. L., Burgess, N. D., . . . Ye, Y. (2014). A mid-term analysis of progress toward international biodiversity targets. *Science, 346*(6206), 241–244. https://doi.org/10.1126/science.1257484

Trisurat, Y. (2006). Community-based wetland management in northern Thailand. *International Journal of Environmental, Cultural, Economic and Social Sustainability, 2*(1), 49–62.

Tsui, C. K., Baschien, C., & Goh, T. K. (2016). Biology and ecology of freshwater fungi. In D. W. Li (Ed.), *Biology of microfungi* (pp. 285–313). Springer.

Vaksmaa, A., Guerrero-Cruz, S., Ghosh, P., Zeghal, E., Hernando-Morales, V., & Niemann, H. (2023). Role of fungi in bioremediation of emerging pollutants. *Frontiers in Marine Science, 10*, 1070905. https://doi.org/10.3389/fmars.2023.1070905

Van Hoewyk, D., Wigand, C., & Groffman, P. M. (2001). Endomycorrhizal colonization of *Dasiphora floribunda*, a native plant species of calcareous wetlands in eastern New York State, USA. *Wetlands, 21*(3), 431–436.

Vijaykrishna, D., & Hyde, K. D. (2006). Inter- and intra-stream variation of lignicolous freshwater fungi in tropical Australia. *Fungal Diversity, 21*, 203–224.

Voglmayr, H. (2011). Phylogenetic relationships and reclassification of *Spirosphaera lignicola*, an enigmatic aeroaquatic fungus. *Mycotaxon, 116*(1), 191–202. https://doi.org/10.5248/116.191

Voigt, K., James, T. Y., Kirk, P. M., Santiago, A. L. M. D. A., Waldman, B., Griffith, G. W., . . . Lee, H. B. (2021). Early-diverging fungal phyla: Taxonomy, species concept, ecology, distribution, anthropogenic impact, and novel phylogenetic proposals. *Fungal Diversity,* 1–40. https://doi.org/10.1007/s13225-021-00494-5

Walker, A. K., & Campbell, J. (2010). Marine fungal diversity: A comparison of natural and created salt marshes of the north-central Gulf of Mexico. *Mycologia, 102*(3), 513–521. https://doi.org/10.3852/09-149

Wang, J. T., Zheng, Y. M., Hu, H. W., Zhang, L. M., Li, J., & He, J. Z. (2015). Soil pH determines the alpha diversity but not beta diversity of soil fungal community along altitude in a typical Tibetan forest ecosystem. *Journal of Soils and Sediments, 15*(5), 1224–1232. https://doi.org/10.1007/s11368-015-1145-x

Wang, L., Liu, J., Zhang, M., Wu, T., & Chai, B. (2023). Ecological processes of bacterial and fungal communities associated with *Typha orientalis* roots in wetlands were distinct during plant development. *Microbiology Spectrum, 11*(1), e05051-22. https://doi.org/10.1128/spectrum.05051-22

Wasko, J. D., McGonigle, T. P., Goldsborough, L. G., Wrubleski, D. A., Badiou, P. H., & Armstrong, L. M. (2022). Use of shoot dimensions and microscopic analysis of leaves to distinguish *Typha latifolia*, *Typha angustifolia*, and their invasive hybrid *Typha* × *glauca*. *Wetlands Ecology and Management, 30*(1), 19–33. https://doi.org/10.1007/s11273-021-09856-0

Watanabe, K., Parbery, D. G., Kobayashi, T., & Doi, Y. (2000). Conidial adhesion and germination of *Pestalotiopsis neglecta*. *Mycological Research, 104*(8), 962–968. https://doi.org/10.1017/S0953756200002570

Wei, D. (2014). *Bamboo inhabiting fungi and their damage to the substrate* (Doctoral dissertation). Staats-und Universitätsbibliothek Hamburg Carl von Ossietzky.

Wimalasena, M. K., Wijayawardene, N. N., Bamunuarachchige, T. C., Zhang, G. Q., Udeni Jayalal, R. G., Bhat, D. J., . . . Dai, D. Q. (2025). *Ectophoma salviniae* sp. nov., *Neottiosporina mihintaleensis* sp. nov. and four other endophytes associated with aquatic plants from Sri Lanka and their extracellular enzymatic potential. *Frontiers in Cellular and Infection Microbiology, 14*, 1475114. https://doi.org/10.3389/fcimb.2025.1475114

Wirsel, S. G. (2004). Homogenous stands of a wetland grass harbour diverse consortia of arbuscular mycorrhizal fungi. *FEMS Microbiology Ecology, 48*(2), 129–138. https://doi.org/10.1016/j.femsec.2004.03.002

Wong, M. K. M., & Hyde, K. D. (2002). Fungal saprobes on standing grasses and sedges in a subtropic aquatic habitat. *Fungal Diversity Research Series, 7*, 195–212.

Wong, M. K., Goh, T. K., Hodgkiss, I. J., Hyde, K. D., Ranghoo, V. M., Tsui, C. K., . . . Yuen, T. K. (1998). Role of fungi in freshwater ecosystems. *Biodiversity & Conservation, 7*, 1187–1206. https://doi.org/10.1023/A:1008870519608

Xing, H., Chen, W., Liu, Y., & Cahill, J. F., Jr. (2024). Local community assembly mechanisms and the size of species pool jointly explain the beta diversity of soil fungi. *Microbial Ecology, 87*(1), 58. https://doi.org/10.1007/s00248-024-02455-3

Yamaguchi, K. (2023). Recent studies on aero-aquatic fungi, with special reference to diversity of conidial morphology and convergent evolution. *Mycoscience, 64*(5), 128–135. https://doi.org/10.1016/j.myc.2023.07.003

Yamaguchi, K., Tsurumi, Y., Suzuki, R., Chuaseeharonnachai, C., Sri-Indrasutdhi, V., Boonyuen, N., . . . Nakagiri, A. (2012). *Trichoderma matsushimae* and *T. aeroaquaticum*: Two aero-aquatic species with Pseudaegerita-like propagules. *Mycologia, 104*(5), 1109–1120. https://doi.org/10.3852/11-337

Yang, J. X., Peng, Y., Yang, J. J., Zhang, Y. H., Dong, Q., Li, Q. S., . . . Gao, C. (2025). Nitrogen addition alters arbuscular mycorrhizal fungi and soil bacteria networks without promoting phosphorus mineralization in a semiarid grassland. *Communications Biology, 8*(1), 1229. https://doi.org/10.1038/s42003-025-01882-3

Yang, J., Wang, Y., Cui, X., Xue, K., Zhang, Y., & Yu, Z. (2019). Habitat filtering shapes the differential structure of microbial communities in the Xilingol grassland. *Scientific Reports, 9*, 19326. https://doi.org/10.1038/s41598-019-55940-y

Yarwood, S. A. (2018). The role of wetland microorganisms in plant-litter decomposition and soil organic matter formation: A critical review. *FEMS Microbiology Ecology, 94*(11), fiy175. https://doi.org/10.1093/femsec/fiy175

Yasanthika, E., Tennakoon, D. S., Farias, A. R. G., Bhat, D. J., & Wanasinghe, D. N. (2022). New soil-inhabiting Chaetosphaeriaceous records from Thailand. *Asian Journal of Mycology, 5*(1), 16–30. https://doi.org/10.5943/ajom/5/1/2

Yu, X. D., Zhang, S. N., Liang, X. D., Zhu, J. T., Hyde, K. D., & Liu, J. K. (2024). Bambusicolous fungi from Southwestern China. *Mycosphere, 15*(1), 5038–5145. https://doi.org/10.5943/mycosphere/15/1/20

Zhang, H., Hyde, K. D., McKenzie, E. H., Bahkali, A. H., & Zhou, D. (2012). Sequence data reveals phylogenetic affinities of *Acrocalymma aquatica* sp. nov., *Aquasubmersa mircensis* gen. et sp. nov. and *Clohesyomyces aquaticus* (freshwater coelomycetes). *Cryptogamie, Mycologie, 33*(3), 333–346. https://doi.org/10.7872/crym.v33.iss3.2012.333

Zhang, Y., Zhang, X., Fournier, J., Chen, J., & Hyde, K. D. (2013). *Lindgomyces griseosporus*, a new aquatic ascomycete from Europe including new records. *Mycoscience, 55*(1), 43–48. https://doi.org/10.1016/j.myc.2013.01.004

Zheng, W., Zhao, Z., Lv, F., Yin, Y., Wang, Z., Zhao, Z., . . . Zhai, B. (2021). Fungal alpha diversity influences stochasticity of bacterial and fungal community assemblies in soil aggregates in an apple orchard. *Applied Soil Ecology, 162*, 103878. https://doi.org/10.1016/j.apsoil.2021.103878

Zhou, D., & Hyde, K. D. (2001). Host-specificity, host-exclusivity, and host-recurrence in saprobic fungi. *Mycological Research, 105*(12), 1449–1457. https://doi.org/10.1017/S0953756201004912

Zhou, B., Tu, T., Kong, F., Wen, J., & Xu, X. (2018). Revised phylogeny and historical biogeography of the cosmopolitan aquatic plant genus *Typha* (Typhaceae). *Scientific Reports, 8,* 813. https://doi.org/10.1038/s41598-018-27279-3

Zhou, X. U., Yihui, B. A. N., Jiang, Y., Zhang, X., & Xiaoying, L. I. U. (2016). Arbuscular mycorrhizal fungi in wetland habitats and their application in constructed wetland: A review. *Pedosphere, 26*(5), 592–617. https://doi.org/10.1016/S1002-0160(15)60091-1

Zhou, Z. F., Zhao, W. X., Lin, R. Z., Huai, W. X., & Yao, Y. X. (2020). Diversity of associated fungi of *Agrilus mali* (Coleoptera: Buprestidae) in wild apple forests of Xinjiang. *Journal Name, Volume* (Issue), pages.

Zhouying, X. U., Yihui, B. A. N., Jiang, Y., Zhang, X., & Xiaoying, L. I. U. (2016). Arbuscular mycorrhizal fungi in wetland habitats and their application in constructed wetland: A review. *Pedosphere, 26*(5), 592–617.

APPENDIX A

CHEMICAL REAGENTS AND MEDIA

1. Potassium hydroxide (KOH) used in the rehydration of dried specimens. 5% aqueous solution

2. Lactoglycerol used for maintaining semipermanent slides

Lactic acid 10 ml

Glycerol 10 ml

Distilled water 10 ml

Mix 10 ml lactic acid, 10 ml glycerol, and add 10 ml distilled water

3. Lactic acid which preserves fungal structures and for getting a true color image of the fungal spore and structures without staining. This is helpful for some of the darker colored organisms.

85% Lactic acid 100 ml

3. Lactophenol-Cotton Blue used to highlight fungal structures for viewing with the compound light microscope. Cotton blue is the most popular stain for observe pseudoparaphyses, septate or ascus walled. This is gives excellent clarity and is also suitable for most fungal groups

Phenol (crystals) 20 g

Lactic acid 16 ml

Glycerol 31 ml

Dissolve phenol in distilled water, add lactic acid, glycerol and 0.05 g of Poirrier's (cotton) blue or acid fuchsin.

4. Melzer's Reagent is a good general mounting medium that clears the material somewhat and allows particularly brilliant resolution with a microscope, and used for identification of ascomycete fungi. Amyloid reaction of asci changed to blue or heavily purple colours.

Chloral hydrate 100 g

Potassium iodide 5 g

Iodine 1.5 g

Distilled water 100 ml

5. Malt Extract Agar (MEA) used for fungal cultivation

Agar 15 g

Peptone 0.78 g

Glycerol 2.35 g

Dextrin 2.75 g

Maltose, Technical 12.75 g

Suspend 33.6 g of malt extract agar in distilled water and mix thoroughly. Heat with frequent agitation and boil for 1 minute to completely dissolve the power and bring volume to 1000 ml. Autoclave at 121^{o}C for 15 minutes

6. Potato dextrose agar (PDA) used for fungal cultivation

Potato starch (from infusion) 4 g

Dextrose 20 g

Agar 15 g

Suspend 39 g of Potato dextrose agar in distilled water and mix thoroughly. Heat with frequent agitation and boil for 1 minute to completely dissolve the power and bring volume to 1000 ml. Autoclave at 121^{o}C for 15 minutes.

APPENDIX B

PUBLICATIONS

Phytotaxa 644 (4): 281–293
https://www.mapress.com/pt/
Copyright © 2024 Magnolia Press

Article

ISSN 1179-3155 (print edition)
PHYTOTAXA
ISSN 1179-3163 (online edition)

https://doi.org/10.11646/phytotaxa.644.4.4

Morphology and multigene phylogeny reveal a novel *Stagonospora* species (*Massarinaceae*, *Dothideomycetes*) from Thailand

AMUHENAGE T. BHAGYA[1,2,5], CHAYANARD PHUKHAMSAKDA[2,6,*], KAZUAKI TANAKA[3,7] & E.B. GARETH JONES[4,8,*]

[1]*School of Science, Mae Fah Luang University, Chiang Rai 57100, Thailand*
[2]*Center of Excellence in Fungal Research, Mae Fah Luang University, Chiang Rai 57100, Thailand*
[3]*Faculty of Agriculture and Life Science, Hirosaki University, 3 Bunkyo-cho, Hirosaki, Aomori 036-8561, Japan*
[4]*Department of Botany and Microbiology, College of Science, King Saud University, P.O Box 2455, Riyadh, 11451, Kingdom of Saudi Arabia*
[5] bhagyatvex@gmail.com; https://orcid.org/0009-0002-3988-298X
[6] chayanard.phu@mfu.ac.th; https://orcid.org/0000-0002-1033-937X
[7] k-tanaka@hirosaki-u.ac.jp; https://orcid.org/0000-0002-7037-0774
[8] torperadgf@gmail.com; https://orcid.org/0000-0002-7286-5471
*Corresponding authors: torperadgf@gmail.com (E.B. Gareth Jones); chayanard.phu@mfu.ac.th (Chayanard Phukhamsakda)

Abstract

Stagonospora is an asexual morph genus that is classified under *Massarinaceae* in *Dothideomycetes*. *Stagonospora* species have been recorded in both tropical and temperate regions. Several species have been reported as saprobic or opportunistic pathogenic lifestyles on grasses and grass-like plants. In this study, *Stagonospora* was collected from a *Typha* species in Sam Roi Yot wetland in central Thailand. Morphological examination was coupled with multi-loci phylogenetic analyses using maximum likelihood and Bayesian interference of a data set containing large subunit ribosomal rDNA (LSU rDNA), internal transcribed spacer (ITS) regions, small subunit ribosomal rDNA (SSU rDNA), and translation elongation factor 1-alpha (*tef1-α*) sequences. Our new taxon is distinguishable from other *Stagonospora* species by having hyaline, one-septate conidia that taper toward the base. This discovery holds significant value in comprehending the fungal diversity within Thailand's wetlands and the specific fungal communities linked to *Typha* plants.

Key words: 1 new species, fungal taxonomy, *Pleosporales*, *Typhaceae*, wetland fungi

Introduction

Stagonospora was introduced by Saccardo & Spegazzini (1884) (Wijayawardene *et al*. 2022) and typified with *Stagonospora paludosa* based on the basionym *Hendersonia paludosa*. *Stagonospora* is an asexual morph, characterized by having immersed, globose, black pycnidia, peridial wall of *textura angularis* cells, with phialidic and hyaline conidiogenous cells, and conidia are guttulate, subcylindrical, (6–)7–8-septate, becoming constricted at septa when mature (Quaedvlieg *et al*. 2013, Jayasiri *et al*. 2015). Phylogenetic studies show that *Stagonospora* is polyphyletic with more than 550 entries listed in MycoBank and Species Fungorum and with sexual morphs in over 20 genera (Quaedvlieg *et al*. 2013, Species Fungorum 2024). Currently, 220 species are accepted in *Stagonospora* (Wijayawardene *et al*. 2022), with hosts in a wide range of plant families, including families under order *Poales*, and often confused with *Septoria*. Quaedvlieg *et al*. (2013) opined that *Stagonospora paludosa* is confined to the plant genus *Carex* and is currently placed in *Massarinaceae*, while other *Stagonospora* species have been referred to many other families, including *Diaporthaceae*, *Didymellaceae*, *Lentitheciaceae*, *Lophiostomataceae*, *Planistromellaceae*, *Sporocadaceae*, and *Teratosphaeriaceae* (Wijayawardene *et al*. 2022).

The sexual morph of *Stagonospora* is distinguishable by globose, brown ascomata that are erumpent on host tissue and have a minute ostiole. The peridium comprises cells of *textura angularis*, with dense, hyaline and septate pseudoparaphyses, bitunicate, clavate asci with eight ascospores, and the ascospores are ellipsoidal, 1-septate, with guttules in each cell (Quaedvlieg *et al*. 2013). *Stagonospora* asexual morphs are characterized by pycnidia that are

Accepted by Eric McKenzie: 26 Mar. 2024; published: 17 Apr. 2024

NEW ZEALAND JOURNAL OF BOTANY
https://doi.org/10.1080/0028825X.2025.2488389

Taylor & Francis
Taylor & Francis Group

RESEARCH ARTICLE

Unveiling a novel *Zopfiella* species (*Lasiosphaeriaceae, Sordariales*): morphological characteristics and multigene phylogeny from *Carex* sp., (Cyperaceae) in Thailand

Amuhenage T. Bhagya[a,b], Chayanard Phukhamsakda[a,b], E. B. Gareth Jones[c] and Kevin D. Hyde[a,b,c]

[a]School of Science, Mae Fah Luang University, Chiang Rai, Thailand; [b]Center of Excellence in Fungal Research, Mae Fah Luang University, Chiang Rai, Thailand; [c]Department of Botany and Microbiology, College of Science, King Saud University, Riyadh, Kingdom of Saudi Arabia

ABSTRACT

Zopfiella is a polyphyletic genus in *Lasiosphaeriaceae, Sordariomycetes*. The habitats of *Zopfiella* species range from aquatic environments to soil, and some are coprophilous. Our isolate was obtained from decomposing submerged Cyperaceae stems in Pranburi Wetland, in central Thailand. The morphological examination including cleistothecial ascomata, evanescent asci and ascospores with hyaline, deliquescing, basal cell are supplemented by phylogenetic analyses using maximum likelihood and Bayesian Interference of the large subunit ribosomal rDNA (LSU), internal transcribed spacer (ITS) regions, β-tubulin (*tub2*), and RNA polymerase II (*rpb2*) loci. *Zopfiella cyperacearum* (MFLUCC 25–0170) is distinct for its pale brown ascomatal hairs protruding from the ascomata, its overall size that is smaller compared to closely related *Zopfiella* species such as *Z. latipes* (IFO 9826) and significant base pair differences in target loci.

ARTICLE HISTORY
Received 27 September 2024
Accepted 9 March 2025
First published online 28 April 2025

HANDLING EDITOR
Milan Samarakoon

KEYWORDS
1 new species; *Cyperaceae*; fungal taxonomy; *Sordariomycetidae*; wetland fungi

Introduction

Genera in the family *Lasiosphaeriaceae* are saprobes on decomposing submerged wood and rotting plant material, including stems, leaves and driftwood (Huang et al. 2021). Several species in this family including species of *Zopfiella* are coprophilous and found on herbivore dung (Maharachchikumbura et al. 2015; Melo et al. 2015; Marin-Felix et al. 2020). The sexual morphs of the family are characterised by globose or subglobose, carbonaceous to coriaceous, perithecial or cleistothecial ascomata. The peridium layers are composed by cells of *textura angularis* and cells of *textura prismatica* (Maharachchikumbura et al. 2015). The hamathecium comprises hyaline, cellular paraphyses, and unitunicate, cylindrical or clavate asci. Ascospores are aseptate or multi-septate, uniformly coloured or showing variation in colour (Maharachchikumbura et al. 2016; Marin-Felix et al. 2020). Asexual morphs produce branched, conidiophores with terminal, enteroblastic or holoblastic conidiogenous cells, which give rise to globose,

CONTACT Chayanard Phukhamsakda chayanard.phu@mfu.ac.th; E. B. Gareth Jones torperadgj@gmail.com

CURRICULUM VITAE

NAME Amuhenage Tharindu Bhagya Maithreepala

EDUCATIONAL BACKGROUND

2019 Maters of Science in Crop Protection and Plant Biotechnology
Faculty of Science
University of Kelaniya

2015 Bachelor of Science in Food Science and Technology
Faculty of Applied Science
Sabaragamuwa University of Sri Lanka

PUBLICATIONS

Bhagya, A. T., Phukhamsakda, C., Tanaka, K., & Jones, E. G. (2024). Morphology and multigene phylogeny reveal a novel Stagonospora species (*Massarinaceae, Dothideomycetes*) from Thailand. *Phytotaxa*, *644*(4), 281-293. https://doi.org/10.11646/phytotaxa.644.4.4

Bhagya, A. T., Phukhamsakda, C., Jones, E. G., & Hyde, K. D. (2025). Unveiling a novel *Zopfiella* species (*Lasiosphaeriaceae, Sordariales*): Morphological characteristics and multigene phylogeny from *Carex* sp., (Cyperaceae) in Thailand. *New Zealand Journal of Botany*, *63*(5), 1419-1430.

Rathnayaka, A. R., Chethana, K. T., Manowong, A., Bhagya, A. T., Win, H., Tun, Z. L., . . . Hyde, K. D. (2025). Taxonomy, phylogeny, and bioactive potential of *Xylariales* (*Sordariomycetes, Ascomycota*) from Thailand: Novel species discovery, new host and geographical records, and antibacterial properties. *MycoKeys*, *120*, 35-117. https://doi.org/10.3897/mycokeys.120.155915

Balagamage, D. T., Maharachchikumbura, S. S. N., Amuhenage, T. B., Phukhamsakda, C., Marin-Felix, Y., Wang, Z.-Y., . . . Liu, J.-K. (2024). Paradictyoarthrinium diffractum, a new host record on Delonix regia in northern Thailand. *Fungal Biotec*, *4*(1), 125-132.

Hyde, K. D., Wijesinghe, S. N., Amuhenage, T. B., Bera, I., Bhunjun, C. S., Chethana, K. W. T., . . . Zhao, H. J. (2024). Current research in applied and environmental mycology fungal profiles 1–30. *Current Research in Environmental & Applied Mycology, 14*(1), 167-266. https://doi.org/10.5943/cream/14/1/11

Hyde, K. D., Abdel-Wahab, M. A., Abdollahzadeh, J., Abeywickrama, P. D., Absalan, S., Afshari, N., . . . Radek, R. (2023). Global consortium for the classification of fungi and fungus-like taxa. *Mycosphere, 14,* 1960-2012. https://doi.org/10.5943/mycosphere/14/1/23

Hyde, K. D., Amuhenage, T. B., Apurillo, C. C. S., Asghari, R., Aumentado, H. D., Bahkali, A. H., . . . Dai, D. Q. (2023). Fungalpedia: An illustrated compendium of the fungi and fungus-like taxa. *Mycosphere, 14*(1), 1835–1959. https://doi.org/10.5943/mycosphere/14/1/22